EMERGING INFECTIOUS DISEASES®

Zoonoses

December 2019

EMERGING INFECTIOUS DISEASES

EDITOR-IN-CHIEF
D. Peter Drotman

DECEMBER 2019 IS EID'S FINAL PRINT ISSUE

Emerging Infectious Diseases will transition to an online-only journal starting with the January 2020 issue, the beginning of Volume 26.

Bookmark the journal's website so you can access and search all of EID*'s* new and archived content, and sign up for email notifications for monthly table of content alerts and topics of interest.

https://wwwnc.cdc.gov/eid/

EMERGING INFECTIOUS DISEASES®

On the Cover

Joan Miró (1893–1983), *The Tilled Field* (*La Terre Labourée*), 1923–1924. Oil on canvas; 26 in × 36.5 in/66 cm × 92.7 cm. © 2018 Successió Miró / Artists Rights Society (ARS), New York / ADAGP, Paris 2019. Photo Credit: The Solomon R. Guggenheim Museum/Art Resource, New York, New York, USA.

About the Cover p. 2344

Dispatches

EMERGING INFECTIOUS DISEASES®

December 2019

2199

EMERGING INFECTIOUS DISEASES®
December 2019

2279

Seroprevalence and Risk Factors Possibly Associated with Emerging Zoonotic Vaccinia Virus in a Farming Community, Colombia

Ashley Styczynski, Jillybeth Burgado, Diana Walteros, José Usme-Ciro, Katherine Laiton, Alejandra Pinilla Farias, Yoshinori Nakazawa, Christina Chapman, Whitni Davidson, Matthew Mauldin, Clint Morgan, Juan Martínez-Cerón, Edilson Patiña, Leidy Laura López Sepúlveda, Claudia Patricia Torres, Anyely Eliana Cruz Suarez, Gina Paez Olaya, Carlos Elkin Riveros, Diana Yaneth Cepeda, Leydi Acosta Lopez, Daniela Gomez Espinosa, Faiber Antonio Gutierrez Lozada, Yu Li, P.S. Satheshkumar, Mary Reynolds, Martha Gracia-Romero, Brett Petersen

In 2014, vaccinia virus (VACV) infections were identified among farmworkers in Caquetá Department, Colombia; additional cases were identified in Cundinamarca Department in 2015. VACV, an orthopoxvirus (OPXV) used in the smallpox vaccine, has caused sporadic bovine and human outbreaks in countries such as Brazil and India. In response to the emergence of this disease in Colombia, we surveyed and collected blood from 134 farmworkers and household members from 56 farms in Cundinamarca Department. We tested serum samples for OPXV antibodies and correlated risk factors with seropositivity by using multivariate analyses. Fifty-two percent of farmworkers had OPXV antibodies; this percentage decreased to 31% when we excluded persons who would have been eligible for smallpox vaccination. The major risk factors for seropositivity were municipality, age, smallpox vaccination scar, duration of time working on a farm, and animals having vaccinia-like lesions. This investigation provides evidence for possible emergence of VACV as a zoonosis in South America.

Vaccinia virus (VACV) is a member of the genus *Orthopoxvirus* within the family *Poxviridae*. Other notable viruses in this lineage include cowpox, monkeypox, and variola (causative agent of smallpox). Because of immunologic cross-reactivity of orthopoxviruses (OPXVs), cutaneous inoculation with VACV through a worldwide vaccination campaign led to the eradication of smallpox in 1980. However, unlike variola virus, VACV can infect nonhuman hosts (*1*). The origin of VACV remains unknown, but the virus is thought to have originated in continental Europe before being isolated and used as the vaccine against smallpox (*2*). Transmission of VACV from humans to cattle was reported during the smallpox eradication campaign, which has engendered debate over whether VACV escaped into animals as a result of vaccination efforts (*3–9*). Regardless of the event that led to zoonotic circulation, recent studies have demonstrated ongoing infections with related VACV

viruses in Brazil, suggesting endemic spread through a common reservoir (*10,11*).

Several sporadic outbreaks of VACV have been reported in humans and cattle in Brazil and India, where mechanisms of transmission have been attributed to cross-inoculation between teats of cows and hands of milkers (*12–19*). Although no reservoir has been identified, data suggest that rodents might be implicated in the transmission and maintenance of the virus (*4,20–23*). Furthermore, laboratory studies have demonstrated the feasibility of rodents as reservoirs (*20,24,25*).

VACV outbreaks have proven hazardous in terms of human health and economic impact (*12,18*), but without an identifiable reservoir, control efforts are limited to hygiene and isolation strategies. In addition, prior smallpox vaccination is not necessarily protective against VACV during outbreaks, likely because of waning immunity (*17*). Another potential concern is the transmission of VACV through the milk of affected cows, which has been experimentally demonstrated by the persistence of viable virus despite heat or refrigeration (*26–30*).

In the course of increased surveillance and education activities, Colombia has confirmed VACV infections in >3 departments; several additional cases of similar pox-like lesions have been reported throughout the country, particularly affecting farmworkers responsible for milking cows (Andres Paez, Instituto Nacional de Salud, pers. comm., email, 2015 Oct 7). Phylogenetic analyses of isolates obtained from case-patients in Colombia demonstrate some differences from strains circulating in Brazil, although limited genetic sequencing precludes definitive determination of the source (*31,32*). This genetic divergence suggests that VACV might be widespread in Colombia; however, its distribution and associated risk factors for transmission have not been systematically evaluated. To help clarify the burden of VACV and risk factors associated with disease exposure, we conducted a serosurvey and risk factor assessment in the municipality of Medina in Cundinamarca Department, Colombia, where several human cases of PCR-confirmed VACV infections had been reported in the preceding year.

Methods

Respondent Selection
During August–September 2016, we performed a serologic investigation of farmworkers and household members in Cundinamarca Department. We selected farms based on respondent availability from a list of farms provided by the local secretary of health. After obtaining informed consent from adults and permission from parents of children <18 years of age, we administered a questionnaire regarding demographic characteristics, exposures, travel history,

Author affiliations: Centers for Disease Control and Prevention, Atlanta, GA, USA (A. Styczynski, J. Burgado, Y. Nakazawa, C. Chapman, W. Davidson, M. Mauldin, C. Morgan, Y. Li, P.S. Satheshkumar, M. Reynolds, B. Petersen); Instituto Nacional de Salud, Bogotá, Colombia (D. Walteros, J. Usme-Ciro, K. Laiton, A.P. Farias, M. Gracia-Romero); Universidad Cooperativa de Colombia, Santa Marta, Colombia (J. Usme-Ciro); Universidad de Antioquia, Medellín, Colombia (J. Martínez-Cerón, E. Patiña, L.L. López Sepúlveda); Secretaria de Salud de Cundinamarca, Bogotá (C.P. Torres, A.E. Cruz Suarez, G.P. Olaya, C.E. Riveros); Hospital Nuestra Señora del Pilar de Medina, Medina, Colombia (D.Y. Cepeda); Vigilancia en Salud Publica, Bogotá (L.A. Lopez); Universidad Javeriana, Bogotá (D.G. Espinosa); Secretaria de Salud de Caquetá, Florencia, Columbia (F.A. Gutierrez Lozada)

DOI: https://doi.org/10.3201/eid2512.181114

and farming practices. We also collected serum samples from interviewees to correlate risk factors with serologic evidence of VACV exposure. We received a total of 134 responses and corresponding specimens from persons on 56 separate farms.

Orthopoxvirus Antibody Detection

We used IgG ELISA to evaluate the presence of orthopoxvirus-specific antibodies (i.e., anti-OPXV) as previously described (33). We coated Immulon II High Binding microtiter plates (ThermoFisher Scientific, https://www.thermofisher.com) with purified VACV DryVax strain at 0.1µg/mL in carbonate buffer, incubated overnight at 4°C, inactivated with 10% formalin, and washed 3 times with PBST (PBS with 0.05% Tween-20) by using a BioTek 405TS plate washer (Biotek, https://www.biotek.com). We then blocked plates at room temperature for 30–60 min with assay diluent containing 5% dried skim milk, 2% normal goat serum, and 2% bovine serum albumin in PBST. After blocking, we washed plates 3 times with PBST, added serum samples at 1:100 dilution in duplicate, and incubated for 1 h at 37°C. We washed plates again and added goat anti-human IgG horseradish peroxidase conjugate (KPL antibodies) (SeraCare, https://www.seracare.com) at 1:2,000 concentration, incubated for 1 h at 37°C, and washed. We then added SureBlue TMB 1-component microwell peroxidase substrate (KPL antibodies) (SeraCare) and developed for 4 min at room temperature before stopping the reaction with addition of equal volume of TMB Stop Solution (SeraCare). We read optical density (OD) on an Enspire plate reader (Perkin Elmer, https://www.perkinelmer.com) at 450 nm.

For the IgM ELISA, we coated microtiter plates (Immulon II) with goat anti-human IgM KPL antibodies at 1:800 dilution in PBS (pH 7.4) and incubated overnight at 4°C. We then washed plates 5 times with PBST by using a plate washer and blocked for 30 min to 1 h at room temperature with assay diluent buffer containing 0.5% gelatin, 2% BSA, 5% skim milk, and 2% normal goat serum in PBST. We added test serum samples at 1:50 dilution in duplicates in assay diluent and incubated for 1 h at 37°C. We washed plates, added antigen (purified VACV) at a concentration of 0.5 µg/mL, and incubated for 1 h at 37°C. We washed plates again and incubated with 1:250 dilution of anti-variola virus hyperimmune mouse polyclonal ascetic fluid for 1 h at 37°C, followed by washing and incubation with 1:6,000 dilution of goat anti-mouse IgG horseradish peroxidase conjugate (KPL antibodies) for 1 h at 37°C. We then washed the plates again and developed with SureBlue TMB 1-component microwell peroxidase substrate for 8 min at room temperature, after which we added equal volume of TMB Stop Solution to each well. We read on an Enspire plate reader at 450 nm.

We averaged OD values for known negative controls and determined a cutoff value by using the equation cutoff value: average negatives + 3 × SD of negatives. We subtracted the cutoff value from the OD values of test samples. If the resulting value was >0.05, we considered the serum sample positive for the presence of OPXV antibodies.

Data Analyses

To identify risk factors associated with OPXV exposure, we performed a nested case–control analysis on the basis of serologic test results. We classified as case-patients those persons with a positive test for OPXV IgM or IgG, which is not specific for VACV but is a reasonable approximation of exposure (either through natural infection or vaccination), given a lack of other known circulating OPXVs in this region. Conversely, we identified as controls those persons without serologic evidence of OPXV exposure. To determine odds ratios (ORs) and 95% CIs, we performed a complex sample analysis to account for clustering of responses and serologic outcomes by farm. Variables found to have a p value <0.1 in bivariate analysis were included in a multivariable model analysis.

We also evaluated the correlation of farm-level characteristics with seropositivity of any persons associated with the farm. We performed bivariate analysis on individual

Table 1. Demographic characteristics of 134 farmworkers and household members from 56 farms in Cundinamarca Department, Colombia, August–September 2016*

Characteristic	Value
Sex	
M	69 (51.5)
F	65 (48.5)
Median age, y (range)	45.5 (12–82)
Municipality of residence	
Medina	114 (85.1)
Ubala	19 (14.2)
Paratebueno	1 (0.7)
Education	
None	25 (18.7)
Primary	67 (50)
Secondary	22 (16.4)
Post-secondary	9 (6.7)
Other	11 (8.2)
Live in rural setting	128 (95.5)
Work outdoors	125 (93.3)
Work with animals	128 (95.5)
Self-report history of smallpox vaccination	46 (34.4)
Eligibility for smallpox vaccine (i.e., respondents age ≥44 y)	76 (56.7)
Seropositivity	
IgM	2 (1.5)
IgG	70 (52.2)
IgM or IgG	70 (52.2)
IgM or IgG among respondents age <44 y	18 (31)
Contact with cows	129 (96.3)
Milk cows	115 (85.8)
Work on multiple farms concurrently	50 (37.3)
Prior knowledge of poxviruses	28 (20.9)

*Values are no. (%) persons except as indicated.

risk factors to determine ORs and 95% CIs. Given that the last smallpox vaccination campaign occurred in Colombia in 1972, we separated persons on the basis of age of eligibility to have received the smallpox vaccine (*34*).

We subsequently built 2 multivariate logistic regression models by using individual-level risk factor data and farm survey data, respectively. We used seropositivity as the outcome variable. Using simple logistic regression, we included all variables found to be statistically significant at an α level of 0.1 in a stepwise model selection procedure. For individual-level risk factor data, we incorporated the variable that was most significant after being solely added to the model (if any were significant at an α level of 0.1) into the model. If any of the tested variables were no longer significant after this addition at an α level of 0.1, we dropped it from the model. This process continued until no variable was found to be significant, after each was solely added to the model. We checked variables for collinearity by using Pearson correlation coefficients; values <0.4 were considered to not be collinear.

We conducted a similar process with the farm survey data. In that case, we also forced into the model the variable indicating whether any animals with a history of vaccinia-like lesions were on the farm. We did this to evaluate the influence of suspected animal vaccinia virus infections on human seropositivity. Afterward, we conducted the same step-wise procedure.

Ethics Statement
Review by the Colombian Instituto Nacional de Salud and a human subjects advisor at the US Centers for Disease Control and Prevention determined that the activities did not meet the definition of research under 45 CFR 46.102(d). All adult participants provided informed written consent before interview participation and collection of specimens. Participants <18 years of age provided age-appropriate assent, and parents or guardians provided consent on their behalf.

Results

Demographics and Descriptive Analysis
Commensurate with the agricultural setting that characterizes Cundinamarca Department, participants in the investigation tended to live in rural environments and had frequent contact with animals (Table 1). Approximately equal numbers of men and women were enrolled; median age was 46 years. Based on the given age threshold (44 years of age), slightly more than half of the participants (57%) would have been eligible to have received a smallpox vaccine before the end of the vaccination campaign. However, only 34% of participants recalled a history of smallpox vaccination.

Nearly all participants (96%) reported contact with cows, and most of these persons participated in the milking process (86%). Thirty-seven percent of participants reported working concurrently on multiple farms, and ≈21% of participants had previously heard of VACV or other poxviruses.

Laboratory analysis demonstrated that 70 (52%) of the 134 participants were OPXV IgG positive, including 2 (1.5%) persons who were also OPXV IgM positive, suggesting a recent exposure (<6 months before). None of the participants was only positive for IgM. Excluding those born in 1972 or earlier, seropositivity for OPXV IgM or IgG was found among 18 (31%) of 58 people included in this category (Appendix Figure 1, https://wwwnc.cdc.gov/EID/article/25/12/18-1114-App1.pdf).

Eighteen seropositive persons also reported a history of a vaccinia-like lesion, primarily occurring on the hand (94.4%), but 3 persons reported eye involvement (Table 2). Of these 18 persons, 12 (67%) were <44 years of age, making them ineligible to have received a smallpox vaccine. The risk for symptomatic vaccinia-like lesions was not statistically different between those who self-reported smallpox vaccination and those who did not recall a

Table 2. Characteristics of 18 OPXV-seropositive persons with history of vaccinia-like lesions among farmworkers and household members from 56 farms in Cundinamarca Department, Colombia, August–September 2016*

Characteristic	Value
Age <44 y	12 (66.6)
Location of lesion(s)†	
Hand	17 (94.4)
Eyes	3 (16.7)
Arm	1 (5.6)
Face or neck	1 (5.6)
Leg	0
Median no. lesions (range)	1.5 (1–6)
Prior injury at site of lesion	5 (27.8)
Residual scar	13 (72.2)
Time off work because of lesion(s), d	10 (55.6)
Median time off work, d (range)	10 (3–15)
Evaluated by physician	11 (61.1)
Hospitalized	2 (11.1)
Lesion symptoms	
Localized pain	18 (100.0)
Pruritus	17 (94.4)
Swelling	15 (83.3)
Warmth	14 (77.8)
Discharge	12 (66.7)
Lymphangitis	11 (61.1)
Constitutional symptoms	
Generalized pain	10 (55.6)
Headache	10 (55.6)
Fever after lesion	10 (55.6)
Fever before lesion	4 (22.2)
Chills or rigors	4 (22.2)
Lymphadenopathy	3 (16.7)
Arthralgias	1 (5.6)
Myalgias	1 (5.6)

*Values are no. (%) persons except as indicated. OPXV, orthopoxvirus.
†Number of lesion locations is >18 because some persons had >1 lesion.

Table 3. Multivariate analysis of OPXV IgM or IgG seropositivity among farmworkers and household members from 56 farms in Cundinamarca Department, Colombia, August–September 2016*

Variable	OR (95% CI)	p value
Individual-level risk factors		
Age (dichotomous)	3.38 (1.31–8.74)	0.01
Smallpox scar	5.18 (1.71–15.66)	<0.01
In-country travel	0.11 (0.03–0.42)	<0.01
Duration of time working at current farm	2.34 (1.03–5.30)	0.04
Residence other than Medina	0.26 (0.07–1.04)	0.01
Farm-level risk factors		
Animals with vaccinia-like lesions	5.71 (0.90–36.19)	0.06
Commercial feed	0.16 (0.03–0.83)	0.03
Cattle fed after milking	0.19 (0.03–1.15)	0.07

*OPXV, orthopoxvirus; OR, odds ratio.

history of vaccination (OR 0.35, 95% CI 0.1–1.3). However, when we compared age of smallpox vaccine eligibility, being <44 years of age was strongly correlated with having a symptomatic vaccinia-like infection (OR 15.3, 95% CI 4.2–56.1).

Symptomatic persons experienced a median of 1.5 lesions, and lesions resulted in scarring in 13 of the 18 patients. Approximately one half of these persons took time off work because of their lesions, for a median of 10 days (range 3–15 days). Eleven people sought care from a physician, and 2 persons were hospitalized.

The lesions were most frequently characterized by localized pain and swelling, pruritus, and increased warmth (Table 2). Two thirds of patients also reported discharge from the lesion and lymphangitis. Many of the patients cited the co-occurrence of other symptoms including fever, malaise, and headache.

In the analysis of farm-level characteristics, 22 (39%) of the 56 farms reported animals with vaccinia-like lesions. Cows were the only domesticated animals noted to have vaccinia-like lesions, with the exception of 1 farm that also recalled pigs having similar lesions. The lesions were located on the udders or teats in all cases; 2 farms also reported oral lesions, and 1 farm reported genital lesions. Twenty (91%) of the 22 farms continued milking their cows in spite of the lesions. Outcomes of the lesions resulted in decreased milk production at 5 farms and caused scarring of the affected cows at 3 farms.

Bivariate Analysis

In the bivariate analysis of individual-level risk factors that we assessed, 13 variables were significantly associated with anti-OPXV seropositivity, including age as a continuous variable or as a dichotomous outcome based on eligibility for smallpox vaccination (Appendix Table 1). Age (dichotomous) and consumption of pork were the variables most strongly associated with seropositivity (OR 4.81 for age, OR 4.86 for pork consumption). Among the other significant factors were municipality of

residence, self-reported history of smallpox vaccination, presence of smallpox vaccination scar, cows living on the property of residence, time spent working on the current farm, previous work on other farms, and consumption of unpasteurized milk or cheese.

In the evaluation of farm-level risk factors, 7 variables were associated with seropositivity among farmworkers at the 0.1 level (Appendix Table 2). These variables included animals with vaccinia-like lesions, type of cattle feed, habitats surrounding the farm, and humans on the farm with vaccinia-like lesions.

Multivariate Analysis

For the multivariate analysis of individual-level risk factors, 5 variables were included in the final model: age (dichotomous), smallpox vaccination scar, in-country travel in the previous 12 months, duration of time spent working on current farm, and municipality of residence. All variables were significant at the p<0.05 level, and none were found to be collinear. Age ≥44 years, presence of a vaccination scar, and longer duration of time working on the current farm were predictive of anti-OPXV seropositivity, whereas in-country travel and residence outside of Medina were protective (Table 3).

Farm-level risk factors in the final model included animals with a history of vaccinia-like lesions, use of commercial feed, and feeding cattle after milking. Variables were significant at the p<0.1 level. Animals having vaccinia-like lesions was predictive of anti-OPXV seropositivity of farmworkers, but the other 2 variables were noted to be protective (Table 3).

Discussion

VACV is probably an emerging zoonosis in Colombia and poses a substantial health risk for the populations affected; namely, farmworkers involved in the dairy industry. In this investigation, OPXV seropositivity along with vaccinia-like symptoms among farmworkers resulted in increased use of healthcare services, loss of productive work days, and dermatologic scarring at the sites of infection. VACV-like infections among cattle resulted in decreased milk production and permanent scarring of teats.

Descriptions of VACV-like infections in this population revealed mostly localized, painful, cutaneous lesions affecting the hands, similar to other descriptions of bovine-related VACV infections (13,17,35). More than half of the patients also reported accompanying systemic symptoms such as fevers and malaise, and most of those affected required medical attention and time off work, indicating substantial economic ramifications. In addition, two thirds of the persons who were seropositive and reported a history of symptomatic lesions were ineligible to have received a smallpox vaccine, supporting the idea that

unvaccinated persons are at greater risk for symptomatic disease (*12*).

Regarding individual-level risk factors, the association of age and smallpox vaccination scar with OPXV seropositivity is expected because these are proxy (albeit imperfect) measures of smallpox vaccination status. Rural areas of the country might have ceased smallpox vaccination before 1972, and smallpox vaccination scars can be confused with bacillus Calmette–Guérin vaccination scars. As such, the actual effect of age on VACV exposure cannot be determined. Increased age might reflect a greater opportunity for exposure, which might explain the correlation with longer duration of working on the current farm, although this correlation might not be relevant if VACV only recently emerged in Colombia. More important, nearly one third of participants who were seropositive would have been ineligible for smallpox vaccination, signifying ongoing risk for population transmission (*36*).

Medina was the center of the VACV outbreak; therefore, living in Medina would be expected to be associated with seropositivity. However, because our investigation was geographically centered on Medina, very few participants resided outside this municipality. A more extensive investigation of other dairy-producing areas in the country might reveal differing results. The finding that in-country travel was protective might suggest that VACV is not extensively circulating in other areas of Colombia.

The reasons for consumption of pork strongly being correlated with seropositivity in the univariate analysis are not clear, given that pigs are not known to be natural hosts of VACV. In addition, few farms in this investigation raised pigs, although nearly all participants reported consuming pork. The fact that 1 farm did report vaccinia-like lesions on pigs might warrant further investigation using PCR testing. Regardless, this variable was excluded through stepwise selection in the multivariate analysis, possibly indicating a measure of confounding.

Among farm-level characteristics, the correlation of human seropositivity with animals having vaccinia-like lesions demonstrates that farmers correctly identified lesions on cattle as being consistent with VACV, although this finding does not answer the question of whether cattle acquired the infection from milkers or vice versa. The observed protective effect of commercial feed might be attributable to commercial feed being less likely to be contaminated by rodent urine and feces, which have been shown to harbor VACV (*24,25*). Reduced VACV exposure by cattle would thus translate into reduced human exposure.

Variables that do not correlate with seropositivity might be as informative as variables that predict seropositivity. In particular, having rodents near the residence, having other household members with VACV-like lesions, consuming unpasteurized dairy products, and having cows that live on the property were not associated with seropositivity in multivariate analysis. These findings underscore that humans are more frequently infected through interaction with cows than with rodents.

VACV has been documented to spread within households, including through household fomites (*31,37,38*), so it is somewhat surprising that having other household members with VACV-like lesions was not identified as a risk factor in this investigation. This finding might indicate that household transmission is not a primary mechanism of VACV spread and that the main means of transmission might be directly from cows to humans. Alternatively, because a high rate of respondents had contact with cows, the significance of transmission only through household contact could not be elucidated. Furthermore, an average of only 2 persons from most households participated in interviews and blood sample collection, so a more dedicated investigation might be needed to evaluate the significance of household spread.

VACV has been detected in unpasteurized dairy products (*24*), but the effect of such contamination on VACV transmission is unknown. In our investigation, consuming unpasteurized dairy products did not correlate with seropositivity, which might indicate that such consumption is not an important mechanism for VACV exposure. Nonetheless, additional population-level studies and testing of dairy products should be performed before negating the consumption of unpasteurized dairy products as a potential risk factor, especially given the high rate of farms that continued milking their cows despite the presence of active lesions. Further assessments regarding dairy products as a potential mechanism of disease spread will be necessary for guiding public health recommendations.

Despite an extensive questionnaire, few farming practices were found to correlate with human seropositivity. This finding could indicate that farming practices do not affect VACV transmission, but, more likely, it reflects homogeneity of farming practices that did not enable distinguishing between specific practices. Of note, all of the surveyed farms had small numbers of cattle and performed manual milking, making the risk for contact transmission either between cattle or between humans and cattle particularly germane. Additional investigation regarding animal seropositivity will be important for gaining insight into the effects of farming practices.

The findings of this investigation are similar to results from studies carried out in Brazil that found a positive correlation between age and seropositivity, although the effect of prior smallpox immunization could not be ruled out. In addition, report of animals with a history of vaccinia-like lesions was predictive of human seropositivity (*39*).

Clinical descriptions of painful, cutaneous lesions with associated systemic symptoms of headache, fever,

and lymphadenopathy align closely with descriptions from Brazil during bovine-associated human outbreaks. Also similar to previous reports, vaccinia-like lesions were reported among persons who would have been age-eligible and self-reported prior smallpox vaccination, implying that prior vaccination might be only partially protective (*12,17,35,40*).

The results of this investigation offer additional insight on the emergence of bovine-associated VACV-like infections in Colombia, which has only recently been described. OPXV seropositivity was linked to VACV-like symptoms in 13% of persons, particularly among those who had not been vaccinated against smallpox, demonstrating a substantial burden of disease in this population. However, these results do not provide a full understanding of the geographic extent of VACV circulation in Colombia, and more widespread assessments that include PCR data will be important for estimating population-level effects.

This outbreak investigation reveals that VACV is likely to become an increasingly important zoonosis in this part of the world, either through independent emergence events or expanding reservoir habitats against a backdrop of waning immunity. Using this type of data to clarify risk factors associated with seropositivity and disease transmission, alongside models that predict areas of disease spread, will be important for directing public health efforts to raise awareness and implement preventive measures to minimize adverse social and economic effects (*36,41*).

About the Author

Dr. Styczynski is an infectious disease fellow at Stanford University in Palo Alto, California, USA. Her primary research interests include global infectious disease epidemiology and emerging infections.

References

1. Essbauer S, Pfeffer M, Meyer H. Zoonotic poxviruses. Vet Microbiol. 2010;140:229–36. https://doi.org/10.1016/j.vetmic.2009.08.026
2. Carroll DS, Emerson GL, Li Y, Sammons S, Olson V, Frace M, et al. Chasing Jenner's vaccine: revisiting cowpox virus classification. PLoS One. 2011;6:e23086. https://doi.org/10.1371/journal.pone.0023086
3. Damaso CR, Esposito JJ, Condit RC, Moussatché N. An emergent poxvirus from humans and cattle in Rio de Janeiro State: Cantagalo virus may derive from Brazilian smallpox vaccine. Virology. 2000;277:439–49. https://doi.org/10.1006/viro.2000.0603
4. Fonseca FG, Lanna MC, Campos MA, Kitajima EW, Peres JN, Golgher RR, et al. Morphological and molecular characterization of the poxvirus BeAn 58058. Arch Virol. 1998;143:1171–86. https://doi.org/10.1007/s007050050365
5. Marques JT, Trindade GD, Da Fonseca FG, Dos Santos JR, Bonjardim CA, Ferreira PC, et al. Characterization of ATI, TK and IFN-alpha/betaR genes in the genome of the BeAn 58058 virus, a naturally attenuated wild orthopoxvirus. Virus Genes. 2001;23:291–301. https://doi.org/10.1023/A:1012521322845
6. Peres MG, Bacchiega TS, Appolinário CM, Vicente AF, Mioni MSR, Ribeiro BLD, et al. Vaccinia virus in feces and urine of wild rodents from São Paulo State, Brazil. Viruses. 2018;10:E51. https://doi.org/10.3390/v10020051
7. Medaglia ML, Moussatché N, Nitsche A, Dabrowski PW, Li Y, Damon IK, et al. Genomic analysis, phenotype, and virulence of the historical Brazilian smallpox vaccine strain IOC: implications for the origins and evolutionary relationships of vaccinia Virus. J Virol. 2015;89:11909–25. https://doi.org/10.1128/JVI.01833-15
8. Gómez Pando V, Hernán López J, Restrepo A, Forero P. Study of an outbreak of vaccinia in dairy cattle of their milkers [in Spanish]. Bol Oficina Sanit Panam. 1967;63:111–21.
9. Lum GS, Soriano F, Trejos A, Llerena J. Vaccinia epidemic and epizootic in El Salvador. Am J Trop Med Hyg. 1967;16:332–8. https://doi.org/10.4269/ajtmh.1967.16.332
10. Trindade GS, Emerson GL, Carroll DS, Kroon EG, Damon IK. Brazilian vaccinia viruses and their origins. Emerg Infect Dis. 2007;13:965–72. https://doi.org/10.3201/eid1307.061404
11. Trindade GS, Lobato ZI, Drumond BP, Leite JA, Trigueiro RC, Guedes MI, et al. Isolation of two vaccinia virus strains from a single bovine vaccinia outbreak in rural area from Brazil: implications on the emergence of zoonotic orthopoxviruses. Am J Trop Med Hyg. 2006;75:486–90. https://doi.org/10.4269/ajtmh.2006.75.486
12. Abrahão JS, Campos RK, Trindade GS, Guimarães da Fonseca F, Ferreira PC, Kroon EG. Outbreak of severe zoonotic vaccinia virus infection, southeastern Brazil. Emerg Infect Dis. 2015;21:695–8. https://doi.org/10.3201/eid2104.140351
13. Nagasse-Sugahara TK, Kisielius JJ, Ueda-Ito M, Curti SP, Figueiredo CA, Cruz AS, et al. Human vaccinia-like virus outbreaks in São Paulo and Goiás States, Brazil: virus detection, isolation and identification. Rev Inst Med Trop São Paulo. 2004; 46:315–22. https://doi.org/10.1590/S0036-46652004000600004
14. de Souza Trindade G, da Fonseca FG, Marques JT, Nogueira ML, Mendes LC, Borges AS, et al. Araçatuba virus: a vaccinialike virus associated with infection in humans and cattle. Emerg Infect Dis. 2003;9:155–60. https://doi.org/10.3201/eid0902.020244
15. Leite JA, Drumond BP, Trindade GS, Lobato ZI, da Fonseca FG, dos SJ, et al. Passatempo virus, a vaccinia virus strain, Brazil. Emerg Infect Dis. 2005;11:1935–8. https://doi.org/10.3201/eid1112.050773
16. Megid J, Borges IA, Abrahão JS, Trindade GS, Appolinário CM, Ribeiro MG, et al. Vaccinia virus zoonotic infection, São Paulo State, Brazil. Emerg Infect Dis. 2012;18:189–91. https://doi.org/10.3201/eid1801.110692
17. Silva-Fernandes AT, Travassos CE, Ferreira JM, Abrahão JS, Rocha ES, Viana-Ferreira F, et al. Natural human infections with vaccinia virus during bovine vaccinia outbreaks. J Clin Virol. 2009;44:308–13. https://doi.org/10.1016/j.jcv.2009.01.007
18. Singh RK, Hosamani M, Balamurugan V, Satheesh CC, Shingal KR, Tatwarti SB, et al. An outbreak of buffalopox in buffalo (*Bubalus bubalis*) dairy herds in Aurangabad, India. Rev Sci Tech. 2006;25:981–7. https://doi.org/10.20506/rst.25.3.1708
19. Yadav S, Hosamani M, Balamurugan V, Bhanuprakash V, Singh RK. Partial genetic characterization of viruses isolated from pox-like infection in cattle and buffaloes: evidence of buffalo pox virus circulation in Indian cows. Arch Virol. 2010;155:255–61. https://doi.org/10.1007/s00705-009-0562-y
20. Abrahão JS, Guedes MI, Trindade GS, Fonseca FG, Campos RK, Mota BF, et al. One more piece in the VACV ecological puzzle: could peridomestic rodents be the link between wildlife and bovine vaccinia outbreaks in Brazil? PLoS One. 2009;4:e7428. https://doi.org/10.1371/journal.pone.0007428
21. Lopesode S, Lacerda JP, Fonseca IE, Castro DP, Forattini OP, Rabello EX. Cotia virus: a new agent isolated from sentinel mice

in Sao Paulo, Brazil. Am J Trop Med Hyg. 1965;14:156–7. https://doi.org/10.4269/ajtmh.1965.14.156

22. da Fonseca FG, Trindade GS, Silva RL, Bonjardim CA, Ferreira PC, Kroon EG. Characterization of a vaccinia-like virus isolated in a Brazilian forest. J Gen Virol. 2002;83:223–8. https://doi.org/10.1099/0022-1317-83-1-223

23. Kroon EG, Mota BE, Abrahão JS, da Fonseca FG, de Souza Trindade G. Zoonotic Brazilian vaccinia virus: from field to therapy. Antiviral Res. 2011;92:150–63. https://doi.org/10.1016/j.antiviral.2011.08.018

24. Abrahão JS, Trindade GS, Ferreira JM, Campos RK, Bonjardim CA, Ferreira PC, et al. Long-lasting stability of vaccinia virus strains in murine feces: implications for virus circulation and environmental maintenance. Arch Virol. 2009;154:1551–3. https://doi.org/10.1007/s00705-009-0470-1

25. Ferreira JM, Abrahão JS, Drumond BP, Oliveira FM, Alves PA, Pascoal-Xavier MA, et al. Vaccinia virus: shedding and horizontal transmission in a murine model. J Gen Virol. 2008;89:2986–91. https://doi.org/10.1099/vir.0.2008/003947-0

26. Abrahão JS, Oliveira TM, Campos RK, Madureira MC, Kroon EG, Lobato ZI. Bovine vaccinia outbreaks: detection and isolation of vaccinia virus in milk samples. Foodborne Pathog Dis. 2009;6:1141–6. https://doi.org/10.1089/fpd.2009.0324

27. de Oliveira TM, Rehfeld IS, Siqueira JM, Abrahão JS, Campos RK, dos Santos AK, et al. Vaccinia virus is not inactivated after thermal treatment and cheese production using experimentally contaminated milk. Foodborne Pathog Dis. 2010;7:1491–6. https://doi.org/10.1089/fpd.2010.0597

28. de Oliveira TM, Guedes MI, Rehfeld IS, Matos AC, Rivetti AV Jr, Alves PA, et al. Detection of vaccinia virus in milk: evidence of a systemic and persistent infection in experimentally infected cows. Foodborne Pathog Dis. 2015;12:898–903. https://doi.org/10.1089/fpd.2015.1974

29. de Oliveira TML, Guedes MIMC, Rehfeld IS, Matos ACD, Rivetti Júnior AV, da Cunha AF, et al. Vaccinia virus detection in dairy products made with milk from experimentally infected cows. Transbound Emerg Dis. 2018;65:e40–7. https://doi.org/10.1111/tbed.12666

30. Rehfeld IS, Fraiha ALS, Matos ACD, Guedes MIMC, Costa EA, de Souza MR, et al. Short communication: survival of vaccinia virus in inoculated cheeses during 60-day ripening. J Dairy Sci. 2017;100:7051–4. https://doi.org/10.3168/jds.2017-12560

31. Usme-Ciro JA, Paredes A, Walteros DM, Tolosa-Pérez EN, Laiton-Donato K, Pinzón MD, et al. Detection and molecular characterization of zoonotic poxviruses circulating in the Amazon

region of Colombia, 2014. Emerg Infect Dis. 2017;23:649–53. https://doi.org/10.3201/eid2304.161041

32. Smithson C, Kampman S, Hetman B, Upton C. Incongruencies in vaccinia virus phylogenetic trees. Computation. 2014;2:182–9. https://doi.org/10.3390/computation2040182

33. Karem KL, Reynolds M, Braden Z, Lou G, Bernard N, Patton J, et al. characterization of acute-phase humoral immunity to monkey-pox: use of immunoglobulin M enzyme–linked immunosorbent assay for detection of monkeypox infection during the 2003 North American outbreak. Clin Diagn Lab Immunol. 2005;12:867–72.

34. Fenner F, Henderson DA, Arita I, Jezek Z, Ladnyi ID. Smallpox and its eradication—South America. Geneva: World Health Organization; 1988.

35. de Souza Trindade G, Drumond BP, Guedes MI, Leite JA, Mota BE, Campos MA, et al. Zoonotic vaccinia virus infection in Brazil: clinical description and implications for health professionals. J Clin Microbiol. 2007;45:1370–2. https://doi.org/10.1128/JCM.00920-06

36. Shchelkunov SN. An increasing danger of zoonotic orthopoxvirus infections. PLoS Pathog. 2013;9:e1003756. https://doi.org/10.1371/journal.ppat.1003756

37. Costa GB, Borges IA, Alves PA, Miranda JB, Luiz AP, Ferreira PC, et al. Alternative routes of zoonotic vaccinia virus transmission, Brazil. Emerg Infect Dis. 2015;21:2244–6. https://doi.org/10.3201/eid2112.141249

38. Assis FL, Borges IA, Mesquita VS, Ferreira PC, Trindade GS, Kroon EG, et al. Vaccinia virus in household environment during bovine vaccinia outbreak, Brazil. Emerg Infect Dis. 2013;19:2045–7. https://doi.org/10.3201/eid1912.120937

39. Peres MG, Bacchiega TS, Appolinário CM, Vicente AF, Allendorf SD, Antunes JM, et al. Serological study of vaccinia virus reservoirs in areas with and without official reports of outbreaks in cattle and humans in São Paulo, Brazil. Arch Virol. 2013;158:2433–41. https://doi.org/10.1007/s00705-013-1740-5

40. Megid J, Appolinário CM, Langoni H, Pituco EM, Okuda LH. Vaccinia virus in humans and cattle in southwest region of São Paulo State, Brazil. Am J Trop Med Hyg. 2008;79:647–51. https://doi.org/10.4269/ajtmh.2008.79.647

41. Quiner CA, Nakazawa Y. Ecological niche modeling to determine potential niche of vaccinia virus: a case only study. Int J Health Geogr. 2017;16:28. https://doi.org/10.1186/s12942-017-0100-1

Address for correspondence: Ashley Styczynski, Stanford University, Infectious Disease, 300 Pasteur Dr, Lane Bldg 134, Palo Alto, CA 94305, USA; email: ashley.styczynski@gmail.com

Patterns of Transmission and Sources of Infection in Outbreaks of Human Toxoplasmosis

Fernanda Pinto-Ferreira, Eloiza Teles Caldart, Aline Kuhn Sbruzzi Pasquali,
Regina Mitsuka-Breganó, Roberta Lemos Freire, Italmar Teodorico Navarro

We report on apparent temporal progression of probable sources of infection and transmission routes for global human toxoplasmosis outbreaks as described in published articles. We searched the Scientific Electronic Library Online, Web of Science, PubMed, and Scopus databases for articles on *Toxoplasma*, toxoplasmosis, and outbreaks. We found that transmission routes for *Toxoplasma gondii* varied by decade. In the 1960s and 1990s, toxoplasmosis outbreaks mainly occurred through ingestion of cysts in meat and meat derivatives; in the 1980s, through milk contaminated with tachyzoites; in 2000, due to the presence of oocysts in water, sand, and soil; and in 2010, due to oocysts in raw fruits and vegetables. Our study suggests a possible change in the epidemiology of reported toxoplasmosis outbreaks. Because of this change, we suggest that greater attention be paid to the disinfection of vegetables, as well as to the quality of water used for drinking and irrigation.

Toxoplasmosis is a zoonotic disease caused by the protozoan *Toxoplasma gondii* of the phylum Apicomplexa, an obligate intracellular parasite with a worldwide distribution that infects mammals and birds (*1*). Warm-blooded animals serve as intermediate hosts for *T. gondii*, but felids are its only definitive host and shed oocysts that result in environmental contamination (*2*).

Because of high exposure to *T. gondii* around the world, humans have a high serologic prevalence, which varies between 10.0% and 97.4% in the adult population. However, cases of clinical disease are less frequent (*3*). Environmental conditions, cultural and eating habits, and fauna are factors in the variability and prevalence of toxoplasmosis in different geographic areas (*4*). Transmission mainly occurs through the ingestion of water, vegetables, or soil contaminated with oocysts (sporozoites) or raw or undercooked meat containing viable tissue cysts (bradyzoites), characterizing this disease as a foodborne zoonosis (*3*).

Better understanding of the patterns of occurrence of human toxoplasmosis outbreaks could lead to more effective and targeted prevention and control measures. We report a possible temporal progression of the probable sources of infection and transmission routes described in articles on human toxoplasmosis outbreaks throughout the world from the 1960s through March 2018.

Materials and Methods

We performed a systematic review by searching the Scientific Electronic Library Online (Scielo), Web of Science, PubMed, and Scopus databases by using the keywords "*Toxoplasma* AND outbreak OR toxoplasmosis AND outbreak." During February–March 2018, we collected data on published toxoplasmosis outbreaks in humans since 1967, when the first relevant article on human infection was published (*5*).

We reviewed published articles to look for changes in the pattern of transmission routes and sources of infection for toxoplasmosis outbreaks in humans around the world. We included articles with at least the abstract in English or Portuguese. We excluded articles on outbreaks of toxoplasmosis in nonhuman species and studies without information about the transmission route.

For each outbreak report, we extracted the year, country of outbreak occurrence, probable source of transmission, number of affected persons, and the affected group. By reviewing the probable source of infection and transmission route defined by the authors of the selected papers, we inferred the parasitic form involved in each case or outbreak report. We used Mendeley (Elsevier, https://www.mendeley.com) software to organize, exclude, and select references. We used Epi Info 3.5.4.4 (*6*) software to tabulate variables obtained from information extracted from the selected articles.

We performed statistical analyses by using χ^2 or Fisher exact tests in R 3.4.1 (http://www.R-project.org) and performed multiple correspondence with the FactoMineR package (http://factominer.free.fr). We chose this technique because it does not rely on statistical tests and provides

visualization of the most relevant relationships in a large set of variables (*7*). It also helps visualize the multivariate relationship between categories of different variables; the geometric proximity of variables in the graph suggests their possible association.

Results

We found a total of 573 articles: 10 in Scielo, 224 in Web of Science, 83 in PubMed, and 256 in Scopus. We excluded articles that did not contain the likely route of transmission, as well as duplicate or incomplete articles, such as those missing titles, authors, or abstracts. We also excluded articles we could not access because they were not available on the Internet or in other sources. For analysis, we selected 33 articles covering 34 reports of outbreaks of acute toxoplasmosis (Figure 1; Appendix Table, https://wwwnc.cdc.gov/EID/article/25/12/18-1565-App1.pdf).

We plotted the geographic distribution of the selected outbreaks on a map (Figure 2). The highest concentration of reported outbreaks, 25/34 (73.5%), occurred in the Americas; Brazil had 35.3% (12/34) of the published outbreaks.

The incidence of cyst-related outbreaks from contaminated meat and its derivatives was 47.1% (16/34), and oocysts were implicated in 44.1% (15/34) of the outbreaks. Transmission through the intake of oocysts in water occurred with a frequency of 20.6% (7/34), through contact with sand and soil with a frequency of 17.6% (6/34), and through consumption of vegetables with a frequency of 5.9% (2/34). Tachyzoites in raw milk caused 8.8% (3/34) of outbreaks. Approximately 1,416 persons were affected in the 15 outbreaks of toxoplasmosis from oocysts (sporozoites), 290 in the 16 outbreaks from tissue cysts (bradyzoites), and 15 in the 3 outbreaks from tachyzoites.

We did not observe a statistical significance in the variables extracted from the articles. Our multiple correspondence analysis shows outbreaks mainly occurred through the ingestion of cysts in meat and its derivatives in the 1960s and 1990s. In the 1980s, milk contaminated with tachyzoites was the primary transmission route. In 2000, outbreaks were caused by oocysts in water and contact with feline feces. Since 2010, outbreaks related to oocyst intake from raw vegetables have increased (Figure 3).

Discussion

Our study had several limitations. Many outbreaks are published only in gray literature, such as in nonindexed journals, on government websites, and in conference abstracts, rather than in peer-reviewed journals such as those we searched. Our search was limited to articles with at least the abstract written in Portuguese or English. Reports had long lag time between an outbreak and the publication of ts occurrence, ranging from 3–7 years. Transmission routes, which can be measured only by means

of epidemiologic investigation (*8,9*), were not always defined in the reports. Although our review searched reports from scientific literature worldwide, it demonstrates much of the reality in Brazil, where we saw the most outbreak reports and the highest numbers of affected persons (776/1,721).

The major clones of *T. gondii*, genotypes I, II, and III, described in the literature differ in virulence and epidemiology (*10–13*). We did not see a clear domain of any genotype in the United States, even though some have relatively higher frequencies (*12*). In Brazil, the seroprevalence of toxoplasmosis in humans ranges from 21.5% to 97.4% (*14*), with more frequent occurrences of atypical genotypes, which might explain reports of the more severe form of the disease (*15*) and the larger numbers of affected persons from this country. In fact, the 2 largest outbreaks of human toxoplasmosis we saw occurred in Brazil. In 2001, an outbreak in Santa Isabel do Ivaí in Paraná State involved >400 persons and was attributed to contamination of the municipal water supply network (*16*). Another outbreak occurred in Santa Maria in Rio Grande do Sul State in 2018 and affected >900 persons; the cause has yet to be determined (*17*).

Oocysts and cysts are the most frequent parasitic form of *T. gondii* transmitted to humans (*8*). According to our results, before 1990, cysts consumed in meat were the main biologic form infecting humans. Beef was the suspected vehicle of transmission in 3 outbreaks: 1 in the United States that affected 5 persons, 1 in Brazil that affected 6 persons, and 1 in Brazil that affected 99 (Appendix). However, because cattle have a low ability to form tissue cysts, beef has less epidemiologic value (Appendix).

Human dietary preferences also can facilitate infection by *T. gondii* (*4*), especially in raw or undercooked meat.
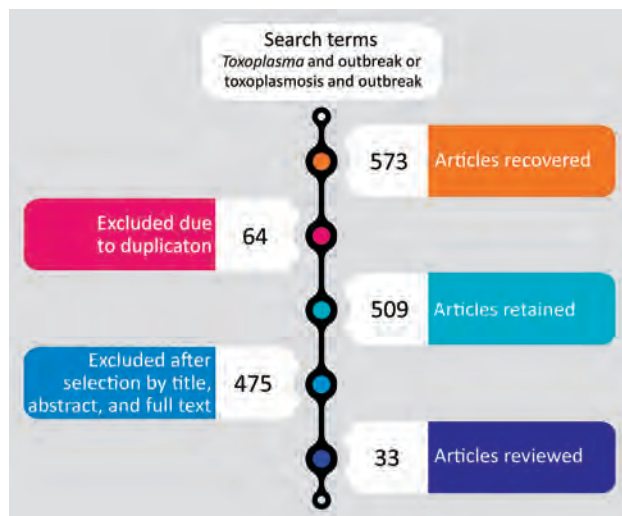
Figure 1. Selection process for articles for systematic review of reports of outbreaks of human toxoplasmosis throughout the world during 1967–March 2018.
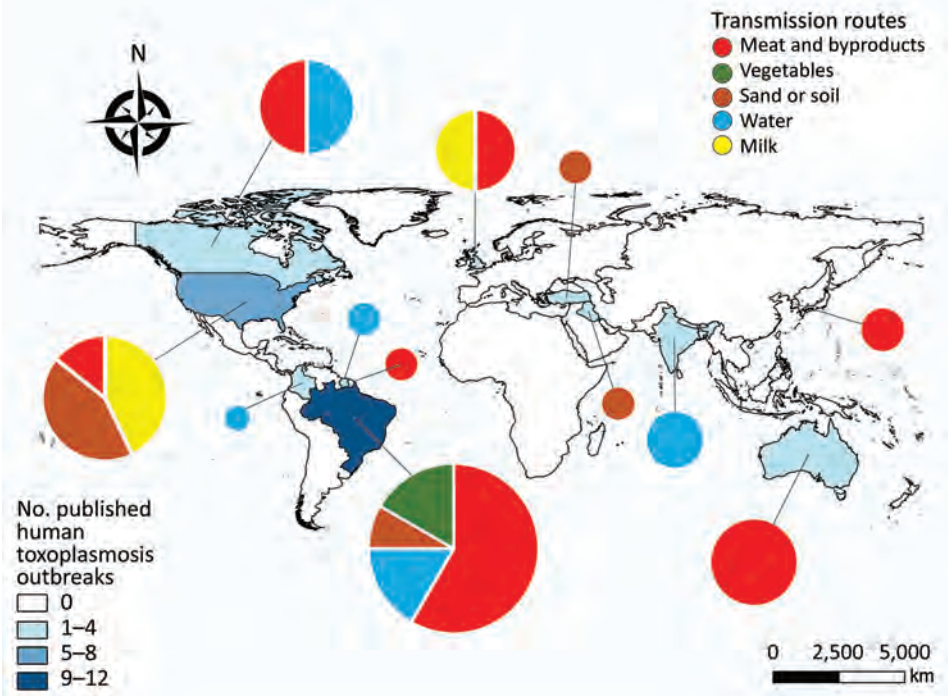
Figure 2. Geographic distribution of 34 outbreaks of human toxoplasmosis worldwide as cited in reports published during 1967–March 2018. Probable and known transmission routes are indicated by color. Circle size corresponds to the number of outbreaks.

For example, consumption of kibbe, a traditional dish in the Middle East made from raw lamb meat, was the cause of 5 outbreaks between 1975 and 2006, 2 in Brazil (*18,19*) and 1 each in England (*20*), the United States (*21*), and Australia (*22*).

Because tissue cysts are sensitive to heat (*23*), properly cooked meat poses less of a risk for *T. gondii* infection in humans. In the 1990s, the government of Brazil implemented a prevention project for another parasitic infection, teniasis-cysticercosis. The project discouraged consumption of raw or undercooked meats, which likely contributed to the decline in *T. gondii* infections from meat consumption (*24*).

In addition, the technology of livestock farming has improved management and reduced pathogenic animal infections, making meat safer. In Brazil, to prevent foodborne diseases, the Ministry of Agriculture, Livestock and Supply, through Administrative Rule no. 46, of February 10, 1998, adopted the hazard analysis and critical control point system as a prerequisite to export meat and to improve good production practices (*25*). In addition, manufacturers improved the practice of freezing meats, to either –10°C degrees for 3 days or –20°C degrees for 2 days, which sufficiently inactivates cysts (*26*). After the improvements in the system, the country saw a reduction in seropositivity to *T. gondii* over the intervening years (*8*).

We noted that consumption of undercooked game meat, such as reindeer, tapir, venison, wild boar, and armadillo, was the cause of *Toxoplasma* infection in several outbreaks globally (*27–30*). Studies have demonstrated that the unusual abundance of atypical *T. gondii* strains found in the wild can cause human toxoplasmosis in its most severe form, even in immunocompetent persons (*16,27,29–33*). The increased severity is caused by poor host adaptation to the circulating *T. gondii* zoonotic neotropical strains (*27*). In 2009, Pino et al. (*32*) described severe cardiac involvement in a military man who consumed untreated water during an operation in the jungle.

In addition, Carme et al. (*27*) reported 16 cases of severe toxoplasmosis in immunocompetent patients hospitalized with nonspecific infectious diseases in French Guiana. Many had severe pulmonary involvement (87.5%), and ≥1 had visceral alteration. *T. gondii* was isolated from 3 patients and characterized as an atypical genotype. Investigators determined game meat was the source of infection in 31.25% (5/16) of cases, likely through consumption of tissue cysts.

Infection through milk consumption was described in 3 outbreaks during 1975–1988, all of which affected intrafamily groups who consumed raw goat milk (*34–36*). Goats are known to secrete tachyzoites in milk (*37,38*), and tachyzoites are resistant to processing in fresh cheeses (*39*). Standard measures to prevent *Listeria monocytogenes, Brucella* spp., and *Mycobacterium* spp. contamination in milk also reduce the risk for human *T. gondii* infection. Practices applied in milk production, such as pasteurization and brucellosis and tuberculosis prevention programs, likely have reduced incidence rates of *T. gondii* infection. We saw fewer outbreaks associated with contaminated milk in the 1990s and 2000s.
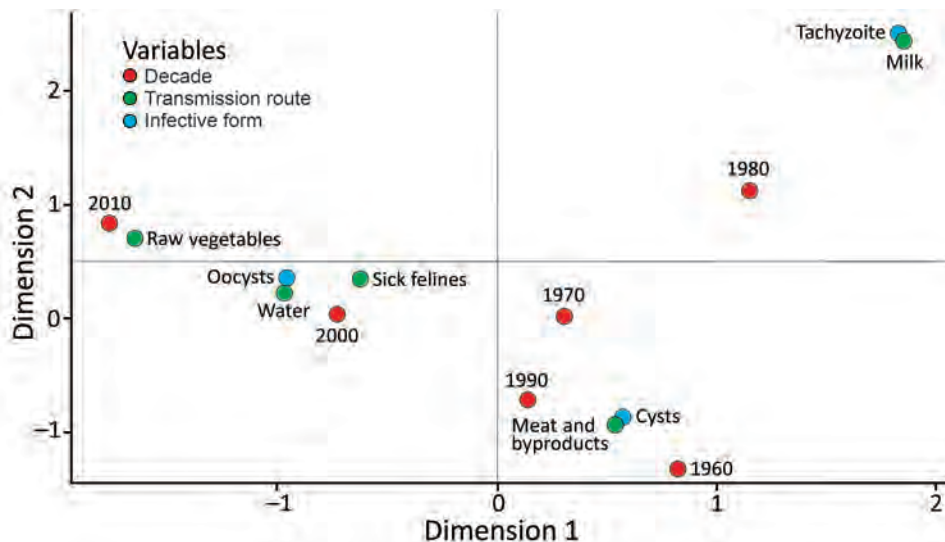
Figure 3. Multiple correspondence analysis of the variables extracted from articles published on human toxoplasmosis outbreaks during 1967–March 2018. The multiple correspondence technique helps to visualize the multivariate relation between the categories of different variables. Proximity of the variables in the graph suggests a possible association between them.

The outbreak in Santa Isabel do Ivaí (*16*) is notable in the history of toxoplasmosis, not only for the high number of cases but also because *T. gondii* was isolated directly from the transmission source, unfiltered municipal water. After this incident, outbreaks were investigated with more attention to this biologic form, a factor that might explain the increase of detected outbreaks of water origin.

One of the main forms of transmission of toxoplasmosis is the fecal-oral route. Felines, definitive hosts for *T. gondii*, eliminate the oocysts in the environment, where they can remain viable for several months in appropriate conditions and cause infection (*2*). Because cats defecate in soil and sand, contact with these sources is a risk factor for infection. Contact with soil and sand was the transmission route in 17.6% (6/34) of human outbreaks reported; 67.0% of those affected were children or adolescents, probably because children play in these environments and indirectly consume oocysts.

In the past 20 years, consumption of healthy foods, such as vegetables, has increased through efforts to change eating habits and combat obesity (*40*). Vegetables provide micronutrients and fiber, which aid in maintaining body weight (*41*). However, increasing reports of toxoplasmosis have coincided with increased consumption of fruits and vegetables. Toxoplasmosis outbreaks related to vegetables generally occurred because of contamination during the production, including planting, harvesting, transport, and distribution, but also during processing and consumption (*42*). In 2009, an investigation of a cluster of 11 cases of acute toxoplasmosis in a factory with 2,300 employees in São Paulo State, Brazil, revealed vegetable ingestion as the suspected transmission route (*43*). In 2013, the municipality of Ponta de Pedras in Pará State, Brazil, was the scene of an outbreak of toxoplasmosis involving 73 cases with clinical and laboratory findings compatible with the

disease. Açaí consumption was identified as the source of the infections. Ponta de Pedras is one of the main producers of açaí in Brazil, but the outbreak occurred during the period when local production of açaí was practically nil. To satisfy the population's demand for the fruit, açaí vendors acquired the fruit from other locations, where it might have been contaminated with atypical *T. gondii* strains for which the urban population had little immunity (*44*).

Such events demonstrate the inadequate sanitation in industrial settings and restaurants and lack of quality control of commercial produce common in developing countries. Considering the increased attention given to safety for food of animal origin in recent years, and the concomitant increase in consumption of raw vegetables and fruits, foods contaminated by oocysts could become the main source for toxoplasmosis outbreaks.

When reviewing the number of cases in toxoplasmosis outbreaks, we noted that oocysts were responsible for outbreaks with high case counts, such as those occurring in city districts or entire municipalities. Although reported outbreaks due to oocysts and cysts occurred at similar rates, outbreaks from oocysts affected many more persons (>1,400) than did outbreaks due to cysts (≈290 persons). Contaminated drinking water was responsible for the largest outbreak of toxoplasmosis described (*16*), but water also serves as a contamination route for vegetables and fruits when used in irrigation (*16,44,45*). Domestic and wild felids are known to have seroprevalence for *T. gondii*, and a single cat can eliminate >100 million oocysts into the environment after primary infection (*46,47*). Such shedding can lead to water dispersion and large-scale outbreaks (Appendix). Cyst infection appears to affect fewer persons in intrafamilial or party-restricted outbreaks (*48,49*).

Public health prevention efforts for toxoplasmosis frequently focus on congenital infections to reduce the

risk of miscarriage in pregnant women. However, with the occurrence of outbreaks in immunocompetent humans, we suggest that infection control and health education also should be directed to the rest of the population. According to World Health Organization estimates, toxoplasmosis is among the leading foodborne parasitic diseases and in recent years has affected >10.3 million persons worldwide (*50*). Because toxoplasmosis is not a notifiable disease in most countries, reports of toxoplasmosis outbreaks in the literature are needed to increase our understanding of transmission and help reduce the number of outbreaks.

Through our review of published data, we believe the epidemiology of reported toxoplasmosis outbreaks has changed over the past 20 years. Consequently, we suggest that greater attention be paid to the production and disinfection of vegetables, to the quality of drinking and irrigation water, and to the adoption of legislation for tracking outbreaks with the aim of eliminating transmission routes, avoiding exposure, or inactivating the parasite before consumption.

About the Author

Dr. Pinto-Ferreira is a professor of veterinary parasitology at the State University of Londrina, Brazil. Her research interests include experience in preventive veterinary medicine, mainly in the areas of geoprocessing applied to public health, epidemiology, and environmental protozoology, toxoplasmosis, giardiasis, cryptosporidiosis, and investigation of waterborne and foodborne outbreaks.

References

1. Jacobs L. The interrelation of toxoplasmosis in swine, cattle, dogs, and man. Public Health Rep. 1957;72:872–82. https://doi.org/10.2307/4589927
2. Dubey JP, Miller NL, Frenkel JK, Frenkel AJK. The *Toxoplasma gondii* oocyst from cat feces. J of Exp Med. 1970;132:636–62. https://doi.org/10.1084/jem.132.4.636
3. Tenter AMM, Heckeroth ARR, Weiss LMM. *Toxoplasma gondii*: from animals to humans. Int J Parasitol. 2000;30:1217–58 . https://doi.org/10.1016/s0020-7519(00)00124-7
4. Dubey JP. Toxoplasma, Hammondia, Besnoitia, Sarcocystis and others tissue cyst-forming coccidia of man and animals. In: Kreier JP, ed. Parasitic Protozoa. 3rd ed. New York: Academic Press; 1977. p. 101–237.
5. Magaldi C, Elkis H, Pattoli D, de Queiróz JC, Coscina AL, Ferreira JM. Outbreak of toxoplasmosis in a Paulist seminary in Braganza (São Paulo state). Clinical, serological and epidemiological aspects [in Portuguese]. Rev Saude Publica. 1967;1:141–71. https://doi.org/10.1590/S0034-89101967000200003
6. Dean AG, Dean JA, Burton AH, Discker RC. Epi-Info: a word processing, database, and statistics program for epidemiology on microcomputers, version 5. Atlanta: Centers for Disease Control and Prevention;1990.
7. Lebart L, Morineau A, Warwick KM. Multivariate descriptive statistical analysis; correspondence analysis and related techniques for large matrices. New York, New York: John Wiley & Sons; 1984.
8. Dubey JP, Lago EG, Gennari SM, Su C, Jones JL. Toxoplasmosis in humans and animals in Brazil: high prevalence, high burden of disease, and epidemiology. Parasitology. 2012;139:1375–424 https://doi.org/10.1017/S0031182012000765
9. Petersen E, Vesco G, Villari S, Buffolano W. What do we know about risk factors for infection in humans with *Toxoplasma gondii* and how can we prevent infections? Zoonoses Public Health. 2010;57:8–17. https://doi.org/10.1111/j.1863-2378.2009.01278.x
10. Sibley LD, Boothroyd JC. Virulent strains of *Toxoplasma gondii* comprise a single clonal lineage. Nature. 1992;359:82–5. https://doi.org/10.1038/359082a0
11. Howe DK, Sibley LD. *Toxoplasma gondii* comprises three clonal lineages: correlation of parasite genotype with human disease. J Infect Dis. 1995;172:1561–6. https://doi.org/10.1093/infdis/172.6.1561
12. Shwab EK, Zhu X-Q, Majumdar D, Pena HFJ, Gennari SM, Dubey JP, et al. Geographical patterns of *Toxoplasma gondii* genetic diversity revealed by multilocus PCR-RFLP genotyping. Parasitology. 2014;141:453–61. https://doi.org/10.1017/S0031182013001844
13. Su C, Khan A, Zhou P, Majumdar D, Ajzenberg D, Darde M-L, et al. Globally diverse *Toxoplasma gondii* isolates comprise six major clades originating from a small number of distinct ancestral lineages. Proc Natl Acad Sci USA. 2012;109:5844–9. https://doi.org/10.1073/pnas.1203190109
14. Dubey JP, Lago EG, Gennari SM, Su C, Jones JL. Toxoplasmosis in humans and animals in Brazil: high prevalence, high burden of disease, and epidemiology. Parasitology. 2012;139:1375–424. https://doi.org/10.1017/S0031182012000765
15. De Salvador-Guillouët F, Ajzenberg D, Chaillou-Opitz S, Saint-Paul MC, Dunais B, Dellamonica P, et al. Severe pneumonia during primary infection with an atypical strain of *Toxoplasma gondii* in an immunocompetent young man. J Infect. 2006;53: e47–50. https://doi.org/10.1016/j.jinf.2005.10.026
16. de Moura L, Bahia-Oliveira LMG, Wada MY, Jones JL, Tuboi SH, Carmo EH, et al. Waterborne toxoplasmosis, Brazil, from field to gene. Emerg Infect Dis. 2006;12:326–9. https://doi.org/10.3201/eid1202.041115
17. Ponte S, Burguez D, Adrioli G. Outbreak of toxoplasmosis in the city of Santa Maria, Brazil. Prehosp. Disaster Med. 2019;34(Suppl. 1):s74. https://doi.org/10.1017/S1049023X19001602
18. Bonametti AM, Passos JN, da Silva EM, Bortoliero AL. Outbreak of acute toxoplasmosis transmitted thru the ingestion of ovine raw meat [in Portuguese]. Rev Soc Bras Med Trop. 1997;30:21–5. https://doi.org/10.1590/S0037-86821997000100005
19. Renoiner EIM, Siqueira AA, Garcia MH, Alves RM, Cardoso ME, Ferreira ABPL, et al. Outbreak of acquired toxoplasmosis, Anápolis-GO, February 2006 [in Porutguese]. Boletim eletrônico epidemiológico da secretária de vigilância em saúde. 2007;(8):1–6 [cited 2019 Oct 13]. https://portalarquivos2.saude.gov.br/images/pdf/2014/julho/16/Ano07-n08-toxoplasmose-adquirida-go-completo.pdf
20. Fertig A, Selwyn S, Tibble MJ. Tetracycline treatment in a food-borne outbreak of toxoplasmosis. Br Med J. 1977;1:1064. https://doi.org/10.1136/bmj.1.6068.1064
21. Masur H, Jones TC, Lempert JA, Cherubini TD. Outbreak of toxoplasmosis in a family and documentation of acquired retinochoroiditis. Am J Med. 1978;64:396–402. https://doi.org/10.1016/0002-9343(78)90218-8
22. De Silva LM, Mulcahy DL, Kamath KR. A family outbreak of toxoplasmosis: a serendipitous finding. J Infect. 1984;8:163–7. https://doi.org/10.1016/S0163-4453(84)92617-3
23. Dubey JP, Kotula AW, Sharar A, Andrews CD, Lindsay DS. Effect of high temperature on infectivity of *Toxoplasma gondii* tissue cysts in pork. J Parasitol. 1990;76:201–4. https://doi.org/10.2307/3283016
24. Ministry of Health, Brazil. Project for the control of the teniasis/cysticercosis complex in Brazil [in Portuguese]. Brasília (Brazil): The Ministry; 1996.

25. Rossi GAM, Hoppe EGL, Martins AMCV, Prata LF. Foodborne parasitic zoonosis: a review of the situation in Brazil [in Portuguese]. Arq Inst Biol (Sao Paulo). 2014;81:290–8 https://doi.org/10.1590/1808-1657000742012

26. El-Nawawi FA, Tawfik MA, Shaapan RM. Methods for inactivation of *Toxoplasma gondii* cysts in meat and tissues of experimentally infected sheep. Foodborne Pathog Dis. 2008;5:687–90. https://doi.org/10.1089/fpd.2007.0060

27. Carme B, Bissuel F, Ajzenberg D, Bouyne R, Aznar C, Demar M, et al. Severe acquired toxoplasmosis in immunocompetent adult patients in French Guiana. J Clin Microbiol. 2002;40:4037–44. https://doi.org/10.1128/JCM.40.11.4037-4044.2002

28. Choi WY, Nam HW, Kwak NH, Huh W, Kim YR, Kang MW, et al. Foodborne outbreaks of human toxoplasmosis. J Infect Dis. 1997;175:1280–2. https://doi.org/10.1086/593702

29. Sacks JJ, Delgado DG, Lobel HO, Parker RL. Toxoplasmosis infection associated with eating undercooked venison. Am J Epidemiol. 1983;118:832–8. https://doi.org/10.1093/oxfordjournals.aje.a113701

30. McDonald JC, Gyorkos TW, Alberton B, MacLean JD, Richer G, Juranek D. An outbreak of toxoplasmosis in pregnant women in northern Québec. J Infect Dis. 1990;161:769–74. https://doi.org/10.1093/infdis/161.4.769

31. Sobanski V, Ajzenberg D, Delhaes L, Bautin N, Just N. Severe toxoplasmosis in immunocompetent hosts: be aware of atypical strains. Am J Respir Crit Care Med. 2013;187:1143–5. https://doi.org/10.1164/rccm.201209-1635LE

32. Pino LE, Salinas JE, López MC. Description of an epidemic outbreak of acute toxoplasmosis in immunocompetent patients from Colombian Armed Forces during jungle operations. Infectio. 2009;13:83–91. https://doi.org/10.1016/S0123-9392(09)70729-5

33. Demar M, Ajzenberg D, Maubon D, Djossou F, Panchoe D, Punwasi W, et al. Fatal outbreak of human toxoplasmosis along the Maroni River: epidemiological, clinical, and parasitological aspects. Clin Infect Dis. 2007;45:e88–95. https://doi.org/10.1086/521246

34. Skinner LJ, Timperley AC, Wightman D, Chatterton JMW, Ho-Yen DO. Simultaneous diagnosis of toxoplasmosis in goats and goatowner's family. Scand J Infect Dis. 1990;22:359–61. https://doi.org/10.3109/00365549009027060

35. Sacks JJ, Roberto RR, Brooks NF. Toxoplasmosis infection associated with raw goat's milk. JAMA. 1982;248:1728–32. https://doi.org/10.1001/jama.1982.03330140038029

36. Chiari CA, Neves DP. Human toxoplasmosis acquired by ingestion of goat's milk [in Portuguese]. Mem Inst Oswaldo Cruz. 1984;79:337–40. https://doi.org/10.1590/S0074-02761984000300007

37. Bezerra MJG, Kim PCP, Moraes ÉPBX, Sá SG, Albuquerque PPF, Silva JG, et al. Detection of *Toxoplasma gondii* in the milk of naturally infected goats in the northeast of Brazil. Transbound Emerg Dis. 2015;62:421–4. https://doi.org/10.1111/tbed.12160

38. Spišák F, Turčeková , Reiterová K, Špilovská S, Dubinský P. Prevalence estimation and genotypization of *Toxoplasma gondii* in goats. Biologia. 2010;65:670–4. https://doi.org/10.2478/s11756-010-0070-2

39. Dubey JP, Verma SK, Ferreira LR, Oliveira S, Cassinelli AB, Ying Y, et al. Detection and survival of *Toxoplasma gondii* in milk and cheese from experimentally infected goats. J Food Prot. 2014;77:1747–53. https://doi.org/10.4315/0362-028X.JFP-14-167

40. Ministry of Health, Brazil. Surveillance of risk factors and protection for chronic diseases by telephone inquiry [in Portuguese] [Internet]. Brasília (Brazil): The Ministry; 2016 [cited 2019 Oct 11]. http://bvsms.saude.gov.br/bvs/publicacoes/vigitel_brasil_2016_saudesuplementar.pdf

41. Ministry of Health, Brazil. Obesity grows 60% in ten years in Brazil [in Portuguese] [Internet]. Brasília (Brazil): The Ministry; 2016 [cited 2017 Nov 13]. http://www.brasil.gov.br/saude/2017/04/obesidade-cresce-60-em-dez-anos-no-brasil

42. Ferreira FP, Caldart ET, Freire RL, Mitsuka-Breganó R, Freitas FM, Miura AC, et al. The effect of water source and soil supplementation on parasite contamination in organic vegetable gardens. Rev Bras Parasitol Vet. 2018;27:327–37. https://doi.org/10.1590/s1984-296120180050

43. Ekman CC, Chiossi MF, Meireles LR, Andrade Júnior HF, Figueiredo WM, Marciano MA, et al. Case-control study of an outbreak of acute toxoplasmosis in an industrial plant in the state of São Paulo, Brazil [in Portuguese]. Rev Inst Med Trop Sao Paulo. 2012;54(5):239–44. https://doi.org/10.1590/s0036-46652012000500001

44. Morais RAPB, Freire ABC, Barbosa DRL, Silva LCT, Pinheiro AF, Costa SS, et al. Acute toxoplasmosis outbreak in the Municipality of Ponta de Pedras, Marajó archipelago, Pará State, Brazil: clinical, laboratory, and epidemiological features [in Portuguese]. Revista Pan-Amazônica de Saúde. 2016;7(esp):143–52. https://doi.org/10.5123/S2176-62232016000500016

45. Dutra LH, Saad E, Alves RM S, Cabral CM, Batista FS, de Lima R, et al. Investigation of an outbreak of toxoplasmosis transmitted by açaí consumption in Rondônia, Brazil, 2011 [in Portuguese]. Annals of the 12th EXPOEPI. Brasília: Ministry of Health; 2012. p. 108–9.

46. Silva JCR, Ogassawara S, Adania CH, Ferreira F, Gennari SM, Dubey JP, et al. Seroprevalence of *Toxoplasma gondii* in captive neotropical felids from Brazil. Vet Parasitol. 2001;102:217–24. https://doi.org/10.1016/S0304-4017(01)00523-4

47. Innes EA, Bartley PM, Maley S, Katzer F, Buxton D. Veterinary vaccines against *Toxoplasma gondii*. Mem Inst Oswaldo Cruz. 2009;104:246–51. http://dx.doi.org/10.1590/S0074-02762009000200018

48. Almeida MABA, Alencar Júnio LR, Carmo GMI, Araújo WNA, Garcia MHO, Reis AK V, et al. Intra-family outbreak of toxoplasmosis, Santa Vitória do Palmar-RS, July 2005 [in Portuguese]. Boletim eletrônico epidemiológico da secretária de vigilância em saúde. 2006;18(3):1–7.

49. Eduardo MB de P, Katsuya EM, Ramos SRTS, Pavanello EI, Paiva OR, Brito S do N, et al. Investigation of the outbreak of toxoplasmosis associated with the consumption of raw meat dish ("steak tartar"), in the municipalities of São Paulo and Guarujá, SP—November 2006 [in Portuguese]. Boletim Epidemiológico Paulista. 2007;4:1–6.

50. Torgerson PR, Devleesschauwer B, Praet N, Speybroeck N, Willingham AL, Kasuga F, et al. World Health Organization estimates of the global and regional disease burden of 11 foodborne parasitic diseases, 2010: a data synthesis. PLoS Med. 2015;12:e1001920. https://doi.org/10.1371/journal.pmed.1001920

Address for correspondence: Fernanda Pinto-Ferreira, Universidade Estadual de Londrina Centro de Ciencias Agrarias, PR, Km 380, 86.057-970 Paraná, Londrina, Brazil; email: fernandaferreira@uel.br

Global Epidemiology of Buruli Ulcer, 2010–2017, and Analysis of 2014 WHO Programmatic Targets

Till F. Omansen, Alfred Erbowor-Becksen, Rie Yotsu, Tjip S. van der Werf,
Alexander Tiendrebeogo, Lise Grout, Kingsley Asiedu

Buruli ulcer is a neglected tropical disease caused by *Mycobacterium ulcerans*; it manifests as a skin lesion, nodule, or ulcer that can be extensive and disabling. To assess the global burden and the progress on disease control, we analyzed epidemiologic data reported by countries to the World Health Organization during 2010–2017. During this period, 23,206 cases of Buruli ulcer were reported. Globally, cases declined to 2,217 in 2017, but local epidemics seem to arise, such as in Australia and Liberia. In 2013, the World Health Organization formulated 4 programmatic targets for Buruli ulcer that addressed PCR confirmation, occurrence of category III (extensive) lesions and ulcerative lesions, and movement limitation caused by the disease. In 2014, only the movement limitation goal was met, and in 2019, none are met, on a global average. Our findings support discussion on future Buruli ulcer policy and post-2020 programmatic targets.

Mycobacterium ulcerans causes the neglected tropical skin disease Buruli ulcer (*1*). The infection manifests as a nonulcerative nodule, plaque, or edema, which ulcerates within 4–6 weeks and develops the characteristic undermined edges and yellowish-white necrotic slough (Figure 1) (*2*). The disease is diagnosed by its characteristic clinical features and confirmed in the laboratory using histopathology, microbiological culture, and PCR for the IS*2404* mycobacterial insertion sequence element (*3*). There is no efficient vaccine for Buruli ulcer (*4*), and disease control strategy focuses on early case detection and comprehensive treatment of

Author affiliations: Bernhard Nocht Institute for Tropical Medicine and University Medical Center Hamburg-Eppendorf, Hamburg, Germany (T.F. Omansen); World Health Organization, Geneva, Switzerland (T.F. Omansen, A. Erbowor-Becksen, L. Grout, K. Asiedu); Indiana University, Indianapolis, Indiana, USA (A. Erbowor-Becksen); Nagasaki University, Nagasaki, Japan (R. Yotsu); National Center for Global Health and Medicine, Tokyo, Japan (R. Yotsu); University of Groningen, Groningen, the Netherlands (T.S. van der Werf); World Health Organization Regional Office for Africa, Brazzaville, Republic of the Congo (A. Tiendrebeogo)

individual patients. Treatment of Buruli ulcer has experienced a paradigm shift during the past 2 decades, from surgery to an 8-week course of the antimicrobial drugs rifampin and clarithromycin (*5,6*). Recent preclinical animal experiments suggest that a higher dose of rifampin can dramatically increase efficacy and reduce treatment duration (*7–9*).

M. ulcerans is an environmental pathogen often associated with aquatic environments. The DNA of the organism has been found in aquatic insects (*10*), mosquitoes (*11*), and domestic animals (*12*). Experimental puncturing injury resulting in introduction of organisms into mouse skin and subcutis led to infection (*13*). However, transmission pathways in nature are complex and multifactorial and depend on the local ecosystem.

A definitive transmission pathway of *M. ulcerans* has not been described. *M. ulcerans* was first described as the causative agent of Buruli ulcer in Victoria, Australia, in 1948 (*14*), while descriptions of ulcerative lesions probably caused by *M. ulcerans* in Africa, namely Uganda, date back to the late 18th century. Formal description and reporting of cases on the continent of Africa occurred during the 1950s and 1960s (*15*). Buruli ulcer has been reported in 33 countries worldwide, occurring mainly in West Africa and southeastern Australia (*1*). The disease occurs in very concentrated, small geographic foci within countries, as described in Cameroon and Australia (*16,17*). Increases in cases have been associated with heavy periods of rainfall in some places (*18–21*). In Africa, landscape fragmentation and destruction has been suggested as a risk factor for Buruli ulcer (*22*).

The niche, ecology, and transmission of the environmental human pathogen *M. ulcerans* are, in summary, poorly understood; close epidemiologic surveillance is important for disease control, and drivers of local occurrence of the disease should be closely investigated. A shift of the endemic focus has been described in Australia (*23*). Because the exact transmission route remains unknown, no clear recommendations can be given on Buruli ulcer prevention. The main strategy for Buruli ulcer disease control is early detection and administration of efficient treatment.

The first global recognition and move toward Buruli ulcer advocacy and research was held in Yamoussoukro, Côte

d'Ivoire, in 1998 and resulted in the Yamoussoukro Declaration on Buruli ulcer (*24*). The meeting leaders stressed the importance of the rising burden of Buruli ulcer cases, particularly in West Africa, and called policy makers to action to support the control of the disease. In 2004, the World Health Assembly (WHA) adopted resolution WHA 57.1, calling for enhanced surveillance and control of the disease (https://www.who.int/neglected_diseases/mediacentre/WHA_57.1_Eng.pdf). In 2009, a second high-level meeting held in Benin resulted in the Cotonou Declaration on Buruli ulcer (*25*), calling for greater political commitment for control through early detection and antimicrobial treatment, as well as support for research. At the 2013 World Health Organization (WHO) meeting on Buruli ulcer control and research in Geneva, Switzerland, participants defined 4 programmatic targets to be met by disease-endemic countries by the end of 2014. The targets addressed PCR confirmation, lesion size, and ulceration as indicators of disease progression or severity (late reporting), as well as functional limitation as a reflection of disability. We discuss the current epidemiology of Buruli ulcer and present an analysis, based on data reported to WHO, on progress toward these programmatic targets.

Materials and Methods

Data Collection

Buruli ulcer is diagnosed clinically in most settings in which it is endemic; where possible, cases are confirmed by PCR targeting the insertion sequence 2404 (IS*2404*). In addition, microscopy, histopathology, and microbiological culture are used to aid in the diagnosis of Buruli ulcer. A suspected Buruli ulcer case is defined as a clinically diagnosed case. Individual data collected for each suspected BU case are standardized throughout the disease-endemic countries and include demographic characteristics, clinical history, referral, clinical presentation, lesion size category, laboratory confirmation (if available), treatment and dosages, and treatment outcome. Lesions are categorized by diameter to reflect severity: category I, <5 cm; category II, 5–15 cm; and category III, >15 cm diameter or presence of multiple lesions at critical anatomic locations affected (e.g., eye, genitalia). Staff record patient data on the paper-based BU01 form (https://www.who.int/buruli/control/ENG_BU_01_N.pdf) and then summarize the data into a BU register, the BU02 form (https://www.who.int/buruli/control/BU02%20form.pdf). The health facility forwards BU02 forms to district public health officers, who enter the data into a digital spreadsheet submitted to the national BU control program. At the national level, all data are compiled, cleaned, aggregated, and analyzed.

Buruli ulcer–endemic countries reported data to WHO annually to assess programmatic indicators. The 4 programmatic targets set in 2013 were as follows: 1) ≥70% of cases

Figure 1. Typical Buruli ulcer lesion on the arm of a patient from Ghana. Central necrosis, yellowish-white slough, and undermined edges surround the wound. Photo courtesy of T.S. van der Werf.

reported from any district or country should have been confirmed by a positive PCR; 2) by the end of 2014, the proportion of category III lesions reported from any district or country should have been reduced from the 2012 average of 33% to <25%; 3) by the end of 2014, the proportion of ulcerative lesions at diagnosis reported from any district or country should have been reduced from the 2012 average of 84% to a maximum of 60%; 4) by the end of 2014, the proportion of patients with limitations of movement at diagnosis reported from any district or country should have been reduced from the 2012 average of 25% to a maximum of 15% (*26*). Countries also reported total number of cases, gender distribution, the proportion of patients <15 years of age, the percentage of cases that are located on the lower limb, and the percentage of patients who completed antimicrobial therapy.

These data concerning the programmatic indicators were retrospectively entered into the WHO integrated data platform (WIDP). The WIDP is a web-based open source platform, District Health Information System 2 (DHIS2) (*27*). WHO further adapted WIDP to streamline global reporting from member states to WHO, integrate data from different sources, and strengthen data collection, analysis, and use in disease-endemic countries.

Data Analysis

We included data reported to WHO during 2010–2017 in this descriptive analysis. We reviewed data from all 33 countries that had ever reported Buruli ulcer, using case numbers, the proportion of patients <15 years of age, sex distribution, lesion location on the lower limb, and antimicrobial treatment completion as descriptive statistics. We calculated incidence rates for Buruli ulcer on the basis of United Nations median population estimates for 2017 (http://data.un.org). Programmatic target indicators are shown per year per country, as available (Table 1); we calculated the global average

Table 1. Overview of status on WHO 2014 programmatic targets for Buruli ulcer*

WHO programmatic targets	2012 data	Target set in 2013	2014 data	2017 data
1. PCR confirmation	50%	≥70%	64%	58%
2. Category III lesions	33%	<25%	37%	31%
3. Ulcerative lesions	84%	≤60%	64%	75%
4. Movement limitation	25%	≤15%	15%	17%

*Targets were formulated at the 2013 WHO Buruli Ulcer Research and Control Meeting (26). Targets were based on the average of data reported from countries in 2012. They were set to be achieved by the end of 2014. Values represent means weighted for case burden of every country, computed from data reported to WHO. For some countries, information on a certain indicator was not available, if this was the case, the case burden was exempted from the calculation for this specific indicator. Red shading indicates failure to meet target; green shading indicates that the target was met. WHO, World Health Organization.

from country means, which were weighted by their population. We performed statistical analysis and graphing using GraphPad Prism version 7.0a (https://www.graphpad.com), quantumGIS version 2.18.13 (https://www.qgis.org), and RStudio version 1.1.456 (https://rstudio.com).

Results

Reporting and Completeness

We analyzed available data from a total of 16 countries: Australia, Democratic Republic of the Congo (DRC), Nigeria, Gabon, Papua New Guinea, Japan, Benin, Cameroon, Côte d'Ivoire, Ghana, Guinea, Liberia, Sierra Leone, South Sudan, Republic of the Congo, and Togo. We excluded Republic of the Congo, Sierra Leone, and South Sudan from the programmatic target analysis because they provided insufficient data; we excluded Burkina Faso, Central African Republic, Sri Lanka, Brazil, Malaysia, China,

Angola, Indonesia, Kenya, Malawi, Peru, Senegal, Suriname, Uganda, and Mexico from the analysis because they had not reported relevant data for the study period.

Decline of Global Buruli Ulcer Cases and Rise of Local Epidemics

During 2010–2017, a total of 23,206 cases of Buruli ulcer were reported to WHO by 16 different countries, 14 in the African Region (AFRO) and 3 in the Western Pacific Region (WPRO). In 2017 alone, 2,217 cases of Buruli ulcer were reported globally, 1,923 in AFRO and 294 in WPRO. Overall, the yearly case burden declined from a maximum of 4,906 cases in 2010 to 1,952 cases in 2016; in 2017, however, the number of cases increased to 2,217 cases (Table 2; Figure 2, panel A), mainly driven by a sharp rise in Australia to 283 cases in 2017. Other than Australia, few cases have been reported in WPRO, from Papua New Guinea and Japan (Table 2; Figure 2, panel B); most cases were reported from AFRO.

Table 2. Epidemiologic data on Buruli ulcer cases reported to the World Health Organization, 2010–2017*

Region and country	No. suspected cases		Total no. cases, 2011–2017	2017 data				
	2010	2017		Incidence, cases/100,000 population	Patients age <15 y, %	Female patients, %	Lesion located on lower limb, %	Completed antimicrobial therapy, %
AFRO region								
Benin	572	267	3,027	2.35	41	50.5	61†	100†
Cameroon	287	No data	1,180	No data	31†	49†	74†	99†
Congo	107	No data	207	No data	No data	No data	No data	No data
Côte d'Ivoire	2,533	344	8,713	1.31	48	52	57†	100†
DRC	136	91	1,535	1.80	33†	44†	72†	100†
Gabon	65	45	402	2.12	40	49	77†	84
Ghana	1,048	538	4,828	1.91	13	48	83†	No data
Guinea	24	98	549	0.83	14†	No data	No data	No data
Liberia	No data	219	353	4.55	14	47	No data	57
Nigeria	7	259	747	0.13	50	57	78†	94
Sierra Leone	No data	No data	28	No data	No data	No data	No data	No data
South Sudan	4	No data	4	No data	No data	No data	No data	No data
Togo	67	62	500	0.76	53	42	54†	86†
AFRO subtotal‡	4,850	1,923	22,073		31	50	71	70
WPRO region								
Australia	42	283	1,033	1.21	10	48	58	100†
Japan	9	6	52	0.0048	17	67	50†	100
Papua New Guinea	5	5	48	0.07	80	60		
WPRO subtotal‡	56	294	1,133		11	49	58	100
Global total	4,906	2,217	23,196		26	50	69	74

*Data from Buruli ulcer–endemic countries that reported continuous data for most of the years assessed. Up-to-date country data on annual reported cases are available at http://apps.who.int/gho/data/node.main.A1631. AFRO, WHO African Region; DRC, Democratic Republic of the Congo; WPRO, WHO Western Pacific Region; WHO, World Health Organization.
†2016 data; 2017 data were not available.
‡Cases and total cases represent sums of countries per region. Programmatic indicators represented mean proportions weighted for case burden in the respective countries.
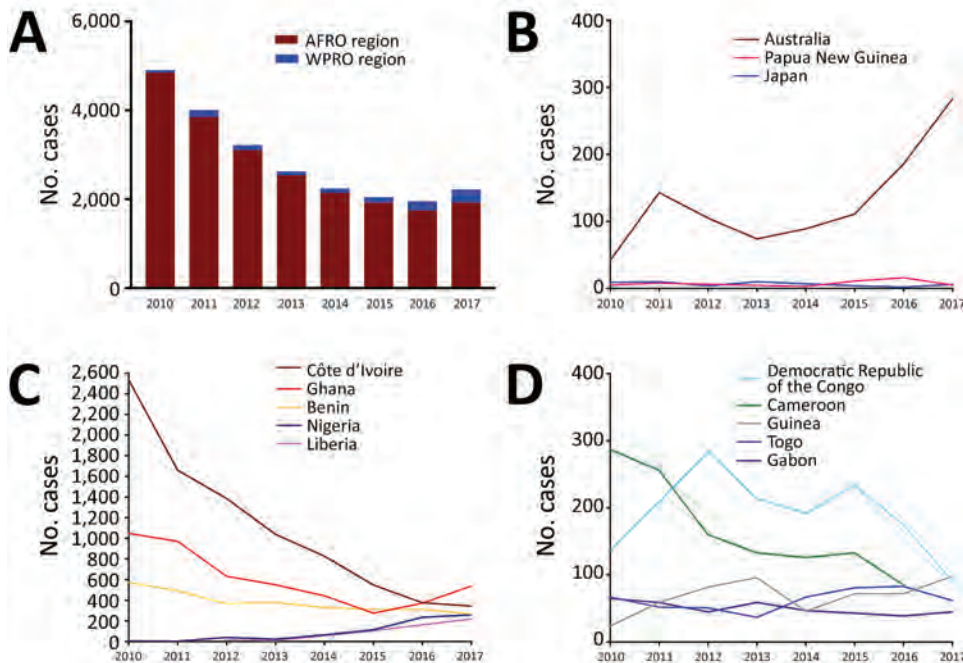
Figure 2. Dynamics of Buruli ulcer epidemiology by cases reported to the World Health Organization (WHO) in 2010–2017. A) Globally, reported cases declined over time, but the proportion of cases reported from WPRO increased. B) WPRO data show an increase in cases in Australia. C) In AFRO, cases drastically declined in Côte d'Ivoire but recently increased in other countries such as Ghana, Nigeria, and Liberia. D) Countries in AFRO that reported fewer cases overall showed stagnant or varying numbers. AFRO, WHO African Region; WPRO, WHO Western Pacific Region.

Countries reporting >200 cases in 2017 (termed high burden; Figures 2, 3) in Africa were Côte d'Ivoire, Ghana, Benin, Nigeria, and Liberia; within these countries, case numbers have increased in Ghana, Nigeria, and Liberia. Cases were constant in Benin; Côte d'Ivoire saw a decline in cases from a historically high-burden country in 2010 (Figure 2, panel C). Case numbers reported from the remaining low-burden countries, DRC, Cameroon, Guinea, Togo, and Gabon, fluctuate around 20–200 cases/year (Figure 2, panel D). We observed the highest incidences in Liberia (4.55 cases/100,000 population), Benin (2.35 cases/100,000 population), Gabon (2.12 cases/100,000 population), Ghana (1.91 cases/100,000 population), and DRC (1.80 cases/100,000 population) (Table 2).

Patient Age and Sex
Age information was available for 18,449 of the 23,206 reported Buruli ulcer cases from 2010–2017. Of these cases, 40% occurred in patients <15 years of age. Countries with >40% of cases occurring in children <15 years of age in 2016–2017 were Benin, Côte d'Ivoire, Gabon, Nigeria, and Togo. Countries with <15% of cases occurring in patients <15 years of age were Liberia, Guinea, Ghana, and Australia. Distribution by sex was even globally, with 50% of reported cases occurring in female and 50% in male case-patients.

Lesion Location
On average, 69% of Buruli ulcer lesions were located on a lower limb. For DRC, Cameroon, Gabon, Nigeria, and Ghana, 70% of recorded lesions were on a lower limb.

The lowest values were reported from Japan (50%), Togo (54%), Côte d'Ivoire (57%), and Australia (58%).

Completion of Antimicrobial Treatment
Most countries that reported data stated that 99%–100% of patients completed antimicrobial treatment in 2016 and 2017. Togo (86%) and Gabon (84%) reported slightly lower rates of patients who completed the regimen. Low levels of completed antimicrobial treatment were reported from Liberia (57%) and Ghana (22%); these low rates may be due to incomplete or inadequate reporting.

Progress toward 2014 WHO Targets
We used data from 2012 as a baseline measure to formulate the programmatic targets. The global average rate of PCR confirmation in 2012 was 50%. Category III lesions were present in 33% of case-patients, ulcerative lesions in 84%, and movement limitations in 25% (Table 1; Figure 4). By 2014, the rate of confirmation by PCR increased globally to 64%, which did not meet the target of ≥70%. The number of category III lesions actually increased to 37%, but ulcerative lesions declined to 64%. The only target met by 2014 was target 4, movement limitations, which were reduced to 15%. Subsequently, in 2017, 58% of Buruli ulcer cases were PCR confirmed, 31% of lesions were category III, 75% of lesions were ulcerative, and 17% of patients had movement limitations, as reported by countries (Table 1). Five countries met the PCR confirmation target, 2 countries met the category III target, 3 countries met the ulcerative lesion target, and 5 countries met the movement limitation target (Figure 4).

We observed many differences at the country level. In general, WPRO countries, particularly Australia and Japan, have had very high rates of PCR confirmation and low rates of category III lesions and movement limitation. In the AFRO countries, PCR confirmation was high in Benin and Togo; we observed improved PCR confirmation rates in DRC and Nigeria. PCR confirmation was low in Cameroon and Gabon and had declined in Ghana from 2012 to 2017. In Côte d'Ivoire, the PCR confirmation rate improved to meet the target in 2014 but then declined again by 2017. Category III lesions were low in Togo and recently also in DRC, meeting the targets in most recent years. Benin, Cameroon, and Nigeria in particular had high rates of category III lesions. Ulcerative lesions were common in all countries in both the WPRO and AFRO regions, with the exception of Togo. Ghana, Togo, and Papua New Guinea had low rates of movement limitation, whereas Nigeria, Cameroon, and Benin's rates of movement limitation exceeded the set target.

We have analyzed data reported through the end of 2018. Figures on the programmatic targets are available on the WIPD web portal (http://extranet.who.int/ntdportal).

Discussion

Even though overall Buruli ulcer cases declined from 2010 until 2017, some countries such as Nigeria, Liberia, and Australia recently reported an increase in cases. The greatest challenge in Buruli ulcer epidemiology and control is that the reservoir and transmission of *M. ulcerans* are unknown. Reporting bias, differences in reporting, or differences in incidence could cause fluctuation in recorded case burden across regions. Nigeria has recently implemented a national Buruli ulcer program; previously, some Buruli ulcer patients had been treated in neighboring Benin (*28,29*). The installation of a formal Buruli ulcer control program and the concurrent intensification of disease control efforts, such as early case finding, might have contributed to increasing reported cases. However, interviewees in a study reported poor knowledge about Buruli ulcer within the local community in one of the affected states of Nigeria, stressing the necessity to further strengthen awareness and control efforts to detect cases (*30*). The number of cases also rose recently in Liberia, the country with the highest incidence of Buruli ulcer (4.55 cases/100,000 population). Underreporting had previously been suggested to be associated with civil war and a lack in knowledge of the disease among healthcare workers (*31*).

In countries such as Benin, Côte d'Ivoire, and Ghana that have well-established facilities for detection and treatment of Buruli ulcer, changes in epidemiology may be due to environmental drivers that are not yet understood, in addition to probable reporting bias. In addition, some countries, such as Uganda, had been endemic for Buruli ulcer but no longer report it, perhaps because of environmental or population changes. In Australia, Buruli ulcer has been known since the 1930s and is a notifiable disease in the state of Victoria; not only an increase in cases but also an increase in severity of the disease have been reported, and the increases may be attributable to a genomic change in *M. ulcerans* (*32*). *M. ulcerans* is a genetically highly clonal organism,
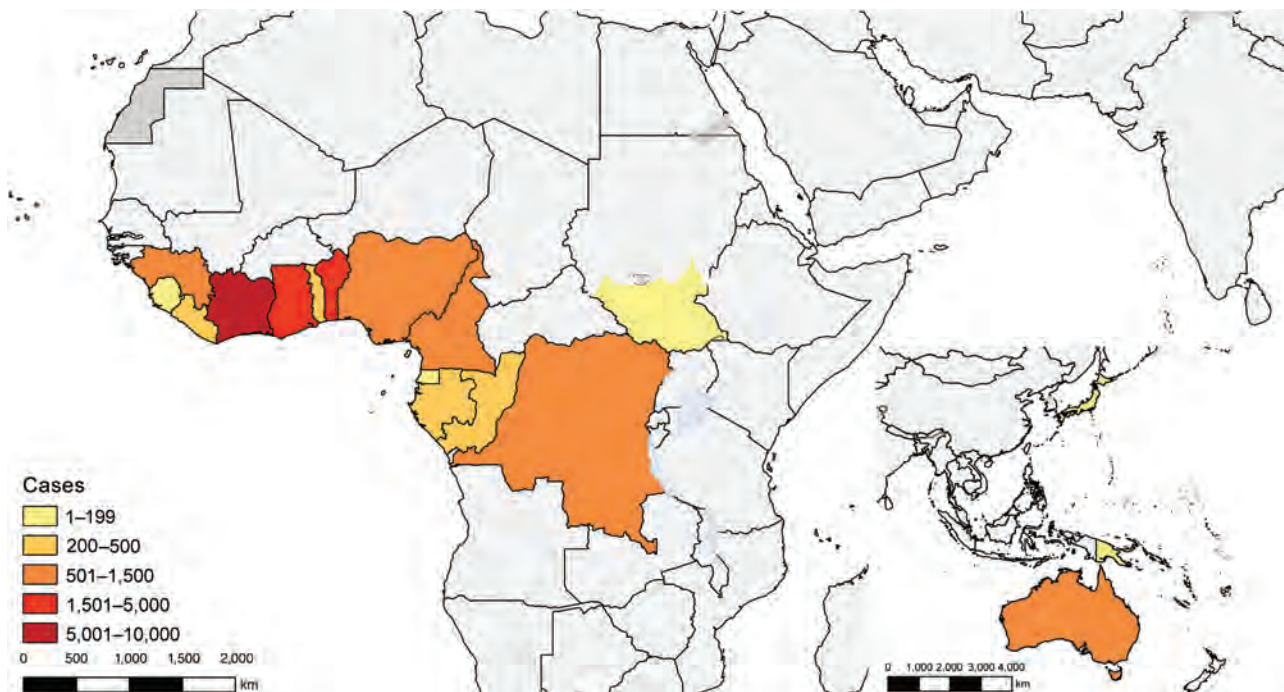
Figure 3. Geographic distribution of Buruli ulcer cases officially reported to World Health Organization during 2010–2017. Concentrations in West Africa and Australia are clearly visible.

and certain genotypes are confined to 1 geographic region (*33,34*). An increase in pathogenicity may be attributed to a genetic shift within the predominant genotype. Changes in the structure of mycolactone or the amount produced could also be driving increased virulence of *M. ulcerans.*

In 2013, WHO formulated programmatic targets to be reached by the end of 2014. The 2014 programmatic targets were defined to ensure good diagnosis (PCR confirmation) and early case finding (fewer category III, ulcerated lesions, movement limitation). Some progress that had been initially achieved toward the programmatic targets was lost soon after, and the situation actually deteriorated below the 2012 average. The overall low rate of 58% of PCR-confirmed infections indicates a need for implementing high-quality PCR locally and training health staff in sample collection, processing, and testing. Of note, PCR diagnosis is universally available in affluent countries, such as Australia. PCR positivity for *M. ulcerans* is part of the case definition in Australia; hence, a rate of 100% PCR confirmation is reported, as expected. In other countries, physicians need to rely on clinical diagnosis or other tests. The PCR for the *M. ulcerans* IS*2404* region has a high sensitivity and specificity to detect Buruli ulcer (*35*). A study in Ghana

showed that >50% of 2,203 clinically diagnosed Buruli ulcer cases were actually not Buruli ulcer, as shown by PCR, culture, and histology (*36*). To avoid overdiagnosis of Buruli ulcer and unnecessary preemptive antimicrobial therapy, we suggest performing PCR in all cases before the initiation of chemotherapy, which is not the current common practice in many countries because of unavailability of the assay and long turnaround time for results where it is available. A point-of-care diagnostic tool is needed and would greatly improve confirmation of Buruli ulcer cases in the field. Currently, simpler methods such as loop-mediated isothermal amplification assay and fluorescent thin layer chromatography are being tested in some treatment centers in Africa (*37*).

Recent advances in our understanding of *M. ulcerans* suggest that lesion size is not necessarily a predictor for delayed manifestation, as was previously thought. It is more of a predictor for treatment outcome, because it reflects disease severity and is associated with increased disabilities and difficulties in treatment (*32,38*). Furthermore, presence of an ulcerative lesion should not be interpreted as caused solely by late reporting. Buruli ulcer can manifest as a nodule, plaque, edematous lesion, or
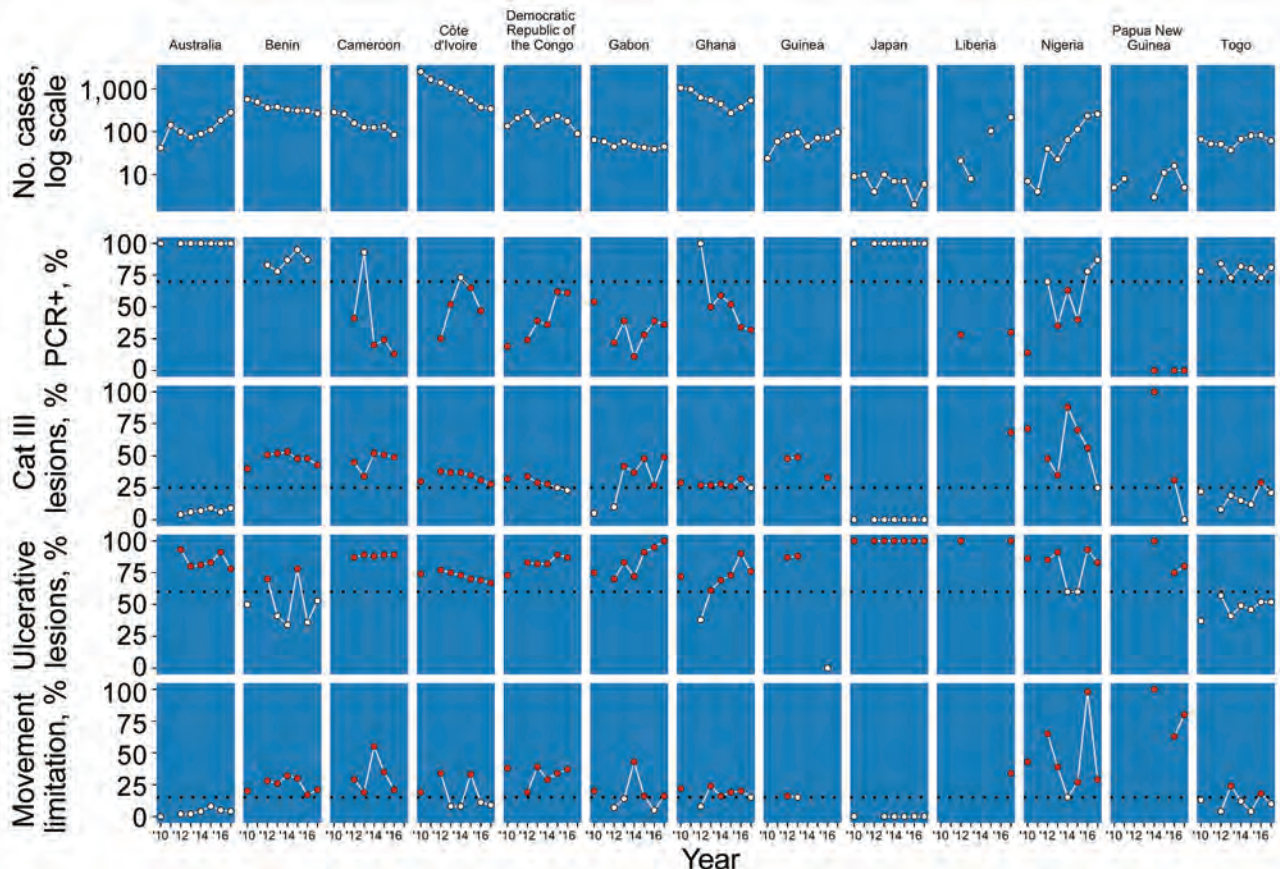
Figure 4. Depiction of progress toward World Health Organization programmatic targets for Buruli ulcer–endemic countries that reported continuous data. Black dotted lines indicate 2014 targets. White dots indicate that the country met the target; red dots indicate that it did not. Cat, category; +, positive.

ulcer, and the factors that contribute to each occurrence are unclear; perhaps the route of transmission and specific host immune response are factors determining this. The ulcer is not necessarily a late stage of either of the other manifestations and can occur without an evident previous nodular stage.

Future programmatic targets should be implemented to assess progress on Buruli ulcer disease control. To address the challenges of Buruli ulcer, these targets should focus on secure diagnosis (PCR confirmation), early case finding (duration of disease reported by patients), case severity (category III lesions), effective treatment (application of oral antimicrobial regimens and 100% completion rate), and reduction of sequelae and disability (scarring, movement limitation). Strengthening active epidemiologic surveillance in underserved areas is as paramount as research into the ecology, transmission, and epidemiology of Buruli ulcer.

This study had several limitations. First, we analyzed only data officially reported to WHO. Buruli ulcer cases did occur in the 2010–2017 period in some other countries than those described in this study, as published literature suggests (*15*), but these cases might not have been reported to WHO for reasons such as local practices, weak health and surveillance systems, or neglect. All countries should be encouraged to report accurate data to WHO so that appropriate support in disease control can be provided. Low case numbers do not always indicate a low disease burden, as in the case of inadequate reporting of disease.

Integrated care for neglected tropical skin diseases is an increasingly popular approach recommended by WHO (*39–41*). We expect integrated case search for these diseases to improve early case detection of Buruli ulcer. An emphasis on precise reporting of cases, with a focus on disease-endemic regions and analysis and mapping of collected data, will ensure sound data for policy planning and Buruli ulcer disease control. As of 2019, countries have been enabled to directly enter Buruli ulcer epidemiologic information into DHIS2, facilitating easier reporting; we expect timeliness, completeness, and use of data to improve. Furthermore, information from the BU02 form is available for most cases from Buruli ulcer–endemic regions; this information, which provides insights into the subnational epidemiology of Buruli ulcer, can give a clearer picture of local epidemiology and would enable comparison of programmatic indicators across health districts or even single health facilities.

Because Buruli ulcer is an environmental disease following unknown ecologic trends, rapid case detection and good treatment are the mainstay components in reducing death and disability associated with the disease. In the framework of universal health coverage, each Buruli ulcer patient should have access to comprehensive treatment, including antimicrobial medication and wound care.

About the Author

Dr. Omansen is a resident doctor in internal medicine and tropical infectious diseases at the Bernhard Nocht Institute for Tropical Medicine and I. Department of Medicine, University Medical Center Hamburg-Eppendorf, Hamburg, Germany. His research focus is the epidemiology and treatment of neglected tropical skin diseases, in collaboration with the World Health Organization.

References

1. Yotsu RR, Suzuki K, Simmonds RE, Bedimo R, Ablordey A, Yeboah-Manu D, et al. Buruli ulcer: a review of the current knowledge. Curr Trop Med Rep. 2018;5:247–56. https://doi.org/10.1007/s40475-018-0166-2
2. van der Werf TS, Stienstra Y, Johnson RC, Phillips R, Adjei O, Fleischer B, et al. *Mycobacterium ulcerans* disease. Bull World Health Organ. 2005;83:785–91.
3. Eddyani M, Sopoh GE, Ayelo G, Brun LVC, Roux J-J, Barogui Y, et al. Diagnostic accuracy of clinical and microbiological signs in patients with skin lesions resembling Buruli ulcer in an endemic region. Clin Infect Dis. 2018;67:827–34.
4. Einarsdottir T, Huygen K. Buruli ulcer. Hum Vaccin. 2011;7:1198–203. https://doi.org/10.4161/hv.7.11.17751
5. Etuaful S, Carbonnelle B, Grosset J, Lucas S, Horsfield C, Phillips R, et al. Efficacy of the combination rifampin-streptomycin in preventing growth of *Mycobacterium ulcerans* in early lesions of Buruli ulcer in humans. Antimicrob Agents Chemother. 2005;49:3182–6. https://doi.org/10.1128/AAC.49.8.3182-3186.2005
6. Nienhuis WA, Stienstra Y, Thompson WA, Awuah PC, Abass KM, Tuah W, et al. Antimicrobial treatment for early, limited *Mycobacterium ulcerans* infection: a randomised controlled trial. Lancet. 2010;375:664–72. https://doi.org/10.1016/S0140-6736(09)61962-0
7. Chauffour A, Robert J, Veziris N, Aubry A, Jarlier V. Sterilizing activity of fully oral intermittent regimens against *Mycobacterium ulcerans* infection in mice. PLoS Negl Trop Dis. 2016; 10:e0005066. https://doi.org/10.1371/journal.pntd.0005066
8. Converse PJ, Almeida DV, Tasneen R, Saini V, Tyagi S, Ammerman NC, et al. Shorter-course treatment for *Mycobacterium ulcerans* disease with high-dose rifamycins and clofazimine in a mouse model of Buruli ulcer. PLoS Negl Trop Dis. 2018;12:e0006728. https://doi.org/10.1371/journal.pntd.0006728
9. Omansen TF, Almeida D, Converse PJ, Li S-Y, Lee J, Stienstra Y, et al. High-dose rifamycins enable shorter oral treatment in a murine model of *Mycobacterium ulcerans* disease. Antimicrob Agents Chemother, 2019;63:e01478–18. https://doi.org/10.1128/aac.01478-18
10. Marsollier L, Robert R, Aubry J, Saint André J-P, Kouakou H, Legras P, et al. Aquatic insects as a vector for *Mycobacterium ulcerans*. Appl Environ Microbiol. 2002;68:4623–8. https://doi.org/10.1128/AEM.68.9.4623-4628.2002
11. Lavender CJ, Fyfe JAM, Azuolas J, Brown K, Evans RN, Ray LR, et al. Risk of Buruli ulcer and detection of *Mycobacterium ulcerans* in mosquitoes in southeastern Australia. PLoS Negl Trop Dis. 2011;5:e1305. https://doi.org/10.1371/journal.pntd.0001305
12. Djouaka R, Zeukeng F, Bigoga JD, Kakou-Ngazoa SE, Akoton R, Tchigossou G, et al. Domestic animals infected with *Mycobacterium ulcerans*—implications for transmission to humans. PLoS Negl Trop Dis. 2018;12:e0006572. https://doi.org/10.1371/journal.pntd.0006572
13. Wallace JR, Mangas KM, Porter JL, Marcsisin R, Pidot SJ, Howden BO, et al. *Mycobacterium ulcerans* low infectious dose and mechanical transmission support insect bites and puncturing

injuries in the spread of Buruli ulcer. PLoS Negl Trop Dis. 2017;11:e0005553. https://doi.org/10.1371/journal.pntd.0005553

14. Maccallum P, Tolhurst JC, Buckle G, Sissons HA. A new mycobacterial infection in man. J Pathol Bacteriol. 1948;60:93–122. https://doi.org/10.1002/path.1700600111

15. O'Brien DP, Jeanne I, Blasdell K, Avumegah M, Athan E. The changing epidemiology worldwide of *Mycobacterium ulcerans*. Epidemiol Infect. 2018;187:1–8.

16. Huang GKL, Johnson PDR. Epidemiology and management of Buruli ulcer. Expert Rev Anti Infect Ther. 2014;12:855–65. https://doi.org/10.1586/14787210.2014.910113

17. Loftus MJ, Tay EL, Globan M, Lavender CJ, Crouch SR, Johnson PDR, et al. Epidemiology of Buruli ulcer infections, Victoria, Australia, 2011–2016. Emerg Infect Dis. 2018;24:1988–97. https://doi.org/10.3201/eid2411.171593

18. Yerramilli A, Tay EL, Stewardson AJ, Fyfe J, O'Brien DP, Johnson PDR. The association of rainfall and Buruli ulcer in southeastern Australia. PLoS Negl Trop Dis. 2018;12:e0006757. https://doi.org/10.1371/journal.pntd.0006757

19. Aboagye SY, Danso E, Ampah KA, Nakobu Z, Asare P, Otchere ID, et al. Isolation of nontuberculous mycobacteria from the environment of Ghanian communities where Buruli ulcer is endemic. Appl Environ Microbiol. 2016;82:4320–9.

20. Aboagye SY, Ampah KA, Ross A, Asare P, Otchere ID, Fyfe J, et al. Seasonal pattern of *Mycobacterium ulcerans*, the causative agent of Buruli ulcer, in the environment in Ghana. Microb Ecol. 2017;74:350–61. https://doi.org/10.1007/s00248-017-0946-6

21. Landier J, Constantin de Magny G, Garchitorena A, Guégan J-F, Gaudart J, Marsollier L, et al. Seasonal patterns of Buruli ulcer incidence, Central Africa, 2002—2012. Emerg Infect Dis. 2015;21:1414–7. https://doi.org/10.3201/eid2108.141336

22. Wu J, Smithwick EAH. Landscape fragmentation as a risk factor for Buruli ulcer disease in Ghana. Am J Trop Med Hyg. 2016;95:63–9. https://doi.org/10.4269/ajtmh.15-0647

23. Buultjens AH, Vandelannoote K, Meehan CJ, Eddyani M, de Jong BC, Fyfe JAM, et al. Comparative genomics shows that *Mycobacterium ulcerans* migration and expansion preceded the rise of Buruli ulcer in southeastern Australia. Appl Environ Microbiol. 2018;84:e02612–7.

24. World Health Organization. The Yamoussoukro declaration on Buruli ulcer. 1998 [cited 2019 Oct 3]. https://www.who.int/buruli/yamoussoukro_declaration/en/

25. World Health Organization. Cotonou declaration on Buruli ulcer. 2009 [cited 2019 Oct 3]. https://www.who.int/neglected_diseases/Benin_declaration_2009_eng_ok.pdf

26. World Health Organization. Recommendations for control of Buruli ulcer. WHO meeting on Buruli ulcer control and research; March 25–27, 2013; Geneva, Switzerland [cited 2019 Oct 3]. https://www.who.int/buruli/Recommendations_Buruli_ulcer_2013.pdf

27. Dehnavieh R, Haghdoost A, Khosravi A, Hoseinabadi F, Rahimi H, Poursheikhali A, et al. The District Health Information System (DHIS2): a literature review and meta-synthesis of its strengths and operational challenges based on the experiences of 11 countries. Health Inf Manag. 2018;48:62–75.

28. Ukwaja KN, Meka AO, Chukwuka A, Asiedu KB, Huber KL, Eddyani M, et al. Buruli ulcer in Nigeria: results of a pilot case study in three rural districts. Infect Dis Poverty. 2016;5:39. https://doi.org/10.1186/s40249-016-0119-8

29. Ayelo GA, Anagonou E, Wadagni AC, Barogui YT, Dossou AD, Houezo JG, et al. Report of a series of 82 cases of Buruli ulcer from Nigeria treated in Benin, from 2006 to 2016. PLoS Negl Trop Dis. 2018;12:e0006358. https://doi.org/10.1371/journal.pntd.0006358

30. Otuh PI, Soyinka FO, Ogunro BN, Akinseye V, Nwezza EE, Iseoluwa-Adelokiki AO, et al. Perception and incidence of Buruli ulcer in Ogun State, South West Nigeria: intensive epidemiological survey and public health intervention recommended. Pan Afr Med J. 2018;29:166. https://doi.org/10.11604/pamj.2018.29.166.10110

31. Kollie K, Amoako YA, Ake J, Mulbah T, Zaizay F, Abass M, et al. Buruli ulcer in Liberia, 2012. Emerg Infect Dis. 2014;20:494–6. https://doi.org/10.3201/eid2003.130708

32. Tai AYC, Athan E, Friedman ND, Hughes A, Walton A, O'Brien DP. Increased severity and spread of *Mycobacterium ulcerans*, southeastern Australia. Emerg Infect Dis. 2018;24:58–64. https://doi.org/10.3201/eid2401.171070

33. Doig KD, Holt KE, Fyfe JAM, Lavender CJ, Eddyani M, Portaels F, et al. On the origin of *Mycobacterium ulcerans*, the causative agent of Buruli ulcer. BMC Genomics. 2012;13:258. https://doi.org/10.1186/1471-2164-13-258

34. Bolz M, Bratschi MW, Kerber S, Minyem JC, Um Boock A, Vogel M, et al. Locally confined clonal complexes of *Mycobacterium ulcerans* in two Buruli ulcer endemic regions of Cameroon. PLoS Negl Trop Dis. 2015;9:e0003802. https://doi.org/10.1371/journal.pntd.0003802

35. Phillips R, Horsfield C, Kuijper S, Lartey A, Tetteh I, Etuaful S, et al. Sensitivity of PCR targeting the IS*2404* insertion sequence of *Mycobacterium ulcerans* in an assay using punch biopsy specimens for diagnosis of Buruli ulcer. J Clin Microbiol. 2005;43:3650–6. https://doi.org/10.1128/JCM.43.8.3650-3656.2005

36. Yeboah-Manu D, Aboagye SY, Asare P, Asante-Poku A, Ampah K, Danso E, et al. Laboratory confirmation of Buruli ulcer cases in Ghana, 2008–2016. PLoS Negl Trop Dis. 2018;12:e0006560. https://doi.org/10.1371/journal.pntd.0006560

37. Wadagni A, Frimpong M, Phanzu DM, Ablordey A, Kacou E, Gbedevi M, et al. Simple, rapid *Mycobacterium ulcerans* disease diagnosis from clinical samples by fluorescence of mycolactone on thin layer chromatography. PLoS Negl Trop Dis. 2015;9:e0004247. https://doi.org/10.1371/journal.pntd.0004247

38. Capela C, Sopoh GE, Houezo JG, Fiodessihoué R, Dossou AD, Costa P, et al. Clinical epidemiology of Buruli ulcer from Benin (2005–2013): effect of time-delay to diagnosis on clinical forms and severe phenotypes. PLoS Negl Trop Dis. 2015;9:e0004005. https://doi.org/10.1371/journal.pntd.0004005

39. World Health Organization African Region. Regional strategy on neglected tropical diseases in the WHO African Region. Document no. AFR/RC63/10. The Organization; 2013 [cited 2019 Oct 15]. https://www.afro.who.int/sites/default/files/sessions/documents/nv-afr-rc63-10-Regional-Strategy-on-NTDs-in-the-WHO-African-Region-2014-2020.pdf

40. World Health Organization. Sixty-sixth World Health Assembly resolution WHA66.12. The Organization; 2013 [cited 2019 Jan 18]. http://apps.who.int/gb/ebwha/pdf_files/WHA66-REC1/WHA66_2013_REC1_complete.pdf

41. World Health Organization. Recognizing neglected tropical diseases through changes on the skin: a training guide for front-line health workers. Document no. WHO/HTM/NTD/2018.03. The Organization; 2018 [cited 2019 Jan 18]. https://www.who.int/neglected_diseases/resources/9789241513531

Address for correspondence: Till F. Omansen, Department of Tropical Medicine, Bernhard Nocht Institute for Tropical Medicine and I. Department of Medicine, University Medical Center Hamburg-Eppendorf, Bernhard-Nocht-Straße 74, Hamburg 20359, Germany; email: till.omansen@bnitm.de.

Cost-effectiveness of Prophylactic Zika Virus Vaccine in the Americas

Affan Shoukat, Thomas Vilches, Seyed M. Moghadas

Zika virus remains a major public health concern because of its association with microcephaly and other neurologic disorders in newborns. A prophylactic vaccine has the potential to reduce disease incidence and eliminate birth defects resulting from prenatal Zika virus infection in future outbreaks. We evaluated the cost-effectiveness of a Zika vaccine candidate, assuming a protection efficacy of 60%–90%, for 18 countries in the Americas affected by the 2015–2017 Zika virus outbreaks. Encapsulating the demographics of these countries in an agent-based model, our results show that vaccinating women of reproductive age would be very cost-effective for sufficiently low (<$16) vaccination costs per recipient, depending on the country-specific Zika attack rate. In all countries studied, the median reduction of microcephaly was >75% with vaccination. These findings indicate that targeted vaccination of women of reproductive age is a noteworthy preventive measure for mitigating the effects of Zika virus infection in future outbreaks.

After the 2013–2014 Zika virus outbreak in French Polynesia (*1,2*), the disease spread to 69 countries and territories worldwide (*3*). The connection of Zika virus infection to prenatal microcephaly and other brain abnormalities (*4–6*) raised a public health emergency of international concern in February 2016 (*7*). Although this concern subsided with declining outbreaks in the Americas, a sizable portion of the population in the tropical world remains at risk for Zika virus infection, especially in countries where the primary transmitting vector (the *Aedes aegypti* mosquito) is abundant (*8*). Furthermore, the economic burden of Zika virus infection is estimated to be substantial, ranging from $7 to $18 billion in short-term costs and $3.2 to $39 billion in long-term costs (*9*), which highlights the need for preventive measures.

The potential for future outbreaks and devastating clinical outcomes with long-term sequelae has directed research efforts to develop an effective Zika virus preventive vaccine (*10–13*). Several vaccine candidates have now advanced to clinical trials and have been shown to be safe and well tolerated in generating humoral immune responses (*14,15*). For the strategic use of a prophylactic vaccine, a vaccine target product profile (VTPP) has been proposed by the World Health Organization and the United Nations Children's Fund, prioritizing women of reproductive age (15–49 years), including pregnant women (*16*). To inform decisions on implementing the recommended VTPP, we evaluated the cost-effectiveness of a potential Zika virus vaccine in 18 countries in the Americas where the estimated attack rates (i.e., the proportion of the population infected) during the 2015–2017 outbreaks were >2% (*17,18*).

Methods

Simulation Model

We adopted a previously established agent-based simulation model for the dynamics of Zika virus infection, incorporating both vector and sexual transmission (*19,20*). For infection dynamics, the human population was divided into susceptible, exposed and incubating, infectious (symptomatic and asymptomatic), and recovered categories (Appendix Figure 1, https://wwwnc.cdc.gov/EID/article/25/12/18-1324-App1.pdf). We stratified the mosquito population into susceptible, exposed and incubating, and infectious groups. We parameterized the model with country-specific demographics (age and sex distributions and fertility rates), and calibrated it to attack rates (*17,18*) estimated for the 2015–2017 outbreaks (Appendix Tables 1–4, Figures 2–4). These attack rates were considered to be the proportion of the population that was infected (representing the level of herd immunity) at the start of simulations for each country in the evaluation of vaccination scenarios. We compiled parameters specific to Zika virus infection in both human and mosquito populations, along with costs associated with the disease and vaccination (Appendix Tables 5, 6). Further details of the model and its implementation are provided in the Appendix; for reproducibility, the computational model can be accessed at https://github.com/affans/zika.

Infection Outcomes

We considered microcephaly and Guillain-Barré syndrome (GBS) as outcomes of infection. The risk for microcephaly was highest (5%–14%) for infections occurring during the

Author affiliations: York University, Toronto, Ontario, Canada (A. Shoukat, S.M. Moghadas); São Paulo State University, Botucatu SP, Brazil (T. Vilches)

first trimester of pregnancy (which ends at 97 days) and decreased to 3%–5% for infections occurring during the second and third trimesters (21–23). We set a probability of 0.798 for survival past the first year of life for infants with microcephaly (24). Life expectancy of infants with microcephaly who survived the first year of life was reduced by 50%, from 70 years to 35 years, on average (25). The risk for GBS with Zika virus infection in adults was 0.025%–0.06% (26).

Vaccination and Cost-effectiveness

We implemented vaccination scenarios corresponding to the recommended strategies in the VTPP (16). The vaccination coverage was set to 60% for women of reproductive age at the onset of simulations. For pregnant women in the same age group, the vaccination coverage was set to 80% initially and continued at 80% throughout the simulations. We also considered a vaccination coverage of 10% for other persons 9–60 years of age. In the absence of efficacy data, we assumed that a single dose of vaccine provides a protection efficacy of 60%–90% against infection, which was sampled for each vaccinated person and implemented as a reduction factor in disease transmission. Infection following vaccination (if it occurred) was assumed to be asymptomatic. Furthermore, we assumed that vaccination has no effect on the risk of microcephaly in pregnant women if infection occurred.

For cost-effectiveness analysis, we considered both short- and long-term medical costs specific to each country (Appendix Table 6) (9). Short-term costs included physician visits and diagnostic tests for symptomatic Zika virus infection in pregnant women. For microcephaly in infants and GBS in adults, we considered lifetime direct medical costs related to hospitalization, treatment, and other associated outcomes. We quantified the long-term sequelae of microcephaly by disability-adjusted life-years (DALYs) with disability weight (i.e., severe intellectual disability) extracted from the Global Burden of Disease study (27). For given vaccination costs per individual (VCPI), we calculated the incremental cost-effectiveness ratios (ICERs) and averaged them over simulations (Appendix). Both DALYs and direct lifetime costs were based on a 3% discounting rate annually (9,25). For cost-effectiveness analysis, we considered the World Health Organization standards of using the per capita gross domestic product (GDP) as a threshold of willingness to pay (28). The vaccination program was considered very cost-effective for ICER values up to the per capita GDP and cost-effective for ICER values up to 3 times the per capita GDP. We also considered a range of willingness to pay values to inform decisions on vaccine cost-effectiveness in settings in which the per capita GDP threshold may not be applicable. Using a nonparametric bootstrap method,

we generated cost-effectiveness acceptability curves for each country and performed cost-effectiveness analysis from a government perspective. All costs are reported in 2015 US dollars.

We ran 2,000 Monte Carlo simulations of Zika virus infection dynamics with a scaled-down population of 10,000 persons for each country. Each simulation was seeded with a single case of Zika virus in the latent stage and run for a time horizon of 1 year with a daily time-step, beginning with a high-temperature season. For each simulation, we recorded the daily incidence of infection and disease outcomes and used them for cost-effectiveness analysis, as well as estimating the percentage reduction of microcephaly attributable to vaccination. DALYs were calculated for the lifetime of each case of microcephaly. Only epidemic curves that had ≥1 secondary cases by the end of simulations were considered in the cost-effectiveness analysis.

Results

We considered a plausible range of $2–$100 for VCPI to account for vaccine dose, wide distribution and administration, and wastage based on the estimates for other flavivirus vaccines (29). Our results show that for a sufficiently low VCPI in this range, a single-dose vaccination program is cost-saving for all countries studied (Figure 1, green). The lowest VCPI was found for Costa Rica, where the vaccine was cost-saving with a probability of ≥90% for VCPI up to $10, derived from the cost-effectiveness acceptability curve (Appendix Figure 5). With the same probability, the highest VCPI under which the vaccine was cost-saving was $25 for Guatemala and Panama. The highest values of VCPI for a cost-saving scenario in other countries were $14–$24.

For positive ICER values, we considered the average per capita GDP of each country in 2015 and 2016 as the threshold for cost-effectiveness (30). For this threshold, the vaccine is very cost-effective with a probability ≥90% at VCPI of ≤$16 in Costa Rica (mean incremental cost of $7,352/DALY averted; 95% CI $1,280–$9,234/DALY averted) and ≤$47 in French Guiana (mean incremental cost of $14,475/DALY averted; 95% CI $10,016–$16,653/DALY averted), with other countries having the highest value of VCPI in this range (Figure 1, red). For the threshold of 3 times the per capita GDP, the vaccine is still cost-effective (with a probability of ≥90%) with VCPI up to $24 (mean incremental cost of $4,829/DALY averted; 95% CI $2,395–$6,068/DALY averted) in Nicaragua and $96 (mean incremental cost of $49,934/DALY averted; 95% CI $36,523–$53,661/DALY averted) in French Guiana, with other countries having the highest value of VCPI in this range (Figure 1, black). We determined the VCPI for scenarios that are cost-saving, very cost-effective, and cost-effective for each country (Table), the corresponding incremental cost per DALY averted with 95% CIs (Table;
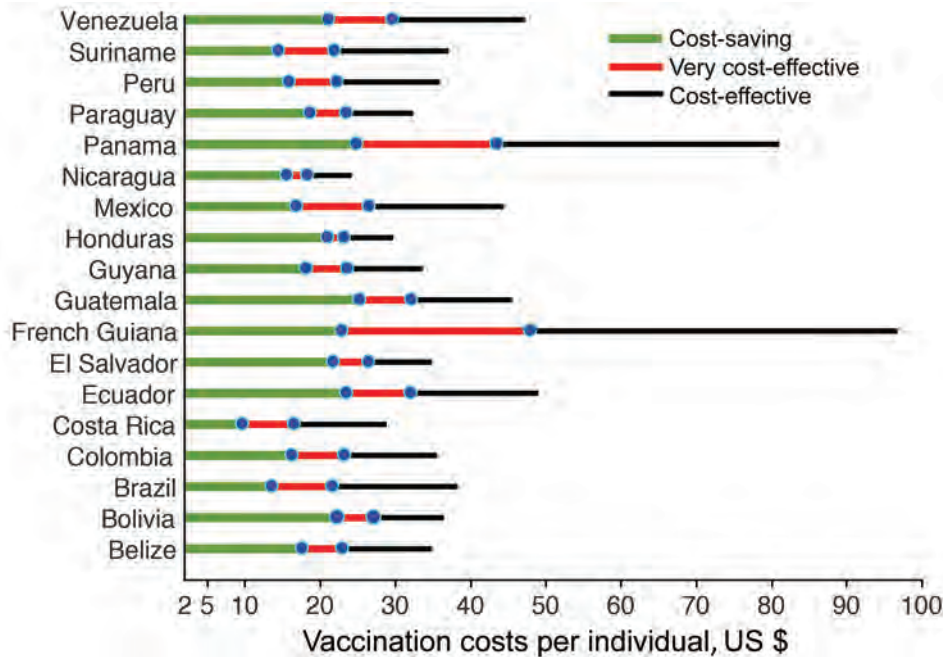
Figure 1. Range of vaccination costs per individual (VCPI; in 2015 US dollars) for the scenarios of whether Zika virus vaccines would be cost-saving (green), very cost-effective (red), and cost-effective (black). All estimates are based on the level of preexisting herd immunity in the population for each country.

Appendix Table 7), and the associated cost-effectiveness acceptability curves (Appendix Figure 5).

We also calculated the reduction of fetal microcephaly during pregnancy by comparing the simulation scenarios in the presence and absence of vaccination. We found a marked reduction in cases of microcephaly, within the range of 74%–92%, attributable to vaccination; the median percentage reduction was >80% in all countries (Figure 2). This finding suggests that a Zika virus vaccine with a pro-

phylactic efficacy as low as 60% could substantially reduce the incidence of microcephaly.

Given that the attack rates in future outbreaks may be different from those estimated for the 2015–2017 outbreaks, we further conducted cost-effectiveness analysis for 2 additional scenarios (Appendix Table 8). In the first scenario, we considered an increase of 4% in the estimated attack rate for each country. We found that vaccination was very cost-effective, with a probability ≥90% at VCPI

Table. Highest values of VCPI (in 2015 US dollars) for a Zika virus vaccine candidate to be cost-saving, very cost-effective, or cost-effective*

Country	Herd immunity, %	Cost-saving, VCPI	Very cost-effective				Cost-effective			
			GDP	VCPI	ICER	95% CI	3×GDP	VCPI	ICER	95% CI
Belize	21	$18	$4,955	$23	$3,516	$144–$4,575	$14,865	$34	$12,092	$7,379–$15,050
Bolivia	10	$22	$3,097	$27	$1,827	$(872)–$2,669	$9,291	$36	$7,038	$4,249–$9,745
Brazil	18	$14	$8,694	$21	$6,356	$1,596–$7,223	$26,082	$38	$21,725	$14,938–$27,441
Colombia	12	$16	$5,900	$23	$4,184	$1,284–$5,349	$17,700	$35	$14,086	$9,447–$16,736
Costa Rica	2	$10	$11,563	$16	$7,352	$1,280–$9,234	$34,689	$29	$29,061	$15,459–$30,561
Ecuador	8	$24	$6,084	$32	$4,451	$1,343–$5,560	$18,252	$48	$15,581	$10,338–$17,576
El Salvador	16	$22	$3,719	$26	$1,379	$(1,884)–$2,826	$11,157	$34	$8,177	$3,408–$9,785
French Guiana	18	$23	$18,036	$47	$14,475	$10,016–$16,653	$54,108	$96	$49,934	$36,523–$53,661
Guatemala	14	$25	$4,032	$32	$2,544	$148–$3,944	$12,096	$45	$9,786	$6,556–$11,859
Guyana	15	$18	$4,325	$23	$2,270	$(285)–$3,717	$12,975	$33	$10,034	$5,884–$12,262
Honduras	14	$21	$2,358	$23	$892	$(1,711)–$1,705	$7,074	$29	$4,992	$1,623–$6,142
Mexico	5	$17	$8,867	$26	$6,362	$2,564–$7,445	$26,601	$44	$21,652	$14,717–$24,875
Nicaragua	17	$16	$2,109	$18	$595	$(1,465)–$1,231	$6,327	$24	$4,829	$2,395–$6,068
Panama	15	$25	$14,009	$43	$11,001	$7,016–$13,486	$42,027	$82	$37,247	$29,096–$43,898
Paraguay	17	$19	$4,094	$23	$2,348	$(305)–$3,332	$12,282	$32	$9,903	$5,028–$10,670
Peru	4	$16	$6,042	$22	$4,332	$1,087–$5,560	$18,126	$35	$14,028	$9,262–$16,432
Suriname	22	$14	$7,298	$21	$4,434	$1,505–$6,235	$21,894	$37	$18,705	$12,714–$22,331
Venezuela	19	$21	$7,766	$29	$4,697	$623–$6,590	$23,298	$47	$19,170	$13,160–$23,579

*Mean ICER values with 95% CI correspond to VCPI values under which the vaccination program is at least 90% cost-effective in each country. The per capita GDP and 3 times the per capita GDP were used as thresholds for very cost-effective and cost-effective analyses, respectively. The dollar values in parentheses indicate that the 95% CI extends to negative ICER values, which is considered cost-saving. GDP, gross domestic product; ICER, incremental cost-effectiveness ratio; VCPI, vaccination cost per individual.
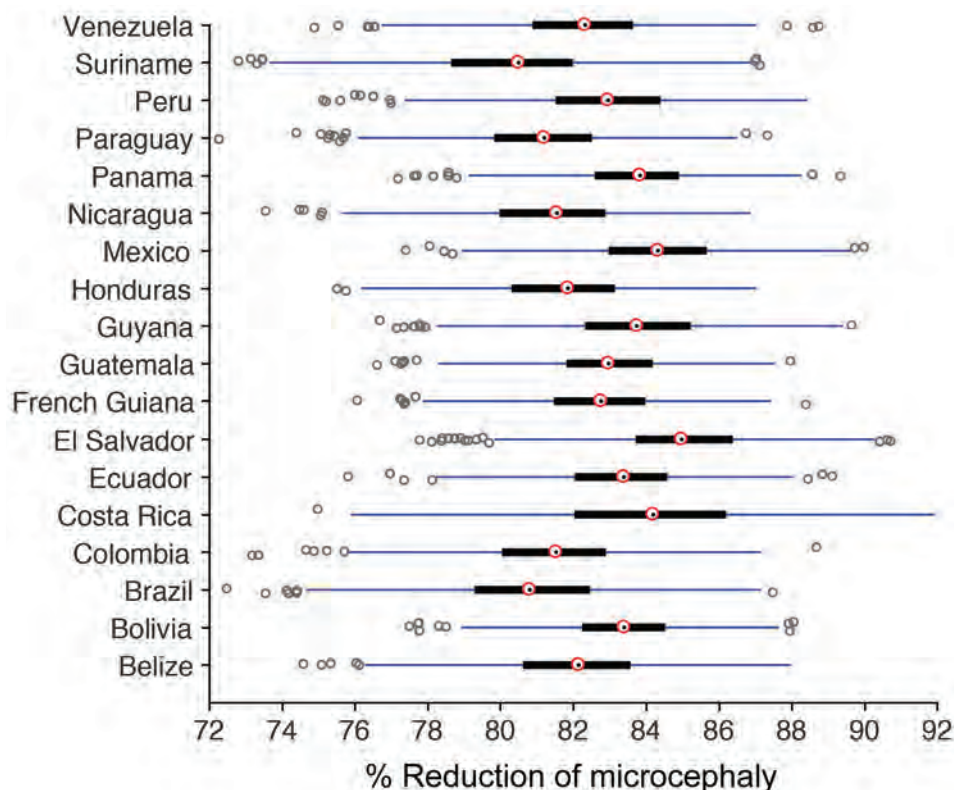
Figure 2. Box plots for the percentage reduction of microcephaly as a result of Zika virus vaccination. Red circles indicate medians; black bars indicate interquartile range (IQR); blue lines indicate extended range, from minimum (25th percentile – 1.5 IQR) to maximum (75th percentile + 1.5 IQR); dark circles indicate outliers.

of ≤$20 in Nicaragua (mean incremental cost of $1,067/DALY averted) and ≤$50 or less in French Guiana (mean incremental cost of $14,914/DALY averted). The highest VCPI for other countries ranged between these values.

In the second scenario, we decreased the attack rates by 4%, with a lower bound of 1% for each country. The results show that vaccination was very cost-effective, with a VCPI of ≤$4 in Mexico (mean incremental cost of $3,054/DALY averted) and ≤$41 in French Guiana (mean incremental cost of $15,037/DALY averted), with other countries having the highest VCPI value in this range (summary of additional results of cost-effectiveness analysis in Appendix Tables 9, 10, and Appendix Figures 6, 7). The median percentage reduction of microcephaly in these scenarios was >75% with vaccination (Appendix Figure 8).

Discussion

We determined the VCPI within the input range of $2–$100, for which vaccination is cost-saving (when ICER values are negative) and is very cost-effective (when ICER values are positive, below the threshold of the per capita GDP) for 18 countries in the Americas. Although several factors (e.g., the level of preexisting herd immunity, attack rate, costs associated with the management of Zika virus infection and its outcomes, and the willingness to pay) are critical in determining VCPI for cost-effectiveness, our results show that targeted vaccination of women of reproductive

age would be cost-effective, and even cost-saving, in all countries studied if VCPI is sufficiently low. Furthermore, vaccination with a protection efficacy of 60%–90% notably reduces the incidence of microcephaly, with a median percentage reduction >75% in simulated scenarios.

Previous work suggests that a prophylactic vaccine with a protection efficacy of 75% reduces the incidence of prenatal infections by ≥94% if 90% of women of reproductive age are vaccinated (31). These estimates are slightly higher than what our model predicts (with a median percentage reduction of 75%–88%) in similar scenarios, which is expected given the deterministic nature of the model used in the previous study (31). Nevertheless, the findings indicate that targeted vaccination is a noteworthy preventive measure for mitigating the impact of Zika virus infection in future outbreaks.

Considering direct medical costs associated with short- and long-term Zika virus infection outcomes, our study provides a cost-effectiveness analysis of a Zika virus vaccine candidate from a government perspective. Several recent modeling studies also evaluate cost-effectiveness of a Zika virus vaccine (20,32). However, these studies have either considered only a few countries in Latin America or relied on homogeneous models. The strength of our study relies on the evaluation of cost-effectiveness for countries affected by Zika virus with estimated attack rates >2% within a single modeling

framework. We based our analysis on an individual-level stochastic approach, accounting for parameter uncertainty and heterogeneities in disease transmission. Because of its dynamic nature, the simulation model also considers the accruing herd immunity during the epidemic that results from the indirect protection effects of naturally acquired immunity in the population.

Our results should be considered within the context of study limitations. First, we note that we based our analysis on estimates of attack rates during the 2015–2017 Zika virus outbreaks in Latin and South America countries (*9,17,18*), and these attack rates were regarded as the levels of preexisting herd immunity in the simulations. Should these levels change as the result of a decline of herd immunity or accumulation of new susceptible persons at the time of vaccine availability in future outbreaks, the expected changes in the VCPI range for cost-effectiveness require further analysis. Second, although the initial phase of clinical trials indicates high levels of neutralizing antibodies (*14,15*), the range of vaccine efficacy has not been ascertained; our estimates rely on the assumption that a single dose of vaccine would provide a protection efficacy of 60%–90%. We assumed that during the epidemic pregnant women are vaccinated (with a coverage of 80%) early in their first trimester, because the highest risk of microcephaly occurs then. However, we understand that because of various factors, including access to healthcare resources and late recognition of pregnancy, vaccination may not occur before any potential Zika virus infection during pregnancy. The risk for microcephaly was not altered if infection occurred following vaccination, but the disease was considered to be asymptomatic. The validation of these assumptions requires efficacy data from clinical trials, which are currently lacking. In our model, the risk of sexual transmission was included only during the infectious period. Although this risk may continue for several days or weeks following recovery (*33,34*), our simplifying assumption is justified because of uncertainty in the duration of sexual transmission at the individual level. Despite these limitations, which warrant further investigation as relevant information and data become available, this study provides estimates for Zika virus vaccine cost-effectiveness to inform decision makers for the implementation of the VTPP strategies in an outbreak response scenario.

About the Author

Dr. Shoukat is a postdoctoral fellow at Yale University, New Haven, CT, USA. His research interests include mathematical and computational modeling of infectious diseases and cost-effectiveness of intervention measures, in particular for vaccine-preventable diseases.

References

1. Aubry M, Teissier A, Huart M, Merceron S, Vanhomwegen J, Roche C, et al. Zika virus seroprevalence, French Polynesia, 2014–2015. Emerg Infect Dis. 2017;23:669–72. https://doi.org/10.3201/eid2304.161549
2. Musso D. Zika virus transmission from French Polynesia to Brazil. Emerg Infect Dis. 2015;21:1887. https://doi.org/10.3201/eid2110.151125
3. World Health Organization. Zika situation report. 2017 [cited 2018 Aug 20]. http://www.who.int/emergencies/zika-virus/situation-report
4. Panchaud A, Stojanov M, Ammerdorffer A, Vouga M, Baud D. Emerging role of Zika virus in adverse fetal and neonatal outcomes. Clin Microbiol Rev. 2016;29:659–94. https://doi.org/10.1128/CMR.00014-16
5. Krauer F, Riesen M, Reveiz L, Oladapo OT, Martínez-Vega R, Porgo TV, et al. Zika virus infection as a cause of congenital brain abnormalities and Guillain–Barré syndrome: systematic review. PLoS Med. 2017;14:e1002203. https://doi.org/10.1371/journal.pmed.1002203
6. Ladhani SN, O'Connor C, Kirkbride H, Brooks T, Morgan D. Outbreak of Zika virus disease in the Americas and the association with microcephaly, congenital malformations and Guillain-Barré syndrome. Arch Dis Child. 2016;101:600–2. https://doi.org/10.1136/archdischild-2016-310590
7. World Health Organization. Fifth meeting of the Emergency Committee under the International Health Regulations (2005) regarding microcephaly, other neurological disorders and Zika virus [cited 2018 Jun 1]. https://www.who.int/news-room/detail/18-11-2016-fifth-meeting-of-the-emergency-committee-under-the-international-health-regulations-(2005)-regarding-microcephaly-other-neurological-disorders-and-zika-virus
8. Bogoch II, Brady OJ, Kraemer MUG, German M, Creatore MI, Kulkarni MA, et al. Anticipating the international spread of Zika virus from Brazil. Lancet. 2016;387:335–6. https://doi.org/10.1016/S0140-6736(16)00080-5
9. United Nations Development Programme. A socio-economic impact assessment of the Zika virus in Latin America and the Caribbean: with a focus on Brazil, Colombia and Suriname. 2017 [cited 2018 Jun 1]. https://www.undp.org/content/undp/en/home/librarypage/hiv-aids/a-socio-economic-impact-assessment-of-the-zika-virus-in-latin-am.html
10. Durbin A, Wilder-Smith A. An update on Zika vaccine developments. Expert Rev Vaccines. 2017;16:781–7. https://doi.org/10.1080/14760584.2017.1345309
11. Lagunas-Rangel FA, Viveros-Sandoval ME, Reyes-Sandoval A. Current trends in Zika vaccine development. J Virus Erad. 2017;3:124–7.
12. Tripp RA, Ross TM. Development of a Zika vaccine. Expert Rev Vaccines. 2016;15:1083–5. https://doi.org/10.1080/14760584.2016.1192474
13. Barouch DH, Thomas SJ, Michael NL. Prospects for a Zika virus vaccine. Immunity. 2017;46:176–82. https://doi.org/10.1016/j.immuni.2017.02.005
14. Gaudinski MR, Houser KV, Morabito KM, Hu Z, Yamshchikov G, Rothwell RS, et al.; VRC 319; VRC 320 study teams. Safety,

tolerability, and immunogenicity of two Zika virus DNA vaccine candidates in healthy adults: randomised, open-label, phase 1 clinical trials. Lancet. 2018;391:552–62. https://doi.org/10.1016/S0140-6736(17)33105-7

15. Barrett ADT. Current status of Zika vaccine development: Zika vaccines advance into clinical evaluation. NPJ Vaccines. 2018;3:24. https://doi.org/10.1038/s41541-018-0061-9

16. World Health Organization. Zika virus (ZIKV) vaccine target product profile (TPP): vaccine to protect against congenital Zika syndrome for use during an emergency. 2017 [cited 2018 Jun 1]. http://www.who.int/immunization/research/development/WHO_UNICEF_Zikavac_TPP_Feb2017.pdf

17. Zhang Q, Sun K, Chinazzi M, Pastore Y Piontti A, Dean NE, Rojas DP, et al. Spread of Zika virus in the Americas. Proc Natl Acad Sci U S A. 2017;114:E4334–43. https://doi.org/10.1073/pnas.1620161114

18. Colón-González FJ, Peres CA, Steiner São Bernardo C, Hunter PR, Lake IR. After the epidemic: Zika virus projections for Latin America and the Caribbean. PLoS Negl Trop Dis. 2017;11:e0006007. https://doi.org/10.1371/journal.pntd.0006007

19. Moghadas SM, Shoukat A, Espindola AL, Pereira RS, Abdirizak F, Laskowski M, et al. Asymptomatic transmission and the dynamics of Zika infection. Sci Rep. 2017;7:5829. https://doi.org/10.1038/s41598-017-05013-9

20. Shoukat A, Vilches T, Moghadas SM. Cost-effectiveness of a potential Zika vaccine candidate: a case study for Colombia. BMC Med. 2018;16:100. https://doi.org/10.1186/s12916-018-1091-x

21. Reynolds MR, Jones AM, Petersen EE, Lee EH, Rice ME, Bingham A, et al.; U.S. Zika Pregnancy Registry Collaboration. Vital signs: update on Zika virus–associated birth defects and evaluation of all U.S. infants with congenital Zika virus exposure—U.S. Zika Pregnancy Registry, 2016. MMWR Morb Mortal Wkly Rep. 2017;66:366–73. https://doi.org/10.15585/mmwr.mm6613e1

22. Honein MA, Dawson AL, Petersen EE, Jones AM, Lee EH, Yazdy MM, et al.; US Zika Pregnancy Registry Collaboration. Birth defects among fetuses and infants of US women with evidence of possible Zika virus infection during pregnancy. JAMA. 2017;317:59–68. https://doi.org/10.1001/jama.2016.19006

23. Johansson MA, Mier-y-Teran-Romero L, Reefhuis J, Gilboa SM, Hills SL. Zika and the risk of microcephaly. N Engl J Med. 2016;375:1–4. https://doi.org/10.1056/NEJMp1605367

24. Nembhard WN, Waller DK, Sever LE, Canfield MA. Patterns of first-year survival among infants with selected congenital anomalies in Texas, 1995–1997. Teratology. 2001;64:267–75. https://doi.org/10.1002/tera.1073

25. Alfaro-Murillo JA, Parpia AS, Fitzpatrick MC, Tamagnan JA, Medlock J, Ndeffo-Mbah ML, et al. A cost-effectiveness tool for informing policies on Zika virus control. PLoS Negl Trop Dis. 2016;10:e0004743. https://doi.org/10.1371/journal.pntd.0004743

26. Cao-Lormeau VM, Blake A, Mons S, Lastère S, Roche C, Vanhomwegen J, et al. Guillain-Barré syndrome outbreak associated with Zika virus infection in French Polynesia: a case-control study. Lancet. 2016;387:1531–9. https://doi.org/10.1016/S0140-6736(16)00562-6

27. Salomon JA, Haagsma JA, Davis A, de Noordhout CM, Polinder S, Havelaar AH, et al. Disability weights for the Global Burden of Disease 2013 study. Lancet Glob Health. 2015;3: e712–23. https://doi.org/10.1016/S2214-109X(15)00069-8

28. Bertram MY, Lauer JA, De Joncheere K, Edejer T, Hutubessy R, Kieny M-P, et al. Cost-effectiveness thresholds: pros and cons. Bull World Health Organ. 2016;94:925–30. https://doi.org/10.2471/BLT.15.164418

29. Zeng W, Halasa-Rappel YA, Baurin N, Coudeville L, Shepard DS. Cost-effectiveness of dengue vaccination in ten endemic countries. Vaccine. 2018;36:413–20. https://doi.org/10.1016/j.vaccine.2017.11.064

30. Marseille E, Larson B, Kazi DS, Kahn JG, Rosen S. Thresholds for the cost-effectiveness of interventions: alternative approaches. Bull World Health Organ. 2015;93:118–24. https://doi.org/10.2471/BLT.14.138206

31. Durham DP, Fitzpatrick MC, Ndeffo-Mbah ML, Parpia AS, Michael NL, Galvani AP. Evaluating vaccination strategies for Zika virus in the Americas. Ann Intern Med. 2018;168:621–30. https://doi.org/10.7326/M17-0641

32. Bartsch SM, Asti L, Cox SN, Durham DP, Randall S, Hotez PJ, et al. What is the value of different Zika vaccination strategies to prevent and mitigate Zika outbreaks? J Infect Dis. 2019;220:920–31. https://doi.org/ 10.1093/infdis/jiy688

33. Counotte MJ, Kim CR, Wang J, Bernstein K, Deal CD, Broutet NJN, et al. Sexual transmission of Zika virus and other flaviviruses: a living systematic review. PLoS Med. 2018;15:e1002611. https://doi.org/10.1371/journal.pmed.1002611

34. Atkinson B, Thorburn F, Petridou C, Bailey D, Hewson R, Simpson AJH, et al. Presence and persistence of Zika virus RNA in semen, United Kingdom, 2016. Emerg Infect Dis. 2017;23:611–5. https://doi.org/10.3201/eid2304.161692

Address for correspondence: Seyed M. Moghadas, York University, Agent-Based Modelling Laboratory, 4700 Keele St, Toronto, ON M3J 1P3, Canada; email: moghadas@yorku.ca

Human Infection with Orf Virus and Description of Its Whole Genome, France, 2017

Julien Andreani, Jessica Fongue, Jacques Y. Bou Khalil, Laurene David, Saïd Mougari,
Marion Le Bideau, Jonatas Abrahão, Philippe Berbis, Bernard La Scola

Zoonotic transmission of parapoxvirus from animals to humans has been reported; clinical manifestations are skin lesions on the fingers and hands after contact with infected animals. We report a human infection clinically suspected as being ecthyma contagiosum. The patient, a 65-year-old woman, had 3 nodules on her hands. She reported contact with a sheep during the Aïd-el-Fitr festival in France during 2017. We isolated the parapoxvirus orf virus from these nodules by using a nonconventional cell and sequenced the orf genome. We identified a novel orf virus genome and compared it with genomes of other orf viruses. More research is needed on the genus *Parapoxvirus* to understand worldwide distribution of and infection by orf virus, especially transmission between goats and sheep.

*P*arapoxvirus is a genus of double-stranded DNA viruses (family *Poxviridae*) that contains 4 virus species: orf virus, bovine papular stomatitis virus, parapoxvirus of red deer, and pseudocowpoxvirus. Recently, a complete genome from a gray seal infected by a parapoxvirus was reported and constituted a putative novel virus in this genus (*1*). Zoonotic transmission of parapoxvirus from animals to humans has been reported in the past few decades; the main human clinical manifestations are skin lesions on the fingers and hands after contact with infected animals (*2–5*).

Most human cases of infection with parapoxvirus reported are caused by orf virus (*2,6,7*), but some human infections are caused by pseudocowpoxviruses (*8,9*). Infection of small ruminants with orf virus is frequent and widely distributed worldwide. Orf virus disease is also known as contagious ecthyma, scabby mouth, sore mouth, or infectious pustular dermatitis. Humans can be infected

Author affiliations: Institut Hospitalo-Universitaire Méditerranée Infection, Marseille, France (J. Andreani, J.Y. Bou Khalil, S. Mougari, M. Le Bideau, B. La Scola); Centre Hospitalier Universitaire Hôpital Nord, Marseille (J. Fongue, L. David, P. Berbis); Universidade Federal de Minas Gerais, Belo Horizonte, Brazil (J. Abrahão)

with orf virus by contact with sheep and goats during religious or cultural practices and during slaughter of animals (*4,10*), and infections appear to be more frequent during the last 3 months of each year (*3*). Human-to-human infection is extremely rare (*11,12*). Vaccination against orf virus is available for animals, although it does not confer long-term protective immunity (*13*). Human infections are relatively frequent when populations are exposed to sheep and goats (occupational disease). However, complete genomes of orf viruses are rarely found in public databases, which results in limited comparative studies in this field.

Diagnosis of human infections with orf virus is usually made by histologic analysis, molecular biology (PCR) studies, or electron microscopy. At least 11 complete orf virus genomes are available, and at least 19 are available for the entire genus *Parapoxvirus*. Nevertheless, a unique orf virus was sequenced after a human case report (*14*) (orf virus strain B029). These data are in contrast with those for orthopoxviruses (another *Poxviridae* genus) in which >300 genomes are available. One of the reasons for limited availability of parapoxvirus genomes is that many of these viruses are not cultivable on most diagnostic laboratories' cell lines (*15*).

In 2017, we identified a 65-year-old woman in France who had 3 nodules on her hands. She was given a diagnosis of ecthyma contagiosum. Genomic and electron microscopy data confirmed the initial diagnosis as infection with orf virus and identified this virus as the etiologic agent. We also isolated this virus on OA3.Ts cells.

Materials and Methods

Case-Patient

A 65-year-old woman came to North Hospital (Marseille, France) because of 3 nodules on her hands. She reported contact 3 weeks earlier with the carcass of a dead sheep during the Aïd-el-Fitr festival (June 25, 2017) in the Bouches-du-Rhones Department in southern France. Clinically, she had 3 painless, well-delimited erythematosus nodules on her fingers with an erythematosus halo (Figure 1). On

Figure 1. Nodules on the A) left thumb and B) left little finger of a 65-year-old woman infected with orf virus during Aïd-el-Fitr festival, France, 2017.

the basis of clinical suspicion of ecthyma contagiosum, we obtained a cutaneous biopsy specimen for biologic confirmations by PCR and histologic analysis. Histopathologic analysis of the skin biopsy specimen showed a moderate epidermal hyperplasia, spongiform degeneration with vacuolated cells, and inflammatory infiltration into the dermis (Figure 2). The patient was given antiseptic and local antimicrobial drug therapy (2% fusidic acid cream) to prevent bacterial superinfection. All skin lesions healed in 3 weeks.

Virus Detection, Isolation, and Production

We performed a parapoxvirus PCR on the cutaneous biopsy sample by using primers forward 5′-CGGTGCAGCACGAGGTC-3′, reverse 5′-CGGCGTATTCTTCTCGGACT-3′, and 6FAM-5′-GCCTAGGAAGCGCTCCGGCG-3′. These primers are specific for the B2L gene, which encodes the major membrane protein of parapoxvirus.

For virus culture, we crushed a biopsy sample and resuspended it in Hanks' balanced salt solution (Thermo Fisher Scientific, https://www.thermofisher.com). We then inoculated 400 µL of this sample onto 2 shell vials (200 µL/vial) (7-mL TRAC bottles; Thermo Fisher Scientific) containing 1 mL of OA3.Ts testes cells from *Ovis aries* sheep (CRL-6546; American Type Culture Collection, https://www.atcc.org) at a concentration of 10^6 cells/ mL. We incubated 1 vial at 32°C and 1 vial at 37°C in an atmosphere of 5% CO_2 and observed daily by inverted microscopy to detect any potential cytopathic effect.

For virus production, we prepared 15 flasks (T75cm^2; Corning, https://www.corning.com) containing OA3.Ts cells and Dulbecco's modified Eagle medium (Thermo Fisher Scientific) plus 10% fetal bovine serum and 1% glutamine. We then incubated the cells, and when they reached a confluence of 80% of confluence, we removed the medium and inoculated the monolayer with 5 mL of virus suspension at a multiplicity of infection of 0.01. We incubated the flasks at 37°C for 1 h to enable adsorption. We then added 20 mL of Dulbecco's modified Eagle medium to the flasks and incubated them for 3 days. On the third day, we discarded the supernatant, washed the cell monolayer 3 times with phosphate-buffered saline, and removed the monolayer by using a scraper. Once all the flasks were scraped and washed twice to collect cells, we transferred all contents to a 50-mL tube and kept the tube on ice.

We then centrifuged the cells at $500 \times g$ for 10 min, removed the supernatant, resuspended the pellet in 10 mL of sterile lysis buffer (1 mmol/L $MgCl_2$, 10 mmol/L Tris, and 10 mmol/L KCl, pH 7.0), and incubated this suspension for 10 min on ice. We performed mechanical lysis by using a sterile douncer device (80 cycles on ice). In parallel, we filtered the entire supernatant by using a 0.45-µm polyvinylidene difluoride membrane (Dutscher, https://www.dutscher.com) and centrifuged the supernatant. Finally, we added 10 mL of 25% sucrose to a plastic centrifugation tube, and slowly transferred the virus mixture from the filtrate to avoid mixing with the sucrose solution (biphasic final solution). We centrifuged the tube at $60,000 \times g$ for 1 h at 4°C, collected the pellet, and stored the pellet at −80°C in small aliquots before genome sequencing.

Sample Embedding and Cell Preparation

We maintained OA3.Ts cells in culture containing minimal essential medium plus 10% fetal bovine serum. We inoculated the cell monolayer with parapoxvirus at a multiplicity of infection of 0.01 and incubated. We then collected the contents after scraping the flask (T-25cm^2) at 24 h postinfection.

We used the protocol of cell embedding as described in Bou Khalil et al. (*16*). We replaced the Epon resin with LR White resin (Agar Scientific, http://www.agarscientific.com). In brief, we fixed cells for 1 h with 2.5% glutaraldehyde in a 0.1 mol/L sodium cacodylate buffer and washed with a mixture of 0.2 mol/L saccharose/0.1 mol/L sodium cacodylate. We then postfixed cells for 1 h with 1% OsO4 diluted in 0.2 mol/L potassium hexacyanoferrate (III)/0.1 mol/L sodium cacodylate solution. After washing the cells with distilled water, we gradually dehydrated them with ethanol, then gradually replaced the ethanol with LR white resin. We performed polymerization for 24 h at 60°C. We obtained ultrathin, 70-nm sections by using a UC7
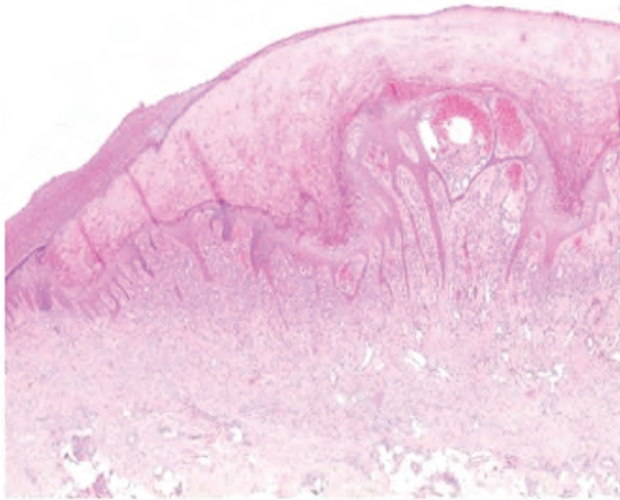
Figure 2. Histopathologic analysis of a skin biopsy specimen from a 65-year-old woman infected with orf virus during Aïd-el-Fitr festival, France, 2017. The specimen shows epidermal hyperplasia with acantolysis and papillomatosis, extensive hyperkeratosis, spongiform degeneration and vacuolated cells, and inflammatory infiltration in the dermis, predominantly by histiocytes and lymphocytes. Hematoxylin and eosin stain, original magnification x100.

ultramicrotome (Leica, https://www.leica-microsystems. com) and placed the sections onto HR25 300-mesh copper/rhodium grids (TAAB, https://www.taab.co.uk). We colored the sections with Reynolds solution. We obtained electron micrographs by using a Tecnai G2 transmission electron microscope (FEI, https://www.fei.com) operated at 200 keV and used ImageJ software (https://imagej.nih. gov) to determine particle size.

Genome Sequencing and Assembling

We sequenced genomic DNA of the parapoxvirus by using MiSeq Technology (Illumina, https://www.illumina.com) and the paired-end strategy. We barcoded sequences and compared them with 19 other genomic projects prepared from Nextera XT DNA Sample Prep Kit (Illumina). We quantified genomic DNA by using the Qubit Assay and the High-Sensitivity Kit (Life Technologies, https://www. thermofisher.com) at a concentration of 43 ng/µL. To prepare the paired-end library, we performed a dilution to obtain 1 ng of each genome as input to prepare the paired-end library. The tagmentation step (Illumina) fragmented and tagged the DNA. Limited cycle PCR amplification (12 cycles) completed the tag adapters and introduced dual-index barcodes. After purification by using AMPure XP Beads (Beckman Coulter Inc., https://www.beckmancoulter. com), we normalized the libraries on specific beads according to the Nextera XT protocol (Illumina). We pooled normalized libraries into a single library for sequencing, then loaded the pooled single-strand library onto the

reagent cartridge and then onto the instrument along with the flow cell. We performed automated cluster generation and paired-end sequencing with dual index reads in a single 39-h run for 2×250 bp.

We obtained total information of 10.2 Gb from 1,140,000 clusters of density/mm^2 and established a cluster passing quality control filters at 91.2% (19,783,000 clusters). Within this run, we determined the index representation for the parapoxvirus to be 5.45%. We filtered the 1,078,648 paired-end reads according to the read qualities.

We assembled paired-end reads by using the Hybrid spades program (*17*) and only paired-end strategy in input. We obtained 1 contig of 132,823 bp with an average coverage of 190 reads/base.

Gene Prediction and Analysis

We used Prodigal software for gene prediction (*18*). For predicted proteins that had lengths <100 amino acids, we used Phyre 2 software to predict the tridimensional fold (*19*). For the 130 initial predicted proteins, we deleted 4 predicted proteins with abnormal folds. We performed a blastp analysis (https://blast.ncbi.nlm.nih.gov/Blast. cgi?PAGE=Proteins&) of all predicted proteins against the nonredundant database at the National Center for Biotechnology Information (https://www.ncbi.nlm.nih.gov) and performed annotation by using delta-blastp results (*20*) and Interproscan version 69.0 (https://www.ebi.ac.uk). To determine average nucleotide values, we compared close phylogenetic strains by using the OrthoANI algorithm (*21*); we compared predicted proteins by using the reciprocal best hit and ProteinOrtho software (*22*) with 80% coverage, 20% identity, and 10^{-2} as an E value cutoff. The genome is available in the EMBL-EBI database (https://www.ebi. ac.uk, accession no. LR594616).

Phylogenetic Analysis

We performed alignment of 22 complete genomes of parapoxviruses with a closely related squirrel poxvirus, by using molluscum contagiosum virus as an outgroup. We computed alignments by using MAFFT version 7 (*23*) with fast Fourier transformation, a heuristic progressive method, and manually controlled alignments in MEGA6.0 (https:// www.megasoftware.net) to delete inverted repeat regions nonaligned at both ends. We conserved 208,216 positions to build a tree by using the general time-reversible model on the PhyML version 3 program (*24*) and visualized trees by using the iTol online program (*25*).

Results

Virus Isolation and Ultrastructure

The cutaneous biopsy specimen from the patient was found to contain parapoxvirus, which was confirmed by using

a quantitative PCR. We inoculated this biopsy specimen onto OA3.Ts cells, and monitored lysis daily by using an inverted microscope. We detected a cytopathic effect at 48 h postinfection. Electron microscopy confirmed the presence of virions in cells at 24 h after reculture and by observations of ultrathin sections (Figure 3).

Characterization of Orf Virus Genome

We obtained a linear complete genome of 132,823 bp with a guanine cytosine–rich content of ≈64.4%. This genome is the third smallest by length among parapoxviruses, after orf virus strain NP and seal parapoxvirus (Table). We propose to name this orf virus strain IHUMI-1.

Genome organization of orthopoxviruses are known to be conserved and follow the typical structure with inverted terminal repeat variations and a conserved central core genome (*33,34*). This structure was also suggested for parapoxviruses (*35*). We investigated synteny by using current complete genome reports. Mauve analysis of 12 complete genomes of orf virus enabled us to observe intraspecies conservation, except at the ends of some genomes (Appendix Figure 1, https://wwwnc.cdc.gov/EID/article/25/12/18-1513-App1.pdf). Moreover, analysis of synteny blocks across parapoxviruses showed the same typical organization (Appendix Figure 2). By using blast and MEGA analysis of the complete genome of orf virus IHUMI-1, we observed matches with all orf virus genomes, a squirrelpox virus genome, and a molluscum contagiosum virus genome (15% coverage and 80% identity). This region between the orf genome and molluscum contagiosum virus genome of ≈3,500 nt (positions on orf virus IHUMI-1 from 97,602 to 101,032) encodes a predicted protein essential for viruses: DNA-directed RNA polymerase subunit RPO132 (*Rbp2*).

Focusing on the 126 predicted proteins of virus strain IHUMI-1, we observed 124 best hits with different strains of orf virus, 1 hit with a hypothetical protein with *Mucor circinelloides* (with an E value of 10^{-3}), and 1 hit with *Ovis aries* sheep, the natural host. The protein showing the best hit with *O. aries* sheep was annotated as the interleukin-10 precursor. The gene for this protein is found in parapoxvirus and was probably acquired from mammals and known as a potential keystone protein that reduces inflammation during the infectious cycle (*36–39*). Despite the position of this gene at the left start region of genomes of parapoxviruses, this protein is highly conserved. The interleukin-10 gene of orf virus IHUMI-1 shows 99% nucleotide sequence identity with other orf virus strains and 79% with *O. aries* sheep and with *Capra hircus* goats; the gene showed, as reported, numerous synonymous mutations and adaptations by orf virus (*39*).
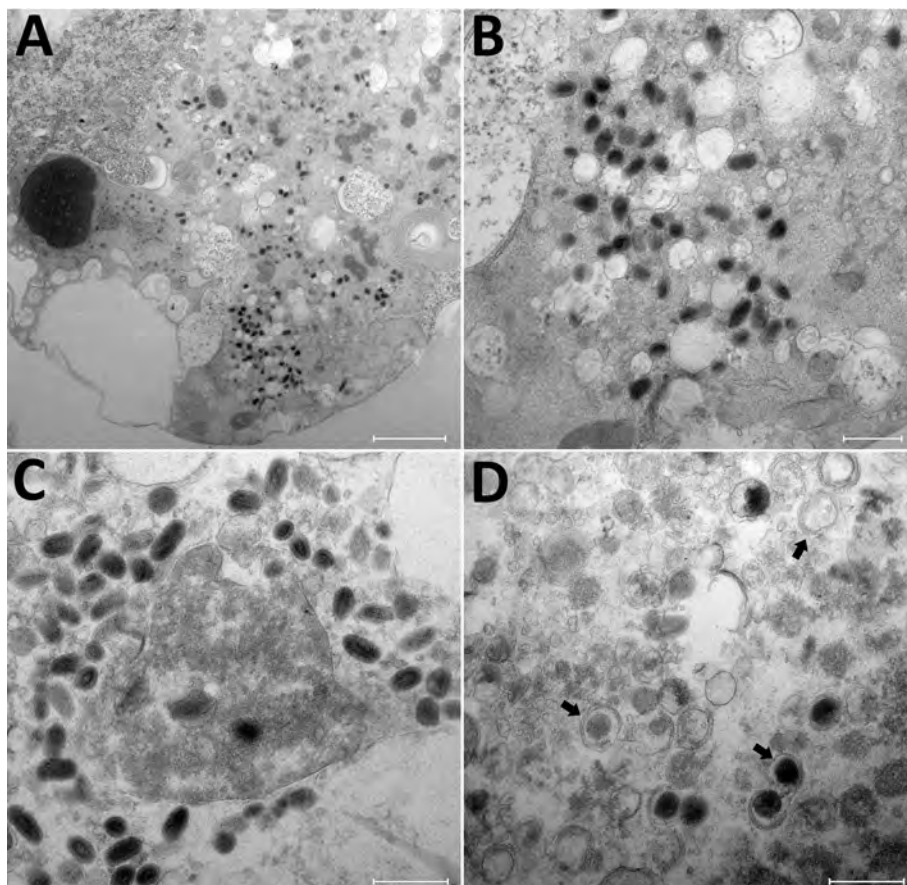
Figure 3. Transmission electron microscopy of OAT3.T cells infected with orf virus IHUMI-1 from a 65-year-old woman in France. A) Ultrathin section of an OAT3.Ts cell at 24 h postinfection harboring orf virus strain IHUMI-1 undergoing its replicative cycle where dense inclusion bodies could be clearly seen in the cell cytoplasm. B, C) Higher magnifications of infected cells showing typical enveloped virions. D) Ultrathin sections of an OAT3.Ts cell showing enveloped particles (arrows). Scale bars indicate 2 μm in panel A, 50 nm in panels B, C, and D.

Table. Genomic characteristics of parapoxviruses used for analysis of an orf virus isolated from a 65-year-old woman infected during Aïd-el-Fïtr, festival, France, 2017

Virus	Genome length, bp	GenBank accession no.	Source of virus	Reference
Orf virus strain PACA France 2017	132,823	LR594616	Hand nodule from human: 2017, France	This study
Orf virus strain OV-IA82	137,241	AY386263.1	Nasal secretion from lamb: 1982, Iowa	(15)
Orf virus strain NZ2	137,820	DQ184476.1	Sheep: New Zealand	(26)
Orf virus strain B029	134,104	KF837136.1	Human: Germany 1996	(14)
Orf virus strain OV-HN3/12	136,643	KY053526.1	Sheep: China 2012	(27)
Orf virus strain NA1/11	137,080	KF234407.1	Sheep: China 2011	(27)
Orf virus strain GO	139,866	KP010354.1	Lamb: Fujian, China, 2012	(27)
Orf virus strain D1701	134,038	HM133903.1	Sheep: Germany	(28)
Orf virus strain SJ1	139,112	KP010356.1	Lamb: Fujian, China, 2012	(27)
Orf virus strain YX	138,231	KP010353.1	Lamb: Fujian, China, 2012	(27)
Orf virus strain OV-SA00	139,962	AY386264.1	Goat kid: 2010, Texas	(15)
Orf virus strain NP	132,111	KP010355.1	Lamb: Fujian, China, 2011	(27)
Pseudocowpox virus strain VR634	145,289	GQ329670.1	Human after contact with contaminated cow: 1963, USA	(29)
Pseudocowpox virus strain F00.120R	133,169	GQ329669.1	Reindeer: Finland, 2009	(29)
Bovine papular stomatitis virus strain BV-TX09c1	135,072	KM875472.1	Domestic cow: 2009, USA	(30)
Bovine papular stomatitis virus strain BV-TX09c15	136,055	KM875470.1	Domestic cow: 2009, USA	(30)
Bovine papular stomatitis virus strain BV-TX09c5	135,635	KM875471.1	Domestic cow: 2009, USA	(30)
Bovine papular stomatitis virus strain BV-AR02	134,431	AY386265.1	Calf (oral lesions): Arkansas, 2004?	(15)
Parapoxvirus red deer/HL953	139,981	KM502564.1	Red deer (tonsil swab): Germany, 2013, subclinical infection	(31)
Seal parapoxvirus isolate AFK76s1	127,941	KY382358.2	Gray seal: Poland, 2015	(1)
Squirrel poxvirus strain red squirrel UK	148,803	HE601899.1	Red squirrel, UK: 2014, outgroup of parapoxvirus	(32)

Virus Clusters and Distribution

Orthopoxviruses, such as various strains of cowpox virus, circulate in Europe, and clusters are well identified with clades and subclades (40,41). Concerning parapoxviruses, a previous study of whole genomes of orf viruses showed that clusters exist and depend on whether the host is a goat or a sheep (27). Our phylogenetic analysis performed on whole genomes of parapoxviruses, which used the maximum-likelihood method, identified clusters with 2 different branches of orf viruses that had a common ancestor. This result is similar to that of Chi et al. (27) and showed 2 branches depending on whether the virus host was a goat or a sheep (Figure 4). In contrast, analysis by using the OrthoANi algorithm enabled us to separate orf viruses that originated
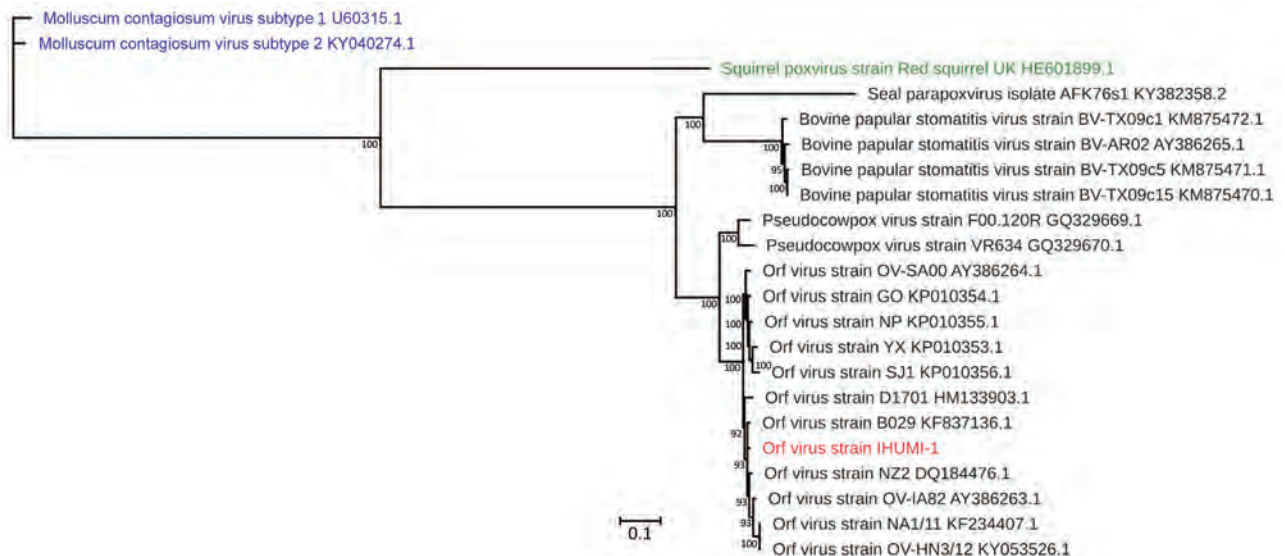
Figure 4. Maximum-likelihood tree based on complete sequences of orf virus IHUMI-1 from a 65-year-old woman in France (red) and 22 other viruses belonging to the family Poxviridae. Tree was constructed by using a general time-reversible model with 100 bootstrap replicates. All branches with bootstrap values <70 were collapsed. Numbers along branches are bootstrap values. Blue indicates 2 chordopoxviruses that served as outgroups, and green indicates a squirrel poxvirus still unclassified but related to the genus Parapoxvirus. GenBank accession numbers are provided for reference isolates. Scale bar indicates nucleotide substitutions per site.

from sheep and those that originated from goats (Figure 5). The only difference we observed was for orf virus strain D1701, which appeared to be an outgroup strain. Nevertheless, when we used the maximum-likelihood method and the OrthoANi algorithm, we found that orf virus IHUMI-1 clustered with orf virus strain B029. These 2 strains were human isolates obtained after infection from sheep.

Reciprocal best hit analysis enabled us to observe a high degree of conservation across orf virus genomes. A total of 102 proteins composed the core genomes of 12 orf viruses, and we did not detect any differences in core genomes of orf virus clusters. All virus proteins known to be essential (e.g., vascular endothelial growth factor, interleukin-10, and nuclear factor-κB inhibitor protein) (*39,42,43*) are present in the genome of orf virus strain IHUMI-1.

Protein analysis showed an absence of a predicted homolog open reading frame 119 in orf virus IHUMI-1. For his region, Chi et al. (*27*) reported numerous deletions and gap sequences (Appendix Figure 3), especially for 3 strains (NP, SJ1, and IHUMI-1). Coverage was <80% in that region for strains SJ1 and IHUMI-1, and the gene was almost completely deleted for strain NP (only 24% coverage) compared with strain OV-SA00. The consequence for orf virus IHUMI-1 is the deletion of the ORF119 gene.

This deletion has been implied in cell apoptosis (*44,45*). Nevertheless, deletion of this gene did not affect the virus cycle and strain virulence (*46*).

Discussion

We determined the complete genome of orf virus strain IHUMI-1 isolated from a human. This virus is the third smallest (by genome length) in the genus *Parapoxvirus*. The genome organization of orf virus IHUMI-1 is extremely similar in its synteny with those of other orf viruses that do not have a genetic inversion. Analysis of the predicted protein highlights strong protein conservation, except for the deletion in the ORF119 gene. The mitochondrial protein coded by this gene was recently described as being capable of increasing cell apoptosis (*44,45*). Despite this finding, our observations and a previous report showed no phenotypic modification in the virus cycle regarding this gene deletion (*46*).

Conversely, phylogenetic analysis of the entire virus genome showed clustering of orf viruses depending on the host (sheep or goats). This result was similar to those of previous analyses performed on different complete genomes by Chi et al. (*27*). Some studies did not report similar results; however, the phylogenetic trees in those studies
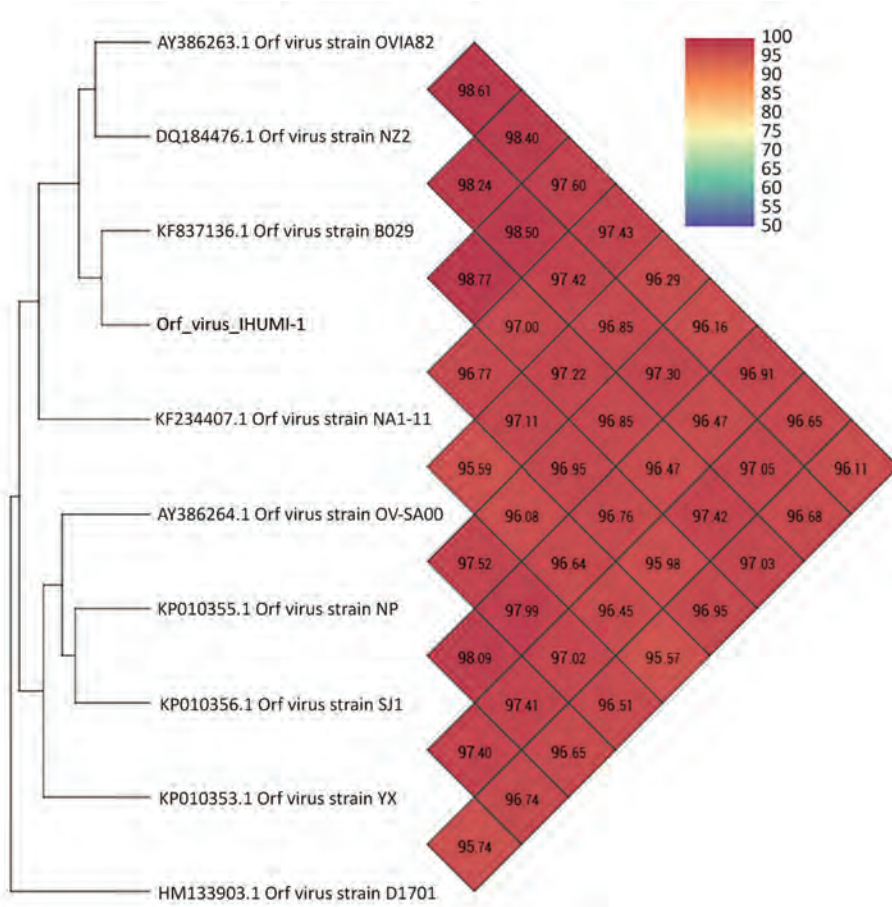
Figure 5. Heatmap representation of strain proximities across complete genomes of orf virus IHUMI-1 from a 65-year-old woman in France (red) and other available orf viruses. Because of the OrthoANi algorithm constraint, we deleted the complete genome of orf virus strain GO (GenBank accession no. KP010354.1) that clusters with orf virus strain NP and the complete genome of orf virus strain OV-HN3/12 (that clusters with NA1-11). GenBank accession numbers are provided for reference isolates. Values indicate percent similarity of nucleotides.

were limited to analysis of a few genes, such as the partial B2L gene (*47–49*). More complete genomes are needed to confirm this trend and verify there are 2 types of orf virus. In addition, we observed clustering on the whole genome between the IHUMI-1 and B029 strains of orf virus after human infection. Further investigations using more complete genome sequences might be able to confirm if some genetically related strains have the potential capacity to cross species barriers.

Numerous strains of parapoxviruses that infect animals are believed to show variable virulence in humans (e.g., orf strain D1701). However, implication of the host immune system in the severity of orf virus disease and in its evolution have been demonstrated (*50*).

Our results highlight the necessity of obtaining more complete genomes for parapoxviruses and retracing the route of infection when humans are infected. Further investigations of parapoxviruses should address the difficulties in isolating and cultivating this fastidious virus by using nonconventional cells for diagnostic analysis. However, recent description of a seal parapoxvirus (*1*) with a high-quality genome sequence obtained directly from a clinical sample could bypass the culture problem. In contrast, isolating the viral particle will always help to improve clinical research and future innovations.

About the Author

Mr. Andreani is a PharmD-PhD student in the Institut National de la Santé et de la Recherche Médicale program at Aix-Marseille University, Marseille, France. His research interests include isolation and genomic characterization of large and giant DNA viruses.

References

1. Günther T, Haas L, Alawi M, Wohlsein P, Marks J, Grundhoff A, et al. Recovery of the first full-length genome sequence of a parapoxvirus directly from a clinical sample. Sci Rep. 2017;7:3734. https://doi.org/10.1038/s41598-017-03997-y
2. Leavell UW Jr, McNamara MJ, Muelling R, Talbert WM, Rucker RC, Dalton AJ. Orf: report of 19 human cases with clinical and pathological observations. JAMA. 1968;204:657–64. https://doi.org/10.1001/jama.1968.03140210011003
3. Johannessen JV, Krogh HK, Solberg I, Dalen A, van Wijngaarden H, Johansen B. Human orf. J Cutan Pathol. 1975;2:265–83. https://doi.org/10.1111/j.1600-0560.1975.tb00179.x
4. Nougairede A, Fossati C, Salez N, Cohen-Bacrie S, Ninove L, Michel F, et al. Sheep-to-human transmission of Orf virus during Eid al-Adha religious practices, France. Emerg Infect Dis. 2013;19:102–5. https://doi.org/10.3201/eid1901.120421
5. Ginzburg VE, Liauchonak I. Human orf: atypical rash in an urban medical practice. Can Fam Physician. 2017;63:769–71.
6. Lederman ER, Green GM, DeGroot HE, Dahl P, Goldman E, Greer PW, et al. Progressive ORF virus infection in a patient with lymphoma: successful treatment using imiquimod. Clin Infect Dis. 2007;44:e100–3. https://doi.org/10.1086/517509
7. Hasheminasab SS, Mahmoodi A, Mahmoodi P, Maghsood H. Orf virus infection in human ecthyma contagiosum: a report of two cases in the West of Iran. Virusdisease. 2016;27:209–10. https://doi.org/10.1007/s13337-016-0304-1
8. Abrahão JS, Silva-Fernandes AT, Assis FL, Guedes MI, Drumond BP, Leite JA, et al. Human vaccinia virus and pseudocowpox virus co-infection: clinical description and phylogenetic characterization. J Clin Virol. 2010;48:69–72. https://doi.org/10.1016/j.jcv.2010.02.001
9. Oğuzoğlu TÇ, Koç BT, Kirdeci A, Tan MT. Evidence of zoonotic pseudocowpox virus infection from a cattle in Turkey. Virusdisease. 2014;25:381–4. https://doi.org/10.1007/s13337-014-0214-z
10. Malik M, Bharier M, Tahan S, Robinson-Bostom L. Orf acquired during religious observance. Arch Dermatol. 2009;145:606–8. https://doi.org/10.1001/archdermatol.2009.69
11. Turk BG, Senturk B, Dereli T, Yaman B. A rare human-to-human transmission of orf. Int J Dermatol. 2014;53:e63–5. https://doi.org/10.1111/j.1365-4632.2012.05669.x
12. Rajkomar V, Hannah M, Coulson IH, Owen CM. A case of human to human transmission of orf between mother and child. Clin Exp Dermatol. 2016;41:60–3. https://doi.org/10.1111/ced.12697
13. Bala JA, Balakrishnan KN, Abdullah AA, Mohamed R, Haron AW, Jesse FFA, et al. The re-emerging of orf virus infection: a call for surveillance, vaccination and effective control measures. Microb Pathog. 2018;120:55–63. https://doi.org/10.1016/j.micpath.2018.04.057
14. Friederichs S, Krebs S, Blum H, Wolf E, Lang H, von Buttlar H, et al. Comparative and retrospective molecular analysis of parapoxvirus (PPV) isolates. Virus Res. 2014;181:11–21. https://doi.org/10.1016/j.virusres.2013.12.015
15. Delhon G, Tulman ER, Afonso CL, Lu Z, de la Concha-Bermejillo A, Lehmkuhl HD, et al. Genomes of the parapoxviruses orf virus and bovine papular stomatitis virus. J Virol. 2004;78:168–77. https://doi.org/10.1128/JVI.78.1.168-177.2004
16. Bou Khalil JY, Benamar S, Di Pinto F, Blanc-Tailleur C, Raoult D, La Scola B. *Protochlamydia phocaeensis* sp. nov., a new *Chlamydiales* species with host dependent replication cycle. Microbes Infect. 2017;19:343–50. https://doi.org/10.1016/j.micinf.2017.02.003
17. Antipov D, Korobeynikov A, McLean JS, Pevzner PA. hybridSPAdes: an algorithm for hybrid assembly of short and long reads. Bioinformatics. 2016;32:1009–15. https://doi.org/10.1093/bioinformatics/btv688
18. Hyatt D, Chen G-L, Locascio PF, Land ML, Larimer FW, Hauser LJ. Prodigal: prokaryotic gene recognition and translation initiation site identification. BMC Bioinformatics. 2010;11:119. https://doi.org/10.1186/1471-2105-11-119
19. Kelley LA, Mezulis S, Yates CM, Wass MN, Sternberg MJ. The Phyre2 web portal for protein modeling, prediction and analysis. Nat Protoc. 2015;10:845–58. https://doi.org/10.1038/nprot.2015.053
20. Boratyn GM, Schäffer AA, Agarwala R, Altschul SF, Lipman DJ, Madden TL. Domain enhanced lookup time accelerated BLAST. Biol Direct. 2012;7:12. https://doi.org/10.1186/1745-6150-7-12
21. Lee I, Ouk Kim Y, Park SC, Chun J. OrthoANI: An improved algorithm and software for calculating average nucleotide identity. Int J Syst Evol Microbiol. 2016;66:1100–3. https://doi.org/10.1099/ijsem.0.000760
22. Lechner M, Findeiss S, Steiner L, Marz M, Stadler PF, Prohaska SJ. Proteinortho: detection of (co-)orthologs in large-scale analysis. BMC Bioinformatics. 2011;12:124. https://doi.org/10.1186/1471-2105-12-124

23. Katoh K, Misawa K, Kuma K, Miyata T. MAFFT: a novel method for rapid multiple sequence alignment based on fast Fourier transform. Nucleic Acids Res. 2002;30:3059–66. https://doi.org/10.1093/nar/gkf436

24. Guindon S, Gascuel O. A simple, fast, and accurate algorithm to estimate large phylogenies by maximum likelihood. Syst Biol. 2003;52:696–704. https://doi.org/10.1080/10635150390235520

25. Letunic I, Bork P. Interactive tree of life (iTOL) v3: an online tool for the display and annotation of phylogenetic and other trees. Nucleic Acids Res. 2016;44:W242–5. https://doi.org/10.1093/nar/gkw290

26. Mercer AA, Ueda N, Friederichs S-M, Hofmann K, Fraser KM, Bateman T, et al. Comparative analysis of genome sequences of three isolates of *Orf virus* reveals unexpected sequence variation. Virus Res. 2006;116:146–58. https://doi.org/10.1016/j.virusres.2005.09.011

27. Chi X, Zeng X, Li W, Hao W, Li M, Huang X, et al. Genome analysis of orf virus isolates from goats in the Fujian Province of southern China. Front Microbiol. 2015;6:1135. https://doi.org/10.3389/fmicb.2015.01135

28. McGuire MJ, Johnston SA, Sykes KF. Novel immune-modulator identified by a rapid, functional screen of the parapoxvirus ovis (*Orf virus*) genome. Proteome Sci. 2012;10:4. https://doi.org/10.1186/1477-5956-10-4

29. Hautaniemi M, Ueda N, Tuimala J, Mercer AA, Lahdenperä J, McInnes CJ. The genome of pseudocowpoxvirus: comparison of a reindeer isolate and a reference strain. J Gen Virol. 2010;91:1560–76. https://doi.org/10.1099/vir.0.018374-0

30. Huang T, Tulman ER, Diel DG, Khatiwada S, Sims W, Edwards JF, et al. Coinfection with multiple strains of bovine papular stomatitis virus. Arch Virol. 2015;160:1527–32. https://doi.org/10.1007/s00705-015-2394-2

31. Friederichs S, Krebs S, Blum H, Lang H, Büttner M. Parapoxvirus (PPV) of red deer reveals subclinical infection and confirms a unique species. J Gen Virol. 2015;96:1446–62. https://doi.org/10.1099/vir.0.000080

32. McInnes CJ, Wood AR, Thomas K, Sainsbury AW, Gurnell J, Dein FJ, et al. Genomic characterization of a novel poxvirus contributing to the decline of the red squirrel (*Sciurus vulgaris*) in the UK. J Gen Virol. 2006;87:2115–25. https://doi.org/10.1099/vir.0.81966-0

33. Mackett M, Archard LC. Conservation and variation in orthopoxvirus genome structure. J Gen Virol. 1979;45:683–701. https://doi.org/10.1099/0022-1317-45-3-683

34. Babkin IV, Babkina IN. The origin of the variola virus. Viruses. 2015;7:1100–12. https://doi.org/10.3390/v7031100

35. Fleming SB, Blok J, Fraser KM, Mercer AA, Robinson AJ. Conservation of gene structure and arrangement between vaccinia virus and orf virus. Virology. 1993;195:175–84. https://doi.org/10.1006/viro.1993.1358

36. Fleming SB, Haig DM, Nettleton P, Reid HW, McCaughan CA, Wise LM, et al. Sequence and functional analysis of a homolog of interleukin-10 encoded by the parapoxvirus orf virus. Virus Genes. 2000;21:85–95. https://doi.org/10.1023/B:VIRU.0000018443.19040.99

37. Fleming SB, Anderson IE, Thomson J, Deane DL, McInnes CJ, McCaughan CA, et al. Infection with recombinant orf viruses demonstrates that the viral interleukin-10 is a virulence factor. J Gen Virol. 2007;88:1922–7. https://doi.org/10.1099/vir.0.82833-0

38. Bennett JR, Lateef Z, Fleming SB, Mercer AA, Wise LM. Orf virus IL-10 reduces monocyte, dendritic cell and mast cell recruitment to inflamed skin. Virus Res. 2016;213:230–7. https://doi.org/10.1016/j.virusres.2015.12.015

39. Fleming SB, Wise LM, Mercer AA. Molecular genetic analysis of orf virus: a poxvirus that has adapted to skin. Viruses. 2015;7:1505–39. https://doi.org/10.3390/v7031505

40. Mauldin MR, Antwerpen M, Emerson GL, Li Y, Zoeller G, Carroll DS, et al. Cowpox virus: what's in a name? Viruses. 2017;9:E101. https://doi.org/10.3390/v9050101

41. Franke A, Pfaff F, Jenckel M, Hoffmann B, Höper D, Antwerpen M, et al. Classification of cowpox viruses into several distinct clades and identification of a novel lineage. Viruses. 2017;9:142. https://doi.org/10.3390/v9060142

42. Diel DG, Luo S, Delhon G, Peng Y, Flores EF, Rock DL. Orf virus ORFV121 encodes a novel inhibitor of NF-kappaB that contributes to virus virulence. J Virol. 2011;85:2037–49. https://doi.org/10.1128/JVI.02236-10

43. Mercer AA, Wise LM, Scagliarini A, McInnes CJ, Büttner M, Rziha HJ, et al. Vascular endothelial growth factors encoded by Orf virus show surprising sequence variation but have a conserved, functionally relevant structure. J Gen Virol. 2002;83:2845–55. https://doi.org/10.1099/0022-1317-83-11-2845

44. Nagendraprabhu P, Khatiwada S, Chaulagain S, Delhon G, Rock DL. A parapoxviral virion protein targets the retinoblastoma protein to inhibit NF-κB signaling. PLoS Pathog. 2017;13:e1006779. https://doi.org/10.1371/journal.ppat.1006779

45. Li W, Chen H, Deng H, Kuang Z, Long M, Chen D, et al. Orf virus encoded protein ORFV119 induces cell apoptosis through the extrinsic and intrinsic pathways. Front Microbiol. 2018;9:1056. https://doi.org/10.3389/fmicb.2018.01056

46. Qiao J, Yang HB, Peng YL, Meng QL, Chen C, Ma Y, et al. Effect of ORF119 gene deletion on the replication and virulence of orf virus. Acta Virol. 2015;59:257–64. https://doi.org/10.4149/av_2015_03_257

47. Billinis C, Mavrogianni VS, Spyrou V, Fthenakis GC. Phylogenetic analysis of strains of *Orf virus* isolated from two outbreaks of the disease in sheep in Greece. Virol J. 2012;9:24. https://doi.org/10.1186/1743-422X-9-24

48. Velazquez-Salinas L, Ramirez-Medina E, Bracht AJ, Hole K, Brito BP, Gladue DP, et al. Phylodynamics of *Parapoxvirus* genus in Mexico (2007–2011). Infect Genet Evol. 2018;65:12–4. https://doi.org/10.1016/j.meegid.2018.07.005

49. Peralta A, Robles CA, Micheluod JF, Rossanigo CE, Martinez A, Carosio A, et al. Phylogenetic analysis of ORF viruses from five contagious ecthyma outbreaks in Argentinian goats. Front Vet Sci. 2018;5:134. https://doi.org/10.3389/fvets.2018.00134

50. de Oliveira CH, Assis FL, Neto JD, Oliveira CM, Lopes CT, Bomjardim HA, et al. Multifocal cutaneous orf virus infection in goats in the Amazon region, Brazil. Vector Borne Zoonotic Dis. 2012;12:336–40. https://doi.org/10.1089/vbz.2011.0725

Address for correspondence: Bernard La Scola, Aix Marseille Université, Institut Hospitalo-Universitaire Méditerranée Infection, 19-21 Bd Jean Moulin, 13005 Marseille, France; email: bernard.la-scola@univ-amu.fr

High Prevalence of Macrolide-Resistant *Bordetella pertussis* and *ptxP1* Genotype, Mainland China, 2014–2016

Lijun Li,[1] Jikui Deng,[1] Xiang Ma,[1] Kai Zhou,[1] Qinghong Meng,
Lin Yuan, Wei Shi, Qing Wang, Yue Li, Kaihu Yao

According to the government of China, reported cases of pertussis have increased remarkably and are still increasing. To determine the genetic relatedness of *Bordetella pertussis* strains, we compared multilocus variable-number tandem-repeat analysis (MLVA) results for isolates from China with those from Western countries. Among 335 isolates from China, the most common virulence-associated genotype was *ptxA1/ptxC1/ptxP1/prn1/fim2–1/fim3A/tcfA2*, which was more frequent among isolates from northern than southern China. Isolates of this genotype were highly resistant to erythromycin. We identified 36 *ptxP3* strains mainly harboring *ptxA1* and *prn2* (35/36); *ptxP3* strains were sensitive to erythromycin and were less frequently from northern China. For all isolates, the sulfamethoxazole/trimethoprim MIC was low, indicating that this drug should be recommended for patients infected with erythromycin-resistant *B. pertussis.* MLVA of 150 clinical isolates identified 13 MLVA types, including 3 predominant types. Our results show that isolates circulating in China differ from those in Western countries.

Whooping cough (pertussis) is a highly contagious respiratory disease mainly transmitted by aerosolized respiratory droplets. The causative agent is a gram-negative bacterium first reported in 1906 and later named *Bordetella pertussis*.

The gradual introduction of whole-cell pertussis vaccines (WCV) worldwide in the mid-1940s (*1*) was followed by a dramatic decrease in illness and death from pertussis. In China, pertussis immunization with WCV was introduced in the early 1960s (*2*). The vaccine is administered as part of a trivalent combined vaccine during the first year of life, at months 3, 4, and 5. Since 1982, many countries have recommended also giving a booster dose to children at 18–24 months of age (*3,4*). However, the side effects and safety of WCV aroused considerable public concern globally, which stimulated the introduction of acellular pertussis vaccines (ACV). In most developed countries, the shift from WCV to ACV was implemented in the 1990s and the early 2000s. In China, both WCV and ACV have been used since 2006 (*5*) and ACV alone since 2013 (*2*). The ACV used in China was made by co-purifying techniques and mainly contained pertussis toxin and filamentous hemagglutinin, as well as a few other antigens that cannot be completely removed.

In the 1990s, however, pertussis began to reemerge in several highly immunized populations, and the number of pertussis cases is still increasing worldwide (*6*). According to the Chinese Center for Disease Control and Prevention (*7*), reported pertussis cases increased substantially after widespread vaccination with ACV and are still increasing (Figure 1). Many factors have contributed to the increase: improved diagnostics, increased awareness, waning immunity, and pathogen adaptation. We aimed to determine molecular evolution and pathogen adaptation of *B. pertussis.*

Macrolides have been used to treat and prevent whooping cough for ≈50 years, but there have been multiple reports of erythromycin resistance (*3,8,9*). Our previous study in northern China showed a strikingly high rate of macrolide resistance (91.9%) in *B. pertussis* (*2*). Whether the high erythromycin resistance rate was also widespread across mainland China or whether it was a temporary epidemic remains unknown. In this study, we recovered 335 *B. pertussis* isolates from patients in mainland China and investigated their susceptibility to erythromycin and other antimicrobial drugs. Our goal was to provide effective treatment guidance in the face of

Author affiliations: Beijing Pediatric Research Institute, Beijing Children's Hospital, Capital Medical University, Beijing, China (L. Li, Q. Meng, L. Yuan, W. Shi, Q. Wang, Y. Li, K. Yao); Shenzhen Children's Hospital, Shenzhen, China (J. Deng); Jinan Children's Hospital, Shandong University, Shandong, China (X. Ma); Nanjing Children's Hospital, Nanjing Medical University, Nanjing, China (K. Zhou)

[1]These authors contributed equally to this article.

erythromycin resistance, because although sulfonamides are the second-line treatment, their use in infants <2 months of age is prohibited. To discern the population structures of *B. pertussis* isolates in China, we also investigated the distribution of virulence-related genotypes by using antigen genotyping for all 335 isolates. To determine the genetic relationship between strains, we then performed multilocus variable-number tandem-repeat analysis (MLVA) on a subset of 150 isolates.

Methods

Bacterial Strains, Patient Demographics, and Clinical Information

From October 2014 through December 2016, all patients suspected to have pertussis were routinely examined by culture of nasopharyngeal swab samples. We included in our study those patients for whom cultures were positive for *B. pertussis*. We analyzed 335 *B. pertussis* isolates
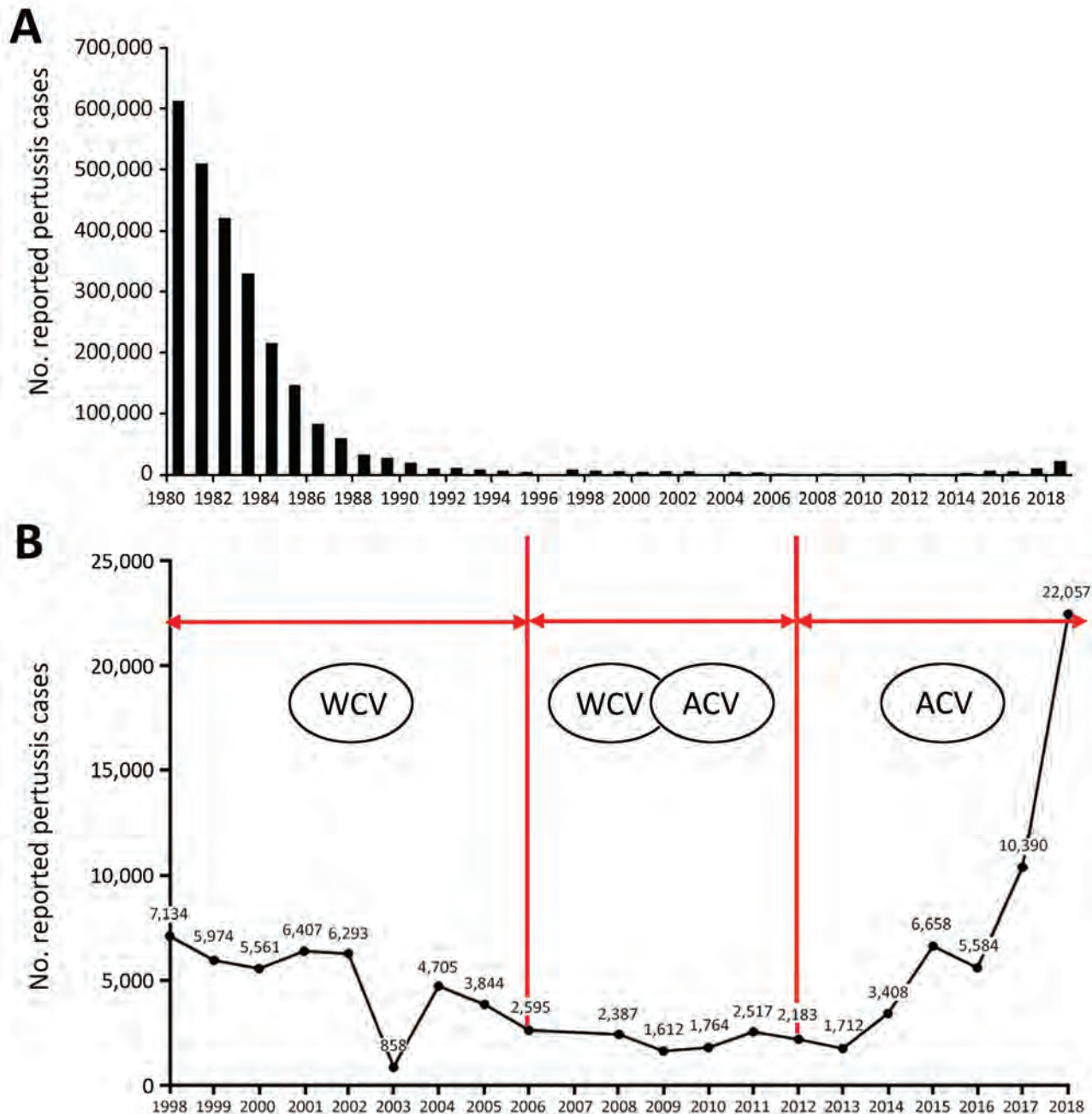
Figure 1. Reported pertussis cases in China, 1980–2018. A) Number of cases 1980–2018. B) Actual numbers of cases (line) according to vaccine type administered during a given period, 1998–2018. ACV, acellular pertussis vaccine; WCV, whole-cell pertussis vaccine.

collected from patients in 4 cities in China: 245 isolates from Beijing Children's Hospital, 21 from Jinan Children's Hospital, 13 from Nanjing Children's Hospital, and 56 from Shenzhen Children's Hospital. We recorded demographic data (e.g., sex, age, and residential address) for all patients with confirmed pertussis. We also recorded clinical information, available for 109 patients at Beijing Children's Hospital (e.g., vaccine history, coughing of family members during the patient's incubation period, leukocyte count, lymphocyte ratio, budesonide aerosol inhalation, and antimicrobial drug use before swab collection). Parents or legal guardians provided informed written consent before nasopharyngeal swab samples were collected. This study was reviewed and approved by the ethics committee of each hospital.

Bacterial Culture

We plated all nasopharyngeal specimens onto charcoal agar (Oxoid; ThermoFisher Scientific, https://www.thermofisher.com) supplemented with 10% defibrinated sheep blood and *Bordetella* selective supplement SR0082E (cephalexin) and incubated the plates at 35–37°C for 3 days. We confirmed suspected *B. pertussis* colonies by the slide agglutination test with *B. pertussis* and *B. parapertussis* antiserum (Remel; ThermoFisher Scientific, http://www.thermofisher.com). We stored all isolates at –80°C until further analysis.

Antimicrobial Susceptibility Testing

We determined antimicrobial susceptibility by E-test and Kirby-Bauer disk diffusion. Before susceptibility testing, we thawed bacterial preservation tubes from a -80°C freezer and performed culture at 35–37°C on the charcoal agar plates containing 10% sheep blood for 72 h. We then subcultured bacterial suspension with 0.5 McFarland turbidity standard on 25 mL charcoal agar containing 10% sheep blood in a 90-mm diameter culture dish. We used the E-test to determine susceptibility to erythromycin, clindamycin, amoxicillin, ampicillin, ceftriaxone, levofloxacin, sulfamethoxazole/trimethoprim, amikacin, clarithromycin, azithromycin, doxycycline, and aztreonam. Because of a lack of adequate E-test strips for some antimicrobials, we tested some isolates against several antimicrobials according to sequential order without any initial selection criteria (i.e., 310 isolates for doxycycline, 222 isolates for amikacin, 86 isolates for aztreonam, 83 isolates for clarithromycin, and 83 isolates for azithromycin). We measured MICs and inhibition zone sizes when the plates were incubated for 4 days. The Clinical and Laboratory Standards Institute and the European Committee on Antimicrobial Susceptibility Testing do not yet provide breakpoint criteria for antimicrobial susceptibility for *B. pertussis*. We report 50% MICs, 90% MICs, and MIC ranges. We also tested susceptibility to erythromycin with Kirby-Bauer disk

diffusion, and according to some studies, an inhibition diameter >42 mm suggested complete susceptibility to erythromycin. MICs <0.12 mg/L are considered susceptible to erythromycin (8). For quality control strains, we included *Haemophilus influenzae* ATCC49247 and *Staphylococcus aureus* ATCC30913 in each batch of susceptibility tests.

Genotyping

We extracted the genomic DNA of isolates by using a DNA extraction kit (SBS Genetic Co. Ltd, http://www.sbsbio.com) according to the manufacturer's instructions. We amplified and sequenced the 7 genes of *B. pertussis* isolates (*ptxA, ptxC, ptxP, prn, fim2, fim3, and tcfA2*) as previously described (2) and identified genotypes by comparison with designated alleles in GenBank.

Sequencing of the *B. pertussis* 23S rRNA Gene

The A2047G mutation has been proven to be the cause of erythromycin resistance of *B. pertussis* (8). We amplified and sequenced domain V of the 23S rRNA gene of 335 isolates as previously described (2). We then compared the sequences with the X68323 sequence and the allele of *B. pertussis* Tohama I strain (accession no. NC_002929.2) in GenBank.

MLVA

We performed MLVA according to the procedures described by Schouls et al (10). We used 5 variable-number tandem-repeats (VNTRs) to characterize 150 randomly selected clinical isolates, which were from 6 geographic areas in China (i.e., 83 from northern, 33 southern, 26 eastern, 3 central, 4 northeastern, and 1 northwestern). We included reference strains (Tohama I) with known MLVA types as positive controls in each run and expressed the results as MLVA types. We assigned MLVA types by using the *B. pertussis* MLVA database (https://www.mlva.net); the assignment of MLVA types was based on the combination of repeat counts for VNTR1, VNTR3a, VNTR3b, VNTR4, VNTR5, and VNTR6. We generated minimum spanning trees from the 6 MLVA loci by using BioNumerics version 7.6 (Applied Maths, http://www.applied-maths.com).

Statistical Analyses

We used SPSS 17.0 (https://www.ibm.com/analytics/spss-statistics-software) for statistical analyses and analyzed the data by using χ^2 or Fisher exact tests, as appropriate. We considered $p<0.05$ to be significant.

Results

Patient Demographic and Clinical Data

The 335 patients (189 male and 146 female) were from Beijing (n = 101), Hebei (n = 91), Guangdong (n = 56),

Shandong (n = 30), Jiangsu (n = 10), Tianjin (n = 9), Inner Mongolia Autonomous Region (n = 7), Henan (n = 6), Shanxi (n = 5), Anhui (n = 5), Jiangxi (n = 4), Zhejiang (n = 3), Heilongjiang (n = 2), Jilin (n = 2), Liaoning (n = 2), Hubei (n = 1), and Ningxia (n = 1). These provinces and municipalities covered 6 geographic areas of China defined by the government. In this study, 213 patients were from northern, 56 southern, 52 eastern, 7 central, 6 northeastern, and 1 northwestern China (Figure 2).

The age distribution of the 335 patients was as follows: 119 (35.5%) were <3 months of age; 113 (33.7%), 3–5 months; 80 (23.9%), 6–18 months; 11 (3.3%), 19 months–2 years; and 12 (3.6%), 3–12 years. Of the 335 patients, 195 were not vaccinated, 32 had received 1 dose of pertussis vaccine, 16 had received 2 doses, and 26 had received 3 or 4 doses. The vaccination history of 66 patients could not be confirmed. For 109 patients, we reviewed hospital medical records carefully for more comprehensive clinical information (Table 1).

Antimicrobial Susceptibility and 23S rRNA Gene Mutations

All 292 isolates with an erythromycin MIC >256 mg/L showed a 6-mm inhibition zone diameter on Kirby-Bauer disk diffusion (Table 2); all of these isolates had the A2047G mutation in the 23S rRNA gene. The remaining 43 isolates had an erythromycin MIC ≤0.125 mg/L, of which only 2 had a MIC of 0.125 mg/L. The diameter of the erythromycin disk was >42 mm for 42 isolates and 36 mm for 1 isolate. Isolates with an erythromycin MIC >256 mg/L had MICs >256 mg/L each for clindamycin, clarithromycin,

and azithromycin. The MIC range for sulfamethoxazole/trimethoprim was low (0.002–0.5 mg/L) (Table 1). The proportions of isolates resistant to erythromycin in northern China (194/213) and southern China (35/56) differed significantly (χ^2 = 28.6; p<0.001).

Genotypes

The most common virulence-associated genotype of all *B. pertussis* strains was *ptxA1/ptxC1/ptxP1/prn1/fim2–1/fim3A/tcfA2;* frequency was 87.2% (292/335) (Table 3). We identified 36 *ptxP3* strains, which mainly harbored *ptxA1* and *prn2* (35/36). The *ptxP3* strains were more frequent in southern than in northern China (16/56 vs. 17/213; χ^2 = 17.5; p<0.001).

All *ptxP3* strains had lower MICs for erythromycin (0.023–0.125 mg/L) and clindamycin (0.094–4 mg/L). The isolates with erythromycin MIC >256 mg/L were all typed as *ptxP1*.

MLVA Combined with Virulence-Associated Genotyping and the A2047G Mutation of 23S rRNA

The 150 isolates typed by MLVA were divided into 13 MLVA types: MT26, MT27, MT29, MT39, MT55, MT104, MT107, MT116, MT195, and 4 new types (N1–N4). The major MLVA types were MT104, MT55, and MT195. Both MT55 and MT195 have a uniform allelic profile: *ptxA1/ptxC1/ptxP1/prn1/fim2–1/ fim3A/tcfA2*. MT104 has 2 profiles; 1 profile was the same as that of isolates of MT55 and MT195, and another is *ptxA1/ptxC2/ptxP1/prn1/fim2–1/fim3A/tcfA2*, which differs only in *ptxC* (Figure 3). The genotypes of MT29
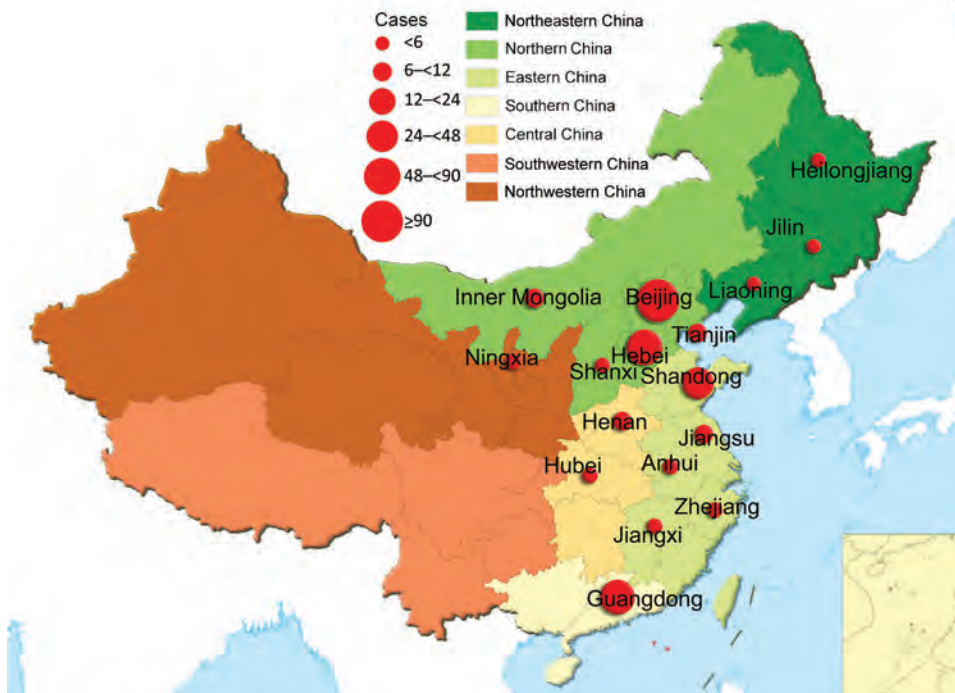
Figure 2. Geographic distribution of 335 patients with pertussis diagnosis, China, 2014–2016. Colors indicate different administrative regions. Red circles indicate numbers of patients; the larger the circle, the more patients in the province.

Table 1. Clinical characteristics of 109 pertussis patients, Bejing Children's Hospital, Beijing, China, October 2014–December 2016*

	No. (%) patients			
Patient characteristic	Total patients, n = 109	Fully vaccinated, n = 17	Not vaccinated or undervaccinated, n = 92	p value
Fever	28 (25.69)	6 (35.29)	22 (23.9)	0.32
Rhinorrhea	47 (43.12)	12 (70.59)	35 (38.0)	0.01
Nasal congestion	50 (45.87)	8 (47.06)	42 (45.65)	0.92
Purulent nasal secretion	5 (4.59)	1 (5.88)	4 (4.35)	1.00
Cough				
Paroxysmal	90 (82.57)	13 (76.47)	77 (83.70)	0.71
Spasmodic	95 (87.16)	13 (76.47)	82 (89.13)	0.30
Whooping	46 (42.20)	9 (52.94)	37 (40.22)	0.33
Excessive phlegm	48 (44.04)	5 (29.41)	43 (46.74)	0.19
Vomiting	66 (60.55)	9 (52.94)	57 (61.96)	0.49
Cyanosis	72 (66.06)	11 (64.71)	64 (69.57)	0.83
Apnea	27 (24.77)	4 (23.53)	20 (21.74)	1.00
Convulsion	1 (0.92)	0	1 (1.09)	1.00
Sweats	25 (22.94)	7 (41.18)	18 (19.57)	0.05
Subconjunctival hemorrhage	4 (3.67)	0 (0.00)	4 (4.35)	0.50
Ulcer of lingual frenum	1 (0.92)	0	1 (1.09)	0.85
Leukocytosis				
>10 × 10^9 cells/L	74 (67.89)	6 (35.29)	68 (73.91)	<0.01
>60 × 10^9 cells/L	2 (1.89)	0	0	NA
Lymphocytosis†	73 (66.97)	8 (47.06)	65 (70.65)	0.06
Antimicrobial drugs prescribed before culture				
Erythromycin	66 (60.55)	7 (41.18)	59 (31.52)	NA
Cephalosporin	77 (70.64)	11 (64.71)	66 (71.74)	NA
Azithromycin	16 (14.68)	4 (23.53)	13 (14.13)	NA
Amoxicillin	8 (7.34)	2 (11.76)	6 (6.52)	NA
Clarithromycin	2 (1.83)	0	0	NA
Mezlocillin	1 (0.92)	0	0	NA
Imipenem	1 (0.92)	0	0	NA
Aztreonam	1 (0.92)	0	0	NA
Household contacts	52 (47.71)	0	0	NA
Culture-based diagnosis for household contacts‡	4 (3.67)	0	0	NA
Reexamination of culture§	4 (3.67)	0	0	NA

*NA, not analyzed.
†Lymphocyte:total leukocyte ratio 66.47% ± 11.47%.
‡Bacterial culture results of the 4 household contacts were negative.
§Reexamination of bacterial culture of 4 patients performed 2 weeks later produced negative results.

isolates (*ptxA1/ptxC1/ptxP1/prn1/fim2–1/fim3A/tcfA2*) differed from MT 55 isolates only in *fim3*. Eight isolates of MT27 had 2 profiles that differed in *ptxC* and *fim3*, *ptxA1/ptxC1/ptxP3/prn2/fim2–1/ fim3A/tcfA2*, and *ptxA1/ptxC2/ptxP3/prn2/fim2–1/ fim3B/tcfA2*. The genotypes of MT26 (*ptxA1/ptxC1/ptxP3/prn2/fim2–1/ fim3A/ tcfA2*) were the same as one of the profiles of isolates of MT27. Although isolates with the same genotype profiles varied in MLVA type, these types were similar for isolates with similar virulence-related genotypes (Figure 3, panel A). Overall, all isolates of MT26, MT27, and MT116 carried *ptxP3/ prn2*, and all isolates of MT55, MT104, and MT195 carried *ptxP1/ prn1*. All isolates of MT55, MT104, MT195, and MT116 had the A2047G mutation of 23S rRNA; no isolates of MT26, MT27, MT29, or MT116 had this mutation (Figure 3, panel B). The MLVA types of isolates with the mutation at the 2047 site of 23S rRNA were closer to each other, and those without the mutation were also linked to each other except for MT39 (Figure 3, panel B).

Discussion

The preferred treatment for persons with pertussis is erythromycin or another macrolide. The first reports of erythromycin-resistant *B. pertussis* in the United States were published in 1994 (*11*). Since then, and not only in the United States, several erythromycin-resistant *B. pertussis* isolates have been reported (*12,13*), but no evidence of an epidemic of erythromycin-resistant pertussis occurred in any other country except China. In 2014, a study in Xi'an, China, detected high prevalence of erythromycin-resistant *B. pertussis;* 85% (85/100) of strains had the A2047G mutation (*5*). In our previous study, the *B. pertussis* isolates from the 1970s and 2000–2008 were susceptible to macrolides, and 91.9% of isolates collected during 2013–2014 were resistant to macrolides (MIC >256 mg/L) (*2*). However, our previous study was performed only at Beijing Children's Hospital, and the number of samples was limited. In the current study, we found that erythromycin-resistant *B. pertussis* strains caused infection in each of the 6 areas in China; 87.5% (292/335) of isolates were resistant

Table 2. Antimicrobial susceptibility test results for *Bordetella pertussis* isolates in study of prevalence of macrolide-resistant *B. pertussis* and *ptxP1* genotype, mainland China, 2014–2016*

Drug	No. isolates	E-test, mg/L			Kirby-Bauer disk diffusion	
		MIC$_{50}$	MIC$_{90}$	MIC range	Range of inhibition zone, mm	Rate of susceptibility, %†
Erythromycin	335	>256	>256	0.032 to >256	668	12.5%
Clindamycin	335	>256	>256	0.25 to >256	NT	NT
Amoxicillin	335	0.5	1	0.125 to 2	NT	NT
Ampicillin	335	0.25	0.5	0.032 to 1	NT	NT
Levofloxacin	335	0.5	1	0.064 to 1	NT	NT
Sulfamethoxazole	335	0.064	0.25	0.002 to 0.5	NT	NT
Ceftriaxone	335	0.25	0.5	0.064 to 2	NT	NT
Amikacin	222	8	8	2 to 32	NT	NT
Clarithromycin	83	>256	>256	0.032 to >256	NT	NT
Azithromycin	83	>256	>256	0.016 to >256	NT	NT
Doxycycline	310	8	8	1 to 16	NT	NT
Aztreonam	86	8	32	4 to 32	NT	NT

*NT, not tested in this study.
†An inhibition diameter >42 mm suggested that the isolate was susceptible to erythromycin.

to erythromycin (MIC >256 mg/L). In 2003, Bartkus et al. confirmed that the 23S rRNA A2047G mutation was a mechanism of erythromycin resistance to *B. pertussis* (*8*). All 292 erythromycin-resistant *B. pertussis* isolates in our study had the 23S rRNA A2047G mutation, a finding that is consistent with other reports. The erythromycin-resistant *B. pertussis* strains were isolated from children in different districts (Figure 4), which means that erythromycin-resistant *B. pertussis* is spread widely across China.

We also found geographic differences in erythromycin resistance among *B. pertussis* isolates. Among those from northern China, the rate reached up to 91.1% (194/213), in accordance with our previous study in 2013–2014 (91.9%, 91/99) (*2*). However, the rate was only 64.3% (36/56) among isolates from southern China. This finding might be associated with differences in antimicrobial drug use between northern and southern China; however, we could not make this comparison because we did not have detailed clinical data for cases in southern China. Because the resistance was closely associated with the *ptxP1* genotype, a geographic difference in *ptxP* genotypes was also found between northern and southern China (Figure 4). Thus, another possible reason for this regional difference is population mobility. Shenzhen is near Hong Kong and Macau, in

the most dynamic and developed region in China in terms of economy. Because daily movement of the population in Shenzhen, Hong Kong, and Macau is large and has become the regular lifestyle, the *ptxP3* strains could be imported more frequently. Shanghai, another economic development area, also had a high proportion of *ptxP3* strains (*14*). The *ptxP3* strains could also be transmitted widely because of less macrolide abuse in southern China.

To better determine the genetic diversity of isolates of different genotypes and erythromycin sensitivities, we analyzed 150 clinical isolates by MLVA type. Compared with other findings for China (*9,15*), our findings showed that the predominant MLVA types of recent isolates were distinct from strains isolated before widespread vaccination with ACV. Some MLVA types that had been prevalent (MT29 and MT33, frequent in the 1950s; MT294 and MT95, frequent during 1962–1986; and MT91, MT136, and MT152, frequent during 1997–2007) (*15*) had disappeared, and others (MT104, MT55, and MT195) had increased. Unlike trends in other countries (*16–18*) that showed that isolates harboring MT27 and MT29 were becoming prevalent over time, isolates from our study were mainly MT55, MT104, and MT195. We found only 8 MT27 isolates and 1 MT29 isolate, which correlates with findings of another study in

Table 3. Genotype profiles for 335 *Bordetella pertussis* isolates from mainland China, 2014–2016

Genotype profile*	No. (%) isolates						
	Total	Year			Region		
		2014	2015	2016	Northern China	Southern China	Other†
ptxA1/ptxC1/ptxP1/prn1/fim2−1/fim3A/tcfA2	5 (1.5)	0	3 (1.7)	2 (1.5)	2 (0.9)	3 (5.4)	0
ptxA1/ptxC2/ptxP1/prn1/fim2−1/fim3A/tcfA2	1 (0.3)	0	1 (0.6)	0	1 (0.5)	0	0
ptxA1/ptxC1/ptxP1/prn3/fim2−1fim3A/tcfA2	1 (0.3)	0	1 (0.6)	0	0	1 (1.8)	0
ptxA1/ptxC2/ptxP3/prn9/fim2−1/fim3A/tcfA2	1 (0.3)	0	0	1 (0.7)	0	1 (1.8)	0
ptxA1/ptxC2/ptxP3/prn2/fim2−1/fim3B/tcfA2	2 (0.6)	1 (3.7)	1 (0.6)	0	2 (0.9)	0	0
ptxA1/ptxC1/ptxP3/prn2/fim2−1/fim3A/tcfA2	5 (1.5)	1 (3.7)	3 (1.7)	1 (0.7)	5 (2.3)	0	0
ptxA1/ptxC2/ptxP3/prn2/fim2−1/fim3A/tcfA2	28 (8.4)	0	8 (4.7)	20 (14.7)	10 (4.7)	15 (26.8)	3 (4.5)
ptxA1/ptxC1/ptxP1/prn1/fim2−1/fim3A/tcfA2	292 (87.2)	25 (92.6)	155 (90.1)	112 (82.4)	193 (90.6)	36 (64.3)	63 (95.5)
Total	335 (100)	27 (100)	172 (100)	136 (100)	213 (100)	56 (100)	66 (100)

*Genotype of vaccine strain in China: *ptxA2/ptxC1/ptxP1/prn1/fim2−1/fim3A/tcfA2*.
†Northeastern, northwestern, eastern, and central southern China.
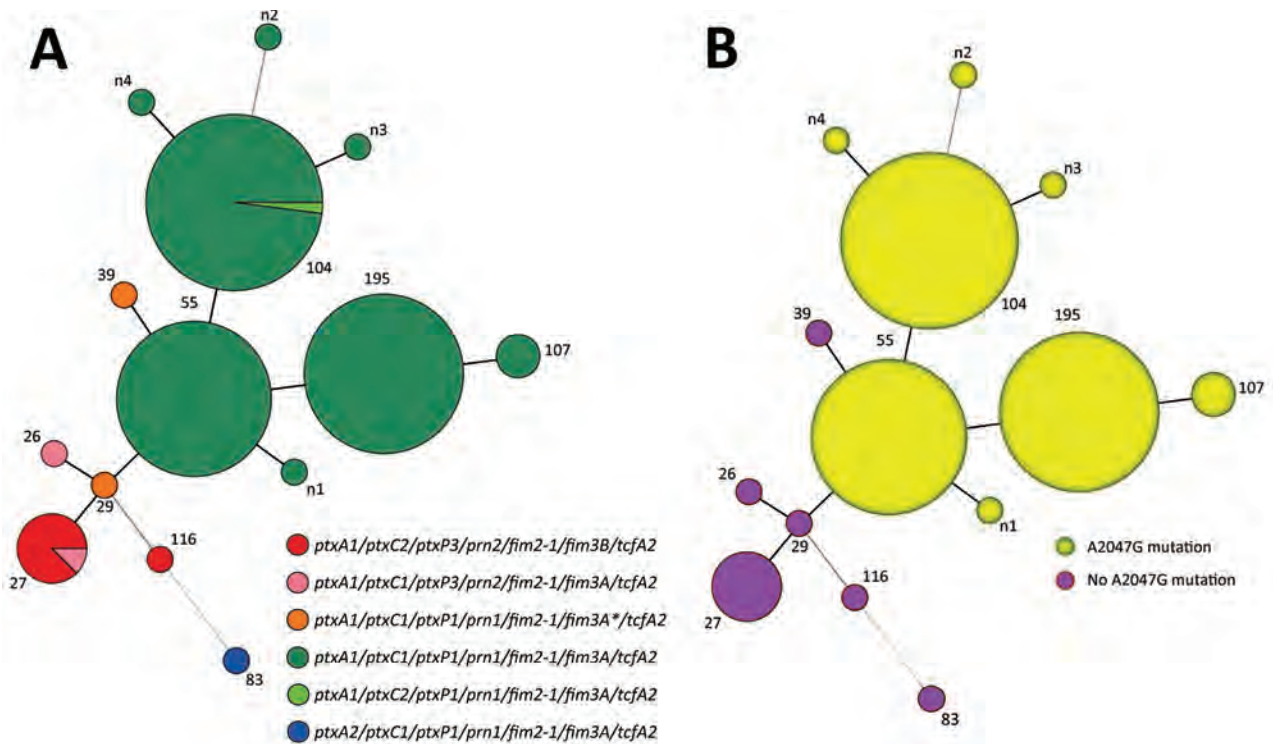
Figure 3. Minimum spanning tree of multilocus variable-number tandem-repeat analysis (MLVA) types of 150 *Bordetella pertussis* isolates collected in China, 2014–2016. Each circle represents an MLVA type, with the number next to the circle. Circle sizes are proportional to the number of isolates belonging to the particular MLVA type. A) Allelic profiles. Circle colors indicate the different allelic profiles of vaccine antigen genes and different erythromycin sensitivities. B) Presence or absence of A2047G mutation.

Xi'an (*9*), in which isolates were collected during 2015–2016 from some parts of northern China. In that study, of 8 MT27 isolates, 5 were from northern China and 3 were from southern China, which was not a significant difference (5/83 vs. 3/22; χ^2 = 3.26; p = 0.07). MT55, MT104, and MT195 were more frequently isolated in northern China (76/83 vs. 22/33; χ^2 = 11.17; p<0.001).

In our study, the 3 predominant MLVA types (MT104, MT55, and MT195) were closely related, with only 1 difference in the number of VNTR6 allele repeats, suggesting that these types could have evolved from closely related strains. *B. pertussis* isolates harboring MT29 were isolated in the 1950s and 1960s but afterward disappeared, according to another study in China (*15*). Whether MT29 existed from the 1950s or was imported from other countries needs further study. Both MT27 and MT55 were related to MT29, but the difference between MT27 and MT29 was in VNTR3a. VNTR3 and VNTR6 were in the pseudogenes. Although pseudogenes do not encode functional genes, they are key in research of bacterial evolution and dynamic genomes and are associated with expression and regulation of functional genes.

Our study lays the foundation for further study of whole-genome sequencing to confirm how much and what kind of genetic changes would happen among *B. pertussis*

isolates. The great heterogeneity of MLVA types was identified among erythromycin-resistant and erythromycin-nonresistant isolates. All MT104, MT55, and MT195 isolates had the same combination of the virulence-related genotypes, *ptxP1/ptxA1/prn1*, and were resistant to erythromycin; this result corroborates results of another study in which isolates were collected from another northern China city with less population movement (*9*). We found MT27, the most common type in other countries, in only 8 isolates; the virulence-related genotypes were similar to those of isolates from other countries, suggesting that MT27 isolates from China are more likely to have been imported into China from other countries than to have arisen from closely related existing strains (*19*). All MT27 isolates were sensitive to erythromycin.

Many studies have shown that *ptxP* may play a role in pathogen adaptation. Strains with *ptxP1* were most common in the early WCV periods but were replaced by *ptxP3* strains in the WCV/ACV periods and ACV periods (*20*). Studies from Finland and Australia suggest that the increase of *ptxP3* strains may be associated with the resurgence of pertussis (*21–23*). The association between virulence-related genotype, erythromycin susceptibility, and MLVA types is in accordance with no resistance epidemic
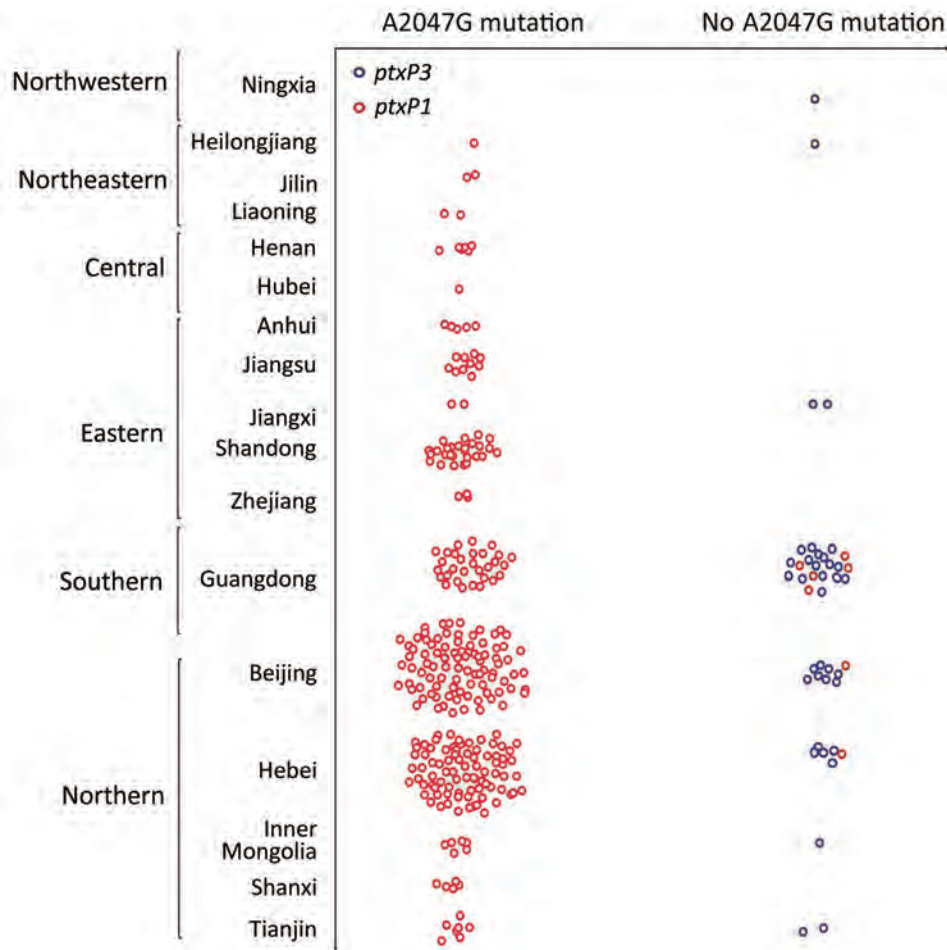
Figure 4. Geographic differences in frequency of erythromycin resistance in Bordetella pertussis isolates, China, 2014–2016.

in other countries, including the United States (*24*), Australia (*22*), and many countries in Europe (*25*), because isolates from those countries mainly harbor *ptxP3* genes, and the prevalent MLVA types were MT27 and MT29.

Because the drug commonly used to treat erythromycin-resistant *B. pertussis* infection is sulfamethoxazole/trimethoprim (*26*), it is reassuring that this drug still shows powerful inhibition of these bacteria. Levofloxacin could be another choice for adult patients, and doxycycline might also be an alternative for adults with pertussis (*27*). Earlier, β-lactams were recommended for pediatric patients with pertussis (*28,29*). The MICs for β-lactams suggest that they could be used; however, their effectiveness for eliminating the bacteria was not comparable to that of macrolides. An explanation is that the local concentrations of β-lactams in the respiratory tract are insufficient (*30*).

It is noteworthy that there is no standard procedure for antimicrobial susceptibility testing for *B. pertussis*. We consider the striking macrolide resistance rates to be reliable because all macrolide-resistant isolates had erythromycin MICs >256 mg/L, no inhibition zone in Kirby-Bauer disk diffusion, and the A2047G mutation in 23S rRNA, which

has been previously reported (*8,31*). To date, the Clinical and Laboratory Standards Institute and the European Committee on Antimicrobial Susceptibility Testing offer no suggestions for macrolides and other drugs that could be used to treat pertussis, even regarding appropriate use and dose. Development of standard methods for antimicrobial susceptibility testing of *B. pertussis* and monitoring the treatment effects of appropriate antimicrobial agents in vivo would be helpful.

Our study had some limitations. First, all patients with clinically suspected pertussis were routinely subjected to nasopharyngeal swab culture in our study. However, the clinical diagnostic standard for pertussis is not specific in China and differs among age groups. Therefore, we did not set specific criteria for enrollment of patients, and the inclusion criteria were based on the subjective judgment of pediatricians. Second, our study was not based on the patient population (no sample collection and follow-up records with clinical information for patients in this study). Thus, we could not precisely evaluate the severity of individual cases and the association between disease severity and drug resistance or genotype. Third, although all clinical samples were collected during 2014–2016, the number of

patients receiving treatment and the duration of recruitment in the included hospitals differed. Therefore, the number of isolates from the participating hospitals does not reflect the actual number of cases in the 17 provinces or municipalities. Fourth, before the patients visited the participating 4 hospitals, Beijing Children's Hospital in particular, they had already received antimicrobial drugs. The high resistance rate may be associated with pretreatment with antimicrobial drugs and therefore may be overestimated. Alternatively, *B. pertussis* isolates with resistance were very common, which implies the failure of treatment with macrolides. Among study patients in Beijing Children's Hospital, 23 were reexamined by culture after 2 weeks of macrolide treatment and 4 were still culture positive. It is conceivable that macrolide treatment could not eliminate the resistant bacteria. More rigorous comparisons should be conducted to interpret the clinical significance of resistance for this self-limiting disease. Last, for some objective reasons, the susceptibility against some drugs was tested in a subset of the present isolates (clarithromycin, azithromycin, and doxycycline in particular).

In conclusion, *B. pertussis* isolates genotyped as *ptxA1/ptxC1/ptxP1/prn1/fim2–1/fim3A/tcfA2* and highly resistant to erythromycin are widespread in China. The *ptxP3* strains sensitive to erythromycin were found mainly in southern China. Sulfamethoxazole/trimethoprim effectively treated pertussis caused by erythromycin-resistant *B. pertussis*. The MLVA profiles of *B. pertussis* isolates currently circulating in China differ from those circulating in other Western countries.

Acknowledgments

About the Author

Ms. Li is a student at the Beijing Key Laboratory of Pediatric Respiratory Infection Diseases, Beijing Pediatric Research Institute, Beijing Children's Hospital, Capital Medical University, National Center for Children's Health, Beijing, China. Her primary research interests include antimicrobial drug resistance in vaccine-preventable infectious diseases.

References

1. Mitka M. Age range widens for pertussis vaccine: boosters advised for adolescents and adults. JAMA. 2006;295:871–2. https://doi.org/10.1001/jama.295.8.871

2. Yang Y, Yao K, Ma X, Shi W, Yuan L, Yang Y. Variation in *Bordetella pertussis* susceptibility to erythromycin and virulence-related genotype changes in China (1970–2014). PLoS One. 2015;10:e0138941. https://doi.org/10.1371/journal.pone.0138941

3. Cherry JD. Pertussis in young infants throughout the world. Clin Infect Dis. 2016;63(suppl 4):S119–22. https://doi.org/10.1093/cid/ciw550

4. Zhang L, Xu Y, Zhao J, Kallonen T, Cui S, Xu Y, et al. Effect of vaccination on *Bordetella pertussis* strains, China. Emerg Infect Dis. 2010;16:1695–701. https://doi.org/10.3201/eid1611.100401

5. Wang Z, Cui Z, Li Y, Hou T, Liu X, Xi Y, et al. High prevalence of erythromycin-resistant *Bordetella pertussis* in Xi'an, China. Clin Microbiol Infect. 2014;20:O825–30. https://doi.org/10.1111/1469-0691.12671

6. Güriş D, Strebel PM, Bardenheier B, Brennan M, Tachdjian R, Finch E, et al. Changing epidemiology of pertussis in the United States: increasing reported incidence among adolescents and adults, 1990-1996. Clin Infect Dis. 1999;28:1230–7. https://doi.org/10.1086/514776

7. Ning G, Gao Y, Wu D, Li J, Li Y, Shao Z, et al. Epidemiology of pertussis in China 2011–2017 [in Chinese]. Zhongguo Yi Miao He Mian Yi. 2018;24:264–7, 273.

8. Bartkus JM, Juni BA, Ehresmann K, Miller CA, Sanden GN, Cassiday PK, et al. Identification of a mutation associated with erythromycin resistance in *Bordetella pertussis*: implications for surveillance of antimicrobial resistance. J Clin Microbiol. 2003;41:1167–72. https://doi.org/10.1128/JCM.41.3.1167-1172.2003

9. Xu Z, Wang Z, Luan Y, Li Y, Liu X, Peng X, et al. Genomic epidemiology of erythromycin-resistant *Bordetella pertussis* in China. Emerg Microbes Infect. 2019;8:461–70. https://doi.org/10.1080/22221751.2019.1587315

10. Schouls LM, van der Heide HG, Vauterin L, Vauterin P, Mooi FR. Multiple-locus variable-number tandem repeat analysis of Dutch *Bordetella pertussis* strains reveals rapid genetic changes during clonal expansion during the late 1990s. J Bacteriol. 2004;186:5496–505. https://doi.org/10.1128/JB.186.16.5496-5505.2004

11. Centers for Disease Control and Prevention. Erythromycin-resistant *Bordetella pertussis*—Yuma County, Arizona, May–October 1994. MMWR Morb Mortal Wkly Rep. 1994;43:807–10.

12. Guillot S, Descours G, Gillet Y, Etienne J, Floret D, Guiso N. Macrolide-resistant *Bordetella pertussis* infection in newborn girl, France. Emerg Infect Dis. 2012;18:966–8. https://doi.org/10.3201/eid1806.120091

13. Yao SM, Liaw GJ, Chen YY, Yen MH, Chen YH, Mu JJ, et al. Antimicrobial susceptibility testing of *Bordetella pertussis* in Taiwan prompted by a case of pertussis in a paediatric patient. J Med Microbiol. 2008;57:1577–80. https://doi.org/10.1099/jmm.0.2008/002857-0

14. Fu P, Wang C, Tian H, Kang Z, Zeng M. *Bordetella pertussis* infection in infants and young children in Shanghai, China, 2016–2017: clinical features, genotype variations of antigenic genes and macrolides resistance. Pediatr Infect Dis J. 2019;38:370–6. https://doi.org/10.1097/INF.0000000000002160

15. Xu Y, Zhang L, Tan Y, Wang L, Zhang S, Wang J. Genetic diversity and population dynamics of *Bordetella pertussis* in China between 1950-2007. Vaccine. 2015;33:6327–31. https://doi.org/10.1016/j.vaccine.2015.09.040

16. Barkoff AM, Mertsola J, Pierard D, Dalby T, Hoegh SV, Guillot S, et al. Surveillance of circulating *Bordetella pertussis* strains in Europe during 1998 to 2015. J Clin Microbiol. 2018;56:e01998-17. https://doi.org/10.1128/JCM.01998-17

17. Wagner B, Melzer H, Freymuller G, Stumvoll S, Rendi-Wagner P, Paulke-Korinek M, et al. Genetic variation of *Bordetella pertussis* in Austria. PLoS ONE. 2015;10:e132623. https://doi.org/10.1371/journal.pone.0132623

18. Bowden KE, Williams MM, Cassiday PK, Milton A, Pawloski L, Harrison M, et al. Molecular epidemiology of the pertussis epidemic in Washington State in 2012. J Clin Microbiol. 2014;52:3549–57. https://doi.org/10.1128/JCM.01189-14

19. Kurniawan J, Maharjan RP, Chan WF, Reeves PR, Sintchenko V, Gilbert GL, et al. *Bordetella pertussis* clones identified by multilocus variable-number tandem-repeat analysis. Emerg Infect Dis. 2010;16:297–300. https://doi.org/10.3201/eid1602.081707

20. Bart MJ, Harris SR, Advani A, Arakawa Y, Bottero D, Bouchez V, et al. Global population structure and evolution of *Bordetella pertussis* and their relationship with vaccination. MBio. 2014;5:e01074. https://doi.org/10.1128/mBio.01074-14

21. Libster R, Edwards KM. Re-emergence of pertussis: what are the solutions? Expert Rev Vaccines. 2012;11:1331–46. https://doi.org/10.1586/erv.12.118

22. Octavia S, Sintchenko V, Gilbert GL, Lawrence A, Keil AD, Hogg G, et al. Newly emerging clones of *Bordetella pertussis* carrying *prn2* and *ptxP3* alleles implicated in Australian pertussis epidemic in 2008-2010. J Infect Dis. 2012;205:1220–4. https://doi.org/10.1093/infdis/jis178

23. Elomaa A, Advani A, Donnelly D, Antila M, Mertsola J, He Q, et al. Population dynamics of *Bordetella pertussis* in Finland and Sweden, neighbouring countries with different vaccination histories. Vaccine. 2007;25:918–26. https://doi.org/10.1016/j.vaccine.2006.09.012

24. Schmidtke AJ, Boney KO, Martin SW, Skoff TH, Tondella ML, Tatti KM. Population diversity among *Bordetella pertussis* isolates, United States, 1935–2009. Emerg Infect Dis. 2012;18:1248–55. https://doi.org/10.3201/eid1808.120082

25. Loconsole D, De Robertis AL, Morea A, Metallo A, Lopalco PL, Chironna M. Resurgence of pertussis and emergence of the *Ptx*p3 toxin promoter allele in South Italy. Pediatr Infect Dis J. 2018;37:e126–31. https://doi.org/10.1097/INF.0000000000001804

26. Tiwari T, Murphy TV, Moran J; National Immunization Program, CDC. Recommended antimicrobial agents for the treatment and postexposure prophylaxis of pertussis: 2005 CDC Guidelines. MMWR Recomm Rep. 2005;54(RR-14):1–16.

27. Zackrisson G, Brorson JE, Björnegård B, Trollfors B. Susceptibility of *Bordetella pertussis* to doxycycline, cinoxacin, nalidixic acid, norfloxacin, imipenem, mecillinam and rifampicin. J Antimicrob Chemother. 1985;15:629–32. https://doi.org/10.1093/jac/15.5.629

28. Hoppe JE, Haug A. Antimicrobial susceptibility of *Bordetella pertussis* (Part I). Infection. 1988;16:126–30. https://doi.org/10.1007/BF01644321

29. Hoppe JE, Haug A. Treatment and prevention of pertussis by antimicrobial agents (Part II). Infection. 1988;16:148–52. https://doi.org/10.1007/BF01644089

30. Trollfors B. Effect of erythromycin and amoxycillin on *Bordetella pertussis* in the nasopharynx. Infection. 1978;6:228–30. https://doi.org/10.1007/BF01642314

31. Fry NK, Duncan J, Vaghji L, George RC, Harrison TG. Antimicrobial susceptibility testing of historical and recent clinical isolates of *Bordetella pertussis* in the United Kingdom using the Etest method. Eur J Clin Microbiol Infect Dis. 2010;29:1183–5. https://doi.org/ 10.1007/s10096-010-0976-1

Address for correspondence: Kaihu Yao, Beijing Pediatric Research Institute, Beijing Children's Hospital, Capital Medical University, No. 56 Nan-li-shi Rd, 100045 Beijing, China; email: yaokaihu@bch.com.cn

EMERGING INFECTIOUS DISEASES®

April 2018

Antimicrobial Resistance

To revisit the April 2018 issue, go to:

https://wwwnc.cdc.gov/eid/articles/issue/24/4/table-of-contents

Avian Influenza A Viruses among Occupationally Exposed Populations, China, 2014–2016

Chuansong Quan,[1] Qianli Wang,[1] Jie Zhang, Min Zhao, Qigang Dai, Ting Huang,
Zewu Zhang, Shenghua Mao, Yifei Nie, Jun Liu, Yun Xie, Baorong Zhang, Yuhai Bi, Weifeng Shi,
Peipei Liu, Dayan Wang, Luzhao Feng, Hongjie Yu, William J. Liu, George F. Gao

To determine the seroprevalence and seroconversion of avian influenza virus (AIV) antibodies in poultry workers, we conducted a seroepidemiologic study in 7 areas of China during December 2014–April 2016. We used viral isolation and reverse transcription PCR to detect AIVs in specimens from live poultry markets. We analyzed 2,124 serum samples obtained from 1,407 poultry workers by using hemagglutination inhibition and microneutralization assays. We noted seroprevalence of AIV antibodies for subtypes H9N2, H7N9, H6N1, H5N1-SC29, H5N6, H5N1-SH199, and H6N6. In serum from participants with longitudinal samples, we noted seroconversion, with ≥4-fold rise in titers, for H9N2, H7N9, H6N1, H5N1-SC29, H6N6, H5N6, and H5N1-SH199 subtypes. We found no evidence of H10N8 subtype. The distribution of AIV antibodies provided evidence of asymptomatic infection. We found that AIV antibody prevalence in live poultry markets correlated with increased risk for H7N9 and H9N2 infection among poultry workers.

Author affiliations: National Institute for Viral Disease Control and Prevention, Chinese Center for Disease Control and Prevention, Beijing, China (C. Quan, J. Zhang, P. Liu, D. Wang, W.J. Liu, G.F. Gao); Shandong First Medical University & Shandong Academy of Medical Sciences, Jinan, China (C. Quan, W. Shi); Fudan University School of Public Health, Shanghai, China (Q. Wang, H. Yu); Institute of Microbiology, Chinese Academy of Sciences, Beijing (M. Zhao, Y. Bi, G.F. Gao); Jiangsu Provincial Center for Disease Control and Prevention, Nanjing, China (Q. Dai); Sichuan Provincial Center for Disease Control and Prevention, Chengdu, China (T. Huang); Dongguan Municipal Center for Disease Control and Prevention, Dongguan, China (Z. Zhang); Shanghai Municipal Center for Disease Control and Prevention, Shanghai (S. Mao); Henan Provincial Center for Disease Control and Prevention, Zhengzhou, China (Y. Nie); Zaozhuang Center for Disease Control and Prevention, Zaozhuang, China (J. Liu); Jiangxi Provincial Center for Disease Control and Prevention, Nanchang, China (Y. Xie); Aviation General Hospital, Beijing (B. Zhang); Chinese Center for Disease Control and Prevention, Beijing (L. Feng, G.F. Gao)

Human infection with avian influenza viruses (AIVs) has been reported in China since the late 1990s. Since then, human infections with subtypes H5N1, H5N6, H6N1, H7N4, H7N9, H9N2, and H10N8 have been reported continuously and are a substantial threat to public health in the country (*1–5*). Birds at wholesale and retail live poultry markets are recognized incubators for novel influenza virus subtypes (*6–9*). Because of special occupational characteristics, poultry workers are at a high risk for repeated exposure to AIV-infected poultry. Most case-patients with H7N9 infection have had a history of contact with live poultry, and poultry workers represent a substantial proportion of cases (*10*). Several studies on AIV seroprevalence in occupationally exposed populations suggest that asymptomatic or clinically mild AIV infections are extensively prevalent among poultry workers (*11–14*). A serologic study of AIV distribution among poultry workers could directly evaluate the potential for AIVs to cross the species barrier to infect humans and might illuminate the current understanding of AIV prevalence in live poultry markets (*15*).

Low pathogenicity avian influenza A(H9N2) virus is distributed widely in domestic poultry around the world. A systematic review reports H9N2 virus seroprevalence in avian-exposed populations ranges from 1% to 43% by hemagglutination inhibition (HI) assays (*16*). Since a 2013 H7N9 infection outbreak in China, caused by a novel reassortant influenza A(H7N9) virus and associated with severe human infections, seroprevalence of the H7N9 subtype has been reported to range from 6% to 14.9% in southern China (*17,18*). In a previous study, the seroprevalence of H5 subtype AIVs in poultry workers was relatively low, whereas a cross-sectional study conducted in Zhejiang Province reported a seroprevalence of 4.7% for H5N1 virus antibodies (*19*).

Few large-scale longitudinal seroepidemiologic studies have included multiple AIV subtypes in diverse epidemic regions, especially after emergence of novel

---

[1]These authors contributed equally to this article.

subtypes. We conducted a prospective seroepidemiologic study in 7 representative areas across China to address gaps in the research. We characterized the seroprevalence profiles of 7 dominant human-infecting AIV subtypes among occupationally exposed workers in live poultry markets. Our aim was to further analyze human AIV infection risks for serotypes common in occupational exposure, including H5N1, H5N6, H6N1, H6N6, H7N9, H9N2, and H10N8 virus subtypes.

Methods

Ethics Approval

This study was approved by the Ethics Review Committee of the National Institute for Viral Disease Control and Prevention, Chinese Center for Disease Control and Prevention. The study was conducted in accordance with the principles of the Declaration of Helsinki and the standards of Good Clinical Practice as defined by the International Conference on Harmonization (https://www.ich.org).

Study Design and Participants

During December 2014–April 2016, we conducted a longitudinal seroepidemiologic study to assess asymptomatic AIV infection levels among poultry workers in China. We defined poultry workers as persons who repeatedly are exposed to poultry and work in wholesale or retail live poultry markets or in backyard farms, including wholesale sellers, retail sellers, transporters, processors, or feeders. The study included 1 municipality, Shanghai, and 6 provinces, Guangdong, Henan, Jiangsu, Jiangxi, Shandong, and Sichuan (Figure 1, panels A and B; Appendix, https://wwwnc.cdc.gov/EID/article/25/12/19-0261-App1.pdf). The study design included 4 serologic surveys. We collected whole blood samples from participating poultry workers at an initial visit in December 2014 and again during 3 consecutive follow-up visits in April 2015, December 2015, and April 2016 (Figure 1, panel C).

We used a standardized questionnaire to collect information at initial participant enrollment and updated participant information at subsequent visits. Participant information collected was demographic data, exposure variables, whether the worker experienced influenza-like illness within the previous month, and whether they received a seasonal influenza vaccination within the previous 12 months (Appendix).

Some poultry workers in China are short-term employees with high population mobility. We attempted to conduct follow-up studies with these employees through assistance from the market managers. To ensure the sample size, we enrolled new participants at each visit to the poultry markets (Figure 2).

We also recruited a control group of 216 outpatients with noninfectious diseases on physical examination at a general hospital in Beijing in October 2015. We collected 216 serum samples from the control group.

Collection of Human Samples

We collected a single venous whole blood sample from each study participant at each visit by using a Vacutainer blood collection tube (Becton Dickinson, https://www.bd.com). We divided serum into 3 aliquots and froze at –80°C until testing.

Serologic Assays

We tested participant serum samples for antibodies against H5N1, H5N6, H6N1, H6N6, H7N9, H9N2, and H10N8 virus subtypes, as well as for antibodies against seasonal influenza A(H1N1)pdm09 (pH1N1) and H3N2 viruses, to exclude cross-reactivity. We selected available representative antigens on the basis of their antigenic characteristics (Table 1) and analyzed the relevant phylogenetic relationship of hemagglutinin (HA) genes (Appendix Figures 1–5).

We performed all serologic assays in a Biosafety Level 2 or 3 laboratory. First, we screened samples by using an HI assay for antibodies, as described previously (20). We tested serum samples at a starting dilution of 1:10, followed by a 2-fold dilution to the endpoint (Appendix). To confirm HI assay results, we performed a microneutralization (MN) assay on serum samples with an HI titer ≥1:20 to H5N1, H5N6, H6N1, H6N6, H7N9, or H10N8 subtypes and those with an HI titer ≥1:40 to H9N2, pH1N1, or H3N2 subtypes, as previously described (20).

We used HI and MN cutoff values in accordance with previously published data (Appendix Table 1). We considered ≥1:20 as the cutoff value for HI and MN titers for positive tests for H5N1, H5N6, H6N1, H6N6, H7N9, and H10N8 virus subtypes (11,12,21) and considered ≥1:40 as the cutoff value for HI titer and ≥1:80 as the cutoff value for MN titer for positive tests for H9N2, pH1N1, and H3N2 virus subtypes (22,23). We set a stricter dilution cutoff value for the H9N2 virus subtype. An HI titer of 1:40 commonly is used and generally is an accepted value for influenza serologic assays used in detection of seasonal influenza and avian influenza H9 infection (24). We considered participants to have seroconversion when they had a ≥4-fold rise in antibody titer measured by HI assay between collection of ≥1 serum samples, plus an MN titer value of the later specimen being ≥1:20 or ≥1:80 for H9N2 subtype only.

Isolation of AIVs from Environmental and Poultry Samples

For environmental and poultry samples, we used previously described sampling and detection methods (25). In brief, we randomly selected environmental sites and poultry to sample by using a multistage sampling strategy. We collected environmental samples by swabbing water
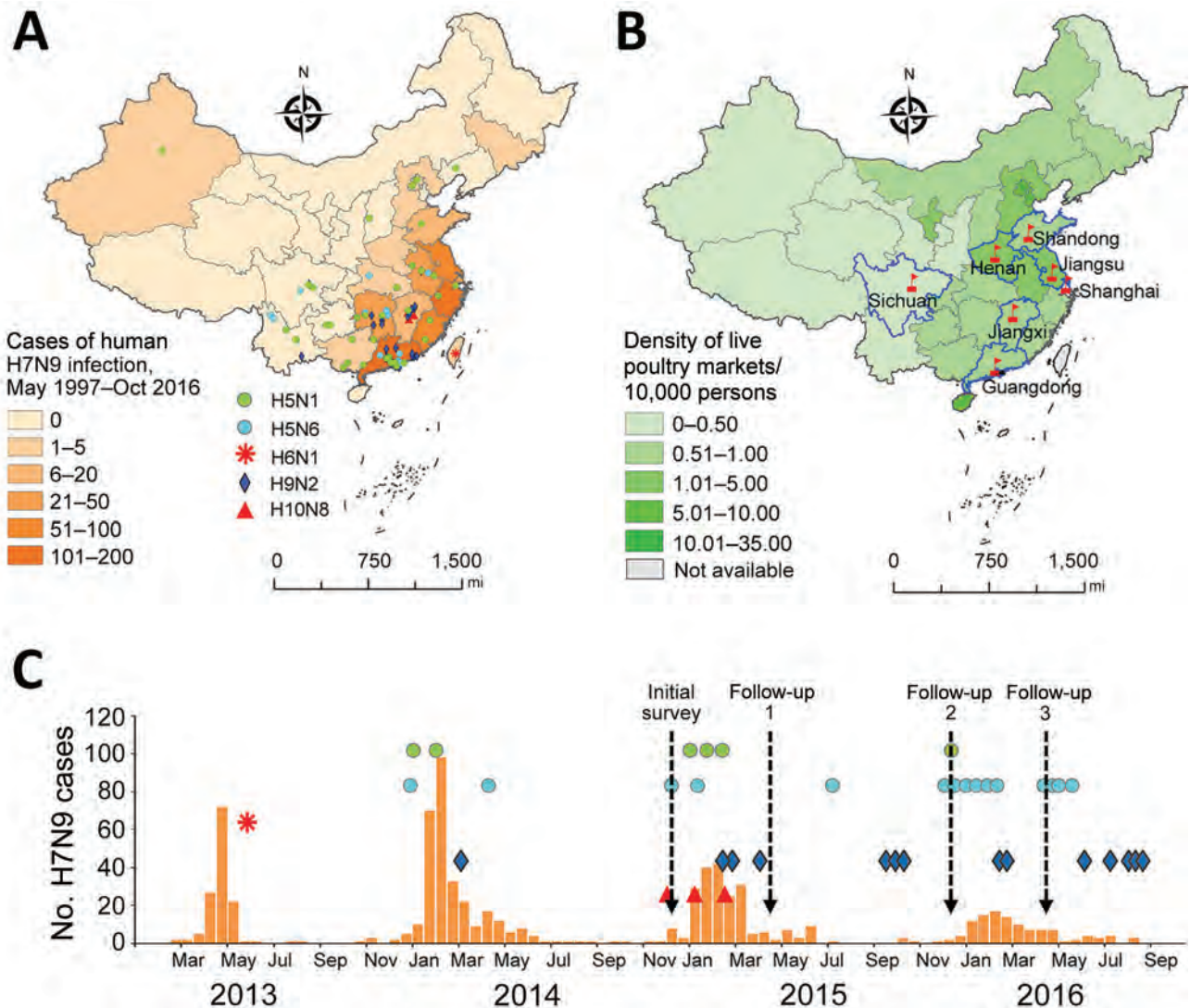
Figure 1. Temporal and spatial distribution of human infections with avian influenza A virus subtypes before and during serosurveillance, China. A) Geographic distribution of avian influenza A(H7N9) virus infection among humans in China during May 1997–October 2016. The number of case-patients in each province is based on data published by the World Health Organization (https://www.who.int/influenza/human_animal_interface/avian_influenza/archive/en/) and the National Health and Family Planning Commission of the Republic of China (http://www.nhc.gov.cn/jkj/s2907/new_list.shtml?tdsourcetag=s_pcqq_aiomsg). Density of shading represents the number of reported avian influenza H7N9 cases in humans in each province. Cases of other AIV subtype infections are represented by other symbols. B) Density of live poultry markets per 10,000 persons in each province included in the study, from data collected during 2013–2014. Red flags indicate locations of poultry markets selected for the serosurveillance study. C) Distribution of biweekly cases of human H7N9 infection before and during serosurveillance study. Orange bars indicate the number of biweekly cases of human H7N9 infection. Dashed lines indicate initial survey and follow-up dates for serosurveys, which were conducted before and after the third and fourth wave H7N9 epidemics. Reported cases of H5N1, H5N6, H6N1, H9N2, and H10N8 infection are noted with symbols as in panel A. AIV, avian influenza virus.

troughs, floors, and drains in poultry enclosures and collected oropharyngeal and cloacal swabs from apparently healthy poultry. We isolated avian influenza viruses in 9- to 10-day-old specific pathogen–free chicken embryos by using viral isolation procedures and following World Health Organization guidelines (*20*). We further analyzed hemagglutinin-positive samples by using reverse transcription PCR (RT-PCR) to identify hemagglutinin (HA) and

neuraminidase (NA) genetic subtypes (*20*). Except for Shandong Province, we detected AIVs from domestic poultry and live poultry market environments in all study areas.

Data Analysis

Our analyses were based on seroepidemiologic studies for influenza published by Horby et al. (*26*). We assigned each participant a unique identifier and used all data collected
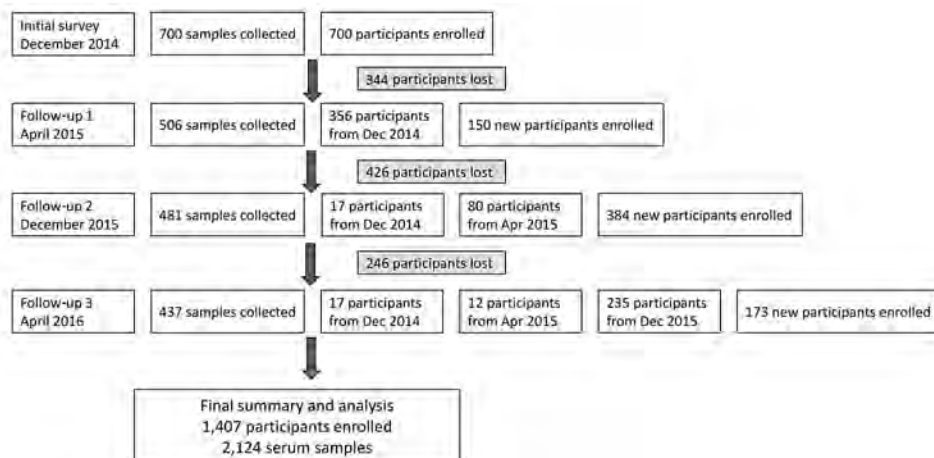
Figure 2. Flowchart of initial participant enrollment and follow-up distribution in 7 areas of China in a study of avian influenza virus seroprevalence during December 2014–April 2016.

with the questionnaire to establish a database. We performed a multivariate logistic regression model to evaluate independent risk factors associated with seroprevalence of antibodies in poultry workers. Risk factors evaluated were age; sex; occupational exposure factors, including processing, selling, transporting, and feeding poultry; and seropositivity to human influenza pH1N1 or H3N2 viruses. For logistic regression analysis, we estimated the maximum likelihood for the odds ratio (OR) and calculated 95% CIs by using the Wald χ^2 test. We used binomial distribution to calculate 95% CIs of rate. We used Spearman correlation analysis to estimate the association between seroprevalence and local epidemic intensity of AIVs in live poultry markets by region. We used 2-tailed p values for all calculations and considered values <0.05 statistically significant. We performed statistical analyses by using SAS 9.4 (SAS Institute, Inc., https://www.sas.com).

Results

Participant Characteristics
We collected 2,124 serum samples from 1,407 participants from 1 municipality, Shanghai, and 6 provinces, Guangdong, Henan, Jiangsu, Jiangxi, Shandong, and Sichuan, in China. We had paired or serial serum samples from 652

participants who had ≥2 visits during the study period. The median age of participants with completed questionnaire information was 46 years (interquartile range [IQR] 36–52 years); 54.0% (1,147/2,124) of samples were from men. The most common category of poultry exposure was poultry seller. We did not see statistically significant differences in the distribution of demographic characteristics of participants, including sex and age, over the 4-period survey. In addition, 2.8% (59/2,124) of samples came from poultry workers who reported receiving a seasonal influenza vaccine within the previous 12 months (Table 2).

Of the 216 participants in control group, the median age was 48 years (IQR 34–59 years); 45.8% were male. We saw no significant differences in their data compared with poultry workers (data not shown).

Seroprevalence of Antibodies against AIVs
In the 2,124 samples, the overall seroprevalence of antibodies was 11.2% for H9N2 subtype and 3.9% for H7N9 subtype. Seroprevalence for H5Nx and H6Nx subtypes was lower, ranging from 1.3% to 2.1% for H5Nx and from 0.4% to 2.5% for H6Nx. We did not observe evidence of H10N8 infection (Table 3).

The seroprevalence profile was geographically distinct (Figure 3). For example, in Shandong Province, H9N2

Table 1. Avian influenza A antigens used in serologic hemagglutinin inhibition and microneutralization assays, China*

Subtype	Virus strain	GISAID number
Avian influenza		
H5N1 clade 2.3.2.1c	A/chicken/Shanghai/02.12 HZ199-P/2015 (SH199)	EPI1544294
H5N1 clade 2.3.4.4	A/pigeon/Sichuan/NCXN29/2014 (SC29)	EPI590898
H5N6 clade 2.3.4.4	A/duck/Guangdong/04.22 DGCP069-O/2015	EPI660071
H6N1	A/Taiwan/2/2013	EPI459855
H6N6	A/duck/Guangxi/04.10 JX031/2015	EPI661887
H7N9	A/chicken/Guangdong/04.22 DGCP098-O/2015	EPI666285
H9N2	A/chicken/Guangdong/04.15 SZBAXQ005/2015	EPI661935
H10N8	A/chicken/Jiangxi /B18/2014	EPI1544302
Seasonal influenza		
H1N1(pdm09)	A/California/04/2009	EPI176470
H3N2	A/Beijing/CAS0001/2007	EPI1544286

*GISAID, https://www.gisaid.org.

Table 2. Characteristics of study participants in serosurveys for avian influenza viruses, China, 2014–2016*

Variables	2014 Dec, n = 700	2015 Apr, n = 506	2015 Dec, n = 481	2016 Apr, n = 437	Total, n = 2,124	χ^2†	p value
Sex, no. (%)							
M	369 (52.7)	264 (52.2)	278 (51.8)	236 (54.0)	1,147 (54.0)	3.94	0.27
F	331 (47.3)	242 (47.8)	203 (42.2)	201 (46.0)	977 (46.0)		
Age, y, no. (%)‡							
<21	10 (1.4)	6 (1.2)	4 (0.8)	11 (2.5)	31 (1.5)	1.43	0.23
21–40	212 (30.3)	144 (28.5)	164 (34.1)	144 (33)	664 (31.3)		
41–60	394 (56.3)	308 (60.9)	254 (52.8)	232 (53.1)	1,188 (55.9)		
>60	78 (11.1)	47 (9.3)	55 (11.4)	50 (11.4)	230 (10.8)		
Missing data	6 (0.9)	1 (0.2)	4 (0.8)	0	11 (0.5)		
Median age (range)§	46 (38–52)	47 (38–52)	45 (35–52)	45 (35–52)	46 (36–52)	6.62	0.08
Type of poultry exposure, no. (%)¶							
Processing	155 (22.1)	107 (21.1)	118 (24.5)	94 (21.5)	474 (22.3)	27.88	0.006
Selling	423 (60.4)	332 (65.6)	299 (62.2)	191 (43.7)	1,243 (58.5)		
Transportation	39 (5.6)	31 (6.1)	24 (5)	21 (4.8)	115 (5.4)		
Feeding	191 (27.3)	125 (24.7)	124 (25.8)	93 (21.3)	533 (25.1)		
Others	59 (8.4)	35 (6.9)	25 (5.2)	48 (11)	167 (7.9)		
Missing data	0	0	2 (0.4)	0	2 (0.1)		
Length of poultry exposure, y (range)§	8 (3–15)	8 (3–15)	5 (2–10)	5 (3–10)	6 (3–13)	61.63	<0.001
Vaccinated against seasonal influenza, no. (%)	23 (3.3)	8 (1.6)	20 (4.2)	8 (1.8)	59 (2.8)	8.20	0.04

*Some participants participated in >1 survey.
†By χ^2 test, unless otherwise indicated.
‡By χ^2_{CMH} test. Missing data were not calculated.
§By Kruskal-Wallis test.
¶Most participants had multiple exposure types. Sums of percentages exceed 2,124. Missing data were not calculated.

virus antibody seroprevalence was 23%, which was higher than in other provinces, especially Sichuan Province, which had only a 4.2% seroprevalence for this subtype. Provinces in the Yangtze River Delta, which were the first to report H7N9 infections in patients during the 2013 outbreak, exhibited higher seroprevalence rates compared with the other provinces. Shanghai had a rate of 10.3% and Jiangsu Province had a rate of 6.9%. In Sichuan Province, where a non–laboratory-confirmed H7N9-infected patient was reported before 2017, no participant tested positive for the H7N9 subtype.

Seroprevalence of H5 and H6 subtypes among poultry workers also were different by region. Detected H5 subtypes included H5N1-SH199 clade 2.3.2.1c in 5.3% of samples from Shandong Province; H5N1-SC29 clade 2.3.4.4 in 3.0% of samples from Jiangsu Province and in 3.3% of samples from Sichuan Province; and H5N6 in 4.9% of samples from Shanghai. We detected H6N1 in 5.2% of samples from Jiangsu Province and in 3.8% from Shanghai and H6N6 in 3.3% of samples from Shanghai (Figure 3).

Among the 216 participants in the control group, we found no evidence of antibodies against H7N9 virus and a lower prevalence (3.7%) of antibodies against H9N2 virus than in the poultry workers. We observed no statistically significant differences in the prevalence of antibodies against other AIV subtypes between the control group and poultry workers (Appendix Table 2).

Seroconversion of Antibodies against AIVs among Poultry Workers

We observed seroconversion in all AIV antigens during the study period, except the H10 subtype, which might represent a new asymptomatic AIV infection among poultry workers (Figure 4, panel A). Among 652 poultry workers with paired or serial serum samples during the study, 3.5% demonstrated seroconversion for H9N2 virus, 1.4% demonstrated seroconversion for H7N9 virus, and <1% demonstrated seroconversion for H5 or H6 viruses (Figure 4, panels B and C; Appendix Tables 3–9). Because we saw no evidence of H10N8 virus, we also

Table 3. Seroprevalence among poultry workers surveyed for avian influenza viruses, China, 2014–2016*

Antigen	No. (%, 95% CI) seropositive participants				
	2014 Dec, n = 700	2015 Apr, n = 506	2015 Dec, n = 481	2016 Apr, n = 437	Total, n = 2,124
Avian influenza serotype					
H5N1-SH199	6 (0.9, 0.2–1.5)	6 (1.2, 0.2–2.1)	10 (2.1, 0.8–3.4)	6 (1.4, 0.3–2.5)	28 (1.3, 0.8–1.8)
H5N1-SC29	22 (3.1, 1.8–4.4)	17 (3.4, 1.8–4.9)	2 (0.4, 0.1–1.5)	3 (0.7, 0.1–2.0)	44 (2.1, 1.5–2.7)
H5N6	28 (4, 2.5–5.5)	11 (2.2, 0.9–3.4)	2 (0.4, 0.1–1.5)	1 (0.2, 0–1.3)	42 (2.0, 1.4–2.6)
H6N1	22 (3.1, 1.8–4.4)	21 (4.1, 2.4–5.9)	5 (1, 0.1–1.9)	5 (1.1, 0.4–2.6)	53 (2.5, 1.8–3.2)
H6N6	0 (0, 0–0.5)	0 (0, 0–0.7)	7 (1.5, 0.4–2.5)	1 (0.2, 0–1.3)	8 (0.4, 0.1–0.6)
H7N9	33 (4.7, 3.1–6.3)	36 (7.1, 4.9–9.4)	6 (1.3, 0.3–2.2)	7 (1.6, 0.4–2.8)	82 (3.9, 3.0–4.7)
H9N2	48 (6.9, 5.0–8.7)	59 (11.7, 8.9–14.5)	64 (13.3, 10.3–16.3)	66 (15.1, 11.7–18.5)	237 (11.2, 9.8–12.5)
Seasonal influenza serotype					
H1N1(pdm09)	94 (13.4, 10.9–16.0)	85 (16.8, 13.5–20.1)	90 (18.7, 15.2–22.2)	79 (18.1, 14.5–21.7)	348 (16.4, 14.8–18.0)
H3N2	237 (33.9, 30.4–37.4)	165 (32.6, 28.5–36.7)	199 (41.4, 37.0–45.8)	171 (39.1, 34.6–43.7)	772 (36.3, 34.3–38.4)
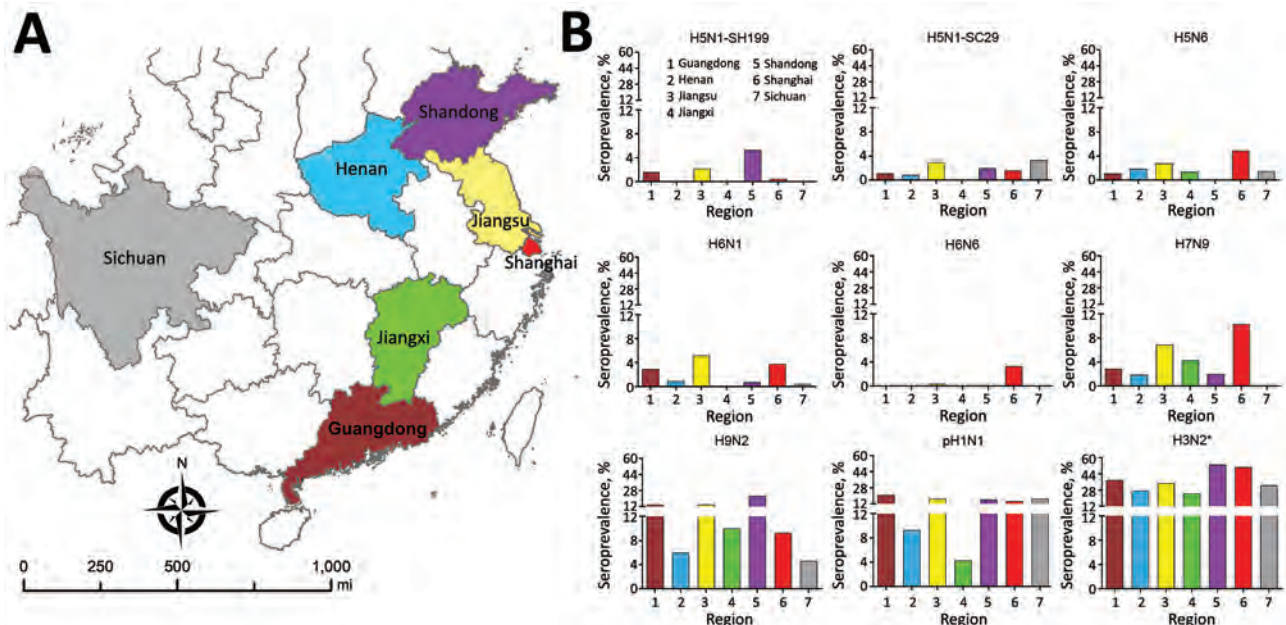
Figure 3. Avian influenza virus seroprevalence in the studied regions of China during December 2014–April 2016. A) Geographic areas included for serosurveillance: 1 municipality, Shanghai, and 6 provinces, Guangdong, Henan, Jiangsu, Jiangxi, Shandong, and Sichuan. B) Seroprevalence against avian influenza A virus subtypes in 4 cross-sectional surveys. Colors on map correspond to colors in bar graphs. *Seasonal influenza virus subtype.

saw no seroconversion for the subtype (Table 4; Figure 4, panel A).

Some participants showed consistently seropositive results, 15 for H7N9 subtype and 41 for H9N2 subtype and a few each for H5N1, H5N6, and H6N1 subtypes (Figure 4, panel B). One participant (no. 14.12GD72) showed HI titers at 1:20 and MN titers at 1:160 to H5N1-SH199 subtype in 4 consecutive surveys (Figure 4, panel C).

Risk Analysis for Asymptomatic AIV Infections
In the multivariable analysis, we identified demographic and occupational risk factors for poultry workers with asymptomatic infections. For instance, the demographic classification female (adjusted OR [aOR] 2.2, 95% CI 1.4–3.6), and occupational classification poultry seller (aOR 4.1, 95% CI 2.2–7.7) appear to be risk factors for H7N9 infection. For H9N2 subtype, female (aOR 1.6, 95% CI 1.2–2.1) and poultry seller (aOR 1.9, 95% CI 1.4–2.6) appear to be risk factors for infection. In addition, the number of years working in poultry-related occupations was associated with seroprevalence. In particular, samples from workers reporting ≥3 years of exposure were associated with seroprevalence of H9N2 subtype. Factors associated with increased risk for H5 infections included being >55 years of age, being exposed to ducks, or being exposed to ill or dead poultry (Table 5).

Our study revealed a correlation between the presence of antibodies and seasonal influenza virus infection. We saw

an association between the presence of pH1N1 virus antibodies and increased seropositivity for H5N1 or H5N6 subtypes, and between occurrence of seasonal H3N2 virus antibodies in humans and positive antibody titers for H7N9 virus subtype. We also saw a positive association between elevated H6N1 seropositivity and the presence of antibodies against pH1N1 (aOR 3.0, 95% CI 1.7–5.4) and H9N2 (aOR 2.6, 95% CI 1.4–5.0) subtypes (Table 5). Seasonal influenza vaccination history was not a significant risk factor for elevated AIV antibody titers, perhaps because of low vaccination rates.

AIV Circulation in Poultry and Markets
We collected 6,207 samples from poultry and the environment for AIV screening and detection in this study. In Shanghai, 4.1% (20/493) of samples were positive for H7N9 subtype, as were 8.6% (41/476) of samples from Jiangsu Province. However, only 0.6% (15/2,308) of samples from Jiangxi Province, 0.6% (12/2,158) of samples from Guangdong Province, and 0.2% (1/516) of samples from Sichuan Province were positive for H7N9 subtype (Appendix Table 10).

For H9N2 subtype, 14.4% (71/493) of samples from Shanghai, 9.5% (45/476) from Jiangsu Province, and 8.3% (180/2,158) of samples from Guangdong Province were positive. However, only 4.4% (102/2,308) of samples from Jiangxi Province and 5.5% (14/256) from Henan Province were positive for H9N2 (Appendix Table 10).

Exploring the correlation between AIV circulation in poultry and seroprevalence in workers in live poultry
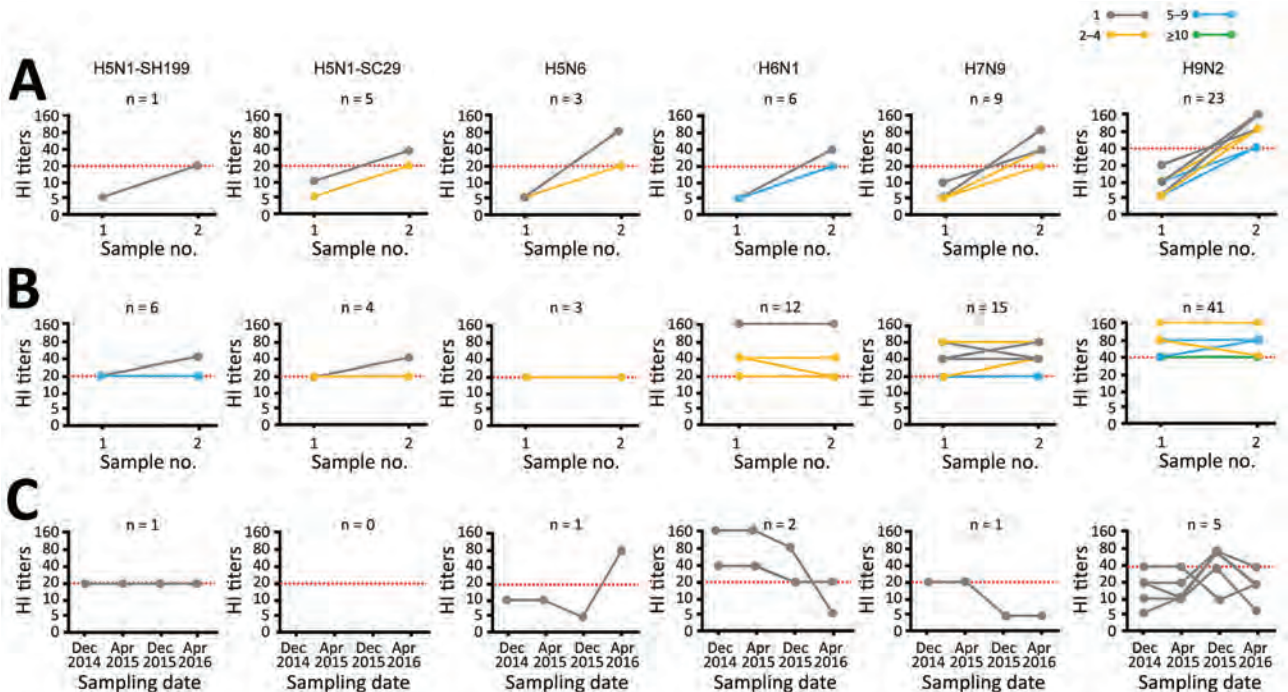
Figure 4. Seroconversion and persistent positivity for avian influenza virus (AIV) A subtypes based on HI titers in a cohort study in China during December 2014–April 2016. Each dot and line connection represents 1 participant. Red dashed lines represent positive cutoff for the HI titers; HI–positive samples were confirmed by a microneutralization assay. A) Comparison of paired samples from participants during 2 surveillance periods showing seroconversion for 6 AIV subtypes. Weighted lines and dots represent participants with seroconversion. B) Number of participants with >2 positive sample who were persistently seropositive for 6 AIV subtypes. Weighted lines and dots represent number of participants with seropositivity. C) Antibody titers of representative participants with >1 positive sample in the 4 serosurveys. HI, hemagglutinin inhibition.

markets revealed a correlation coefficient of 0.8 (p = 0.04) for H7N9 virus and 0.5 (p = 0.28) for H9N2 virus, indicating that prevalence of local AIVs was statistically correlated with H7N9 subtype seroprevalence. Our results also revealed that AIV prevalence in the different provinces was a key determinant of seroprevalence in the corresponding poultry workers. However, we did not observe a similar trend with other seroepidemic subtypes.

Discussion

We conducted a longitudinal seroepidemiologic study of occupationally exposed poultry workers in China during December 2014–April 2016. We investigated antibody

Table 4. Seroconversion and persistently positive findings for avian influenza virus among 652 participants with paired or serial serum samples, China, 2014–2016*

Subtype	No. (%, 95% CI) participants	
	Seroconversion	Persistently positive
H5N1-SH199	1 (0.2, 0–0.9)	6 (0.9, 0.3–2.0)
H5N1-SC29	5 (0.8, 0.2–1.8)	4 (0.6, 0.2–1.6)
H5N6	3 (0.5, 0.0–1.3)	3 (0.5, 0.0–1.3)
H6N1	6 (0.9, 0.3–2.0)	12 (1.8, 0.8–2.9)
H6N6	4 (0.6, 0.2–1.7)	0 (0.0, 0.0–0.6)
H7N9	9 (1.4, 0.5–2.3)	15 (2.3, 1.1–3.5)
H9N2	23 (3.5, 2.1–4.9)	41 (6.3, 4.4–8.2)
H10N8	0 (0–0.6)	0 (0–0.6)

profiles of 7 AIV subtypes that have crossed the species barrier to infect humans, H5N1, H5N6, H6N1, H7N9, H9N2 and H10N8 subtypes, and H6N6 subtype, which is a potential risk to humans. We assessed seroconversion by analyzing paired serum samples from poultry workers and detecting AIV in poultry and the environment in live poultry markets.

H9N2 virus, which plays a role at the animal–human interface, serves as gene donor for H7N9 and H10N8 viruses that infect humans (*27*). We used a Y280/G9 lineage antigen isolated in samples from Guangdong Province in 2015 as a reference, and its seroprevalence was higher than all other AIV subtypes in our study (Appendix Figure 4). Previous serologic studies also have reported that this strain's seroprevalence consistently is higher than other AIV subtypes in most provinces surveyed in China, reflecting the association between prevalent asymptomatic infections and frequent poultry exposure (*12,16,28*).

Overall, seroprevalence of antibodies against H9N2 subtype in this study was higher than reported in previous serologic studies in China and the seroprevalence was highest in Shandong Province compared with other provinces. Li et al. reported a 3.04% seroprevalence between 2009 and 2011 in occupationally exposed populations (*29*), and Yu

Table 5. Risk analysis for seropositive participants in surveys for avian influenza subtypes among poultry workers, China, 2014–2016*

Subtypes and variables	Seropositive, no. (%)	Seronegative, no. (%)	p value†	OR (95% CI)	Adjusted OR (95% CI)
H5Nx‡					
Age, y					
<35	8 (10.8)	442 (21.7)	<0.001	Referent	Referent
35–55	40 (54.1)	1,231 (60.4)		1.8 (0.8–3.9)	2.3 (1.0–4.9)
>55	26 (35.1)	366 (18.0)		3.9 (1.8–8.8)	4.7 (2.1–10.7)
Exposed to ducks					
Yes	34 (45.3)	651 (31.8)	0.014	1.8 (1.1–2.8)	1.6 (1.0–2.5)
No	41 (54.7)	1,398 (68.2)		Referent	Referent
Exposed to ill or dead poultry					
Yes	15 (20.0)	221 (10.8)	0.013	2.1 (1.2–3.7)	2.3 (1.3–4.2)
No	60 (80.0)	1826 (89.2)		Referent	Referent
Seropositivity for H1N1(pdm09) virus					
Positive	24 (32.0)	316 (16.4)	<0.001	2.6 (1.6–4.3)	3.1 (1.8–4.5)
Negative	51 (68.0)	1,733 (84.6)		Referent	Referent
H7N9					
Sex					
F	53 (64.6)	924 (45.2)	<0.001	2.2 (1.4–3.5)	2.2 (1.4–3.6)
M	29 (35.4)	1,118 (54.8)		Referent	Referent
Poultry seller§					
Yes	70 (85.4)	1,173 (57.5)	<0.001	4.3 (2.3–8.0)	4.1 (2.2–7.7)
No	12 (14.6)	867 (42.5)		Referent	Referent
No. years of work at live poultry market					
<3	11 (13.4)	561 (27.5)	0.017	Referent	Referent
3–10	46 (56.1)	924 (45.3)		2.0 (1.1–3.5)	1.8 (1.0–3.2)
>10	25 (30.5)	557 (27.3)		1.7 (0.9–3.2)	1.3 (0.7–2.5)
Seropositivity for seasonal H3N2 virus					
Positive	44 (53.7)	743 (36.4)	0.002	2.0 (1.3–3.2)	1.9 (1.2–2.9)
Negative	38 (46.4)	1,299 (63.6)		Referent	Referent
H9N2					
Age, y§					
<35	56 (23.6)	394 (21.0)	0.004	2.1 (1.3–3.4)	1.9 (1.1–3.3)
35–55	156 (65.8)	1,115 (59.4)		2.1 (1.3–3.2)	1.6 (1.0–2.5)
>55	25 (10.6)	367 (19.6)		Referent	Referent
Sex					
F	134 (56.5)	843 (44.7)	<0.001	1.6 (1.2–2.1)	1.6 (1.2–2.1)
M	103 (43.5)	1,044 (55.3)		Referent	Referent
Poultry seller§					
Yes	175 (73.8)	1,068 (56.7)	<0.001	2.2 (1.6–2.9)	1.9 (1.4–2.6)
No	62 (26.2)	817 (43.3)		Referent	Referent
Poultry processor§					
Yes	67 (28.3)	407 (21.6)	0.02	1.4 (1.1–1.9)	1.3 (1.0–1.7)
No	170 (71.7)	1,478 (78.4)		Referent	Referent
No. years of work at live poultry market					
<3	37 (15.6)	535 (28.4)	<0.001	Referent	Referent
3–10	126 (53.2)	844 (44.7)		2.6 (1.8–3.7)	2.4 (1.6–3.5)
>10	74 (31.2)	508 (26.9)		2.2 (1.5–3.2)	3.0 (1.3–3.1)
H6N1					
Seropositivity for H1N1(pdm09) virus					
Positive	19 (35.9)	321 (15.5)	<0.001	3.0 (1.7–5.4)	3.0 (1.7–5.4)
Negative	34 (64.1)	1,750 (84.5)		Referent	Referent
Seropositivity for H9N2 virus					
Positive	13 (24.5)	224 (10.8)	0.002	2.7 (1.4–5.1)	2.6 (1.4–5.0)
Negative	40 (75.5)	1,847 (89.2)		Referent	Referent

*Results represent only statistically significant factors from analysis of questionnaire data.
†By χ^2 test.
‡Combined the H5N1-SC29 and H5N6 data.
§Missing data.

et al. reported 4.6% of poultry workers in their study had antibodies against H9N2 virus in 2013 (*30*). Another previous serologic study in Tai'an, Shandong Province, reported the prevalence of antibodies against H9 subtypes among poultry workers was ≤8.5% during January 2011–December 2013 (*31*). Because no uniform standard antibody titer cutoff is available for H9N2 seropositivity, we used a stricter cutoff value for HI titers, ≥1:40, and for MN titers, ≥1:80, for seroprevalence to avoid overestimation and reduce cross-reactivity with seasonal influenza viruses (*32*).

The higher seroprevalence in Shandong Province could be explained by 2 possibilities. Participants in this province were all poultry sellers in live poultry markets, an occupation that we noted as a statistically high risk factor

for seroprevalence. Shandong is ranked as the one of the largest egg-producing provinces in China, and it has a high prevalence of H9N2 in local chicken flocks (*33,34*), which could indicate that more people are exposed to AIV from the poultry industry in general.

Logistic regression analysis of risk factors showed that occupational characteristics might increase risk for infection. Seropositive participant characteristics and related AIV information provided pivotal seroevidence for subclinical AIV infection risk factors. We noted that the participant characteristics female and poultry seller were risk factors for H7N9 and H9N2 infection, which coincides with results of previous studies (*18,35*). Further risk factor analysis indicated that seropositivity for pH1N1 virus was a risk factor for H5 infections with H5N1 and H5N6 subtypes and for H6N1 infection and that seropositivity for H3N2 subtype was a risk factor for H7N9 infection. In addition, seroprevalence for H6N1 infection also was affected by seropositivity for H9N2 subtypes. Our results might be explained partially by cross-reactivity between HA antigen from different AIV subtypes (*36,37*). We noted that the prevalence of H7N9 and H9N2 viruses in poultry from local markets was associated closely with seroprevalence for these subtypes in poultry workers. We also noted that the low seasonal influenza vaccination rate (2.8%) in poultry workers might have a limited effect on potential cross-reactions between pH1N1 and H5 subtypes and between H3N2 and H7N9 subtypes.

We observed higher prevalence for certain AIV subtypes and seroprevalence for certain AIV antibodies in live poultry markets, providing further evidence of cross-species transmission from birds to humans. Since the H7N9 outbreaks of 2013, consensus that AIV was transmitted from birds to humans led the government of China to implement epidemic control measures. The measures, such as closing live poultry markets during influenza season, cleaning and disinfecting live poultry markets daily, and vaccinating poultry, have effectively reduced the chances for human exposure to AIV-contaminated environments and ill poultry (*38,39*). Our results demonstrate that epidemic control measures aimed at live poultry markets, including their closure, can be highly effective in human AIV infection control (*9,38*).

Many participants with seropositivity were residents of southern and eastern provinces. Several determinants could account for this observation. First, the high density of live poultry markets, high population density, and expansive live poultry transportation network in these regions could favor large-scale and transboundary AIV spread in poultry, thereby increasing the risk for human infection (*40*). Second, these regions are rich in water resources, including the Yangtze and Pearl Rivers, as well as many lakes, which are natural habitats for waterfowl and wild birds that serve as natural hosts for various AIV subtypes, including H5Nx and H9N2 viruses, and that continually generate biological threats to public health (*41,42*). Studies suggest that migratory birds play a role in the evolution and spread of various zoonotic agents, and southeast China is located along the East Asian-Australian flyway, a migratory route for many bird species (*43,44*).

Our study had several limitations. Despite serious efforts to collect samples from the same participants during follow-up sampling, movement of vendors and poultry workers from target poultry markets reduced the possibility of obtaining paired samples. In addition, the relatively small sample size and use of only 1 location for the control group, Beijing in 2015, could be potential sources of bias.

In conclusion, our study provides serologic evidence of subclinical human AIV infection in an occupationally exposed population of poultry workers and corresponding AIV infection risk factors. Because novel influenza viruses continue to emerge, our results show the need for enhanced etiologic surveillance of AIVs in live poultry markets and humans. Implementing poultry vaccination would also reduce human infection risk. Finally, our results demonstrate the need for active surveillance to foresee dynamic AIV epidemics and inform influenza vaccine development.

About the Author

Dr. Quan was a medical student at the National Institute for Viral Disease Control and Prevention, Chinese Center for Disease Control and Prevention, Beijing, China, during the study. His primary research interests include etiology and serology of influenza viruses and other emerging and reemerging viruses.

References

1. Su S, Bi Y, Wong G, Gray GC, Gao GF, Li S. Epidemiology, evolution, and recent outbreaks of avian influenza virus in China. J Virol. 2015;89:8671–6. https://doi.org/10.1128/JVI.01034-15

2. Gao GF. From "A"IV to "Z"IKV: Attacks from emerging and re-emerging pathogens. Cell. 2018;172:1157–9. https://doi.org/10.1016/j.cell.2018.02.025

3. Huo X, Cui L, Chen C, Wang D, Qi X, Zhou M, et al. Severe human infection with a novel avian-origin influenza A(H7N4) virus. Sci Bull. 2018;63:1043–50. https://doi.org/10.1016/j.scib.2018.07.003

4. Wei SH, Yang JR, Wu HS, Chang MC, Lin JS, Lin CY, et al. Human infection with avian influenza A H6N1 virus: an epidemiological analysis. Lancet Respir Med. 2013;1:771–8. https://doi.org/10.1016/S2213-2600(13)70221-2

5. Han M, Gu J, Gao GF, Liu WJ. China in action: national strategies to combat against emerging infectious diseases. Sci China Life Sci. 2017;60:1383–5. https://doi.org/10.1007/s11427-017-9141-3

6. Liu D, Shi W, Shi Y, Wang D, Xiao H, Li W, et al. Origin and diversity of novel avian influenza A H7N9 viruses causing human infection: phylogenetic, structural, and coalescent analyses. Lancet. 2013;381:1926–32. https://doi.org/10.1016/S0140-6736(13)60938-1

7. Liu J, Xiao H, Wu Y, Liu D, Qi X, Shi Y, et al. H7N9: a low pathogenic avian influenza A virus infecting humans. Curr Opin Virol. 2014;5:91–7. https://doi.org/10.1016/j.coviro.2014.03.001

8. Quan C, Huang T, Chen X, Zhang J, Wang Q, Zhang C, et al. Genomic characterizations of H4 subtype avian influenza viruses from live poultry markets in Sichuan Province of China, 2014–2015. Sci China Life Sci. 2018;61:1123–6. https://doi.org/10.1007/s11427-018-9327-4

9. Gao GF. Influenza and the live poultry trade. Science. 2014;344:235. https://doi.org/10.1126/science.1254664

10. Cui B, Liao Q, Lam WWT, Liu ZP, Fielding R. Avian influenza A/H7N9 risk perception, information trust and adoption of protective behaviours among poultry farmers in Jiangsu Province, China. BMC Public Health. 2017;17:463–76. https://doi.org/10.1186/s12889-017-4364-y

11. Bai T, Zhou J, Shu Y. Serologic study for influenza A (H7N9) among high-risk groups in China. N Engl J Med. 2013;368:2339–40. https://doi.org/10.1056/NEJMc1305865

12. Wang M, Fu C-X, Zheng B-J. Antibodies against H5 and H9 avian influenza among poultry workers in China. N Engl J Med. 2009;360:2583–4. https://doi.org/10.1056/NEJMc0900358

13. Ma C, Cui S, Sun Y, Zhao J, Zhang D, Zhang L, et al. Avian influenza A (H9N2) virus infections among poultry workers, swine workers, and the general population in Beijing, China, 2013–2016: A serological cohort study. Influenza Other Respir Viruses. 2019;13:415–25. https://doi.org/10.1111/irv.12641

14. Xin L, Bai T, Zhou JF, Chen YK, Li XD, Zhu WF, et al. Seropositivity for avian influenza H6 virus among humans, China. Emerg Infect Dis. 2015;21:1267–9. https://doi.org/10.3201/eid2107.150135

15. Sikkema RS, Freidl GS, de Bruin E, Koopmans M. Weighing serological evidence of human exposure to animal influenza viruses–a literature review. Euro Surveill. 2016;21:30388. https://doi.org/10.2807/1560-7917.ES.2016.21.44.30388

16. Khan SU, Anderson BD, Heil GL, Liang S, Gray GC. A systematic review and meta-analysis of the seroprevalence of influenza A(H9N2) infection among humans. J Infect Dis. 2015;212:562–9. https://doi.org/10.1093/infdis/jiv109

17. Yang S, Chen Y, Cui D, Yao H, Lou J, Huo Z, et al. Avian-origin influenza A(H7N9) infection in influenza A(H7N9)-affected areas of China: a serological study. J Infect Dis. 2014;209:265–9. https://doi.org/10.1093/infdis/jit430

18. Wang X, Fang S, Lu X, Xu C, Cowling BJ, Tang X, et al. Seroprevalence to avian influenza A(H7N9) virus among poultry workers and the general population in southern China: a longitudinal study. Clin Infect Dis. 2014;59:e76–83. https://doi.org/10.1093/cid/ciu399

19. Li LH, Yu Z, Chen WS, Liu SL, Lu Y, Zhang YJ, et al. Evidence for H5 avian influenza infection in Zhejiang province, China, 2010–2012: a cross-sectional study. J Thorac Dis. 2013;5:790–6. https://doi.org/10.3978/j.issn.2072-1439.2013.12.45

20. World Health Organization. Manual for the laboratory diagnosis and virological surveillance of influenza. Geneva: The Organization; 2011 [cited 2019 Feb 10]. https://www.who.int/influenza/gisrs_laboratory/manual_diagnosis_surveillance_influenza/en

21. Qi W, Su S, Xiao C, Zhou P, Li H, Ke C, et al. Antibodies against H10N8 avian influenza virus among animal workers in Guangdong Province before November 30, 2013, when the first human H10N8 case was recognized. BMC Med. 2014;12:205. https://doi.org/10.1186/s12916-014-0205-3

22. Gomaa MR, Kayed AS, Elabd MA, Zeid DA, Zaki SA, El Rifay AS, et al. Avian influenza A(H5N1) and A(H9N2) seroprevalence and risk factors for infection among Egyptians: a prospective, controlled seroepidemiological study. J Infect Dis. 2015;211:1399–407. https://doi.org/10.1093/infdis/jiu529

23. Liu WJ, Tan S, Zhao M, Quan C, Bi Y, Wu Y, et al. Cross-immunity against avian influenza A(H7N9) virus in the healthy population is affected by antigenicity-dependent substitutions. J Infect Dis. 2016;214:1937–46. https://doi.org/10.1093/infdis/jiw471

24. Pawar SD, Tandale BV, Raut CG, Parkhi SS, Barde TD, Gurav YK, et al. Avian influenza H9N2 seroprevalence among poultry workers in Pune, India, 2010. PLoS One. 2012;7:e36374. https://doi.org/10.1371/journal.pone.0036374

25. Bi Y, Chen Q, Wang Q, Chen J, Jin T, Wong G, et al. Genesis, evolution and prevalence of H5N6 avian influenza viruses in China. Cell Host Microbe. 2016;20:810–21. https://doi.org/10.1016/j.chom.2016.10.022

26. Horby PW, Laurie KL, Cowling BJ, Engelhardt OG, Sturm-Ramirez K, Sanchez JL, et al.; CONSISE Steering Committee. CONSISE statement on the reporting of seroepidemiologic studies for influenza (ROSES-I statement): an extension of the STROBE statement. Influenza Other Respir Viruses. 2017;11:2–14. https://doi.org/10.1111/irv.12411

27. Sun Y, Liu J. H9N2 influenza virus in China: a cause of concern. Protein Cell. 2015;6:18–25. https://doi.org/10.1007/s13238-014-0111-7

28. Wang Q, Ju L, Liu P, Zhou J, Lv X, Li L, et al. Serological and virological surveillance of avian influenza A virus H9N2 subtype in humans and poultry in Shanghai, China, between 2008 and 2010. Zoonoses Public Health. 2015;62:131–40. https://doi.org/10.1111/zph.12133

29. Li X, Tian B, Jianfang Z, Yongkun C, Xiaodan L, Wenfei Z, et al. A comprehensive retrospective study of the seroprevalence of H9N2 avian influenza viruses in occupationally exposed populations in China. PLoS One. 2017;12:e0178328. https://doi.org/10.1371/journal.pone.0178328

30. Yu Q, Liu L, Pu J, Zhao J, Sun Y, Shen G, et al. Risk perceptions for avian influenza virus infection among poultry workers, China. Emerg Infect Dis. 2013;19:313–6. https://doi.org/10.3201/eid1901.120251

31. Li S, Zhou Y, Song W, Pang Q, Miao Z. Avian influenza virus H9N2 seroprevalence and risk factors for infection in occupational poultry-exposed workers in Tai'an of China. J Med Virol. 2016;88:1453–6. https://doi.org/10.1002/jmv.24483

32. World Health Organization. Recommendations and laboratory procedures for detection of avian influenza A(H5N1) virus in specimens from suspected human cases. Geneva: The Organization; 2007. [cited 2019 Aug 12]. https://www.who.int/influenza/resources/documents/h5n1_laboratory_procedures

33. National Bureau of Statistics of China. Statistical Yearbook of China [in Chinese]. Beijing: The Bureau; 2014. [cited 2019 Aug 12]. http://www.stats.gov.cn/tjsj/ndsj/2014/indexch.htm

34. Li Y, Liu M, Sun Q, Zhang H, Zhang H, Jiang S, et al. Genotypic evolution and epidemiological characteristics of H9N2 influenza virus in Shandong Province, China. Poult Sci. 2019;98(9):3488-95. PubMed https://doi.org/10.3382/ps/pez151

35. Ma MJ, Zhao T, Chen SH, Xia X, Yang XX, Wang GL, et al. Avian influenza A virus infection among workers at live poultry markets, China, 2013–2016. Emerg Infect Dis. 2018;24:1246–56. https://doi.org/10.3201/eid2407.172059

36. Khuntirat BP, Yoon IK, Blair PJ, Krueger WS, Chittaganpitch M, Putnam SD, et al. Evidence for subclinical avian influenza virus infections among rural Thai villagers. Clin Infect Dis. 2011; 53:e107–16. https://doi.org/10.1093/cid/cir525

37. Kallewaard NL, Corti D, Collins PJ, Neu U, McAuliffe JM, Benjamin E, et al. Structure and function analysis of an antibody recognizing all influenza A subtypes. Cell. 2016;166:596–608. https://doi.org/10.1016/j.cell.2016.05.073

38. Yuan J, Lau EH, Li K, Leung YH, Yang Z, Xie C, et al. Effect of live poultry market closure on avian influenza A(H7N9) virus activity in Guangzhou, China, 2014. Emerg Infect Dis. 2015;21:1784–93. https://doi.org/10.3201/eid2110.150623

39. Peiris JSM, Cowling BJ, Wu JT, Feng L, Guan Y, Yu H, et al. Interventions to reduce zoonotic and pandemic risks from avian influenza in Asia. Lancet Infect Dis. 2016;16:252–8. https://doi.org/10.1016/S1473-3099(15)00502-2

40. Fournié G, Guitian J, Desvaux S, Cuong VC, Dung H, Pfeiffer DU, et al. Interventions for avian influenza A (H5N1) risk management in live bird market networks. Proc Natl Acad Sci U S A. 2013;110:9177–82. https://doi.org/10.1073/pnas.1220815110

41. Wang D, Yang L, Zhu W, Zhang Y, Zou S, Bo H, et al. Two outbreak sources of influenza A (H7N9) viruses have been established in China. J Virol. 2016;90:5561–73. https://doi.org/10.1128/JVI.03173-15

42. Gao GF. For a better world: Biosafety strategies to protect global health. Biosaf Health. 2019;1(1):1-3. https://doi.org/10.1016/j.bsheal.2019.03.001

43. Tian H, Zhou S, Dong L, Van Boeckel TP, Cui Y, Newman SH, et al. Avian influenza H5N1 viral and bird migration networks in Asia. Proc Natl Acad Sci U S A. 2015;112:172–7. https://doi.org/10.1073/pnas.1405216112

44. Bi Y, Shi W, Chen J, Chen Q, Ma Z, Wong G, et al. CASCIRE surveillance network and work on avian influenza viruses. Sci China Life Sci. 2017;60:1386–91. https://doi.org/10.1007/s11427-017-9251-2

Address for correspondence: George F. Gao or William J. Liu, Chinese Center for Disease Control and Prevention, 155 Changbai Rd, Changping District, Beijing 102206, China; email: gaofu@chinacdc.cn or liujun@ivdc.chinacdc.cn; Hongjie Yu, Fudan University School of Public Health, No. 138 Yixueyuan Rd, Xuhui District, Shanghai, 200032, China; email: yhj@fudan.edu.cn

Genomic Analysis of Fluoroquinolone- and Tetracycline-Resistant *Campylobacter jejuni* Sequence Type 6964 in Humans and Poultry, New Zealand, 2014–2016

Nigel P. French, Ji Zhang, Glen P. Carter, Anne C. Midwinter, Patrick J. Biggs, Kristin Dyet, Brent J. Gilpin, Danielle J. Ingle, Kerry Mulqueen, Lynn E. Rogers, David A. Wilkinson, Sabrina S. Greening, Petra Muellner, Ahmed Fayaz, Deborah A. Williamson

In 2014, antimicrobial drug–resistant *Campylobacter jejuni* sequence type 6964 emerged contemporaneously in poultry from 3 supply companies in the North Island of New Zealand and as a major cause of campylobacteriosis in humans in New Zealand. This lineage, not previously identified in New Zealand, was resistant to tetracycline and fluoroquinolones. Genomic analysis revealed divergence into 2 major clades; both clades were associated with human infection, 1 with poultry companies A and B and the other with company C. Accessory genome evolution was associated with a plasmid, phage insertions, and natural transformation. We hypothesize that the *tetO* gene and a phage were inserted into the chromosome after conjugation, leaving a remnant plasmid that was lost from isolates from company C. The emergence and rapid spread of a resistant clone of *C. jejuni* in New Zealand, coupled with evolutionary change in the accessory genome, demonstrate the need for ongoing *Campylobacter* surveillance among poultry and humans.

Author affiliations: Massey University, Palmerston North, New Zealand (N.P. French, J. Zhang, A.C. Midwinter, P.J. Biggs, L.E. Rogers, D.A. Wilkinson, S.S. Greening, A. Fayaz); New Zealand Food Safety Science and Research Centre, Palmerston North (N.P. French, D.A. Wilkinson); The University of Melbourne, Melbourne, Victoria, Australia (G.P. Carter, D.J. Ingle, D.A. Williamson); Institute of Environmental Science and Research Limited, Christchurch, New Zealand (K. Dyet, B.J. Gilpin); Australian National University, Canberra, Australian Capital Territory, Australia (D.J. Ingle); Poultry Industry Association of New Zealand, Auckland, New Zealand (K. Mulqueen); EPI-interactive, Wellington, New Zealand (P. Muellner)

Campylobacteriosis caused by *Campylobacter jejuni* is one of the most common zoonotic diseases; in many countries, incidence is increasing (*1*). Typically, human infection with *C. jejuni* results in an acute, self-limiting gastroenteritis, and treatment is largely supportive. However, antimicrobial drug treatment is indicated for patients who have invasive infection, have severe and persistent gastroenteritis, or are immunocompromised. The mainstays of therapy are macrolides and fluoroquinolones; however, resistance to these drugs, particularly fluoroquinolones, is common in many parts of the world and precludes their clinical usefulness (*2*).

Among industrialized countries, one of the highest rates of campylobacteriosis is found in New Zealand. In 2017, there were 6,482 notified cases in New Zealand, representing an incidence of ≈150 cases/100,000 population (*3*). The high proportion of cases in New Zealand is thought to result from ingestion of contaminated food, typically undercooked poultry, which has prompted regulatory and voluntary implementation of control measures along the poultry supply chain (*4*).

Poultry production in New Zealand is dominated by 3 major supply companies and several smaller companies. No fresh chicken meat is imported into New Zealand (*5*). Studies in New Zealand have identified dominant multilocus sequence types (STs) of *C. jejuni* associated with poultry from particular companies; the most prevalent ST associated with human cases during 2005–2008, ST474, was predominant in poultry from 1 company (*5–7*). The vertically contained nature of the New Zealand poultry supply, which involves minimal transfer of birds between poultry companies, is considered to be a major contributor to the dominance of particular strains at individual companies (*5*).

In May 2014, a previously unreported *C. jejuni* clone of ST6964, a member of a poultry-associated clonal complex (CC), CC354 (*8*), resistant to fluoroquinolones and tetracyclines, was isolated from poultry carcasses at a *Campylobacter* sentinel surveillance site (*9*) on the North Island of New Zealand. Concurrently, throughout 2014 and 2015, sporadic and outbreak-associated human cases of campylobacteriosis associated with resistant ST6964 were identified across New Zealand. Subsequent cross-sectional studies of poultry and humans suggested that fluoroquinolone resistance in *C. jejuni* had increased from <5% to 19% over 1 year (*10*). The unprecedented rapid emergence and geographic spread of this resistant strain has widespread implications. A marked shift from low to relatively high levels of antimicrobial drug resistance in *Campylobacter* spp. in New Zealand is a concern for food safety and public health. Furthermore, evidence of very rapid spread across the vertically contained poultry companies requires reevaluation of biosecurity measures in the industry. To determine which factors may have contributed to the dissemination of this clone in New Zealand, we undertook a detailed genomic analysis of ST6964 isolates from humans and poultry collected during 2014–2016.

Methods

Ethics Statement
Approval from the Multi-Region Ethics Committee, New Zealand, is provided for work related to the *Campylobacter* sentinel surveillance site (application no. MEC/10/16/EXP). Isolates were collected and analyzed through routine public health investigation activities. The 2006 guidelines from the National Ethics Advisory Committee, Ministry of Health, Wellington, New Zealand, state that these activities do not require ethics committee review.

Setting and Sampling Strategies
The 2014 isolation of antimicrobial drug–resistant *C. jejuni* ST6964 from humans and poultry led to systematic surveys of cases in humans and poultry aimed at determining the extent of spread of this lineage into the food supply and the origin of human cases. During 2014–2016, we collected antimicrobial drug–resistant *C. jejuni* ST6964 isolates from 4 sources. The first source was whole poultry carcasses and fecal samples from humans with campylobacteriosis at the sentinel site from May 1, 2014, through December 31, 2015 (*9*). The second source was a cross-sectional survey of human cases conducted from May 1 through October 31, 2015 (*10*). Five community diagnostic laboratories, covering all major population centers in the North and South Islands, were asked to refer *C. jejuni* isolates from humans to the Institute of Environmental Science and Research Ltd (ESR),

Wellington, New Zealand, for the survey. The third source was samples submitted directly to ESR from humans with antimicrobial drug–resistant campylobacteriosis. The fourth source was 2 cross-sectional studies of pooled cecal samples from slaughtered poultry from the major companies (Appendix Figure 1, https://wwwnc.cdc.gov/EID/article/25/12/19-0267-App1.pdf). A total of 227 isolates were included in the analysis.

Microbiological Testing
We isolated *C. jejuni* from whole poultry carcasses and fecal samples from humans at the sentinel site as described previously (*11*). Isolates from pooled cecal samples came from swab samples taken from the pooled ceca of 5 chickens that were from the same poultry shed and slaughtered in a commercial poultry factory. Swabs in Amies with charcoal transport media (Copan, https://www.copangroup.com) were transported chilled to ᵐEpiLab (Massey University, Palmerston North, New Zealand) for microaerobic culture at 42°C in a microaerobic incubator (Don Whitley Scientific, https://www.dwscientific.com) on modified charcoal cefoperazone deoxycholate agar (mCCDA; Fort Richard, https://www.fortrichard.com) and mCCDA-cip/tet (LabM Ltd., http://www.labm.com) containing 1 μg/mL ciprofloxacin and 4 μg/mL tetracycline (Sigma-Aldrich, https://www.sigmaaldrich.com). We subcultured colonies that resembled *C. jejuni* on the mCCDA-cip/tet plates onto Columbia horse blood agar plates (Fort Richard) and incubated them microaerobically at 42°C. All isolates from poultry carcasses and human fecal samples and a subset of those isolated from mCCDA-cip/tet from pooled chicken ceca were speciated by PCR (*12*). We determined susceptibility to ciprofloxacin and tetracycline according to Clinical and Laboratory Standards Institute (CLSI) methods, by using disk diffusion (*13*).

For human clinical isolates from the cross-sectional survey and direct submissions to ESR, we determined susceptibility to ciprofloxacin, erythromycin, and tetracycline by using the methods described by the CLSI, with either Etests or disk diffusion (13). Tests were performed on Mueller-Hinton agar with 5% sheep blood and incubated microaerobically at 36°C–37°C for 48 h. We interpreted MICs according to CLSI breakpoints (13) and disk-diffusion results according to European Committee on Antimicrobial Susceptibility Testing clinical breakpoints (14). We subtyped *C. jejuni* isolates from humans and fresh chicken carcasses and a subset of those from pooled chicken ceca by multilocus sequence typing (MLST) (15) as described (11).

Whole-Genome Sequencing
For Illumina sequencing, we extracted genomic DNA from bacterial isolates on a JANUS automated workstation (PerkinElmer, https://www.perkinelmer.com) by

using Chemagic magnetic bead technology, according to the manufacturer's instructions. We prepared DNA libraries by using a NexteraXT DNA preparation kit (Illumina, https://www.illumina.com) and performed 2 × 100 bp sequencing on the NextSeq 500 platform (Illumina), as previously described (*16*). Four representative *C. jejuni* isolates also underwent whole-genome sequencing on the Pacific Biosciences, Inc., RS II platform (https://www.pacb.com). For this, genomic DNA was extracted from overnight cultures by using the Genelute bacterial genomic DNA kit (Sigma Aldrich). DNA libraries were prepared according to the 20 kb Template Preparation using the BluePippin DNA Size Selection system protocol (Pacific Biosciences, Inc). Sequence data are available from GenBank BioProject ID PRJNA520992 and PubMLST (https://pubmlst.org/campylobacter) nos. 70207–12, 70229, 70230, 70232, 70233, 70252, 70253, and 78631–845.

Genome Assembly

For processing and quality control of the Illumina reads, we used QCtool pipeline (https://github.com/mtruglio/QCtool). To assemble the processed reads, we used the SPAdes genome assembler version 3.12.0 (*17*).

Whole-Genome MLST Phylogeny

To define whole-genome MLST allelic profiles, we used Fast Genome Profiler (Fast-GeP, https://github.com/jizhang-nz/fast-GeP) (*18*) and the complete chromosome sequence of isolate 15AR0984 (generated in this study) as a reference. Phylogenetic relationships were displayed as NeighborNets by using SplitsTree 4 (*19*). The whole-genome polymorphic sites–based phylogeny was inferred from the concatenated sequences of the coding sequences shared by all the whole-genome sequences. We predicted and eliminated all regions with elevated densities of base substitutions and reconstructed the phylogenetic relationship of the remaining recombination-free sequences by using Gubbins version 2.3.4 with the default settings (*20*). We further examined the relationship by using the 1,343 genes in the *C. jejuni* core-genome MLST scheme version 1.0 (*21*) on the *Campylobacter* PubMLST website (https://pubmlst.org/campylobacter).

Single-Nucleotide Polymorphism Phylogeny

We mapped 227 genomes to complete chromosome reference 15AR0984 (completed with PacBio sequencing, https://www.pacb.com) by using Snippy version 4.3.5 with mincov (the minimum number of reads covering a site to be considered) of 10 and minfrac (the minimum proportion of those reads that must differ from the reference) of 0.9 (https://github.com/tseemann/snippy). We filtered the resulting single-nucleotide polymorphism (SNP) alignment for recombination by using Gubbins (*20*), allowing for 50 iterations and specifying the weighted Robinson-Foulds convergence method. We extracted core SNPs by using SNP sites (*22*), giving a final total of 70 SNPs in the core genome. We then used the filtered alignment as input for IQtree (*23,24*) along with a general time reversible plus gamma 4 model, constant sites (606841, 268757, 264881, 606654), ultrafast bootstrapping with 1,000 replicates, and the SH-aLRT parameter with 1,000 bootstrap replicates to infer phylogenetic structure. We visualized the phylogeny in R (https://www.r-project.org) by using the package *ggtree* (*25*). We investigated pairwise SNP distances by using HarrietR (https://github.com/andersgs/harrietr). We visualized the recombination regions detected in the 227 genomes from Gubbins (*20*) by using Phandango (*26*) and annotated the reference chromosome 15AR0984 using Prokka version 1.13 (*27*).

Comparative Genomics of Mobile Elements

The reference genome 15AR0984 contained a plasmid (15AR0984-m) that was 43,680-bp long. We calculated the likelihood of this plasmid and other chromosomally integrated mobile elements being in each of the 227 genomes by using a method described previously (*28*). We considered the mobile elements CJIE1, CJIE2, CJIE3, and CJIE4 from the reference genome RM1221 (*29*) and a variant of CJIE1, named CJIE1v, which was also present in the reference genome 15AR0984. We plotted these data against the inferred phylogenetic tree in R by using *ggtree* (*25*). We examined the locations of chromosomally integrated mobile elements in the 4 PacBio complete genomes (15AR0984, 15AR0917, 15AR0919, and 15AR1555) and the reference strain RM1221 by using Mauve (*30*) and BLAST Ring Image Generator (*31*).

To find closely related plasmids to 15AR0984-m, we used the complete sequence as a query to BLAST (https://blast.ncbi.nlm.nih.gov/Blast.cgi) against the GenBank Nucleotide collection (nr/nt) database. We performed phylogenetic analyses of the most similar plasmids (Appendix Table 1) by using the whole-genome MLST method described and using the 15AR0984-m plasmid as the reference and presented as a NeighborNet using SplitsTree (*19*).

Results

Rapid Emergence of *C. jejuni* ST-6964 in Humans and Poultry

C. jejuni ST6964 with dual resistance to ciprofloxacin and tetracycline was first identified through sentinel surveillance in May 2014 in 2 retail poultry carcasses sampled in Palmerston North, Manawatu, New Zealand. The only other members of CC354 identified in the country to date are at least 2 locus variants of ST6964, according to the 7-gene

MLST scheme, and only 1 other ST-6964 isolate has been reported outside of New Zealand, originating from China (https://pubmlst.org/campylobacter).

By July 2014, *C. jejuni* ST6964 had been identified in 3 poultry companies, and by August 2014, the first human case was observed at the sentinel site. A total of 3 (1.8%) of 165 human cases at the sentinel site were identified as being caused by ST6964 in 2014 and 4 (3.3%) of 122 human cases in 2015. A total of 10 (13.9%) of 72 retail poultry carcasses at the sentinel site were positive for ST6964 in 2014 and 25 (34.7%) of 72 in 2015. A total of 41 isolates from unique samples (7 human and 34 poultry) from the sentinel site underwent whole-genome sequencing and were included in this study.

In light of findings from the sentinel site, ESR conducted a national survey of antimicrobial-resistant *C. jejuni* in human patients in New Zealand during May–October 2015 (*10*). A total of 297 isolates were referred from 5 clinical laboratories: 3 in the North Island and 2 in the South Island. This survey provided 22 of the *C. jejuni* ST6964 isolates included in this study; 21 were from patients in the North Island and 1 was from a patient in the South Island. In addition to the survey, another 28 isolates from human patients on the North Island were included in this study from samples submitted directly to ESR from diagnostic laboratories.

To assess the extent of spread of *C. jejuni* ST6964 in poultry, we undertook 2 systematic surveys of poultry carcasses from slaughter plants servicing poultry companies A–D. Only samples from companies A, B, and C, which

are based in the North Island, were positive for this ST; these companies accounted for 136 of the isolates included in this study.

All sequenced *C. jejuni* ST6964 isolates were confirmed as phenotypically resistant to ciprofloxacin and tetracycline. All tetracycline-resistant ST6964 isolates harbored the *tetO* gene, which was located at a previously described insertion site, between the *kdsB* and CJE0905 genes (*32*). The C257T (Thr86Ile) mutation in *gyrA*, associated with fluoroquinolone resistance (*33*), was present in all ciprofloxacin-resistant isolates.

Relationship between Core Genomes of *C. jejuni* ST6964 from Humans and Poultry

We used 3 complementary approaches to assess relatedness of human and poultry isolates: whole-genome MLST using Fast-GeP (*18*), core-genome MLST using the *Campylobacter* PubMLST scheme (*21*), and SNP-based phylogeny. Fast-GeP analysis found 1,363 complete coding sequences that were single copy and shared by all 227 isolates. Most of the loci were identical across isolates (n = 1,163 loci), and NeighborNet distances and a NeighborNet network revealed 2 clades, 1 associated with poultry companies A and B and 1 with company C. A similar relationship was evident after removal of hypothetical recombination regions (Figure 1; Appendix Table 2). A similar NeighborNet profile and distribution among poultry companies resulted from the core-genome MLST results (Appendix Figure 2); 954 of the loci were identical and 389 were polymorphic.
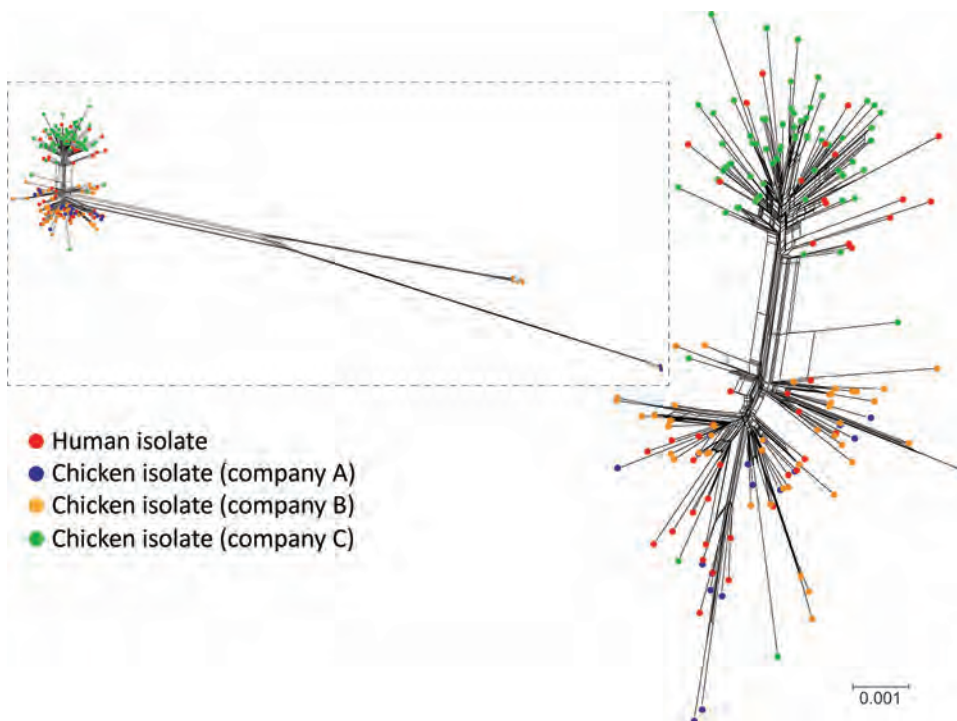
Figure 1. NeighborNet phylogenies generated from the allele profiles identified in the whole-genome multilocus sequence typing analysis of 227 sequence type 6964 *Campylobacter jejuni* isolates from humans and poultry, New Zealand, 2014–2016. The corrected NeighborNet network was generated after eliminating the 87 loci that were identified in predicted recombinant regions (Appendix Table 1, https://wwwnc.cdc.gov/EID/article/25/12/19-0267-App1.pdf). Inset shows the uncorrected NeighborNet network, generated with the original 1,363-loci allele profiles. Scale bar indicates the whole-genome multilocus sequence typing distance, which represents the number of allelic differences per shared locus.

We constructed an SNP-based phylogeny after removal of recombinant regions (Figure 2) and identified recombinant block and associated genes (Appendix Table 1, Figure 3). We found a maximum of 13 SNPs between any single pair of isolates in the 70 shared-SNP loci present in non-recombinant regions. The lower genetic diversity between isolates in the SNP analysis compared with the allele-based analysis was attributable to the removal of insertion and deletion mutations and loci subject to recombination. In the SNP analysis, isolates were again segregated into distinct clades strongly associated with poultry companies and carriage of mobile elements (Figure 2). Isolates from humans admixed with isolates from poultry in all clades, suggesting that the human infections were linked to poultry from all supply companies.

Plasmid Sequences Associated with Distinct ST6964 Lineages

We identified high mobile element likelihood scores (>90) for plasmid 15AR0984-m in 131 (58%) of the isolates. Plasmid sequences were strongly associated with the core phylogeny and 2 of the 3 poultry companies, A and B (Figure 2). Plasmid 15AR0984-m showed high sequence and structural similarities with other previously described *tetO* carrying pTet plasmids and shares the same backbone as *tetO* plasmids pcjDM, S3, and pRM4661 (Figure 3; Appendix Table 1, Figure 4).

The plasmid 15AR0984-m was most closely related to the *tetO* megaplasmid pcjDM (Appendix Figure 4), which also contains a prophage (*34*) that shows sequence homology with integrated elements found in multiple ST6964
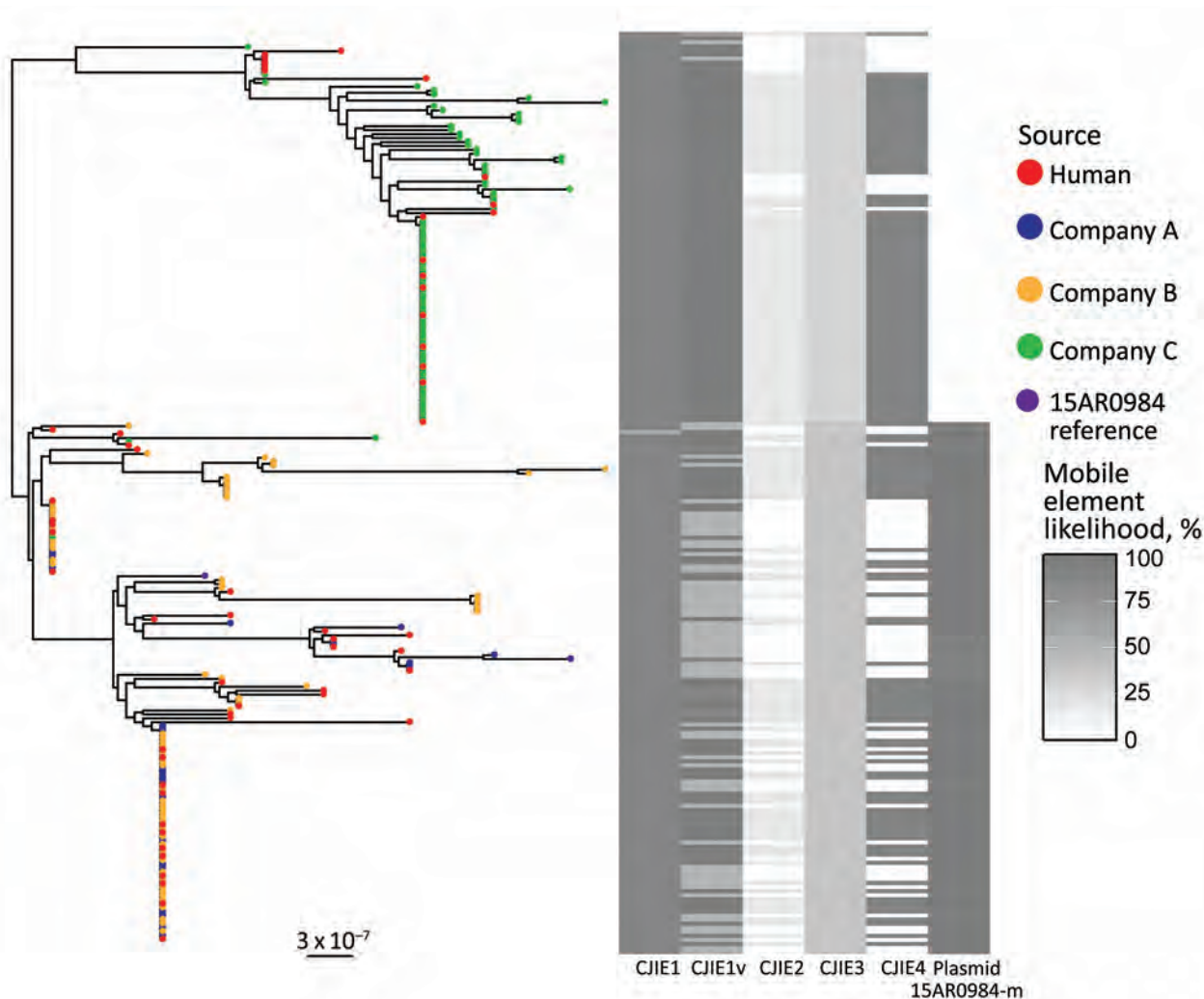
Figure 2. Population structure of 227 sequence type 6964 *Campylobacter jejuni* isolates from humans and poultry, New Zealand, 2014–2016. The tree is the inferred midpoint rooted phylogeny of the isolates, including the reference 15AR0984 genome. The tips are colored by source of the *C. jejuni* isolate. The heatmap indicates the likelihoods of the presence of mobile elements including CJIE1 variant (cjie1_15AR0984), CJIEs 1–4, and the plasmid 15AR0984-m. Dark shading on the heatmap indicates 100% likelihood; white indicates absence. Scale bar indicates nucleotide substitutions per site.
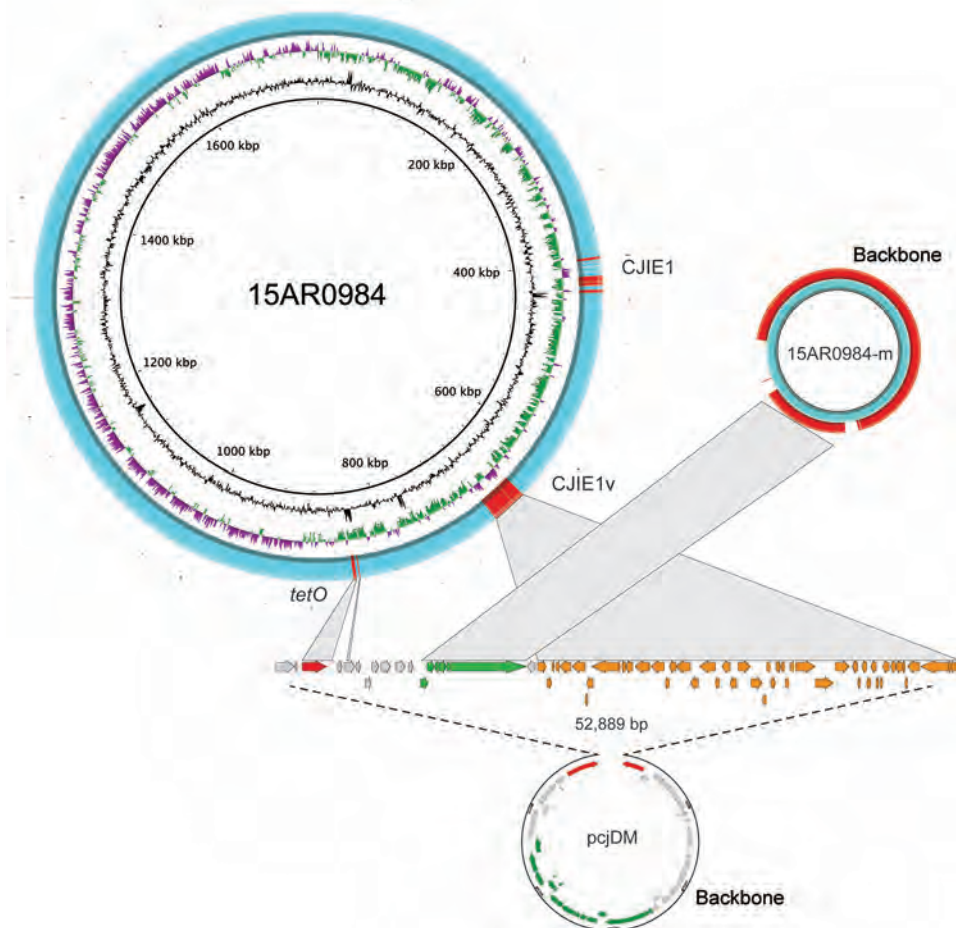
Figure 3. Genome structures of the complete *Campylobacter jejuni* strain 15AR0984 chromosome and plasmid (15AR0984-m) isolated from humans and poultry, New Zealand, 2014–2016, compared with the closest plasmid (pcjDM) sequence found in GenBank. High-scoring segment pairs between the 15AR0984 genome and the plasmid pcjDM ware connected with gray bars to illustrate the similar shared regions except for the backbone regions, which were highly conserved across the pTet-like plasmid genomes.

isolates. These elements are labeled CJIE1 and CJIE1v (a variant of CJIE1), and the latter was most similar to the prophage in plasmid pcjDM. Both prophage integrated elements bear similarities to integrated element CJIE1 identified in *C. jejuni* isolate RM1221 (*29,35*). All but 1 isolate (H2239a) contained CJIE1, and all were identified at the same location in the chromosome of the 4 isolates sequenced with PacBio. In contrast, 71% (162/227) of the isolates contained CJIE1v, as did 3 of the 4 complete genomes (15AR0984, 15AR0919, and 15AR1555). Although CJIE1 was located at the same chromosomal position in all 4 complete genomes, CJIE1v was located at a different position in the chromosome of 3 of the 4 that contained this mobile element (Appendix Figure 5).

In addition to the 2 CJIE1-like elements, 65% (148/227) of genomes showed evidence of a previously described integrated element CJIE4 (*29*), located in the same chromosomal location in 2 of 4 complete genomes (15AR0984 and 15AR0919) and the reference genome *C. jejuni* RM1221 (*29*) (Appendix Figure 6). CJIE4 was identified in isolates from all poultry companies and in 26 of 57 isolates from humans. The *dns* gene (CJE0256), encoding for an extracellular desoxyribonuclease, was carried in CJIE1 in all but 1 of our isolates (H2239a). However, none of the CJIE1v elements contained the *dns* gene (CJE0256). Although 149 of 227 *C. jejuni* ST6964 isolates carried CJIE4, none of the CJIE4 elements had the DNA/RNA nonspecific endonuclease gene (CJE1441) present in the CJIE4 element of strain RM1221.

Discussion

Data from the 4 sources, (i.e., sentinel surveillance, human case survey, direct submission of samples from humans, and samples from poultry) demonstrated rapid emergence of a resistant lineage of *C. jejuni* among isolates from humans and poultry in New Zealand from 2014 on, indicating how rapidly national levels of resistance can change through the introduction of a successful bacterial clone. Despite high rates of campylobacteriosis in New Zealand, rates of *C. jejuni* antimicrobial drug resistance have been considered extremely low; during 2000–2013, prevalence of fluoroquinolone resistance in *Campylobacter* spp. isolated from humans was reportedly <6% (*36*). During 2005–2006, no resistance to tetracyclines or fluoroquinolones was found in 193 *C. jejuni* isolates from poultry (*37*); a 2009 systematic survey of

antimicrobial drug resistance in animal (calves and poultry) isolates of *C. jejuni* found no resistance to erythromycin, 0.3% resistance to tetracycline, and only 2.3% resistance to fluoroquinolones (*38*). The emergence of this lineage is unlikely to be the result of fluoroquinolone use in the food chain because the poultry industry in New Zealand does not use fluoroquinolones (*39,40*).

Our data demonstrate the utility of systematic phenotypic surveillance of antimicrobial drug resistance in *C. jejuni,* which is becoming increasingly necessary as laboratories adopt routine culture-independent diagnostic testing for enteric pathogens. The use of phenotypic surveillance is particularly relevant for *Campylobacter*, for which culture-independent diagnostic testing is replacing culture-based diagnosis in many settings (*41,42*). Although recent whole-genome sequencing–based work demonstrated good concordance between antimicrobial-resistance genotype and phenotype in *Campylobacter* spp. (*43*), uncharacterized mutations are unlikely to be detected and isolates are still required for whole-genome sequencing analysis. To ensure ongoing culture capability and the capacity to undertake periodic phenotypic antimicrobial-resistance testing, close liaison between clinical and public health laboratories is needed.

Both the *tetO* gene and the prophage-integrated element CJIE1v may have originated on the remnant plasmid and been inserted into the genome of ST6964. One possible scenario is that the common ancestor of ST6964 acquired a plasmid similar to megaplasmid pcjDM, which carried the *tetO* gene and a phage. Under this scenario, the *tetO* gene was then inserted into the genome at a single site and the phage element was inserted into multiple sites, leaving the remnant plasmid with the backbone minus the *tetO* and CJIE1v sequences. We propose that the remnant plasmid was then lost from a common ancestor of isolates in poultry company C (Figure 3).

Although the *tetO* flanking genes in the chromosome differ from the *tetO* cargo in megaplasmid pcjDM, evidence that these came from the plasmid comes from isolate 15AR1747, which contains additional chromosomal genes adjacent to the *tetO* sequence that are identical to those found in the remnant plasmid of all other plasmid-bearing *C. jejuni* ST6964 isolates. Furthermore, these genes are absent from the smaller remnant plasmid identified in 15AR1747 (Appendix Figure 6).

Both CJIE1 and CJIE4 are prophages (*29*). CJIE1 has been associated with increased adherence and invasion (*44*) and differences in protein expression under different conditions (*45*). The multiple locations of prophage-integrated element CJIE1 has been identified in previous studies (*29*). Previous studies have shown that both CJIE1 and CJIE4 encode nucleases that hydrolyze DNA and inhibit natural transformation (*46,47*). Prophage-integrated elements in addition to the plasmid may have played some role in the evolution of ST6964 in New Zealand, potentially stabilizing lineages by reducing transformability (*47*); however, what may have influenced their frequency and distribution among poultry companies and hosts is unclear.

Conclusions

The emergence of antimicrobial-drug resistant *C. jejuni* ST6964 in New Zealand poultry and transmission to humans via the food chain underlines the role of the fresh poultry supply as a source of human cases of campylobacteriosis and how rapidly new clones can evolve and spread. We provide evidence that this clone has undergone rapid evolution in New Zealand through multiple mechanisms, including mutations/substitutions, conjugation, natural transformation, and the incorporation of prophages into the chromosome. Given its speed of emergence and its spread across vertically integrated poultry companies, it is imperative that ongoing periodic surveillance of antimicrobial drug resistance in *Campylobacter* and other relevant bacterial pathogens is supported by government agencies to better track the emergence and possible further spread of resistance in New Zealand. This surveillance includes gathering information at the farm level to determine the relative roles of different transmission pathways that could account for spread within and between poultry companies.

Ongoing work indicates that *C. jejuni* ST6964 is persisting in the poultry supply and continuing to make a considerable contribution to the country's disease burden. This finding has implications for the use of antimicrobial drugs; for example, fluoroquinolones are likely to be ineffective for treatment of severe and invasive campylobacteriosis. To control and mitigate the spread of this clone, appropriate source control measures and increased public awareness of appropriate food hygiene should be considered by the government and the poultry industry, along with the development of rapid, less costly diagnostic assays, which could be facilitated by data derived from whole-genome sequencing.

About the Author

Dr. French is chief scientist of the New Zealand Food Safety Science and Research Centre and chair of Food Safety and Veterinary Public Health at Massey University, New Zealand. He is also co-director of One Health Aotearoa and executive director of the Infectious Disease Research Centre at Massey University.

References

1. Kaakoush NO, Castaño-Rodríguez N, Mitchell HM, Man SM. Global epidemiology of *Campylobacter* infection. Clin Microbiol Rev. 2015;28:687–720. https://doi.org/10.1128/CMR.00006-15

2. Sproston EL, Wimalarathna HML, Sheppard SK. Trends in fluoroquinolone resistance in *Campylobacter*. Microb Genom. 2018;4. https://doi.org/10.1099/mgen.0.000198

3. The Institute of Environmental Science and Research Ltd. Notifiable diseases in New Zealand: annual report 2017 [cited 2019 Oct 9]. https://surv.esr.cri.nz/surveillance/annual_surveillance.php

4. Sears A, Baker MG, Wilson N, Marshall J, Muellner P, Campbell DM, et al. Marked campylobacteriosis decline after interventions aimed at poultry, New Zealand. Emerg Infect Dis. 2011;17:1007–15. https://doi.org/10.3201/eid1706.101272

5. Müllner P, Collins-Emerson JM, Midwinter AC, Carter P, Spencer SE, van der Logt P, et al. Molecular epidemiology of *Campylobacter jejuni* in a geographically isolated country with a uniquely structured poultry industry. Appl Environ Microbiol. 2010;76:2145–54. https://doi.org/10.1128/AEM.00862-09

6. McTavish SM, Pope CE, Nicol C, Sexton K, French N, Carter PE. Wide geographical distribution of internationally rare *Campylobacter* clones within New Zealand. Epidemiol Infect. 2008;136:1244–52. https://doi.org/10.1017/S0950268807009892

7. Mullner P, Spencer SEF, Wilson DJ, Jones G, Noble AD, Midwinter AC, et al. Assigning the source of human campylobacteriosis in New Zealand: a comparative genetic and epidemiological approach. Infect Genet Evol. 2009;9:1311–9. https://doi.org/10.1016/j.meegid.2009.09.003

8. Sheppard SK, Cheng L, Méric G, de Haan CP, Llarena A-K, Marttinen P, et al. Cryptic ecology among host generalist *Campylobacter jejuni* in domestic animals. Mol Ecol. 2014;23:2442–51. https://doi.org/10.1111/mec.12742

9. Bolwell CF, Gilpin BJ, Campbell D, French NP. Evaluation of the representativeness of a sentinel surveillance site for campylobacteriosis. Epidemiol Infect. 2015;143:1990–2002. https://doi.org/10.1017/S0950268814003173

10. Williamson D, Dyet K, Heffernan H. Antimicrobial resistance in human isolates of *Campylobacter jejuni*, 2015 [cited 2019 Oct 9]. https://surv.esr.cri.nz/PDF_surveillance/Antimicrobial/CAMPY/CampyFQRfinalreport2015.pdf

11. Nohra A, Grinberg A, Midwinter AC, Marshall JC, Collins-Emerson JM, French NP. Molecular epidemiology of *Campylobacter coli* strains isolated from different sources in New Zealand between 2005 and 2014. Appl Environ Microbiol. 2016;82:4363–70. https://doi.org/10.1128/AEM.00934-16

12. Wang G, Clark CG, Taylor TM, Pucknell C, Barton C, Price L, et al. Colony multiplex PCR assay for identification and differentiation of *Campylobacter jejuni, C. coli, C. lari, C. upsaliensis,* and *C. fetus* subsp. *fetus*. J Clin Microbiol. 2002;40:4744–7. https://doi.org/10.1128/JCM.40.12.4744-4747.2002

13. Clinical and Laboratory Standards Institute. Methods for antimicrobial dilution and disk susceptibility testing of infrequently isolated or fastidious bacteria, 3rd edition (M45). Wayne (PA): The Institute; 2016.

14. The European Committee on Antimicrobial Susceptibility Testing. Breakpoint tables for interpretation of MICs and zone diameters. Version 5.0. 2015 [cited 2018 Oct 10]. http://www.eucast.org/fileadmin/src/media/PDFs/EUCAST_files/Breakpoint_tables/v_5.0_Breakpoint_Table_01.pdf

15. Dingle KE, McCarthy ND, Cody AJ, Peto TE, Maiden MC. Extended sequence typing of *Campylobacter* spp., United Kingdom. Emerg Infect Dis. 2008;14:1620–2. https://doi.org/10.3201/eid1410.071109

16. Baines SL, Howden BP, Heffernan H, Stinear TP, Carter GP, Seemann T, et al. Rapid emergence and evolution of *Staphylococcus aureus* clones harboring *fusC*-containing staphylococcal cassette chromosome elements. Antimicrob Agents Chemother. 2016;60:2359–65. https://doi.org/10.1128/AAC.03020-15

17. Bankevich A, Nurk S, Antipov D, Gurevich AA, Dvorkin M, Kulikov AS, et al. SPAdes: a new genome assembly algorithm and its applications to single-cell sequencing. J Comput Biol. 2012;19:455–77. https://doi.org/10.1089/cmb.2012.0021

18. Zhang J, Xiong Y, Rogers L, Carter GP, French N. Genome-by-genome approach for fast bacterial genealogical relationship evaluation. Bioinformatics. 2018;34:3025–7. https://doi.org/10.1093/bioinformatics/bty195

19. Huson DH, Bryant D. Application of phylogenetic networks in evolutionary studies. Mol Biol Evol. 2006;23:254–67. https://doi.org/10.1093/molbev/msj030

20. Croucher NJ, Page AJ, Connor TR, Delaney AJ, Keane JA, Bentley SD, et al. Rapid phylogenetic analysis of large samples of recombinant bacterial whole genome sequences using Gubbins. Nucleic Acids Res. 2015;43:e15. https://doi.org/10.1093/nar/gku1196

21. Cody AJ, Bray JE, Jolley KA, McCarthy ND, Maiden MCJ. Core genome multilocus sequence typing scheme for stable, comparative analyses of *Campylobacter jejuni* and *C. coli* human disease isolates. J Clin Microbiol. 2017;55:2086–97. https://doi.org/10.1128/JCM.00080-17

22. Page AJ, Taylor B, Delaney AJ, Soares J, Seemann T, Keane JA, et al. *SNP-sites*: rapid efficient extraction of SNPs from multi-FASTA alignments. Microb Genom. 2016;2:e000056. https://doi.org/10.1099/mgen.0.000056

23. Nguyen LT, Schmidt HA, von Haeseler A, Minh BQ. IQ-TREE: a fast and effective stochastic algorithm for estimating maximum-likelihood phylogenies. Mol Biol Evol. 2015;32:268–74. https://doi.org/10.1093/molbev/msu300

24. Minh BQ, Nguyen MA, von Haeseler A. Ultrafast approximation for phylogenetic bootstrap. Mol Biol Evol. 2013;30:1188–95. https://doi.org/10.1093/molbev/mst024

25. Yu G, Lam TT, Zhu H, Guan Y. Two methods for mapping and visualizing associated data on phylogeny using *ggtree*. Mol Biol Evol. 2018;35:3041–3. https://doi.org/10.1093/molbev/msy194

26. Hadfield J, Croucher NJ, Goater RJ, Abudahab K, Aanensen DM, Harris SR. Phandango: an interactive viewer for bacterial population genomics. Bioinformatics. 2017. [Epub ahead of print].

27. Seemann T. Prokka: rapid prokaryotic genome annotation. Bioinformatics. 2014;30:2068–9. https://doi.org/10.1093/bioinformatics/btu153

28. Llarena A-K, Zhang J, Vehkala M, Välimäki N, Hakkinen M, Hänninen M-L, et al. Monomorphic genotypes within a generalist lineage of *Campylobacter jejuni* show signs of global dispersion. Microb Genom. 2016;2:e000088. https://doi.org/10.1099/mgen.0.000088

29. Parker CT, Quiñones B, Miller WG, Horn ST, Mandrell RE. Comparative genomic analysis of *Campylobacter jejuni* strains reveals diversity due to genomic elements similar to those present in *C. jejuni* strain RM1221. J Clin Microbiol. 2006;44:4125–35. https://doi.org/10.1128/JCM.01231-06

30. Darling AC, Mau B, Blattner FR, Perna NT. Mauve: multiple alignment of conserved genomic sequence with rearrangements. Genome Res. 2004;14:1394–403. https://doi.org/10.1101/gr.2289704

31. Alikhan NF, Petty NK, Ben Zakour NL, Beatson SA. BLAST Ring Image Generator (BRIG): simple prokaryote genome comparisons. BMC Genomics. 2011;12:402. https://doi.org/10.1186/1471-2164-12-402

32. Poly F, Read TD, Chen YH, Monteiro MA, Serichantalergs O, Pootong P, et al. Characterization of two *Campylobacter jejuni* strains for use in volunteer experimental-infection studies. Infect Immun. 2008;76:5655–67. https://doi.org/10.1128/IAI.00780-08

33. Wang Y, Huang WM, Taylor DE. Cloning and nucleotide sequence of the *Campylobacter jejuni gyrA* gene and characterization of quinolone resistance mutations. Antimicrob Agents Chemother. 1993;37:457–63. https://doi.org/10.1128/AAC.37.3.457

34. Marasini D, Fakhr MK. Whole-genome sequencing of a *Campylobacter jejuni* strain isolated from retail chicken meat

reveals the presence of a megaplasmid with Mu-like prophage and multidrug resistance genes. Genome Announc. 2016;4:e00460-16. https://doi.org/10.1128/genomeA.00460-16

35. Fouts DE, Mongodin EF, Mandrell RE, Miller WG, Rasko DA, Ravel J, et al. Major structural differences and novel potential virulence mechanisms from the genomes of multiple *Campylobacter* species. PLoS Biol. 2005;3:e15. https://doi.org/10.1371/journal.pbio.0030015

36. The Institute of Environmental Science and Research Ltd. General antimicrobial susceptibility data collected from hospital and community laboratories [cited 2018 Aug 1]. https://surv.esr.cri.nz/antimicrobial/general_antimicrobial_susceptibility.php

37. Pleydell EJ, Rogers L, Kwan E, French NP. Low levels of antibacterial drug resistance expressed by Gram-negative bacteria isolated from poultry carcasses in New Zealand. N Z Vet J. 2010;58:229–36. https://doi.org/10.1080/00480169.2010.69297

38. Heffernen H, Wong T, Lindsay J, Bowen B, Woodhouse R. A baseline survey of antimicrobial resistance in bacteria from selected New Zealand foods, 2009–2010 [cited 2019 Oct 9]. https://www.mpi.govt.nz/dmsdocument/21464-a-baseline-survey-of-antimicrobial-resistance-in-bacteria-from-selected-new-zealand-foods-2009-2010

39. New Zealand Food Safety. Antibiotic sales analysis 2014–2016. Technical paper no. 2018/08 [cited 2019 Oct 9]. https://www.fisheries.govt.nz/dmsdocument/31920/direct

40. Ministry for Primary Industries. 2011–2014 Antibiotic Sales Analysis. MPI technical paper no. 2016/65 [cited 2019 Oct 9]. https://www.mpi.govt.nz/dmsdocument/14497-2011-2014-antibiotic-sales-analysis

41. Huang JY, Henao OL, Griffin PM, Vugia DJ, Cronquist AB, Hurd S, et al. Infection with pathogens transmitted commonly through food and the effect of increasing use of culture-independent diagnostic tests on surveillance—Foodborne Diseases Active Surveillance Network, 10 U.S. Sites, 2012–2015. MMWR Morb Mortal Wkly Rep. 2016;65:368–71. https://doi.org/10.15585/mmwr.mm6514a2

42. May FJ, Stafford RJ, Carroll H, Robson JM, Vohra R, Nimmo GR, et al. The effects of culture independent diagnostic testing on the diagnosis and reporting of enteric bacterial pathogens in Queensland, 2010 to 2014. Commun Dis Intell Q Rep. 2017;41:E223–30.

43. Whitehouse CA, Young S, Li C, Hsu CH, Martin G, Zhao S. Use of whole-genome sequencing for *Campylobacter* surveillance from NARMS retail poultry in the United States in 2015. Food Microbiol. 2018;73:122–8. https://doi.org/10.1016/j.fm.2018.01.018

44. Clark CG, Grant CC, Pollari F, Marshall B, Moses J, Tracz DM, et al. Effects of the *Campylobacter jejuni* CJIE1 prophage homologs on adherence and invasion in culture, patient symptoms, and source of infection. BMC Microbiol. 2012;12:269. https://doi.org/10.1186/1471-2180-12-269

45. Clark CG, Chong PM, McCorrister SJ, Simon P, Walker M, Lee DM, et al. The CJIE1 prophage of *Campylobacter jejuni* affects protein expression in growth media with and without bile salts. BMC Microbiol. 2014;14:70. https://doi.org/10.1186/1471-2180-14-70

46. Gaasbeek EJ, Wagenaar JA, Guilhabert MR, van Putten JP, Parker CT, van der Wal FJ. Nucleases encoded by the integrated elements CJIE2 and CJIE4 inhibit natural transformation of *Campylobacter jejuni*. J Bacteriol. 2010;192:936–41. https://doi.org/10.1128/JB.00867-09

47. Gaasbeek EJ, Wagenaar JA, Guilhabert MR, Wösten MM, van Putten JP, van der Graaf-van Bloois L, et al. A DNase encoded by integrated element CJIE1 inhibits natural transformation of *Campylobacter jejuni*. J Bacteriol. 2009;191:2296–306. https://doi.org/10.1128/JB.01430-08

Address for correspondence: Nigel P. French, Massey University, New Zealand Food Safety Science and Research Centre, Hopkirk Institute, Palmerston North 4410, New Zealand; email n.p.french@massey.ac.nz

Streptococcus suis–Associated Meningitis, Bali, Indonesia, 2014–2017

Ni Made Susilawathi, Ni Made Adi Tarini, Ni Nengah Dwi Fatmawati, Putu I.B. Mayura,
Anak Agung Ayu Suryapraba, Made Subrata, Anak Agung Raka Sudewi, Gusti Ngurah Mahardika

Medscape EDUCATION ACTIVITY

In support of improving patient care, this activity has been planned and implemented by Medscape, LLC and Emerging Infectious Diseases. Medscape, LLC is jointly accredited by the Accreditation Council for Continuing Medical Education (ACCME), the Accreditation Council for Pharmacy Education (ACPE), and the American Nurses Credentialing Center (ANCC), to provide continuing education for the healthcare team.

Medscape, LLC designates this Journal-based CME activity for a maximum of 1.00 **AMA PRA Category 1 Credit(s)™**. Physicians should claim only the credit commensurate with the extent of their participation in the activity.

Successful completion of this CME activity, which includes participation in the evaluation component, enables the participant to earn up to 1.0 MOC points in the American Board of Internal Medicine's (ABIM) Maintenance of Certification (MOC) program. Participants will earn MOC points equivalent to the amount of CME credits claimed for the activity. It is the CME activity provider's responsibility to submit participant completion information to ACCME for the purpose of granting ABIM MOC credit.

All other clinicians completing this activity will be issued a certificate of participation. To participate in this journal CME activity: (1) review the learning objectives and author disclosures; (2) study the education content; (3) take the post-test with a 75% minimum passing score and complete the evaluation at http://www.medscape.org/journal/eid; and (4) view/print certificate. For CME questions, see page 2355.

Release date: November 15, 2019; Expiration date: November 15, 2020

Learning Objectives

Upon completion of this activity, participants will be able to:

- Describe the epidemiology and clinical signs of *Streptococcus suis* meningitis, according to a case series in Bali, Indonesia

- Determine laboratory findings and microbiology of *S. suis* meningitis, according to a case series in Bali, Indonesia

- Identify clinical and public health implications of findings from this case series of *S. suis* meningitis in Bali, Indonesia

CME Editor

Karen L. Foster, Technical Writer/Editor, Emerging Infectious Diseases. *Disclosure: Karen L. Foster has disclosed no relevant financial relationships.*

CME Author

Laurie Barclay, MD, freelance writer and reviewer, Medscape, LLC. *Disclosure: Laurie Barclay, MD, has disclosed no relevant financial relationships.*

Authors

Disclosures: ***Ni Made Susilawathi, MD; Ni Made Adi Tarini, MD; Ni Nengah Dwi Fatmawati, MD, PhD; I Putu Bayu Mayura, MD; Anak Agung Ayu Suryapraba, MD; Made Subrata, DVM; Anak Agung Raka Sudewi, MD, PhD;*** *and* ***Gusti Ngurah Mahardika, DVM, PhD****, have disclosed no relevant financial relationships.*

Streptococcus suis is an emerging agent of zoonotic bacterial meningitis in Asia. We describe the epidemiology of *S. suis* cases and clinical signs and microbiological findings in persons with meningitis in Bali, Indonesia, using patient data and bacterial cultures of cerebrospinal fluid collected during 2014–2017. We conducted microbiological assays using the fully automatic VITEK 2 COMPACT system. We amplified and sequenced gene fragments of glutamate dehydrogenase and recombination/repair protein and conducted PCR serotyping to confirm some serotypes. Of 71 cases, 44 were confirmed as *S. suis*; 29 isolates were serotype 2. The average patient age was 48.1 years, and 89% of patients were male. Seventy-seven percent of patients with confirmed cases recovered without complications; 11% recovered with septic shock, 7% with deafness, and 2% with deafness and arthritis. The case-fatality rate was 11%. Awareness of *S. suis* infection risk must be increased in health promotion activities in Bali.

Author affiliation: Udayana University, Denpasar, Bali, Indonesia

Community-acquired bacterial meningitis is a serious infectious disease with high rates of illness and death worldwide, even in the era of effective antimicrobial drugs (1). The disease is classified as a neurologic emergency; thus, immediate diagnosis and accurate treatment are vital to save the patient's life (2). Gram-positive, coccus-shaped *Streptococcus suis* (3) is the most common causative agent of zoonotic bacterial meningitis; pigs are the primary source of infection. *S. suis* is an important pathogen in community-acquired bacterial meningitis (2,4,5).

Human *S. suis* infections are mostly associated with pig husbandry and eating pork-derived products. Since 2010, the number of reported *S. suis* infections in humans has increased substantially; most cases have originated in Southeast Asia, where the density of pigs is high (6). Moreover, >1,600 *S. suis* infections have been reported in 30 countries worldwide (7). Previously considered to be sporadic, *S. suis* meningitis can cause epidemics, as occurred in Thailand, Vietnam, and China (3). The presence of this bacterium is likely to be inevitable in areas with dense pig populations, including the province of Bali in Indonesia. We describe data on the epidemiology, clinical signs, and microbiology of *S. suis* from meningitis cases in Bali.

Materials and Methods

Data Collection
We obtained medical records of persons who had suspected bacterial meningitis during 2014–2017 from the Sanglah Provincial Referral Hospital (SPRH; Denpasar, Bali, Indonesia). SPRH is a 760-bed national referral hospital for eastern Indonesia with >600,000 annual visits.

Cerebrospinal fluid (CSF) was collected from each patient at admission. Recorded data included patient demographics and clinical signs indicating bacterial meningitis, such as altered mental status, fever, headache, and neck stiffness (8). Other data were CSF laboratory test results, therapy history, and outcomes.

Laboratory Investigation
We cultured CSF samples from patients with suspected meningitis on a 5% defibrinated sheep blood agar plate (DSBAP) and incubated in 5% CO_2 at 37°C for 18–24 h (9). We isolated colonies for identification and drug susceptibility testing using fully automatic VITEK 2 COMPACT system (bioMérieux, https://www.biomerieux.com) based on Clinical and Laboratory Standards Institute guidelines (10). Upon positive detection, we grew selected colonies in tryptic soy broth, incubated at 37°C for 18–24 h, and preserved at −80°C in 50% glycerol. We cultured 44 glycerol stock isolates of *S. suis* on DSBAP and incubated in 5% CO_2 at 37°C for 18–24 h for further study. We reconfirmed the bacterial identity using VITEK 2 COMPACT.

PCR and Sequencing
We suspended 6–8 colonies grown on DSBAP in 200 μL of phosphate buffered saline (pH 7.3) and then isolated bacterial DNA using a Roche High Pure PCR Template Isolation Kit (Roche Life Science, https://www.roche.com). DNA was eluted with 50 μL of elution buffer. We confirmed all isolates by PCR using glutamate dehydrogenase (GDH) and recombination/repair protein (recN) primer sets, as described previously (11,12). We commercially sequenced selected PCR products in 1stBase (Selangor, Malaysia), aligned them using MEGA 6.0 (https://www.megasoftware.net), and subjected them to BLAST search (https://blast.ncbi.nlm.nih.gov/Blast.cgi). We inferred phylogenetic reconstruction of GDH sequence using the unweighted pair group method with arithmetic mean (13). We downloaded the GDH or parts of complete genomes of *S. suis* from GenBank for reference and included 1 sequence of *S. pneumoniae* in the phylogenetic analysis. We conducted PCR serotyping to confirm serotype 2 and 1/2, as well as 1 and 14, using published primer sets (14). Further differentiation of serotype 2 to serotype 1/2 was based on BLAST of recN.

Ethics Approval
The Research Ethics Committee of the Faculty of Medicine, Udayana University (Denpasar, Bali, Indonesia), approved this study (no. 691/UN.14.2/KEP/2017, dated April 7, 2017). In accordance with the standard operation procedure of the SPRH, CSF was collected after informed consent.

Results
Of 71 acute bacterial meningitis cases, *S. suis* was confirmed in CSF culture of 44 patients (Table 1). The median time from illness onset to hospital admission was 2 days (range 1–14 days). Thirty-nine (89%) patients were male; the average patient age ± SD was 48.1 ± 11.5 (range 28–77 years). The most common 3 municipalities/regencies of origin of patients were Denpasar (28 [64%] confirmed cases), Badung (5 [11%]), and Gianyar (4 [9%]) (Figure 1). Patient occupations were private sector employees (57%), unemployed (14%), farmers (11%), entrepreneurs (11%), and government employees (7%).

The 4 most frequent clinical signs in patients with acute *S. suis* meningitis were fever (91%), neck stiffness (86%), altered mental status (86%), and headache (82%) (Table 2). Septic shock was documented in 5 (11%) cases and sensorineural hearing loss in 4 (9%); seizure, ataxia, and hemiparesis were each recorded in 3 cases (7%) and arthritis in 2 (5%).

All patients were treated intravenously with 2 g of ceftriaxone every 12 hours for 14 days and 10 mg of dexamethasone every 6 hours for 4 days. In 2 patients, meningitis relapsed after 14 days of ceftriaxone treatment, but they

Table 1. Demographic data for patients confirmed to have *Streptococcus suis* meningitis, Sanglah Provincial Referral Hospital, Bali, Indonesia, 2014–2017*

Variable	Value
Onset of illness before hospital admission, median d (range)	2 (1–14)
Sex	
M	39 (88.6)
F	5 (11.4)
Age, y, mean ± SD (range)	48.1 ± 11.5 (28–77)
Origin	
Denpasar	28 (63.6)
Badung	5 (11.4)
Gianyar	4 (9.1)
Buleleng	2 (4.5)
Karangasem	2 (4.5)
Tabanan	2 (4.5)
Klungkung	1 (2.3)
Jembrana	0
Bangli	0
Employment	
Private sector employee	25 (56.8)
Unemployed	6 (13.6)
Farmer	5 (11.4)
Entrepreneur	5 (11.4)
Government employee	3 (6.8)

*Values are no. (%) patients unless otherwise indicated.

recovered after 3 additional weeks of ceftriaxone therapy. The case-fatality rate (CFR) was 11%; moderate disabilities occurred in 16% of survivors in the form of sensorineural deafness (4 patients) and hemiparesis (3 patients).

Complete blood counts showed leukocytosis (mean ± SD 24.4 ± 10.5 × 10^3 cells/µL) (Table 3). The neutrophil differential count was 88.4% ± 9.8%, and the lymphocyte count was 4.9% ± 4.7%. The mean platelet count was 196.4 ± 100.2 × 10^3 cells/µL. CSF analysis showed pleocytosis (median 799 cells/µL; range 92–8,510 cells/µL); CSF neutrophil count was 60%, and lymphocyte count was 40%. Glucose levels were low (median 5 mg/dL; range 0–78

mg/dL); the CSF/blood glucose ratio was 0.4; and protein levels were increased (median 198 mg/dL; range 64–855 mg/dL). CSF culture was positive for *S. suis* and sensitive to ceftriaxone, benzyl-penicillin, ampicillin, levofloxacin, erythromycin, vancomycin, and linezolid (data not shown).

PCR results for GDH and recN of all samples produced specific single bands of expected sizes (data not shown). Five GDH and 3 recN PCR products were sequenced. The sequences of GDH and recN generated in this study are available in GeneBank (accession nos. MK161045–54). All GDH and recN sequences of *S. suis* generated in our study were identical. BLAST analysis of the GDH sequence, using blastn (*15*), demonstrated that the sequence had query cover of 100% and an identity score of 94%–100% with the complete *S. suis* genome, GDH complete or partial cDNA sequences (CDS). *S. pneumoniae* and *S. marmotae* had a 99%–100% query cover and an identity score of 86%. For recN, the sequence from the isolates had query cover of 100% and identity of 95%–99% with the *S. suis* complete genome and *S. suis* recN partial CDS. The next closest query cover of 54% with identity score of 83% was with the recN CDS of *S. parasuis*. Phylogenetic analysis of GDH (Figure 2) showed that the isolates were identical with 20 GDH and part of complete genome sequences of *S. suis*.

PCR serotyping showed that 29 (66%) of the 44 isolates were positive in PCR using primer pair for serotype 2 or 1/2, which amplifies *cps2I* gene, whereas none were positive using primer pair for serotypes 1 and 14 detecting *cps1I*, as previously published (*14*). The sequence of *cps2I* of our isolates are available in GenBank (accession nos. MN395406–34). The readable length of sequences was 284 bp. The sequences were identical to *S. suis cps2I* gene of the reference sequence (GenBank accession no. KC537364) (*14*). BLAST analysis showed the recN of our
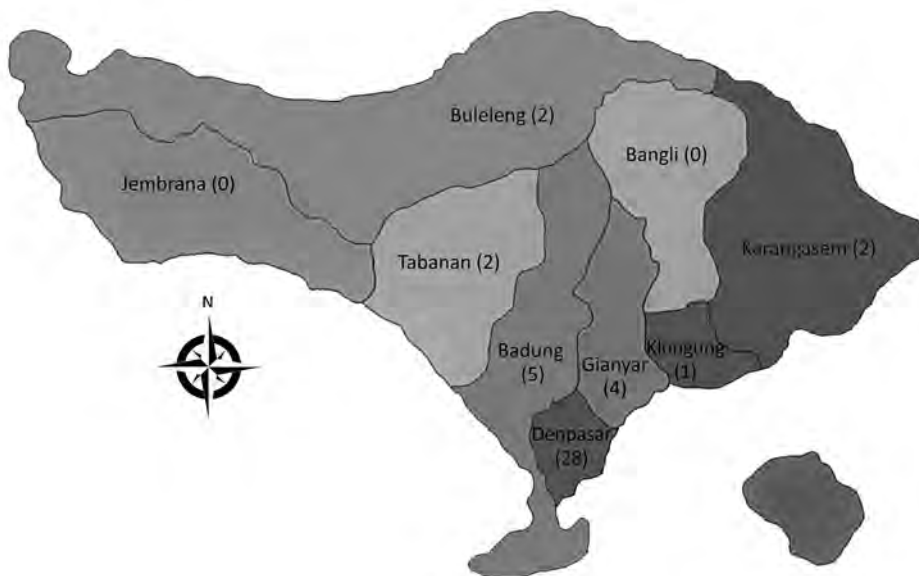
Figure 1. Geographic origin of patients in each regency/municipality confirmed to have *Streptococcus suis* meningitis in Sanglah Provincial Referral Hospital, Denpasar, Bali, Indonesia, 2014–2017. Numbers of patients are shown in parentheses.

isolates were distancing 3.7% to the strain 2651 (GenBank accession no. AB724091), which was annotated as serotype 1/2 (*19*).

Discussion

Our study confirms that *S. suis* is present and infects human in Bali. This finding should alert other provinces in Indonesia. The bacterium has been isolated previously in other provinces (*20,21*), but the cases of human *S. suis* meningitis we report extend the known range of *S. suis* in Indonesia. Pigs are raised in many provinces in Indonesia, and densities differ. In 13 provinces, pig populations were >100,000 head in 2017 (https://www.bps.go.id). The presence of *S. suis* in other provinces needs to be confirmed. Pigs or pig products are thought to be the main source of human infection (*6*) because evidence on the role of other species is unavailable. The awareness will be invaluable in avoiding human suffering and death because medical services will be fully informed and aware of the risk posed by *S. suis* and thus better equipped to save lives.

We based this study on medical records of persons with suspected bacterial meningitis during 2014–2017 at SPRH. All patients with suspected meningitis in the province are referred to this hospital for a definitive diagnosis. Although the presence of *S. suis* has been confirmed only since 2014, suspected bacterial meningitis had been suspected before then and diagnosed as *S. viridans* group. The installment of VITEK 2 COMPACT testing confirmed *S. suis* in 2014. Although cases from many districts in Bali might have been underdiagnosed, we believe that the number of confirmed cases in this report represents most human cases in the province.

Handling pigs or pork products seems to be the major risk factors for human transmission of *S. suis* (*22*). Pork products can originate from slaughterhouses, as has been described in Vietnam (*23*), or from backyard slaughter of dead or sick pigs, as reported in China (*24*). The risk also seems to increase when raw pork products are eaten. Furthermore, eating raw or medium-cooked pork-derived food containing blood, tonsil, tongue, intestine, and uterus has been indicated as an important risk factor for *S. suis* meningitis (*25,26*). A history of ingesting raw pork, pig's blood, or both was found in most cases in Thailand (*27,28*).

Table 2. Clinical signs and outcomes of patients with confirmed *Streptococcus suis* meningitis, Sanglah Provincial Referral Hospital, Bali, Indonesia, 2014–2017

Variable	No. (%) patients
Sign	
Fever	40 (90.9)
Neck stiffness	38 (86.4)
Altered mental status	38 (86.4)
Headache	36 (81.8)
Nausea/vomiting	13 (29.5)
Septic shock	5 (11.4)
Sensorineural hearing loss	4 (9.1)
Seizure	3 (6.8)
Ataxia	3 (6.8)
Hemiparesis	3 (6.8)
Septic arthritis	2 (4.5)
Definitive diagnosis *S. suis* acute bacterial meningitis with:	
No complications	34 (77.3)
Septic shock	5 (11.4)
Deafness	3 (6.8)
Signs of relapse*	2 (4.5)
Deafness and arthritis	1 (2.3)
Outcome	
Full recovery	32 (72.7)
Moderate disability	7 (15.9)
Death	5 (11.4)

*Relapsed meningitis: not recovered after 14 d treatment, but responded well after prolonged (3 weeks) ceftriaxone treatment.

Eating raw meat with fresh blood from sick or subclinically infected pigs might be a major risk factor for *S. suis* transmission in humans in Bali, Indonesia. Most (88%) confirmed *S. suis* meningitis patients in our study were men. This finding was similar to that of *S. suis* infection in Thailand (*28*). The average age and the proportion of men is consistent with the results of a systematic review of studies published during 1980–2015 (*2*). The link of traditional pork consumption and pig handling to the risk for contracting *S. suis* needs to be elucidated further in Bali.

S. suis was predominant as the causal agent of acute bacterial meningitis in our study. Our finding shows it was confirmed in 44 (62%) of 71 acute bacterial meningitis cases. The percentage might have been higher because the *S. suis*–negative patients received antimicrobial therapy before sampling. Human infection with this bacterium needs immediate interventions. Recent data from SPRH showed 20 confirmed cases in 2018 and 13 as of July 2019.

Table 3. Laboratory findings in *Streptococcus suis* meningitis patients, Sanglah Provincial Referral Hospital, Bali, Indonesia, 2014–2017

Parameters	Finding	Reference values
Blood		
Leukocytes, × 1,000/μL, mean ± SD	24.4 ± 10.5	4.1–11.0
Neutrophils, no. (%)	88.4 (9.8)	47–80
Lymphocytes, no. (%)	4.9 (4.7)	13–40
Platelet count, × 1,000/μL, no. (%)	196.4 (100.2)	140–440
Cerebrospinal fluid, median (range)		
Cell count, cells/μL	799 (92–8,510)	0–5
Glucose, mg/dL	5 (1–78)	60–80
Blood/glucose ratio	0.4 (0.1–74)	>0.66
Protein, mg/dL	198 (64–855)	<45

Figure 2. Phylogenetic relationships of the glutamate dehydrogenase gene fragment of *Streptococcus suis i*solated from humans in Denpasar, Bali, Indonesia (BL1-BL6 taxa), with sequences data of S. suis available in GenBank. The phylogeny was inferred using unweighted pair group method with arithmetic mean (13). The GenBank accession number and strain name are written as taxon name. To minimize crowding, some tree branches were condensed. The number of taxa in each condensed branch is indicated. The location of standard American Type Culture Collection isolate (GenBank accession no. EF198476) is shown. Respective gene sequence of full-genome data of *S. pneumoniae* (accession no. LR129844) was co-analyzed as outgroup. The percentage of replicate trees in which the associated taxa clustered in the bootstrap test (1,000 replicates) are shown next to the branches (16). Bootstrap values of <50% are not shown. The genetic distances were computed using the Kimura 2-parameter method (17). Phylogenetic analyses were conducted in MEGA6 (18). Scale bar indicates nucleotide substitutions per site.
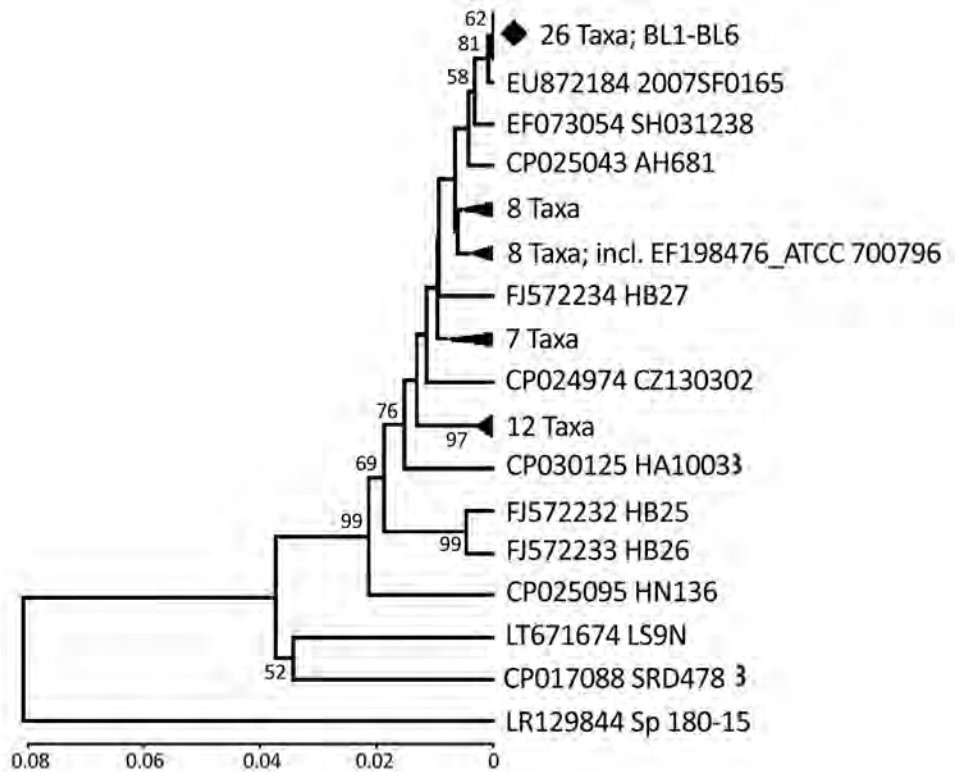
Clinical signs of *S. suis* meningitis recorded in this study resemble those of general bacterial meningitis (*2,4,6,29*). All cases were of acute infection. The median time from illness onset to hospital admission in our study was 2 days (range 1–14 days). The 4 most frequent clinical signs were fever or history of fever, neck stiffness, altered mental status, and headache; these signs correspond to the 3 most frequent globally reported symptoms of meningitis: fever, headache, and neck stiffness (*2,30*).

Initially, some patients did not demonstrate overt neurologic symptoms and thus were admitted under nonneurologic diagnoses. One patient was admitted to the Ear, Nose and Throat Department for sensorineural bilateral deafness, and another was admitted as having an ischemic stroke. Another patient was admitted with suspected dengue fever, which later developed into clinical meningitis. Such misadmission is understandable and may be more widespread because infection with *S. suis* has been reported to cause other syndromes, such as arthritis, endocarditis, peritonitis, and endophthalmitis (*29–31*).

If we grade outcomes according to the Glasgow Outcome Scale (*32*), 73% of the patients in our study had favorable outcomes. All 44 patients were intravenously treated for bacterial meningitis with 2 g of ceftriaxone every 12 hours for 14 days and 10 mg of dexamethasone every 6 hours for 4 days, in accordance with SPRH protocol. Ceftriaxone is a third-generation cephalosporin, which is recommended as the drug of choice for bacterial meningitis (*6,8*).

The CFR in our study was 11%; death was caused by septic shock, which has been attributed to *S. suis* infection (*2,33*). The CFR here is slightly higher than the globally reported CFR of ≈3% (*2*). The reported CFR for *S. suis* meningitis is lower than for other bacterial meningitis, such as pneumococcal (20%) and *Listeria monocytogenes* (36%) meningitis (*2*). The relatively high CFR seems to be related to the late admission of some patients in our study. A high CFR has also been reported in Thailand (*34*).

Four (9%) patients reported hearing loss in our study. This percentage is lower than that from previous findings. In a systematic review and meta-analysis to summarize global estimates of the epidemiology, clinical characteristics, and outcomes of *S. suis* infection, hearing loss was reported in ≈40% 50% of cases and vestibular dysfunction in >20% (*2,29*). This discrepancy might be due to early administration of antimicrobial drugss, so *S. suis* was uncultivable. Also, we excluded unconfirmed cases from our study.

Laboratory findings in the CSF were leukocytosis (predominantly neutrophil), low glucose levels, and

increased protein content. These findings resemble typical bacterial meningitis (*1,8*).

Of all *S suis* serotypes, serotype 2 is recognized as the most common pig and human pathogen (*23,35*). However, other serotypes should not be ignored, as evidenced by serotype 5 in Japan (*36*), serotype 9 in Thailand (*37*), serotype 16 in Vietnam (*38*), serotype 21 in Argentina (*39*), serotypes 24 (*40*) and 31 (*41*) in Thailand, and many more. PCR serotyping indicated that 29 of 44 isolates were positive in PCR using a primer set to detect serotypes 2 and 1/2 (*14*) but not serotypes 1 and 14. We focused on serotypes 2 and 1/2 because *S. suis* serotype 2 is the most common cause of human cases (*42*); serotypes 1, 4, 14, and 16 infection can lead to severe illness, but fewer cases are reported than for serotype 2 (*38*). We confirmed those PCR-positive isolates in our study to be serotype 2 or 1/2. The readable sequences were identical to *S. suis cps2I* gene of the reference sequence (GenBank accession no. KC537364) (*14*). Although the existing PCR serotyping is unable to differentiate between serotype 2 and 1/2 (*14*), the nucleotide sequences of recN of our isolates are distancing 3.7% to the 2651 strain (GenBank accession no. AB724091), which was annotated as serotype 1/2 (*19*). Therefore, we proposed those PCR-positive isolates were serotype 2. Samples should be sent to a reference laboratory to be tested using a panel of standard antiserum (*6*), and the complete primer sets for PCR serotyping (*14*) serotypes of all isolates should be made available. The knowledge gained will convey important epidemiologic picture for human prevention.

We confirmed *S. suis* in this study after applying a standard method with fully automatic equipment. Performing PCR and sequencing of GDH and recN further confirmed the species identification. Both gene fragments are proposed as an appropriate PCR system for the reclassification of *S. suis* (*11*) or as a specific PCR system for *S. suis* (*12*).

BLAST search of the GDH sequences showed high coverage and identity with the *S. suis* complete genome and GDH partial CDS available in the database. The closest identity score of 86% was to *S. pneumoniae* and *S. marmotae*. Phylogenetic analysis (Figure 2) also confirmed that our isolates are *S. suis.* The recN had high sequence coverage and high identity to the *S. suis* database, too., The closest sequence data of *S. parasuis* have an identity score of 83% to the recN of *S. suis*. Sequencing of PCR products to confirm detected genetic sequences should limit or reduce misidentification. We did not sequence all PCR products because sequencing was conducted only to determine the specificity of the PCR. We propose implementation of GDH and recN as diagnostic tools in elucidating the distribution of *S. suis* in Indonesia.

Misidentification of *S. suis* is common. This bacterium is frequently misidentified as *S. viridans* (*43*) and has also

been misidentified as *S. bovis*, *S. pneumoniae*, *S. faecalis*, and *S. acidominimus* (*29,44*). Misidentification of *S. suis* also has been reported in Canada, which raises suspicion that human *S. suis* infections might be underdiagnosed in North America (*45*). We found 1 case of suspected *S. mitis* infection using the VITEK 2 COMPACT system. However, PCR and sequencing confirmed this to be *S. suis*.

Published reports of animal cases and isolation of *S. suis* from animals in Bali are not available. Isolation of *S. suis* from tonsil samples has been reported from Papua, Indonesia (*21*). Another group in Udayana University is working to isolate and detect *S. suis* from sick pigs in Bali, further suggesting that *S. suis* is present in the island (K. Besung, Udayana University, pers. comm., 2018 Oct 1). As indicated elsewhere that pig and pork products are the primary sources of human infection (*2,4,5*), so is the source of *S. suis* in humans in our study most likely to be pigs and pork products.

In conclusion, we confirmed *S. suis* meningitis in humans in Bali, Indonesia. Of 44 cases, 29 human isolates were serotype 2. Because human infections are mostly associated with pig husbandry and eating pork-derived products, the distribution of *S. suis* in the country needs to be fully elucidated. The risk factor of eating raw pork and pig blood in traditional delicacies seems to be valid, although this point requires further investigation. Our study contributes to enhancing knowledge of *S. suis* distribution and risk factors in Bali. By increasing awareness of *S. suis* infection, medical services will be better prepared to alleviate human suffering and death from *S. suis* meningitis.

About the Author

Dr. Susilawathi is a lecturer at the Faculty of Medicine, Udayana University, and is undertaking a doctoral degree in the School of Post Graduate Studies of Udayana University. Her primary research interests include neurologic infection and pathogenesis.

References
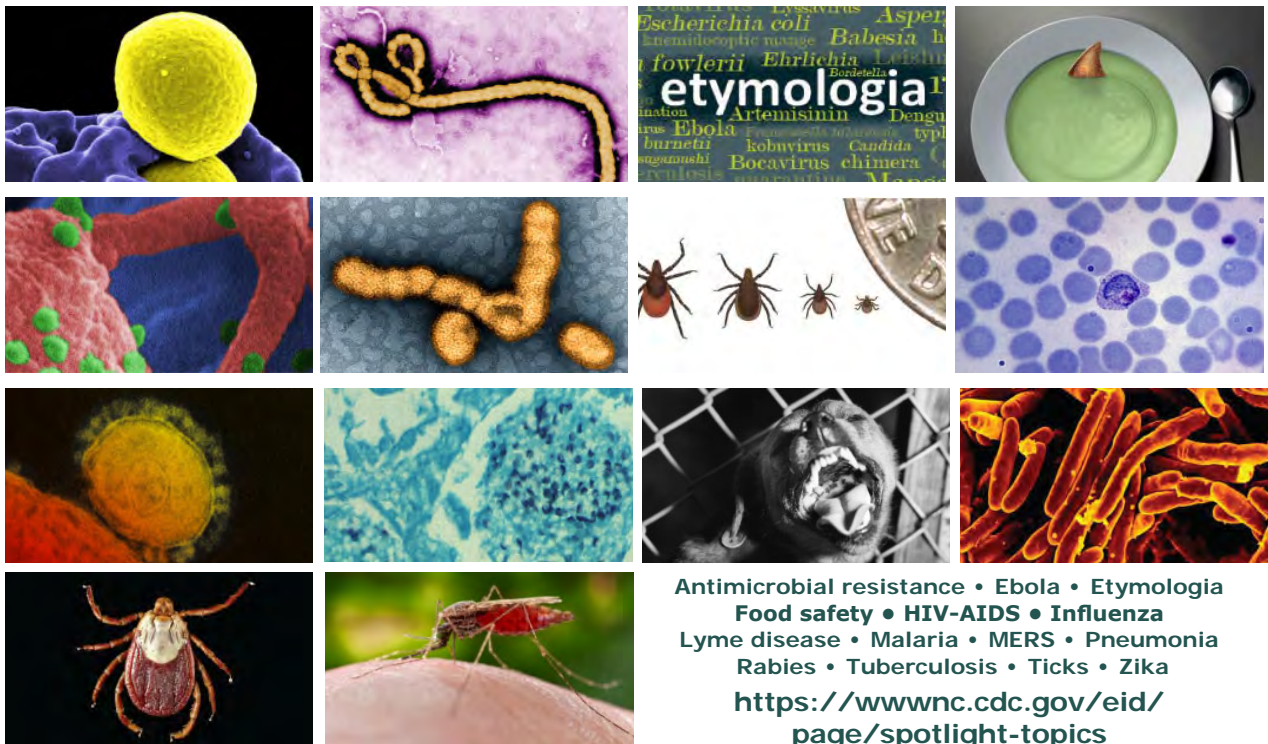
1. van de Beek D, Brouwer M, Hasbun R, Koedel U, Whitney CG, Wijdicks E. Community-acquired bacterial meningitis. Nat Rev Dis Primers. 2016;2:16074. http://dx.doi.org/10.1038/nrdp.2016.74
2. van Samkar A, Brouwer MC, Schultsz C, van der Ende A, van de Beek D. *Streptococcus suis* meningitis: a systematic review and meta-analysis. PLoS Negl Trop Dis. 2015;9:e0004191. http://dx.doi.org/10.1371/journal.pntd.0004191
3. Feng Y, Zhang H, Wu Z, Wang S, Cao M, Hu D, et al. *Streptococcus suis* infection: an emerging/reemerging challenge of

bacterial infectious diseases? Virulence. 2014;5:477–97. http://dx.doi.org/10.4161/viru.28595

4. van Samkar A, Brouwer MC, van der Ende A, van de Beek D. Zoonotic bacterial meningitis in human adults. Neurology. 2016; 87:1171–9. http://dx.doi.org/10.1212/WNL.0000000000003101

5. Gottschalk M, Fittipaldi N, Segura M. *Streptococcus suis* meningitis. In: Christodoulides M, editor. Meningitis: cellular and molecular basis. Oxford (UK): CAB International; 2013. p. 184–98.

6. Wertheim HF, Nghia HD, Taylor W, Schultsz C. *Streptococcus suis*: an emerging human pathogen. Clin Infect Dis. 2009;48:617–25. http://dx.doi.org/10.1086/596763

7. Goyette-Desjardins G, Auger JP, Xu J, Segura M, Gottschalk M. *Streptococcus suis*, an important pig pathogen and emerging zoonotic agent-an update on the worldwide distribution based on serotyping and sequence typing. Emerg Microbes Infect. 2014;3:e45. http://dx.doi.org/10.1038/emi.2014.45

8. Scarborough M, Thwaites GE. The diagnosis and management of acute bacterial meningitis in resource-poor settings. Lancet Neurol. 2008;7:637–48. http://dx.doi.org/10.1016/S1474-4422(08)70139-X

9. Lehman DC, Mahon CR, Suvarna K. *Streptococcus, Enterococcus*, and other catalase-negative, gram-positive cocci. In: Mahon CR, Lehman DC, Manuselis G, editors. Textbook of diagnostic microbiology. 5th ed. Maryland Heights (MO): Saunders Elsivier; 2016. p. 328–48.

10. Clinical and Laboratory Standards Institute. Performance standards for antimicrobial susceptibility testing; twenty-fifth informational supplement (M100-S27). Wayne (PA): The Institute; 2017. p. 250.

11. Ishida S, Tien HT, Osawa R, Tohya M, Nomoto R, Kawamura Y, et al. Development of an appropriate PCR system for the reclassification of *Streptococcus suis*. J Microbiol Methods. 2014;107:66–70. http://dx.doi.org/10.1016/j.mimet.2014.09.003

12. Okwumabua O, O'Connor M, Shull E. A polymerase chain reaction (PCR) assay specific for *Streptococcus suis* based on the gene encoding the glutamate dehydrogenase. FEMS Microbiol Lett. 2003;218:79–84. http://dx.doi.org/10.1111/j.1574-6968.2003.tb11501.x

13. Sneath PHA, Sokal RR. Numerical taxonomy. San Francisco: Freeman; 1973.

14. Liu Z, Zheng H, Gottschalk M, Bai X, Lan R, Ji S, et al. Development of multiplex PCR assays for the identification of the 33 serotypes of *Streptococcus suis*. PLoS One. 2013;8:e72070. http://dx.doi.org/10.1371/journal.pone.0072070

15. Altschul SF, Madden TL, Schäffer AA, Zhang J, Zhang Z, Miller W, et al. Gapped BLAST and PSI-BLAST: a new generation of protein database search programs. Nucleic Acids Res. 1997;25:3389–402. http://dx.doi.org/10.1093/nar/25.17.3389

16. Felsenstein J. Confidence limits on phylogenies: an approach using the bootstrap. Evolution. 1985;39:783–91. http://dx.doi.org/10.1111/j.1558-5646.1985.tb00420.x

17. Kimura M. A simple method for estimating evolutionary rates of base substitutions through comparative studies of nucleotide sequences. J Mol Evol. 1980;16:111–20. http://dx.doi.org/10.1007/BF01731581

18. Tamura K, Stecher G, Peterson D, Filipski A, Kumar S. MEGA6: Molecular Evolutionary Genetics Analysis version 6.0. Mol Biol Evol. 2013;30:2725–9. http://dx.doi.org/10.1093/molbev/mst197

19. Tien HT, Nishibori T, Nishitani Y, Nomoto R, Osawa R. Reappraisal of the taxonomy of *Streptococcus suis* serotypes 20, 22, 26, and 33 based on DNA-DNA homology and sodA and recN phylogenies. Vet Microbiol. 2013;162:842–9. http://dx.doi.org/10.1016/j.vetmic.2012.11.001

20. Southeast Asia Infectious Disease Clinical Research Network. Causes and outcomes of sepsis in southeast Asia: a multinational multicentre cross-sectional study. Lancet Glob Health. 2017;5: e157–67. http://dx.doi.org/10.1016/S2214-109X(17)30007-4

21. Nugroho W, Cargill CF, Putra IM, Kirkwood RN, Trott DJ, Salasia SI, et al. Investigations of selected pathogens among village pigs in Central Papua, Indonesia. Trop Anim Health Prod. 2016;48:29–36. http://dx.doi.org/10.1007/s11250-015-0913-5

22. Zalas-Wiecek P, Michalska A, Grabczewska E, Olczak A, Pawlowska M, Gospodarek E. Human meningitis caused by *Streptococcus suis*. J Med Microbiol. 2013;62:483–5. http://dx.doi.org/10.1099/jmm.0.046599-0

23. Ngo TH, Tran TB, Tran TT, Nguyen VD, Campbell J, Pham HA, et al. Slaughterhouse pigs are a major reservoir of *Streptococcus suis* serotype 2 capable of causing human infection in southern Vietnam. PLoS One. 2011;6:e17943. http://dx.doi.org/10.1371/journal.pone.0017943

24. Yu H, Jing H, Chen Z, Zheng H, Zhu X, Wang H, et al.; Streptococcus suis study groups. Human Streptococcus suis outbreak, Sichuan, China. Emerg Infect Dis. 2006;12:914–20. http://dx.doi.org/10.3201/eid1206.051194

25. Nghia HD, Tu TP, Wolbers M, Thai CQ, Hoang NV, Nga TV, et al. Risk factors of *Streptococcus suis* infection in Vietnam. A case-control study. Erratum in: PLoS One. 2011;6(4); 2012;7(5). PLoS One. 2011;6:e17604.

26. Takeuchi D, Kerdsin A, Akeda Y, Chiranairadul P, Loetthong P, Tanburawong N, et al. Impact of food safety campaign on *Streptococcus suis* infection in humans in Thailand. Am J Trop Med Hyg. 2017;96:1370–7. http://dx.doi.org/10.4269/ajtmh.16-0456

27. Navacharoen N, Chantharochavong V, Hanprasertpong C, Kangsanarak J, Lekagul S. Hearing and vestibular loss in *Streptococcus suis* infection from swine and traditional raw pork exposure in northern Thailand. J Laryngol Otol. 2009;123:857–62. http://dx.doi.org/10.1017/S0022215109004939

28. Takeuchi D, Kerdsin A, Pienpringam A, Loetthong P, Samerchea S, Luangsuk P, et al. Population-based study of *Streptococcus suis* infection in humans in Phayao Province in northern Thailand. PLoS One. 2012;7:e31265. http://dx.doi.org/10.1371/journal.pone.0031265

29. Huong VT, Ha N, Huy NT, Horby P, Nghia HD, Thiem VD, et al. Epidemiology, clinical manifestations, and outcomes of *Streptococcus suis* infection in humans. Emerg Infect Dis. 2014;20:1105–14. http://dx.doi.org/10.3201/eid2007.131594

30. Teekakirikul P, Wiwanitkit V. *Streptococcus suis* infection: overview of case reports in Thailand. Southeast Asian J Trop Med Public Health. 2003;34(Suppl 2):178–83.

31. Heidt MC, Mohamed W, Hain T, Vogt PR, Chakraborty T, Domann E. Human infective endocarditis caused by *Streptococcus suis* serotype 2. J Clin Microbiol. 2005;43:4898–901. http://dx.doi.org/10.1128/JCM.43.9.4898-4901.2005

32. van de Beek D, de Gans J, Spanjaard L, Weisfelt M, Reitsma JB, Vermeulen M. Clinical features and prognostic factors in adults with bacterial meningitis. N Engl J Med. 2004;351:1849–59. http://dx.doi.org/10.1056/NEJMoa040845

33. Fillo S, Mancini F, Anselmo A, Fortunato A, Rezza G, Lista F, et al. Draft genome sequence of *Streptococcus suis* strain SsRC-1, a human isolate from a fatal case of toxic shock syndrome. Genome Announc. 2018;6:e00447–18. http://dx.doi.org/10.1128/genomeA.00447-18

34. Wangsomboonsiri W, Luksananun T, Saksornchai S, Ketwong K, Sungkanuparph S. *Streptococcus suis* infection and risk factors for mortality. J Infect. 2008;57:392–6. http://dx.doi.org/10.1016/j.jinf.2008.08.006

35. Robertson ID, Blackmore DK. Experimental studies on the comparative infectivity and pathogenicity of *Streptococcus suis* type 2. I. Porcine and human isolates in pigs. Epidemiol Infect. 1990;105:469–78. http://dx.doi.org/10.1017/S0950268800048081

36. Taniyama D, Sakurai M, Sakai T, Kikuchi T, Takahashi T. Human case of bacteremia due to *Streptococcus suis* serotype 5 in

Japan: the first report and literature review. IDCases. 2016;6:36–8. http://dx.doi.org/10.1016/j.idcr.2016.09.011

37. Kerdsin A, Hatrongjit R, Gottschalk M, Takeuchi D, Hamada S, Akeda Y, et al. Emergence of *Streptococcus suis* serotype 9 infection in humans. J Microbiol Immunol Infect. 2017;50:545–6. http://dx.doi.org/10.1016/j.jmii.2015.06.011

38. Nghia HD, Hoa NT, Linh D, Campbell J, Diep TS, Chau NV, et al. Human case of *Streptococcus suis* serotype 16 infection. Emerg Infect Dis. 2008;14:155–7. http://dx.doi.org/10.3201/eid1401.070534

39. Callejo R, Prieto M, Salamone F, Auger JP, Goyette-Desjardins G, Gottschalk M. Atypical *Streptococcus suis* in man, Argentina, 2013. Emerg Infect Dis. 2014;20:500–2. http://dx.doi.org/10.3201/eid2003.131148

40. Kerdsin A, Gottschalk M, Hatrongjit R, Hamada S, Akeda Y, Oishi K. Fatal septic meningitis in child caused by *Streptococcus suis* serotype 24. Emerg Infect Dis. 2016;22:1519–20. http://dx.doi.org/10.3201/eid2208.160452

41. Hatrongjit R, Kerdsin A, Gottschalk M, Takeuchi D, Hamada S, Oishi K, et al. First human case report of sepsis due to infection with *Streptococcus suis* serotype 31 in Thailand. BMC Infect Dis. 2015;15:392. http://dx.doi.org/10.1186/s12879-015-1136-0

42. Lun ZR, Wang QP, Chen XG, Li AX, Zhu XQ. *Streptococcus suis*: an emerging zoonotic pathogen. Lancet Infect Dis. 2007;7:201–9. http://dx.doi.org/10.1016/S1473-3099(07)70001-4

43. Fongcom A, Pruksakorn S, Netsirisawan P, Pongprasert R, Onsibud P. *Streptococcus suis* infection: a prospective study in northern Thailand. Southeast Asian J Trop Med Public Health. 2009;40:511–7.

44. Tsai HY, Liao CH, Liu CY, Huang YT, Teng LJ, Hsueh PR. *Streptococcus suis* infection in Taiwan, 2000–2011. Diagn Microbiol Infect Dis. 2012;74:75–7. http://dx.doi.org/10.1016/j.diagmicrobio.2012.05.013

45. Gomez-Torres J, Nimir A, Cluett J, Aggarwal A, Elsayed S, Soares D, et al. Human case of *Streptococcus suis* disease, Ontario, Canada. Emerg Infect Dis. 2017;23:2107–9. http://dx.doi.org/10.3201/eid2312.171005

Address for correspondence: Gusti N. Mahardika, Udayana University, Animal Biomedical and Molecular Biology Laboratory, Faculty of Veterinary Medicine, Jl Sesetan-Markisa #6, Denpasar, 80226, Bali, Indonesia; email: gnmahardika@unud.ac.id

Epidemiologic, Entomologic, and Virologic Factors of the 2014–15 Ross River Virus Outbreak, Queensland, Australia

Cassie C. Jansen, Martin A. Shivas, Fiona J. May, Alyssa T. Pyke,
Michael B. Onn, Kerryn Lodo, Sonja Hall-Mendelin, Jamie L. McMahon,
Brian L. Montgomery, Jonathan M. Darbro, Stephen L. Doggett, Andrew F. van den Hurk

Australia experienced its largest recorded outbreak of Ross River virus (RRV) during the 2014–15 reporting year, comprising >10,000 reported cases. We investigated epidemiologic, entomologic, and virologic factors that potentially contributed to the scale of the outbreak in Queensland, the state with the highest number of notifications (6,371). Spatial analysis of human cases showed that notifications were geographically widespread. In Brisbane, human case notifications and virus detections in mosquitoes occurred across inland and coastal locations. Viral sequence data demonstrated 2 RRV lineages (northeastern genotypes I and II) were circulating, and a new strain containing 3 unique amino acid changes in the envelope 2 protein was identified. Longitudinal mosquito collections demonstrated unusually high relative abundance of *Culex annulirostris* and *Aedes procax* mosquitoes, attributable to extensive freshwater larval habitats caused by early and persistent rainfall during the reporting year. Increased prevalence of these mosquitoes probably contributed to the scale of this outbreak.

Ross River virus (RRV; family *Togaviridae*, genus *Alphavirus*) is distributed throughout Australasia and has caused outbreaks involving thousands of humans in the western Pacific (*1*). RRV is the most commonly reported endemic arboviral infection in Australia; a mean of 4,541 cases/year

Author affiliations: Communicable Diseases Branch, Queensland Government Department of Health, Herston, Queensland, Australia (C.C. Jansen, K. Lodo); Brisbane City Council, Fortitude Valley, Queensland, Australia (M.A. Shivas, M.B. Onn); Metro North Hospital and Health Service, Windsor, Queensland, Australia (F.J. May); Forensic and Scientific Services, Queensland Government Department of Health, Coopers Plains, Queensland, Australia (A.T. Pyke, S. Hall-Mendelin, J.L. McMahon, A.F. van den Hurk); Metro South Hospital and Health Service, Coopers Plains (B.L. Montgomery); Queensland Institute of Medical Research Berghofer, Herston (J.M. Darbro); University of Sydney and Westmead Hospital, Sydney, New South Wales, Australia (S.L. Doggett)

were recorded during 2000–2016 (*2*). Cases are reported from every state and territory of Australia, and Queensland accounts for a large percentage (40%–65% during 2000–2006) (*2*).

Similar to the disease spectrum of related chikungunya virus, RRV infection causes polyarthritis and, in some cases, fever, maculopapular rash, fatigue, myalgia, lethargy, and headache (*3,4*). Many infections are asymptomatic and do not result in clinical disease (*5*), but debilitating arthritis of 3–6 months' duration can occur in some patients (*5–7*). RRV ecology is complex, involving zoonotic transmission between multiple mosquitoes and vertebrates (*8*). Although numerous species may be hosts for RRV, the predominant vertebrate hosts are considered to be macropods (e.g., kangaroos and wallabies) (*1,9,10*). Humans have been implicated as hosts in outbreaks where macropods were absent (*11,12*). Overall, >40 mosquito species have yielded RRV isolates, although *Aedes vigilax*, *Aedes camptorhynchus*, and *Culex annulirostris* mosquitoes are considered the key vectors (*13*). Other species can be involved in specific locations (*8,14*), and transmission dynamics appear locally unique.

During the 2014–15 reporting year (i.e., July 1, 2014–June 30, 2015), a widespread RRV epidemic occurred in Australia; 10,074 cases were reported to the National Notifiable Diseases Surveillance System (*15*). This epidemic represented the highest number of RRV notifications ever reported in a season since 1993, when human RRV infection became nationally notifiable. In total, 63% (6,371) of notifications were from Queensland, Australia's third-most populous state (*15*). We investigated the epidemiologic, entomologic, and virologic characteristics of the outbreak in Brisbane, the Queensland capital.

Methods

Study Area

Brisbane is situated at 27°28′S and 153°01′E on Australias' eastern coast. The Brisbane local government area (LGA)

comprises $1,367$ km^2 and, on June 30, 2015, had an estimated residential population of 1,165,437 (16). Brisbane has a subtropical climate (Köppen climate classification Cfa); monthly average temperatures are 10°C–22°C in winter and 20°C–29°C in summer. Approximately two thirds of the annual mean rainfall (1,149 mm) falls during November–March (17).

Human Case Notifications

The Queensland Notifiable Conditions Surveillance System (18) houses data on notifiable conditions in Queensland as outlined in the Public Health Act 2005 (19). We defined an RRV notification as the national case definition (i.e., a laboratory diagnosis of RRV) (20), but in 2016, this definition was changed to reduce the effect of false-positive notifications resulting from single IgM-positive test results. Thus, notifications reported herein might include false-positives. We assigned an LGA to notified cases using patient residential addresses. We extracted notification data, including date of specimen collection (used as a proxy for illness onset because this information was not systematically collected), residential address, and LGA, from the Notifiable Conditions Surveillance System for the period January 1, 1990–June 30, 2015. We present data as annual totals by reporting year, defined as July 1 of one year through June 30 of the next year, to reflect seasonality of mosquito abundance and mosquitoborne disease notifications and provide consistency with the national reporting convention. We numbered weeks as specified by ISO 8601:2004 (21), with week 1 starting on a Monday and containing the first Thursday of the calendar year.

We tabulated RRV notifications in the Brisbane LGA by week of specimen collection and Australian Statistical Geography Standard statistical area level 2 (22) and visualized using QGIS 2.18.1 (https://qgis.org). Because locations of exposures were unknown, we used patient residential address to map the spatial distribution of notifications. We performed all case data analyses in Stata SE 15 (https://www.stata.com) and calculated rates (per 100,000 population) using estimated Queensland residential population data (23). We obtained ethics approval to conduct this research through the Children's Health Queensland Hospital and Health Service Human Research Ethics Committee (reference no. HREC/15/QRCH/230).

Mosquito Collections

We collected mosquitoes weekly at 9 sites representing the larval habitat diversity of implicated RRV vectors and their proximity to human habitation. Trap sites varied by distance to larval habitats. Four sites were within 500 m of a saltmarsh, and 5 were close to freshwater habitats; some freshwater habitats were also near urban areas and considered suburban larval habitats (Table 1; Figure

Table 1. Mosquito trap site location and type, Brisbane local government area, Queensland, Australia

Site name, suburb	Geolocation	Dominant habitat type
Ascot	−27.431441, 153.051788	Suburban hilltop, freshwater
Bracken Ridge	−27.307225, 153.040433	Saltmarsh
Banyo	−27.369166, 153.072694	Saltmarsh
Corinda	−27.549861, 152.994836	Suburban, freshwater
Hemmant	−27.451706, 153.123781	Saltmarsh
Indooroopilly	−27.511639, 152.984458	Suburban riparian
Lota	−27.469912, 153.18057	Saltmarsh
The Gap	−27.450889, 152.937806	Suburban, freshwater
Fig Tree Pocket	−27.539056, 152.969333	Suburban, freshwater

1). We collected mosquitoes using PB light traps (Pacific BioLogics, http://www.pacificbiologics.com.au) baited with carbon dioxide (2-kg dry ice pellets) and 1-octen-3-ol (24) operated 4:00 PM–7:00 AM.

To account for occasional variation in the number of traps set (resulting from trap failures and prohibitive weather), for each week, we calculated the mean count of all mosquito species per trap and mean relative abundance of each mosquito species per trap. We compared the mean count of all mosquitoes per trap in the 2014–15 season with those of the other reporting years using Poisson regression. We compared the mean relative abundance of mosquito species comprising >5% of the total trap catch in 2014–15 with their mean relative abundances in the previous 2 reporting years using the 2-sample test of proportions. We considered p values <0.05 significant for all statistical tests.

For each week, we compared the number of human cases notified in the Brisbane LGA with the mean total mosquito count per trap and the mean relative abundance of frequently collected mosquitoes (i.e., those comprising >5% of the total trap catch in 2014–15) using Spearman rank correlation. We similarly compared the lag time of 0–8 weeks between mosquito counts and human case notifications.

Virus Detection in Mosquito Saliva and Mosquito Pools

We used 2 methods to acquire mosquito samples for RRV screening (Appendix, https://wwwnc.cdc.gov/EID/article/25/12/18-1810-App1.pdf). The first method was the sugar-based system described by Flies et al. (25), which involves collecting mosquito saliva expectorated during feedings (26). We deployed traps containing honey-soaked Flinders Technology Associates (FTA) cards (Whatman International Ltd, https://www.gelifesciences.com) overnight on 15 occasions at weekly intervals during February 3–May 20, 2015 (weeks 6–21), excluding week 18. For the second method, we pooled whole mosquitoes collected in traps during February 3–March 10, 2015 (weeks 6–11), by species, trap, and trap night into groups of ≤100 mosquitoes.
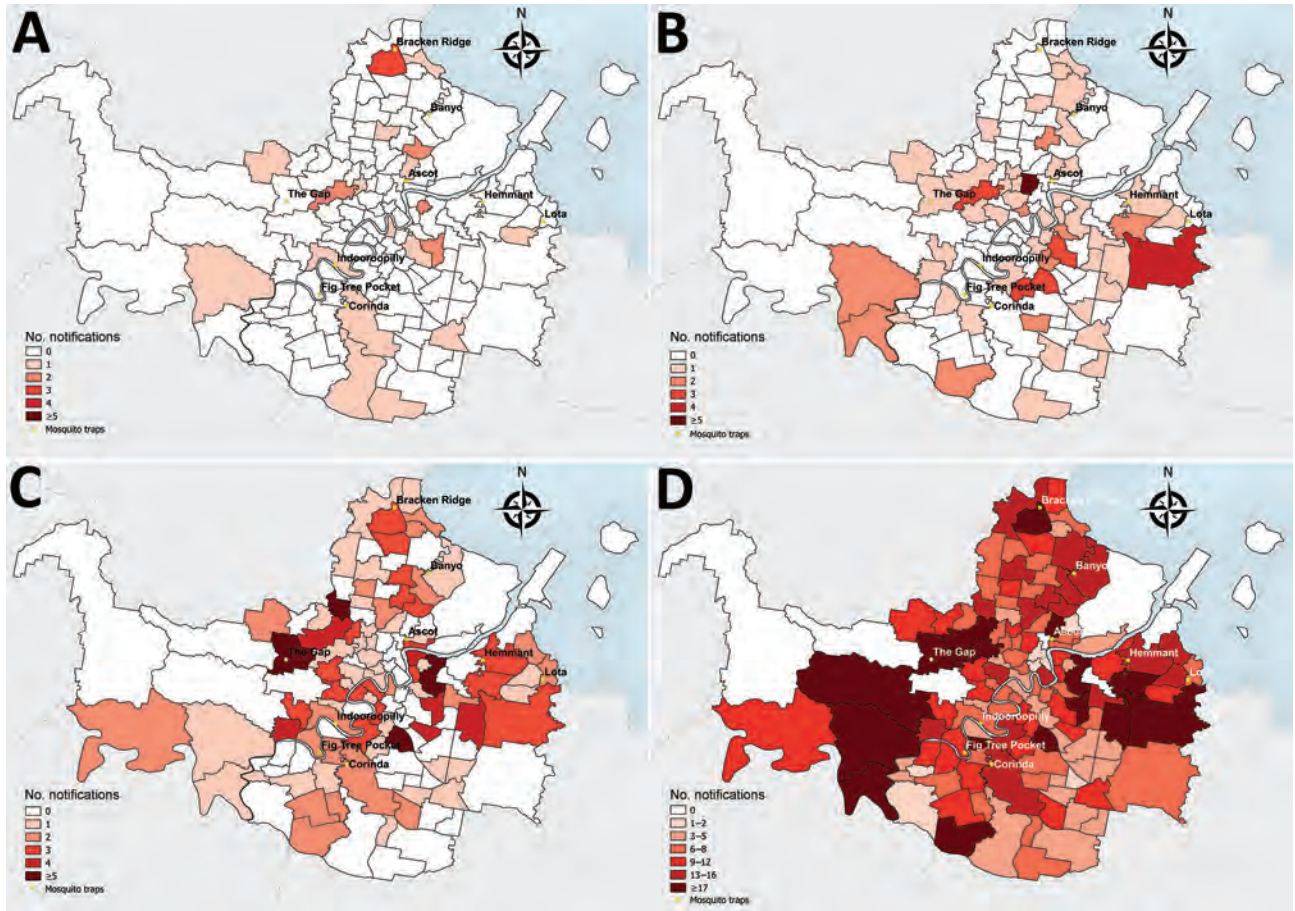
Figure 1. Spatial distribution of Ross River virus notifications by patient residential address and Australian Statistical Geography Standard statistical area level 2 (22) and mosquito trap sites, Brisbane local government area, Queensland, Australia, 2015. A) Week 2 (first week with an increased number of cases); B) week 6 (early in outbreak); C) week 9 (peak of notified cases); and D) weeks 2–20 combined (entire outbreak period).

We used a cell culture ELISA (27) to detect RRV in mosquito pools. We used an RRV-specific TaqMan real-time reverse transcription PCR (rRT-PCR) (28) to detect RRV RNA extracted from FTA cards and RRV RNA from mosquito pools acquired from traps that yielded RRV-positive FTA cards. We also performed rRT-PCR on mosquito samples derived from traps where a high level of mosquito death was observed during the 24-hour holding period after trap collection. Mosquito death compromises virus integrity and subsequent detection in the cell culture ELISA.

Sequence Analysis

We extracted virus RNA from patient serum samples, mosquito homogenates, FTA cards, and infected C6/36 cell culture supernatants. We amplified and sequenced the complete envelope (E) 3 and E2 gene regions (1,458 nt in total) using RRV-specific primers (Appendix Table 2) and 2 overlapping RT-PCR reactions (Appendix). We phylogenetically compared the RRV E3 and E2 sequences from samples collected in Brisbane during the 2014–15 outbreak with those of archived viruses from Brisbane and other locations around Australia isolated during 1959–2016 (Appendix Table 1).

Results

Study Area Climate

The weather of southeast Queensland during the 2014–15 reporting year was characterized by early and consistent weekly rainfall from mid-November through late February (17), followed by drier weather interspersed with several large rain events. A total of 1,595 mm of rain fell, representing 152% of the Brisbane long-term average (Table 2). Of note, the preceding reporting year was unusually dry; only 55% of the long-term average rainfall fell.

Human Case Notifications

In the 2014–15 reporting year, 10,074 RRV notifications were reported nationally through the National Notifiable Diseases Surveillance System. The number of notifications in

Table 2. Total rainfall in Brisbane local government area, Queensland, Australia, 2011–2015, compared with long-term average

Reporting year	Rainfall, mm*	% Long-term average rainfall†
2011–12	1,305	124
2012–13	1,159	110
2013–14	582	55
2014–15	1,595	152

*Rainfall values from the Bureau of Meteorology (*17*).
†The long-term average rainfall for the reporting years 2000–2015 was 1,049 mm.

Queensland was 6,371, considerably higher than the mean of 1,854 cases reported annually over the previous 5 years and the largest number reported since statewide RRV surveillance began in 1990. Despite being the highest number of annual RRV notifications reported, the Queensland notification rate in 2014–15 (135 notifications/100,000 population) was lower than that in 1995–96 (150 notifications/100,000 population; Figure 2), a finding attributable to an increase in population over time. However, the mean rate for the 5 years before the 2014–15 outbreak was 41 notifications/100,000 population.

The 2014–15 notification rates varied by Queensland LGA (Figure 3). In total, 1,454 RRV notifications were reported in the Brisbane LGA in 2014–15. The number of weekly notifications first increased in Brisbane in week 2 of 2015 (25 cases; Figure 1, panel A; Figure 4). A marked increase occurred in week 6 (79 cases, compared with the average of 16.8 cases of the preceding 5 weeks), and the highest number occurred in week 9 (177 cases; Figure 1, panels B, C; Figure 4). The number of weekly case notifications returned to pre-outbreak levels by week 21 (Figure 4).

Notifications were widespread across Brisbane throughout the outbreak (Figure 1, panels A–D). No spatial clustering by statistical area level 2 was observed for notifications at any time during the outbreak.

Mosquito Collections

During 2014–15, a total of 411,328 mosquitoes (mean 877 mosquitoes per trap night) comprising >35 species were collected (Appendix Table 3). This number is a significant increase compared with the 204,220 (mean 498 mosquitoes/trap night) collected during the 2012–13 reporting year and 108,422 (mean 232 mosquitoes/trap night) collected during the 2013–14 reporting year (p<0.001). *Ae. vigilax*, *Cx. annulirostris*, and *Aedes procax* mosquitoes were the only species that comprised >5% of the trap catch during the 2014–15 reporting year. *Ae. vigilax* populations dominated collections in all years. Only *Cx. annulirostris* and *Ae. procax* mosquitoes significantly increased in abundance during the 2014–15 reporting year compared with previous reporting years (p<0.001). The relative abundance of all other species was not significantly increased in 2014–15 compared with previous years.

Cx. annulirostris populations accounted for 34% (140,287/411,328) of the total trap catch in 2014–15, a relative abundance significantly higher than those recorded for the 2012–13 (20%, 39,858/204,220; p<0.001) and 2013–14 (12%, 12,650/108,422; p<0.001) reporting years. During 2014–15, *Cx. annulirostris* mosquitoes showed an earlier than usual increase in abundance, and elevated counts were sustained throughout the outbreak (data not shown). The initial increase in weekly collections of this mosquito population observed starting week 50 of 2014 coincided with an increased number of weekly case notifications. The correlation between the mean relative abundance of *Cx. annulirostris* populations and RRV notifications was strong and significant (Spearman rank correlation coefficient $\rho = 0.6190$; p<0.001) only when a 3-week lag from mosquito abundance to human case notifications was applied.
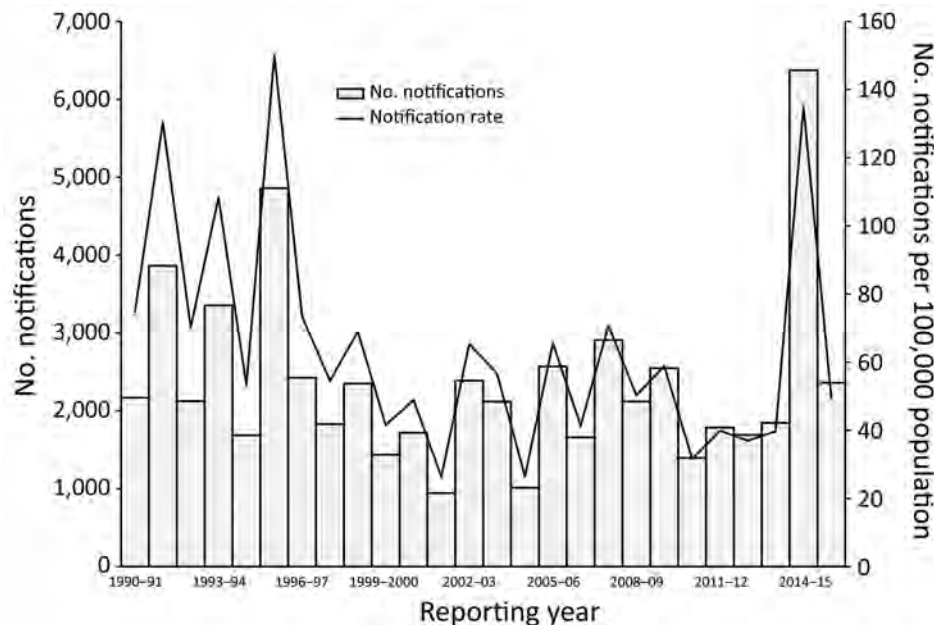
Figure 2. Number of notifications and notification rate of Ross River virus infections by reporting year, Queensland, Australia, 1990–2016. Reporting year is defined as July 1 of one year to June 30 of the next year.
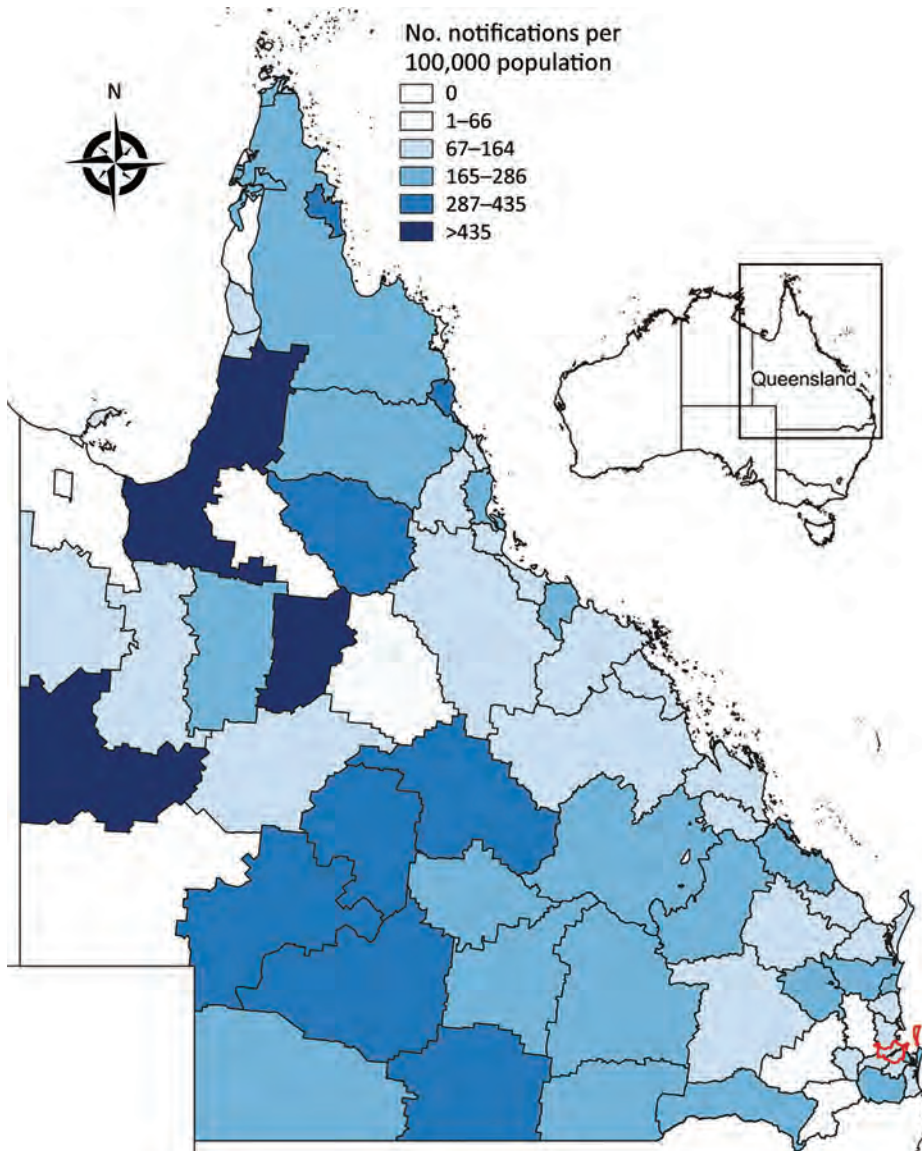
Figure 3. Ross River virus notification rate by local government area, Queensland, Australia, July 1, 2014–June 30, 2015. Brisbane local government area (red outline) is indicated. Inset map shows the location of Queensland in Australia.

No correlation between the mean relative abundance of *Cx. annulirostris* mosquitoes and RRV notifications was observed in other reporting years (data not shown).

The *Ae. procax* population accounted for 6.4% (26,408/411,328) of the total trap catch in 2014–15, a relative abundance significantly higher than those recorded for the 2012–13 (2.3%, 4,654/204,220; p<0.001) and 2013–14 (1.4%, 1,570/108,422; p<0.001) reporting years. As with *Cx. annulirostris* mosquitoes, *Ae. procax* mosquito abundance increased starting week 50 of 2014 but did not reach a sustained peak until week 10 of 2015 and did not decrease until week 18 of 2015 (data not shown). As a result, *Ae. procax* mosquito mean relative abundance only moderately correlated with RRV notifications; a 2-week lag produced the highest correlation (ρ = 0.5543; p<0.001). No correlation was observed in any other reporting year (data not shown).

More *Ae. vigilax* mosquitoes were collected in 2014–15 than in other years. However, the relative abundance was only 51% (211,008/411,328) of the total trap catch, significantly lower than that of 2012–13 (60%, 123,024/204,220; p<0.001) and 2013–14 (78%, 84,133/108,422; p<0.001). *Ae. vigilax* mosquito numbers peaked in December 2014 (data not shown) but returned to typical numbers by early January, consistent with a weak negative correlation with RRV notifications (ρ = –0.3553, p = 0.009).

Virus Detection in Mosquito Pools and FTA Cards

A total of 135 honey-soaked FTA cards were deployed in mosquito traps during February 3–May 20, 2015, and we detected RRV RNA on 12 (8.9%) of them (Figure 4, panel B). On the first week of deployment (week 6 of 2015), 4 cards were positive for RRV RNA. Except for week 10,
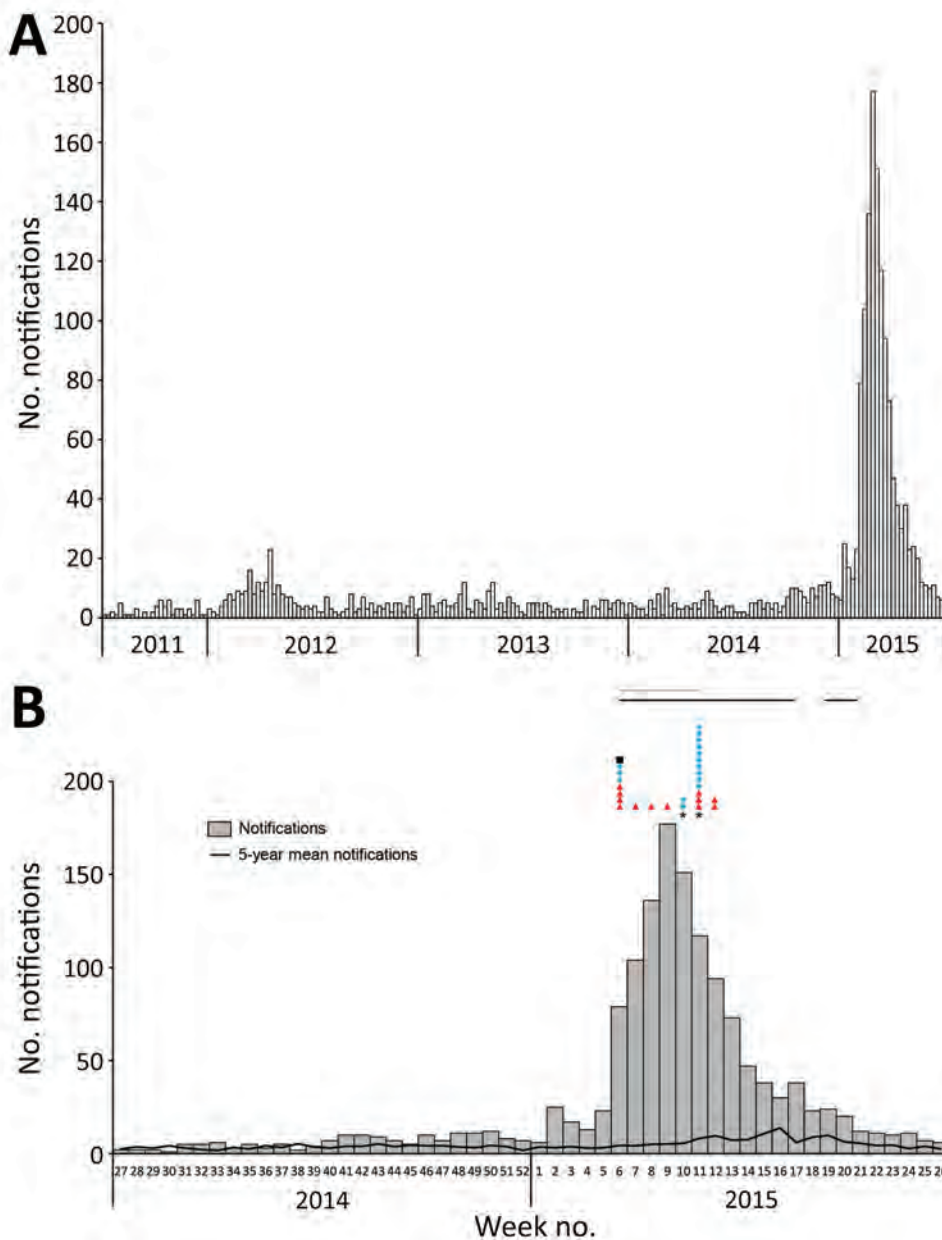
Figure 4. Ross River virus (RRV) notifications by week, Brisbane local government area, Queensland, Australia, July 1, 2011–June 30, 2015 (A), and July 1, 2014–June 30, 2015 (B). Symbols in panel B represent single detection events: red triangles, RRV RNA detection from Flinders Technology Associates cards by real-time reverse transcription PCR; blue diamonds, RRV RNA detection from mosquito pools by real-time reverse transcription PCR; and black square, RRV detection from mosquito pools by cell culture ELISA. Also in panel B, the black line above the graph indicates when Flinders Technology Associates cards were deployed and gray line when mosquito pools were being collected and screened for RRV infection. Mosquitoes acquired from traps in weeks 10 and 11 were damaged by rain; thus, RRV-positive mosquito parts might have stuck to RRV-negative mosquitoes and turned some pools artificially positive.

≥1 card was positive each week during weeks 6–12, after which RRV was not detected. RRV was detected 3 times from FTA cards deployed March 11, 2015 (week 11), and 2 times from cards deployed March 18, 2015 (week 12; Figure 4, panel B). Except for Fig Tree Pocket, RRV RNA was detected ≥1 time from each trap location.

We processed 21,250 mosquitoes (5% of total collected in 2014–15), representing ≥20 species, for RRV detection (Appendix Table 4). Mosquitoes were combined into 385 pools and screened by cell culture ELISA. We also processed 155 pools, representing 10,112 mosquitoes, for rRT-PCR. A single pool of 68 *Cx. annulirostris* mosquitoes collected from Lota in week 6 of 2015 was positive by cell culture ELISA and rRT-PCR. One pool each of *Ae. vigilax* and *Culex orbostiensis* mosquitoes collected in the same trap on the same trap night as the *Cx. annulirostris* population were positive by rRT-PCR. RRV was also detected in a pool of 4 *Mansonia uniformis* mosquitoes collected in week 10 of 2015 at Hemmant. Viral RNA was detected in an additional 11 pools comprising mosquitoes from the trap deployed at Hemmant in weeks 10 (1 pool) and 11 (10 pools) of 2015. However, the species of mosquitoes in these pools could not be identified morphologically because rain permeated the traps and damaged the samples. Thus, the high number of RRV-positive pools from these traps could represent cross-contamination caused by parts

of RRV-positive mosquitoes sticking to RRV-negative mosquitoes. Regardless, these data are evidence that RRV was present at Hemmant during these weeks.

Virus Nucleotide Sequence Phylogenetic Analysis

We determined the complete E3 and E2 gene sequences of 32 RRV samples and phylogenetically compared them with 9 additional RRV sequences from GenBank (accession nos. HM234643, M20162, GQ433354–60). The maximum-likelihood phylogenetic tree inferred from these sequences demonstrated all isolates belonged to the northeastern genotype (Figure 5). The 32 RRV sequences sampled over a 27-year period grouped within 1 of 2 major northeastern lineages, designated I and II (Figure 5). The phylogenetic groupings of BNE2015b (human origin, GenBank accession no. KX757013) and BNE-2885 (mosquito origin, GenBank accession no. KX757014) from Brisbane into lineage I and BNE2015a (human origin, accession no. KX757012) from Brisbane and 19661 (mosquito origin, accession no. KY290883) from Tweed, New South Wales, Australia, into lineage II demonstrate co-circulation of both lineages in southeast Queensland and northeast New South Wales during the 2014–15 outbreak.

Sequences of the outbreak isolates BNE2015b (lineage I) and BNE2015a (lineage II) were highly similar (98.4% nucleotide identity, 99.0% amino acid identity). Within lineage I, 2 sublineages (Ia and Ib) were demonstrated (Figure 5). In a comparison of amino acid sequences, except for the 203769 isolate (Queensland 2015) sequence, which was most similar to the LGRH-7021 (Longreach, Queensland, 2013) isolate sequence, the 2015 and 2016 sublineage Ib sequences all contained an A389T substitution within E2. Within lineage II, the E3 and E2 sequences of isolates 19661 (from an FTA card) and BNE2015a (from a patient) sampled during the 2014–15 outbreak shared 100% nucleotide and amino acid identities. Of note, these 2 sequences contained 3 unique amino acid substitutions in the E2 gene (A369T, M376I, T384A). Another unique E2 amino acid substitution, M45K, was demonstrated in 3 New South Wales 2015 RRV sequences obtained from mosquitoes (188448–50).

Discussion

Outbreaks of RRV involving hundreds to thousands of cases have been reported from all mainland states of Australia (29). The 2014–15 outbreak was unprecedented in the high number of cases reported and large area of the eastern seaboard affected. Our investigations confirmed that human case notifications were distributed across the Brisbane LGA throughout the season, including before the outbreak, early in the outbreak, and at the peak of notifications. The concurrent detection of virus from mosquitoes across Brisbane provides compelling evidence that RRV activity was widespread and the exposure risk for humans high across all suburbs and districts. We suggest that a combination of ecologic factors contributed to the magnitude of the RRV outbreak in Brisbane in 2014–15.

Previous RRV outbreaks in Australia were preceded by above-average rainfall (29,30). The weather in Brisbane during 2014–15 was unusual, characterized by early elevated rainfall that persisted throughout the summer and resulted in total rainfall exceeding the historical mean. These conditions provided temporary freshwater larval habitats for many mosquito species, including *Cx. annulirostris* populations, for an unusually long period. The early increase in *Cx. annulirostris* abundance, which remained high, coupled with a correlation with RRV notifications, suggest that this species was a key vector during the outbreak. In addition, the widespread geographic distribution of *Cx. annulirostris* mosquitoes (data not shown), which reflected the distribution of human notifications, further supports the involvement of this species in the outbreak. The *Cx. annulirostris* mosquito is a competent laboratory vector of RRV that has yielded numerous field isolates in previous studies (31,32) and yielded field isolates in our study. Furthermore, evidence has implicated *Cx. annulirostris* mosquito involvement in RRV outbreaks in New South Wales in 2014–15 (33) and New South Wales and Victoria in 2016–17 (34,35).

On the basis of their temporal and spatial abundance, *Ae. procax* mosquitoes also showed a moderate correlation with human RRV notifications in 2014–15, albeit at a lower relative abundance than *Cx. annulirostris* mosquitoes. Although RRV was not detected in the *Ae. procax* populations herein, this species has previously yielded relatively high numbers of field isolates (when compared with the number of specimens tested) and demonstrates high vector competence for RRV in the laboratory (32). Like *Cx. annulirostris* mosquitoes, *Ae. procax* mosquitoes feed on a range of mammals (36), so they might play a greater role in urban transmission of arboviruses than previously considered (32,37,38).

The most abundant saltmarsh mosquito in southeast Queensland, *Ae. vigilax*, reached notably high numbers in 2014–15. However, this mosquito's relative abundance was significantly lower in 2014–15 than in previous years. Furthermore, the temporal abundance of *Ae. vigilax* populations peaked earlier and had a weak and negative correlation with human case notifications, suggesting that even if involved in enzootic transmission this species was unlikely responsible for sustained transmission to humans throughout the outbreak. In addition, in previous years, high numbers of *Ae. vigilax* mosquitoes were present in the Brisbane LGA without increased numbers of RRV notifications (e.g., 2012–13 and 2013–14), and low numbers

were present in years when RRV notifications were above average (e.g., 2011–12).

Given the complexity of RRV transmission cycles, the role of other common species should not be discounted. Of the remaining 2 species from which RRV was detected during this study, *Ma. uniformis* mosquitoes have previously yielded isolates and been shown to transmit the virus in laboratory experiments (*32*). In contrast, RRV has not been detected in *Cx. orbostiensis* mosquitoes previously, despite extensive testing for

field isolates in New South Wales since 1988, so its status as an RRV vector is unknown.

In Australia, RRV comprises 3 distinct genotypes, western, northeastern, and southeastern, named for the location in which they predominate (*39,40*). The finding of northeastern genotype lineage I and II sequences in human and mosquito samples suggests both lineages contributed to the 2014–15 outbreak and confirms their persistent transmission in eastern Australia. Our results are consistent with previous studies suggesting that the distribution of lineages
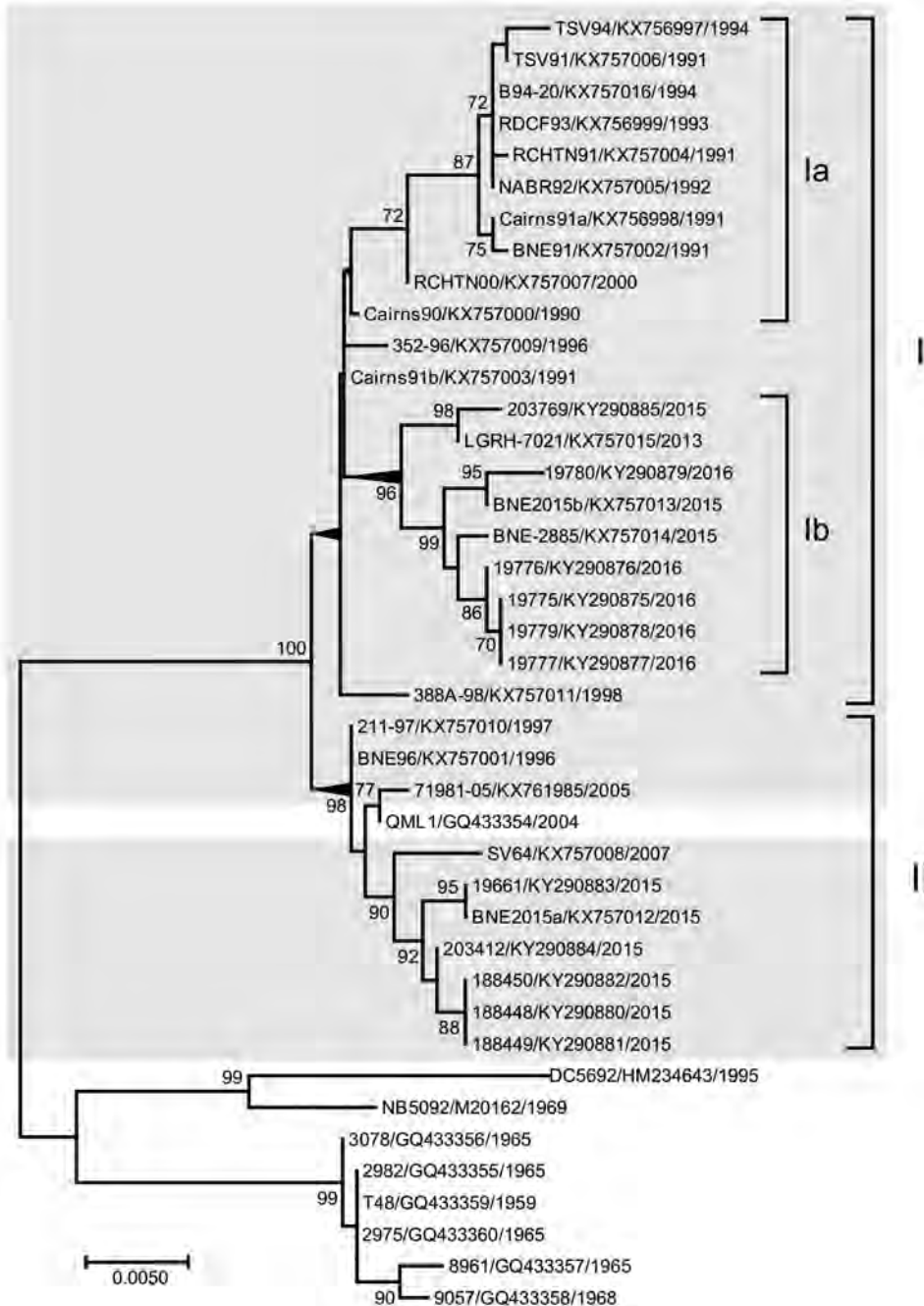
Figure 5. Maximum-likelihood phylogenetic tree of 41 complete Ross River virus envelope (E) 3 and E2 gene nucleotide sequences (1,458 nt), 32 from isolates collected in Queensland and New South Wales, Australia, during January 1, 1990–June 30, 2015 (gray shading), and 9 reference sequences. Tree was constructed by using MEGA 7.0 (https://megasoftware.net) with bootstrap support (1,000 replications). The tree is midpoint rooted for clarity. Circulating northeastern lineages I and II are shown together with sublineages Ia and Ib. Percentage bootstrap support values determined from 1,000 replicates are shown for key nodes. GenBank accession numbers are provided. Scale bar indicates nucleotide substitutions per site.

I and II in eastern Australia are not constrained by geographic distance or location.

We detected several amino acid substitutions in E2 of most 2015 and 2016 RRV isolates, including 3 (A369T, M376I, T384A) in a strain represented by isolates 19661 and BNE2015a. Of note, A369T, M376I, T384A, and A389T all occurred within the putative E2 C-terminal anchor sequence comprising amino acids 365–90 (*41*). Whether these amino acid changes are pleiotropic or represent adaptive changes related to the interaction of E2 with E1 or other structural proteins during viral assembly is unknown.

We investigated entomologic, epidemiologic, and virologic factors associated with the 2014–15 RRV outbreak in Brisbane. A missing factor in the investigation of this and previous outbreaks is the contribution of nonhuman hosts to epidemic transmission. Numerous vertebrate species are likely involved in RRV maintenance (*10*), and the role of each species during outbreaks is probably complex. The widespread distribution of RRV during 2014–15 suggests the involvement of a common ubiquitous species or several reservoir species. Furthermore, limited RRV activity in the preceding years might have increased the pool of nonimmune hosts, contributing to the scale of the outbreak.

Overall, early and consistent rainfall in 2014–15 in southeast Queensland probably contributed to a high abundance and the survival of adult mosquitoes, providing ideal conditions for the largest recorded outbreak of RRV. As demonstrated by the spatial distribution of RRV patients and virus detections in mosquitoes, virus activity was widespread across the Brisbane LGA. Notwithstanding the potential role of other mosquito species in ongoing transmission of RRV, we propose that freshwater species (particularly *Cx. annulirostris* and *Ae. procax* mosquitoes) were likely key drivers of the outbreak activity in Brisbane in 2014–15. We demonstrate that the risk for RRV infection in humans is widespread and driven by complex factors in Queensland.

About the Author

Dr. Jansen is the state consultant medical entomologist for the Communicable Diseases Branch of the Department of Health, Queensland Government, Australia. Dr. Jansen's research interests span various aspects of medical entomology, including the development of preparedness and mitigation strategies for exotic arboviruses and invasive mosquitoes and the description of transmission cycles of endemic and exotic arboviruses.

References

1. van den Hurk AF, Jansen CC. Arboviruses of Oceania. In: Loukas A, editor. Neglected tropical diseases—Oceania. Cham (Switzerland): Springer International Publishing; 2016. p. 193–235.
2. Australian Government Department of Health. Introduction to the National Notifiable Diseases Surveillance System. 2015 Jun 9 [cited 2017 Oct 23]. http://www.health.gov.au/internet/main/publishing.nsf/Content/cda-surveil-nndss-nndssintro.htm
3. Fraser JR. Epidemic polyarthritis and Ross River virus disease. Clin Rheum Dis. 1986;12:369–88.
4. Flaxman JP, Smith DW, Mackenzie JS, Fraser JRE, Bass SP, Hueston L, et al. A comparison of the diseases caused by Ross River virus and Barmah Forest virus. Med J Aust. 1998;169:159–63. https://doi.org/10.5694/j.1326-5377.1998.tb116019.x
5. Harley D, Sleigh A, Ritchie S. Ross River virus transmission, infection, and disease: a cross-disciplinary review. Clin Microbiol Rev. 2001;14:909–32. https://doi.org/10.1128/CMR.14.4.909-932.2001
6. Harley D, Bossingham D, Purdie DM, Pandeya N, Sleigh AC. Ross River virus disease in tropical Queensland: evolution of rheumatic manifestations in an inception cohort followed for six months. Med J Aust. 2002;177:352–5.
7. Mylonas AD, Brown AM, Carthew TL, McGrath B, Purdie DM, Pandeya N, et al. Natural history of Ross River virus-induced epidemic polyarthritis. Med J Aust. 2002;177:356–60.
8. Claflin SB, Webb CE. Ross River virus: many vectors and unusual hosts make for an unpredictable pathogen. PLoS Pathog. 2015;11:e1005070. https://doi.org/10.1371/journal.ppat.1005070
9. Kay BH, Hall RA, Fanning ID, Mottram P, Young PL, Pollitt CC. Experimental infection of vertebrates with Murray Valley encephalitis and Ross River viruses. Arbovirus Res Aust. 1986;4:71–5.
10. Stephenson EB, Peel AJ, Reid SA, Jansen CC, McCallum H. The non-human reservoirs of Ross River virus: a systematic review of the evidence. Parasit Vectors. 2018;11:188. https://doi.org/10.1186/s13071-018-2733-8
11. Tesh RB, McLean RG, Shroyer DA, Calisher CH, Rosen L. Ross River virus (*Togaviridae*: *Alphavirus*) infection (epidemic polyarthritis) in American Samoa. Trans R Soc Trop Med Hyg. 1981;75:426–31. https://doi.org/10.1016/0035-9203(81)90112-7
12. Lindsay MD, Johansen C, Broom AK, D'Ercole M, Wright AE, Condon R, et al. The epidemiology of outbreaks of Ross River virus infection in Western Australia in 1991–1992. Arbovirus Res Aust. 1993;6:72–6.
13. Russell RC. Ross River virus: ecology and distribution. Annu Rev Entomol. 2002;47:1–31. https://doi.org/10.1146/annurev.ento.47.091201.145100
14. Harley D, Ritchie S, Phillips D, van den Hurk A. Mosquito isolates of Ross River virus from Cairns, Queensland, Australia. Am J Trop Med Hyg. 2000;62:561–5. https://doi.org/10.4269/ajtmh.2000.62.561
15. Knope KE, Doggett SL, Jansen CC, Johansen CA, Kurucz N, Feldman R, et al. Arboviral diseases and malaria in Australia,

2014–15: annual report of the National Arbovirus and Malaria Advisory Committee. Commun Dis Intell. 2019;43. https://doi.org/10.33321/cdi.2019.43.14

16. Queensland Treasury. Population estimate. Regions. Estimated resident population by local government area (LGA), Queensland, 1991 to 2018. 2019 Mar 29 [cited 2019 Oct 15]. http://www.qgso.qld.gov.au/products/tables/erp-lga-qld/index.php?region=brisbane

17. Australian Government Bureau of Meteorology. Climate statistics for Australian locations. Monthly climate statistics. 2017 [cited 2017 Jun 13]. http://www.bom.gov.au/climate/averages/tables/cw_040913.shtml

18. Queensland Government Department of Health. Notifiable conditions register. 2016 Feb 3 [cited 2017 Oct 23]. https://www.health.qld.gov.au/clinical-practice/guidelines-procedures/diseases-infection/notifiable-conditions/register

19. Queensland Health. Public Health Act 2005. 2019 Oct 11 [cited 2019 Oct 15]. https://www.health.qld.gov.au/system-governance/legislation/specific/public-health-act

20. Australian Government Department of Health. Ross River virus infection case definition. Australian national notifiable diseases case definitions. 2016 Jan 1 [cited 2019 Oct 15]. http://www.health.gov.au/internet/main/publishing.nsf/content/cda-surveil-nndss-casedefs-cd_rrv.htm

21. International Organization for Standardization. ISO 8601:2004. Data elements and interchange formats—information interchange—representation of dates and times. 2004 Dec [cited 2017 Oct 23]. https://www.iso.org/standard/40874.html

22. Australian Bureau of Statistics. 1270.0.55.001-Australian Statistical Geography Standard (ASGS): volume 1-main structure and greater capital city statistical areas, July 2011. 2016 Jul 11 [cited 2017 Oct 23]. http://www.abs.gov.au/ausstats/abs@.nsf/Latestproducts/88F6A0EDEB8879C0CA257801000C64D9

23. Australian Bureau of Statistics. Australian Demographic Statistics Mar 2017. 2017 Dec 13 [cited 2017 Dec 23]. http://www.abs.gov.au/AUSSTATS/abs@.nsf/DetailsPage/3101.0Mar%202017

24. van Essen PH, Kemme JA, Ritchie SA, Kay BH. Differential responses of *Aedes* and *Culex* mosquitoes to octenol or light in combination with carbon dioxide in Queensland, Australia. Med Vet Entomol. 1994;8:63–7. https://doi.org/10.1111/j.1365-2915.1994.tb00387.x

25. Flies EJ, Toi C, Weinstein P, Doggett SL, Williams CR. Converting mosquito surveillance to arbovirus surveillance with honey-baited nucleic acid preservation cards. Vector Borne Zoonotic Dis. 2015;15:397–403. https://doi.org/10.1089/vbz.2014.1759

26. Hall-Mendelin S, Ritchie SA, Johansen CA, Zborowski P, Cortis G, Dandridge S, et al. Exploiting mosquito sugar feeding to detect mosquito-borne pathogens. Proc Natl Acad Sci U S A. 2010;107:11255–9. https://doi.org/10.1073/pnas.1002040107

27. Broom AK, Hall RA, Johansen CA, Oliveira N, Howard MA, Lindsay MD, et al. Identification of Australian arboviruses in inoculated cell cultures using monoclonal antibodies in ELISA. Pathology. 1998;30:286–8. https://doi.org/10.1080/00313029800169456

28. Hall RA, Prow NA, Pyke AT. Ross River virus. In: Liu D, editor. Molecular detection of human viral pathogens. Boca Raton (FL): CRC Press; 2011. p. 349–59.

29. Kelly-Hope LA, Purdie DM, Kay BH. Ross River virus disease in Australia, 1886–1998, with analysis of risk factors associated with outbreaks. J Med Entomol. 2004;41:133–50. https://doi.org/10.1603/0022-2585-41.2.133

30. Woodruff RE, Guest CS, Garner MG, Becker N, Lindesay J, Carvan T, et al. Predicting Ross River virus epidemics from regional weather data. Epidemiology. 2002;13:384–93. https://doi.org/10.1097/00001648-200207000-00005

31. Ritchie SA, Fanning ID, Phillips DA, Standfast HA, McGinn D, Kay BH. Ross River virus in mosquitoes (Diptera:*Culicidae*) during the 1994 epidemic around Brisbane, Australia. J Med Entomol. 1997;34:156–9. https://doi.org/10.1093/jmedent/34.2.156

32. Ryan PA, Do KA, Kay BH. Definition of Ross River virus vectors at Maroochy Shire, Australia. J Med Entomol. 2000;37:146–52. https://doi.org/10.1603/0022-2585-37.1.146

33. Doggett S, Haniotis J, Clancy J, Webb C, Toi C, Hueston L, et al. The New South Wales Arbovirus Surveillance and Mosquito Monitoring Program, 2014–2015 annual report. 2015 [cited 2019 Oct 15]. http://medent.usyd.edu.au/arbovirus/information/arbovirus_annual_reports_pdfs/arbovirus_annual_report_2014_2015.pdf

34. Wong S, Brown K, Crowder J, Chea S, Mee P, Batovska J, et al. Victorian Arbovirus Disease Control Program annual report 2016–2017. Melbourne (VIC, Australia): Agriculture Victoria; 2017.

35. Doggett S, Haniotis J, Clancy J, Webb C, Toi C, Hueston L, et al. The New South Wales Arbovirus Surveillance and Mosquito Monitoring Program, 2016–2017 annual report. 2017 [cited 2019 Oct 15]. https://www.health.nsw.gov.au/environment/pests/vector/Publications/nswasp-annual-report-2016-2017.pdf

36. Kay BH, Boyd AM, Ryan PA, Hall RA. Mosquito feeding patterns and natural infection of vertebrates with Ross River and Barmah Forest viruses in Brisbane, Australia. Am J Trop Med Hyg. 2007;76:417–23. https://doi.org/10.4269/ajtmh.2007.76.417

37. Doggett SL, Clancy J, Haniotis J, Webb CE, Hueston L, Marchetti M, et al. Arbovirus and vector surveillance in New South Wales, 2004/5–2007/8. Arbovirus Res Aust. 2009;10:28–37.

38. Webb CE, Jansen CC, van den Hurk AF, Russell RC. Is *Aedes procax* (Skuse) emerging as an important vector of arboviruses in coastal NSW? Arbovirus Res Aust. 2009;10:182.

39. Sammels LM, Coelen RJ, Lindsay MD, Mackenzie JS. Geographic distribution and evolution of Ross River virus in Australia and the Pacific Islands. Virology. 1995;212:20–9. https://doi.org/10.1006/viro.1995.1449

40. Jones A, Lowry K, Aaskov J, Holmes EC, Kitchen A. Molecular evolutionary dynamics of Ross River virus and implications for vaccine efficacy. J Gen Virol. 2010;91:182–8. https://doi.org/10.1099/vir.0.014209-0

41. Strauss EG, Lenches EM, Strauss JH. Molecular genetic evidence that the hydrophobic anchors of glycoproteins E2 and E1 interact during assembly of alphaviruses. J Virol. 2002;76:10188–94. https://doi.org/10.1128/JVI.76.20.10188-10194.2002

Address for correspondence: Andrew F. van den Hurk, Queensland Government Department of Health, Public Health Virology, Forensic and Scientific Services, 39 Kessels Rd, Coopers Plains, QLD 4108 Australia; email: andrew.vandenhurk@health.qld.gov.au

Multicountry Analysis of Spectrum of Clinical Manifestations in Children <5 Years of Age Hospitalized with Diarrhea

Jillian Murray, S. Yati Soenarto,
Nenny S. Mulyani, Pushpa S. Wijesinghe,
Evans M. Mpabalwani, Julia C. Simwaka,
Belem Matapo, Jason M. Mwenda,
Gayane Sahakyan, Svetlana Grigoryan,
Artavazd Vanyan, Sergey Khactatryan,
Jennifer Sanwogou, Lúcia Helena de Oliveira,
Gloria Rey-Benito, Gagandeep Kang,
Fatima Serhan, Jacqueline E. Tate,
Negar Aliabadi, Adam L. Cohen, and the
Global Rotavirus Surveillance Network
Clinical Presentation Group[1]

After introduction of rotavirus vaccine, other pathogens might become leading causes of hospitalizations for severe diarrhea among children <5 years of age. Our study in 33 hospitals in 7 countries found acute gastroenteritis accounted for most (84%) reported hospitalizations of children with diarrhea. Bloody and persistent diarrhea each accounted for <1%.

Diarrhea is a leading cause of illness and death in children <5 years of age globally. The most common

Author affiliations: World Health Organization, Geneva, Switzerland (J. Murray, F. Serhan, A.L. Cohen); Universitas Gadjah Mada/Dr. Sardjito Hospital, Yogyakarta, Indonesia (S.Y. Soenarto, N.S. Mulyani); World Health Organization, South-East Asia Regional Office, New Delhi, India (P.S. Wijesinghe); University Teaching Hospital, Lusaka, Zambia (E.M. Mpabalwani, J.C. Simwaka); World Health Organization Country Office, Lusaka (B. Matapo); World Health Organization Regional Office for Africa, Brazzaville, Republic of the Congo (J.M. Mwenda); National Immunization Program, Yerevan, Armenia (G. Sahakyan); National Centre of Disease Control and Prevention, Yerevan (G. Sahakyan, S. Grigoryan, A. Vanyan); Ministry of Health of Armenia, Yerevan (G. Sahakyan, S. Grigoryan, A. Vanyan, S. Khactatryan); Immunization and Epidemiology of Vaccine-Preventable Diseases Program, Yerevan (S. Grigoryan); Pan American Health Organization, Washington, DC, USA (J. Sanwogou, L.H. de Oliveira, G. Rey-Benito); Christian Medical College, Vellore, India (G. Kang); Centers for Disease Control and Prevention, Atlanta, Georgia, USA (J.E. Tate, N. Aliabadi)

cause is rotavirus. Persons infected with this virus typically have acute watery diarrhea and gastroenteritis (*1–4*). As rotavirus vaccines are increasingly incorporated into national immunization programs globally and the proportion of diarrhea caused by rotavirus decreases, other causes of pediatric diarrhea (such as *Shigella* spp.) are responsible for an increasing proportion of diarrhea, and these pathogens might have different clinical manifestations (*5–7*).

Because of this evolving etiology of diarrhea in children, it is necessary to clarify the spectrum of clinical manifestations of diarrhea to better inform interventions and surveillance systems, particularly in low- and middle-income countries (LMICs), where the burden of diarrhea is highest (*1–4*). We report a spectrum of clinical manifestations for diarrheal illness reported in hospitalized children <5 years of age in 7 countries.

The Study

Data collection and reporting to the Global Rotavirus Surveillance Network occurs as part of routine public health surveillance in participating countries and does not require human subjects review. As part of a larger study on the etiology of pediatric diarrhea in LMICs, we conducted a retrospective review of ward admission logbooks and electronic databases from 33 hospitals with pediatric services that conduct sentinel surveillance for rotavirus. Hospitals were chosen for this analysis from the World Health Organization (WHO)–coordinated Global Rotavirus Surveillance Network and the Indian National Rotavirus Surveillance Network (*8–10*).

A convenience sample of countries was chosen by using the following inclusion criteria: countries had ≥1 sentinel hospital reporting data to one of the surveillance networks above, sentinel sites in the country had 12 consecutive months of available logbook data for each year included in the analysis, and individual sentinel sites in the country enrolled ≥100 diarrhea case-patients each year. Sites were not eligible for inclusion in the larger study, and therefore our convenience sample, if they had participated in the Global Enteric Multicenter Study (*11*). We used a convenience sample to ensure that sites

selected were available and able to perform the retrospective logbook review.

Participating countries performed retrospective manual reviews of admissions logbooks. All countries used paper-based surveillance logbooks except countries in the Americas and Zambia, which have electronic databases. Data were abstracted by hospital data managers for total diarrhea admissions for children <5 years of age in at least 2–3 of the previous 5 years for the following mutually exclusive clinical surveillance categories: acute gastroenteritis (watery, nonbloody diarrhea); bloody diarrhea (dysentery); persistent (chronic, nonacute) diarrhea; and other, nonspecified diarrhea (12). The other, nonspecified diarrhea category contains admissions that did not meet criteria for acute watery, bloody, or persistent diarrhea or for which the logbook information was insufficient to classify the case into a specific category. Aggregate numbers of diarrheal admissions were tallied for each category by month and year.

For countries with prevaccine and postvaccine introduction data, we compared the proportions of admissions for each diarrheal category in the preintroduction and postintroduction periods by using the χ^2 test. We used Stata version 12 (https://www.stata.com) for all analyses.

We included 7 countries that had 33 sentinel surveillance hospitals in this analysis. Acute gastroenteritis accounted for most (median 84%) of hospitalized case-patients with diarrhea overall. Bloody diarrhea accounted for a median <1%, and persistent diarrhea accounted for a median of 0% (Table 1). The proportion of diarrhea cases classified as acute gastroenteritis varied from 41% to 96%; acute gastroenteritis also accounted for most cases in each country except for El Salvador, where 59% of cases were categorized as other, nonspecified. Four countries provided data disaggregated by sentinel site (Table 2). The proportion of total diarrhea admissions due to acute gastroenteritis varied within sites from year to year and between sites within the same country.

The proportions of bloody and persistent diarrhea were similar across years in the same country, but there were some differences in bloody diarrhea proportions between sites in the same country. In Indonesia, 4 sites had average proportions of <10% bloody diarrhea, but 1 site had an average of 28% across both years. Overall, a median of 11% of diarrheal cases were categorized as other, nonspecified.

Zambia provided 3 years of data from before and 2 years of data from after rotavirus vaccine introduction (Table 1). The proportion of diarrhea caused by acute gastroenteritis decreased from 86% in the preintroduction era to 70% in the postintroduction era (p<0.01). There was a concomitant increase in other, nonspecified diarrhea cases, from 14% to 29%, over the same period (p<0.01).

Conclusions

The most common clinical manifestations of children with cases of diarrhea were acute watery diarrhea and gastroenteritis in the LMICs analyzed; cases classified as bloody and persistent diarrhea cases were rare. However, the proportions of different clinical manifestations of pediatric diarrhea varied between sentinel sites within a country and between countries and regions. Differences between sites within the same country could be caused by different hospital-specific practices for describing the clinical manifestation of diarrheal disease, disease referral and healthcare use patterns, or relative uptake of rotavirus vaccine in countries that have introduced vaccine.

In the period before a country introduces rotavirus vaccine, one of the main objectives of rotavirus surveillance

Table 1. Characteristics of children <5 y of age hospitalized for diarrhea in selected countries from the WHO-coordinated Global Rotavirus Sentinel Surveillance Network and the Indian National Rotavirus Surveillance Network, 2009–2016*

Vaccine status and country/WHO region	No. sites (no. years data)	No. diarrhea cases	Clinical manifestations of diarrhea			
			Acute watery	Bloody	Persistent	Other, nonspecified†
Overall	33‡ (23)	42,632	29,853	358	1,467	10,954
Before§	13 (8)	11,637	10,396	321	55	865
India/SEAR	7 (3)	5,261	4,940 (94)	196 (4)	20 (<1)	105 (2)
Indonesia/SEAR	5 (2)	1,995	1,695 (85)	110 (6)	35 (2)	155 (8)
Zambia/AFR	1 (3)	4,381	3,761 (86)	15 (<1)	0 (0)	605 (14)
Median proportion	NA	NA	86	4	<1	8
After§	21 (15)	30,995	19,457	37	1,412	10,089
Armenia/EUR	2 (3)	8,938	7,414 (83)	0 (0)	1,412 (16)	112 (1)
Bolivia/AMR	6 (3)	4,505	3,229 (72)	0 (0)	0 (0)	1,276 (28)
El Salvador/AMR	8 (3)	13,321	5,466 (41)	0 (0)	0 (0)	7,855 (59)
Paraguay/AMR	4 (3)	1,515	1,454 (96)	0 (0)	0 (0)	61 (4)
Zambia/AFR	1 (2)	2,716	1,894 (70)	37 (1)	0 (0)	785 (29)
Median proportion	NA	NA	72	0	0	28
Overall median proportion	NA	NA	84	<1	0	11

*Values are no. (%) unless otherwise indicated. AFR, African region; AMR, Americas region; EUR, European region; SEAR, Southeast Asian region; WHO, World Health Organization; NA, not applicable.
†Other category contains admissions that did not meet criteria for acute gastroenteritis, bloody or persistent diarrhea, or the logbook information was insufficient to classify the case into a specific category.
‡Includes only 1 site for Zambia, which has data both preintroduction and postintroduction.
§Excludes year of vaccine introduction for Armenia, Bolivia, El Salvador, Paraguay, and Zambia.

Table 2. Proportion of children <5 years of age hospitalized for diarrhea who also had acute gastroenteritis at sentinel sites from the WHO-coordinated Global Rotavirus Sentinel Surveillance Network, 2013–2015*

Country	Year of vaccine introduction	National rotavirus vaccine coverage, 2016, % (13)	Site	Acute gastroenteritis, %†			
				2013	2014	2015	Weighted mean
Bolivia	2008	99	1	82	65	72	74
			2	81	82	96	85
			3	76	65	100	78
			4	56	49	46	52
			5	93	99	88	95
			6	53	50	37	48
			Total	74	68	71	72
El Salvador	2006	92	1	28	49	57	40
			2	40	38	24	35
			3	48	41	41	44
			4	51	34	30	40
			5	59	46	75	61
			6	44	29	19	30
			7	22	6	NA	14
			8	62	54	54	57
			Total	45	35	43	41
Paraguay	2009	93	1	96	97	100	98
			2	100	84	NA	89
			3	78	100	100	94
			4	100	97	100	99
			Total	92	97	100	96
Indonesia	NA	NA	1	NA	98	95	97
			2	NA	95	91	93
			3	NA	97	99	98
			4	NA	61	70	66
			5	NA	68	58	63
			Total	NA	83	86	85

*NA, not available; WHO, World Health Organization.
†These calculations include nonspecified diarrhea in the denominator. Thus, individual site years might have higher percentage acute gastroenteritis if this category is excluded.

is to provide data on burden of disease and to describe rotavirus disease epidemiology (12). In the period after rotavirus vaccine introduction, one of the main objectives of surveillance is to assess the effect of vaccine. Although patient admissions for bloody and persistent diarrhea constitute a smaller proportion of pediatric case-patients with diarrhea, excluding these patients in pediatric diarrhea surveillance might overestimate the proportion of total diarrhea cases as being positive for rotavirus. Although WHO recommends surveillance for acute watery diarrhea to monitor rotavirus disease, the case definition of diarrheal cases enrolled needs to be expanded to fully capture the changing etiology of disease in the post–rotavirus vaccine era (12,14).

Our study and analysis have several limitations, many of which are caused by the retrospective nature of logbook reviews. First, the review was conducted as a convenience sample of 7 countries. Therefore, findings might not be generalizable to every country. There are regional variations in the case definitions based on the practices of clinicians at individual sentinel hospitals. Large proportions of diarrhea cases were also categorized as other, nonspecified, which might have been defined differently locally or over time; logbooks often have inadequate information to classify each case into one of the specified categories used for this analysis. In addition, age

stratification <5 years of age for diarrhea hospitalizations was not available. Last, site-specific differences, such as disease classification practices and healthcare use patterns, and regional differences, such as rurality, socioeconomic status, and prevalence of malnutrition, might also play a role in intracountry differences, and data on these characteristics for the hospitals included in this analysis were not available.

Monitoring bloody and persistent pediatric diarrhea in addition to acute gastroenteritis is useful for fully understanding the burden and etiology of diarrhea in children, especially after introduction of rotavirus vaccine. Expanding the case definition recommended by WHO for pediatric diarrhea surveillance to include other types of diarrhea would facilitate more robust disease estimates and monitor the rollout and effect of these vaccines once they are introduced.

About the Author

Ms. Murray is an epidemiologist at the World Health Organization, Geneva, Switzerland. Her primary research interest is vaccine-preventable diseases.

References

1. Wang H, Naghavi M, Allen C, Barber RM, Bhutta ZA, Carter A, et al.; GBD 2015 Mortality and Causes of Death Collaborators. Global, regional, and national life expectancy, all-cause mortality, and cause-specific mortality for 249 causes of death, 1980–2015: a systematic analysis for the Global Burden of Disease Study 2015. Lancet. 2016;388:1459–544. https://doi.org/10.1016/S0140-6736(16)31012-1
2. Tate JE, Burton AH, Boschi-Pinto C, Steele AD, Duque J, Parashar UD; WHO-Coordinated Global Rotavirus Surveillance Network. 2008 estimate of worldwide rotavirus-associated mortality in children younger than 5 years before the introduction of universal rotavirus vaccination programmes: a systematic review and meta-analysis. Lancet Infect Dis. 2012;12:136–41. https://doi.org/10.1016/S1473-3099(11)70253-5
3. World Health Organization. Rotavirus vaccines. WHO position paper, January 2013. Wkly Epidemiol Rec. 2013;88:49–64.
4. Operario DJ, Platts-Mills JA, Nadan S, Page N, Seheri M, Mphahlele J, et al. Etiology of severe acute watery diarrhea in children in the global rotavirus surveillance network using quantitative polymerase chain reaction. J Infect Dis. 2017;216:220–7. https://doi.org/10.1093/infdis/jix294
5. Banajeh SM, Abu-Asba BA. The epidemiology of all-cause and rotavirus acute gastroenteritis and the characteristics of rotavirus circulating strains before and after rotavirus vaccine introduction in Yemen: analysis of hospital-based surveillance data. BMC Infect Dis. 2015;15:418. https://doi.org/10.1186/s12879-015-1165-8
6. Becker-Dreps S, Bucardo F, Vilchez S, Zambrana LE, Liu L, Weber DJ, et al. Etiology of childhood diarrhea after rotavirus vaccine introduction: a prospective, population-based study in Nicaragua. Pediatr Infect Dis J. 2014;33:1156–63. https://doi.org/10.1097/INF.0000000000000427
7. Aliabadi N, Antoni S, Mwenda JM, Weldegebriel G, Biey JN, Cheikh D, et al. Global impact of rotavirus vaccine introduction on rotavirus hospitalisations among children under 5 years of age, 2008-16: findings from the Global Rotavirus Surveillance Network. Lancet Glob Health. 2019;7:e893–903. https://doi.org/10.1016/S2214-109X(19)30207-4
8. Agócs MM, Serhan F, Yen C, Mwenda JM, de Oliveira LH, Teleb N, et al.; Department of Immunization, Vaccines, and Biologicals, World Health Organization (WHO), Geneva, Switzerland; Centers for Disease Control and Prevention (CDC). WHO global rotavirus surveillance network: a strategic review of the first 5 years, 2008–2012. MMWR Morb Mortal Wkly Rep. 2014;63:634–7.
9. Mehendale S, Venkatasubramanian S, Girish Kumar CP, Kang G, Gupte MD, Arora R. Expanded Indian National Rotavirus Surveillance Network in the context of rotavirus vaccine introduction. Indian Pediatr. 2016;53:575–81. https://doi.org/10.1007/s13312-016-0891-3
10. World Health Organization Vaccine-Preventable Surveillance Team. WHO Global Invasive Bacterial Vaccine-Preventable Disease and Rotavirus Surveillance Network Bulletin; 2017 [cited 2019 Jan]. https://mailchi.mp/9379015a2472/who-ib-vpd-and-rotavirus-surveillance-bulletin-june-1737585
11. Kotloff KL, Nataro JP, Blackwelder WC, Nasrin D, Farag TH, Panchalingam S, et al. Burden and aetiology of diarrhoeal disease in infants and young children in developing countries (the Global Enteric Multicenter Study, GEMS): a prospective, case–control study. Lancet. 2013;382:209–22. https://doi.org/10.1016/S0140-6736(13)60844-2
12. World Health Organization. Vaccine-preventable disease surveillance standards: rotavirus; 2018 [cited 2019 Jul 17]. https://www.who.int/immunization/monitoring_surveillance/burden/vpd/WHO_SurveillanceVaccinePreventable_19_Rotavirus_R2.pdf
13. World Health Organization. WHO/UNICEF estimates of national immunization coverage; 2017 [cited 2017 Sep 13]. http://www.who.int/immunization/monitoring_surveillance/routine/coverage/en/index4.html
14. Lanata CF, Fischer-Walker CL, Olascoaga AC, Torres CX, Aryee MJ, Black RE; Child Health Epidemiology Reference Group of the World Health Organization and UNICEF. Global causes of diarrheal disease mortality in children <5 years of age: a systematic review. PLoS One. 2013;8:e72788. https://doi.org/10.1371/journal.pone.0072788

Address for correspondence: Adam L. Cohen, World Health Organization, Ave Appia 20, CH-1211, 1202 Geneva, Switzerland; email: cohena@who.int

Sheep as Host Species for Zoonotic *Babesia venatorum*, United Kingdom

Alexander Gray, Paul Capewell, Colin Loney,
Frank Katzer, Brian R. Shiels, William Weir

Babesia venatorum is an increasingly prominent zoonotic parasite that predominantly infects wild deer. Our molecular examination of *Babesia* infecting mammals in the United Kingdom identified 18S sequences in domestic sheep isolates identical to zoonotic *B. venatorum*. Identification of this parasite in livestock raises concerns for public health and farming policy in Europe.

Babesiosis, an economically consequential animal disease caused by a wide range of tick-transmitted *Babesia* spp. parasites, is recognized as an emerging infection in humans (*1*). *Babesia venatorum* (formerly *Babesia* sp. EU1) is notable in that it appears able to infect humans without immune suppression or splenectomy and can present with more severe symptoms (*2,3*). However, the higher prevalence in healthy persons may be a consequence of intensive active sampling; understanding the true impact on healthy patients requires further investigation. Nevertheless, the parasite is increasingly reported in Europe, with 3 confirmed human infections (*3,4*). Babesiosis is treatable in most cases (*5*), although successful treatment depends on rapid and accurate diagnosis of the correct *Babesia* species. Diagnosis may be complicated by possible serologic cross-reactivity in laboratory diagnostic tests; *B. venatorum* infections may have been overlooked or misdiagnosed (*1*). Recent serologic reexamination of human babesiosis cases using *B. venatorum* antigen derived from a cloned isolate found that *Babesia* isolates from Europe could be typed without cross-reactivity, indicating the potential for more refined tests (*6*).

Despite identification across continental Europe, *B. venatorum* infecting vertebrate hosts has not been reported in the United Kingdom. Six 18S small subunit (SSU) rRNA sequences with high similarity to *B. venatorum* (99%) have been amplified from ticks infesting dogs and cats in the United Kingdom, but no infected mammalian hosts have been detected despite intensive sampling (*7,8*). In continental Europe, roe deer are believed to be the primary vertebrate host (*9,10*), although it is possible that livestock could represent a source of infection, as *B. venatorum* has been detected in ticks collected from sheep in Switzerland (*11*) and cattle in Belgium (*12*). Even so, *B. venatorum* infecting these hosts has not been reported, and livestock are not considered a major factor in disease epidemiology.

The Study

To confirm that *B. venatorum* is present in the United Kingdom and to identify putative vertebrate hosts, we collected blood from sheep (n = 93) and cattle (n = 107) at 2 farms in northeastern Scotland (Appendix Figure, https://wwwnc.cdc.gov/EID/article/25/12/19-0459-App1.pdf), selected because of previous reports of tickborne disease, including red water in cattle (*Babesia divergens* infection) and tickborne fever (*Anaplasma phagocytophilum* infection) and louping ill (ovine encephalomyelitis) in sheep. We also collected blood postmortem from culled wild red deer at site A (n = 24) and 6 surrounding areas (n = 60; Appendix Figure). To provide temporal information, we sampled 34 sheep at site B in both June and November 2014 and sampled 12 sheep in either June or November. The study was approved by the Ethics and Welfare Committee of the University of Glasgow School of Veterinary Medicine (Ref. 15a/13).

We prepared smears from sheep blood and stained them with May-Grünwald Giemsa stain. We extracted DNA using a Wizard Genomic DNA Purification Kit (Promega, https://www.promega.com) with prior homogenization and incubation with proteinase K (Invitrogen, https://www.thermofisher.com). We amplified the informative hypervariable V4 region of the 18S SSU rRNA gene using nested PCR and previously validated primers/conditions (outer: BT1-F 5′-GGTTGATCCTGCCAGTAGT and BTH-1R 5′-TTGCGACCATACTCCCCCCA [*13*]; inner: RLB-F2 5′-GACACAGGGAGGTAGTGACAAG and RLB-R2 5′-CTAAGAATTTCACCTCTGACAGT [*14*]). We separated amplicons of the predicted size using agarose gel electrophoresis, purified them using a QIAquick PCR purification kit (QIAGEN, https://www.qiagen.com), and had them sequenced commercially (Eurofins Genomics, https://www.eurofinsgenomics.com). We deposited the sequences into GenBank (accession ns. MK641004–18) and

Author affiliations: University of Glasgow, Glasgow, Scotland, UK
(A. Gray, P. Capewell, C. Loney, B.R. Shiels, W. Weir);
Moredun Research Institute, Penicuik, Scotland, UK (F. Katzer)

compared them with the National Center for Biotechnology Information nonredundant database using BLAST (https://blast.ncbi.nlm.nih.gov). We aligned high-scoring hits and constructed a neighbor-joining tree using ClustalW (https://www.genome.jp/tools-bin/clustalw). We assessed tree stability with 1,000 bootstrapping replicates and visualized it using FigTree version 1.4.2 (https://github.com/rambaut/figtree/releases). We included the bovine 18S SSU rRNA sequence as a root.

Initial blood smears from sheep revealed the presence of a small *Babesia* species displaying ring and pyriform morphology in 3 samples (Figure 1). Further PCR and sequencing revealed 11 positive samples that were identical to 30 *Babesia* 18S SSU rRNA sequences in the National Center for Biotechnology Information database annotated as *Babesia* sp. EU1 or *B. venatorum* (Figure 2). These sequences had been amplified from human patients in Austria, Italy, and China. These data demonstrate that *B. venatorum* is indeed present in the United Kingdom and that domestic sheep are a host.

At the site sampled on 2 separate occasions, most (85%) ewes were negative in June and November 2014 and none were positive at both times. Four (12%) were negative in June and became positive in November, whereas 1 was positive on first sampling but negative on the second. These findings indicate that *B. venatorum* infection is persistent but dynamic within the sheep population; new animals are infected over time, and previously infected animals become PCR negative.

A separate group of 4 sequences distinct from *B. venatorum* was also obtained in the study and showed high identity to the sheep apicomplexan parasite *Sarcocystis tenella* (Figure 2). No *B. venatorum* infections were detected in the cattle population, despite sharing pasture with infected sheep, and no *B. venatorum* infections were detected in any of the culled red deer.

Conclusions

This study confirms that *B. venatorum* is present in the United Kingdom, but it remains unclear how the parasite entered the country, because there was no history of imported animals at either farm surveyed. However, the survey sites are situated near the main landing areas for migratory birds coming to the United Kingdom from continental Europe,
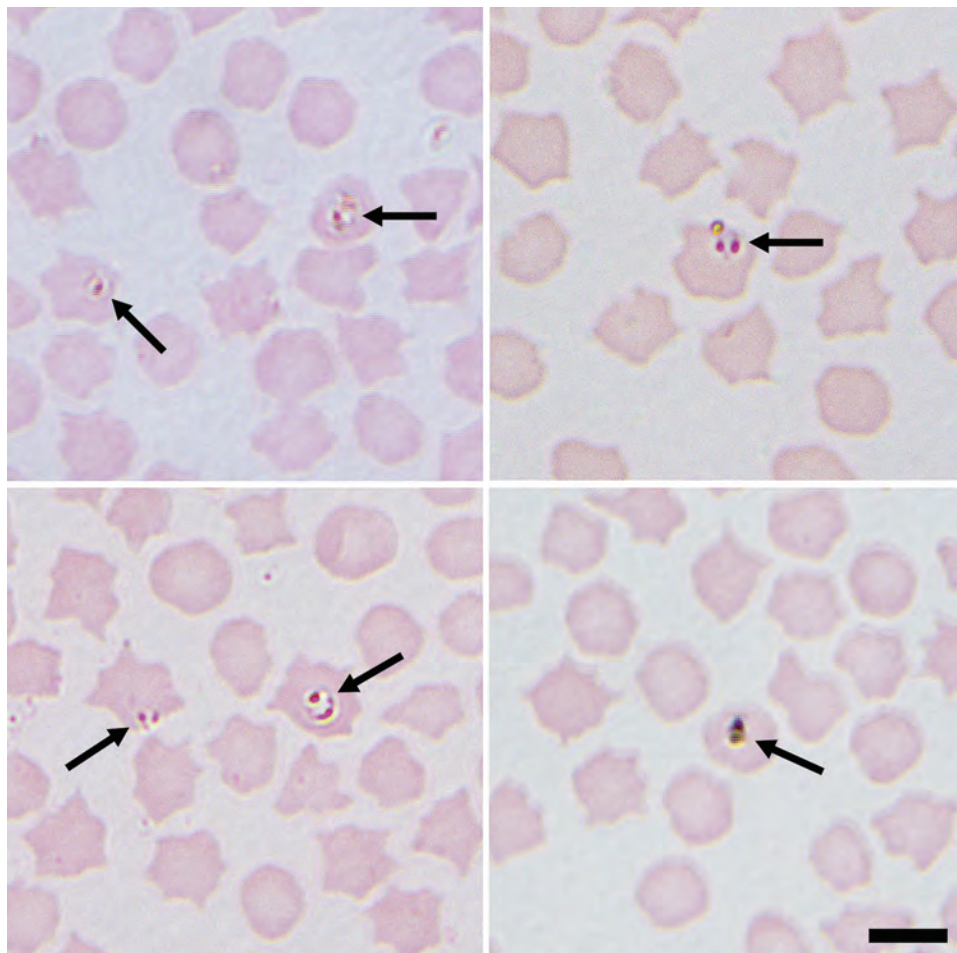
Figure 1. Representative images of small intracellular *Babesia* (arrows) identified in sheep erythrocytes from several sites in northeastern Scotland, UK. Both paired pyroforms and ring forms are visible. Images were taken at ×1,000 magnification with oil immersion. Scale bar indicates 5 μm.
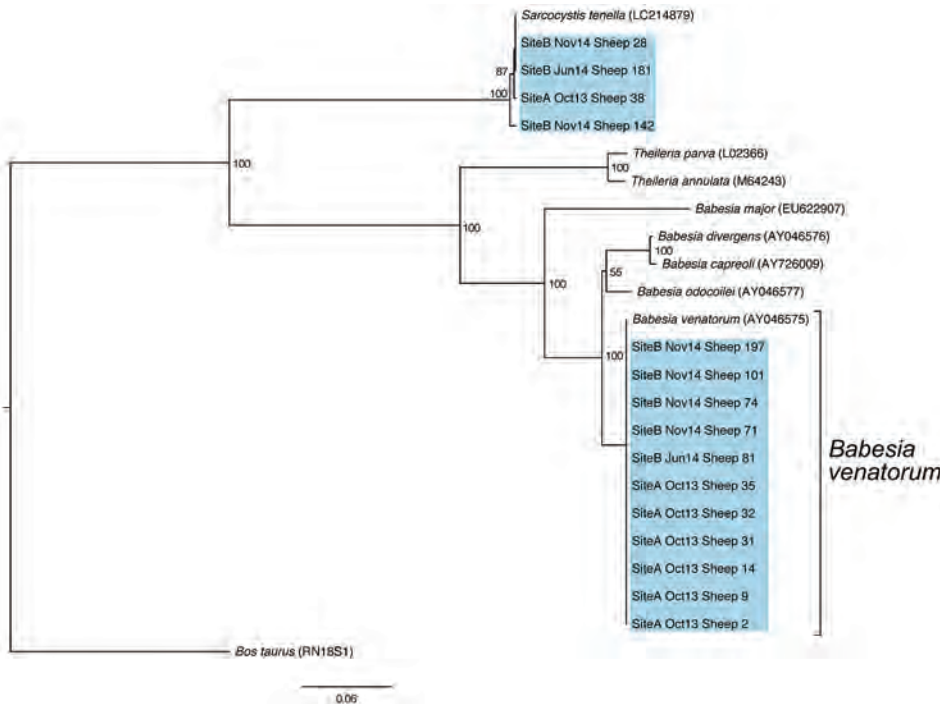
Figure 2. A neighbor-joining tree of 18S small subunit rRNA amplicon sequences obtained from sheep at sites A and B in northeastern Scotland, UK. Blue shading indicates sequences obtained in this study. Previously published *Babesia* and *Theileria* sequences include *B. venatorum* (GenBank accession no. AY046575), *B. divergens* (AY046576), *B. capreoli* (AY726009), *B. odocoilei* (AY046577), *B. major* (EU622907), *Theileria parva* (L02366), and *T. annulata* (M64243). In addition, a *Sarcocystis tenella* (LC214879) isolate was included because of the presence of a similar parasite identified in the sheep population. A *Bos taurus* 18S small subunit rRNA sequence (RN18S1) was used to root the tree.

particularly Norway, and *B. venatorum* has been found in ticks collected from the environment and in migratory birds in Scandinavia (*15*). We postulate that birds could act as an import vector for ticks carrying *B. venatorum*.

The presence of *B. venatorum* in the United Kingdom represents a new risk to humans working, living, or hiking in areas harboring infected ticks and livestock, particularly sheep. As such, local health and veterinary professionals will need to be aware of the disease if the risk for tick-borne disease in the United Kingdom is to be fully understood. Current UK medical inclusion criteria for babesiosis focus on identifying cattleborne *B. divergens*. Going forward, consideration of *B. venatorum,* through careful morphologic description of blood smears and sequencing of informative regions of the 18S SSU rRNA gene, will be necessary for accurate diagnosis and correctly targeted treatment regimens.

Our study has revealed that sheep are a natural host for *B. venatorum* in the United Kingdom. Previously, roe deer were believed to be the main vertebrate host for this parasite in Europe (*9,10*). It is unclear why *B. venatorum* has not previously been detected in sheep, although it may be that infection in this host species occurs only in particular foci or is limited to the United Kingdom. Thus, ongoing active surveillance of *Babesia* species in UK livestock would be useful to fully understand the prevalence and transmission of the disease. Such information may be critical for controlling the spread of babesiosis, because sheep are routinely transported large distances (including across international borders) and are closely associated with tick

habitats. Our study also suggests that the role that livestock play in *B. venatorum* transmission in continental Europe should be reassessed.

In summary, we have demonstrated that *B. venatorum* is present in the UK sheep population. This finding represents a novel potential threat to animal and human health and demonstrates that livestock may act as a major host for *B. venatorum*, affecting the spread of babesiosis across Europe.

Acknowledgments

About the Author

Dr. Gray leads the veterinary postmortem facility at the University of Glasgow, Scotland, UK. His research interests include tickborne pathogens affecting livestock in Scotland, particularly the potential role of such livestock as reservoirs for zoonotic pathogens.

References

1. Hildebrandt A, Gray JS, Hunfeld K-P. Human babesiosis in Europe: what clinicians need to know. Infection. 2013;41:1057–72. https://doi.org/10.1007/s15010-013-0526-8

2. Jiang J-F, Zheng Y-C, Jiang R-R, Li H, Huo Q-B, Jiang B-G, et al. Epidemiological, clinical, and laboratory characteristics of

48 cases of "*Babesia venatorum*" infection in China: a descriptive study. Lancet Infect Dis. 2015;15:196–203. https://doi.org/10.1016/S1473-3099(14)71046-1

3. Herwaldt BL, Cacciò S, Gherlinzoni F, Aspöck H, Slemenda SB, Piccaluga P, et al. Molecular characterization of a non–*Babesia divergens* organism causing zoonotic babesiosis in Europe. Emerg Infect Dis. 2003;9:942–8. https://doi.org/10.3201/eid0908.020748

4. Häselbarth K, Tenter AM, Brade V, Krieger G, Hunfeld KP. First case of human babesiosis in Germany—clinical presentation and molecular characterisation of the pathogen. Int J Med Microbiol. 2007;297:197–204. https://doi.org/10.1016/j.ijmm.2007.01.002

5. Babesiosis: Clinical manifestations and diagnosis—UpToDate; 2019 [cited 2019 Mar 6]. https://www.uptodate.com/contents/babesiosis-clinical-manifestations-and-diagnosis

6. Lempereur L, Shiels B, Heyman P, Moreau E, Saegerman C, Losson B, et al. A retrospective serological survey on human babesiosis in Belgium. Clin Microbiol Infect. 2015;21:96.e1–7. https://doi.org/10.1016/j.cmi.2014.07.004

7. Smith FD, Wall LE. Prevalence of *Babesia* and *Anaplasma* in ticks infesting dogs in Great Britain. Vet Parasitol. 2013;198:18–23. https://doi.org/10.1016/j.vetpar.2013.08.026

8. Davies S, Abdullah S, Helps C, Tasker S, Newbury H, Wall R. Prevalence of ticks and tick-borne pathogens: *Babesia* and *Borrelia* species in ticks infesting cats of Great Britain. Vet Parasitol. 2017;244:129–35. https://doi.org/10.1016/j.vetpar.2017.07.033

9. Michel AO, Mathis A, Ryser-Degiorgis M-P. *Babesia* spp. in European wild ruminant species: parasite diversity and risk factors for infection. Vet Res (Faisalabad). 2014;45:65. https://doi.org/10.1186/1297-9716-45-65

10. Zanet S, Trisciuoglio A, Bottero E, de Mera IG, Gortazar C, Carpignano MG, et al. Piroplasmosis in wildlife: *Babesia* and *Theileria* affecting free-ranging ungulates and carnivores in the Italian Alps. Parasit Vectors. 2014;7:70. https://doi.org/10.1186/1756-3305-7-70

11. Hilpertshauser H, Deplazes P, Schnyder M, Gern L, Mathis A. *Babesia* spp. identified by PCR in ticks collected from domestic and wild ruminants in southern Switzerland. Appl Environ Microbiol. 2006;72:6503–7. https://doi.org/10.1128/AEM.00823-06

12. Lempereur L, Lebrun M, Cuvelier P, Sépult G, Caron Y, Saegerman C, et al. Longitudinal field study on bovine *Babesia* spp. and *Anaplasma phagocytophilum* infections during a grazing season in Belgium. Parasitol Res. 2012;110:1525–30. https://doi.org/10.1007/s00436-011-2657-0

13. Criado-Fornelio A, Martinez-Marcos A, Buling-Saraña A, Barba-Carretero JC. Molecular studies on *Babesia, Theileria* and *Hepatozoon* in southern Europe: part I. Epizootiological aspects. Vet Parasitol. 2003;113:189–201. https://doi.org/10.1016/S0304-4017(03)00078-5

14. Georges K, Loria GR, Riili S, Greco A, Caracappa S, Jongejan F, et al. Detection of haemoparasites in cattle by reverse line blot hybridisation with a note on the distribution of ticks in Sicily. Vet Parasitol. 2001;99:273–86. https://doi.org/10.1016/S0304-4017(01)00488-5

15. Hasle G, Leinaas HP, Røed KH, Øines Ø. Transport of *Babesia venatorum*-infected *Ixodes ricinus* to Norway by northward migrating passerine birds. Acta Vet Scand. 2011;53:41. https://doi.org/10.1186/1751-0147-53-41

Address for correspondence: William Weir, University of Glasgow School of Veterinary Medicine, College of Medical, Veterinary and Life Sciences, 464 Bearsden Rd, Glasgow, Scotland G61 1QH, UK; email: willie.weir@glasgow.ac.uk

September 2018

EMERGING INFECTIOUS DISEASES®

Vectorborne Infections

To revisit the September 2018 issue, go to:
https://wwwnc.cdc.gov/eid/articles/issue/24/9/table-of-contents

Half-Life of African Swine Fever Virus in Shipped Feed

Ana M.M. Stoian, Jeff Zimmerman, Ju Ji, Trevor J. Hefley, Scott Dee, Diego G. Diel, Raymond R.R. Rowland, Megan C. Niederwerder

African swine fever virus is transmissible through animal consumption of contaminated feed. To determine virus survival during transoceanic shipping, we calculated the half-life of the virus in 9 feed ingredients exposed to 30-day shipment conditions. Half-lives ranged from 9.6 to 14.2 days, indicating that the feed matrix environment promotes virus stability.

African swine fever virus (ASFV) is the most significant threat to pork production worldwide. Over the past year, the virus has emerged in new countries and continents, including Belgium (*1*), and has rapidly disseminated throughout China and several other countries in Asia (*2,3*). Without effective vaccines or treatment, infection with ASFV results in severe disease in swine, high mortality rates, and preventive culling to halt virus spread. Since the 2013 introduction of porcine epidemic diarrhea virus in the United States, feed and feed ingredients have been recognized as potential routes for transboundary spread of swine diseases (*4*). Recent work has demonstrated that the stability of ASFV strain Georgia 2007 across animal feed ingredients is broad and that the virus survives in ingredients subjected to environmental conditions mimicking transAtlantic shipment (*5*). Furthermore, experimental infection with ASFV Georgia 2007 can occur through the natural consumption of contaminated plant-based feed; the likelihood of infection increases after repeated consumption of a batch of feed (*6*). Field reports have also implicated contaminated feed as playing a role in the introduction and transmission of ASFV on farms in China and Latvia (*7–9*).

We previously evaluated the stability of ASFV in various feed ingredients during a simulated 30-day transAtlantic voyage. We used those data to prepare rough estimates for the half-life of ASFV in each ingredient (*5,10*).

Author affiliations: Kansas State University, Manhattan, Kansas, USA (A.M.M. Stoian, T.J. Hefley, R.R.R. Rowland, M.C. Niederwerder); Iowa State University, Ames, Iowa, USA (J. Zimmerman, J. Ji); Pipestone Applied Research, Pipestone, Minnesota, USA (S. Dee); Cornell University, Ithaca, New York, USA (D.G. Diel)

However, half-life calculations were based on the limited data available at the time, including 2 time points representing inoculation dose and titers at the conclusion of the study and insufficient replicates from which to calculate SEs or 95% CIs around the half-life estimates. For this study, our objective was to improve the accuracy of ASFV half-life estimates by increasing the number of time points and replicates in the same trans-Atlantic model.

The Study

We used 9 feeds or feed ingredients for this study. We programmed an environmental chamber with the environmental conditions of humidity and temperature, which fluctuated every 6 hours, over a 30-day simulated trans-Atlantic shipment (*11*). We added 5 g of each gamma-irradiated feed ingredient to 50-mL conical tubes before inoculating them with 100 μL of 10^5 50% tissue culture infective dose (TCID$_{50}$) of ASFV. We used ASFV Georgia 2007/1 (*12*) because of its similarity to currently circulating isolates (*3*). Negative controls consisted of complete feed samples in meal form with 100 μL of sterile phosphate-buffered saline (PBS) added. Positive controls consisted of 5 mL of RPMI 1640 medium (Gibco, https://www.thermofisher.com) lacking feed with 100 μL of 10^5 TCID$_{50}$ ASFV. After addition of virus or PBS, we vortexed samples for 10 s and covered each tube with a vented cap for incubation. After removing the samples from the environmental chamber, we added 15 mL of sterile PBS and replaced the vented caps with solid caps. We organized samples in duplicate into 4 replicate batches representing 4 time points and simulated the trans-Atlantic shipping model over 2 separate 30-day periods. We used 144 titrations for the half-life calculations in feed (4 time points × 4 replicates = 16 titers/feed ingredient) and duplicate titers over 4 time points to calculate half-life in RPMI medium. We tested samples for ASFV on days 1, 8, 17, and 30 after contamination. The first sample was collected at 1 day after contamination to allow the virus to stabilize within each matrix.

ASFV was quantified by virus titration as described previously (*5*). We vortexed samples for 10 s and then centrifuged at $10,000 \times g$ for 5 min at 4°C. Supernatant from each sample was stored at −80°C. We collected porcine alveolar macrophages for virus isolation by lung lavage of 3–5-week-old pigs and cultured for 1 day in RPMI medium supplemented with 10% fetal bovine serum and antibiotics

in a 37°C 5% CO_2 incubator. We prepared 2-fold serial dilutions in RPMI medium in triplicate, added dilutions to monolayers of porcine alveolar macrophages in 96-well plates, and incubated for 1 h at 37°C. Cells were washed again and RPMI medium replaced. After 4 days at 37°C, the cells were fixed with 80% acetone for 10 min and stained with mouse anti-p30 primary monoclonal antibody (1:6,000 dilution). We incubated plates at 37°C for 1 h and washed 3 times with PBS before addition of goat anti-mouse Alexa Fluor 488 secondary antibody (Invitrogen, https://www.thermofisher.com; 1:400 dilution), followed by 1-h incubation at 37°C. We viewed cells under a fluorescence microscope and calculated the $\log_{10}$ $TCID_{50}$/mL according to the Spearman-Karber method (13).

For all sample types, we calculated the half-life and corresponding 95% CI. The half-life analysis was performed by fitting a linear regression model to the data by using R version 3.5.2 (https://www.r-project.org), with the natural log of the virus endpoint titers as the response variables and time as the explanatory variables. We estimated the slope and SE of the respective lines by using these regression models and half-lives calculated as $-\log_e(2)$/slope as previously described (14). We calculated the SE for each half-life by multiplying the SE of the slope by log(2) divided by the square of the slope. We calculated the upper and lower bounds of the 95% CI as the estimated half-life plus/minus the product of the SE times the critical value of a t distribution with quantile as 0.025 and degrees of freedom as n – 2, where n is the sample size for that ingredient (14).

Environmental conditions during the course of the trans-Atlantic model (Figure, panel A) were a mean ± SD temperature of 12.3 ± 4.7°C (range 0–26°C) and a mean ± SD humidity of 74.1% ± 19.2% (range 20%–100%). Negative control samples remained negative. All ASFV-inoculated samples showed detectable quantities of infectious ASFV (Figure, panel B). The half-life estimate in the RPMI-positive control was shorter than that for all feed ingredients tested: 8.3 ± 0.3 days (95% CI 7.7–9.0 days)
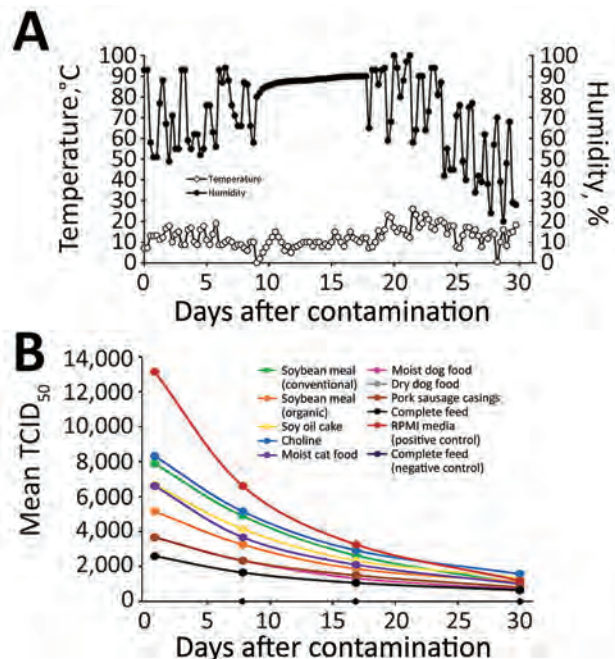
Figure. Decay of African swine fever virus (ASFV) Georgia 2007 in feed ingredients exposed to temperature and humidity conditions simulating a 30-day trans-Atlantic shipment. A) Temperature and humidity conditions, which fluctuated every 6 hours during the course of the 30-day environmental model. Environmental conditions were based on the availability of historical data logged from April 5, 2011, through May 4, 2011 (5,11) to model trans-Atlantic shipment from Warsaw, Poland, to Des Moines, Iowa, USA. B) Mean $TCID_{50}$ of ASFV Georgia 2007 quantified on porcine alveolar macrophages at 1, 8, 17, and 30 days after contamination for different types of feed and controls. Feed ingredients were inoculated with 10^5 $TCID_{50}$ ASFV based on previous half-life calculations (5,10) and the infectious dose in feed (6). $TCID_{50}$, 50% tissue culture infective dose.

(Table). The virus half-life was longest in complete feed: 14.2 ± 0.8 days (95% CI 12.4–15.9 days). Of note, for conventional versus organic soybean meal, the half-life of ASFV differed by >3 days: 9.6 ± 0.4 days (conventional

Table. Half-life of African swine fever virus Georgia 2007 in animal feed ingredients subjected to temperature and humidity conditions simulating a 30-d transoceanic shipment*

Feed or feed ingredient	Mean titer on day 30†	Half-life ± SE	95% CI for half-life estimates	Previous titer on day 30 (5,10)†	Previous half-life estimates (5,10)
Soybean meal (conventional)	$10^{3.0}$	9.6 ± 0.4	8.7–10.4	$10^{3.0}$	4.6
Soybean meal (organic)	$10^{3.0}$	12.9 ± 0.6	11.5–14.3	$10^{3.1}$	4.7
Soy oil cake	$10^{3.1}$	12.4 ± 0.9	10.4–14.3	$10^{3.2}$	5.0
Choline	$10^{3.2}$	11.9 ± 0.5	10.9–12.9	$10^{3.2}$	5.1
Moist cat food	$10^{3.0}$	10.6 ± 0.5	9.5–11.7	$10^{3.0}$	4.6
Moist dog food	$10^{2.8}$	11.7 ± 0.4	10.8–12.6	$10^{2.8}$	4.2
Dry dog food	$10^{2.7}$	13.1 ± 0.4	12.3–14.0	$10^{2.8}$	4.1
Pork sausage casings	$10^{2.9}$	13.1 ± 0.7	11.6–14.6	$10^{2.9}$	4.4
Complete feed	$10^{2.7}$	14.2 ± 0.8	12.4–15.9	$10^{2.9}$	4.3
RPMI medium	Not determined	8.3 ± 0.3	7.7–9.0	$10^{3.0}$	4.7

*Values listed in days unless otherwise indicated. Feed ingredient selection based on use in swine feed or volume of ingredient imported into the United States from China each year (5). Samples subjected to temperature (mean 12.3°C) and relative humidity (mean 74.1%) conditions in an environmental chamber programmed to simulate transoceanic shipment. Complete feed samples were in meal form.
†Mean titer of duplicate samples listed as 50% tissue culture infective dose.

soybean meal) and 12.9 ± 0.6 days (organic soybean meal). The relative stability in feed may be the result of variable protein, fat, or moisture content among ingredients. Overall, the mean half-life for ASFV in all animal feed ingredients was 12.2 days.

Conclusions

Although the high stability of ASFV in contaminated pork products and blood has been appreciated for decades (15), the stability of ASFV in plant-based feed has been recognized only recently (5). Our previous estimation of the half-life of ASFV in feed ingredients was based on the limited data we had available, including inoculation dose and 18 titers quantified at 1 time point during the 30-day model (5,10). In this study, we quantified viral decay at several time points over the 30-day model and increased sample size, which enabled us to calculate SEs and 95% CIs around the half-life estimates. In general, this updated modeling approach resulted in longer half-life estimates across all matrices.

This study provides quantitative data on the half-life of ASFV Georgia 2007 in animal feed ingredients exposed to moderate temperature and humidity conditions simulating transoceanic shipment. The longer virus half-lives in feed compared with half-lives in media support the concept that the feed matrix provides an environment that increases ASFV stability. Furthermore, these data provide additional evidence supporting the ability of plant-based feed ingredients to promote survival of ASFV should these products become contaminated.

About the Author

Ms. Stoian is a PhD student in the College of Veterinary Medicine at Kansas State University, Manhattan, Kansas. Her research is focused on understanding virus replication in gene-edited animals and on feed biosecurity for prevention and control of foreign and endemic infectious diseases.

References

1. Forth JH, Tignon M, Cay AB, Forth LF, Höper D, Blome S, et al. Comparative analysis of whole-genome sequence of African swine fever virus Belgium 2018/1. Emerg Infect Dis. 2019;25:1249–52. https://doi.org/10.3201/eid2506.190286
2. Le VP, Jeong DG, Yoon SW, Kwon HM, Trinh TBN, Nguyen TL, et al. Outbreak of African swine fever, Vietnam, 2019. Emerg Infect Dis. 2019;25:1433–5. https://doi.org/10.3201/eid2507.190303
3. Zhou X, Li N, Luo Y, Liu Y, Miao F, Chen T, et al. Emergence of African swine fever in China, 2018. Transbound Emerg Dis. 2018;65:1482–4. https://doi.org/10.1111/tbed.12989
4. Niederwerder MC, Hesse RA. Swine enteric coronavirus disease: a review of 4 years with porcine epidemic diarrhoea virus and porcine deltacoronavirus in the United States and Canada. Transbound Emerg Dis. 2018;65:660–75. https://doi.org/10.1111/tbed.12823
5. Dee SA, Bauermann FV, Niederwerder MC, Singrey A, Clement T, de Lima M, et al. Survival of viral pathogens in animal feed ingredients under transboundary shipping models. PLoS One. 2018;13:e0194509. https://doi.org/10.1371/journal.pone.0194509
6. Niederwerder MC, Stoian AMM, Rowland RRR, Dritz SS, Petrovan V, Constance LA, et al. Infectious dose of African swine fever virus when consumed naturally in liquid or feed. Emerg Infect Dis. 2019;25:891–7. https://doi.org/10.3201/eid2505.181495
7. Zhai SL, Wei WK, Sun MF, Lv DH, Xu ZH. African swine fever spread in China. Vet Rec. 2019;184:559. https://doi.org/10.1136/vr.l1954
8. Oļševskis E, Guberti V, Seržants M, Westergaard J, Gallardo C, Rodze I, et al. African swine fever virus introduction into the EU in 2014: experience of Latvia. Res Vet Sci. 2016;105:28–30. https://doi.org/10.1016/j.rvsc.2016.01.006
9. Wen X, He X, Zhang X, Zhang X, Liu L, Guan Y, et al. Genome sequences derived from pig and dried blood pig feed samples provide important insights into the transmission of African swine fever virus in China in 2018. Emerg Microbes Infect. 2019;8:303–6. https://doi.org/10.1080/22221751.2019.1565915
10. Dee SA, Bauermann FV, Niederwerder MC, Singrey A, Clement T, de Lima M, et al. Correction: survival of viral pathogens in animal feed ingredients under transboundary shipping models. PLoS One. 2019;14:e0214529. https://doi.org/10.1371/journal.pone.0214529
11. Dee SA, Bauermann FV, Niederwerder MC, Singrey A, Clement T, de Lima M, et al. Correction: survival of viral pathogens in animal feed ingredients under transboundary shipping models. PLoS One. 2018;13:e0208130. https://doi.org/10.1371/journal.pone.0208130
12. Rowlands RJ, Michaud V, Heath L, Hutchings G, Oura C, Vosloo W, et al. African swine fever virus isolate, Georgia, 2007. Emerg Infect Dis. 2008;14:1870–4. https://doi.org/10.3201/eid1412.080591
13. Finney DJ. The Spearman-Karber method. In: Finney DJ, editor. Statistical method in biological assay. 2nd ed. London: Charles Griffin; 1964. p. 524–30.
14. Bryan M, Zimmerman JJ, Berry WJ. The use of half-lives and associated confidence intervals in biological research. Vet Res Commun. 1990;14:235–40. https://doi.org/10.1007/BF00347743
15. Niederwerder MC, Rowland RR. Is there a risk for introducing porcine reproductive and respiratory syndrome virus (PRRSV) through the legal importation of pork? Food Environ Virol. 2017;9:1–13. https://doi.org/10.1007/s12560-016-9259-z

Address for correspondence: Megan C. Niederwerder, Kansas State University, College of Veterinary Medicine, L-227 Mosier Hall, 1800 Denison Ave, Manhattan, KS 66506, USA; email: mniederwerder@vet.k-state.edu

Zika Virus IgM 25 Months after Symptom Onset, Miami-Dade County, Florida, USA

Isabel Griffin, Stacey W. Martin, Marc Fischer,
Trudy V. Chambers, Olga L. Kosoy,
Cynthia Goldberg, Alyssa Falise,
Vanessa Villamil, Olga Ponomareva,
Leah D. Gillis, Carina Blackmore, Reynald Jean

We assessed IgM detection in Zika patients from the 2016 outbreak in Miami-Dade County, Florida, USA. Of those with positive or equivocal IgM after 12–19 months, 87% (26/30) had IgM 6 months later. In a survival analysis, ≈76% had IgM at 25 months. Zika virus IgM persists for years, complicating serologic diagnosis.

Diagnosis of Zika virus infection is accomplished by testing for viral RNA or IgM and neutralizing antibodies (*1*). A cohort study of 62 confirmed Zika virus cases from the 2016 outbreak in Miami-Dade County, Florida, USA, demonstrated that Zika virus IgM remains detectable in most (92%) persons 12–19 months after symptom onset (*2*). We estimated the proportion of persons with detectable Zika virus IgM up to 25 months after initial illness onset.

The Study

We included persons residing in Miami-Dade County who had confirmed Zika virus disease with symptom onset during June–October 2016 and had participated in a previous prospective cohort study (*2*). Of the original 62 patients, we asked all 57 patients with positive or equivocal Zika virus IgM results at 12–19 months after symptom onset to provide another specimen 6 months later. We obtained written consent for the additional specimen from study participants. We tested all serum specimens at the Centers for Disease Control and Prevention (Fort Collins, Colorado, USA) by the IgM capture ELISA for Zika virus (*3–5*).

Author affiliations: Florida Department of Health in Miami-Dade County, Miami, Florida, USA (I. Griffin, C. Goldberg, A. Falise, V. Villamil, O. Ponomareva, R. Jean); Centers for Disease Control and Prevention, Fort Collins, Colorado, USA (S.W. Martin, M. Fischer, T.V. Chambers, O.L. Kosoy); Bureau of Public Health Laboratories, Miami (L.D. Gillis); Florida Department of Health, Tallahassee, Florida, USA (C. Blackmore)

We used SAS version 9.4 (https://www.sas.com) to manage and analyze the data and performed a nonparametric survival analysis (i.e., PROC ICLIFETEST) for interval-censored data to estimate the duration of Zika virus IgM detection. For this procedure, we considered survival to be the detection of Zika virus IgM (a positive or equivocal result). We included the IgM results of specimens from all 62 original participants collected 12–19 months after symptom onset and the IgM results from all follow-up specimens acquired in the survival analysis. The Florida Health Institutional Review Board (Tallahassee, Florida, USA) approved this study.

Of 57 persons with positive or equivocal Zika virus IgM results at 12–19 months after symptom onset, 30 (53%) provided a follow-up specimen. The median time of specimen collection after symptom onset was 21 (range 18–25) months; 5 (17%) patients provided a specimen at 18 months after symptom onset, 1 (3%) at 19 months, 6 (20%) at 20 months, 9 (30%) at 21 months, 3 (10%) at 22 months, 3 (10%) at 23 months, 1 (3%) at 24 months, and 2 (7%) at 25 months.

Demographics and clinical characteristics of the 62 participants in the original study were previously reported (*6*). Of the 30 who provided an additional follow-up specimen, the median age at symptom onset was 45 (range 22–70) years; all were adults >18 years of age. Fifteen (50%) were female, and 14 (47%) were Hispanic. After reviewing case investigations, we found that 13 (43%) of these participants reported no international travel (outside of the continental United States) during the 2 years before collection of the last specimen.

Of the 30 participants who provided a follow-up specimen, 19 (63%) were positive for Zika virus IgM, 7 (23%) had an equivocal result, and 4 (13%) were IgM seronegative. Compared with results from the specimen collection 6 months earlier, 20 (67%) remained positive for Zika virus IgM, 2 (7%) remained Zika virus IgM equivocal, 4 (13%) transitioned from Zika virus IgM positive to equivocal, and 4 (13%) transitioned from Zika virus IgM equivocal to negative; no participants switched from Zika virus IgM positive to negative. Because of the small sample size, we were unable to assess whether age group, race, or ethnicity was associated with Zika virus IgM results. When we used all available test results from the 62 participants, a survival
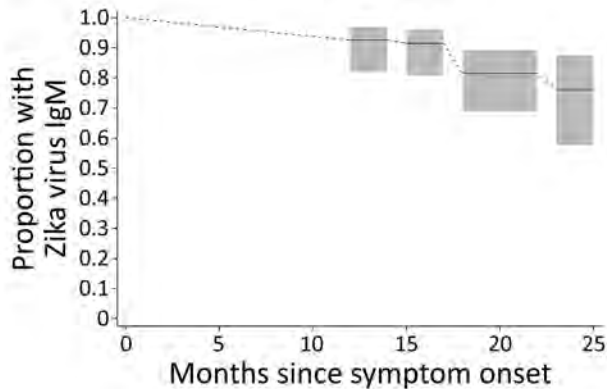
Figure. Estimated proportion of persons with detectable Zika virus IgM up to 25 months after symptom onset among persons with PCR-confirmed Zika virus disease, Miami-Dade County, Florida, USA. Detectable Zika virus IgM was defined as a positive or equivocal result on IgM capture ELISA. Interval-censored nonparametric survival analysis probability estimates and 95% CIs (gray boxes) are shown.

analysis indicated that 93% (95% CI 82%–97%) of participants had detectable (positive or equivocal) Zika virus IgM at 14 months after symptom onset, 91% (95% CI 81%–96%) at 17 months, 81% (95% CI 69%–89%) at 22 months, and 76% (95% CI 57%–88%) at 25 months (Figure).

Conclusions
Our findings suggest that approximately three quarters of persons with PCR-confirmed symptomatic Zika disease still have detectable IgM at 25 months after initial illness onset. The prolonged detection of IgM after Zika virus infection is consistent with previous findings for related flaviviruses (*6–10*). Our findings are specific to the Centers for Disease Control and Prevention IgM capture ELISA for Zika virus, which targets the premembrane and envelope glycoproteins; other available IgM serologic assays targeting other Zika virus proteins might not produce comparable findings (*3*). In addition, these results are only representative of symptomatic Zika cases; whether persons with asymptomatic Zika virus infections exhibit similar Zika virus IgM persistence is unknown. IgM persistence needs to be assessed with other serologic assays for both symptomatic and asymptomatic Zika virus cases to determine the full duration of Zika virus IgM after infection.

About the Author
Dr. Griffin is an outbreak epidemiologist at the Florida Department of Health in Miami, Florida, USA. Her primary research interest is emerging infectious diseases.

References
1. Rabe IB, Staples JE, Villanueva J, Hummel KB, Johnson JA, Rose L, et al.; MTS. Interim guidance for interpretation of Zika virus antibody test results. MMWR Morb Mortal Wkly Rep. 2016;65:543–6. https://doi.org/10.15585/mmwr.mm6521e1
2. Griffin I, Martin SW, Fischer M, Chambers TV, Kosoy O, Falise A, et al. Zika virus IgM detection and neutralizing antibody profiles 12–19 months after illness onset. Emerg Infect Dis. 2019;25:299–303. https://doi.org/10.3201/eid2502.181286
3. Martin DA, Muth DA, Brown T, Johnson AJ, Karabatsos N, Roehrig JT. Standardization of immunoglobulin M capture enzyme-linked immunosorbent assays for routine diagnosis of arboviral infections. J Clin Microbiol. 2000;38:1823–6.
4. Lanciotti RS, Kosoy OL, Laven JJ, Velez JO, Lambert AJ, Johnson AJ, et al. Genetic and serologic properties of Zika virus associated with an epidemic, Yap State, Micronesia, 2007. Emerg Infect Dis. 2008;14:1232–9. https://doi.org/10.3201/eid1408.080287
5. Theel ES, Hata DJ. Diagnostic testing for Zika virus: a postoutbreak update. J Clin Microbiol. 2018;56:e01972-17. https://doi.org/10.1128/JCM.01972-17
6. Prince HE, Tobler LH, Yeh C, Gefter N, Custer B, Busch MP. Persistence of West Nile virus-specific antibodies in viremic blood donors. Clin Vaccine Immunol. 2007;14:1228–30. https://doi.org/10.1128/CVI.00233-07
7. Roehrig JT, Nash D, Maldin B, Labowitz A, Martin DA, Lanciotti RS, et al. Persistence of virus-reactive serum immunoglobulin M antibody in confirmed West Nile virus encephalitis cases. Emerg Infect Dis. 2003;9:376–9. https://doi.org/10.3201/eid0903.020531
8. Gibney KB, Edupuganti S, Panella AJ, Kosoy OI, Delorey MJ, Lanciotti RS, et al. Detection of anti-yellow fever virus immunoglobulin M antibodies at 3–4 years following yellow fever vaccination. Am J Trop Med Hyg. 2012;87:1112–5. https://doi.org/10.4269/ajtmh.2012-0182
9. Busch MP, Kleinman SH, Tobler LH, Kamel HT, Norris PJ, Walsh I, et al. Virus and antibody dynamics in acute West Nile virus infection. J Infect Dis. 2008;198:984–93. https://doi.org/10.1086/591467
10. Poland JD, Calisher CH, Monath TP, Downs WG, Murphy K. Persistence of neutralizing antibody 30–35 years after immunization with 17D yellow fever vaccine. Bull World Health Organ. 1981;59:895–900.

Address for correspondence: Isabel Griffin, Florida Department of Health in Miami-Dade County, Department of Epidemiology, Disease Control, and Immunization Services, 8175 NW 12th St, Ste 314, Miami, FL 33126, USA; email: griffin.isabel@gmail.com

Divergent Barmah Forest Virus from Papua New Guinea

Leon Caly, Paul F. Horwood,
Dhanasekaran Vijaykrishna, Stacey Lynch,
Andrew R. Greenhill, William Pomat,
Glennis Rai, Debbie Kisa, Grace Bande,
Julian Druce, Mohammad Y. Abdad

We report a case of Barmah Forest virus infection in a child from Central Province, Papua New Guinea, who had no previous travel history. Genomic characterization of the virus showed divergent origin compared with viruses previously detected, supporting the hypothesis that the range of Barmah Forest virus extends beyond Australia.

Barmah Forest virus (BFV) is an arbovirus that is pathogenic to humans and is traditionally considered to be endemic only to Australia (*1*). BFV is a member of the Semliki Forest virus complex of the family *Togaviridae* (genus *Alphavirus*) that comprises several human arboviruses, including Ross River virus (RRV), Sindbis virus, and chikungunya virus. BFV was first isolated in 1974 from *Culex annulirostris* mosquitoes collected in the Barmah Forest within the state of Victoria and simultaneously from mosquitoes collected in southwest Queensland, Australia (*2*). Since then, it has been isolated in numerous other mosquitoes, including the coastal species *Aedes vigilax* (New South Wales) and *Ae. camptorhynchus* (Victoria), found in salt marshes and from the midge *Culicoides marksi* in Northern Territory (*3–5*). Subsequently, BFV has been detected in humans in most parts of mainland Australia, and serologic surveys have shown that this virus causes widespread infection (*6–8*).

Author affiliations: Victorian Infectious Diseases Reference Laboratory of Royal Melbourne Hospital at the Peter Doherty Institute for Infection and Immunity, Melbourne, Victoria, Australia (L. Caly, J. Druce); James Cook University, Townsville, Queensland, Australia (P.F. Horwood); Monash University, Clayton, Victoria, Australia (D. Vijaykrishna); AgriBio Centre for AgriBioscience, Bundoora, Victoria, Australia (S. Lynch); Federation University Australia, Gippsland, Victoria, Australia (A.R. Greenhill); Papua New Guinea Institute of Medical Research, Goroka, Papua New Guinea (W. Pomat, G. Rai, D. Kisa); Divine Word University, Madang, Papua New Guinea (G. Bande); National Centre for Infectious Diseases, Singapore (M.Y. Abdad)

BFV is transmitted to humans through bite from an infected mosquito, resulting in a mild disease and symptoms similar to those of RRV infection, including rash, fever, muscle tenderness, and polyarthralgia. Although the fever will generally pass within a week, muscle and joint pain may persist for $\geq$6 months (*9*), making BFV an infection of public concern. We report a case of infection with BFV in a child in Papua New Guinea.

The Study

In April 2014, a boy (5 years, 11 months of age) who had no history of international travel came to an outpatient health clinic in a coastal village northwest of Port Moresby, Central Province, Papua New Guinea, because of an undifferentiated fever. Rash, muscle pain, and polyarthralgia were not noted at that time. Blood samples (containing EDTA anticoagulant) were collected as part of ongoing febrile illness surveillance and transferred to the Port Moresby laboratory of the Papua New Guinea Institute of Medical Research, where extraction of nucleic acids was performed.

We screened eluates by using a real-time reverse transcription PCR (RT-PCR) for a range of pathogens known to cause febrile illnesses, including BFV, chikungunya virus, dengue virus, Japanese encephalitis virus, RRV, West Nile (Kunjin) virus, Zika virus, *Orientia tsutsugamushi*, *Leptospira* sp., and *Rickettsia* sp. All test results were negative, except for a BFV TaqMan RT-PCR, which showed a positive result.

We isolated BFV by inoculating 100 µL of patient serum onto cultured Vero cells (strain PNG_BFV) and extracting and assessing the nucleic acid content of the harvested cell culture material by using a BFV-specific real-time RT-PCR. The result was positive, suggesting viral replication in culture and confirming the presence of BFV within the specimen of the patient.

We extracted RNA from the isolate material, prepared an RNASeq library by using the Scriptseq Version 2 Kit (http://www.epibio.com), and subjected this library to whole-genome sequencing by using the MiSeq System (https://www.illumina.com). We obtained 32 million paired-end reads and mapped them to the only available full-length (11,488-nt) BFV reference genome sequence (RefSeq accession no. NC_001786.1, strain ID BH2193) (*10*), which resulted in a complete PNG_BFV genome (GenBank accession no. MN115377) of 11,480 nt.

Comparison of PNG_BFV with the reference genome showed the presence of 343 nt differences, which constitutes a 2.98% pairwise difference between PNG_BFV and prototype strain BH2193 (Table). Most changes were single-nucleotide polymorphisms, although these changes included multiple-nucleotide substitutions, and insertions and deletions (indels). A large number of these changes (219 nt) were found in the nonstructural polyprotein coding region 1–4, of which 23 were nonsynonymous, resulting in 19 aa changes (Figure 1).

In addition, 91 nt changes occurred within the structural polyprotein coding region, 10 of which were nonsynonymous, resulting in 9 aa changes (Figure 1). We also observed an additional 33 nt substitutions in the 3′ noncoding end of the genome. The biologic context of these amino acid substitutions and their effects on virus pathogenicity, infectivity, and antigenicity remains to be determined and will be explored in further studies.

To determine the evolutionary relationship of the PNG_BFV strain with those detected in Australia, we estimated their phylogenetic relationships by using the maximum-likelihood method and the time to most recent common ancestor of each node by using Bayesian methods. We aligned the complete envelope (E2) sequences of all currently available BFV strains (n = 7) in the Virus Pathogen Resource database (https://www.viprbrc.org/brc/home.spg?decorator = vipr) and an isolate from Victoria (M4208_16/17) with the newly generated PNG_BFV envelope (E2) protein gene sequence of 1,263 nt.

Table. Synonymous and nonsynonymous differences between Barmah Forest virus isolate PNG_BFV from a child in Papua New Guinea and prototype strain BH2193*

Genome region	nsP1–4	Structural	3′
Synonymous	196	81	–
Nonsynonymous	23	10	–
Total	219	91	33

*Prototype strain, RefSeq accession no. NC_001786.1. nsP, nonstructural protein; –, none.

Phylogenetic analysis showed that PNG_BFV is divergent from known BFV strains from Australia, suggesting that the strain was not a recent introduction from Australia but has been evolving independently as a separate BFV clade for quite some time (Figure 2, panel A). Furthermore, we observed a greater nucleotide diversity of the E2 gene between the BFV reference strain (BH2139) and the Papua New Guinea strain (2.85%) than between all strains collected in Australia during 1974–2016 (1.50%–1.90%).

In an effort to determine the time of divergence of the Papua New Guinea strain from known strains from Australia, we first estimated a root-to-tip regression model to explore the temporal structure of the 8 BFV sequences by using Tempest version 1.5 (13). This estimation showed a slope of 1.98×10^{-4}, which was comparable to nucleotide substitution rates of the surface proteins of RNA viruses (14) and also showed that this dataset contained adequate temporal signal for a robust estimation of substitution rates and divergence times (Figure 2, panel B).

PNG_BFV amino acid substitutions

Protein	Mutation
nsP1	D184N
	S461P
	A471E
	V491A
	E521D
nsP2	T484M
	L764F
nsP3	G244S
	G359V
	I364T
nsP4	H93R
	P94S
	V104A
	D111I
	L112R
	K119E
	R168K
	W460C
	P461A

Protein	Mutation
Capsid (C)	S89P
E3	E52D
E2	A24T
	A221T
	V281A
	S303N
E1	G26A
	N72S
	I260V
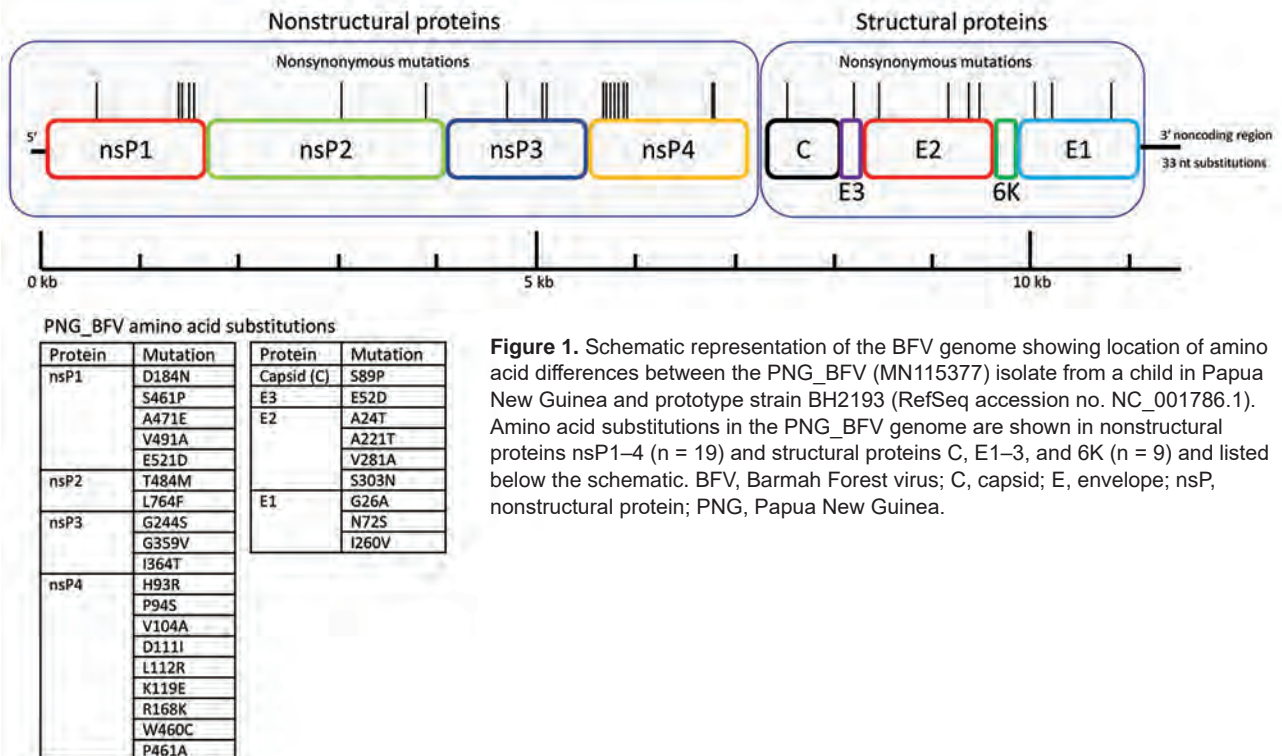
Figure 1. Schematic representation of the BFV genome showing location of amino acid differences between the PNG_BFV (MN115377) isolate from a child in Papua New Guinea and prototype strain BH2193 (RefSeq accession no. NC_001786.1). Amino acid substitutions in the PNG_BFV genome are shown in nonstructural proteins nsP1–4 (n = 19) and structural proteins C, E1–3, and 6K (n = 9) and listed below the schematic. BFV, Barmah Forest virus; C, capsid; E, envelope; nsP, nonstructural protein; PNG, Papua New Guinea.
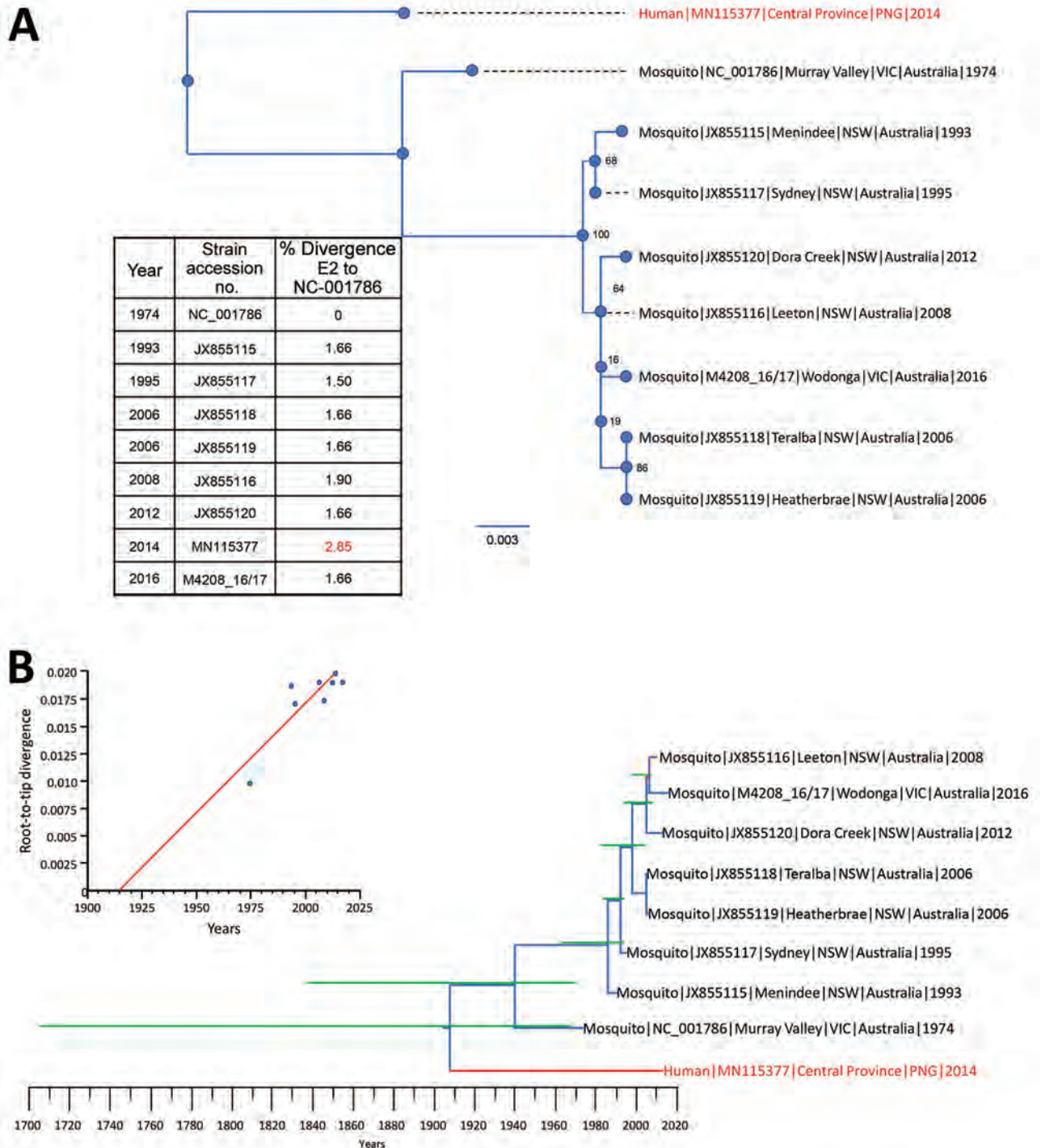
Figure 2. Phylogenetic relationships between 9 full-length (1,263 nt) Barmah Forest virus (BFV) envelope (E) protein genes. A) Maximum-likelihood phylogenetic tree constructed from 8 full-length Australia BFV E2 sequences (blue) and a BFV E2 sequence from an isolate from a child in Papua New Guinea (red) by using the best-fit nucleotide substitution model in IQ-Tree version 1.5 (*11*). Bootstrap values were estimated by using 1,000 replicates; percentages are indicated on branch nodes. Inset table shows E2 nucleotide divergence compared with that for prototype strain BH2193 (RefSeq accession no. NC_001786.1). Scale bar indicates nucleotide substitutions per site. B) Molecular clock analysis using the Bayesian Markov chain Monte Carlo method in BEAST (*12*) for 9 complete BFV E2 sequences (blue) spanning 1974–2016. Red indicates BFV from an isolate from a child in Papua New Guinea. Green lines indicate 95% CIs. Inset shows temporal analysis of root-to-tip linear regression by using TempEst version 1.5 (*13*). Slope, 1.98×10^{-4}; X-intercept, 1914.2; correlation coefficient, 0.86; R^2, 0.743; residual mean squared, 2.76×10^{-6}. NSW, New South Wales; VIC, Victoria.

Subsequently, we estimated the molecular clock for the final dataset of 8 complete E2 protein sequences with a sampling range of 1974–2016, under a stick clock model; a constant coalescent population size and the Hasegawa, Kishino, and Yano substitution model by using the Bayesian Markov chain Monte Carlo method in BEAST version 1.8 (*12*) (Figure 2, panel B). We determined the median root age to be during 1906 (95% CI 1703–1969) with a calculated mean nucleotide substitution rate of 1.7×10^{-4} (95% CI 5.4×10^{-12}–3.3×10^{-4}). The wide CIs suggest that sampling was inadequate to provide a precise estimate of the time of divergence and evolutionary rate, which would be greatly improved with access to additional BFV whole-genome sequences and full-length E2 gene sequences, which are currently not available for public access.

Conclusions

We report a case of infection with BFV in a child who had no travel history from the Central Province of Papua New Guinea. BFV has been traditionally believed to be endemic only to Australia. Whole-genome sequencing, followed by phylogenetic analysis, showed that this strain was highly divergent from known strains from Australia. These findings placed the Papua New Guinea virus strain within its own clade and supported the hypothesis that the range of BFV extends beyond Australia. Molecular clock analysis indicates that the virus strains from Papua New Guinea and Australia probably diverged during or before the early 1900s, raising questions on the origins and the overall genetic diversity of BFV. On the basis of currently available data, the probable origins of these viruses, either from Australia or neighboring northern countries, such as Papua New Guinea, are inconclusive.

The timeline of divergence suggests that this divergence could have occurred by movement of humans, livestock, or mosquitoes from or to Australia during the early 1900s by trade routes or movement of troops during World War I. Increased mosquito surveillance and serosurveys of the population in Papua New Guinea is needed to determine the endemic nature of BFV, which is likely to extend beyond the single detection noted within the Central Province.

About the Author

Dr. Caly is a virologist at the Victorian Infectious Diseases Reference Laboratory, Melbourne, Victoria, Australia. His research interests include virus discovery and evolution, long-read and short-read whole-genome sequencing, and phylogenetic approaches.

References

1. Mackenzie JS, Lindsay MD, Coelen RJ, Broom AK, Hall RA, Smith DW. Arboviruses causing human disease in the Australasian zoogeographic region. Arch Virol. 1994;136:447–67. https://doi.org/10.1007/BF01321074
2. Marshall ID, Woodroofe GM, Hirsch S. Viruses recovered from mosquitoes and wildlife serum collected in the Murray Valley of South-eastern Australia, February 1974, during an epidemic of encephalitis. Aust J Exp Biol Med Sci. 1982; 60:457–70. https://doi.org/10.1038/icb.1982.51
3. Doggett SL, Russell RC, Clancy J, Haniotis J, Cloonan MJ. Barmah Forest virus epidemic on the south coast of New South Wales, Australia, 1994–1995: viruses, vectors, human cases, and environmental factors. J Med Entomol. 1999;36:861–8. https://doi.org/10.1093/jmedent/36.6.861
4. Ryan PA, Kay BH. Vector competence of mosquitoes (Diptera: Culicidae) from Maroochy Shire, Australia, for Barmah Forest virus. J Med Entomol. 1999;36:856–60. https://doi.org/10.1093/jmedent/36.6.856
5. Jeffery JA, Ryan PA, Lyons SA, Kay BH. Vector competence of *Coquillettidia linealis* (Skuse) (Diptera: Culicidae) for Ross River and Barmah Forest viruses. Australian Journal of Entomology. 2002;41:339–44. https://doi.org/10.1046/j.1440-6055.2002.00316.x
6. Quinn HE, Gatton ML, Hall G, Young M, Ryan PA. Analysis of Barmah Forest virus disease activity in Queensland, Australia, 1993–2003: identification of a large, isolated outbreak of disease. J Med Entomol. 2005;42:882–90. https://doi.org/10.1093/jmedent/42.5.882
7. Ehlkes L, Eastwood K, Webb C, Durrheim D. Surveillance should be strengthened to improve epidemiological understandings of mosquito-borne Barmah Forest virus infection. Western Pac Surveill Response J. 2012;3:63–8. https://doi.org/10.5365/wpsar.2012.3.1.004
8. Knope K, Doggett SL, Jansen CC, Johansen CA, Kurucz N, Feldman R, et al. Arboviral diseases and malaria in Australia, 2014–15. Annual report of the National Arbovirus and Malaria Advisory Committee. Communicable Diseases Intelligence (2018). 2019;Apr 15:43.
9. Flexman JP, Smith DW, Mackenzie JS, Fraser JR, Bass SP, Hueston L, et al. A comparison of the diseases caused by Ross River virus and Barmah Forest virus. Med J Aust. 1998;169:159–63. https://doi.org/10.5694/j.1326-5377.1998.tb116019.x
10. Lee E, Stocks C, Lobigs P, Hislop A, Straub J, Marshall I, et al. Nucleotide sequence of the Barmah Forest virus genome. Virology. 1997;227:509–14. https://doi.org/10.1006/viro.1996.8343
11. Nguyen LT, Schmidt HA, von Haeseler A, Minh BQ. IQ-TREE: a fast and effective stochastic algorithm for estimating maximum-likelihood phylogenies. Mol Biol Evol. 2015;32:268–74. https://doi.org/10.1093/molbev/msu300
12. Drummond AJ, Suchard MA, Xie D, Rambaut A. Bayesian phylogenetics with BEAUti and the BEAST 1.7. Mol Biol Evol. 2012;29:1969–73. https://doi.org/10.1093/molbev/mss075
13. Rambaut A, Lam TT, Max Carvalho L, Pybus OG. Exploring the temporal structure of heterochronous sequences using TempEst (formerly Path-O-Gen). Virus Evol. 2016;2:vew007. https://doi.org/10.1093/ve/vew007
14. Sanjuán R, Domingo-Calap P. Mechanisms of viral mutation. Cell Mol Life Sci. 2016;73:4433–48. https://doi.org/10.1007/s00018-016-2299-6

Address for correspondence: Leon Caly, Victorian Infectious Diseases Reference Laboratory, Royal Melbourne Hospital, Peter Doherty Institute for Infection and Immunity, 792 Elizabeth St, Melbourne, VIC 3000, Australia; email: leon.caly@mh.org.au or Mohammad Y. Abdad, Infectious Disease Research Laboratory, National Centre for Infectious Diseases, 16 Jln Tan Tock Seng, 308442, Singapore; email: yazid_abdad@ncid.sg

Animal Exposure and Human Plague, United States, 1970–2017

**Stefanie B. Campbell, Christina A. Nelson,
Alison F. Hinckley, Kiersten J. Kugeler**

Since 1970, >50% of patients with plague in the United States had interactions with animals that might have led to infection. Among patients with pneumonic plague, nearly all had animal exposure. Improved understanding of the varied ways in which animal contact might increase risk for infection could enhance prevention messages.

Plague is a rare, life-threatening zoonosis caused by *Yersinia pestis* that occurs globally in discrete foci, including the western United States (*1*). The bacterium is maintained in an enzootic cycle of rodents and their fleas (*2*). Periodically, the cycle intensifies, leading to epizootic events characterized by localized small mammal die-offs. During epizootics, the risk for incidental human infection increases (*2*). Humans are exposed to *Y. pestis* most commonly through flea bites but also through contact with tissues of infected animals or inhalation of infectious droplets.

Clinical manifestations of plague in humans are associated with route of exposure. Primary pneumonic plague, the most severe and rapidly fatal form of the disease, occurs after direct inhalation of infectious droplets coughed by infected animals or humans (*3*). Human exposure to *Y. pestis* results from direct and indirect interactions with animals. Improved understanding of the role of animals in human exposure to *Y. pestis* may foster more refined prevention messages in plague-endemic areas.

The Study

Plague is a nationally notifiable condition in the United States (*4*). State and local health jurisdictions report human cases to the Centers for Disease Control and Prevention. Case records typically include supplemental information on possible sources of exposure, clinical course, and outcome. We reviewed data from all reported human plague cases during 1970–2017 that were characterized by a clinically compatible illness and presumptive or confirmatory laboratory evidence as defined previously (*5*). For this analysis, we considered only the primary clinical manifestation of illness.

Author affiliation: Centers for Disease Control and Prevention, Fort Collins, Colorado, USA

We created a data extraction tool to capture details on patient–animal interactions in the 2 weeks preceding illness onset. If animal exposure had occurred, we classified the type of animal(s) involved as domestic or wild and the interactions as directly or indirectly associated with exposure to *Y. pestis*. We grouped animal exposures into categories based on authors' judgment regarding risk for transmission. From high-risk to low-risk, the categories were animal bite, scratch, lick, or cough; skinning of a deceased animal; providing care to or handling a sick or deceased animal; co-sleeping; casual handling or touching; and other (walking, feeding, or contact type unspecified). If a patient had ≥1 animal interaction, the interaction recorded is that of the higher-risk category.

During 1970–2017, a total of 482 human plague cases were reported in the United States. Median case-patient age was 31 (range <1–94) years; 58% were male patients (Table 1). Bubonic plague was the predominant primary clinical manifestation of illness (n = 364, 76%), followed by septicemic plague (n = 91, 19%) and pneumonic plague (n = 15, 3%) (Table 1). Outcomes were known for 465 patients; 65 (14%) reportedly died from their illness.

Animal exposure that was plausibly related to plague transmission was identified in 258 (54%) records. The median case-patient age was greater among those with animal exposure (33 years) than those without animal exposure (24 years) (p<0.05). The frequency of known flea bite and mortality rate did not differ between patients with animal exposures and those without animal exposures (Table 1). After peaking in the 1980s, frequency of human plague decreased (Figure). However, the proportion of plague cases with animal exposure seemingly increased over time, from 52% in the years before 2000 to 63% since 2000 (p = 0.07) (Figure).

Of the 258 plague patients with animal exposures, 154 (60%) had contact with domestic animals before illness, including 121 with dogs and 102 with cats. The types of interactions included casual handling or touching (n = 55, 36%); co-sleeping (n = 31, 20%); caring for or handling a sick or dead animal (n = 29, 19%); bite, scratch, lick, or cough (n = 20, 13%); or other (n = 19, 12%) (Table 2). Among those with domestic animal contact, 65 (42%) had exposure to a domestic animal that brought home dead wild animals and 21 (14%) to a domestic animal with evidence of fleas.

Table 1. Characteristics of reported human plague case-patients, United States, 1970–2017*

| Characteristic | Total | Animal exposure before illness | |
		Yes	No
Case-patients	482 (100)	258 (54)	224 (46)
Sex			
M	278 (58)	152 (59)	126 (56)
F	204 (42)	106 (41)	98 (44)
Median age, y (range)	31 (<1–94)	33 (2–85)	24 (<1–94)
Race/ethnicity†‡			
White	220 (46)	135 (52)	85 (38)
American Indian/Alaska Native	114 (24)	52 (20)	62 (28)
Not specified	94 (20)	45 (17)	49 (22)
Hispanic	51 (11)	25 (10)	26 (12)
Asian	3 (<1)	1 (<1)	2 (1)
Primary clinical form†			
Bubonic	364 (76)	200 (78)	164 (73)
Septicemic	91 (19)	41 (16)	50 (22)
Pneumonic	15 (3)	13 (5)	2 (<1)
Pharyngeal	3 (<1)	2 (<1)	1 (<1)
Gastrointestinal	2 (<1)	1 (<1)	1 (<1)
Other and unknown	7 (1)	1 (<1)	6 (3)
Died	65 (14)	40 (16)	25 (11)
Known flea bite	104 (22)	49 (19)	55 (25)
State of exposure			
New Mexico	253 (52)	124 (48)	129 (58)
Colorado	66 (14)	44 (17)	22 (10)
Arizona	62 (13)	33 (13)	29 (13)
Other and unknown	101 (21)	57 (22)	44 (20)

*Values are no. (%) unless otherwise indicated.
†Indicates statistically significant difference ($\alpha = 0.05$) in proportion with characteristic between patients with animal exposure and those without animal exposure.
‡Several established race and ethnicity categories were absent among reported case-patient records and therefore not included.

A total of 134 (52%) patients had exposure to wild animals before illness. Common wild animal exposures were to sciurid rodents (e.g., squirrels, prairie dogs, gophers) (n = 58), lagomorphs (n = 50), other rodents (n = 40), wild carnivores (n = 15), and cervids (e.g., antelope, deer) (n = 9). Types of interactions identified were skinning (n = 54, 40%); handling a sick or dead animal (n = 37, 24%); casual handling or touching (n = 29, 22%); other type of contact (n = 12, 9%); and bite, scratch, lick, or cough (n = 2, 1%) (Table 2). Wild animal interactions were generally higher-risk, more direct exposures.

Pneumonic plague occurred more frequently among patients with animal exposure (n = 13, 5%) than among those without animal exposure (n = 2, 1%) (p<0.05); most patients had a history of contact with domestic animals (n = 11, 73%). Of 6 pneumonic plague cases associated with occupational exposures, 5 were among veterinarians or veterinary technicians providing care to plague-infected animals. The proportions of bubonic (n = 205, 77% vs. n = 162, 75%) and septicemic (n = 42, 16% vs. n = 49, 23%) cases were similar between patients with and without these exposures (Table 1).
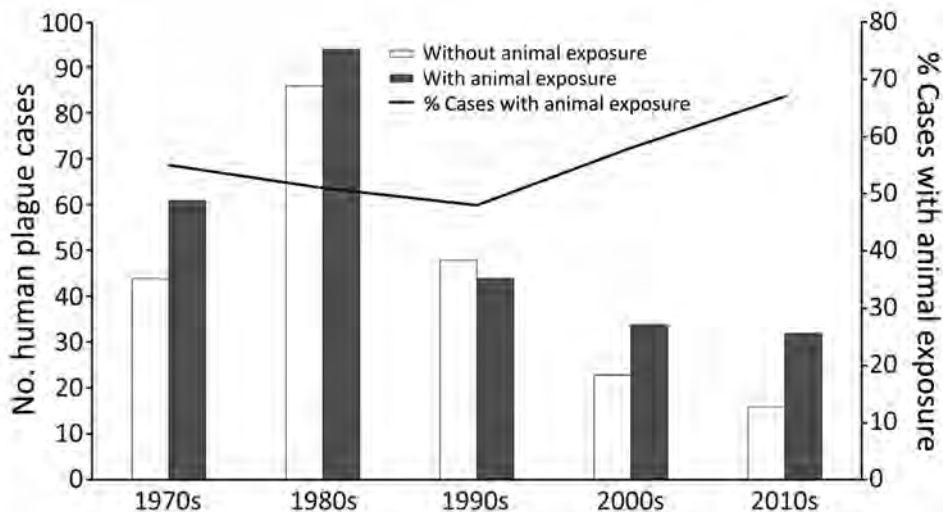
Figure. Frequency of animal exposure among human plague cases, by decade, United States, 1970–2017.

Table 2. Animal type and nature of interaction for 258 human plague case-patients with identified animal exposures, United States, 1970–2017

Category of animal interaction	Domestic animal, n = 154, no. (%)*	Wild animal, n = 134, no. (%)*
Bite, scratch, lick, cough	20 (13)	2 (1)
Skinning	0 (0)	54 (40)
Handling a sick or dead animal	29 (19)	37 (24)
Co-sleeping	31 (20)	0 (0)
Casual handling or touching	55 (36)	29 (22)
Other†	19 (12)	12 (9)

*Interaction ordered from highest to lowest risk.
†Walking, feeding, or nature of interaction not specified.

Conclusions

More than 50% of patients in the United States with plague since 1970 had animal interaction that might have directly or indirectly led to their exposure to *Y. pestis*. Animals are associated with human plague transmission in varied ways, ranging from direct exposure, such as caring for a plague-infected animal, to more subtle indirect encounters with infected fleas, such as by co-sleeping with a flea-infested pet in an area with epizootic plague. Nearly all patients with pneumonic plague had animal interaction before illness, and several occurred in an occupational setting. Although the frequency of human plague in the United States has decreased, the proportion of human cases potentially related to animal exposure has concomitantly increased.

Cat-associated and wild animal–associated human plague have been documented in previous reports (*6–9*). More recently, the severity of plague illness in dogs and the role these animals might play in human plague have been recognized (*10*). A cluster of pneumonic plague in Colorado was linked to a dog with pneumonic plague (*11*), and a recent case of canine plague resulted in the potential exposure of ≥116 persons at a veterinary clinic (*12*). Gould et al. found that co-sleeping with a dog occurred more frequently among human plague case-patients than among neighborhood controls (*13*).

Limitations of our analysis include the possibility that human plague cases might have gone undiagnosed and thus were not captured. Our findings might underrepresent animal-associated plague because case records contain variable levels of detail. Thus, some patients might have had animal exposures that were not captured. In many instances, we could not determine which exposure contributed to human illness, if any at all. Therefore, this analysis is meant to describe the potential rather than definitive scope of animal-related human plague.

This report offers perspective on frequency and diversity of animal interaction as possible means of human exposure to *Y. pestis* in the United States. Given that most human plague worldwide is caused by flea bites, animal-associated prevention messages have been geared toward hunters and trappers, including the use of gloves when handling or skinning wild animals. Our findings highlight One Health–oriented opportunities to maximize plague prevention through communication with veterinarians in plague-endemic areas. Veterinarians play an integral role in plague prevention for animals and humans by increasing use of flea prevention products, promoting basic precautions among pet owners caring for sick pets, and encouraging use of appropriate personal protective equipment in the veterinary community.

About the Author

At the time of this study, Dr. Campbell was an Epidemic Intelligence Service Officer in the Division of Vector-Borne Diseases, National Center for Emerging and Zoonotic Infectious Diseases, Centers for Disease Control and Prevention, Fort Collins, CO. She is currently a veterinary epidemiologist in the National Center for Emerging and Zoonotic Infectious Diseases, Centers for Disease Control and Prevention, Atlanta, GA. Her research interests include zoonotic and infectious diseases.

References

1. Pollitzer R. Plague. World Health Organization monograph series; 1954 [cited 2019 Jan 15]. http://apps.who.int/iris/bitstream/10665/41628/1/WHO_MONO_22.pdf?ua=1
2. Gage KL, Kosoy MY. Natural history of plague: perspectives from more than a century of research. Annu Rev Entomol. 2005;50:505–28. https://doi.org/10.1146/annurev.ento.50.071803.130337
3. Mandell GL, Bennett JE, Dolin R, editors. Principles and practice of infectious diseases. Philadelphia: Churchill Livingstone Elsevier; 2010.
4. Centers for Disease Control and Prevention. National notifiable diseases surveillance system. Plague (*Yersinia pestis*) 1996 case definition [cited 2019 Sep 4]. https://wwwn.cdc.gov/nndss/conditions/plague/case-definition/1996
5. Kugeler KJ, Staples JE, Hinckley AF, Gage KL, Mead PS. Epidemiology of human plague in the United States, 1900–2012. Emerg Infect Dis. 2015;21:16–22. https://doi.org/10.3201/eid2101.140564
6. Gage KL, Dennis DT, Orloski KA, Ettestad P, Brown TL, Reynolds PJ, et al. Cases of cat-associated human plague in the

western US, 1977–1998. Clin Infect Dis. 2000;30:893–900. https://doi.org/10.1086/313804

7. Eidson M, Tierney LA, Rollag OJ, Becker T, Brown T, Hull HF. Feline plague in New Mexico: risk factors and transmission to humans. Am J Public Health. 1988;78:1333–5. https://doi.org/10.2105/AJPH.78.10.1333

8. Wong D, Wild MA, Walburger MA, Higgins CL, Callahan M, Czarnecki LA, et al. Primary pneumonic plague contracted from a mountain lion carcass. Clin Infect Dis. 2009;49:e33–8. https://doi.org/10.1086/600818

9. Doll JM, Zeitz PS, Ettestad P, Bucholtz AL, Davis T, Gage K. Cat-transmitted fatal pneumonic plague in a person who traveled from Colorado to Arizona. Am J Trop Med Hyg. 1994;51:109–14. https://doi.org/10.4269/ajtmh.1994.51.109

10. Nichols MC, Ettestad PJ, Vinhatton ES, Melman SD, Onischuk L, Pierce EA, et al. *Yersinia pestis* infection in dogs: 62 cases (2003–2011). J Am Vet Med Assoc. 2014;244:1176–80. https://doi.org/10.2460/javma.244.10.1176

11. Runfola JK, House J, Miller L, Colton L, Hite D, Hawley A, et al.; Centers for Disease Control and Prevention. Outbreak of human pneumonic plague with dog-to-human and possible human-to-human transmission—Colorado, June–July 2014. MMWR Morb Mortal Wkly Rep. 2015;64:429–34.

12. Schaffer PA, Brault SA, Hershkowitz C, Harris L, Dowers K, House J, et al. Pneumonic plague in a dog and widespread potential human exposure in a veterinary hospital, United States. Emerg Infect Dis. 2019;25:800–3. https://doi.org/10.3201/eid2504.181195

13. Gould LH, Pape J, Ettestad P, Griffith KS, Mead PS. Dog-associated risk factors for human plague. Zoonoses Public Health. 2008;55:448–54.

Address for correspondence: Kiersten J. Kugeler, Centers for Disease Control and Prevention, 3156 Rampart Rd, Fort Collins, CO 80521, USA; email: bio1@cdc.gov

EMERGING INFECTIOUS DISEASES®

June 2018

Zoonoses

To revisit the June 2018 issue, go to:

Sentinel Listeriosis Surveillance in Selected Hospitals, China, 2013–2017

Weiwei Li, Li Bai, Xiaochen Ma, Xiuli Zhang, Xinpeng Li, Xiaorong Yang, Jennifer Y. Huang, Séamus Fanning, Yunchang Guo

During 2013–2017, a total of 211 cases of listeriosis were reported by 64 sentinel hospitals in China to a national food-borne disease surveillance network. The average case-fatality rate was 31.2% for perinatal cases and 16.4% for nonperinatal cases. Sequence types 87 and 8 were the most prevalent types.

Listeriosis is caused by the gram-positive bacterium *Listeria monocytogenes*, which is ubiquitous in the environment and a foodborne pathogen of importance to public health. Listeriosis occurs sporadically and mainly in high-risk groups, such as pregnant women, neonates, and immunocompromised and elderly persons (*1*). Although listeriosis occurs rarely in humans, it has a high case-fatality rate of 20%–50% (*2*). Nearly all reported listeriosis cases are transmitted to humans via food (*3*), and *L. monocytogenes* can grow at refrigeration temperatures, which makes it particularly challenging to control (*4*).

In China, surveillance of *L. monocytogenes* in food products was launched in 2000 (*5*); however, as yet, listeriosis is not a notifiable disease in China. The National Foodborne Disease Surveillance Plan was implemented in 2011 (*6,7*). Human listeriosis surveillance was included as a special pilot project in 2013. We provide an overview of the listeriosis sentinel surveillance data for the period 2013–2017. We summarize the demographic and clinical characteristics of patients with listeriosis and analyze the prevalent sequence types (STs) of all identified isolates.

Author affiliations: China National Center for Food Safety Risk Assessment, Beijing, China (W. Li, L. Bai, Y. Guo); Beijing Center for Disease Control and Prevention, Beijing (X. Ma); Henan Provincial Center for Disease Control and Prevention, Zhengzhou, China (X. Zhang); Shandong Provincial Center for Disease Control and Prevention, Jinan, China (X. Li); Sichuan Provincial Center for Disease Control and Prevention, Chengdu, China (X. Yang); Centers for Disease Control and Prevention, Atlanta, Georgia, USA (J.Y. Huang); University College Dublin, Dublin, Ireland (S. Fanning)

The Study

In 2013, listeriosis surveillance started in 6 selected provinces in China. The target was to detect whether human listeriosis existed in China and to determine illness and death rates for listeriosis. In 2017, this pilot surveillance had expanded to 12 provinces with the additional objectives to investigate high-risk factors and detect potential outbreaks (Figure). A total of 78 sentinel hospitals were selected using convenient sampling: 40 general hospitals, 28 maternity hospitals, and 10 children's hospitals.

We defined invasive listeriosis as the isolation of *L. monocytogenes* from a normally sterile site (e.g., blood or cerebrospinal fluid) or products of conception (e.g., placental or fetal tissue) (*8*). Pregnancy-associated patients were considered perinatal case-patients, including pregnant women, fetuses, or infants ≤28 days of age; maternal–fetal infections were counted as a single case. We defined stillbirths and miscarriages as deaths, which were tallied in case-fatality rates. Pregnant women and neonates were the focused population groups, with immunocompromised and older adults also included. All demographic data, clinical manifestations, and laboratory tests were submitted to the China National Center for Food Safety Risk Assessment (CFSA) through the National Foodborne Disease Reporting System. All confirmed isolates were finally referred to CFSA for pulsed-field gel electrophoresis and whole-genome sequencing analysis through the National Molecular Tracing Network for Foodborne Disease Surveillance (TraNet).

During 2013–2017, a total of 211 listeriosis cases were diagnosed and reported by 64 sentinel hospitals, 138 (65.4%) perinatal cases and 73 (34.6%) nonperinatal cases. All case-patients were hospitalized; 55 deaths or fetal losses (case-fatality rate 26.1%) were reported, and 43 (78.2%) fatal cases occurred among fetuses and neonates. The average case-fatality rates were 31.2% (43/138) for perinatal and 16.4% (12/73) for nonperinatal cases. No maternal death was reported. Seventy-four (35.1%) case-patients acquired listeriosis in the summer (June–August).

Of the 138 perinatal infections, the median age of the mother was 29 years (range 20–41 years), and the median gestational age was 32 weeks (range 8–40 weeks). Preterm labor (<37 weeks gestational age) was reported in 63 (45.7%) pregnant women with listeriosis. Clinical signs in pregnant women included intrauterine
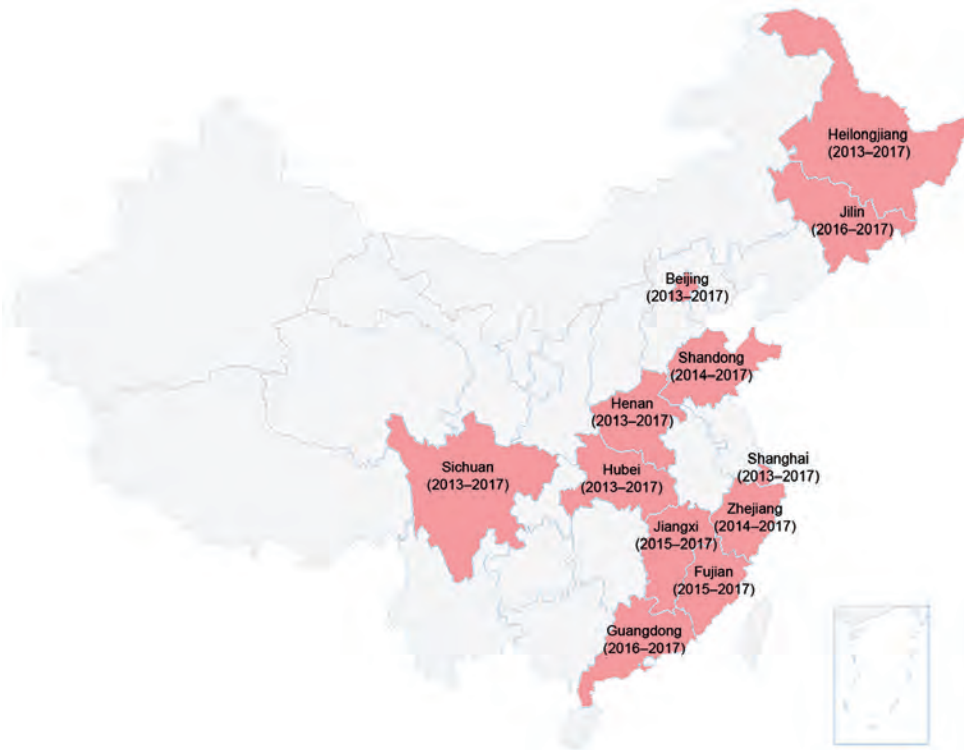
Figure. Geographic distribution of 12 selected provinces (red shading) included in human listeriosis surveillance, China, 2013–2017

infection, abortion, preterm labor, and influenza-like symptoms. Clinical manifestations and outcomes of infection in neonates included neonatal sepsis, asphyxia, pneumonia, meningitis, aspiration of amniotic fluid, meconium syndrome, and death.

Of the 73 nonperinatal infections, 45 (61.6%) cases were bloodstream infections such as septicemia and bacteremia, 20 (27.4%) were central nervous system infections, 6 (8.2%) were acute gastroenteritis, and 2 (2.7%) were focal infections. The median age of nonperinatal case-patients was 53 years (range 2 months–102 years); 22.9% were >65 years of age. The sex ratio was 1:1. Fifty-seven (78.1%) patients had positive blood samples, 11 (15.1%) had positive cerebrospinal fluid, and 15 (6.9%) were positive in other specimens, such as pleural effusion, cystic liquid, bone marrow, and feces (Table 1). The all-cause

immunosuppression rate was 28.8% (21/73 cases). We detected the following underlying immunosuppression conditions: hematologic malignancy, systemic lupus erythematosus, chronic obstructive pulmonary disease, chronic kidney disease, liver disease, organ tumor, lung transplantation, and tuberculosis.

Of the reported listeriosis cases, 28.9% (61/211) were followed up with epidemiologic investigation, and 18.0% (11/61) yielded positive results for *L. monocytogenes* in suspicious food, chopping boards, refrigerators, or kitchen sinks. However, the pulsed-field gel electrophoresis patterns were not identical to those of clinical isolates, and >100 allele differences were found by using the core genome multilocus sequence typing (MLST) profile of 1,748 loci (*9*). These results showed no links between food, environmental, and clinical isolates.

Table 1. Demographic data of 211 listeriosis case-patients reported by 64 sentinel hospitals, by risk group, China, 2013–2017*

Characteristic	Pregnancy-associated, no. (%)	Not pregnancy-associated, no. (%)	Total, no. (%)
Total	138 (65.4)	73 (34.6)	211 (100.0)
Sex			
F	138 (100.0)	36 (49.3)	174 (82.5)
M	0	0	0
Specimen source			
Blood	86 (62.3)	57 (78.1)	143 (67.8)
CSF	8 (5.8)	11 (15.1)	19 (9.0)
Other†	NA	5 (6.9)	5 (2.4)
Product of conception	44 (31.9)	NA	44 (20.9)
Death or fetal loss	43 (31.2)	12 (16.4)	55 (26.1)

*CSF, cerebrospinal fluid; NA, nonapplicable.
†Including pleural effusion, cystic liquid, bone marrow, and feces.

Table 2. Distribution of PCR serogroups and ST types identified among 108 isolates from listeriosis case-patients, by risk group, China, 2013–2017*

Characteristic	Pregnancy-associated, no. (%)	Not pregnancy-associated, no. (%)	Total, no. (%)
Total	76 (70.4)	32 (29.6)	108 (100.0)
PCR serogroups			
IIa	30 (39.5)	15 (46.9)	45 (41.7)
IIb	32 (42.1)	13 (40.6)	45 (41.7)
IVb	13 (17.1)	3 (9.4)	16 (14.8)
IIc	1 (1.3)	1 (3.1)	2 (1.9)
MLST types			
ST87	14 (18.4)	3 (9.4)	17 (15.7)
ST8	11 (14.5)	4 (12.5)	15 (13.9)
ST619	4 (5.3)	4 (12.5)	8 (7.4)
ST155	2 (2.6)	4 (12.5)	6 (5.6)
Other STs	45 (59.2)	17 (53.1)	62 (57.4)

*MLST, multilocus sequencing typing; ST, sequence type.

A total of 116 isolates isolated during 2013–2016 were submitted to CFSA for whole-genome sequencing analysis: 108 from human listeriosis and 8 from the environment and suspicious food. The distribution of these 108 clinical *L. monocytogenes* clones was determined by MLST. A previous study reported that clonal complex (CC) 1, CC2, CC121, and CC155 were frequent clones in eastern Asia (*10*). We found that sequence type (ST) 87 (lineage I) and ST8 (lineage II) were the predominant STs; 15.7% of isolates were ST87 and 13.9% were ST8. The prevalences of ST87 in clinical isolates (*11*) and in domestic food products were also reported previously (*12*). ST87 was seldom linked to human listeriosis in other countries; only 2 outbreaks (both in Spain) were associated with ST87 strains (*13*). The most common PCR serogroups were IIb and IIa (Table 2). A total of 89 different core genome MLST types were identified as groups that differ by up to 7 allelic mismatches among the clinical isolates.

Conclusions

Our study describes epidemiologic characteristics of listeriosis from sentinel surveillance in China. An estimated 1,662 cases of listeriosis occur each year in the United States (*3*); a detailed analysis should be expedited in China to estimate incidence. The Universal Two-Child Policy was proposed and passed in 2015, which likely will increase the number of pregnancies and births in China and might therefore increase the incidence of listeriosis.

This study has limitations (*1*). All cases came from sentinel hospitals but were not a complete picture of listeriosis occurrence because of the gradual increase of provinces included in surveillance (from 6 to 12 provinces), which meant the population served by selected hospitals could not be estimated accurately (*2*). All case-patients might be the most ill patients; cases might have been missed because those patients with milder illness might not go to the hospital and therefore will not be reflected in the data (*3*). The number of perinatal cases was nearly twice the number of nonperinatal cases, which cannot represent the actual illness and death rates because perinatal infection is given more attention in some sentinel hospitals (*4*). The case-fatality rates might be underestimated because all live-born infants, premature infants, and case-patients who did not complete follow-up surveillance were assumed to survive unless they were reported to have died.

In summary, health education and reasonable diet advice regarding listeriosis prevention should be provided to high-risk groups in China, and a focus on *L. monocytogenes* infection should be strengthened in hospitals. Moreover, *L. monocytogenes* is common in domestic food products in mainland China, especially in meat, poultry, seafood, and Chinese salad (*14,15*). An urgent need exists for improving surveillance of food and humans, exploring the mechanisms of pathogenesis, determining higher-risk foods, detecting potential outbreaks, and implementing control measures to protect vulnerable populations.

About the Author

Mrs. Weiwei Li is an associate researcher in the Department of Risk Surveillance, China National Center for Food Safety Risk Assessment, Beijing, China. Her research interests include foodborne disease surveillance and molecular epidemiology of bacterial pathogens.

References

1. Lamont RF, Sobel J, Mazaki-Tovi S, Kusanovic JP, Vaisbuch E, Kim SK, et al. Listeriosis in human pregnancy: a systematic review. J Perinat Med. 2011;39:227–36. https://doi.org/10.1515/jpm.2011.035

2. Swaminathan B, Gerner-Smidt P. The epidemiology of human listeriosis. Microbes Infect. 2007;9:1236–43. https://doi.org/10.1016/j.micinf.2007.05.011

3. Scallan E, Hoekstra RM, Angulo FJ, Tauxe RV, Widdowson MA, Roy SL, et al. Foodborne illness acquired in the United States—major pathogens. Emerg Infect Dis. 2011;17:7–15. https://doi.org/10.3201/eid1701.P11101

4. de Noordhout CM, Devleesschauwer B, Angulo FJ, Verbeke G, Haagsma J, Kirk M, et al. The global burden of listeriosis: a systematic review and meta-analysis. Lancet Infect Dis. 2014;14:1073–82. https://doi.org/10.1016/S1473-3099(14)70870-9

5. Pei X, Li N, Guo Y, Liu X, Yan L, Li Y, et al. Microbiological food safety surveillance in China. Int J Environ Res Public Health. 2015;12:10662–70. https://doi.org/10.3390/ijerph120910662

6. Li W, Wu S, Fu P, Liu J, Han H, Bai L, et al. National molecular tracing network for foodborne disease surveillance in China. Food Control. 2018;88:28–32. https://doi.org/10.1016/j.foodcont.2017.12.032

7. Liu J, Bai L, Li W, Han H, Fu P, Ma X, et al. Trends of foodborne diseases in China: lessons from laboratory-based surveillance since 2011. Front Med. 2018;12:48–57. https://doi.org/10.1007/s11684-017-0608-6

8. Silk BJ, Date KA, Jackson KA, Pouillot R, Holt KG, Graves LM, et al. Invasive listeriosis in the Foodborne Diseases Active Surveillance Network (FoodNet), 2004–2009: further targeted prevention needed for higher-risk groups. Clin Infect Dis. 2012;54(Suppl 5):S396–404. https://doi.org/10.1093/cid/cis268

9. Moura A, Criscuolo A, Pouseele H, Maury MM, Leclercq A, Tarr C, et al. Whole genome-based population biology and epidemiological surveillance of Listeria monocytogenes. Nat Microbiol. 2016;2:16185. https://doi.org/10.1038/nmicrobiol.2016.185

10. Chenal-Francisque V, Lopez J, Cantinelli T, Caro V, Tran C, Leclercq A, et al. Worldwide distribution of major clones of Listeria monocytogenes. Emerg Infect Dis. 2011;17:1110–2. https://doi.org/10.3201/eid1706.101778

11. Wang Y, Jiao Y, Lan R, Xu X, Liu G, Wang X, et al. Characterization of Listeria monocytogenes isolated from human Listeriosis cases in China. Emerg Microbes Infect. 2015;4:e50. https://doi.org/10.1038/emi.2015.50

12. Wang Y, Zhao A, Zhu R, Lan R, Jin D, Cui Z, et al. Genetic diversity and molecular typing of Listeria monocytogenes in China. BMC Microbiol. 2012;12:119. https://doi.org/10.1186/1471-2180-12-119

13. Pérez-Trallero E, Zigorraga C, Artieda J, Alkorta M, Marimón JM. Two outbreaks of Listeria monocytogenes infection, Northern Spain. Emerg Infect Dis. 2014;20:2155–7. https://doi.org/10.3201/eid2012.140993

14. Wu S, Wu Q, Zhang J, Chen M, Yan ZA, Hu H. Listeria monocytogenes prevalence and characteristics in retail raw foods in China. PLoS One. 2015;10:e0136682. https://doi.org/10.1371/journal.pone.0136682

15. Chen J, Zhang X, Mei L, Jiang L, Fang W. Prevalence of Listeria in Chinese food products from 13 provinces between 2000 and 2007 and virulence characterization of Listeria monocytogenes isolates. Foodborne Pathog Dis. 2009;6:7–14. https://doi.org/10.1089/fpd.2008.0139

Address for correspondence: Yunchang Guo, China National Center for Food Safety Risk Assessment, No. 37, Bldg 2, Guangqulu, Chaoyang District, Beijing 100022, China; email: gych@cfsa.net.cn
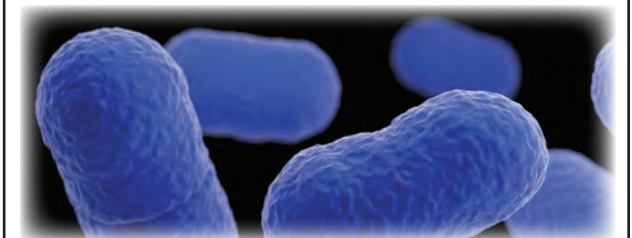
Economic Effect of Confiscation of Cattle
Viscera Infected with Cystic Echinococcosis, Huancayo Province, Peru

**J. Raúl Lucas, Carmen A. Arias,
Stephanie S. Balcázar-Nakamatsu,
Alejandro P. Rodríguez, Karen A. Alroy,
Cesar M. Gavidia**

We report cystic echinococcosis (CE) prevalence in Huancayo Province, Peru, and the associated economic effect of bovine organ condemnation. CE prevalence during the 16-month study period was 42.8% and caused $14,595 in economic losses. CE threatens food security in the region by reducing farmers' income and viscera supply in markets.

*E*chinococcus granulosus is a parasitic flatworm found in the small intestines of canids. The metacestode of this parasite (hydatid cyst) can infect various organs of intermediate hosts (mainly livers and lungs), causing cystic echinococcosis (CE) (*1*). The parasite also can infect humans. Intermediate hosts are commonly asymptomatic; however, CE causes economic losses in livestock because of organ condemnation, decreased productivity, and decreased reproductive performance (*2,3*).

Slaughterhouse records have been used as an inexpensive method to record CE data for livestock. These data serve as the foundation for estimating the effects of disease in different endemic regions and can potentially help guide implementation of control programs or serve as an indicator to assess control measures (*4*). We aimed to determine the CE prevalence in cattle slaughtered in a province in the central Andes of Peru and to assess the economic losses and potential food security effects from a multisectoral perspective (e.g., farmers, meat industry, and consumers).

The Study

We conducted a 2-phased study in 1 of 3 official bovine slaughterhouses (authorized by the Peruvian Ministry of Agriculture) in Huancayo Province (altitude 3,263 m, latitude 12°4′S, longitude 75°13′W), a CE-endemic region of

Author affiliations: Universidad Nacional Mayor de San Marcos, Lima, Peru (J.R. Lucas, C.A. Arias, S.S. Balcázar-Nakamatsu, C.M. Gavidia); Servicio Nacional de Sanidad Agraria, Junin, Peru (A.P. Rodríguez); Johns Hopkins Bloomberg School of Public Health, Baltimore, Maryland, USA (K.A. Alroy)

Peru, where prevalence of human CE is >4% (*5*). In this region, cattle are raised primarily for milk production, and the predominant breed is a criollo (i.e., mixed) breed.

In the first phase, we conducted a retrospective review of abattoir meat inspection reports from September 2013–December 2014 to estimate the 16-month offal prevalence and identify the affected organs and sex of the animals. CE-infected organs can be easily distinguished macroscopically, either by palpation and visual inspection (Figure) or, when necessary, by performing incisions in accordance with World Health Organization guidelines (*6*). We evaluated and categorized the records into 4-month periods: September–December 2013, January–April 2014, May–August 2014, and September–December 2014. The cost of noninfected viscera was also recorded from the slaughterhouse register.

In the second phase, initiated in January 2015, we determined the average weight of infected viscera. We then estimated the economic losses by multiplying the number of condemned organs by the average viscera weight and the selling price. In addition, we estimated the total amount of confiscated viscera (expressed as tons of viscera destroyed) for September 2013–December 2014.

We conducted statistical analysis by using Stata 10 (StataCorp, https://www.stata.com). We obtained CE prevalence, 95% CIs, and the prevalence differences between infected organs by χ^2 test. To estimate the risk for infection, we constructed a multivariate logistic regression model that included as variables the sex of the animal and the month and year of slaughter.

We evaluated data for 7,046 animals during the study period (September 2013–December 2014). The overall 16-month prevalence of CE was 42.8% (95% CI 41.64%–43.96%). We determined specific organ infection by sex and period (Table 1). CE infection of lungs was significantly higher (p<0.001) than in other organs. The sex of the animal and time of year was associated with the presence of CE (Table 2); for example, the odds of CE in ≥1 infected organ in male animals was 27% lower than that in female animals (p<0.001). In addition, the odds of detecting CE in animals slaughtered during January–April was 3.2 times higher than for May–August 2014 (p<0.001) (Table 2).

Mean weight of affected organs was 2.73 kg (SD ± 0.85 kg) for lungs, 4.19 kg (SD ± 1.28 kg) for liver, and 1.00 kg (SD ± 0.51 kg) for heart. The total weight of
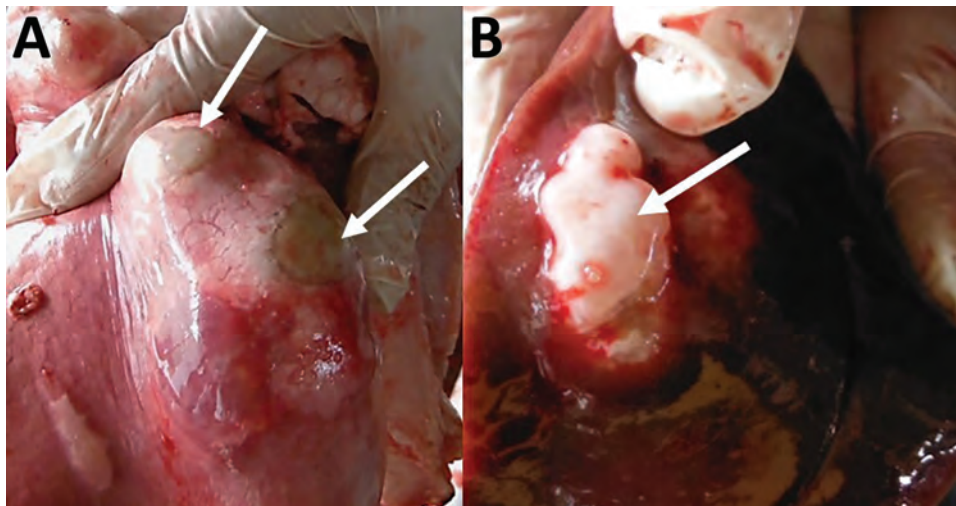
Figure. Lung (A) and liver (B) parenchyma infected with hydatid cysts (white arrows) detected during veterinary inspection at slaughterhouse and before the entire organ was confiscated and destroyed by incineration, Huancayo Province, Peru.

destroyed organs during the 16-month period was 11.12 metric tons. The estimated 16-month total economic loss was USD $14,595 (95% CI $12,713–$16,488).

Our results showed that CE infection in slaughtered cattle remains very high in areas like the central Peruvian Andes. Previous reports also described endemic cattle CE in this region with 68% prevalence (17/25 cattle were CE infected) (*5*). With no control program in place in this region of Peru, animal CE has achieved one of the highest infection rates in the world (*4,7–12*). The large numbers of dogs around the slaughterhouses and traditional human practices are factors that contribute to the high CE infection rates in rural areas (*5,7,13*).

Pulmonary CE infection was ≈3-fold higher than hepatic CE infection in this study. Multiple studies have indicated that lungs are the most affected organs by CE in ruminants (*5,9,11*). In contrast, other studies indicate that livers are the most commonly affected organs (*8,12*). Although the *E. granulosus* oncospheres first reach hepatic capillaries, lungs have the largest capillary beds in mammals, which might explain the higher prevalence of pulmonary CE infection (*9*). Increased volume and dilation of pulmonary capillaries, associated with the physiologic adaptive response to high altitude in humans (*14*), might also be occurring in cattle in this region.

Similar to our results, other reports have shown that female cattle are more prone to acquire CE than male cattle

(*10,11*). A biologic explanation for this apparent female susceptibility might exist, but further investigation is required. Husbandry practices in the Andes of Peru might provide another possible explanation because cows commonly remain in production longer than male cattle; consequently, older animals would have a longer exposure time (*4,8,11*).

May–August is the dry season in the Andes of Peru, and pastures are scarce. Therefore, during this period, slaughtering young cattle instead of older animals is more profitable. This factor would explain the temporal variation observed (Table 2), but concluding that seasonality (e.g., humidity and temperature) plays a role in CE prevalence in the Andes is difficult. However, studies have indicated a higher CE frequency during months of higher humidity in some regions of Iran and Kazakhstan (*10,12*).

In South America, the viscera of ≈2 million cattle and ≈3.5 million sheep are condemned in slaughterhouses yearly, which represents a loss of >$6 million USD (*3*). We calculated a 16-month economic loss of $14,595. Previously, the economic loss attributable to ovine and bovine hepatic CE in Peru was reported as $196,681 annually (*13*). Moreover, the loss of livestock to hepatic CE is estimated to be $141,605,195 worldwide (*15*). The economic loss described in our study is from just 1 official abattoir, so when considering farm animal slaughter, unofficial abattoirs, and the remaining slaughterhouses throughout the country, this estimated economic effect might represent just a small

Table 1. Prevalence of cystic echinococcosis among cattle and number of infected animals, by 4-month period, sex, and organ type, Huancayo Province, Peru, September 2013–December 2014

Period	% Infected (no. infected animals)						Total prevalence, % (no. infected animals)
	Female			Male			
	Lung	Liver	Heart	Lung	Liver	Heart	
2013 Sep–Dec	48.97 (592)	9.18 (111)	0.17 (2)	41.92 (280)	7.93 (53)	0.15 (1)	49.55 (930)
2014 Jan–Apr	50.46 (383)	14.36 (109)	0.13 (1)	55.19 (351)	12.42 (79)	0.16 (1)	58.64 (818)
2014 May–Aug	32.34 (305)	9.86 (93)	0.32 (3)	24.52 (180)	6.54 (48)	0.14 (1)	31.13 (522)
2014 Sep–Dec	31.98 (433)	21.94 (297)	0.52 (7)	19.52 (145)	15.48 (115)	0.27 (2)	35.72 (749)
2013 Sep–2014 Dec	40.16 (1,713)	14.30 (610)	0.31 (13)	34.38 (956)	17.62 (490)	0.18 (5)	42.85 (3,019)

Table 2. Prevalence of cystic echinococcosis among cattle in multivariate logistic regression model, by sex and 4-month period, Huancayo Province, Peru, September 2013–December 2014*

Characteristic	Presence of CE†		Lung CE‡		Hepatic CE†	
	OR (95% CI)	p value	OR (95% CI)	p value	OR (95% CI)	p value
Sex						
F	Referent	NA	Referent	NA	Referent	NA
M	0.73 (0.66–0.81)	0.00	0.75 (0.68–0.83)	0.00	0.73 (0.62–0.84)	0.00
Four-month period§						
Sep–Dec 2013	2.1 (1.85–2.44)	0.00	2.1 (1.82–2.40)	0.00	1.0 (0.80–1.29)	0.89
Jan–Apr 2014	3.2 (2.73–3.69)	0.00	2.8 (2.73–3.20)	0.00	1.7 (1.35–2.15)	0.00
Sep–Dec 2014	1.2 (1.05–1.38)	0.00	0.9 (0.79–1.05)	0.21	2.6 (2.12–3.19)	0.00

*CE, cystic echinococcosis; NA, not applicable; OR, odds ratio.
†Pearson χ^2 goodness-of-fit test value of p<0.05.
‡Pearson χ^2 goodness-of-fit test value of p = 0.3845.
§Reference period is May–August 2014.

portion of the actual effect in Peru. However, we have no information from other slaughterhouses because abattoir information is often unavailable or underestimated. These challenges have been observed in other studies for which similar estimations are performed (*15*).

Conclusions

The direct economic effects associated with confiscation of infected offal represents only part of the overall losses attributable to CE. Other losses, such as reduction of protein sources and decreased animal productivity, are important components to consider in a global estimation. The central Andes of Peru require interventions aimed at strengthening food security and reducing undernutrition. As demonstrated in this 16-month study, >11 metric tons of viscera were destroyed because of CE infection. Viscera, particularly lungs and livers, are inexpensive sources of protein for human consumption in poor and rural areas of Peru and in other developing countries. Bovine CE infection limits the supply of this protein in local markets and could also result in reduced nutritional quality of carcasses of infected animals (*12*) and in increased prices of suitable noninfected viscera.

Contributions to this manuscript by Karen A. Alroy were done in her personal capacity.

About the Author

Dr. Lucas is a professor of food security at the Universidad Nacional Mayor de San Marcos, Lima, Peru. His research interests focus on food security, with an emphasis on the epidemiology of foodborne illnesses.

References

1. Craig PS, McManus DP, Lightowlers MW, Chabalgoity JA, Garcia HH, Gavidia CM, et al. Prevention and control of cystic echinococcosis. Lancet Infect Dis. 2007;7:385–94. https://doi.org/10.1016/S1473-3099(07)70134-2
2. Benner C, Carabin H, Sánchez-Serrano LP, Budke CM, Carmena D. Analysis of the economic impact of cystic echinococcosis in Spain. Bull World Health Organ. 2010;88:49–57. https://doi.org/10.2471/BLT.09.066795
3. Battelli G. Echinococcosis: costs, losses and social consequences of a neglected zoonosis. Vet Res Commun. 2009;33(Suppl 1):47–52. https://doi.org/10.1007/s11259-009-9247-y
4. Yang S, Wu W, Tian T, Zhao J, Chen K, Wang Q, et al. Prevalence of cystic echinococcosis in slaughtered sheep as an indicator to assess control progress in Emin County, Xinjiang, China. Korean J Parasitol. 2015;53:355–9. https://doi.org/10.3347/kjp.2015.53.3.355
5. Moro PL, McDonald J, Gilman RH, Silva B, Verastegui M, Malqui V, et al. Epidemiology of *Echinococcus granulosus* infection in the central Peruvian Andes. Bull World Health Organ. 1997;75:553–61.
6. World Health Organization. Guidelines for surveillance, prevention and control of echinococcosis/hydatidosis. Geneva: The Organization; 1984.
7. Acosta-Jamett G, Cleaveland S, Bronsvoort BM, Cunningham AA, Bradshaw H, Craig PS. *Echinococcus granulosus* infection in domestic dogs in urban and rural areas of the Coquimbo region, north-central Chile. Vet Parasitol. 2010;169:117–22. https://doi.org/10.1016/j.vetpar.2009.12.005
8. Azlaf R, Dakkak A. Epidemiological study of the cystic echinococcosis in Morocco. Vet Parasitol. 2006;137:83–93. https://doi.org/10.1016/j.vetpar.2006.01.003
9. Getaw A, Beyene D, Ayana D, Megersa B, Abunna F. Hydatidosis: prevalence and its economic importance in ruminants slaughtered at Adama municipal abattoir, Central Oromia, Ethiopia. Acta Trop. 2010;113:221–5. https://doi.org/10.1016/j.actatropica.2009.10.019
10. Daryani A, Alaei R, Arab R, Sharif M, Dehghan MH, Ziaei H. The prevalence, intensity and viability of hydatid cysts in slaughtered animals in the Ardabil province of Northwest Iran. J Helminthol. 2007;81:13–7. https://doi.org/10.1017/S0022149X0720731X
11. Pour AA, Hosseini SH, Shayan P. The prevalence and fertility of hydatid cysts in buffaloes from Iran. J Helminthol. 2012;86:373–7. https://doi.org/10.1017/S0022149X11000514
12. Valieva Z, Sarsembaeva N, Valdovska A, Ussenbayev AE. Impact of echinococcosis on quality of sheep meat in the south eastern Kazakhstan. Asian-Australas J Anim Sci. 2014;27:391–7. https://doi.org/10.5713/ajas.2013.13386
13. Moro PL, Budke CM, Schantz PM, Vasquez J, Santivañez SJ, Villavicencio J. Economic impact of cystic echinococcosis in Peru. PLoS Negl Trop Dis. 2011;5:e1179. https://doi.org/10.1371/journal.pntd.0001179
14. Naeije R. Physiological adaptation of the cardiovascular system to high altitude. Prog Cardiovasc Dis. 2010;52:456–66. https://doi.org/10.1016/j.pcad.2010.03.004
15. Budke CM, Deplazes P, Torgerson PR. Global socioeconomic impact of cystic echinococcosis. Emerg Infect Dis. 2006;12:296–303. https://doi.org/10.3201/eid1202.050499

Address for correspondence: J. Raúl Lucas, Universidad Nacional Mayor de San Marcos, Av Circunvalación 2800, San Borja, Lima, Perú; email: jrlucas.pe@gmail.com

Predicting Dengue Outbreaks in Cambodia

**Anthony Cousien, Julia Ledien, Kimsan Souv,
Rithea Leang, Rekol Huy, Didier Fontenille,
Sowath Ly, Veasna Duong, Philippe Dussart,
Patrice Piola,[1] Simon Cauchemez,[1]
Arnaud Tarantola[1]**

In Cambodia, dengue outbreaks occur each rainy season (May–October) but vary in magnitude. Using national surveillance data, we designed a tool that can predict 90% of the variance in peak magnitude by April, when typically <10% of dengue cases have been reported. This prediction may help hospitals anticipate excess patients.

Dengue is endemic to Cambodia; outbreaks are seasonal, occurring during the rainy season (May–October). However, the magnitude of outbreaks varies from year to year. When the epidemic is particularly large, the influx of patients with severe dengue in pediatric hospitals may saturate the healthcare system and negatively affect quality of care. However, adequate supportive care is crucial for patients with severe dengue and can decrease the fatality rate to <1% (*1*). Early prediction of the size of nascent dengue epidemics may improve healthcare planning and optimize allocation of healthcare resources. We used surveillance data to build a simple early warning tool based on the reported number of cases early in the season. Compared with other approaches used to predict dengue epidemics (*2–6*), this one is characterized by its simplicity because it relies only on the number of cases reported early in the season to predict the magnitude of the epidemic.

The Study

We used the monthly number of probable dengue cases reported by the National Dengue Surveillance System (NDSS) in Cambodia during 2004–2016. The NDSS includes passive surveillance of probable dengue pediatric inpatients reported by public hospitals to the Communicable Diseases Center of the Ministry of Health and a sentinel, pediatric hospital–based active surveillance system managed by the National Dengue Control Program of the National Center for Parasitology, Entomology and Malaria Control, Ministry of Health. A probable dengue case was defined as an acute febrile illness with ≥2 of the following: headache, retro-orbital pain, myalgia, arthralgia, rash, hemorrhage, and leukopenia, combined with either 1) a posteriori virologic confirmation, serologic confirmation, or both or 2) presence of ≥1 laboratory-confirmed case at the same location and time (*7*).

From January 2004 through December 2016, NDSS reported 215,574 probable dengue cases (Figure 1). During this period, we observed 2 outbreaks of particularly high magnitude, in 2007 (dengue virus serotype 3) and 2012 (dengue virus serotype 1). The magnitude of these outbreaks reached ≈10,000 cases versus the usual number of <5,000 cases. Incidence was always lowest during the dry season (i.e., November–April); the nadirs usually occurred in February and the peaks in July (8 times), August (4 times), and June (1 time, in 2007). On average, only 6.1% of the cases reported during a season (i.e., from February through January of the following year) are observed before the end of April (range 2.7%–9.0% of cases). We wanted to ascertain whether the small number of cases reported at the season's onset (i.e., up to April) could be used as an early warning tool for predicting the magnitude of that season's epidemic.

We observed a strong linear correlation between the magnitude of the peak and the number of cases reported at the beginning of the season, in February (Pearson correlation coefficient r = 0.78), March (r = 0.88), April (r = 0.95), February–March (r = 0.86), March–April (r = 0.95), and February–April (r = 0.94). Fitting a simple linear regression model to the data, we estimated that the number of cases reported explained the following parts of the variance in the peak magnitude for February (61%), March (78%), April (91%), February–March (73%), March–April (90%), and February–April (88%). The magnitude was therefore best predicted by the number of dengue cases reported in April. This simple model offered excellent accuracy for predicting the magnitude of the peak; mean absolute percentage error for 2007 was 2.5% and for 2012 was 1.9% (Figure 2, panel A). Predictions relying on data from March were also acceptably accurate; the error was larger, but the model was able to predict a larger than usual magnitude (Appendix Figure 1, https://wwwnc.cdc.gov/EID/article/25/12/18-1193-App1.pdf).

Author affiliations: Institut Pasteur du Cambodge, Phnom Penh, Cambodia (A. Cousien, J. Ledien, K. Souv, D. Fontenille, S. Ly, V. Duong, P. Dussart, P. Piola); Institut Pasteur, Paris, France (A. Cousien, S. Cauchemez); CNRS, Paris (A. Cousien, S. Cauchemez); National Center for Entomology, Parasitology and Malaria Control, Phnom Penh (R. Leang, R. Huy); Institut Pasteur, Noumea, New Caledonia (A. Tarantola)

[1]These senior authors contributed equally to this article.
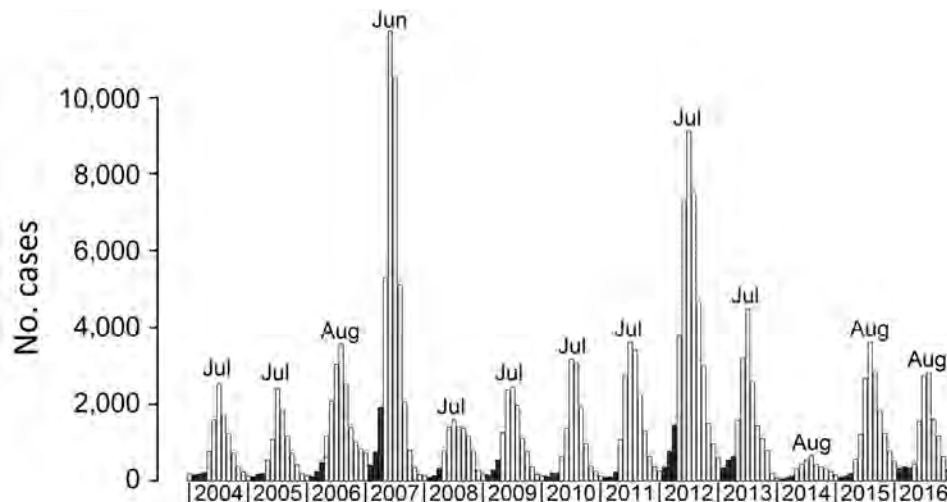
Figure 1. Monthly number of probable dengue cases reported to the National Dengue Surveillance System in Cambodia, 2004–2016. Dark gray bars represent the 3 months (February, March, and April) used as predictors for the magnitude of the following peak. For each year, the month corresponding to the peak of the epidemic is indicated.

To evaluate the performance of our model in a real-life situation, when the outcome of the ongoing epidemic remains unknown, we used a leave-one-out cross-validation procedure (*8–10*). We obtained the predicted value for season *s* by fitting our regression model to the 12 other seasons (i.e., excluding season *s* from the set of observations used to fit the parameters of the model [the training dataset]). The predictive power of our best fitting model remained very high; it was able to explain 90% of the variance of the magnitude of epidemics (Figure 2, panel B).

Our dataset contains information for only 2 large epidemics (2007 and 2012). If we trained the model on these 2 large epidemics only, performance would remain very good (98% variance explained). In contrast, when both epidemics were excluded from the training dataset, their magnitude was underestimated by 35% (2007) and 32% (2012). As expected, to be properly calibrated, the model needs to be trained on a mix of small and large epidemics; if 1 category is excluded from the training dataset, performance may be substantially degraded.

Of note, this loss of accuracy is mostly an issue for large epidemics. Given the small number of such epidemics in our dataset, robustly demonstrating predictability from this dataset alone remains difficult. We therefore explored whether similar patterns could be observed in 4 other countries in South Asia: Thailand, Vietnam, Laos, and the Philippines (*11–14*). To be comparable with our analysis for Cambodia, we used the month at which >5% of cases have been observed on average (Appendix Tables 4, 5). The results were promising for Vietnam (variance explained in the leave-one-out procedure was 64.3%), the Philippines (45.8%), and Thailand (33.4%) but bad for Laos (–53.5%) (Appendix Figures 3–6). This variability could be explained by several factors: national surveillance system characteristics, demographics, land cover, healthcare systems, or climate; all of these factors can affect dengue epidemiology and reporting. This analysis confirms the observation made for Cambodia that the number of dengue cases reported early in the epidemic year may provide early insight into the probable scale of the forthcoming epidemic.
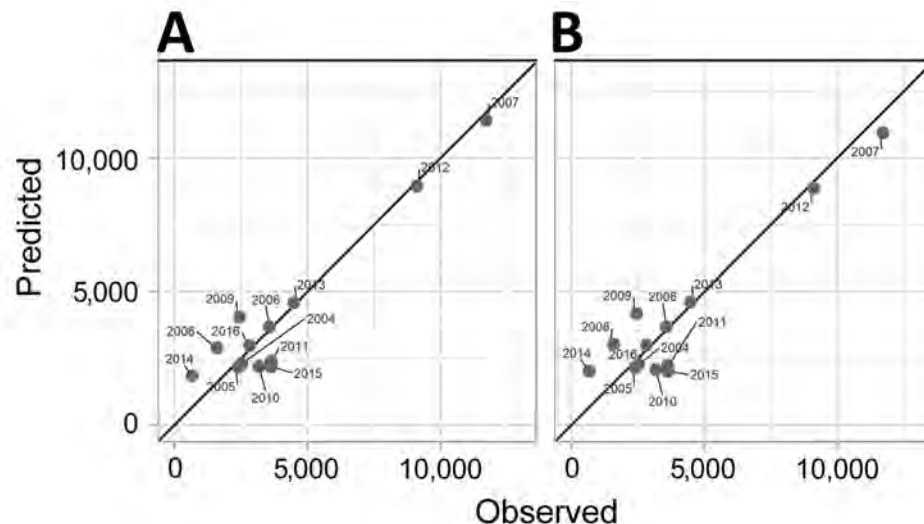
Figure 2. Dengue cases in Cambodia, 2004–2016. A) Observed versus predicted magnitude of the peak for each dengue season. We used a simple linear regression model, $M = \alpha + \beta N$, in which *M* indicates the magnitude of the peak and *N* the number of reported dengue-like cases in April. The black line represents the expected results with perfect prediction. B) Results for the leave-one-out cross-validation procedure.

Conclusions

The correlation between the number of patients hospitalized with probable dengue during the interepidemic period (i.e., the dry season) and the magnitude of the next outbreak peak during the rainy season was strong, even from February, which corresponds to the nadir of the incidence curves. Using dengue surveillance data for the end of the dry season (April), we were able to predict the magnitude of the peak for the next dengue outbreak, when typically <10% of cases have been observed and the peak is 2–3 months away. These results suggest that the intensity of rainfalls during the rainy season is not a major determinant of the occurrence of major outbreaks in Cambodia and that the outbreaks could be explained by conditions already present during the early stages of the outbreak (i.e., the part of the population immune to the circulating strains or weather conditions during the dry season). Our analysis is limited by the small number of epidemic seasons that are available to train our model for Cambodia (in particular, the small number of large epidemics), but similar patterns were observed in some other countries in South Asia.

In a setting where resources are limited and where pediatric hospitals face several other health issues (diarrheal diseases, other infectious diseases), the amount of available beds, medical supplies, and medical staff are usually appropriate for an average dengue outbreak. This simple and easy tool can help hospitals to plan in accordance with the predicted magnitude of the seasonal outbreak.

About the Author

Dr. Cousien is a postdoctoral researcher at the Institut Pasteur. His research interests include the modeling of arbovirus epidemics.

References

1. World Health Organization. Dengue and severe dengue [cited 2017 Sep 7]. http://www.who.int/mediacentre/factsheets/fs117
2. Lowe R, Gasparrini A, Van Meerbeeck CJ, Lippi CA, Mahon R, Trotman AR, et al. Nonlinear and delayed impacts of climate on dengue risk in Barbados: a modelling study. PLoS Med. 2018;15:e1002613. https://doi.org/10.1371/journal.pmed.1002613
3. Lowe R, Barcellos C, Coelho CAS, Bailey TC, Coelho GE, Graham R, et al. Dengue outlook for the World Cup in Brazil: an early warning model framework driven by real-time seasonal climate forecasts. Lancet Infect Dis. 2014;14:619–26. https://doi.org/10.1016/S1473-3099(14)70781-9
4. Lauer SA, Sakrejda K, Ray EL, Keegan LT, Bi Q, Suangtho P, et al. Prospective forecasts of annual dengue hemorrhagic fever incidence in Thailand, 2010–2014. Proc Natl Acad Sci U S A. 2018;115:E2175–82. https://doi.org/10.1073/pnas.1714457115
5. Johansson MA, Reich NG, Hota A, Brownstein JS, Santillana M. Evaluating the performance of infectious disease forecasts: a comparison of climate-driven and seasonal dengue forecasts for Mexico. Sci Rep. 2016;6:33707. https://doi.org/10.1038/srep33707
6. Reich NG, Lauer SA, Sakrejda K, Iamsirithaworn S, Hinjoy S, Suangtho P, et al. Challenges in real-time prediction of infectious disease: a case study of dengue in Thailand. PLoS Negl Trop Dis. 2016;10:e0004761. https://doi.org/10.1371/journal.pntd.0004761
7. Cambodian Ministry of Health. Standard Operating Procedures of the National Dengue Sentinel Surveillance System, National Dengue Control Program. Phnom Penh (Cambodia): The Ministry; 2010.
8. Stone M. Cross-validatory choice and assessment of statistical predictions. J R Stat Soc B. 1974;36:111–33. https://doi.org/10.1111/j.2517-6161.1974.tb00994.x
9. Allen DM. The relationship between variable selection and data augmentation and a method of prediction. Technometrics. 1974;16:125–7. https://doi.org/10.1080/00401706.1974.10489157
10. Geisser S. The predictive sample reuse method with applications. J Am Stat Assoc. 1975;70:320–8. https://doi.org/10.1080/01621459.1975.10479865
11. Van Panhuis W, Cross A, Burke D, Choisy M. Project Tycho: Philippines (dengue) dataset: 1955–2010: Project Tycho [cited 2019 Sep 13]. https://www.tycho.pitt.edu/dataset/PH.38362002
12. Van Panhuis W, Cross A, Burke D, Choisy M. Project Tycho: Thailand (dengue) dataset: 1958–2010 [cited 2019 Sep 13]. https://www.tycho.pitt.edu/dataset/TH.38362002
13. Van Panhuis W, Cross A, Burke D, Choisy M. Project Tycho: Lao People's Democratic Republic (dengue) dataset 1979–2010: Project Tycho [cited 2019 Sep 13]. https://www.tycho.pitt.edu/dataset/LA.38362002
14. Van Panhuis W, Cross A, Burke D, Choisy M. Project Tycho: Vietnam (dengue) dataset: 1960–2010 [cited 2019 Sep 13]. https://www.tycho.pitt.edu/dataset/VN.38362002

Address for correspondence: Patrice Piola, Institut Pasteur du Cambodge, Epidemiology and Public Health Unit, 5 Blvd Monivong, BP 983, Phnom Penh, Cambodia; email: ppiola@pasteur-kh.org

Cat-to-Human Transmission of *Mycobacterium bovis*, United Kingdom

Catherine M. O'Connor, Muhammad Abid,[1]
Amanda L. Walsh, Behrooz Behbod,[2]
Tony Roberts, Linda V. Booth, H. Lucy Thomas,
Noel H. Smith, Eleftheria Palkopoulou,
James Dale, Javier Nunez-Garcia,[3] Dilys Morgan

Human infection with *Mycobacterium bovis* is reported infrequently in the United Kingdom. Most cases involve previous consumption of unpasteurized milk. We report a rare occurrence of 2 incidents of cat-to-human transmission of *M. bovis* during a cluster of infection in cats.

In the United Kingdom, *Mycobacterium bovis* infection in humans is relatively rare (*1*), and most cases involve previous exposure to well-recognized risk factors, such as unpasteurized milk (*2*). However, with >4,500 new cases reported in cattle herds each year during 2014–2018 (*3*), *M. bovis* remains a major issue for animal health in large parts of England and Wales.

Cats are considered spillover hosts of *M. bovis* in the United Kingdom. During 2002–2010, <30 feline cases of *M. bovis* infection were confirmed by laboratory culture each year by the Animal and Plant Health Agency *M. bovis* Reference Laboratory (*4*). Cases of *M. bovis* infection in cats are generally restricted to areas to which bovine tuberculosis (TB) is endemic (*5*), where infected cattle and wildlife have the potential to introduce *M. bovis* into cat populations. Most reported feline cases of *M. bovis* infection in the United Kingdom are sporadic, and outside the occasional household-linked cases, spatially or temporally linked clusters are unusual.

The potential for cat-to-human transmission of *M. bovis* has always been recognized. Although concurrent infection in cats and humans in the same household has been reported (*6*), and reports of potential transmission exist (*7*), documented transmission events have not been clearly described. We report a rare occurrence of microbiologically and genetically confirmed cat-to-human transmission of *M. bovis*.

The Study

During December 2012–March 2013, a veterinary practice in Berkshire, England, diagnosed 7 confirmed (culture from lesions or wounds) and 2 suspected (clinically compatible) cases of *M. bovis* disease in domestic cats. One additional suspected case was identified after an interview with an affected household. No samples were available from any of the suspected cases for confirmation for this study. The 10 cats belonged to 9 separate households, of which 6 were ≤250 m from each other. All cats had severe systemic infection, including discharging lymph nodes, nonhealing or discharging infected wounds, and radiographic pulmonary signs. Isolates from the culture-confirmed cases were of the same genotype (10:u), were similar by whole-genome sequencing, and separated into 2 clusters by a single informative polymorphism (*8*). Veterinary investigations did not determine the source of infection, but the source was believed to be infected wildlife, most likely rodents or badgers, for at least some of the cats. Further information on the investigation into this cluster of infection in cats has been reported (*8*).

The unusual size and severity of the cluster of feline *M. bovis* cases led to the decision that TB screening (*9*) would be offered to all human household members and others who had close contact with the infected cats. Local Health Protection Teams of Public Health England identified 39 human contacts; 24 accepted TB screening. Three persons (person A, 13 years of age; person B, 18 years of age; and person C, 39 years of age) were positive for latent TB infection (LTBI) by a combination of interferon-γ release assays and Mantoux screening tests; none showed evidence of active disease.

These 3 persons with LTBI reported close contact with 2 cats with culture-confirmed *M. bovis* infection while the

Author affiliations: Public Health England, London, UK (C.M. O'Connor, A.L. Walsh, H.L. Thomas, D. Morgan); Public Health England, Chilton, UK (M. Abid, B. Behbod); Animal and Plant Health Agency, Oxford, UK (T. Roberts); Public Health England, Fareham, UK (L.V. Booth); Animal and Plant Health Agency, Weybridge, UK (N.H. Smith, E. Palkopoulou, J. Dale, J. Nunez-Garcia)

[1]Current affiliation: United Arab Emirates University, Al Ain, United Arab Emirates.

[2]Current affiliations: Communicable Disease Surveillance Centre, Public Health Wales, Cardiff, Wales, UK, and Cardiff University, Cardiff.

[3]Current affiliation: Genomics Medicine Ireland, Dublin, Ireland.

cats had clinical disease (1 had a discharging nonhealing wound and 1 had a discharging lymph node). Apart from contact with the infected cats, no other risk factors for *M. bovis* or *M. tuberculosis* exposure were identified. Because it was not possible to isolate the causative organism from cats or persons with LTBI or identify the likely exposure or source of infection, it was not possible to determine whether transmission of *M. bovis* from these affected cats to their human contacts had occurred. All 3 persons with LTBI were offered chemoprophylaxis, but only 1 (person A) accepted. All 3 persons were advised to go to local health services if any symptoms potentially indicative of active TB developed.

Six months after initial screening, person B was medically assessed because of nonspecific abdominal pain. Chest radiographs showed evidence of pathologic changes potentially indicative of TB. *M. bovis* was isolated from pleural biopsy samples. Shortly after person B had clinical illness, a nonhousehold human contact (person D, 20 years of age) of person B and their cat also had *M. bovis* isolated from pleural biopsy samples after reporting chest pain and fever. Person D had initially declined screening. Persons B and D had close contact with the infected cat while it was systemically ill (including a discharging wound). The cat died before *M. bovis* infection was diagnosed. Both persons completed a 9-month course of rifampin, isoniazid, pyrazinamide, and ethambutol and responded well to treatment (*10*).

Molecular analysis showed that persons B and D, who had active *M. bovis* disease, and the cat all had *M. bovis* isolates of the same genotype. Whole-genome sequencing of samples from one of the humans and the cat showed that their isolates were indistinguishable (Figure). (Sequencing was not possible for the isolate from the second human patient.) This evidence, coupled with the timeline of onset of disease in the cat (March 2013) and its human contacts (October 2013), and the lack of any other risk factors for exposure to *M. bovis*, indicated that the cat was the likely source of infection for these 2 affected persons.

Conclusions

Before this incident, the absence of confirmed reports of human cases of *M. bovis* infection acquired from pet cats led us to believe that the risk for cat-to-human transmission was negligible. Thus, no public health action was warranted. However, with the evidence of transmission from 1 cat to these 2 patients, the risk for spread of *M. bovis* from cats to their human contacts was increased from negligible to low (*11*). Cats with clinical signs compatible with disseminated disease are believed to have the greatest risk to humans, most likely by ingestion from a contaminated environment, following handling of discharges from exudative tuberculous lesions, or
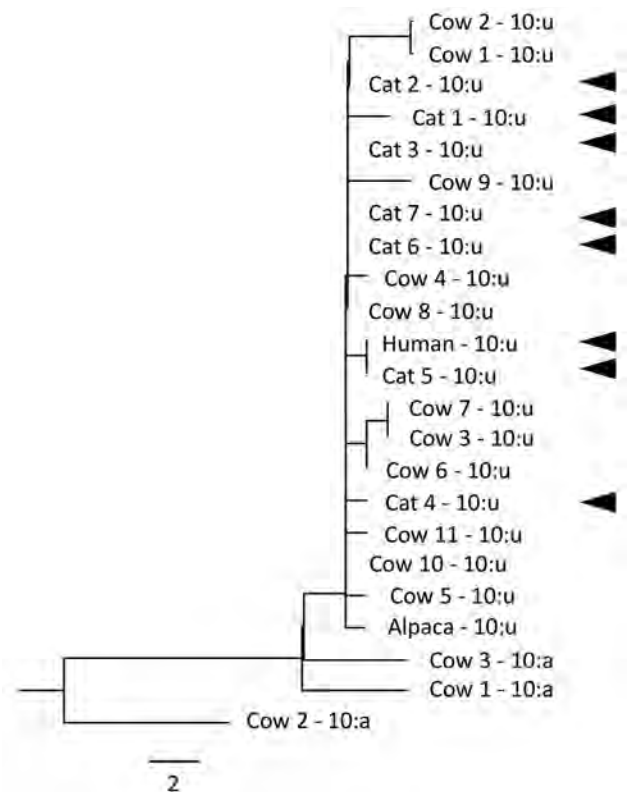
Figure. Whole-genome sequencing phylogenetic relationship of genotype 10:u isolates of *Mycobacterium bovis* from 1 human, 7 cats, 11 cattle, and 1 alpaca, and 10:a isolates from 3 cattle (maximum-likelihood tree of all single-nucleotide polymorphisms [SNPs]). Cat and human isolates are indicated by solid arrowheads. Heat-killed cultures were sequenced by using a MiSeq Sequencer (Illumina, https://www.illumina.com), and reads were mapped by using reference strain AF2122. The average coverage ranged from 23.9-fold to 88.8-fold. The human and their household cat contact (cat 5) isolates were indistinguishable in their genome sequences. Scale bar indicates SNPs.

by aerosols from cats with respiratory signs or aerosol-generating procedures.

Public Health England now advises that all close contacts of household companion animals with confirmed *M. bovis* infections should be assessed by a public health professional and receive guidance on how to best minimize zoonotic transmission (*12,13*). In addition, as part of an enhanced surveillance system in England and Wales, newly diagnosed human case-patients with *M. bovis* infection are now also asked explicitly about contact with pets with suspected or confirmed *M. bovis* disease (*14*).

In summary, *M. bovis* disease in companion animals, particularly cats with severe systemic features including exudative lesions, can no longer be regarded as posing a negligible public health risk. Guidance should be provided to minimize the risk for transmission to human contacts.

About the Author

Ms. O'Connor is an epidemiologist in the National Infection Service at Public Health England, London, UK. Her primary research interests are epidemic intelligence, risk assessment, and emerging zoonotic infections.

References

1. Public Health England. Tuberculosis caused by *Mycobacterium bovis* (*M. bovis*): notification data; 2018 [cited 2018 Nov 13]. https://www.gov.uk/government/publications/mycobacterium-bovis-mbovis-tuberculosis-annual-data
2. Davidson JA, Loutet MG, O'Connor C, Kearns C, Smith RM, Lalor MK, et al. Epidemiology of *Mycobacterium bovis* disease in Humans in England, Wales, and Northern Ireland, 2002–2014. Emerg Infect Dis. 2017;23:377–86. https://doi.org/10.3201/eid2303.161408
3. Department for Environment, Food, and Rural Affairs. Tuberculosis (TB) in cattle in Great Britain (update 17 October 2018); 2018 [cited 2018 Nov 13]. https://www.gov.uk/government/statistical-data-sets/tuberculosis-tb-in-cattle-in-great-britain
4. Department for Environment, Food, and Rural Affairs. Incidents of *M. bovis* infection in non-bovine domestic animals and wild deer in GB confirmed by laboratory culture; 2015 [cited 2018 Dec 3]. www.gov.uk/government/uploads/system/uploads/attachment_data/file/232602/bovinetb-otherspecies-27aug13.xls
5. Gunn-Moore DA, McFarland SE, Brewer JI, Crawshaw TR, Clifton-Hadley RS, Kovalik M, et al. Mycobacterial disease in cats in Great Britain: I. Culture results, geographical distribution and clinical presentation of 339 cases. J Feline Med Surg. 2011;13:934–44. https://doi.org/10.1016/j.jfms.2011.07.012
6. Ramdas KE, Lyashchenko KP, Greenwald R, Robbe-Austerman S, McManis C, Waters WR. *Mycobacterium bovis* infection in humans and cats in same household, Texas, USA, 2012. Emerg Infect Dis. 2015;21:480–3. https://doi.org/10.3201/eid2103.140715
7. Lewis-Jonsson J. Transmission of tuberculosis from cats to human beings. Acta Tuberculosea et Pneumologica Scandinavica. 1946;20:102.
8. Roberts T, O'Connor C, Nuñez-Garcia J, de la Rua-Domenech R, Smith NH. Unusual cluster of *Mycobacterium bovis* infection in cats. Vet Rec. 2014;174:326. https://doi.org/10.1136/vr.102457
9. Public Health England. Tuberculosis screening; 2018 [cited 2019 Jul 30]. https://www.gov.uk/guidance/tuberculosis-screening
10. Talwar A, McGown A, Langham T, Abid M, Pilling J; Department of Respiratory Medicine, Royal Berkshire Hospital. A very strange tail. Thorax. 2014;69:1159–60. https://doi.org/10.1136/thoraxjnl-2014-206033
11. Human Animal Infections and Risk Surveillance group (HAIRS). Qualitative assessment of the risk that cats infected with *Mycobacterium bovis* present to human health; 2014 [cited 2018 Dec 3]. https://www.gov.uk/government/publications/hairs-risk-assessment-mycobacterium-bovis-in-cats
12. Public Health England. Bovine tuberculosis: guidance on management of the public health consequences of tuberculosis in cattle and other animals (England); 2014 [cited 2018 Dec 3]. https://www.gov.uk/government/publications/bovine-tuberculosis-tb-public-health-management
13. UK Government. Bovine tuberculosis in domestic pets; 2014 [cited 2019 Jul 30]. https://assets.publishing.service.gov.uk/government/uploads/system/uploads/attachment_data/file/596240/AG-TBYP-01e.pdf
14. Public Health England. *Mycobacterium bovis* (*M. bovis*): enhanced surveillance questionnaire; 2016 [cited 2018 Dec 3]. https://www.gov.uk/government/publications/mycobacterium-bovis-m-bovis-enhanced-surveillance-questionnaire

Address for correspondence: Catherine M. O'Connor, TARGET, Emerging Infections and Zoonoses Team, National Infection Service, Public Health England, 61 Colindale Ave, London NW9 5EQ, UK; email: catherine.oconnor@phe.gov.uk

Evolution of Highly Pathogenic Avian Influenza A(H5N1) Virus in Poultry, Togo, 2018

Maxime Fusade-Boyer, Pidemnéwé S. Pato,
Mathias Komlan, Koffi Dogno, Trushar Jeevan,
Adam Rubrum, Casimir K. Kouakou,
Emmanuel Couacy-Hymann, Daniel Batawui,
Emilie Go-Maro, Pamela McKenzie,
Richard J. Webby, Mariette F. Ducatez

In 2015, highly pathogenic avian influenza A(H5N1) viruses reemerged in poultry in West Africa. We describe the introduction of a reassortant clade 2.3.2.1c virus into Togo in April 2018. Our findings signal further local spread and evolution of these viruses, which could affect animal and human health.

Relatively little is known about the emergence, prevalence, and circulation of animal influenza viruses in Africa. Highly pathogenic avian influenza (HPAI) H5N1 clade 2.2 viruses emerged in Africa in 2006 (cases were reported from Egypt, Nigeria, Côte d'Ivoire, Benin, Togo, Ghana, Sudan, Djibouti, and Cameroon), although the virus was only maintained long term in Egypt (*1,2*). We conducted surveillance in domestic poultry in Côte d'Ivoire, Benin, and Togo during 2008–2010 but were unable to find virologic or serologic evidence for influenza A virus circulation. Several factors, such as type of hosts, climate, and animal density, might have provided unfavorable conditions for the virus' circulation in the region (*3*).

In early 2015, HPAI H5N1 viruses of clade 2.3.2.1c were reported in Nigeria (*4*), followed closely by detections in Burkina Faso, Côte d'Ivoire, Ghana, Niger, Cameroon, and Togo (*2*). These viruses could be clustered into 2 genetic subgroups (*5*); cluster WA1 viruses were detected in Ghana, Burkina Faso, Côte d'Ivoire, Nigeria, and Niger, and cluster WA2 viruses were detected in Niger, Côte d'Ivoire, and Nigeria (*6,7*). In this study, we aimed to

Author affiliations: Université de Toulouse, Toulouse, France
(M. Fusade-Boyer, M.F. Ducatez); Laboratoire Central Vétérinaire
de Lomé, Lomé, Togo (P.S. Pato, M. Komlan, K. Dogno,
D. Batawui, E. Go-Maro); St. Jude Children's Research Hospital,
Memphis, Tennessee, USA (T. Jeevan, A. Rubrum, P. McKenzie,
R.J. Webby); Central Laboratory for Animal Diseases, Bingerville,
Côte d'Ivoire (C.K. Kouakou, E. Couacy-Hymann)

determine the origin and evolution of HPAI A(H5N1) viruses responsible for poultry outbreaks in Togo in April 2018 in the context of viruses from surrounding countries.

The Study

In April 2018, high mortality rates were reported in chickens (84%) and quails (27%) on a farm with 4,371 domestic birds and 89 swine in Lacs Province in the south of Togo. Necropsies revealed petechiae and hemmorrhages in tracheas, bursa of Fabricius, lungs, and livers. We suspected influenza A virus, which we subsequently confirmed by using the Flu Detect rapid test (Synbiotics Corporation, http://www.synbiotics.com) according to the manufacturer's instructions. We collected 15 samples, including cloacal and tracheal swab specimens and tissues (liver, trachea, lung, and spleen), from euthanized chickens with clinical signs and confirmed the presence of H5 by using reverse transcription PCR. As a precaution, all the animals on the farm (including swine) were slaughtered, even if clinical signs were observed only in birds. Humans in contact with animals on the farm were put under surveillance by public health services (no samples were collected but medical checkup was offered).

To determine the relationship of the viruses from Togo with viruses from neighboring countries, we also analyzed samples collected during April 2015–October 2016 during HPAI A(H5N1) outbreaks in Côte d'Ivoire. We successfully isolated 15 viruses from Togo and 32 viruses from Côte d'Ivoire. We performed hemagglutination inhibition assays, as previously described (*8*); these assays indicated a similar antigenic profile of viruses from the 2 countries. The noticeable exception was that most viruses from Côte d'Ivoire reacted more robustly to antiserum derived from the 2.3.2.1a virus A/duck/Bangladesh/19097/2013 (Appendix Table, https://wwwnc.cdc.gov/EID/article/25/12/19-0054-App1.pdf). We obtained full hemagglutinin (HA) and neuraminidase (NA) gene segment sequences by using Sanger sequencing (GenBank accession nos. MK071279 and MK084618). These sequences clustered with clade 2.3.2.1c HPAI A(H5N1) viruses from western Africa when analyzed using maximum-likelihood phylogenies (Appendix Figures 1, 2).

All the isolates from Togo were closely related to each other, which can be explained by the limited duration

of the outbreak, and clustered with WA2 2.3.2.1c viruses on the basis of their HA sequence but with WA1 2.3.2.1c viruses on the basis of their NA sequence; the highest similarities in both cases were to viruses from Nigeria. Such reassortants have been previously observed in Nigeria and Cameroon (7,9), providing further support for Nigeria (and not Côte d'Ivoire) as a possible source of the Togo virus. Although most similar to sequences from viruses in Nigeria, the sequences from Togo displayed a degree of divergence (1.3% as calculated with the maximum composite distance) from their closest relatives as evidenced by tree topologies (Appendix Figures 1, 2). On the basis of HA sequences, the time to the most recent common ancestor (tMRCA) of the Togo 2018 viruses was estimated as November 2017 (95% highest posterior density [HPD] interval May 2017–April 2018), as determined in a relaxed molecular clock method under the Bayesian Markov chain Monte Carlo framework in BEAST 1.7.1 (10) and implemented on a Galaxy workbench (http://galaxy-workbench.toulouse.inra.fr) with parameters previously described (11). The tMRCA of the viruses from Togo, Nigeria, and Cameroon was estimated as September 2015 (95% HPD interval August–November 2015), suggesting a gap in surveillance and sequence data in the region during 2015–2018 (Appendix Figure 3). Whether outbreaks went unnoticed or unreported in the region or whether specific selection pressures might have existed in Togo still requires further investigation.

We observed higher genetic diversity among the sequences of the 2015–2016 isolates from Côte d'Ivoire than among the isolates from Togo. Most viruses from Côte d'Ivoire that we sequenced in this study belonged to the subcluster WA1 (on the basis of their HA and NA gene segments) and were closely related to viruses from Burkina Faso, Nigeria, and Ghana (closest strain was A/domestic bird/Burkina Faso/15VIR1774-22/2015) (Appendix Figures 1, 2). Two isolates from Côte d'Ivoire clustered with WA2 viruses from the same outbreak from Côte d'Ivoire and viruses from Nigeria in both HA and NA phylogenies (Appendix Figures 1, 2). We also identified WA1 HA and WA2 NA reassortants. Full genome sequencing of these isolates from Togo and Côte d'Ivoire is warranted to allow for a full assessment of recent genetic reassortments in the region.

On the basis of HA sequences, we estimated the tMRCA of the WA2 strains from Côte d'Ivoire (as well as those from the closely related strains previously reported from Nigeria and Côte d'Ivoire) as January 2015 (95% HPD interval July 2014–February 2015), and we estimated the tMRCA of the WA1 strains from Côte d'Ivoire (and their related counterparts from Nigeria and Burkina Faso) as February 2015 (95% HPD interval December 2014–March 2015) (Appendix Figure 3). Both the phylogeny and the molecular clock analyses show multiple introductions of HPAI A(H5N1) clade 2.3.2.1c viruses into Côte d'Ivoire during the 18 months of the outbreaks (April 2015–October 2016). Although we performed limited (and not randomized) sampling, which probably yielded results that are not representative of the complete epidemiologic context, we nevertheless observed substantial virus diversity in the region.

Conclusions

After a period of absence, HPAI clade 2.3.2.1c H5 viruses have spread in sub-Saharan Africa in the past 3 years. A single introduction of virus into the region might have occurred, followed by local spread, leading to genetic and antigenic diversification. The high prevalence of these viruses in countries with large commercial poultry industries, such as Nigeria and Côte d'Ivoire, has resulted in reassortment between local viral lineages. Adding to the complexity, HPAI A(H5N8) viruses from clade 2.3.4.4 have recently been reported in Cameroon and Nigeria (2,12), and low-pathogenicity avian influenza H9N2 viruses have also spread from northern to western Africa in 2017–2018 (with a report from Burkina Faso) (13–15). If these viruses also establish endemicity, the avian influenza situation in western Africa will be in stark contrast to the situation over the past decade or more, when limited virus circulation occurred. The threat to animal and public health should therefore be seriously reconsidered, especially because veterinary services in the region might not operate at the efficiency required to quickly identify and contain outbreaks.

About the Author

Mr. Fusade-Boyer is a PhD student at the UMR Interactions Hôtes Agents Pathogènes in Toulouse, France. His primary research interests include influenza viruses at the animal–human interface.

References

1. World Health Organization. Update on human cases of highly pathogenic avian influenza A (H5N1) infection: 2009. Wkly Epidemiol Rec. 2010;85:49–51.

2. OIE. Animal health in the world—update on avian influenza. 2016 [cited 2019 Oct 11]. http://www.oie.int/animal-health-in-the-world/update-on-avian-influenza

3. Couacy-Hymann E, Kouakou VA, Aplogan GL, Awoume F, Kouakou CK, Kakpo L, et al. Surveillance for influenza viruses in poultry and swine, West Africa, 2006–2008. Emerg Infect Dis. 2012;18:1446–52. https://doi.org/10.3201/eid1809.111296

4. Monne I, Meseko C, Joannis T, Shittu I, Ahmed M, Tassoni L, et al. Highly pathogenic avian influenza A(H5N1) virus in poultry, Nigeria, 2015. Emerg Infect Dis. 2015;21:1275–7. https://doi.org/10.3201/eid2107.150421

5. Tassoni L, Fusaro A, Milani A, Lemey P, Awuni JA, Sedor VB, et al. Genetically different highly pathogenic avian influenza A(H5N1) viruses in West Africa, 2015. Emerg Infect Dis. 2016;22:2132–6. https://doi.org/10.3201/eid2212.160578

6. Shittu I, Meseko CA, Gado DA, Olawuyi AK, Chinyere CN, Anefu E, et al. Highly pathogenic avian influenza (H5N1) in Nigeria in 2015: evidence of widespread circulation of WA2 clade 2.3.2.1c. Arch Virol. 2017;162:841–7. https://doi.org/10.1007/s00705-016-3149-4

7. Laleye A, Joannis T, Shittu I, Meseko C, Zamperin G, Milani A, et al. A two-year monitoring period of the genetic properties of clade 2.3.2.1c H5N1 viruses in Nigeria reveals the emergence and co-circulation of distinct genotypes. Infect Genet Evol. 2018;57:98–105. https://doi.org/10.1016/j.meegid.2017.10.027

8. World Health Organization Global Influenza Surveillance Network. Manual for the laboratory diagnosis and virological surveillance of influenza. 2011 [cited 2019 Oct 11]. http://apps.who.int/iris/bitstream/handle/10665/44518/9789241548090_eng.pdf

9. Wade A, Taïga T, Fouda MA, MaiMoussa A, Jean Marc FK, Njouom R, et al. Highly pathogenic avian influenza A/H5N1 clade 2.3.2.1c virus in poultry in Cameroon, 2016–2017. Avian Pathol. 2018;47:559–75. https://doi.org/10.1080/03079457.2018.1492087

10. Drummond AJ, Rambaut A. BEAST: Bayesian evolutionary analysis by sampling trees. BMC Evol Biol. 2007;7:214. https://doi.org/10.1186/1471-2148-7-214

11. Twabela AT, Tshilenge GM, Sakoda Y, Okamatsu M, Bushu E, Kone P, et al. Highly pathogenic avian influenza A(H5N8) virus, Democratic Republic of the Congo, 2017. Emerg Infect Dis. 2018;24:1371–4. https://doi.org/10.3201/eid2407.172123

12. Wade A, Jumbo SD, Zecchin B, Fusaro A, Taiga T, Bianco A, et al. Highly pathogenic avian influenza A(H5N8) virus, Cameroon, 2017. Emerg Infect Dis. 2018;24:1367–70. https://doi.org/10.3201/eid2407.172120

13. El Houadfi M, Fellahi S, Nassik S, Guérin JL, Ducatez MF. First outbreaks and phylogenetic analyses of avian influenza H9N2 viruses isolated from poultry flocks in Morocco. Virol J. 2016;13:140. https://doi.org/10.1186/s12985-016-0596-1

14. Zecchin B, Minoungou G, Fusaro A, Moctar S, Ouedraogo-Kaboré A, Schivo A, et al. Influenza A(H9N2) virus, Burkina Faso. Emerg Infect Dis. 2017;23:2118–9. https://doi.org/10.3201/eid2312.171294

15. Nagy A, Mettenleiter TC, Abdelwhab EM. A brief summary of the epidemiology and genetic relatedness of avian influenza H9N2 virus in birds and mammals in the Middle East and North Africa. Epidemiol Infect. 2017;145:3320–33. https://doi.org/10.1017/S0950268817002576

Address for correspondence: Mariette F. Ducatez, Institut National de la Recherche Agronomique, Animal Health, 23 Chemin des Capelles, 31300, Toulouse, Occitanie, France; email: m.ducatez@envt.fr
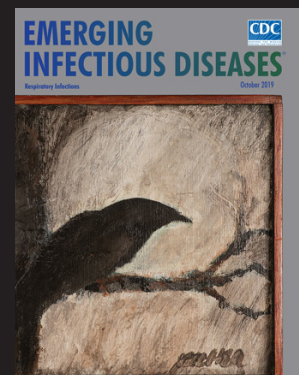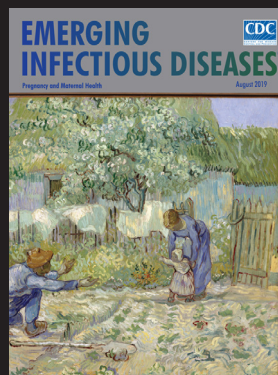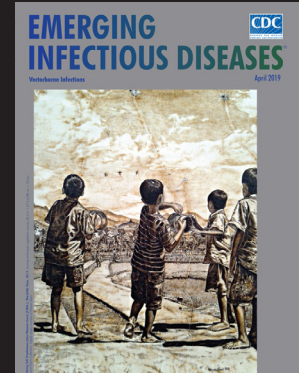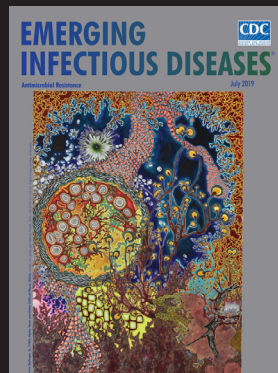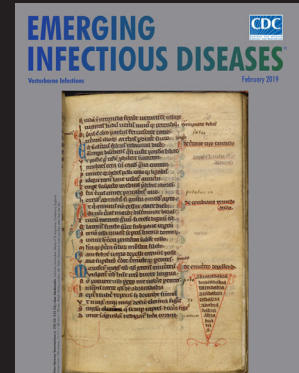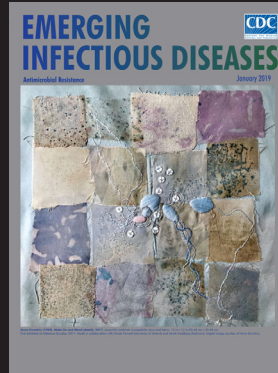
West Nile Virus in Wildlife and Nonequine Domestic Animals, South Africa, 2010–2018

Jumari Steyn, Elizabeth Botha,
Voula I. Stivaktas, Peter Buss,
Brianna R. Beechler, Jan G. Myburgh,
Johan Steyl, June Williams, Marietjie Venter

West Nile virus (WNV) lineage 2 is associated with neurologic disease in horses and humans in South Africa. Surveillance in wildlife and nonequine domestic species during 2010–2018 identified WNV in 11 (1.8%) of 608 animals with severe neurologic and fatal infections, highlighting susceptible hosts and risk for WNV epizootics in Africa.

West Nile virus (WNV) is associated with febrile disease, meningoencephalitis, and death in humans and horses (*1,2*). WNV infections are recognized on most continents but remain underreported in Africa. An 8-year study in horses with fever, neurologic signs, or both in South Africa described WNV lineage 2 as the cause of annual outbreaks; 93.7% of WNV-positive horses displayed neurologic signs, resulting in a 34.2% fatality rate (*3*). In the United States, clinical WNV disease has been reported in several nonequine species: birds, crocodiles, bats, wolves, cats, dogs, cattle, and sheep (*4*). The disease susceptibility of wildlife species in Africa and the role they play in amplifying the virus is unknown. We conducted surveillance for neurologic disease and death in animals other than horses in South Africa during 2010–2018 to determine potential WNV reservoir species, identify susceptible hosts, and highlight potential areas for targeted surveillance.

The Study

A total of 608 specimens comprising central nervous system tissue, visceral organs, and whole blood from wildlife; nonequine domestic animals; and birds with neurologic, febrile, or respiratory signs or sudden unexpected death were submitted to the Centre for Viral Zoonoses, University of Pretoria (Pretoria, South Africa), during February 2010–June 2018. We extracted RNA from the samples using the

Author affiliations: University of Pretoria, Pretoria, South Africa (J. Steyn, E. Botha, V.I. Stivaktas, J.G. Myburgh, J. Steyl, J. Williams, M. Venter); South African National Parks, Kruger National Park, South Africa (P. Buss); Oregon State University, Corvallis, Oregon, USA (B.R. Beechler)

QIAamp viral RNA (QIAGEN, https://www.qiagen.com) (blood) or RNeasy (QIAGEN) (tissue) mini-kits under Biosafety Level 3 conditions. All specimens were subjected to 1-step nested real-time reverse transcription PCR (RT-PCR) targeting WNV (LightCycler FastStart DNA Master HybProbe; Roche Applied Science, https://www.life-science.roche.com) (*5*).

Eleven (1.8% [95% CI 0.8%–2.9%]) of the 608 animals tested positive for WNV. A total of 519 (84.5%) specimens were from animals that died, of which 78 were found dead and classified as sudden unexpected death. WNV was detected in 6 (1.7% [95% CI 0.3%–3.0%]) of 361 wildlife and 5 (1.5% [95% CI 0%–3.3%]) of 196 nonequine domestic animals but in 0 of 51 birds (Table 1). We detected WNV RNA in 2 (2%) of 93 domestic cattle (*Bos taurus*), 1 (2%) of 54 African buffalo (*Syncerus caffer*), 1 (5%) of 22 domestic dogs (*Canis lupus familiaris*), 1 (33%) of 3 exotic fallow deer (*Dama dama*), 1 (9%) of 6 giraffes (*Giraffa camelopardalis*), 1 (9%) of 11 domestic goats (*Capra aegagrus hircus*), 1 (11%) of 9 lions (*Panthera leo*), 1 (2%) of 45 domestic sheep (*Ovis aries*), and 2 (7%) of 28 roan antelope (*Hippotragus equinus*) (Table 1). Only 2 of 11 infected animals survived: 1 domestic bovid and the exotic fallow deer.

Virus isolation identified African horse sickness virus as a co-infection in the WNV-positive dog (ZRU358_17), confirmed by the Equine Research Centre (*6*) (Table 1). WNV neutralizing antibodies have previously been reported among dogs in South Africa, although no active infection has been described (*7*). The domestic bovid (ZRU181_12_1) and buffalo (ZRU161_18) had Middleburg virus co-infections, and the giraffe had Shuni virus co-infection confirmed by differential testing (*8–10*) at the Centre for Viral Zoonoses (Table 1). In these animals, clinical signs and death could not be attributed to any of the detected viruses alone.

Positive WNV infections were detected in the Free State (2/45, 4%), Gauteng (5/192, 3%), North West (1/47, 2%), Limpopo (2/132, 2%), and Mpumalanga provinces (1/82, 1%) (Figure 1). Most positive animals were reported during March–June, corresponding to the arbovirus season in South Africa (Appendix, https://wwwnc.cdc.gov/EID/article/25/12/19-0572-App1.pdf).

We detected WNV in lung (5/11, 45%), brain (4/11, 36%), and spleen (2/11, 18%) tissue and in blood (2/11,

Table 1. West Nile virus detected in specimens from animals with neurologic disease or unexplained death using real-time reverse transcription PCR, South Africa, 2010–2018*

Animal	Identifier	Origin of sample, province	No. positive/animal type (%) [95% CI]	Specimen testing positive	Co-infection (tissue source)
Domestic bovid (*Bos taurus*)	ZRU181/12/1† ZRU176/14/2	Gauteng Free State	2/93 (2.2) [0.0–5.1]	Brain blood	MIDV (spleen)
African buffalo (*Syncerus caffer*)	ZRU161/18†	Limpopo	1/54 (1.9) [0.0–5.5]	Lung	MIDV (lung, blood)
Domestic dog (*Canis lupus familiaris*)	ZRU358/17†	Gauteng	1/22 (4.6) [0.0–13.3]	Brain, lung	AHSV (brain, lung, spleen)
Fallow deer (*Dama dama*)	ZRU174/14	Gauteng	1/3 (33.3) [0.0–86.7]	Blood	
Giraffe (*Giraffa giraffa*)	ZRU87/18†	North West	1/6 (9.1) [0.0–46.5]	Lung	SHUV (blood)
Domestic goat (*Capra aegagrus hircus*)	ZRU192/14	Gauteng	1/11 (9.1) [0.0–26.1]	Brain, spleen	
Lion (*Panthera leo*)	ZRU297/17†	Mpumalanga	1/9 (11.1) [0.0–31.2]	Brain	
Domestic sheep (*Ovis aries*)	ZRU159/18†	Gauteng	1/45 (2.2) [0.0–6.6]	Spleen	
Roan antelope (*Hippotragus equinus*)	ZRU061/16/2† ZRU165/16	Free State Limpopo	2/28 (7.1) [0.0–16.7]	Lung Lung	
Wildlife			6/361 (1.6) [0.3–2.9]		
Domestic animals			5/196 (2.6) [0.3–4.8]		
Birds			0/51		
Total			11/608 (1.8) [0.5–2.9]		

*Identifiers are ZRU laboratory number/year/sample number. AHSV, African horse sickness virus; MIDV, Middleburg virus; SHUV, Shuni virus; ZRU, Zoonosis Research Unit (now CVZ, Centre for Viral Zoonoses).
†Sequence data available.

18%) (Table 1). Clinical signs noted in WNV-positive animals included neurologic (4/8, 50%) and respiratory (3/8, 38%); 2 animals with neurologic signs also had pyrexia (Table 2). The lion (ZRU297_17) and giraffe (ZRU87_18) were found dead (2/11, 18%); thus, no clinical signs were reported. The WNV-positive sheep (ZRU159_18), an indigenous Dorper, was a stillborn fetus with cerebral edema. In sheep, WNV is reported to cause neurologic symptoms (*11*) but has not been associated with stillbirths. The roan antelope (ZRU61_16_2), the domestic bovid (ZRU181_12_1),

and the sheep fetus represented WNV-positive specimens among a cluster of animals with similar signs potentially representing larger outbreaks in these areas. Despite extensive screening for arboviruses, the causative link between the clinical presentation of the various species and the evidence of WNV infection must be regarded with caution because we could not exclude all other possible infectious and noninfectious etiologies.

We subjected positive specimens to Sanger sequencing (Inqaba biotech, https://www.inqababiotec.co.za) and
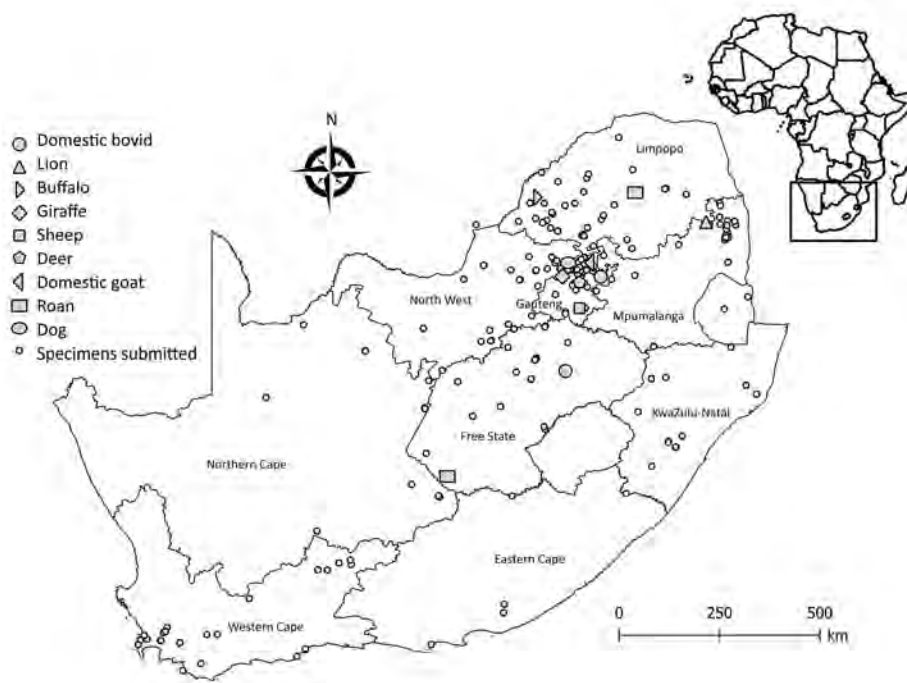
Figure 1. Areas where West Nile virus infections were detected in wildlife and nonequine domestic animals, South Africa, 2010–2018. Insert indicates location of South Africa in Africa.

Table 2. Clinical signs and outcomes in wildlife and nonequine domestic animals tested for WNV upon submission to Centre for Viral Zoonoses, South Africa, 2010–2018*

Variable	No. WNV positive/total no. animals (%)	No. WNV negative/total no. animals (%)	Odds ratio (95% CI)	p value†
Sign				
Fever	2/8 (25.0)	44/496 (8.9)	3.4 (0.7–17.2)	0.2
Neurologic signs	4/8 (50.0)	422/496 (85.1)	0.2 (0.0–0.6)	<0.05
Ataxia	2/8 (25.0)	102/496 (20.6)	1.3 (0.3–6.3)	1.0
Paralysis	1/8 (12.5)	63/496 (12.7)	0.9 (0.1–8.0)	1.0
Hind leg paralysis	1/8 (12.5)	22/496 (4.4)	3.0 (0.4–25.7)	0.3
Paresis	2/8 (25.0)	118/496 (23.8)	1.1 (0.2–5.3)	1.0
Tongue paralysis	0/8	4/496 (0.8)	Undefined	1
Recumbency	2/8 (25.0)	103/496 (20.8)	1.3 (0.3–6.3)	0.7
Dyspnea	3/8 (37.5)	78/496 (15.7)	3.2 (0.7–13.5)	0.1
Hemorrhage	0/8	11/496 (2.2)	Undefined	1
Blindness	0/8	11/496 (2.2)	Undefined	1
Icterus	0/8	2/496 (0.4)	Undefined	1
Seizure	0/8	30/496 (6.0)	Undefined	1
Outcome‡				
Sudden unexpected death	2/11 (18.2)	76/608 (12.5)	1.5 (0.3–7.2)	0.4
Stillborn	1/11 (9.1)	15/608 (2.5)	3.9 (0.5–32.3)	0.3
Abortion	0/11	24/608 (4.0)	Undefined	1
Congenital deformities	0/11	11/608 (1.8)	Undefined	1
Death	9/11 (81.8)	510/608 (84.4)	0.8 (0.2–3.6)	0.4

*WNV, West Nile virus.
†p values <0.05 are significant.
‡Sudden unexplained death indicates animals found dead without an obvious reason; stillborn, abortion, and congenital deformities are related to potential cross-placental transmission; death refers to sick animals that subsequently died.

conducted sequence analysis with CLC-genomic workbench (https://www.qiagenbioinformatics.com), MAFFT (Multiple Alignment using Fast Fourier Transform) version 7 (http://mafft.cbrc.jp/alignment/server), and MEGA6.06 (https://www.megasoftware.net). We used RAxML (https://cme.h-its.org/exelixis/web/software/raxml) for maximum-likelihood phylogenetic analysis of the partial nonstructural protein 5 gene region (215 nt) and confirmed the RT-PCR results and WNV lineages (Figure 2). The lion from Kruger National Park (KNP) clustered with lineage 1 (bootstrap = 70), and all other animals clustered with lineage 2 strains from South Africa (bootstrap = 67) (Figure 2). One previous report found a lineage 1 strain that clustered with lineage 1 strains previously identified in South Africa (*12*).

We used an epitope-blocking ELISA (*13*) to screen serum for WNV antibodies in 50 white rhinoceros (*Ceratotherium simum*) collected by the South African National Parks in March 2014 and 45 African buffalo in June 2016, all from KNP, and from 34 Nile crocodiles (*Crocodylus niloticus*) collected from northern KwaZulu-Natal during 2009–2012. We coated flat-bottom 96-well microtiter plates (CELLSTAR, Sigma Aldricht, https://www.sigmaaldrich.com) with 1:800 dilution of WNV cell lysate antigen, prepared according to (*14*) using strain HS101/08, passage 6, South Africa and WNV hyperimmune mouse ascites fluid polyclonal antibody (FC-M30200-06-1, Centers for Disease Control and Prevention, https://www.cdc.gov/ncezid/dvbd/specimensub/arc) diluted 1:400 and horseradish peroxidase–conjugated rabbit antimouse IgG (BioRad Laboratories, https://www.bio-rad.com) (1:2000 dilution). We calculated the percentage inhibition of

antibody binding with a cutoff value of 40% and confirmed positive reactions by microtiter virus neutralization test using a 10^3 50% tissue culture infectious dose stock culture (MRM61C, passage 6) (*15*). We detected WNV-specific antibodies in serum of 25 (50%) of white rhinoceros, of which 20 (80%) demonstrated neutralization at all 3 dilutions (1:8, 1:16, and 1:32) and 5 showed no neutralization, suggesting high-level WNV exposure. This finding highlights the prevalence of WNV in KNP despite a low number of reported clinical infections. No buffaloes or crocodiles were seropositive.

Conclusions

We recorded WNV (lineages 1 and 2) in wildlife and nonequine domestic animals in South Africa. Seroconversion to WNV was demonstrated in asymptomatic white rhinoceros from KNP. The data suggest severe disease and neurologic signs occur in species other than horses; these signs may be used for surveillance in areas of Africa where horses are less common to predict WNV outbreaks and predict spillover events into the human population. Wildlife and nonequine domestic animals are not as closely monitored for WNV as horses, and early detection is less likely. The short viremia associated with WNV infection may result in underreporting of positive animals if only RT-PCR is used for diagnosis, but a lack of conjugates for wildlife species complicates development of IgM ELISA. The epitope-blocking ELISA and microtiter virus neutralization test can be used for seroprevalence studies in animals other than horses because they are species-independent but do not differentiate between IgM and IgG and are not quantitative.
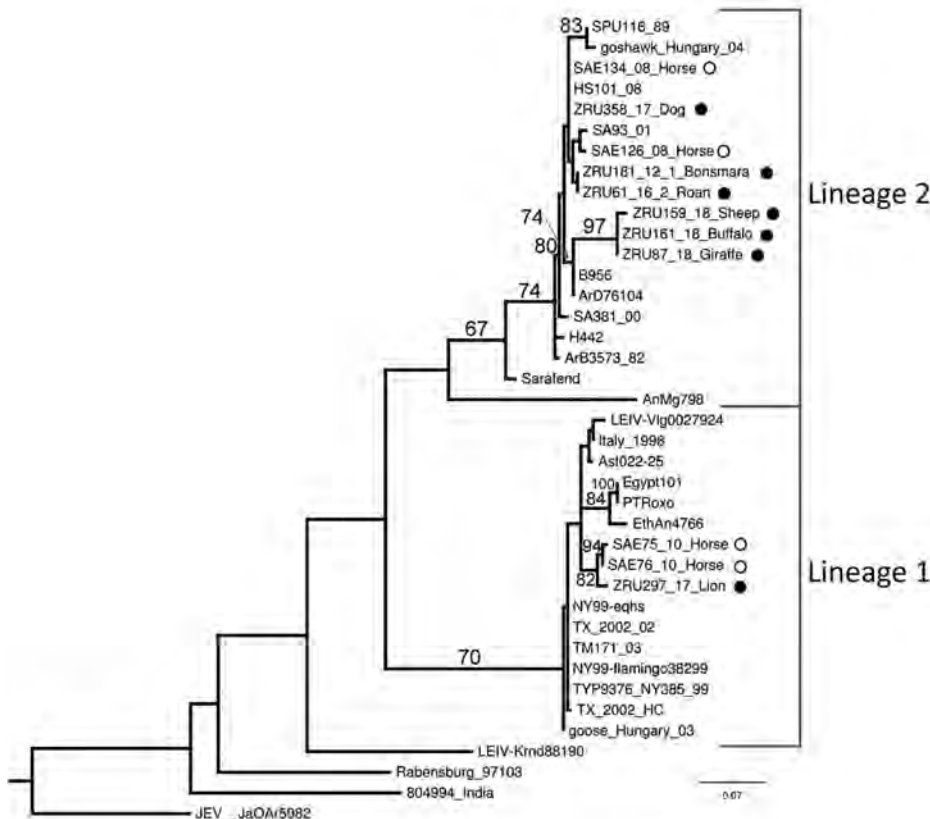
Figure 2. Maximum-likelihood phylogram of the partial (215-nt) nonstructural protein gene used for identification of West Nile virus infection in wildlife and nonequine domestic animals, South Africa, 2010–2018. Tree was generated with RAXML (https://cme.h-its.org/exelixis/web/software/raxml) using the general time-reversible plus gamma model with 39 taxa and the AutoMRE bootstopping function invoked (bootstraps >65 as branch support). Black circles indicate wildlife and nonequine domestic animal sequences from this study; open circles indicate horse sequences (*3,12*). Reference strains, GenBank accession numbers, and origins are as indicated in (*4*). GenBank accession numbers for the newly sequenced strains are ZRU87_18, MN270988; ZRU159_18_SA, MN270989; ZRU161_18_SA, MN27099; and ZRU181_12_1, KY176733. The sequences for strains ZRU358/17, ZRU061/16/2, and ZRU297/17 were <200 bp long and therefore could not be submitted to GenBank; the sequence data are available from the authors. Scale bar indicates nucleotide substitutions per site.

Future work should focus on assay development for species other than horses.

Acknowledgments

About the Author

Dr. Steyn is a virologist and PhD candidate at the Centre for Viral Zoonoses at the University of Pretoria. Her primary research focuses on investigating arboviruses with zoonotic potential at human–animal interface areas.

References

1. Murray KO, Walker C, Gould E. The virology, epidemiology, and clinical impact of West Nile virus: a decade of advancements in research since its introduction into the Western Hemisphere. Epidemiol Infect. 2011;139:807–17. https://doi.org/10.1017/S0950268811000185
2. Pauli G, Bauerfeind U, Blümel J, Burger R, Drosten C, Gröner A, et al. West Nile virus. Transfus Med Hemother. 2013;40:265–84.
3. Venter M, Pretorius M, Fuller JA, Botha E, Rakgotho M, Stivaktas V, et al. West Nile virus lineage 2 in horses and other animals with neurologic disease, South Africa, 2008–2015. Emerg Infect Dis. 2017;23:2060–4. https://doi.org/10.3201/eid2312.162078
4. Gould LH, Fikrig E. West Nile virus: a growing concern? J Clin Invest. 2004;113:1102–7. https://doi.org/10.1172/JCI21623
5. Zaayman D, Human S, Venter M. A highly sensitive method for the detection and genotyping of West Nile virus by real-time PCR.

J Virol Methods. 2009;157:155–60. https://doi.org/10.1016/j.jviromet.2008.12.014

6. O'Dell N, Arnot L, Janisch CE, Steyl JC. Clinical presentation and pathology of suspected vector transmitted African horse sickness in South African domestic dogs from 2006 to 2017. Vet Rec. 2018;182:715. https://doi.org/10.1136/vr.104611

7. Blackburn NK, Reyers F, Berry WL, Shepherd AJ. Susceptibility of dogs to West Nile virus: a survey and pathogenicity trial. J Comp Pathol. 1989;100:59–66. https://doi.org/10.1016/0021-9975(89)90090-X

8. van Niekerk S, Human S, Williams J, van Wilpe E, Pretorius M, Swanepoel R, et al. Sindbis and Middelburg Old World alphaviruses associated with neurologic disease in horses, South Africa. Emerg Infect Dis. 2015;21:2225–9. https://doi.org/10.3201/eid2112.150132

9. Van Eeden C, Zaayman D, Venter M. A sensitive nested real-time RT-PCR for the detection of Shuni virus. J Virol Methods. 2014;195:100–5. https://doi.org/10.1016/j.jviromet.2013.10.008

10. van Niekerk M, Freeman M, Paweska JT, Howell PG, Guthrie AJ, Potgieter AC, et al. Variation in the NS3 gene and protein in South African isolates of bluetongue and equine encephalosis viruses. J Gen Virol. 2003;84:581–90. https://doi.org/10.1099/vir.0.18749-0

11. Yaeger M, Yoon K-J, Schwartz K, Berkland L. West Nile virus meningoencephalitis in a Suri alpaca and Suffolk ewe. J Vet Diagn Invest. 2004;16:64–6. https://doi.org/10.1177/104063870401600111

12. Venter M, Human S, van Niekerk S, Williams J, van Eeden C, Freeman F. Fatal neurologic disease and abortion in mare infected with lineage 1 West Nile virus, South Africa. Emerg Infect Dis. 2011;17:1534–6. https://doi.org/10.3201/eid1708.101794

13. Blitvich BJ, Marlenee NL, Hall RA, Calisher CH, Bowen RA, Roehrig JT, et al. Epitope-blocking enzyme-linked immunosorbent assays for the detection of serum antibodies to West Nile virus in multiple avian species. J Clin Microbiol. 2003;41:1041–7. https://doi.org/10.1128/JCM.41.3.1041-1047.2003

14. Ksiazek TG, West CP, Rollin PE, Jahrling PB, Peters CJ. ELISA for the detection of antibodies to Ebola viruses. J Infect Dis. 1999;179(Suppl 1):S192–8. https://doi.org/10.1086/514313

15. Zaayman D, Venter M. West Nile virus neurologic disease in humans, South Africa, September 2008–May 2009. Emerg Infect Dis. 2012;18:2051–4. https://doi.org/10.3201/eid1812.111208

Address for correspondence: Marietjie Venter, Centre for Viral Zonooses, Department Medical Virology, Faculty of Health Science, University of Pretoria, Rm 2-67, Pathology Bldg, Prinshof Campus, University of Pretoria, PO Box 323, Arcadia, 0007, South Africa; email: marietjie.venter@up.ac.za

Highly Pathogenic Avian Influenza A(H5N8) Virus in Gray Seals, Baltic Sea

Dai-Lun Shin, Ursula Siebert,
Jan Lakemeyer, Miguel Grilo, Iwona Pawliczka,
Nai-Huei Wu, Peter Valentin-Weigand,
Ludwig Haas,[1] Georg Herrler

We detected a highly pathogenic avian influenza A(H5N8) virus in lung samples of 2 gray seals (*Halichoerus grypus*) stranded on the Baltic coast of Poland in 2016 and 2017. This virus, clade 2.3.4.4 B, was closely related to avian H5N8 viruses circulating in Europe at the time.

In 1996, emerging highly pathogenic avian influenza (HPAI) viruses caused outbreaks in domestic poultry in China. The ancestral virus (A/goose/Guangdong/1/1996(H5N1); gs/Gd) and the related reassortant viruses have continued to cause outbreaks in birds and have been associated with human infections. Multiple genetic linages of the hemagglutinin (HA) gene are clustered into 10 clades (*1*). In 2014, gs/Gd-lineage H5Nx HPAI viruses belonging to clade 2.3.4.4 were detected in Eurasia, followed by a novel lineage 2.3.4.4 B of H5N8 viruses detected in wild birds in 2016. This reassortant H5N8 virus is widespread among wild birds worldwide, causing mass deaths in waterfowl, its natural reservoir (*2*). No natural transmission of this virus from birds to marine mammals has been reported.

In 2014, an epizootic among harbor seals infected with avian influenza viruses (AIV) of subtype H10N7 was reported at the coast of northern Europe. Infected seals displayed multifocal pyogranulomatous to necrotizing pneumonia, which led to death (*3–5*). Various outbreaks of H3N8, H7N7, and H4N6 low pathogenicity avian influenza (LPAI) viruses have occurred in harbor seals along the New England coast of the United States (*6*). Yet, the exact route of viral transmission from bird to seal remains unclear. Avian, but not human, influenza viruses have been reported to attach to cells of the respiratory tract of seals (*7*). The limited studies do not provide a comprehensive picture about the abundance of avian-type α2,3-linked sialic acid receptor molecules on the airway epithelium of seals (*8*).

Author affiliations: University of Veterinary Medicine Hannover, Hannover, Germany (D.-L. Shin, U. Siebert, J. Lakemeyer, M. Grilo, N.-H. Wu, P. Valentin-Weigand, L. Haas, G. Herrler); University of Gdańsk, Gdańsk, Poland (I. Pawliczka)

The Study

On November 27, 2016, an immature male gray seal estimated to be 20 months old was found dead on the Baltic coast of Poland; it was in a state of initial decomposition and displayed poor nutritional status. Pathologic findings included a parasitic infestation (*Halarachne halichoeri*) in the nasal cavity, lung, and gastrointestinal tract; agonal changes, including pulmonary edema and emphysema, were observed. A second male seal with estimated age of 2 months was found on April 21, 2017; it was emaciated and showed several signs of trauma. It had mild to severe parasitic infestation in the digestive tract. Bacteriologic investigation provided evidence for the presence of several different bacteria.

We obtained a lung sample from each animal for virologic analysis. PCR results were negative for phocine distemper virus and phocine herpesvirus 1 in the lung tissues of both animals. However, we detected influenza A virus RNA using a real-time reverse transcription PCR targeting the NP gene (provided by Timm Harder, Friedrich-Loeffler-Institut, Greifswald-Riems, Germany). We isolated and propagated the virus from the lung of the older seal by using MDCK cells and designated the isolate as A/gray seal/BalticPL/361-10/2016 (GISAID [https://www.gisaid.org] accession no. EPI_ISL_322984). We sequenced HA, NA, and internal segments using Sanger sequencing. The isolation of the virus from the other animal failed; however, we were able to perform direct sequencing of the HA and NA genes (A/gray seal/BalticPL/361-13/2017; GISAID accession no. EPI_ISL_362127). The results confirmed that both animals were infected by the same H5N8 virus (H5N8/seal) with a multibasic cleavage site of PLREKRRKR/GLF in its HA protein, which fits the consensus sequence of a clade 2.3.4. HPAI virus (*1*). Phylogenetic analysis of the HA and NA segments using the GISAID EpiFLU database further revealed that the isolate belonged to the clade 2.3.4.4 B group of H5 HPAI viruses (Figure). Results of a homology BLAST search (https://blast.ncbi.nlm.nih.gov/Blast.cgi) showed that this H5N8/seal virus had a nucleotide homology of 99.7%–100% to viruses that were circulating in aquatic wild bird species during the avian influenza outbreaks in 2016 and 2017. Alignment of viral RNA using ClustalW (http://www.clustal.org) showed that no coding mutation was found

---

[1]Deceased.
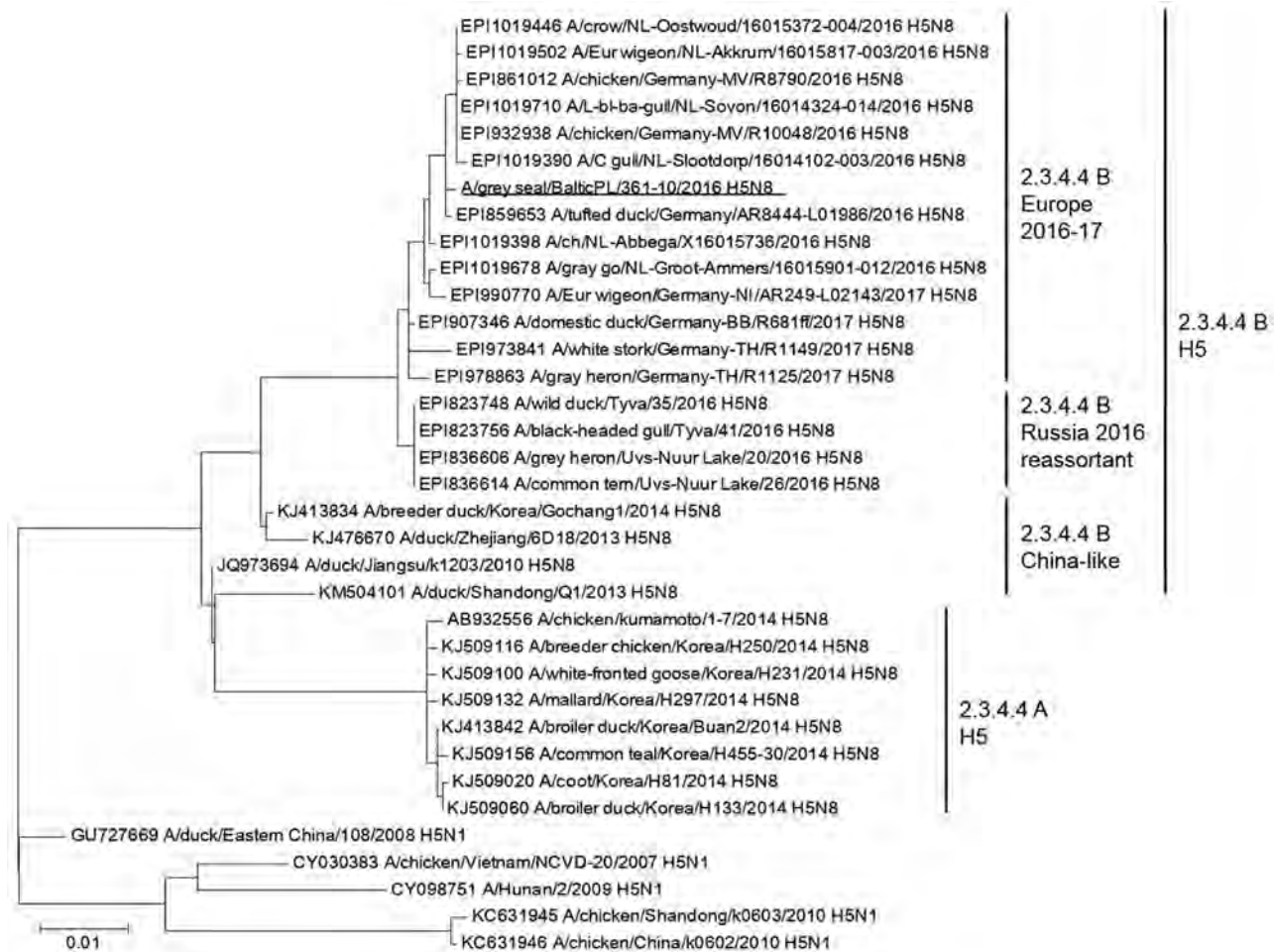
Figure. Maximum-likelihood phylogenetic tree for the hemagglutinin genes of a highly pathogenic avian influenza A(H5N8) virus isolated from a seal in the Baltic Sea region of Poland (underlined) and reference sequences. Different clades and the subclades of 2.3.4.4 are marked. Accession numbers for reference sequences are provided; numbers beginning with EPI are from the GISAID EpiFLU database (https://www.gisaid.org), others from GenBank. Scale bar indicates nucleotide substitutions per site.

in the H5N8/seal virus compared with A/tufted duck/ Germany/AR8444/2016 (H5N8).

Conclusions

We report the case of a clade 2.3.4.4 B group HPAI H5N8 virus able to infect marine mammals. The isolated H5N8/ seal virus showed 99%–100% identity to the avian strains that were circulating in Europe during 2016–2017. HPAI H5N8 2.3.4.4 B virus infections are associated with severe symptoms in infected waterfowl or wild birds. The AIV AR8444 strain in the EpiFLU database with the highest homology to H5N8/seal was isolated from a dead tufted duck found in Lake Plön, Schleswig-Holstein, in northern Germany. Experimental infection of ducks with the AR8444 strain resulted in a mortality rate of 33% 4–8 days postinfection (9).

Pinnipeds, including seals, are susceptible to various viral pathogens, such as influenza A and B viruses,

morbillivirus, and herpesvirus. Most of the influenza viruses isolated from harbor seals were closely related to avian influenza viruses, such as H7N7 (10), H3N8 (8), and H10N7, of which there was an outbreak in 2014 (5). However, the exact transmission pathway of AIV from birds to seals is still unknown, and to our knowledge, HPAI viruses have not been isolated from seals.

We describe findings from 2 dead seals collected during the avian influenza outbreaks of 2016 and 2017 by the Prof. Krzysztof Skóra Hel Marine Station; these 2 were positive for AIV by real-time reverse transcription PCR. Examination of the lungs by gross pathology and histopathology did not reveal any suspicious lesions that indicated an influenza virus infection. No evidence of a related outbreak or mass deaths has been observed in the Baltic seal population. The positive samples appear to be the result of HPAI spillovers from birds to the gray seals. The finding of 2 seals infected 5 months apart suggests that such cross-species transmissions

Table. Molecular markers for enhancing interspecies transmission ability of highly pathogenic avian influenza A(H5N8) virus to seals, Poland*

| Subtype | Location | Year isolated | PB2 | | | PB1 | PA | HA† | |
			17C	E627K	D701N	453S	192H	226L	228S
H5N8‡	Baltic Sea	2016	R	E	D	A	R	Q	G
H10N7§	North Sea	2015	C	E	D	S	H	L	G
H3N8¶	North Atlantic Ocean	2011	R	E	N	A	R	Q	G
H4N5#	North Atlantic Ocean	1982	R	E	D	A	R	Q	G
H7N7**	North Atlantic Ocean	1980	R	E	D	A	R	Q	G

*HA, hemagglutinin; PB1, polymerase basic 1; PB2, polymerase basic 2; PA, polymerase.
†All HA genes are in H3 numbering.
‡Strain destination: A/gray seal/BalticPL/361–10/2016 (this study).
§Strain destination: A/harbor seal/Netherlands/PV14–221_ThS/2015.
¶Strain destination: A/harbor seal/New Hampshire/179629/2011.
#Strain destination: A/harbor seal/Massachusetts/133/1982.
**Strain destination: A/harbor seal/Massachusetts/1/1980.

can occur sporadically, but we cannot exclude the possibility of seal-to-seal transmission. There is no evidence that this virus is highly pathogenic for seals.

Studies have shown that some mutations known to enhance the transmissibility of H5N1 HPAI viruses may increase the ability of LPAI viruses to be transmitted from bird to marine mammal (*11–13*). These factors include the change of sialic acid receptor binding affinity (*11*) and adaptive mutations in the vRNP complex for replication and virus spread in the seal population (*12*). In the H5N8/seal isolate, we detected no molecular markers previously associated with the transmission of avian-derived influenza viruses to marine mammals (*13*) in the viral PB2, PB1, PA, or HA segments (Table). Thus, it appears that no adaptive mutations have occurred in the gray seal analyzed in this study.

Most reports on influenza viruses in seals are related to outbreaks in harbor seals and not gray seals. However, seroprevalences against H10N7 influenza A virus were described in gray seals in the Netherlands (*14*). In addition, influenza A virus matrix RNA (without further characterization) was detected in swab samples of 9.0% of apparently healthy weaned gray seal pups live-captured in the North Atlantic (*15*). In adult seals, seroprevalence was 50%; the authors suggest a possible role of gray seals as a wild reservoir of influenza A virus. These reports indicate that the gray seal can be infected by influenza viruses. Because we describe a naturally occurring spillover of HPAI virus to a marine mammal, future surveillance programs should continue to monitor gray seals and harbor seals as possible reservoirs of AIV.

About the Author

Dr. Shin is a veterinarian at the University of Veterinary Medicine, Hannover, Germany. His primary research interest is the pathogenesis of influenza virus infection in different animal species.

References

1. World Organisation for Animal Health. Manual of diagnostic tests and vaccines for terrestrial animals: OIE terrestrial manual. 2018 [cited 2019 Sep 16]. https://www.oie.int/en/standard-setting/terrestrial-manual/access-online
2. Lee DH, Bertran K, Kwon JH, Swayne DE. Evolution, global spread, and pathogenicity of highly pathogenic avian influenza H5Nx clade 2.3.4.4. J Vet Sci. 2017;18(S1):269–80. https://doi.org/10.4142/jvs.2017.18.S1.269
3. Bodewes R, Bestebroer TM, van der Vries E, Verhagen JH, Herfst S, Koopmans MP, et al. Avian Influenza A(H10N7) virus–associated mass deaths among harbor seals. Emerg Infect Dis. 2015;21:720–2. https://doi.org/10.3201/eid2104.141675
4. Krog JS, Hansen MS, Holm E, Hjulsager CK, Chriél M, Pedersen K, et al. Influenza A(H10N7) virus in dead harbor seals, Denmark. Emerg Infect Dis. 2015;21:684–7. https://doi.org/10.3201/eid2104.141484
5. Zohari S, Neimanis A, Härkönen T, Moraeus C, Valarcher JF. Avian influenza A(H10N7) virus involvement in mass mortality of harbor seals (*Phoca vitulina*) in Sweden, March through October 2014. Euro Surveill. 2014;19:pii=20967. https://doi.org/10.2807/1560-7917.ES2014.19.46.20967
6. Short KR, Richard M, Verhagen JH, van Riel D, Schrauwen EJ, van den Brand JM, et al. One health, multiple challenges: the inter-species transmission of influenza A virus. One Health. 2015;1:1–13. https://doi.org/10.1016/j.onehlt.2015.03.001
7. Ramis AJ, van Riel D, van de Bildt MW, Osterhaus A, Kuiken T. Influenza A and B virus attachment to respiratory tract in marine mammals. Emerg Infect Dis. 2012;18:817–20. https://doi.org/10.3201/eid1805.111828
8. Anthony SJ, St. Leger JA, Pugliares K, Ip HS, Chan JM, Carpenter ZW, et al. Emergence of fatal avian influenza in New

England harbor seals. MBio. 2012;3:e00166–12. https://doi.org/10.1128/mBio.00166-12

9. Grund C, Hoffmann D, Ulrich R, Naguib M, Schinköthe J, Hoffmann B, et al. A novel European H5N8 influenza A virus has increased virulence in ducks but low zoonotic potential. Emerg Microbes Infect. 2018;7:1–14. https://doi.org/10.1038/s41426-018-0130-1

10. Webster RG, Hinshaw VS, Bean WJ, Van Wyke KL, Geraci JR, St. Aubin DJ, et al. Characterization of an influenza A virus from seals. Virology. 1981;113:712–24. https://doi.org/10.1016/0042-6822(81)90200-2

11. Karlsson EA, Ip HS, Hall JS, Yoon SW, Johnson J, Beck MA, et al. Respiratory transmission of an avian H3N8 influenza virus isolated from a harbour seal. Nat Commun. 2014;5:4791. https://doi.org/10.1038/ncomms5791

12. Bodewes R, Zohari S, Krog JS, Hall MD, Harder TC, Bestebroer TM, et al. Spatiotemporal analysis of the genetic diversity of seal influenza A(H10N7) virus, northwestern Europe. J Virol. 2016;90:4269–77. https://doi.org/10.1128/JVI.03046-15

13. Lloren KKS, Lee T, Kwon JJ, Song MS. Molecular markers for interspecies transmission of avian influenza viruses in mammalian hosts. Int J Mol Sci. 2017;18:2706. https://doi.org/10.3390/ijms18122706

14. Bodewes R, Rubio García A, Brasseur SM, Sanchez Conteras GJ, van de Bildt MW, Koopmans MP, et al. Seroprevalence of antibodies against seal influenza A(H10N7) virus in harbor seals and gray seals from the Netherlands. PLoS One. 2015;10:e0144899. https://doi.org/10.1371/journal.pone.0144899

15. Puryear WB, Keogh M, Hill N, Moxley J, Josephson E, Davis KR, et al. Prevalence of influenza A virus in live-captured North Atlantic gray seals: a possible wild reservoir. Emerg Microbes Infect. 2016;5:1–9. https://doi.org/10.1038/emi.2016.77

Address for correspondence: Georg Herrler, University of Veterinary Medicine Hannover, Institute of Virology, Buenteweg 17, 30559 Hannover, Germany; email: Georg.Herrler@tiho-hannover.de

etymologia

Markov Chain Monte Carlo

Ronnie Henry

A Markov chain Monte Carlo (MCMC) simulation is a method of estimating an unknown probability distribution for the outcome of a complex process (a posterior distribution). Prior (capturing the concept *prior* to seeing any data) distributions are used to simulate sampling from variables that have known or closely approximated distributions in the complex process. Thus, the prior distributions are known probability distributions that represent uncertainty about a particular attribute of a population prior to data sampling, and the posterior distribution represents estimated uncertainty about a population attribute after data sampling and is conditional on the observed data.

Figure: Andrey Markov (1856–1922), photographer unknown, public domain, https://commons.wikimedia.org/w/index.php?curid=1332494

Monte Carlo (named for the casino in Monaco) methods estimate a distribution by random sampling. Many samples of the prior distributions must be obtained (e.g., many rolls of the dice) to obtain a stable and accurate posterior distribution. The modern version of the Monte Carlo was invented by Stanislaw Ulam and developed early on by John von Neumann and Nicholas Metropolis, the latter of whom suggested the name, as part of follow-on work to the Manhattan Project. Ulam was trying to calculate the probability of laying out a winning game of solitaire from a shuffled deck of 52 cards. Because of the complexity of the calculations, he decided it would be easier to play 100 games of solitaire and count the percentage that won.

In a Markov chain (named for Russian mathematician Andrey Markov), the probability of the next computed estimated outcome depends only on the current estimate and not on prior estimates. For example, if you shuffle a deck of cards 3 times, the outcome of the third shuffle depends only on the state of the cards at the second shuffle, not at the first shuffle. Markov chain Monte Carlo simulations allow researchers to approximate posterior distributions that cannot be directly calculated.

Sources

1. Eckhardt R. Stan Ulam, John von Neumann, and the Monte Carlo method. Los Alamos Science. 1987;15:131–7.
2. Hamra G, MacLehose R, Richardson D. Markov chain Monte Carlo: an introduction for epidemiologists. Int J Epidemiol. 2013;42:627–34. https://doi.org/10.1093/ije/dyt043
3. van Ravenzwaaij D, Cassey P, Brown SD. A simple introduction to Markov chain Monte-Carlo sampling. Psychon Bull Rev. 2018;25:143–54. https://doi.org/10.3758/s13423-016-1015-8

Address for correspondence: Ronnie Henry, Centers for Disease Control and Prevention, 1600 Clifton Rd NE, Mailstop E28, Atlanta, GA 30329-4027, USA; email: boq3@cdc.gov

Bagaza Virus in Himalayan Monal Pheasants, South Africa, 2016–2017

Jumari Steyn,[1] Elizabeth M. Botha,[1]
Carina Lourens, Jacobus A.W. Coetzer,
Marietjie Venter

Bagaza virus (BAGV) has not been reported in birds in South Africa since 1978. We used phylogenetic analysis and electron microscopy to identify BAGV as the likely etiology in neurologic disease and death in Himalayan monal pheasants in Pretoria, South Africa. Our results suggest circulation of BAGV in South Africa.

The flavivirus genus of family *Flaviviridae* consists of 53 virus species, including arboviruses of medical and veterinary relevance, such as West Nile virus and Bagaza virus (BAGV). BAGV was isolated in 1966 from *Culex* mosquitoes in the Bagaza district of Central African Republic (*1*). In 1978, BAGV was isolated from turkeys with clinical signs similar to Israel turkey meningoencephalitis virus (ITV) in South Africa (*2*). BAGV infection causes neurologic disease in avian species, especially turkeys and other members of the *Phasianidae* family; 1 report suggests that BAGV and ITV are the same viral species (*3*).

BAGV also has been detected in various mosquito species in western Africa (*4,5*), India (*6*), and the Arabian Peninsula (*7*) and in wild partridges in Spain (*8*). No evidence of the virus has been reported in other parts of Africa. Zoonotic transmission was reported in India after patients with acute encephalitis demonstrated 15% positivity for BAGV neutralizing antibodies (*6*). We report detection of BAGV in fatalities in Himalayan monal pheasants in South Africa during 2016–2017.

The Study

In April 2016, two Himalayan monal pheasants (*Lophophorus impejanus*) and 1 tragopan pheasant (*Tragopan melanocephalus*) suddenly died on a property northeast of Pretoria, Gauteng Province, South Africa. In June 2017, this property had another 4 monal pheasants that displayed signs of lethargy and ataxia and died within a day. Around the same time, a residence in the northern suburbs of Pretoria had 5 monal and 2 tragopan pheasants that exhibited neurologic signs and died. That residence had another incidence in 2018 when a monal pheasant exhibited neurologic disease. Also in 2018, a monal pheasant was found dead in North West Province, South Africa. The cause of these deaths was unknown. All the birds were adults that were locally bred from parents imported from Belgium >2 years before.

Brain tissue from the 16 birds was sent to the Department of Veterinary Tropical Diseases (DVTD), University of Pretoria, (Pretoria, South Africa), for virus isolation and to the Centre for Viral Zoonoses (CVZ), University of Pretoria for zoonotic arbovirus investigations. At the CVZ, we extracted RNA from the brain tissues by using the RNeasy Mini Kit (QIAGEN, https://www.qiagen.com) according to manufacturer's instructions under Biosafety Level 3 conditions. We used nested real-time reverse transcription Pan-Flavi assay targeting the nonstructural coding gene 5 (NS5) (*9*) to identify the etiologic agent (*10,11*). To obtain a larger NS5 gene segment, we performed additional PCR using SuperScript III/Platinum Taq Mix (Invitrogen, https://www.thermofisher.com) and the MAMD (*9*) and FLAVI-2 (*10*) primers with the following cycling conditions: 50°C for 30 min; 94°C for 15 min; 35 cycles of 94°C for 45 s, 50°C for 45 s, 72°C for 1 min; and 72°C for 10 min. We successfully obtained a larger NS5 gene segment for phylogenetic analyses, but only for 4 positive birds.

We assembled and edited sequence data by using CLC Main WorkBench (https://www.qiagenbioinformatics.com) and performed multiple sequence alignments using the online version of MAFFT (http://mafft.cbrc.jp/alignment/server/index.html) with default parameters. We used MEGA 6.06 (https://www.megasoftware.net) to view, edit, and truncate the datasets. We downloaded reference sequences for the flavivirus genus from GenBank (*12*). We conducted maximum likelihood analysis in RAxML (*13*), invoking the autoMRE bootstopping function applying a general time-reversible plus gamma model with default 4 rate categories on both datasets. We performed an analysis on the longer dataset by using BEAST version 1.8 (http://beast.community) and a relaxed log-normal clock, general time-reversible plus gamma model, and default priors to generate a maximum clade credibility tree (MCC). We ran a Markov chain Monte Carlo analysis for 10^6 generations,

[1]These authors contributed equally to this article.

saving every 1,000th tree. We estimated effective sample size by using Tracer version 1.6 (https://tree.bio.ed.ac.uk/software/tracer) with an effective sample size value >200. We used TreeAnnotator version 1.8 (http://beast.community) to generate the MCC tree and discarded 15% as burn-in. We displayed bootstrap and posterior probabilities on RAxML topology.

We performed virus isolation on all PCR-positive samples. We inoculated brain tissue supernatant onto a confluent monolayer of baby hamster kidney fibroblast cells (BHK-21 line) in 25 cm² tissue culture flasks and incubated at 37°C for 1 h. Then we added Dulbecco's Minimum Essential Medium (ThermoFisher Scientific, https://www.thermofisher.com) containing 2% fetal bovine serum and 0.1 mg/mL gentamycin. We harvested cells and supernatant when 80% of the cell monolayer showed cytopathic effect and sent these to the Electron

Microscopy Unit of the University of Pretoria and to the CVZ for molecular identification.

The Pan-Flavi assay targeting the NS5 gene resulted in amplicons of the expected size in 8/13 (61.5%, 95% CI 35.1%–88.0%) Himalayan monal pheasants but not in the 3 tragopan pheasants tested. Neurologic signs were reported before death in 7/8 (87.5%, 95% CI 0.5%–66.5%) positive birds, but 1/8 (12.5%, 95% CI 0–2.1%) was found dead and its clinical signs are unknown. Inqaba Biotec (https://www.inqababiotec.co.za) performed Sanger sequencing; we confirmed all positive samples as BAGV using phylogenetic analysis of the flavivirus genus NS5 PCR regions at CVZ. Phylogenetic analyses were based on partial nucleotide sequences of NS5 from genomic positions 9091–9280 (166 nt) and 9030–10109 (1,079 nt) and were used to compare the identified strains with other flaviviruses. Analyses confirmed the molecular results from all 8 Himalayan monals as BAGV
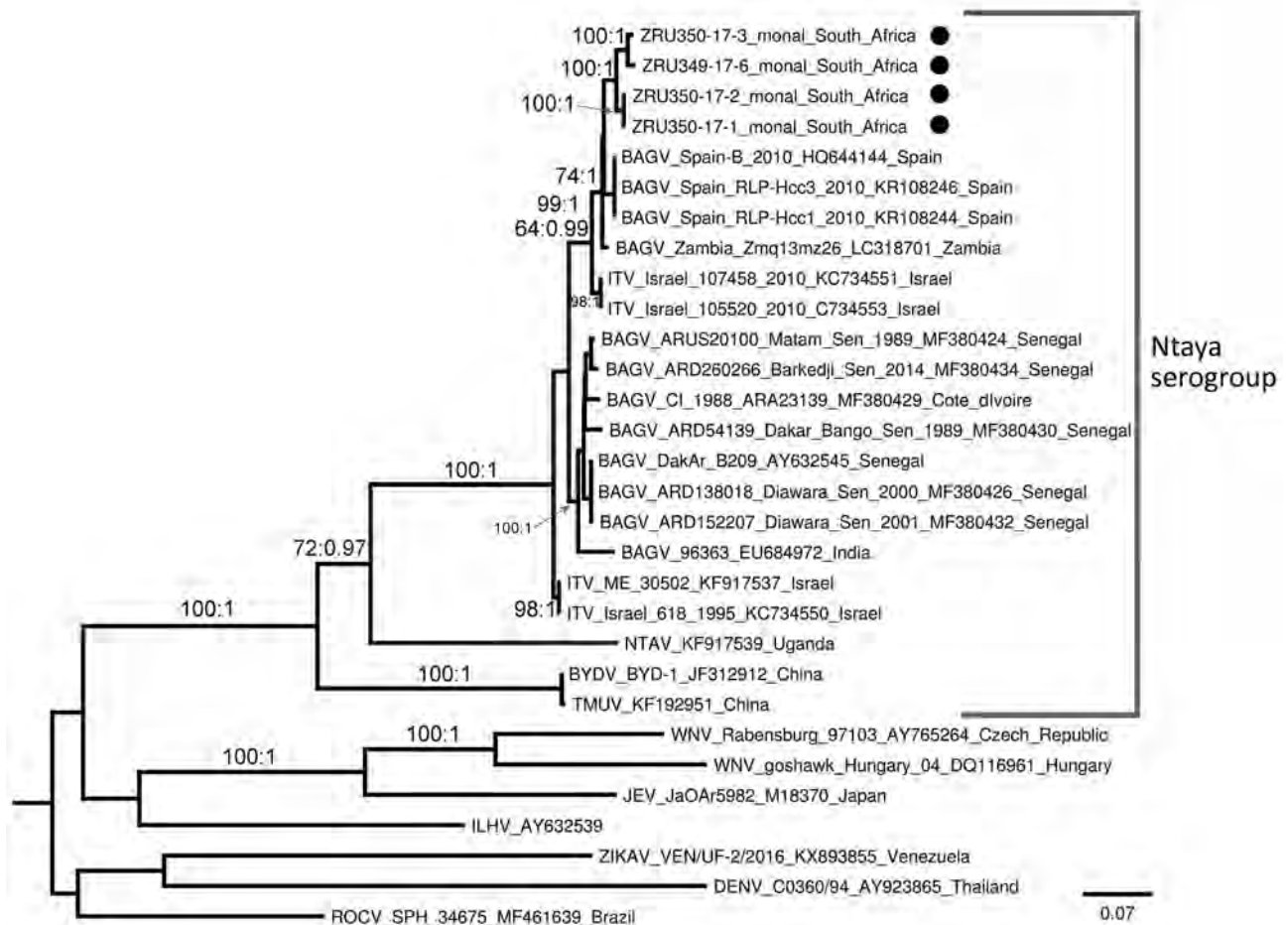
Figure 1. Maximum-likelihood phylogram of BAGV isolated in samples from Himalayan monal pheasants (black dots), South Africa, 2016–2017. Phylogram represents partial (1,079 nt) nonstructural coding gene 5 (NS5; taxa = 30). Bootstrap support with values >60 indicated on branches with posterior probabilities >0.95 from a maximum clade credibility tree. BAGV strains from this study are available in GenBank under the following accession nos.: ZRU349/17/6, no. MN329586; ZRU350/17/1, no. MN329584; ZRU350/17/2, no. MN329585; ZRU350/17/3, no. MN329587. Scale bar indicates nucleotide substitutions per site. BAGV, Bagaza virus; BYDV, Baiyangdian virus; DENV, Dengue virus; ILHV, Ilheus virus; ITV, Israel turkey meningoencephalitis virus; JEV, Japanese encephalitis virus; NTAV, Ntaya virus; ROCV, Rocio virus; TMUV, Tembusu virus; WNV, West Nile virus; ZIKAV, Zika virus.

in the Ntaya virus group with a bootstrap value of 92, sister to BAGV strains from Spain (bootstrap value 68) (Appendix Figure, http://wwwnc.cdc.gov/EID/article/25/12/19-0756-App1.pdf). The 4 strains for which we amplified a larger region (1,079 nt) formed 2 well-supported sister groups, both with a bootstrap value of 100 and phylogenetic probability of 1, with nucleotide similarities of 97.7%–99.7%, and highest nucleotide identity (96.7%–97.7%) to strain Zambia_Zmq13mz26 (GenBank accession no. LC318701.1) isolated from a mosquito (Figure 1).

Electron microscopy on 3 BAGV cultures (sample nos. ZRU350_17_1, ZRU350_17_2, and ZRU349_17_6) (Appendix Table) from 2017 confirmed the presence of *Flaviviridae* particles (Figure 2). We observed fringed isometric and free-lying smooth-surfaced particles typical of *Flaviviridae* (Figure 2, panels B and C).

Conclusions

We detected BAGV in the offspring of monal pheasants imported from Belgium to South Africa. We sequenced BAGV strains and found they monophyletically clustered with strains from Spain rather than strains from West Africa. However, nucleotide similarities in the large gene segment were highest when compared with a strain from Zambia that was isolated from a *Cx. quinquefasciatus* mosquito (GenBank accession no. LC318701.1; *14*), an endemic species in South Africa that could be a BAGV vector. We noted 2 distinct monophyletic clusters of BAGV, a cluster composed of strains from West Africa and older strains and a cluster containing the newly sequenced birds with BAGV from Spain and more recent strains that could indicate several circulating strains or genotypes.
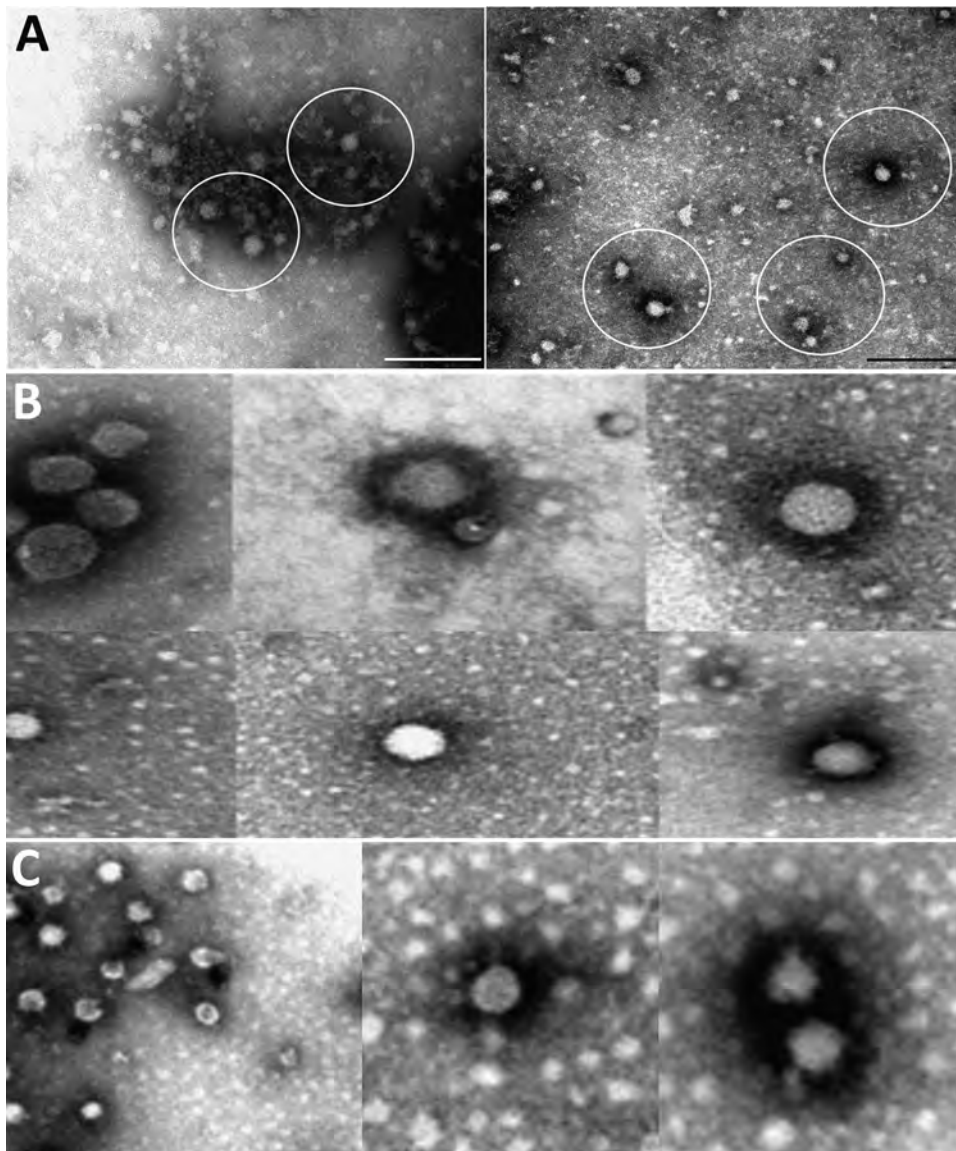
Figure 2. Electron microscopy of Bagaza virus isolated in samples from Himalayan monal pheasants, South Africa, 2016–2017. A) Circles indicate occasional particles with size range and approximate morphology of *Flaviviridae* observed in samples ZRU350_17_1 and ZRU350_17_2. Scale bars indicate 200 nm. B) A few isolated fringed isometric particles of 40–65 nm (top row) and free-lying smooth-surfaced particles of 25–40 nm (bottom row) of suspected *Flaviviridae* observed in sample ZRU349_17_6. C) A few free-lying smooth-surfaced particle cores of 30–40 nm (C1) and a cluster of fringed isometric particles of 40–50 nm (C2–3) of suspected *Flaviviridae* observed in sample ZRU349_17_6.

We used virus isolation and electron microscopy results to confirm the etiology of the agent as a flavivirus. The causative link between the clinical symptoms of the monal pheasants and evidence of BAGV infection should be regarded with caution because we did not exclude other possible infectious and noninfectious etiologies. However, detection of BAGV in the brain suggests crossing of the blood–brain barrier and exclusion of other flaviviruses, arboviruses, and orthobunyaviruses suggests BAGV as a probable cause. Future work will focus on next-generation sequencing to obtain full genomes because initial attempts were unsuccessful. More data are needed to determine the endemicity of BAGV and the reservoir host and vectors of BAGV in South Africa and to define the seroprevalence of these infections in birds and possibly in humans.

About the Authors

Ms. Steyn is a virologist and PhD candidate at the Centre for Viral Zoonoses at the University of Pretoria, Pretoria, South Africa. Her primary research focuses on investigating arboviruses with zoonotic potential at human–animal interface areas. Mrs. Botha was a master's student and research assistant in the Centre for Viral Zoonoses at the University of Pretoria and currently is employed at a private pathology laboratory. Her primary interest is flaviviruses.

References

1. Digoutte JP. Bagaza (BAG) strain: Dak Ar B 209. Am J Trop Med Hyg. 1978;27:376–7. https://doi.org/10.4269/ajtmh.1978.27.376
2. Barnard BJ, Buys SB, Du Preez JH, Greyling SP, Venter HJ. Turkey meningo-encephalitis in South Africa. Onderstepoort J Vet Res. 1980;47:89–94.
3. Fernández-Pinero J, Davidson I, Elizalde M, Perk S, Khinich Y, Jiménez-Clavero MA. Bagaza virus and Israel turkey meningo-encephalomyelitis virus are a single virus species. J Gen Virol. 2014;95:883–7. https://doi.org/10.1099/vir.0.061465-0
4. Diallo M, Nabeth P, Ba K, Sall AA, Ba Y, Mondo M, et al. Mosquito vectors of the 1998–1999 outbreak of Rift Valley Fever and other arboviruses (Bagaza, Sanar, Wesselsbron and West Nile) in Mauritania and Senegal. Med Vet Entomol. 2005;19:119–26. https://doi.org/10.1111/j.0269-283X.2005.00564.x
5. Traore-Lamizana M, Zeller HG, Mondo M, Hervy JP, Adam F, Digoutte JP. Isolations of West Nile and Bagaza viruses from mosquitoes (Diptera: *Culicidae*) in central Senegal (Ferlo). J Med Entomol. 1994;31:934–8. https://doi.org/10.1093/jmedent/31.6.934
6. Bondre VP, Sapkal GN, Yergolkar PN, Fulmali PV, Sankararaman V, Ayachit VM, et al. Genetic characterization of Bagaza virus (BAGV) isolated in India and evidence of anti-BAGV antibodies in sera collected from encephalitis patients. J Gen Virol. 2009;90:2644–9. https://doi.org/10.1099/vir.0.012336-0
7. Camp JV, Karuvantevida N, Chouhna H, Safi E, Shah JN, Nowotny N. Mosquito biodiversity and mosquito-borne viruses in the United Arab Emirates. Parasit Vectors. 2019;12:153. https://doi.org/10.1186/s13071-019-3417-8
8. Agüero M, Fernández-Pinero J, Buitrago D, Sánchez A, Elizalde M, San Miguel E, et al. Bagaza virus in partridges and pheasants, Spain, 2010. Emerg Infect Dis. 2011;17:1498–501. https://doi.org/10.3201/eid1708.110077
9. Zaayman D, Human S, Venter M. A highly sensitive method for the detection and genotyping of West Nile virus by real-time PCR. J Virol Methods. 2009;157:155–60. https://doi.org/10.1016/j.jviromet.2008.12.014
10. Scaramozzino N, Crance JM, Jouan A, DeBriel DA, Stoll F, Garin D. Comparison of flavivirus universal primer pairs and development of a rapid, highly sensitive heminested reverse transcription-PCR assay for detection of flaviviruses targeted to a conserved region of the NS5 gene sequences. J Clin Microbiol. 2001;39:1922–7. https://doi.org/10.1128/JCM.39.5.1922-1927.2001
11. Ayers M, Adachi D, Johnson G, Andonova M, Drebot M, Tellier R. A single tube RT-PCR assay for the detection of mosquito-borne flaviviruses. J Virol Methods. 2006;135:235–9. https://doi.org/10.1016/j.jviromet.2006.03.009
12. Benson DA, Karsch-Mizrachi I, Lipman DJ, Ostell J, Sayers EW. GenBank. Nucleic Acids Res. 2010;38(suppl_1):D46–51. https://doi.org/10.1093/nar/gkp1024
13. Stamatakis A. RAxML version 8: a tool for phylogenetic analysis and post-analysis of large phylogenies. Bioinformatics. 2014;30:1312–3. https://doi.org/10.1093/bioinformatics/btu033
14. Orba Y, Hang'ombe BM, Mweene AS, Sasaki, M, Eshita Y, Sawa H. Bagaza virus genomic RNA, nearly complete genome, strain: Zmq13mz26. GenBank;2017. PubMed

Address for correspondence: Marietjie Venter, University of Pretoria Zoonotic Arbo- and Respiratory Virus Program, Centre for Viral Zoonoses, Rm 2-76.1, Pathology Bldg, 5 Bophelo Rd, Prinshof Campus, Corner of Beatrix and Dr. Savage St, Pretoria 0001, South Africa; email: marietjie.venter@up.ac.za

Influenza A(H1N1)pdm09 Virus Infection in a Captive Giant Panda, Hong Kong

Paolo Martelli,[1] Jade L.L. Teng,[1]
Foo-Khong Lee, Kai-Yan Yeong,
Jordan Y.H. Fong, Suk-Wai Hui,
Kwok-Hung Chan, Susanna K.P. Lau,
Patrick C.Y. Woo

We report influenza A(H1N1)pdm09 virus infection in a captive giant panda in Hong Kong. The viral load peaked on day 1 and became undetectable on day 5, and an antibody response developed. Genome analysis showed 99.3%–99.9% nucleotide identity between the virus and influenza A(H1N1)pdm09 virus circulating in Hong Kong.

Since 2009, influenza A(H1N1)pdm09 virus (pH1N1) has been circulating seasonally worldwide and causing substantial illness, hospitalization, and death in humans every year. The virus has also caused infection in mammals and birds in addition to humans (*1–3*).

The giant panda (*Ailuropoda melanoleuca*) is considered a National Treasure of China with the highest legal protection and dedicated recovery programs. Any emerging infection in giant pandas is of utmost importance because they may not have adequate immunity against the pathogen, implying that such infection may rapidly spread to other giant pandas, leading to large outbreaks and fatalities (*4*). In this article, we describe a case of pH1N1 infection in a captive giant panda in an oceanarium in Hong Kong, China.

The Study

Ocean Park Hong Kong is a financially independent not-for-profit zoological park, oceanarium, and amusement park housing >5,000 marine and terrestrial animals of >500 species. There are 2 buildings for giant pandas in the park; 1 houses a 32-year-old male giant panda and the other a breeding pair.

On November 14, 2018, the 13-year-old male panda of the breeding pair was lethargic and had low appetite. Examination showed yellowish-brown mucoid nasal discharge, tachypnea (respiratory rate >60 breaths/min), and abdominal breathing. On day 2, his condition worsened, and he showed little appetite, persistent nasal discharge, and cough. Attempts at rectal temperature measurement and blood collection were unsuccessful in the first 2 days. We initiated treatment with ciprofloxacin, carprofen, bromhexine, and β-glucan and fogged his living quarters twice daily with F10 antiseptic solution (1:250 dilution) containing benzalkonium chloride and polyhexanide. Clinical surveillance performed on staff members of the park at the time when the giant panda was ill revealed that none of the animal caretakers had influenza-like illness around that time. Additional measures included placing rat traps to test resident rodents for influenza and increased biosecurity to limit contact between the breeding pair and between the staff and giant pandas at both panda facilities.

On day 3, the panda's conditions and appetite improved. Nasal discharge was unchanged, but he only coughed occasionally. Rectal temperature was normal. Blood examination revealed leukocytosis with marked neutrophilia and lymphopenia, hypoferremia, and increased fibrinogen and globulins. He gradually improved in the next 5 days and has remained asymptomatic for 9 months after the onset of illness.

On day 1 of his illness, we collected nasal swab specimens for virologic studies; we collected additional nasal samples on days 2, 3, and 5 for viral load measurement. We took serial serum samples before and after the illness for serologic studies. Veterinary surgeons performed all sample collection.

We performed rapid antigen detection using BinaxNOW Influenza A & B Card (Alere, https://www.alere.com) and determined viral loads by quantitative real-time reverse transcription PCR (RT-PCR) targeting the M gene (*5*). We performed cell culture using MDCK cells inoculated with the first nasal swab sample; we examined it for cytopathic effect at 72 h. We performed serologic analyses using hemagglutination inhibition (HI) and microneutralization (MN) assays (*6,7*). We determined the complete

Author affiliations: Ocean Park Corporation, Hong Kong, China (P. Martelli, F.-K. Lee, S.-W. Hui); The University of Hong Kong, Hong Kong (J.L.L. Teng, K.-Y. Yeong, J.Y.H. Fong, K.-H. Chan, S.K.P. Lau, P.C.Y. Woo); State Key Laboratory of Emerging Infectious Diseases at the University of Hong Kong, Hong Kong (J.L.L. Teng, K.-H. Chan, S.K.P. Lau, P.C.Y. Woo); Collaborative Innovation Center for Diagnosis and Treatment of Infectious Diseases at the University of Hong Kong, Hong Kong (S.K.P. Lau, P.C.Y. Woo)

[1]These authors contributed equally to this article.

Figure 1. Viral load and serologic response to influenza A(H1N1)pdm09 in nasal and serum samples from an infected giant panda in Hong Kong, China. Hemagglutination inhibition (red) and microneutralization (green) antibody titers are shown on a $\log_2$ scale, and viral load (blue) shown as mean viral load ± SD ($\log_{10}$ M gene copies/mL).

genome sequencing of the culture isolate by Illumina HiSeq1500 (https://www.illumina.com) as described previously (*8,9*). We deposited the genome sequence in the GISAID database (http://platform.gisaid.org; accession no. EPI1493152 and nos. EPI1493160–6).

Rapid antigen detection on the nasal swab specimen collected on day 1 was positive for influenza A virus. The viral load (± SD) in the nasal swabs on day 1 of the illness was $5.84 \pm 0.07 \log_{10}$ copies/mL; on day 2, $5.81 \pm 0.05 \log_{10}$ copies/mL; and on day 3, $2.83 \pm 0.16 \log_{10}$ copies/mL. On day

5, viral loads became undetectable (Figure 1). MDCK cells inoculated with the nasal sample showed cytopathic effect on day 3 of incubation with cell rounding, progressive degeneration, and detachment. Serologically, HI and MN antibodies against pH1N1 were undetectable >40 days before the onset of the illness and on days 1 and 4 of the illness, but high titers (HI, 1:320; MN, 1:160) were detected in the second and the fourth week after the onset of the illness (Figure 1). The other 2 giant pandas did not develop any clinical signs, and their nasal swab specimens remained negative by RT-PCR.

Table. Comparison of influenza A(H1N1)pdm09 isolated from a giant panda (A/giant panda/Hong Kong/MISO20/2018) with other representative H1N1 subtype isolates by gene segment*

Isolate	Nucleotide identity, %							
	PB2	PB1	PA	HA	NP	NA	M	NS
A/Hong Kong/2272/2018	99.90	99.90	99.90	99.80	99.80	99.70	99.80	99.70
A/Hainan-Xiuying/11613/2018	99.90	99.70	99.90	99.80	99.70	99.70	99.70	99.80
A/Victoria/2102/2018	99.80	99.60	99.80	99.70	99.60	99.90	99.60	99.60
A/Hong Kong/1125/2018	99.30	99.50	99.50	99.40	99.50	99.50	99.60	99.70
A/Guangdong/GLW/2018	98.90	99.50	99.60	99.00	99.40	99.50	99.30	99.70
A/Zhejiang-Yuecheng/SWL143/2018	99.10	99.20	99.40	98.80	99.30	99.10	99.20	99.50
A/Sichuan-Qingyang/11819/2018	99.00	99.10	99.00	98.50	99.00	98.30	99.20	99.60
A/Hong Kong/111/2019	99.00	98.90	99.40	98.70	99.00	99.00	99.20	99.30
A/Indiana/04/2019	99.90	99.70	99.80	99.70	99.70	99.70	99.70	99.80
A/Arizona/15/2017	98.80	99.00	99.10	98.10	98.90	98.70	99.00	99.20
A/Georgia/01/2016	99.00	99.10	99.20	98.40	99.10	98.70	99.10	99.50
A/Hong Kong/1682/2016	98.90	99.10	99.00	98.20	99.10	98.70	99.00	99.60
A/Hong Kong/95/2016	99.00	99.10	99.30	98.40	99.00	98.70	99.10	99.50
A/Bangkok/SIMI506/2010	97.00	97.30	97.70	96.40	97.50	96.00	97.80	96.80
A/Hong Kong/H090–751-V20/2009	97.30	97.60	97.60	96.60	97.70	96.90	98.10	96.90
A/Shanghai/37T/2009	97.30	97.60	97.70	96.60	97.70	97.00	98.10	96.70
A/Fuzhou/01/2009	97.40	97.60	97.70	96.60	97.70	97.00	98.10	92.60
A/Sichuan-Wenjiang/SWL456/2009	97.40	97.70	97.70	96.60	97.70	96.90	98.10	96.90
A/Hong Kong/H090–770-V10/2009	97.30	97.70	97.70	96.50	97.60	97.00	98.10	96.90
A/giant panda/Ya'an/01/2009	97.30	97.50	97.50	96.40	97.50	96.70	98.10	96.80
A/panda/Sichuan/01-GG/2009	97.30	97.50	97.50	96.40	97.50	96.70	98.10	96.80
A/Niigata/08F188/2009	82.80	80.10	82.50	76.20	83.30	78.00	86.70	80.50
A/Thailand/CU-H565/2009	82.70	80.00	82.60	75.90	83.30	77.90	86.60	81.00
A/swine/Guangdong/05/2009	82.20	79.60	81.60	88.90	92.10	79.30	86.80	91.30
A/Hong Kong/1870/2008	82.70	80.60	82.70	76.00	83.60	77.70	87.00	81.70
A/swine/Hong Kong/1733/2002	81.70	79.30	81.30	89.20	92.60	79.50	86.00	90.40
A/swine/Hong Kong/158/1993	82.10	79.70	82.00	90.20	93.50	79.30	87.20	96.70
A/AA/Huston/1945	84.80	81.80	83.40	78.30	85.10	80.20	88.90	83.60

*HA, hemagglutinin; M, matrix; NA, neuraminidase; NP, nucleoprotein; NSP, nonstructural protein; PA, polymerase; PB1, polymerase basic 1; PB2, polymerase basic 2.

Whole-genome sequence analysis showed that the influenza virus we isolated from the giant panda (A/giant panda/Hong Kong/MISO20/2018) was closely related to other pH1N1 viruses circulating among humans in 2018, sharing 99.3%–99.9% nucleotide identities (Table). Phylogenetic analyses based on the hemagglutinin (HA) and neuraminidase (NA) gene sequences showed that A/giant panda/Hong Kong/MISO20/2018 was most closely related to the human pH1N1 strain A/Hong Kong/2272/2018, which was circulating in Hong Kong at the time at which the giant panda acquired the infection (Figure 2; Appendix Figure, https://wwwnc.cdc.gov/EID/article/25/12/19-1143-App1.pdf). There were only 2 bases difference between the HA genes and 4 bases difference between the NA genes of A/giant panda/Hong Kong/MISO20/2018 and A/Hong Kong/2272/2018, but 60 bases difference between the HA genes and 45 bases difference between the NA genes of A/giant panda/Hong Kong/MISO20/2018 and A/giant panda/01/Ya'an/2009, a pH1N1 virus previously isolated in giant panda in China (1). Phylogenetic analyses based on the other gene segments displayed similar topologies (Appendix Figure). Detailed annotation of the genome sequence of the giant panda isolate revealed features essential for transmission and replication of pH1N1 in other mammalian species. For example, A/giant panda/Hong Kong/MISO20/2018 also possessed glutamine at position 226 (H3 numbering) in HA and alanine at position 271 in polymerase protein 2 (1).

Conclusions

We documented a case of influenza infection caused by pH1N1 virus in a captive giant panda in Hong Kong. The viral load was $>6 \times 10^5$ copies/mL during the first 2 days of the illness and decreased to an undetectable level on day 5. The decrease in viral load was coupled with development of antibody response. Complete genome sequencing and phylogenetic analysis showed that the pH1N1 virus from the giant panda differed from the influenza virus circulating in Hong Kong at that time by only 2–24 bases. In 2014, pH1N1 infection was reported in giant pandas at the Conservation and Research Center for the Giant Panda in Sichuan (1). That pH1N1 virus, A/giant panda/01/Ya'an/2009, was also closely related to the pH1N1 strains circulating in humans during 2009 (1).

These findings show that influenza A virus infection in this giant panda was not an isolated case and that these infections have happened not only in mainland China. Our findings indicate that the influenza virus in giant pandas was most likely directly or indirectly from humans with seasonal influenza. Of interest, respiratory infection in a sloth bear due to pH1N1 has also been observed in a zoo in the United States in 2014, indicating that pH1N1 can probably infect a variety of bears (2).
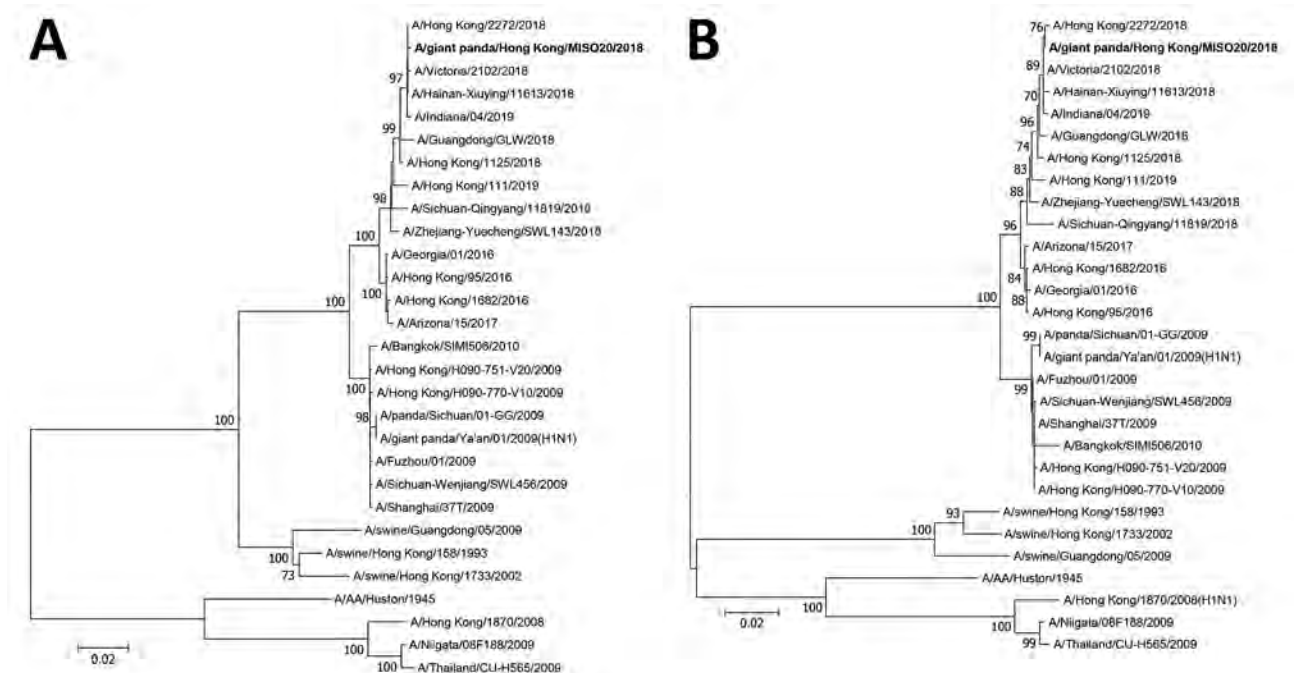
Figure 2. Phylogenetic analyses of (A) hemagglutinin and (B) neuraminidase gene sequences of influenza A(H1N1)pdm09 (A/giant panda/Hong Kong/MISO20/2018) isolated from a giant panda in Hong Kong, China (bold), and other previously characterized strains retrieved from GISAID. The trees were constructed by the neighbor-joining method using Kimura 2-parameter in MEGA6 (http://www.megasoftware.net). A total of 1,691 nt positions in hemagglutinin and 1,404 in neuraminidase genes were included in the analyses. Bootstrapping was performed with 1,000 replicates; only bootstrap values ≥700 are shown. Scale bars indicate nucleotide substitutions per site.

In animal species with no preexisting immunity against an infectious agent, a new intrusion of the pathogen may result in high fatalities. Transmission of a new strain of influenza from birds and poultry to humans has resulted in many epidemics (*10–15*). Because the inactivated vaccine against pH1N1 has been widely used in humans and is effective in mice, pigs, and ferrets, it might be worthwhile to test its immunogenicity in giant pandas. Moreover, caretakers working at these parks who are infected with influenza, even with mild illness or in recovery, should not work near the animals.

About the Author

Dr. Martelli, a zoological veterinarian, is currently Director of Veterinary Services at Hong Kong Ocean Park.

References

1. Li D, Zhu L, Cui H, Ling S, Fan S, Yu Z, et al. Influenza A(H1N1) pdm09 virus infection in giant pandas, China. Emerg Infect Dis. 2014;20:480–3. https://doi.org/10.3201/eid2003.131531
2. Boedeker NC, Nelson MI, Killian ML, Torchetti MK, Barthel T, Murray S. Pandemic (H1N1) 2009 influenza A virus infection associated with respiratory signs in sloth bears (*Melursus ursinus*). Zoonoses Public Health. 2017;64:566–71. https://doi.org/10.1111/zph.12370
3. Keenliside J. Pandemic influenza A H1N1 in swine and other animals. In: Richt JA, Webby RJ, editors. Swine influenza. Current topics in microbiology and immunology, vol 370. Heidelberg: Springer; 2012. https://doi.org/10.1007/82_2012_301
4. Feng N, Yu Y, Wang T, Wilker P, Wang J, Li Y, et al. Fatal canine distemper virus infection of giant pandas in China. Sci Rep. 2016;6:27518. https://doi.org/10.1038/srep27518
5. To KK, Chan KH, Li IW, Tsang TY, Tse H, Chan JF, et al. Viral load in patients infected with pandemic H1N1 2009 influenza A virus. J Med Virol. 2010;82:1–7. https://doi.org/10.1002/jmv.21664
6. Chan KH, To KK, Hung IF, Zhang AJ, Chan JF, Cheng VC, et al. Differences in antibody responses of individuals with natural infection and those vaccinated against pandemic H1N1 2009 influenza. Clin Vaccine Immunol. 2011;18:867–73. https://doi.org/10.1128/CVI.00555-10
7. Hung IF, To KK, Lee CK, Lin CK, Chan JF, Tse H, et al. Effect of clinical and virological parameters on the level of neutralizing antibody against pandemic influenza A virus H1N1 2009. Clin Infect Dis. 2010;51:274–9. https://doi.org/10.1086/653940
8. Guan TP, Teng JLL, Yeong KY, You ZQ, Liu H, Wong SSY, et al. Metagenomic analysis of Sichuan takin fecal sample viromes reveals novel enterovirus and astrovirus. Virology. 2018;521:77–91. https://doi.org/10.1016/j.virol.2018.05.027
9. Woo PC, Lau SK, Teng JL, Tsang AK, Joseph M, Wong EY, et al. Metagenomic analysis of viromes of dromedary camel fecal samples reveals large number and high diversity of circoviruses and picobirnaviruses. Virology. 2014;471-473:117–25. https://doi.org/10.1016/j.virol.2014.09.020
10. Refaey S, Azziz-Baumgartner E, Amin MM, Fahim M, Roguski K, Elaziz HA, et al. Increased number of human cases of influenza virus A(H5N1) infection, Egypt, 2014–15. Emerg Infect Dis. 2015;21:2171–3. https://doi.org/10.3201/eid2112.150885
11. Wei SH, Yang JR, Wu HS, Chang MC, Lin JS, Lin CY, et al. Human infection with avian influenza A H6N1 virus: an epidemiological analysis. Lancet Respir Med. 2013;1:771–8. https://doi.org/10.1016/S2213-2600(13)70221-2
12. Goneau LW, Mehta K, Wong J, L'Huillier AG, Gubbay JB. Zoonotic influenza and human health—part 1: virology and epidemiology of zoonotic influenzas. Curr Infect Dis Rep. 2018;20:37. https://doi.org/10.1007/s11908-018-0642-9
13. Ke C, Lu J, Wu J, Guan D, Zou L, Song T, et al. Circulation of reassortant influenza A(H7N9) viruses in poultry and humans, Guangdong Province, China, 2013. Emerg Infect Dis. 2014;20:2034–40. https://doi.org/10.3201/eid2012.140765
14. Zhang T, Bi Y, Tian H, Li X, Liu D, Wu Y, et al. Human infection with influenza virus A(H10N8) from live poultry markets, China, 2014. Emerg Infect Dis. 2014;20:2076–9. https://doi.org/10.3201/eid2012.140911
15. Nga VT, Ngoc TU, Minh LB, Ngoc VTN, Pham VH, Nghia LL, et al. Zoonotic diseases from birds to humans in Vietnam: possible diseases and their associated risk factors. Eur J Clin Microbiol Infect Dis. 2019;38:1047–58. https://doi.org/10.1007/s10096-019-03505-2

Address for correspondence: Patrick C.Y. Woo or Susanna K.P. Lau, Queen Mary Hospital, Department of Microbiology, 19/F, Block T, 102 Pokfulam Rd, Hong Kong, China; email: pcywoo@hku.hk or skplau@hku.hk

Middle East Respiratory Syndrome Coronavirus Seropositivity in Camel Handlers and Their Families, Pakistan

Jian Zheng,[1] Sohail Hassan,[1]
Abdulaziz N. Alagaili, Abeer N. Alshukairi,
Nabil M.S. Amor, Nadia Mukhtar,
Iqra Maleeha Nazeer, Zarfishan Tahir,
Nadeem Akhter, Stanley Perlman, Tahir Yaqub

A high percentage of camel handlers in Saudi Arabia are seropositive for Middle East respiratory syndrome coronavirus. We found that 12/100 camel handlers and their family members in Pakistan, a country with extensive camel MERS-CoV infection, were seropositive, indicating that MERS-CoV infection of these populations extends beyond the Arabian Peninsula.

Middle East respiratory syndrome (MERS) coronavirus (MERS-CoV), identified in 2012, causes a highly lethal pneumonia with a 34.5% mortality rate (https://www.who.int/emergencies/mers-cov). As of July 31, 2019, a total of 2,458 cases and 848 deaths have been reported to the World Health Organization, with all cases in the Middle East or in travelers from this region or their contacts (1). MERS cases fall into 2 categories, primary and secondary. Secondary cases, which result most commonly from human-to-human transmission in hospitals, were most prominent during the early years of the outbreak. However, as stringent infection control measures have been followed more closely, a greater proportion of cases are classified as primary. Camels are believed to be the zoonotic source for primary infections, but a large proportion of patients describe no camel contact, raising the question of how they acquired the disease (2).

To determine the source of the infection, several studies have focused on a potential role in transmission for camel handlers. These reports indicate that the percentage of MERS-CoV–immune camel handlers is much greater than in the general population of Saudi Arabia, the country with the largest number of MERS cases. These studies have reported that 3%–67% of camel handlers in this country are MERS-CoV exposed, compared with 0.15% of the general population (3–5). In Saudi Arabia, much of camel farming is labor intensive, and many camel owners hire camel handlers, generally from outside of the country, to tend to them (6). To determine the generalizability of these observations, we tested blood samples from 100 camel handlers and their families in the Cholistan desert in Punjab, Pakistan, a country with no reported human MERS (7).

The Study

We chose Cholistan as the study site because it is the most important region of Pakistan for the camel industry, and handlers and their families are in close contact with dromedaries. We engaged study participants in the Bahawalnagar and Bahawalpur districts, located in southern Punjab Province, Pakistan. The Institutional Ethical Review Board (IERB) of the Institute of Public Health, Government of Punjab, Lahore, Pakistan, approved the study. We obtained written informed consent from all study participants.

Camel handlers in Cholistan differ from those in Saudi Arabia in that they own their camels, along with cows, goats, and sheep, and they and their families take care of these animals. Both men and women are responsible for grazing, feeding, milking, and waste disposal. In addition, they live in close proximity to camels and share similar water sources (8–10). Camel handlers in Cholistan are either nomadic, seminomadic, or sedentary, with varying degrees of exposure to camels. Nomads live with their camels in the desert and migrate throughout Cholistan, whereas seminomads tend to live at a base camp and migrate depending on availability of fodder and water. Nomadic camel handlers and their families have the highest exposure to camels, whereas sedentary ones have the least exposure.

During 2017–2018, we obtained blood samples from 100 participants from nomadic, seminomadic, and sedentary populations. The age range was 8–76 years (average

Author affiliations: University of Iowa, Iowa City, Iowa, USA
(J. Zheng, S. Perlman); University of Veterinary and Animal
Sciences, Lahore, Pakistan (S. Hassan, I.M. Nazeer, T. Yaqub);
King Saud University, Riyadh, Saudi Arabia (A.N. Alagaili,
N.M.S. Amor); King Faisal Specialist Hospital and Research
Centre, Jeddah, Saudi Arabia (A.N. Alshukairi); Government of
Punjab, Lahore (N. Mukhtar, Z. Tahir, N. Akhter); The First
Affiliated Hospital of Guangzhou Medical University, Guangzhou,
China (S. Perlman)

[1]These first authors contributed equally to this article.

Table 1. Characteristics of participants in study of Middle East respiratory syndrome coronavirus seropositivity in camel handlers and their families, Pakistan

Characteristic	No. (%) participants
Lifestyle	
Sedentary	10 (10)
Seminomadic	64 (64)
Nomadic	26 (26)
Concurrent conditions	21 (21)
Consumption of unpasteurized camel milk	98 (98)
Tobacco use	38 (38)

30.1 years). We obtained demographic and clinical information at sampling by written questionnaire, including participant age, lifestyle (nomadic, seminomadic, sedentary), role in family (husband, wife, child, etc.), underlying medical conditions, numbers of camels owned, history of tobacco use (smoking or chewing), and consumption of camel products (milk) (Table 1; Appendix Table, https://wwwnc.cdc.gov/EID/article/25/12/19-1169-App1.pdf). We transported samples to the microbiology department at the University of Veterinary and Animal Sciences (Lahore, Punjab, Pakistan). We prepared serum samples, stored them at –80°C, and shipped them to the University of Iowa (Iowa City, Iowa, USA) for analysis.

We tested all the samples for MERS-CoV–specific antibodies by ELISA and 50% reduction plaque-reduction neutralization test ($PRNT_{50}$). Of 91 participants examined by a commercially available ELISA, 49 were positive for MERS-CoV–specific antibody. Twelve had $PRNT_{50}$ titers >1:20 and were considered positive; of these, 5 were also positive by ELISA. In addition, 10/12 were positive by immunofluorescence assay. Of the 12 $PRNT_{50}$-positive participants, 3 were women and 1 was an 8-year-old child (Table 2).

All but 2 of the study participants were exposed to camels. There was no significant correlation (p>0.5) between MERS-CoV seropositivity and lifestyle, presence of concurrent conditions, drinking unpasteurized camel milk, or tobacco use, with the caveat that the sample size was small.

Conclusions

In general, nomads had the most and sedentary populations had the least camel contact, although nearly all family members were exposed to and took care of camels. Of 100 participants, we identified 12 who were MERS-CoV seropositive, as measured by the presence of $PRNT_{50}$ antibody. Of note, several $PRNT_{50}$-positive samples were negative by ELISA, but most were positive by immunofluorescence assay. This lack of concordance between ELISA and $PRNT_{50}$ titers was observed previously (3,11) and may reflect lower sensitivity of the commercial ELISA kit (12). Other coronaviruses circulate in camel populations (13), and it is conceivable that the high rate of ELISA seropositivity resulted from immune responses to other, possibly MERS-like, coronaviruses present in Pakistan. Thus, it will be important to assess camel (and human) populations for other coronaviruses that might elicit a cross-reactive response.

The mechanism of MERS-CoV transmission from camels to humans in Pakistan is not established, but most camel handlers and their families drink fresh camel milk, obtained after young camels have finished nursing. Juvenile camels demonstrate the highest rate of seroconversion and of MERS-CoV positivity (6,14), so it is possible that drinking fresh milk is a source of infection. In this region of Pakistan, camel handlers and their families also share water sources with camels, which probably

Table 2. Characteristics of camel handlers and their families positive for Middle East respiratory syndrome coronavirus in study in Pakistan*

Patient no.	Family no.	Age, y/ sex	Camel contact†	Smoking	Concurrent conditions	Lifestyle	$PRNT_{50}$	ELISA result/ value‡	IFA result/ titer§
SH94	F2	20/M	Direct/daily	Yes	None	Nomadic	211	–/0.78	+/1:80
SH85	F2	21/M	Direct/daily	Yes	None	Nomadic	32	+/1.51	+/1:40
SH100	F1	8/M	Direct/daily	No	None	Nomadic	72	–/0.64	+/1:40
SH71	F9	35/F	Indirect	No	HPT, renal and respiratory disease	Seminomadic	33	Borderline/ 0.99	+/1:20
SH74	F9	40/F	Indirect	No	HPT	Seminomadic	40	+/2.18	+/1:80
SH63	F13	35/F	Direct/monthly	No	None	Seminomadic	27	Borderline/ 0.92	+/1:10
SH57	F14	20/M	Direct	No	None	Seminomadic	51	+/3.11	+/1:80
SH58	F16	28/M	Direct	Yes	None	Seminomadic	68	+/1.74	+/1:160
SH21	None	17/M	Direct/seasonal	Yes	None	Seminomadic	80	–/0.36	–/<1:10
SH65	None	20/M	D/daily	No	None	Seminomadic	65	+/1.13	+/1:80
SH43	None	34/M	Direct	No	None	Sedentary	1,600	–/0.76	+/1:160
SH44	None	40/M	Direct	Yes	None	Sedentary	89	–/0.48	–/<1:10

*All 12 patients tested positive by $PRNT_{50}$. IFA, immunofluorescence assay; HPT, hypertension; $PRNT_{50}$, 50% reduction plaque reduction neutralization assay.
†Direct indicates camel herders with direct camel contact but extent of exposure is not known; direct/daily, camel herders with daily direct camel contact; direct/monthly, camel herders with monthly direct camel contact; direct/seasonal, camel herders with seasonal direct camel contact; indirect, family members of camel herders.
‡Positive result is >1.1; borderline, 0.8–1.1; negative, <0.8, as defined by the test manufacturer.
§Negative test result is <1:10, as defined by the test manufacturer.

contributes to virus transmission. Zohaib et al. identified a 75.6% MERS seroprevalence in camels throughout Pakistan, but 0% seropositivity in humans, including some with camel contact (*7*).

Medical services in Cholistan and adjacent areas are limited, making MERS diagnosis and transmission studies difficult. Our findings show a need for additional studies to confirm the absence of clinically apparent MERS in this region and to determine whether epidemiologic, technical, or other factors caused differences in seropositivity between our study and that of Zohaib et al.

Our study, by demonstrating a low but detectable rate of MERS-CoV seropositivity in camel handlers and their families, indicates that this population could contribute to MERS-CoV transmission to the broader community in Pakistan. We previously showed that measurement of T cell responses identified additional MERS-CoV–immune persons (*3*,*11*), suggesting that our results may underestimate the prevalence of MERS-CoV infection. Our results also illustrate the importance of educating camel herders and their families about proper infection control measures, including handwashing, to diminish the likelihood of MERS-CoV transmission.

Acknowledgments

About the Author

Dr. Zheng is a postdoctoral researcher in the Department of Microbiology and Immunology, University of Iowa. His research interests are in respiratory viruses, such as human coronaviruses and influenza viruses. Dr. Hassan is a lecturer in microbiology, University of Veterinary and Animal Sciences, Lahore, Pakistan. His primary research interests are emerging viral infections and zoonoses at the animal–human interface.

References

1. Hui DS, Azhar EI, Kim YJ, Memish ZA, Oh MD, Zumla A. Middle East respiratory syndrome coronavirus: risk factors and determinants of primary, household, and nosocomial transmission. Lancet Infect Dis. 2018;18:e217–27. https://doi.org/10.1016/S1473-3099(18)30127-0

2. Conzade R, Grant R, Malik MR, Elkholy A, Elhakim M, Samhouri D, et al. Reported direct and indirect contact with dromedary camels among laboratory-confirmed MERS-CoV cases. Viruses. 2018;10:425. https://doi.org/10.3390/v10080425

3. Alshukairi AN, Zheng J, Zhao J, Nehdi A, Baharoon SA, Layqah L, et al. High prevalence of MERS-CoV infection in camel workers in Saudi Arabia. MBio. 2018;9:e01985–18. 10.1128/mBio.01985-18 https://doi.org/10.1128/mBio.01985-18

4. Khudhair A, Killerby ME, Al Mulla M, Abou Elkheir K, Ternanni W, Bandar Z, et al. Risk factors for MERS-CoV seropositivity among animal market and slaughterhouse workers, Abu Dhabi, United Arab Emirates, 2014–2017. Emerg Infect Dis. 2019;25:927–35. https://doi.org/10.3201/eid2505.181728

5. Müller MA, Meyer B, Corman VM, Al-Masri M, Turkestani A, Ritz D, et al. Presence of Middle East respiratory syndrome coronavirus antibodies in Saudi Arabia: a nationwide, cross-sectional, serological study. Lancet Infect Dis. 2015;15:559–64. https://doi.org/10.1016/S1473-3099(15)70090-3

6. Hemida MG, Elmoslemany A, Al-Hizab F, Alnaeem A, Almathen F, Faye B, et al. Dromedary camels and the transmission of Middle East respiratory syndrome coronavirus (MERS-CoV). Transbound Emerg Dis. 2017;64:344–53. https://doi.org/10.1111/tbed.12401

7. Zohaib A, Saqib M, Athar MA, Chen J, Sial AU, Khan S, et al. Countrywide survey for MERS-coronavirus antibodies in dromedaries and humans in Pakistan. Virol Sin. 2018;33:410–7. https://doi.org/10.1007/s12250-018-0051-0

8. Ali I, Chaudhry MS, Farooq U. Camel rearing in Cholistan Desert of Pakistan. Pak Vet J. 2009;29:85–92.

9. Khan AA, Khan K. Women's role in livestock economy of Cholistan Desert, Pakistan. Global Journal of Human-Social Science: E Economics. 2015;15:29–39 [cited 2019 Oct 18]. https://globaljournals.org/GJHSS_Volume15/4-Womens-Role-in-Livestock-Economy.pdf

10. Amin H, Ali T, Ahmad M, Zafar M. Gender and development: roles of rural women in livestock production in Pakistan. Pak J Agric Sci. 2010;47:32–6.

11. Zhao J, Alshukairi AN, Baharoon SA, Ahmed WA, Bokhari AA, Nehdi AM, et al. Recovery from the Middle East respiratory syndrome is associated with antibody and T-cell responses. Sci Immunol. 2017;eaan5393. https://doi.org/10.1126/sciimmunol.aan5393

12. Okba NMA, Raj VS, Widjaja I, GeurtsvanKessel CH, de Bruin E, Chandler FD, et al. Sensitive and specific detection of low-level antibody responses in mild Middle East respiratory syndrome coronavirus infections. Emerg Infect Dis. 2019;25:1868–77. https://doi.org/10.3201/eid2510.190051

13. Sabir JSM, Lam TT-Y, Ahmed MMM, Li L, Shen Y, Abo-Aba SEM, et al. Co-circulation of three camel coronavirus species and recombination of MERS-CoVs in Saudi Arabia. Science. 2016;351:81–4. https://doi.org/10.1126/science.aac8608

14. Wernery U, Lau SK, Woo PC. Middle East respiratory syndrome (MERS) coronavirus and dromedaries. Vet J. 2017;220:75–9. https://doi.org/10.1016/j.tvjl.2016.12.020

Address for correspondence: Stanley Perlman, University of Iowa, Department of Microbiology and Immunology, 51 Newton Rd, Iowa City, IA 52242, USA; email: stanley-perlman@uiowa.edu; Sohail Hassan, University of Veterinary and Animal Sciences, Department of Microbiology, Lahore 54000, Pakistan; email: sohail.hassan@uvas.edu.pk

Distantly Related Rotaviruses in Common Shrews, Germany, 2004–2014

Reimar Johne, Simon H. Tausch,
Josephine Grützke, Alexander Falkenhagen,
Corinna Patzina-Mehling, Martin Beer,
Dirk Höper, Rainer G. Ulrich

We screened samples from common shrews (*Sorex araneus*) collected in Germany during 2004–2014 and identified 3 genetically divergent rotaviruses. Virus protein 6 sequence similarities to prototype rotaviruses were low (64.5% rotavirus A, 50.1% rotavirus C [tentative species K], 48.2% rotavirus H [tentative species L]). Shrew-associated rotaviruses might have zoonotic potential.

Rotaviruses are a major cause of diarrhea in young children, causing an estimated 215,000 deaths worldwide every year (1). These viruses are nonenveloped and have a genome consisting of 11 segments of double-stranded RNA (2); each segment codes for either 1 of the structural proteins, virus protein (VP) 1–7, or 1 or 2 of the nonstructural proteins (NSPs), NSP1–6. Rotaviruses are classified into species A–I or the tentative species J on the basis of the amino acid sequence similarity of the conserved structural protein VP6 and the conserved nucleotide sequence of the genome segment ends (3–5). For rotavirus A, further classification into genome segment–specific genotypes has been established (6). Rotaviruses can infect a wide diversity of animals, and zoonotic transmission of rotaviruses has been reported (7).

Shrews are small insectivorous mammals that have been previously identified as reservoirs for other pathogens (e.g., hantaviruses and *Leptospira* spp.) (8–10). In this investigation, we aimed to determine whether common shrews (*Sorex araneus*, order Eulipotyphla) are also a reservoir for rotaviruses and, if so, assess the genetic variability of the viruses found in this species.

The Study

During 2004–2014, small mammals were caught in different regions of Germany as part of local monitoring or

pest control measures (9,10). From these animal collections, we acquired samples (intestine contents) collected from 49 common shrews (Figure 1). We combined these samples almost equally into 2 pools and performed RNA extraction followed by next-generation sequencing (NGS) using the Ion Torrent Personal Genome Machine system (ThermoFisher Scientific, https://www.thermofisher.com; Appendix, https://wwwnc.cdc.gov/EID/article/25/12/19-1225-App1.pdf). By applying the RIEMS data analysis pipeline (11), we identified 3 short contigs with low sequence similarities to rotavirus H in both pools. To identify the positive animals, we extracted RNA from individual samples and screened for rotavirus RNA using reverse transcription PCR (RT-PCR) with primers specific to 1 of the 3 rotavirus H contigs we previously obtained (Appendix Table 1). In total, 7 (15.2%) of 46 samples turned out to be positive for species H–like rotavirus (Table 1); 2 samples, KS/12/0644 and KS/11/2281, generated the strongest signal on ethidium bromide staining. We subjected these 2 samples to RNase and DNase treatment followed by RNA extraction and NGS using the NextSeq 500 sequencing system (Illumina, https://www.illumina.com); 8,576,782 read pairs for KS/12/0644 and 6,168,437 for KS/11/2281 were generated. After a RAMBO-K analysis (12) suggested a low abundance of highly deviant rotavirus sequences, we performed data analysis and contig assembly using a newly generated pipeline (Appendix). By this method, contig lengths were 164–3,017 nt, and we obtained 48 contigs with sequence similarities to rotavirus A, 17 with low sequence similarities to rotavirus C, and 23 with low sequence similarities to rotavirus H (Appendix Table 2). Because contigs of homologous genes from each of the 3 viruses were detected in these samples, we concluded 3 different rotaviruses were present in both.

We then performed RT-PCR with all samples using primers specific to the species A and species C–like rotavirus contigs from the previous analysis, and 21.7% (10/46) were positive for species A rotavirus and 10.9% (5/46) for species C–like rotavirus; rotavirus co-infections were also identified (Table 1). An analysis of the geographic distribution of shrew rotaviruses in Germany shows that species C–like rotaviruses were mainly located in the northeast and Southwest, species H–like rotaviruses mainly in the south,

and species A rotaviruses broadly throughout (Figure 1). At the monitoring site in Baden-Württemberg (southwest Germany), frequent detections of different rotaviruses and multiple co-infections were observed.

Despite several efforts, we could delineate only partial genomic sequences of rotaviruses from the NGS data. By application of primer ligation, rapid amplification of cDNA ends, and degenerated primer RT-PCR strategies, we acquired the complete open reading frames of VP1, VP6, and NSP5 of most viruses (Table 2). In addition, we reamplified and sequenced the VP6 genes of all viruses by dideoxy chain–termination sequencing and confirmed the VP6 sequences obtained. Sequence analysis of these genes and in silico translation indicated 14.1%–65.6% amino acid sequence similarity to the respective proteins of other rotavirus species (Table 2). The Rotavirus Classification Working Group reviewed the sequences of the shrew rotavirus A genes in sample KS/11/2281 and designated the new genotypes R23 for VP1, I27 for VP6, and H23 for NSP5. The maximum amino acid sequence similarities to established
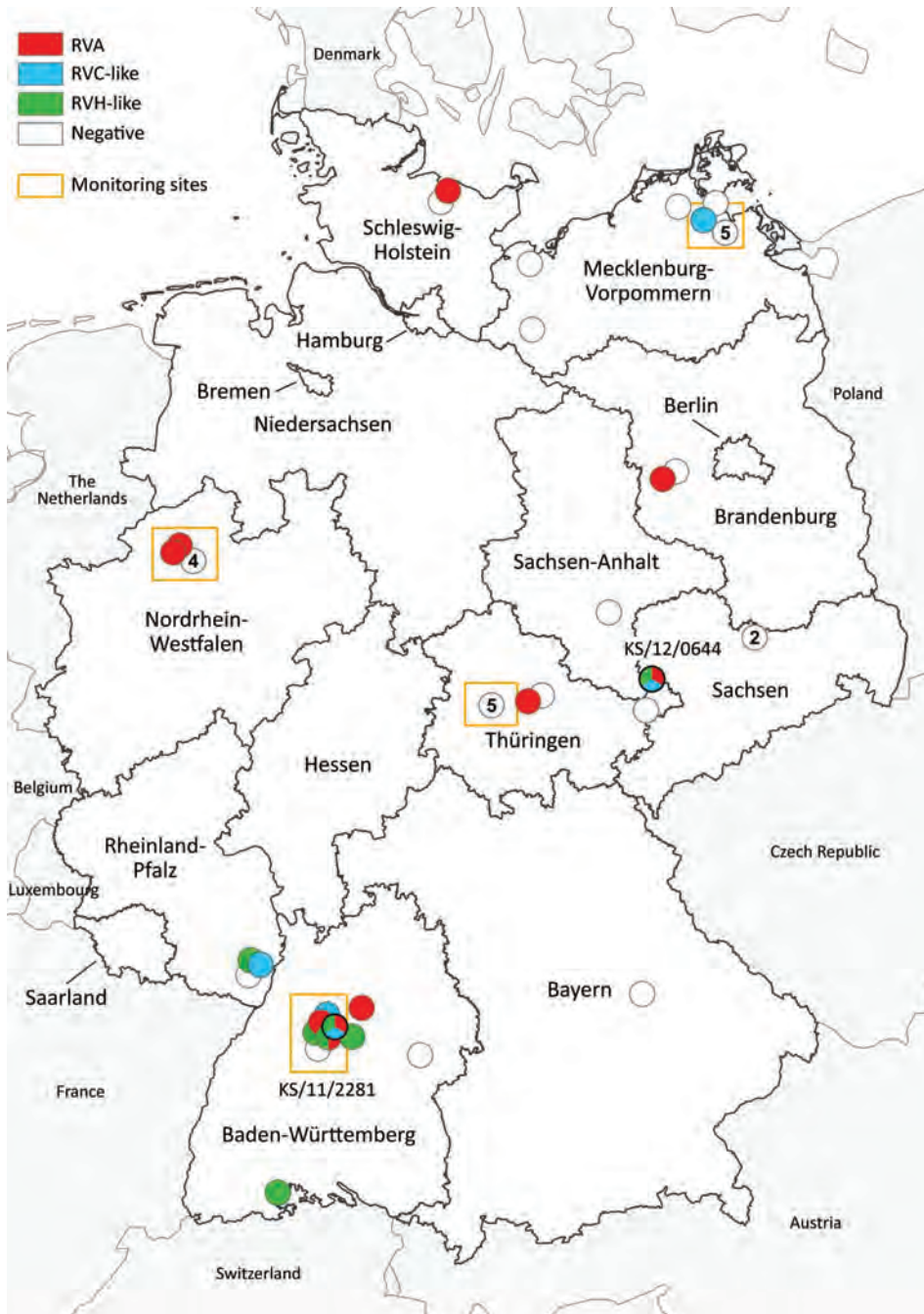
Figure 1. Distribution of common shrews (*Sorex araneus*) collected at monitoring sites (*9*) and additional sites (*10*) in Germany, 2004–2014, positive and negative for RVA, RVC-like, and RVH-like species by reverse transcription PCR. Numbers in white circles indicate the number of negative samples at that collection site; white circles without numbers indicate 1 negative sample at that site. Circles with multiple colors indicate animals with co-infections. The collection sites of the 2 samples analyzed in detail by next-generation sequencing (KS/12/0644 and KS/11/2281; tricolored circles) are indicated. RVA, rotavirus A; RVC, rotavirus C; RVH, rotavirus H.

Table 1. Rotavirus infections detected in common shrews (*Sorex araneus*) sampled in Germany, 2004–2014*

Virus species	Monoinfections	RVA	RVC	RVH	RVA and RVC	RVC and RVH	RVA and RVH	Total infections
				Co-infections with				
RVA	7/46 (15.2)	NA	0/46	1/46 (2.2)	NA	2/46 (4.3)	NA	10/46 (21.7)
RVC-like	3/46 (6.5)	0/46	NA	0/46	NA	NA	2/46 (4.3)	5/46 (10.9)
RVH-like	4/46 (4.3)	1/46 (2.2)	0/46	NA	2/46 (4.3)	NA	NA	7/46 (15.2)

*Samples from shrews were examined by reverse transcription PCRs specific for RVA, RVC-like, and RVH-like species. Values are no. positive/total (%). NA, not applicable; RVA, rotavirus A; RVC, rotavirus C; RVH, rotavirus H.

rotavirus type species of 50.1% for VP6 of species C–like rotavirus and 48.2% (species H) or 48.3% (species J) for VP6 of species H–like rotavirus suggest that these viruses should be classified as novel (tentative) rotavirus species (Table 2).

Phylogenetic analyses of the VP1, VP6, and NSP5 proteins indicate a consistent branching of shrew rotavirus A with other rotavirus A species and shrew species C–like rotavirus with other rotavirus C species. However, the species H–like rotavirus branches more variably within the rotavirus B-G-H-I-J cluster (Figure 2). A more detailed phylogenetic analysis of complete and additional partial genome segment nucleotide sequences of the shrew rotavirus A showed a basal branching at the cluster of other species A rotavirus sequences for most genes (Appendix Figure 1). In addition, phylogenetic analyses of partial amino acid sequences deduced from other genes of the shrew species C–like and H–like rotaviruses confirmed the relationship evident from analyses of the 3 completely sequenced open reading frames (Appendix Figure 2–4).

Shrews have been analyzed infrequently for rotaviruses. In 1 study, rotavirus antigen was detected in wild Chinese tree shrews (*Tupaia chinensis*, order Scandentia) (*13*), and in another study, species A rotaviruses not identical to those of our study (Appendix Figure 1) were identified in house shrews (*Suncus murinus*, order Eulipotyphla) from China (*14*). Here, a broader rotavirus screening of common shrew samples resulted in the identification of novel rotaviruses. The rotavirus detection rate of 10.9%–21.7% in the analyzed samples from animals from different regions of Germany suggests a wide circulation of rotaviruses in

shrews, although more samples should be analyzed in the future to clarify the association of rotaviruses with these animals. We also identified co-infections with >1 rotavirus, a regular finding in other animal host species (*15*).

The shrew rotavirus A sequences showed low similarities with other species A rotaviruses, resulting in the assignment of novel genotypes and suggesting a long-term separate evolution of these viruses in this shrew species. The 2 other rotaviruses identified showed even lower sequence similarities to the known rotavirus species. According to the cutoff value of 53% suggested for the differentiation of rotavirus species on the basis of the encoded VP6 amino acid sequence (*5*), both viruses should be considered new rotavirus species, which we tentatively designate rotavirus species K (for the rotavirus C–like species) and L (for the rotavirus H–like species). However, because their complete genome sequences have not been determined, a final classification of these viruses remains to be accomplished. At least the 5′ and 3′ termini of these rotavirus genome segments, which are conserved within known rotavirus species (*2*), should be determined. The low virus amounts in samples, restricted available sample volumes, presence of multiple viruses in single samples, and low sequence similarities for some virus genes might help explain the failure to generate complete genome sequences in our study.

Conclusions

We identified multiple, genetically divergent rotavirus species in common shrews in Germany. These animals should be further investigated as a potential reservoir for rotaviruses capable of infecting humans.

Table 2. Sequence similarities of deduced VP1, VP6, and NSP5 amino acid sequences of rotaviruses from common shrews (*Sorex araneus*), Germany, 2004–2014*

Comparator rotavirus species and strain	A (KS/11/2281)			C-like (KS/11/2281)			H-like (KS/12/0644)		
	VP1	VP6	NSP5	VP1†	VP6‡	NSP5	VP1	VP6	NSP5
A, SA11	65.6	64.5	47.6	48.6	40.2	24.5	26.8	20.3	17.6
B, WH-1	27.4	17.1	15.9	24.9	14.7	17.6	55.5	39.2	32.9
C, Bristol	48.0	42.8	24.6	63.2	50.1	31.5	25.8	20.0	16.8
D, 05V0059	51.8	39.8	18.2	48.3	36.1	17.8	25.7	20.3	14.5
F, 03V0568	57.5	34.1	20.2	48.5	32.3	22.8	26.0	15.2	17.4
G, 03V0567	26.4	19.1	12.4	25.9	17.1	17.1	56.1	40.7	34.8
H, J19	27.3	17.3	18.8	25.7	17.4	15.1	63.1	48.2	38.2
I, KE135/2012	26.2	17.6	14.1	26.0	13.8	15.9	59.0	44.5	33.3
J, BO4351/Ms/2014	27.0	18.1	15.2	25.2	14.5	14.1	63.0	48.3	43.9

*Values are % sequence similarities. NSP, nonstructural protein; VP, virus protein.
†Incomplete at N terminus (≈70 aa residues missing) and C terminus (≈10 aa residues missing).
‡Incomplete at N terminus (≈40 aa residues missing).
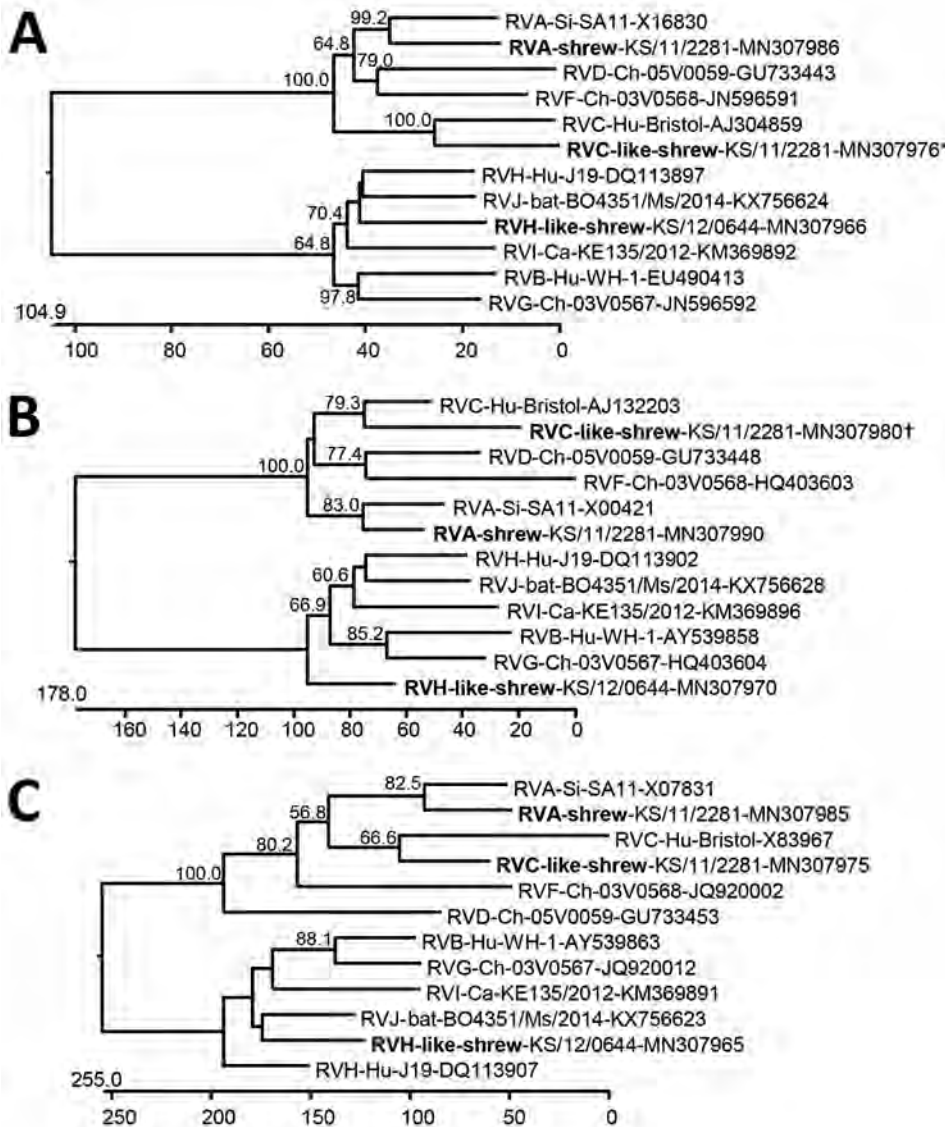
Figure 2. Phylogenetic relationship of shrew rotaviruses (bold), Germany, 2011–2012, with RVA–RVJ determined by using the deduced amino acid sequences of virus protein 1 (A), virus protein 6 (B), and nonstructural protein 5 (C). Trees were constructed by using a neighbor-joining method implemented in the MegAlign module of DNASTAR (https://www.dnastar.com) and a bootstrap analysis with 1,000 trials and 111 random seeds. Bootstrap values of >50% are shown. The rotavirus species, host, strain or sample designation, and GenBank accession number are indicated at each branch. Scale bars indicate amino acid substitutions per 100 residues. *Sequence incomplete at N terminus (≈70 aa residues missing) and C terminus (≈10 aa residues missing). †Sequence incomplete at N terminus (≈40 aa residues missing). Ca, canine; Ch, chicken; Hu, human; RVA, rotavirus A; RVB, rotavirus B; RVC, rotavirus C; RVD, rotavirus D; RVF, rotavirus F; RVG, rotavirus G; RVH, rotavirus H; RVI, rotavirus I; RVJ, rotavirus J; Si, simian.

Acknowledgments

About the Author

Dr. Johne is a senior scientist at the German Federal Institute for Risk Assessment, Berlin, Germany. His research interests are the epidemiology, molecular evolution, pathogenesis, and transmission pathways of foodborne viruses.

References

1. Tate JE, Burton AH, Boschi-Pinto C, Parashar UD; World Health Organization–Coordinated Global Rotavirus Surveillance Network. Global, regional, and national estimates of rotavirus mortality in children <5 years of age, 2000–2013. Clin Infect Dis. 2016; 62(Suppl 2):S96–105. https://doi.org/10.1093/cid/civ1013
2. Attoui H, Mertens PPC, Becnel J, Belaganahalli S, Bergoin M, Brussaard CP, et al. Family: *Reoviridae*. In: King AMQ, Adams MJ, Carstens EB, Lefkowitz EJ, editors. Virus taxonomy: ninth report of the International Committee on Taxonomy of Viruses. Amsterdam: Elsevier Academic Press; 2012. p. 541–637.

3. Bányai K, Kemenesi G, Budinski I, Földes F, Zana B, Marton S, et al. Candidate new rotavirus species in Schreiber's bats, Serbia. Infect Genet Evol. 2017;48:19–26. https://doi.org/10.1016/j.meegid.2016.12.002

4. International Committee on Taxonomy of Viruses. Taxonomic information. Virus taxonomy: 2018b release. 2018 Jul [cited 2019 Aug 21]. https://talk.ictvonline.org/taxonomy

5. Matthijnssens J, Otto PH, Ciarlet M, Desselberger U, Van Ranst M, Johne R. VP6-sequence-based cutoff values as a criterion for rotavirus species demarcation. Arch Virol. 2012;157:1177–82. https://doi.org/10.1007/s00705-012-1273-3

6. Matthijnssens J, Ciarlet M, Rahman M, Attoui H, Bányai K, Estes MK, et al. Recommendations for the classification of group A rotaviruses using all 11 genomic RNA segments. Arch Virol. 2008;153:1621–9. https://doi.org/10.1007/s00705-008-0155-1

7. Martella V, Bányai K, Matthijnssens J, Buonavoglia C, Ciarlet M. Zoonotic aspects of rotaviruses. Vet Microbiol. 2010;140:246–55. https://doi.org/10.1016/j.vetmic.2009.08.028

8. Schlegel M, Radosa L, Rosenfeld UM, Schmidt S, Triebenbacher C, Löhr PW, et al. Broad geographical distribution and high genetic diversity of shrew-borne Seewis hantavirus in Central Europe. Virus Genes. 2012;45:48–55. https://doi.org/10.1007/s11262-012-0736-7

9. Fischer S, Mayer-Scholl A, Imholt C, Spierling NG, Heuser E, Schmidt S, et al. *Leptospira* genomospecies and sequence type prevalence in small mammal populations in Germany. Vector Borne Zoonotic Dis. 2018;18:188–99. https://doi.org/10.1089/vbz.2017.2140

10. Mayer-Scholl A, Hammerl JA, Schmidt S, Ulrich RG, Pfeffer M, Woll D, et al. *Leptospira* spp. in rodents and shrews in Germany.

Int J Environ Res Public Health. 2014;11:7562–74. https://doi.org/10.3390/ijerph110807562

11. Scheuch M, Höper D, Beer M. RIEMS: a software pipeline for sensitive and comprehensive taxonomic classification of reads from metagenomics datasets. BMC Bioinformatics. 2015;16:69. https://doi.org/10.1186/s12859-015-0503-6

12. Tausch SH, Renard BY, Nitsche A, Dabrowski PW. RAMBO-K: rapid and sensitive removal of background sequences from next generation sequencing data. PLoS One. 2015;10:e0137896. https://doi.org/10.1371/journal.pone.0137896

13. Wang XX, Li JX, Wang WG, Sun XM, He CY, Dai JJ. Preliminary investigation of viruses to the wild tree shrews (*Tupaia belangeri chinese*) [in Chinese]. Dongwuxue Yanjiu. 2011;32:66–9.

14. Li K, Lin XD, Huang KY, Zhang B, Shi M, Guo WP, et al. Identification of novel and diverse rotaviruses in rodents and insectivores, and evidence of cross-species transmission into humans. Virology. 2016;494:168–77. https://doi.org/10.1016/j.virol.2016.04.017

15. Otto PH, Rosenhain S, Elschner MC, Hotzel H, Machnowska P, Trojnar E, et al. Detection of rotavirus species A, B, and C in domestic mammalian animals with diarrhoea and genotyping of bovine species A rotavirus strains. Vet Microbiol. 2015;179:168–76. https://doi.org/10.1016/j.vetmic.2015.07.021

Address for correspondence: Reimar Johne, German Federal Institute for Risk Assessment, Diedersdorfer Weg 1, Berlin 12277, Germany; email: reimar.johne@bfr.bund.de

etymologia revisited

Rotavirus

[ro′tə-vi″rəs]

From the Latin *rota,* wheel, plus *virus*. After viewing the virus through an electron microscope in 1974, Flewett et al. suggested the name rotavirus on the basis of the pathogen's shape. The International Committee on Taxonomy of Viruses approved the name 4 years later.

Source: Dorland's illustrated medical dictionary. 31st edition. Philadelphia: Saunders, 2007; Flewett TH, Bryden AS, Davies H, Woode GN, Bridger JC, Derrick JM. Relation between viruses from acute gastroenteritis of children and newborn calves. Lancet. 1974;304:61–3. doi:10.1016/S0140-6736(74)91631-6; Matthews RE. Third report of the International Committee on Taxonomy of Viruses. Classification and nomenclature of viruses. Intervirology. 1979;12:129–296. doi:10.1159/000149081

DOI: 10.3201/eid1708.ET1708

Originally published in August 2011

https://wwwnc.cdc.gov/eid/articles/issue/17/8/table-of-contents

Molecular Confirmation of *Rickettsia parkeri* in *Amblyomma ovale* Ticks, Veracruz, Mexico

Sokani Sánchez-Montes, Gerardo G. Ballados-González, Alejandra Hernández-Velasco, Héctor M. Zazueta-Islas, Marlene Solis-Cortés, Haydee Miranda-Ortiz, Julio C. Canseco-Méndez, Edith A. Fernández-Figueroa,[1] Pablo Colunga-Salas, Andrés M. López-Pérez, Jesús Delgado-de la Mora, Jesús D. Licona-Enriquez, David Delgado-de la Mora, Sandor E. Karpathy, Christopher D. Paddock, Claudia Rangel-Escareño[1]

Author affiliations: Universidad Nacional Autónoma de México, Mexico City, Mexico (S. Sánchez-Montes, H.M. Zazueta-Islas, M. Solis-Cortés, E.A. Fernández-Figueroa, P. Colunga-Salas, A.M. López-Pérez); Universidad Veracruzana, Veracruz, Mexico (G.G. Ballados-González, A. Hernández-Velasco); Instituto Nacional de Medicina Genómica, Mexico City (H. Miranda-Ortiz, J.C. Canseco-Méndez, E.A. Fernández-Figueroa, C. Rangel-Escareño); University of California, Davis, California, USA (A.M. López-Pérez); Instituto Nacional de Ciencias Médicas y Nutrición Salvador Zubirán, Mexico City (J. Delgado-de la Mora); Centro Médico Nacional Siglo XXI, Mexico City (J.D. Licona-Enriquez); Instituto Tecnológico de Sonora, Sonora, Mexico (D. Delgado-de la Mora); Centers for Disease Control and Prevention, Atlanta, Georgia, USA (S.E. Karpathy, C.D. Paddock)

We found *Rickettsia parkeri* in *Amblyomma ovale* ticks collected in Veracruz, Mexico, in 2018. We sequenced gene segments of *gltA*, *htrA*, *sca0*, and *sca5*; phylogenetic reconstruction revealed near-complete identity with *R. parkeri* strain Atlantic Rainforest. Enhanced surveillance is needed in Mexico to determine the public health relevance of this bacterium.

Amblyomma ovale hard ticks are located predominantly in South and Central America but can also be found in areas of the nearctic, particularly Mexico and the southern United States (*1,2*). Immature stages of this species parasitize many mammal and bird species, and adults complete their life cycle on artiodactyls and carnivores, particularly canids (*1,3*). *A. ovale* ticks have been collected predominantly in sylvatic areas, but because free-roaming dogs often enter sylvatic habitats and return to peridomestic settings with attached ticks, these ticks have become distributed into transitional and rural environments (*3*).

In Brazil, this species has been implicated as the main vector of the *Rickettsia parkeri* strain Atlantic Rainforest, an eschar-associated spotted fever pathogen (*3,4*). Since its discovery, strain Atlantic Rainforest has been detected in other hard tick species, including *A. aureolatum* and *Rhipicephalus sanguineus* sensu lato in Argentina, Colombia, and Belize (*4–6*).

In Mexico, *A. ovale* ticks have been collected from 8 species of mammals in 10 of 32 states (*2*). Despite the wide distribution of *A. ovale* ticks in Mexico, attempts to identify *R. parkeri* strain Atlantic Rainforest in this species are lacking.

During July–August 2018, we collected *A. ovale* ticks from dogs in 3 municipalities, Alvarado (18°46′52″N, 95°45′26″W), Catemaco (18°30′36.30″N, 95°02′08.61″W), and Martínez de la Torre (20°04′00″N, 97°03′00″W), in the state of Veracruz, Mexico (Figure, panel A). Ticks were harvested from owned dogs during their evaluations at veterinary clinics and from free-roaming dogs during vaccination campaigns conducted by local rabies vaccination programs. We identified ticks morphologically using a standard taxonomic key (*2*), fixed them in absolute ethanol, and stored them at 4°C.

To extract DNA, we used the Cheelex-100 protocol as previously reported (*7,8*). To evaluate the DNA quality of samples, we amplified a 400-bp segment of the ixodid 16S rRNA gene (*5*). We screened DNA extracts for *Rickettsia* species using a PCR targeting an 800-bp segment of the citrate synthase (*gltA*) gene. With *gltA*-positive samples, we performed PCRs amplifying segments of the *htrA* (549-bp), *sca0* (532-bp), and *sca5* (862-bp) genes (*7,8*). We purified PCR products using Agencourt AMPure XP (https://www.beckman.com) and sequenced amplicons on the ABI 3730xL DNA Analyzer (https://www.thermofisher.com) at the Sequencing Unit of the National Institute of Genomic Medicine (Mexico City, Mexico). We generated consensus sequences using Geneious 2019.1.3 (https://www.geneious.com) and compared these sequences with those of validated *Rickettsia* species deposited in GenBank using the blastn tool (https://blast.ncbi.nlm.nih.gov). We performed global alignments using ClustalW (http://www.clustal.org), concatenated sequences in BioEdit (https://bioedit.org), and then constructed phylogenetic trees in MEGA 6.0 (https://megasoftware.net) using the maximum-likelihood method and 10,000 bootstrap replicates.

We collected 22 adult (16 female, 6 male) *A. ovale* ticks from 6 dogs (tick density of 2–5 ticks per dog). We could amplify ixodid 16S sequences from all samples. We sequenced the 16S gene of 1 female (GenBank accession no. MK792953) and 1 male tick, and both exhibited 99.5% (404/406 bp) sequence identity with sequences of *A. ovale* ticks from Colombia (GenBank accession nos.

---

[1]These authors were co–principal investigators.
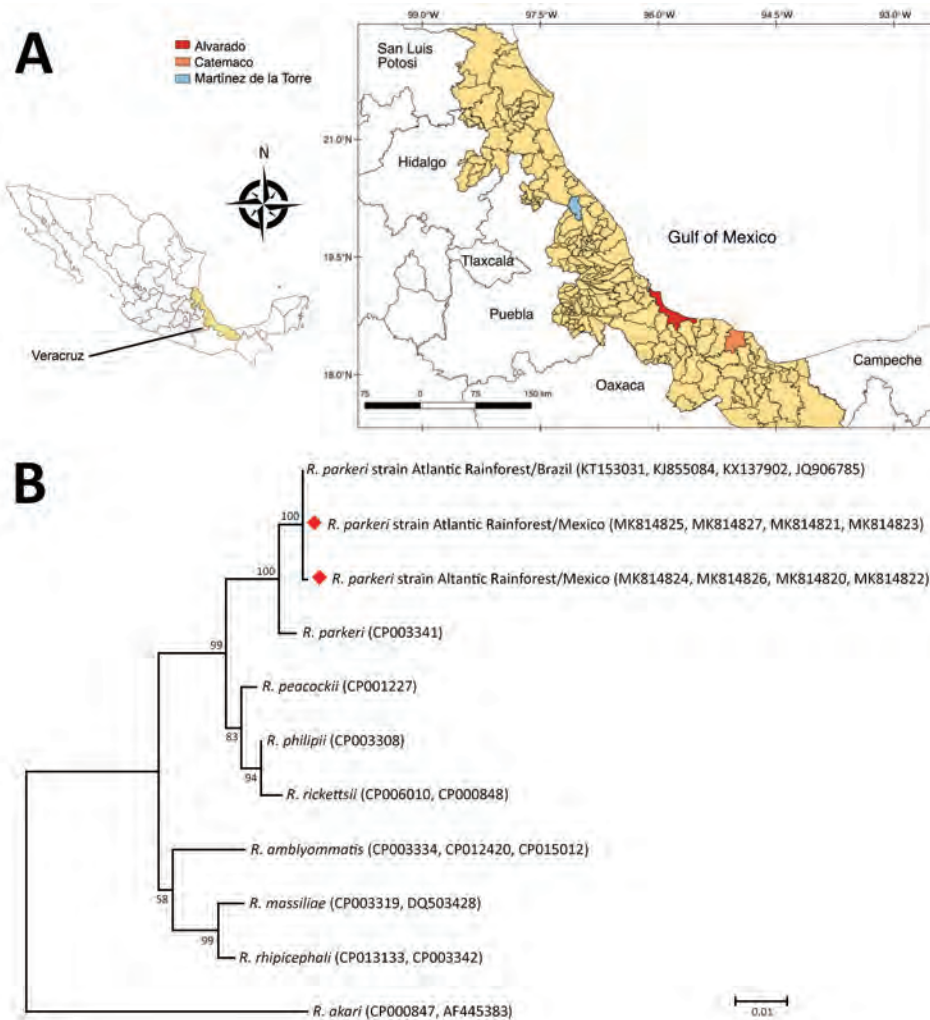
Figure. *Amblyomma ovale* tick sampling sites and phylogenetic analysis of tickborne *Rickettsia parkeri* strain Atlantic Rainforest isolates (diamonds), state of Veracruz, Mexico, July–August 2018. A) Sites where *A. ovale* ticks were collected from dogs to assess prevalence of *R. parkeri* strain Atlantic Rainforest. Inset shows location of Veracruz state in Mexico. QGis (https://www.qgis.org) was used for map construction. B) Maximum-likelihood phylogenetic tree generated with concatenated segments of the *gltA*, *htrA*, *sca0*, and *sca5* genes (2,476 bp total) of several members of spotted fever group *Rickettsia*. Bootstrap values >50 are indicated at nodes. GenBank accession numbers are provided. Scale bar indicates nucleotide substitutions per site.

MF353104.1–5.1). Six (27.3%) specimens tested positive for *Rickettsia* DNA, including 1 female specimen from Alvarado, 2 female specimens from Martínez de la Torre, and 2 female specimens and 1 male specimen from Catemaco. The *gltA*, *htrA*, *sca0*, and *sca5* gene segments could be amplified for all 6 samples. Each gene segment was 99%–100% identical to that of the *R. parkeri* strain Atlantic Rainforest from Brazil and Argentina (Figure, panel B; data not shown). Phylogenetic analysis corroborated the presence of 2 *R. parkeri* strain Atlantic Rainforest haplotypes: 1 for the northern region (Martínez de la Torre; GenBank accession nos. MK844821, MK844823, MK844825, MK844827) and 1 for the central and southern regions (Alvarado and Catemaco; GenBank accession nos. MK844820, MK844822, MK844824, MK844826) of Veracruz. With a bootstrap value of 100, both haplotypes clustered in a clade comprising other *R. parkeri* strains.

Our findings document *R. parkeri* strain Atlantic Rainforest farther north than previous reports (*4–6*). The discovery of this pathogen in ticks associated with dogs in different localities of Veracruz has implications for public health safety. In this state, the Ministry of Health reported 22 cases of spotted fever during 2015–2017 (*9*). *R. rickettsii*, the etiologic agent of Rocky Mountain spotted fever, has been previously described in *A. mixtum* (formerly *A. cajennense*) ticks collected from Veracruz (*10*), suggesting the potential for co-circulation of *R. rickettsii* and *R. parkeri* in ticks in this state. Two other *R. parkeri* lineages have been detected circulating in Mexico: *R. parkeri* strain black gap in the rabbit tick (*Dermacentor parumapertus*) in Sonora and Chihuahua (*7*) and *R. parkeri* sensu stricto associated with *A. maculatum* ticks (*8*). These findings emphasize the need for enhanced surveillance studies of these rickettsia in Mexico to better elucidate the evolutionary, ecologic, and public health relevance of the various *R. parkeri* strains.

About the Author

Dr. Sanchez-Montes is a biologist at the Tropical Medicine Center of the Universidad Nacional Autónoma de México, Mexico City, Mexico, in charge of detecting rickettsial agents. His interests are the identification of rickettsial agents, pathogen–host interactions, and epidemiology of zoonotic emerging diseases.

References

1. Guglielmone AA, Robbins RG, Apanaskevich DA, Petney TN, Estrada-Peña A, Horak IG. The hard ticks of the world. Dordrecht (the Netherlands): Springer; 2014. p. 978–94.
2. Guzmán-Cornejo C, Robbins RG, Guglielmone AA, Montiel-Parra G, Pérez TM. The *Amblyomma* (Acari: Ixodida: *Ixodidae*) of Mexico: identification keys, distribution and hosts. Zootaxa. 2011;2998:16–38.
3. Bitencourth K, Amorim M, de Oliveira SV, Voloch CM, Gazêta GS. Genetic diversity, population structure and rickettsias in *Amblyomma ovale* in areas of epidemiological interest for spotted fever in Brazil. Med Vet Entomol. 2019;33:256–68. https://doi.org/10.1111/mve.12363
4. Nieri-Bastos FA, Marcili A, De Sousa R, Paddock CD, Labruna MB. Phylogenetic evidence for the existence of multiple strains of *Rickettsia parkeri* in the New World. Appl Environ Microbiol. 2018;84:e02872-17. https://doi.org/10.1128/AEM.02872-17
5. Lopes MG, Junior JM, Foster RJ, Harmsen BJ, Sanchez E, Martins TF, et al. Ticks and rickettsiae from wildlife in Belize, Central America. Parasit Vectors. 2016;9:62. https://doi.org/10.1186/s13071-016-1348-1
6. Lamattina D, Tarragona EL, Nava S. Molecular detection of the human pathogen *Rickettsia parkeri* strain Atlantic Rainforest in *Amblyomma ovale* ticks in Argentina. Ticks Tick Borne Dis. 2018;9:1261–3. https://doi.org/10.1016/j.ttbdis.2018.05.007
7. Sánchez-Montes S, López-Pérez AM, Guzmán-Cornejo C, Colunga-Salas P, Becker I, Delgado-de la Mora J, et al. *Rickettsia parkeri* in *Dermacentor parumapertus* ticks, Mexico. Emerg Infect Dis. 2018;24:1108–11. https://doi.org/10.3201/eid2406.180058
8. Delgado-de la Mora J, Sánchez-Montes S, Licona-Enríquez JD, Delgado-de la Mora D, Paddock CD, Beati L, et al. *Rickettsia parkeri* and *Candidatus* Rickettsia andeanae in tick of the *Amblyomma maculatum* group, Mexico. Emerg Infect Dis. 2019;25:836–8. https://doi.org/10.3201/eid2504.181507
9. Dirección General de Epidemiología. Anuarios de morbilidad 1984–2018. 2019 Jun 26 [cited 2019 Sep 18]. https://www.gob.mx/salud/acciones-y-programas/anuarios-de-morbilidad-1984-2018
10. Bustamante ME, Varela G. Estudios de fiebre manchada en México: hallazgo del *Amblyomma cajennense* naturalmente infectado en Veracruz. Rev Inst Salubr Enferm Trop. 1946;7:75–8.

Rhombencephalitis and Myeloradiculitis Caused by a European Subtype of Tick-Borne Encephalitis Virus

Lorna Neill, Anna M. Checkley, Laura A. Benjamin, M. Trent Herdman, Daniel P. Carter, Steven T. Pullan, Emma Aarons, Katie Griffiths, Bernadette Monaghan, Kushan Karunaratne, Olga Ciccarelli, Jennifer Spillane, David A.J. Moore, Dimitri M. Kullmann

Author affiliations: University College London Hospitals, London, UK (L. Neill, A.M. Checkley, L.A. Benjamin, M.T. Herdman, B. Monaghan, K. Karunaratne, O. Ciccarelli, J. Spillane, D.A.J. Moore, D.M. Kullmann); University College London, London (L.A. Benjamin, O. Ciccarelli, J. Spillane, D.M. Kullmann); Public Health England, Porton Down, UK (M.T. Herdman, D.P. Carter, S.T. Pullan, E. Aarons, K. Griffiths); London School of Hygiene and Tropical Medicine, London (D.A.J. Moore)

We report a case of a previously healthy man returning to the United Kingdom from Lithuania who developed rhombencephalitis and myeloradiculitis due to tick-borne encephalitis. These findings add to sparse data on tick-borne encephalitis virus phylogeny and associated neurologic syndromes and underscore the importance of vaccinating people traveling to endemic regions.

Tick-borne encephalitis virus (TBEV) is an emerging disease caused by a neurotropic flavivirus; its incidence is increasing in north, central, and eastern Europe (*1,2*). Typical resulting neurologic illnesses include meningitis or meningoencephalitis (*3*). Cases peak in the summer, when contact between humans and tick vectors is highest, and infection is associated with time spent in meadows and forests (*1,2*). We report a previously healthy 38-year-old man from the United Kingdom who had unusual neurologic manifestations of TBEV after travel to Lithuania.

The patient, who had received no travel-related vaccinations, traveled to the Kaunas region, where he visited woodlands. He reported having received insect bites on his feet. Seven days after arriving in Lithuania, he developed influenza-like symptoms, which continued after his return to the United Kingdom. Ten days later, he reported neck stiffness, photophobia, slurred speech, tongue deviation to the left, and left leg weakness; the next day, progressive bilateral lower limb weakness in his hips, urinary retention, and constipation developed. At that time, he sought treatment at a hospital.

On examination, the patient was febrile (38.0°C) and had a peripheral leukocyte count of 15×10^9 cells/L and C-reactive protein of 120 mg/L. Cauda equina syndrome was ruled out by using lumbar-sacral magnetic resonance imaging; results of a computed tomography scan of the head were unremarkable. Pleocytosis was identified in the cerebrospinal fluid (CSF), and the patient was empirically treated with ceftriaxone and acyclovir (Appendix Table, https://wwwnc.cdc.gov/EID/article/25/12/19-1017-App.pdf).

Two days after neurologic signs began, the patient became breathless and drowsy. Neurologic examination revealed dysarthria, interrupted saccades, and difficulty with alternating lateral tongue movements. He exhibited a pout reflex and a brisk jaw jerk. Upper limbs had normal tone; power was graded 4+/5 on the Medical Research Council (MRC) scale (https://mrc.ukri.org/research/facilities-and-resources-for-researchers/mrc-scales/mrc-muscle-scale) for shoulder abduction and elbow extension bilaterally but was otherwise normal. The patient had reduced tone in his lower limbs and bilateral proximal muscle weakness affecting hip and knee flexors (MRC grade 1–2/5); distal limb power was less affected (MRC grade 4/5). He was areflexic and had bilateral flexor plantars. Pinprick testing indicated dermatomal sensory loss isolated from L2 to L5 on the left. Forced vital capacity was 800 mL (reference >1,700 mL); therefore, due to respiratory muscle weakness, he was intubated and transferred to a neurology hospital. Repeat CSF testing showed a profile similar to the initial test (Appendix Table). Antituberculosis therapy was added because of the enigmatic etiology.

Magnetic resonance imaging of the brain and spinal cord demonstrated long-segment myelitis with high T2 signal in the central cord extending from C2 through T12; no intracranial lesions or pathological enhancement were seen (Figure). Neurophysiology test results pointed to a preganglionic lesion, with decreased compound muscle action potentials in the L4–S1 myotomes, in the context of a normal motor conduction velocity and sensory nerve action potential. Mild denervation affecting L4–S1 roots did not explain the patient's degree of weakness. His neurologic syndrome was consistent with rhombencephalitis and myeloradiculitis. High-dose steroid was added to cover the possibility of neuromyelitis optica.

Blood and CSF were screened for inflammatory and infective etiologies (Appendix Table). Serum and urine samples were sent to the Rare and Imported Pathogens Laboratory (Porton Down, UK) for serologic and PCR testing for alphaviruses, flaviviruses, and rickettsial infections. Serum and urine PCR results were positive for TBEV RNA; serum and CSF results were positive for TBEV IgG (Appendix Table). Metagenomic RNA sequencing confirmed TBEV. A total of 129 reads (0.01% of total reads) were identified

as TBEV, sufficient to elucidate the full envelope gene sequence at a minimum coverage depth of 5× (when mapped to reference sequence GenBank accession no. KC154190.1). No reads were observed for other pathogens. Phylogenetic analysis of the envelope gene revealed the isolate was most closely related to the European TBEV clade (GenBank accession no. MK992869) (Appendix Figure).

Detection of TBEV RNA from both blood and urine is diagnostic of acute TBEV infection (1). On day 14, antibiotics, antivirals, and steroids were stopped; antituberculosis therapy had been halted earlier. The patient was extubated on day 17 and has slowly recovered. However, he has residual profound proximal left leg weakness and bladder and bowel dysfunction.
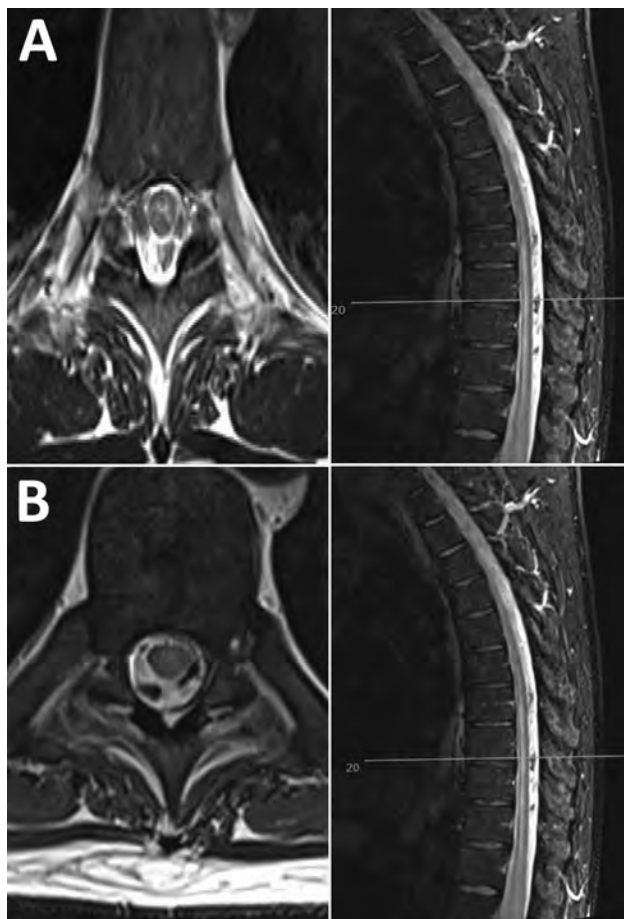
Figure. Neurologic manifestations of tick-borne encephalitis in a 38-year-old man from the United Kingdom after travel to Lithuania. A) Magnetic resonance imaging of the brain and spinal cord at onset of neurologic signs, showing possible longitudinal extensive transverse myelitis in the cervical and thoracic cord, with involvement of the central gray matter. B) One month later, increased T2 signal and mild swelling of the central gray matter of the cervical cord have both regressed, with some residual subtle signal changes throughout the spinal cord. Left, axial images; right, sagittal images.

Several subtypes of TBEV cause disease: European, Siberian, and Far Eastern (*1*). Siberian and Far Eastern have been associated with worse outcomes (*1*), but the potentially fatal neurologic complications in this patient are consistent with emerging data indicating that the European subtype causes more severe disease than previously thought (*4–6*). In <10% of cases, TBEV targets the anterior horn of the spinal cord, resulting in flaccid poliomyelitis-like paralysis (*3,7*), or, rarer still, as in this case, in paralysis of respiratory muscles, requiring artificial ventilation (*3,8,9*).

Treatment of TBEV is supportive only; vaccination and avoiding mosquito bites are key to disease prevention and control. Although some TBEV-endemic countries have vaccination programs, level of uptake varies (*10*). Public health experts recommend that travelers undertaking high-exposure activities in endemic countries get vaccinated. This case underscores the importance of vaccination among groups of susceptible people and improved awareness of this emerging disease.

About the Author

Dr. Neill is a junior doctor currently working at University College Hospital London. Her research interests include infectious diseases and hematological malignancy.

References

1. Taba P, Schmutzhard E, Forsberg P, Lutsar I, Ljøstad U, Mygland Å, et al. EAN consensus review on prevention, diagnosis and management of tick-borne encephalitis. Eur J Neurol. 2017;24:1214–e61. https://doi.org/10.1111/ene.13356
2. European Centre for Disease Prevention and Control. Tick-borne encephalitis. In: Annual epidemiological report for 2016. Stockholm: The Centre; 2018.
3. Kaiser R. The clinical and epidemiological profile of tick-borne encephalitis in southern Germany 1994–98: a prospective study of 656 patients. Brain. 1999;122:2067–78. https://doi.org/10.1093/brain/122.11.2067
4. Mansfield KL, Johnson N, Phipps LP, Stephenson JR, Fooks AR, Solomon T. Tick-borne encephalitis virus—a review of an emerging zoonosis. J Gen Virol. 2009;90:1781–94. https://doi.org/10.1099/vir.0.011437-0
5. Kuivanen S, Smura T, Rantanen K, Kämppi L, Kantonen J, Kero M, et al. Fatal tick-borne encephalitis virus infections caused by Siberian and European subtypes, Finland, 2015. Emerg Infect Dis. 2018;24:946–8. https://doi.org/10.3201/eid2405.171986
6. Bender A, Schulte-Altedorneburg G, Walther EU, Pfister HW. Severe tick borne encephalitis with simultaneous brain stem, bithalamic, and spinal cord involvement documented by MRI. J Neurol Neurosurg Psychiatry. 2005;76:135–7. https://doi.org/10.1136/jnnp.2004.040469
7. Beer S, Brune N, Kesselring J. Detection of anterior horn lesions by MRI in central European tick-borne encephalomyelitis. J Neurol. 1999;246:1169–71. https://doi.org/10.1007/s004150050537
8. Lenhard T, Ott D, Jakob NJ, Pham M, Bäumer P, Martinez-Torres F, et al. Predictors, neuroimaging characteristics and long-term outcome of severe European tick-borne encephalitis: a prospective cohort study. PLoS ONE. 2016;11:e0154143. https://doi.org/10.1371/journal.pone.0154143
9. Schellinger PD, Schmutzhard E, Fiebach JB, Pfausler B, Maier H, Schwab S. Poliomyelitic-like illness in central European encephalitis. Neurology. 2000;55:299–302. https://doi.org/10.1212/WNL.55.2.299
10. Jacob L, Kostev K. Compliance with vaccination against tick-borne encephalitis virus in Germany. Clin Microbiol Infect. 2017;23:460–3. https://doi.org/10.1016/j.cmi.2017.01.012

Address for correspondence: Laura A. Benjamin, UCL Queen Square Institute of Neurology, Stroke Research Centre, Department of Brain Repair and Rehabilitation, Russell Square House, 10-12 Russell Sq, London WC1B 5EH, UK; email: l.benjamin@ucl.ac.uk

Aspergillus felis in Patient with Chronic Granulomatous Disease

Olivier Paccoud, Romain Guery, Sylvain Poirée, Grégory Jouvion, Marie Elisabeth Bougnoux, Emilie Catherinot, Olivier Hermine, Olivier Lortholary, Fanny Lanternier

Author affiliations: Hôpital Necker-Enfants Malades, Paris, France (O. Paccoud, R. Guery, S. Poirée, M.E. Bougnoux, O. Hermine, O. Lortholary, F. Lanternier); Institut Pasteur, Paris (G. Jouvion, O. Lortholary, F. Lanternier); Hôpital Foch, Université Versailles-Saint-Quentin-en-Yvelines, Versailles, France (E. Catherinot)

We report a case of *Aspergillus felis* infection in a patient with chronic granulomatous disease who had overlapping features of invasive pulmonary aspergillosis and allergic bronchopulmonary aspergillosis. Identifying the species responsible for aspergillosis by molecular methods can be crucial for directing patient management and selection of appropriate antifungal agents.

A 42-year-old man with X-linked chronic granulomatous disease (CGD) sought care at a hospital in Paris, France, for a 2-week history of cough and night sweats. He had been receiving long-term prophylaxis with itraconazole (400 mg/d) and had normal trough levels (1,240 µg/L) 1 month before his hospital visit.

At admission, blood counts showed mild leukocytosis (leukocytes 9.6×10^9 cells/L, reference range $4–10 \times$

Table. Defining features of invasive pulmonary aspergillosis and allergic bronchopulmonary aspergillosis in a 42-year-old man with X-linked chronic granulomatous disease, Paris, France*

Category	Defining features			
	IPA (oncohematologic setting)	IPA during CGD	Patient in this study	ABPA
Underlying disease	Neutropenia	CGD, particularly X-linked CGD	X-linked CGD	Asthma, cystic fibrosis
Mechanisms of disease	Angioinvasion	Tissue invasion, little or no angioinvasion	No angioinvasion	Exaggerated inflammatory response to *Aspergillus*
Course of infection	Acute, single event	Subacute or chronic, single event	Subacute, single event	Chronic with exacerbations
Radiographic findings	Cavitation, pulmonary infarction, air crescent sign, halo sign	Single or multiple nodules and consolidations	Single consolidation	Central bronchiectasis, pulmonary infiltrates, mucus plugs
Galactomannan testing	Positive	Positive or negative	Negative	Negative
Total serum IgE	Normal	Normal	Elevated (1,410 IU/L)	Elevated (>1,000 IU/L)
Aspergillus species-specific IgE or skin test reactivity	Negative	Negative	Positive (7 IU/mL)	Positive (>0.1 IU/mL)
Aspergillus IgG	Negative	Negative	Positive (54 IU/mL)	Positive (>10 IU/mL)
Precipitating antibodies to *Aspergillus*	Negative	Negative	Positive (2 arcs of precipitation)	Positive (>1 arc of precipitation)
Blood eosinophilia	Absent	Absent; reported only during "fulminant mulch pneumonia"	Present (2.2×10^9 cells/L)	Present ($>0.5 \times 10^9$ cells/L)
First-line treatment	Antifungal treatment	Antifungal treatment	Antifungal treatment	Systemic or inhaled corticosteroids

*ABPA, allergic bronchopulmonary aspergillosis; CGD, chronic granulomatous disease; IPA, invasive pulmonary aspergillosis.

10^9 cells/L), with neutrophils at 6.1×10^9 cells/L (reference range 1.5–7×10^9 cells/L) and eosinophils at 2×10^9 cells/L (reference $<0.5 \times 10^9$ cells/L). Computed tomography (CT) revealed an upper left lobe consolidation (Appendix Figure, https://wwwnc.cdc.gov/EID/article/25/12/19-1020-App1.pdf). We administered broad-spectrum antimicrobial drugs (2 g meropenem 3×/d and 20 mg/kg/d amikacin). Results of bacterial and mycological cultures from sputum were negative, as was serum galactomannan.

The patient's condition did not improve, so we administered liposomal amphotericin B (5 mg/kg/d) and caspofungin (70 mg/d loading dose followed by 50 mg/d). Bronchoalveolar lavage demonstrated hypercellularity (1.22×10^6 cells/mL); manual differential showed 12% macrophages and 76% eosinophils. Results of bacterial, mycological, and mycobacterial cultures were negative. Pathology studies from a transbronchial biopsy revealed numerous eosinophilic granulomas alongside Charcot-Leyden crystals (Appendix Figure). Grocott methenamine silver staining revealed rare septated filamentous hyphae, but results of mycological cultures were negative. The patient had elevated total serum IgE (1,210 IU/mL, reference <114 IU/mL), elevated serum *A. fumigatus* IgE (7 IU/mL, reference <0.1 IU/mL) and *A. fumigatus* IgG (54 IU/mL, reference <5 IU/mL), and precipitating antibodies to *A. fumigatus* (2 arcs of precipitation in immunoelectrophoresis). Results of parasitologic examination of fecal samples and serologic testing for alternative causes of eosinophilia were negative.

Eosinophilia persisted (1.8–2×10^9 cells/L) despite antiparasitic treatment with ivermectin (5 mg/kg/d at days 1 and 7) and albendazole (400 mg/d for 7 d). Pathology findings from a transthoracic percutaneous biopsy revealed granulomas with Grocott-positive septated hyphae. Result of an *Aspergillus* section Fumigati PCR on a biopsy specimen were positive, and mycological cultures yielded a mold morphologically identified as *Aspergillus*. After 5 weeks of liposomal amphotericin B therapy (including 2 weeks of combination therapy with caspofungin), we switched treatment to oral voriconazole (loading dose of 400 mg 2×/d, followed by 200 mg 2×/d). Normalization of eosinophilia occurred at 6 weeks.

We sent mycological cultures from the biopsy specimens to the French National Center for Invasive Mycoses and Antifungals (Paris). Molecular identification based on the partial sequence of the internal transcribed spacer 2, 5.8S ribosomal RNA gene, and internal transcribed spacer 2 (525/526 bp; 99% similarity to the type strain, CBS 130245; GenBank accession no. KF558318.1) and the β-tubulin target gene enabled the identification of *Aspergillus felis* (109/109 bp; 100% similarity to the type strain, CBS DTO_131-E3 β-tubulin [*benA*] gene, partial cds; GenBank accession no. KY808576.1). The European Committee for Antimicrobial Susceptibility Testing (EUCAST) MICs with broth microdilution methods (*1*) were 4 μg/L for voriconazole, 4 μg/L for itraconazole, 0.25 μg/L for posaconazole, 2 μg/L for caspofungin, and 4 μg/L for amphotericin B. Based on EUCAST MIC breakpoints for *A. fumigatus* (*2*), we switched treatment to oral posaconazole (loading dose of 300 mg 2×/d,

followed by 300 mg/d). Chest CT performed 12 months after treatment initiation showed noticeable improvement of pulmonary lesions.

Invasive pulmonary aspergillosis (IPA) remains a leading cause of death during CGD, and typically manifests as subacute pneumonia, with little or no angioinvasion (*3*). This patient had pulmonary infection caused by *A. felis* with overlapping features of IPA and allergic bronchopulmonary aspergillosis (ABPA) (*4*). Sensitization to *Aspergillus* spp. in patients with CGD (*5*) and tissue eosinophilia in lung pathology studies during invasive fungal infections (*6*) have been reported but do not seem to be common features of IPA in patients with CGD (*3,7*). There was some uncertainty about whether *A. felis* was responsible for this overlapping phenotype between IPA and ABPA (Table).

A. felis is a member of the *A. viridinutans* complex, a group of cryptic species belonging to *Aspergillus* section Fumigati (*8*). Such fumigati-mimetic molds are increasingly being recognized as sporadic causes of IPA (*9*). *A. felis* has been reported as a cause of sino-orbital aspergillosis in cats, but less frequently in humans (*8*). In one such case of IPA, and in the few reported cases in patients with CGD of IPA caused by the closely related *A. pseudoviridinutans* and *A. udagawae*, the course of infection was more protracted than for *A. fumigatus* infections, and dissemination occurred in a contiguous manner (*10*). Nonfumigatus *Aspergillus* spp. exhibit decreased in vitro susceptibility to commonly used antifungal drugs. Most previously reported antifungal susceptibilities from *A. felis* isolates showed high MICs for voriconazole and itraconazole but lower MICs for posaconazole (*8*).

Because isolates may be misidentified as *A. fumigatus*, culture-based morphological identification of invasive fungal infections in CGD may sometimes be insufficient. In cases of breakthrough fungal infections, or when faced with an atypical or refractory course of infection, identification of the fungus at a species level by molecular methods appears to be critical to guiding proper patient management.

Acknowledgments

About the Author

Dr. Paccoud is an infectious diseases resident at Necker Hospital, Paris, France. His primary interests include care for immunocompromised patients, fungal infections, and infectious disease epidemiology.

References

1. Subcommittee on Antifungal Susceptibility Testing of the ESCMID European Committee for Antimicrobial Susceptibility Testing. EUCAST technical note on the method for the determination of broth dilution minimum inhibitory concentrations of antifungal agents for conidia-forming moulds. Clin Microbiol Infect. 2008;14:982–4. https://doi.org/10.1111/j.1469-0691.2008.02086.x
2. EUCAST. Antifungal agents: breakpoint tables for interpretation of MICs. 2018 [cited 2019 Aug 24]. http://www.eucast.org/fileadmin/src/media/PDFs/EUCAST_files/AFST/Clinical_breakpoints/Antifungal_breakpoints_v_9.0_180212.pdf
3. Henriet S, Verweij PE, Holland SM, Warris A. Invasive fungal infections in patients with chronic granulomatous disease. Adv Exp Med Biol. 2013;764:27–55. https://doi.org/10.1007/978-1-4614-4726-9_3
4. Greenberger PA, Bush RK, Demain JG, Luong A, Slavin RG, Knutsen AP. Allergic bronchopulmonary aspergillosis. J Allergy Clin Immunol Pract. 2014;2:703–8. https://doi.org/10.1016/j.jaip.2014.08.007
5. Eppinger TM, Greenberger PA, White DA, Brown AE, Cunningham-Rundles C. Sensitization to *Aspergillus* species in the congenital neutrophil disorders chronic granulomatous disease and hyper-IgE syndrome. J Allergy Clin Immunol. 1999;104:1265–72. https://doi.org/10.1016/S0091-6749(99)70023-0
6. Moskaluk CA, Pogrebniak HW, Pass HI, Gallin JI, Travis WD. Surgical pathology of the lung in chronic granulomatous disease. Am J Clin Pathol. 1994;102:684–91. https://doi.org/10.1093/ajcp/102.5.684
7. Beauté J, Obenga G, Le Mignot L, Mahlaoui N, Bougnoux M-E, Mouy R, et al.; French PID Study Group CEREDIH. Epidemiology and outcome of invasive fungal diseases in patients with chronic granulomatous disease: a multicenter study in France. Pediatr Infect Dis J. 2011;30:57–62. https://doi.org/10.1097/INF.0b013e3181f13b23
8. Barrs VR, van Doorn TM, Houbraken J, Kidd SE, Martin P, Pinheiro MD, et al. *Aspergillus felis* sp. nov., an emerging agent of invasive aspergillosis in humans, cats, and dogs. PLoS One. 2013;8:e64871. https://doi.org/10.1371/journal.pone.0064871
9. Seyedmousavi S, Lionakis MS, Parta M, Peterson SW, Kwon-Chung KJ. Emerging *Aspergillus* species almost exclusively associated with primary immunodeficiencies. Open Forum Infect Dis. 2018;5:ofy213. https://doi.org/10.1093/ofid/ofy213
10. Vinh DC, Shea YR, Sugui JA, Parrilla-Castellar ER, Freeman AF, Campbell JW, et al. Invasive aspergillosis due to *Neosartorya udagawae*. Clin Infect Dis. 2009;49:102–11. https://doi.org/10.1086/599345

Address for correspondence: Fanny Lanternier, Hôpital Necker-Enfants Malades, Service de Maladies Infectieuses et Tropicales, 149 Rue de Sèvres, 75015 Paris, France; email: fanny.lanternier@aphp.fr

Fatal Brazilian Spotted Fever Associated with Dogs and *Amblyomma aureolatum* Ticks, Brazil, 2013

Elisa S.M.M. Savani, Francisco B. Costa,
Elisabete A. Silva, Ana C.F. Couto,
Melanie Gutjahr, Juliana N.M.O. Alves,
Fabiana C.P. Santos, Marcelo B. Labruna

Author affiliations: Prefeitura de São Paulo, São Paulo, Brazil
(E.S.M.M. Savani, E.A. Silva, A.C.F. Couto, M. Gutjahr,
J.N.M.O. Alves); Universidade de São Paulo, São Paulo
(F.B. Costa, M.B. Labruna); Instituto Adolfo Lutz, São Paulo
(F.C.P. Santos)

In São Paulo metropolitan area, Brazil, *Amblyomma aureolatum* ticks are the main vector of *Rickettsia rickettsii*, which causes Brazilian spotted fever. In 2013, a boy in São Paulo died of Brazilian spotted fever associated with household dogs and *A. aureolatum* ticks. Prompt recognition and treatment of this illness might prevent deaths.

The bacterium *Rickettsia rickettsii* is the etiologic agent of Rocky Mountain spotted fever; in Brazil, this illness is called Brazilian spotted fever and is a national notifiable tickborne disease with fatality rates ≈50% (*1,2*). Since the 1920s, the vector of *R. rickettsii* in the southern São Paulo metropolitan area has been the *Amblyomma aureolatum* tick (*3,4*). In this area, free-roaming domestic dogs (major hosts of *A. aureolatum* ticks) are presumed to play a role in carrying *R. rickettsii*–infected ticks from forest fragments (*A. aureolatum* tick habitat) to household interiors (*4,5*). Dogs could thus be associated with the higher incidence of Brazilian spotted fever in women and children, who usually spend more time indoors, in close contact with dogs (*5*).

In November 2013, a 12-year-old boy died after 8 days of an acute febrile illness. He lived in the neighborhood of Sete Praias, near Atlantic forest remnants in the southern São Paulo metropolitan area. On day 3 of illness, he was admitted to the Nasf-Unifesp Hospital in the city of São Paulo with fever (temperature 39.5°C), headache, nausea, asthenia, and abdominal rash. The patient's mother informed the physician that her son had been bitten by a tick on his nape ≈1 week before disease onset; the tick was removed and discarded. The boy was medicated with dipyrone and sent home. On day 6, the patient was returned to the hospital, unconscious, with jaundice and seizures. He was transferred to the intensive care unit; meningitis was suspected. The next day, his condition worsened, and

when hematologic and biochemical examinations indicated thrombocytopenia and hepatic alterations, meningitis was ruled out. A blood serum sample was submitted for leptospirosis and spotted fever testing by serologic and molecular analysis, respectively. Results for leptospirosis were negative. The patient died on day 8 of illness. While the body was being prepared for the funeral, a tick was found attached behind the ear and was sent to the laboratory of the Prefeitura de São Paulo, where it was identified as an *A. aureolatum* unengorged female.

DNA extracted from the serum sample by use of Pure-Link Viral RNA/DNA Mini Kit (Invitrogen, https://www.thermofisher.com) was positive by Taqman real-time PCR for the genus *Rickettsia* (*6*). We therefore next performed 2 conventional PCRs, 1 targeting a 401-bp fragment of the rickettsial *gltA* gene (*7*) and the other targeting a 631-bp fragment of the rickettsial *ompA* gene (*8*). Both yielded amplicons that, after DNA sequencing, had sequences 100% identical to *R. rickettsii* (GenBank accession no. CP003305) by BLAST analyses (http://blast.ncbi.nlm.nih.gov/Blast.cgi).

Immediately after the patient's death, the hospital notified the São Paulo Board of Health of this case, and we performed an epidemiologic investigation. In the patient's household, we collected blood samples from 3 dogs and 11 cats, all adults, born and raised in the area, with free access to surrounding forests and the dwelling interior. Direct contact between the patient and his pets was reportedly common. Serum from the dogs and cats was tested for *R. rickettsii* IgG by immunofluorescence assay, as described (*3*). Seroreactivity was detected in the 3 dogs (endpoint titers 512, 2,048, and 4,096) and 3 of the cats (titers 64, 64, and 512).

During animal sampling, we collected 13 ticks from 1 dog and 1 tick from 1 cat; all ticks were *A. aureolatum* adults. These 14 ticks, plus the 1 from the patient's body, were submitted for DNA extraction (*5*) and tested by the same 2 conventional PCRs. Two ticks (1 from the dog and the 1 from the patient) yielded *gltA* and *ompA* amplicons, which generated DNA sequences 100% identical to *R. rickettsii* (CP003305).

This fatal case of Brazilian spotted fever was epidemiologically associated with *A. aureolatum* ticks and domestic dogs. Because the patient had no recent history of traveling outside his neighborhood, we infer that he acquired the infection in his neighborhood, where *R. rickettsii* was circulating between ticks and his dogs. Although the *A. aureolatum* tick collected postmortem from the patient harbored *R. rickettsii*, we cannot be sure that this particular tick was the primary vector of the bacterium to the patient because the tick would certainly have been exposed to an infected blood meal during the last days of the patient's life. We can, however, confirm that the patient was exposed in his neighborhood to *A. aureolatum* ticks, competent vectors of *R. rickettsii* (*5*). Because fed adult *A. aureolatum* ticks need only 10 minutes of attachment to transmit *R. rickettsii* to hosts (*5*), the likelihood

of such transmission for this patient was high, considering his close contact with his pets. Had the physicians suspected Brazilian spotted fever when the boy was first admitted to the hospital on day 3 of febrile illness, treatment with appropriate antimicrobial drugs might have prevented his death (*9*).

This work was performed at the University of São Paulo, Prefeitura de São Paulo, and Adolfo Lutz Institute, São Paulo, SP, Brazil.

About the Author

Dr. Savani is an epidemiologist at the São Paulo City Board of Health. Her research interests are epidemiology and control of urban zoonoses.

References

1. Parola P, Paddock CD, Socolovschi C, Labruna MB, Mediannikov O, Kernif T, et al. Update on tick-borne rickettsioses around the world: a geographic approach. Clin Microbiol Rev. 2013;26:657–702. https://doi.org/10.1128/CMR.00032-13
2. de Oliveira SV, Guimarães JN, Reckziegel GC, Neves BM, Araújo-Vilges KM, Fonseca LX, et al. An update on the epidemiological situation of spotted fever in Brazil. J Venom Anim Toxins Incl Trop Dis. 2016;22:22.4 https://doi.org/10.1186/s40409-016-0077-4
3. Ogrzewalska M, Saraiva DG, Moraes-Filho J, Martins TF, Costa FB, Pinter A, et al. Epidemiology of Brazilian spotted fever in the Atlantic Forest, state of São Paulo, Brazil. Parasitology. 2012;139:1283–300. https://doi.org/10.1017/S0031182012000546
4. Scinachi CA, Takeda GACG, Mucci LF, Pinter A. Association of the occurrence of Brazilian spotted fever and Atlantic rain forest fragmentation in the São Paulo metropolitan region, Brazil. Acta Trop. 2017;166:225–33. https://doi.org/10.1016/j.actatropica.2016.11.025
5. Saraiva DG, Soares HS, Soares JF, Labruna MB. Feeding period required by *Amblyomma aureolatum* ticks for transmission of *Rickettsia rickettsii* to vertebrate hosts. Emerg Infect Dis. 2014;20:1504–10. PubMed https://doi.org/10.3201/eid2009.140189
6. dos Santos FC, do Nascimento EM, Katz G, Angerami RN, Colombo S, de Souza ER, et al. Brazilian spotted fever: real-time PCR for diagnosis of fatal cases. Ticks Tick Borne Dis. 2012;3:312–4. https://doi.org/10.1016/j.ttbdis.2012.10.027
7. Labruna MB, Whitworth T, Horta MC, Bouyer DH, McBride JW, Pinter A, et al. *Rickettsia species* infecting *Amblyomma cooperi* ticks from an area in the state of São Paulo, Brazil, where Brazilian spotted fever is endemic. J Clin Microbiol. 2004;42:90–8. https://doi.org/10.1128/JCM.42.1.90-98.2004
8. Eremeeva ME, Bosserman EA, Demma LJ, Zambrano ML, Blau DM, Dasch GA. Isolation and identification of *Rickettsia massiliae* from *Rhipicephalus sanguineus* ticks collected in Arizona. Appl Environ Microbiol. 2006;72:5569–77. https://doi.org/10.1128/AEM.00122-06
9. Vilges de Oliveira S, Nogueira Angerami R. Timeliness in the notification of spotted fever in Brazil: evaluating compulsory reporting strategies and digital disease detection. Int J Infect Dis. 2018;72:16–8. https://doi.org/10.1016/j.ijid.2018.04.4317

Phylogenetic Analysis of Bird-Virulent West Nile Virus Strain, Greece

George Valiakos, Konstantinos Plavos, Alexandros Vontas, Marina Sofia, Alexios Giannakopoulos, Themis Giannoulis, Vassiliki Spyrou, Constantina N. Tsokana, Dimitrios Chatzopoulos, Maria Kantere, Vasilis Diamantopoulos, Angeliki Theodorou, Spyridoula Mpellou, Athanasios Tsakris, Zissis Mamuris, Charalambos Billinis

Author affiliations: University of Thessaly, Karditsa, Greece (G. Valiakos, K. Plavos, A. Vontas, M. Sofia, A. Giannakopoulos, T. Giannoulis, V. Spyrou, C.N. Tsokana, D. Chatzopoulos, M. Kantere, Z. Mamuris, C. Billinis); Public Health Director, Region of Peloponnese, Tripoli, Greece (V. Diamantopoulos); Directorate-General for Regional Agricultural Economics and Veterinary, Region of Peloponnese, Nafplio, Greece (A. Theodorou); Bioefarmoges Eleftheriou LP—Integrated Mosquito Control, Marathon, Greece (S. Mpellou); University of Athens, Athens, Greece (A. Tsakris)

We report the full polyprotein genomic sequence of a West Nile virus strain isolated from Eurasian magpies dying with neurologic signs in Greece. Our findings demonstrate the local genetic evolution of the West Nile virus strain responsible for a human disease outbreak in the country that began in 2010.

West Nile virus (WNV) is the etiologic agent of an ongoing human disease outbreak in Greece since 2010. Until 2014, successive yearly outbreaks occurred mainly in central and northeastern Greece (*1*). After a 2-year hiatus, during July–October 2017, an outbreak of the disease occurred in the Peloponnese region in southern Greece that resulted in 48 laboratory-confirmed cases and 5 human deaths (*2*). In 2018, cases further expanded, with a total of 243 human cases and 50 deaths reported from various areas of Greece (*3*).

In June 2017, one month before human cases occurred, dead wild birds were reported in the Argolida regional unit in the Peloponnese region of Greece. Through mid-July, local residents noticed a reduction of the native wild bird population, especially Eurasian magpies (*Pica pica*), hooded crows (*Corvus cornix*), sparrows (*Passer domesticus*), and Eurasian collared doves (*Streptopelia decaocto*). Our team verified the presence of Eurasian magpies with neurologic signs in the area; affected birds were lethargic and

unable to fly, stayed low to the ground, and had no reaction to external stimuli (i.e., human presence).

During July and August 2017, we collected a total of 29 dead Eurasian magpies in the study area (Appendix Figure, https://wwwnc.cdc.gov/EID/article/25/12/18-1225-App1.pdf), as part of a monitoring program conducted and supported by the local prefecture since 2016. Twelve of the carcasses were in a condition appropriate for laboratory investigation.

We extracted brain tissue samples during necropsy for inoculation in Vero cell culture. We vortexed brain homogenates in phosphate-buffered saline and centrifuged them at $4,000 \times g$ for 10 min at 4°C. We filtrated 1 mL of brain tissue supernatant with 0.22-μm filters, inoculated it in 75-cm^2 flasks with 80% Vero cell confluence, and incubated it at 37°C with 5% CO_2 in the appropriate growth medium. We observed the monolayer daily. When we detected cytopathic effect (in 8/12 samples) ≈48 hours after infection, we transferred the flasks to –20°C for 4 hours. After thawing the supernatant and cells, we performed total RNA extraction using the PureLink RNA Mini Kit (Invitrogen, https://www.thermofisher.com).

We amplified the WNV genome by PCR using a set of 14 primer pairs, newly designed or preexisting from related studies targeting overlapping sequences in the WNV genome (Appendix). Amplicons underwent bidirectional sequencing using the fluorescent BigDye Terminator v3.1 Cycle Sequencing Kit (Applied Biosystems, https://www.thermofisher.com), followed by fragment separation with a 3730xl DNA Analyzer (Applied Biosystems). We verified all nucleotide changes from other WNV strains detected in the 8 positive WNV RNA culture extracts by PCR using the corresponding primers on the tissue extracts. We submitted the consensus sequence, obtained by alignment and assembling in MEGA version 7 software (4), to GenBank (accession no. MH549209) and named it Argolida-Greece-2017.

Results of BLAST sequencing (https://blast.ncbi.nlm.nih.gov/Blast.cgi) showed that the Argolida-Greece-2017 strain had the highest sequence similarity (99.79%) to the Nea Santa-Greece-2010 strain (5) responsible for the largest WNV human disease outbreak since 2010. Phylogenetic analysis confirmed this closer relatedness to the Nea Santa strain than to other strains within the Hungary/04 cluster (Figure). Our findings indicated possible introduction of the Nea Santa strain in the area of southern Greece and the local genetic evolution that took place before reemergence.

The Argolida-Greece-2017 has a total of 23 nt substitutions (3 of them in the 3′ untranslated region of the viral genome) and 4 amino acid changes compared with the phylogenetically closer Nea Santa strain. Amino acid changes include the I159M in the envelope gene near the NYS glycosylation motif, the H22Y and A298V in the nonstructural (NS) 1 gene, and the K805R mutation in NS5 gene. We predicted that all amino acid changes in the polyprotein gene are tolerated in accordance with the Sorting Tolerant From Intolerant algorithm (6). Although these changes do not seem to affect genetic determinants of virulence as was previously reported (7), further investigation is needed.
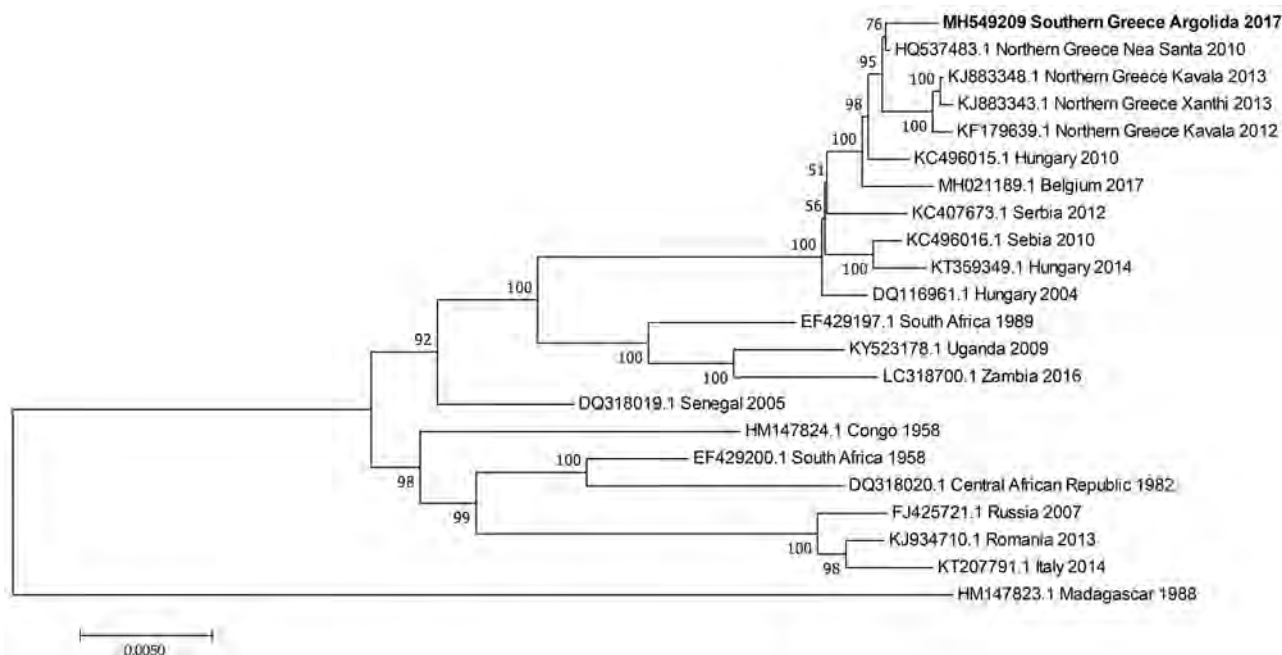
Figure. Phylogenetic tree of West Nile virus lineage 2 strains from a Eurasian magpie in Greece (bold) compared with reference strains. Each strain is listed by GenBank accession number, geographic origin, and collection date. Bootstrap values are shown as percentages at each tree node. Scale bar indicates substitutions per site.

The presence of proline at the 249 aa position of the NS3 gene is a mutation related to increased viremia potential and virus transmission rates in corvids (*8*).

In a recent study, Jiménez de Oya et al. performed experimental infection of Eurasian magpies with 2 WNV strains currently circulating in Europe; they found magpies to be highly susceptible to WNV infection, with low survival rates for both strains (*9*). No WNV-associated bird death had been reported in Greece previously, which could be attributed to the lack of an organized wild bird surveillance system in the country. Nevertheless, mass deaths of Eurasian magpies showing neurologic signs, 1 month earlier than a human neuroinvasive outbreak in the area, demonstrate that monitoring sick birds (e.g., using oral swabs or feather pulp) or carcasses of dead wild birds, in an active and passive surveillance system, could benefit public health by recognizing areas in which prevention measures could be implemented to minimize the impact of WNV human disease outbreaks.

About the Author

Dr. Valiakos is an assistant professor in the Department of Microbiology and Parasitology, Faculty of Veterinary Medicine, University of Thessaly, Greece. His primary research interests include zoonoses and wildlife animal species that play an important epidemiological role in the transmission of zoonotic diseases, in a One Health approach.

References

1. Gossner CM, Marrama L, Carson M, Allerberger F, Calistri P, Dilaveris D, et al. West Nile virus surveillance in Europe: moving towards an integrated animal-human-vector approach. Euro Surveill. 2017;22:30526. https://doi.org/10.2807/1560-7917.ES.2017.22.18.30526
2. Hellenic Centre for Disease Control & Prevention. Annual epidemiological report for West Nile virus human infection, Greece, 2017. 2017 [cited 2019 Oct 1]. https://eody.gov.gr/wp-content/uploads/2019/01/Annual_Report_WNV_2017_ENG_revised_final.pdf
3. Hellenic Centre for Disease Control & Prevention. Annual epidemiological report for West Nile virus human infection, Greece, 2017. 2018 [cited 2019 Oct 9]. https://eody.gov.gr/wp-content/uploads/2019/04/Annual_Report_WNV_2018_ENG.pdf
4. Kumar S, Stecher G, Tamura K. MEGA7: Molecular Evolutionary Genetics Analysis version 7.0 for bigger datasets. Mol Biol Evol. 2016;33:1870–4. https://doi.org/10.1093/molbev/msw054
5. Papa A, Bakonyi T, Xanthopoulou K, Vázquez A, Tenorio A, Nowotny N. Genetic characterization of West Nile virus lineage 2, Greece, 2010. Emerg Infect Dis. 2011;17:920–2. https://doi.org/10.3201/eid1705.101759
6. Kumar P, Henikoff S, Ng PC. Predicting the effects of coding nonsynonymous variants on protein function using the SIFT algorithm. Nat Protoc. 2009;4:1073–81. https://doi.org/10.1038/nprot.2009.86
7. Botha EM, Markotter W, Wolfaardt M, Paweska JT, Swanepoel R, Palacios G, et al. Genetic determinants of virulence in pathogenic lineage 2 West Nile virus strains. Emerg Infect Dis. 2008; 14:222–30. https://doi.org/10.3201/eid1402.070457
8. Brault AC, Huang CY, Langevin SA, Kinney RM, Bowen RA, Ramey WN, et al. A single positively selected West Nile viral mutation confers increased virogenesis in American crows. Nat Genet. 2007;39:1162–6. https://doi.org/10.1038/ng2097
9. Jiménez de Oya N, Camacho MC, Blázquez AB, Lima-Barbero JF, Saiz JC, Höfle U, et al. High susceptibility of magpie (*Pica pica*) to experimental infection with lineage 1 and 2 West Nile virus. PLoS Negl Trop Dis. 2018;12:e0006394. https://doi.org/10.1371/journal.pntd.0006394

Address for correspondence: George Valiakos, University of Thessaly, Department of Microbiology and Parasitology, Faculty of Veterinary Medicine, Trikalon 224, 43100, Karditsa, Greece; email: georgevaliakos@uth.gr

Hemorrhagic Fever with Renal Syndrome, Russia

Evgeniy A. Tkachenko, Aydar A. Ishmukhametov, Tamara K. Dzagurova, Alla D. Bernshtein, Viacheslav G. Morozov, Alexandra A. Siniugina, Svetlana S. Kurashova, Alexandra S. Balkina, Petr E. Tkachenko, Detlev H. Kruger, Boris Klempa

Author affiliations: Russian Academy of Sciences, Moscow, Russia (E.A. Tkachenko, A.A. Ishmukhametov, T.K. Dzagurova, A.D. Bernshtein, A.A. Siniugina, S.S. Kurashova, A.S. Balkina); Sechenov First Moscow State Medical University, Moscow (E.A. Tkachenko, A.A. Ishmukhametov, P.E. Tkachenko); Gepatolog, LLC, Samara, Russia (V.G. Morozov); Institute of Virology, Helmut-Ruska-Haus, Charité Medical School, Berlin, Germany (D.H. Kruger, B. Klempa); Biomedical Research Center, Slovak Academy of Sciences, Bratislava, Slovakia (B. Klempa)

In Russia, 131,590 cases of hemorrhagic fever with renal syndrome caused by 6 different hantaviruses were reported during 2000–2017. Most cases, 98.4%, were reported in western Russia. The average case-fatality rate was 0.4%, and strong regional differences were seen, depending on the predominant virus type.

Hemorrhagic fever with renal syndrome (HFRS) is caused by hantaviruses (order *Bunyavirales*, family *Hantaviridae*), enveloped, single-strand, negative-sense RNA viruses, predominantly carried by rodents and insectivores. In Asia, the primary HFRS pathogens are Hantaan virus (HTNV), Amur virus (AMRV), and Seoul virus (SEOV); in Europe, the primary pathogens are Puumala virus (PUUV) and Dobrava-Belgrade virus (DOBV) (*1*).

Russia, bordered by Europe in the west and Asia in the east, included HFRS in the official reporting system of the Ministry of Public Health in 1978 (*2*). Clinical and laboratory diagnoses for reported cases are confirmed serologically by indirect immunofluorescence assay (Diagnostikum HFRS; Federal Scientific Center for Research and Development of Immune and Biological Products of the Russian Academy of Sciences, http://chumakovs.ru).
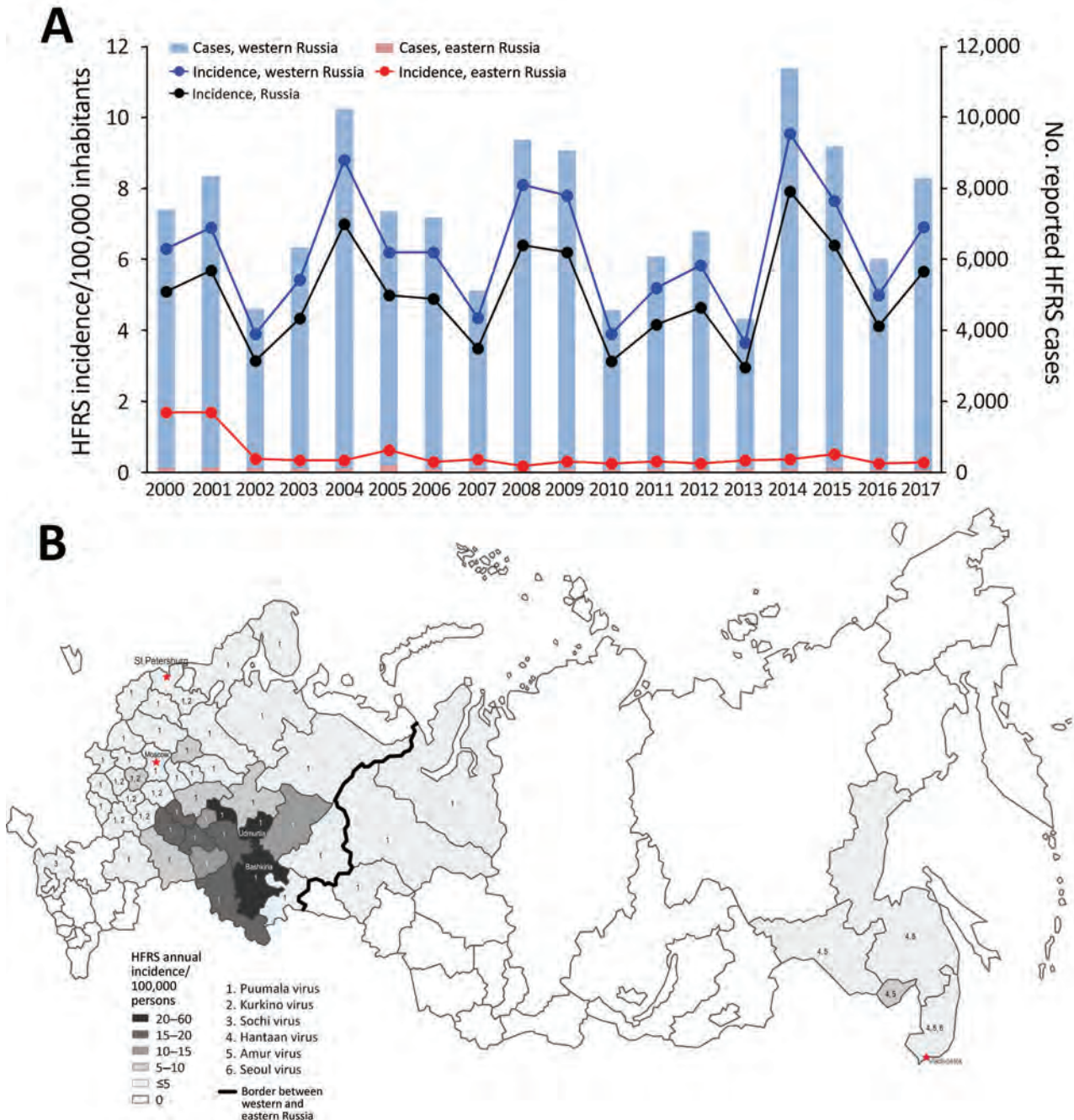
Figure. Distribution of hemorrhagic fever with renal syndrome caused by hantavirus in Russia, 2000–2017. A) Mean number of reported cases and incidence of disease, by region; B) geographic distribution and incidence rate of causative agents (indicated by numbers). Red stars indicate primary cities in Russia.

HFRS has the highest incidence rate of all reportable zoonotic viral diseases in Russia. In the west, in administrative regions close to the border with Europe, reported cases mainly are caused by PUUV carried by bank voles (*Myodes glareolus*) and to a lesser extent by 2 types of DOBV, Kurkino virus (KURV) and Sochi virus (SOCV) (*3*). Vectors for DOBV subtypes in western Russia are the western subtype of striped field mouse (*Apodemus agrarius agrarius*), which hosts KURV, in the central regions; and the Black Sea field mouse (*A. ponticus*), which hosts SOCV, in southern regions. In eastern Russia, near the border with Asia, HFRS cases primarily are caused by HTNV carried by the eastern subtype of striped field mouse (*A. agrarius mantchuricus*), AMRV carried by the Korean field mouse (*A. peninsulae*), and, less frequently, SEOV carried by the Norway rat (*Rattus norvegicus*) (*4*,*5*).

During 2000–2017, a total of 68 of Russia's 85 administrative regions reported 131,590 HFRS cases, an annual average rate of 4.9 cases/100,000 inhabitants (Figure 1, panel A). Annual incidence rates varied greatly, and epidemics occurred every 2–4 years with occasional 2-year peaks, such as in 2008–2009 and 2014–2015. This phenomenon is related to sequential independent epidemic years in 2 distinct, highly affected regions rather than geographically synchronized hantavirus activity on a nationwide scale.

HFRS cases were distributed unevenly throughout Russia. Western Russia reported 129,530 (98.4%) cases in 52/60 regions and an average annual incidence of 6.0 cases/100,000 persons. Eastern Russia reported only 2,060 (1.6%) cases in 16/25 regions and an average annual incidence of 0.4 cases/100,000 persons (*2*). The Ural and Ural-Volga-Viatka foothill areas, which encompass 11 administrative regions of western Russia, had the highest HFRS incidence rates, ≥10 cases/100,000 persons (Figure 1, panel B). Overall, 77% of HFRS cases in Russia were reported from these 11 regions, which are characterized by lime forests that provide suitable habitat for the bank vole, the reservoir host of PUUV. Among these regions, 2 had the highest incidence rates in the country: Udmurtia had 61.4 cases/100,000 persons and Bashkiria 47.5 cases/100,000 persons.

In eastern Russia, the 4 administrative regions closest to Asia reported HFRS cases. Vladivostok reported 1,089 cases and an incidence rate of 3.0 cases/100,000 persons; Khabarovsk reported 519 cases and an incidence rate of 2.1 cases/100,000 persons; Amur reported 71 cases and an incidence rate of 0.4 cases/100,000 persons; and Jewish Autonomous Region reported 189 cases and an incidence rate of 5.8 cases/100,000 persons. Siberia reported only 179 cases, mainly from western Siberia, which likely were imported cases in temporary oil and gas field workers from other hantavirus-endemic regions, such as the neighboring Udmurtia and Bashkiria.

During 2000–2017, Russia had 564 fatal cases of HFRS, 483 in the east and 81 in the west. The overall case-fatality rate was 0.4%, but rates varied by region. Central regions of western Russia had case-fatality rates of 0.3%, but the Black Sea coastal area of western Russia, where highly pathogenic SOCV occurs, had a 14% HFRS case-fatality rate. The far eastern regions, which have endemic highly pathogenic HTNV, had a 7% case-fatality rate (*6*–*9*).

HFRS appears to affect persons 20–50 years of age most frequently (65%), and ≈80% of cases in Russia were in men. Only 3,157 (2.4%) cases were reported among children ≤14 years of age. Most HFRS cases in western Russia occurred during the summer and autumn, but cases in the far eastern part of the country occurred in autumn and winter (*4*,*5*).

Comparative analyses of clinical courses indicated that even though infections by all recognized causative agents can cause mild, moderate, and severe clinical forms of HFRS, the frequency differs depending on the causative agent. SOCV infections had greater incidence of severe HRFS and high case-fatality rates (14%) and HTNV infections had case-fatality rates of 5%–8%, whereas PUUV, SEOV, and KURV infections had case-fatality rates ≤1% (*8*–*10*). Of note, 97.7% of HFRS cases in Russia are reportedly caused by PUUV (*5*), possibly explaining the overall low case-fatality rate in the country. Nevertheless, considering the high case numbers reported from the west, HFRS remains a public health threat in Russia.

About the Author

Dr. Tkachenko is a head of scientific direction in the Chumakov Federal Scientific Center for Research and Development of Immune and Biological Products of the Russian Academy of Sciences, Moscow, Russia. His major research interests include hantavirus ecology and epidemiology, devising hantavirus laboratory diagnostic methods, and developing vaccines against hantaviruses.

References

1. Kruger DH, Figueiredo LT, Song JW, Klempa B. Hantaviruses–globally emerging pathogens. J Clin Virol. 2015;64:128–36. https://doi.org/10.1016/j.jcv.2014.08.033
2. Federal Service for Surveillance on Consumer Rights Protection and Human Wellbeing. Statistical materials 2000–2017 [in Russian]. Moscow: The Service; 2000–2017 [cited 2018 Oct 20]. https://www.rospotrebnadzor.ru/activities/statistical-materials
3. Klempa B, Avsic-Zupanc T, Clement J, Dzagurova TK, Henttonen H, Heyman P, et al. Complex evolution and epidemiology of Dobrava-Belgrade hantavirus: definition of genotypes and their characteristics. Arch Virol. 2013;158:521–9. https://doi.org/10.1007/s00705-012-1514-5

4. Tkachenko EA, Bershtein AD, Dzagurova TK, Morozov VG, Slonova RA, Ivanov LI, et al. Actual problems of hemorrhagic fever with renal syndrome [in Russian]. Zh Mikrobiol Epidemiol Immunobiol. 2013;1:51–8. PubMed

5. Tkachenko EA, Dzagurova TK, Bernstein AD, Korotina NA, Okulova NM, Mutnikh ES, et al. Hemorrhagic fever with renal syndrome (history, problems and study perspectives) [in Russian]. Epidemiology and Vaccine Prophylaxis. 2016;15:23–34. https://doi.org/10.31631/2073-3046-2016-15-3-23-34

6. Dzagurova TK, Tkachenko EA, Yunicheva YV, Morozov VG, Briukhanov AF, Bashkirtsev VN, et al. Detection, clinical and etiological characteristics of HFRS in the subtropical zone of the Krasnodar region [in Russian]. Zh Mikrobiol Epidemiol Immunobiol. 2008;1:12–6.

7. Klempa B, Tkachenko EA, Dzagurova TK, Yunicheva YV, Morozov VG, Okulova NM, et al. Hemorrhagic fever with renal syndrome caused by 2 lineages of Dobrava hantavirus, Russia. Emerg Infect Dis. 2008;14:617–25. https://doi.org/10.3201/eid1404.071310

8. Kruger DH, Tkachenko EA, Morozov VG, Yunicheva YV, Pilikova OM, Malkin G, et al. Life-threatening Sochi virus infections, Russia. Emerg Infect Dis. 2015;21:2204–8. https://doi.org/10.3201/eid2112.150891

9. Morozov VG, Ishmukhametov AA, Dzagurova TK, Tkachenko EA. Clinical features of hemorrhagic fever with renal syndrome in Russia [in Russian]. Medical Council. 2017;5:156–61. https://doi.org/10.21518/2079-701X-2017-5-156-161

10. Dzagurova TK, Klempa B, Tkachenko EA, Slyusareva GP, Morozov VG, Auste B, et al. Molecular diagnostics of hemorrhagic fever with renal syndrome during a Dobrava virus infection outbreak in the European part of Russia. J Clin Microbiol. 2009;47:4029–36. https://doi.org/10.1128/JCM.01225-09

Laboratory-Confirmed Avian Influenza A(H9N2) Virus Infection, India, 2019

Varsha Potdar, Dilip Hinge, Ashish Satav, Eric F. Simões, Pragya D. Yadav, Mandeep S. Chadha

Author affiliations: National Institute of Virology, Pune, India (V. Potdar, D. Hinge, P.D. Yadav, M.S. Chadha); Mahan Trust Melghat, Amravati, India (A. Satav); University of Colorado School of Medicine, Aurora, Colorado, USA (E.F. Simões)

A 17-month-old boy in India with severe acute respiratory infection was laboratory confirmed to have avian influenza A(H9N2) virus infection. Complete genome analysis of the strain indicated a mixed lineage of G1 and H7N3. The strain also was found to be susceptible to adamantanes and neuraminidase inhibitors.

Low-pathogenicity avian influenza A(H9N2) viruses have a wide host range, and outbreaks in poultry have been recorded since the 1990s in China (*1*). In India, avian specimens indicated no serologic evidence of H5N1 and H9N2 during 1958–1981 (*2*); however, 5%–6% persons with direct exposure to poultry had H9N2 antibodies (*3*). Human cases of influenza H9N2 virus infection have been observed in Hong Kong, China, Bangladesh, and Pakistan (*4*–*7*).

An institutional review board approved an ongoing community-based surveillance in 93 villages of Korku tribes in Melghat District, Maharashtra State, India, to determine incidence of respiratory syncytial virus (RSV)–associated deaths among children <2 years of age. A total of 2,085 nasopharyngeal swabs from children with severe or fatal pneumonia were transported to India's National Institute of Virology to test for influenza, RSV, and other respiratory viruses. A nasopharyngeal swab from a 17-month-old boy received on February 12, 2019, tested positive by PCR for influenza A(H9N2) virus.

The child, a resident of Melghat, had fever, cough, breathlessness, and difficulty feeding for 2 days after illness onset on January 31, 2019. His high intermittent grade fever had no diurnal variation and no association with rash or mucocutaneous lesions. Examination revealed a conscious, restless child with a respiratory rate of 48 breaths/min and lower chest wall in-drawing with intermittent absence of breathing for ≥ 20 seconds. He was fully immunized for his age, with bacillus Calmette–Guérin, diphtheria, hepatitis B, poliovirus, and measles vaccines. Both length and weight for age were less than –3 SD. History of travel with his parents to a local religious gathering 1 week before symptom onset was elicited. The father had similar symptoms on return from the gathering but could not undergo serologic testing because of his migrant work. No history of poultry exposure was elicited. The child received an antibacterial drug and antipyretics and recovered uneventfully.

We tested the clinical sample using duplex real-time PCR for influenza A/B, H3N2, and 2009 pandemic H1N1 viruses; RSV A/B; human metapneumovirus; parainfluenza virus types 1–4; rhinovirus; and adenovirus. The sample was strongly positive for influenza A virus (cycle threshold value 20) but negative for seasonal influenza viruses and all respiratory viruses. Real-time PCR analysis for avian influenza viruses H5N1, H7N9, H10N8, and H9N2

revealed positivity for H9N2 virus (cycle threshold value for H9 was 25). We confirmed this result by sequencing the matrix (M) and hemagglutinin (HA) genes of the isolate, designated A/India/TCM2581/2019/(H9N2); the M gene (260 bp) had 97.27% nucleotide identity with A/chicken/India/99321/2009(H9N2), and the HA gene (225,478 bp) had 96.93% nucleotide identity with A/chicken/India/12CL3074/2015(H9N2).

We then generated whole-genome sequences by using the Miniseq NGS Platform (Illumina, https://www.illumina.com) and a de novo assembly program (CLC Genomics Software 10.1.1 [8]). We used MEGA7 (https://megasoftware.net) with a Tamura-Nei nucleotide substitution model including 1,000 replicates bootstrap support (9) for evolutionary analysis of 8 genes of A/India/TCM2581/2019/(H9N2) (submitted to GenBank under accession nos. MK673893–900). The HA, neuraminidase, and nucleoprotein gene phylogeny of A/India/TCM2581/2019/(H9N2) grouped with the dominant G1 lineage (h94.1.1) and clustered with poultry strains from India and human strains from Bangladesh (Figure). The M, nonstructural, polymerase basic 1, polymerase basic 2, and polymerase acidic genes were related to an H7N3 isolate from Pakistan (10) (Appendix Figure 1, https://wwwnc.cdc.gov/EID/article/25/12/19-0636-App1.pdf). We confirmed that the A/India/TCM2581/2019(H9N2) strain had low pathogenicity, showing a KSKR/GLF amino acids motif at the cleavage site of HA (335-341 [H9 numbering]).

We observed 6 potential glycosylation sites (11, 87, 123, 280, 287, and 472 [H9 numbering]) and loss of 2 sites (208 and 218 [H9 numbering]) in the HA gene of A/India/TCM2581/2019(H9N2) with respect to G1 viruses.

The virus was susceptible to adamantanes with S31 and to neuraminidase inhibitor with R292 and E119 (N2 numbering) (11). A/India/TCM2581/2019(H9N2) had Q226L and I155T in HA gene, which promote the human receptor binding. Compared with G1 vaccine strain A/Hong Kong/1073/99, the study strain had multiple mammalian-specific mutations that already exist in poultry-adapted H9N2. The study strain had amino acid changes R207K, H436Y, and M677T in the polymerase basic 1 gene; A515T in the polymerase acidic 1 gene; N30D, T215A, and T139A (all H3 numbering) in the matrix 1 gene; and P42S in the nonstructural 1 gene, all of which are known to be associated with mammalian host specificity and increased virulence in ferrets and mice (12). Known markers for virulence and transmission (E627K and D701N) in the polymerase basic 2 gene in the study strain were absent (Appendix Table 1).

Bayesian evolutionary analyses using BEAST version 1.8.1 (13) of the HA gene of H9N2 poultry strains from India indicated 3 clusters of multiple introductions at the estimated node age of 2000–2001 (Appendix Figure 2). Human strain A/India/TCM2581/2019(H9N2) and the other poultry viruses from India evolved with 5.163×10^{-3} substitutions/site/year.
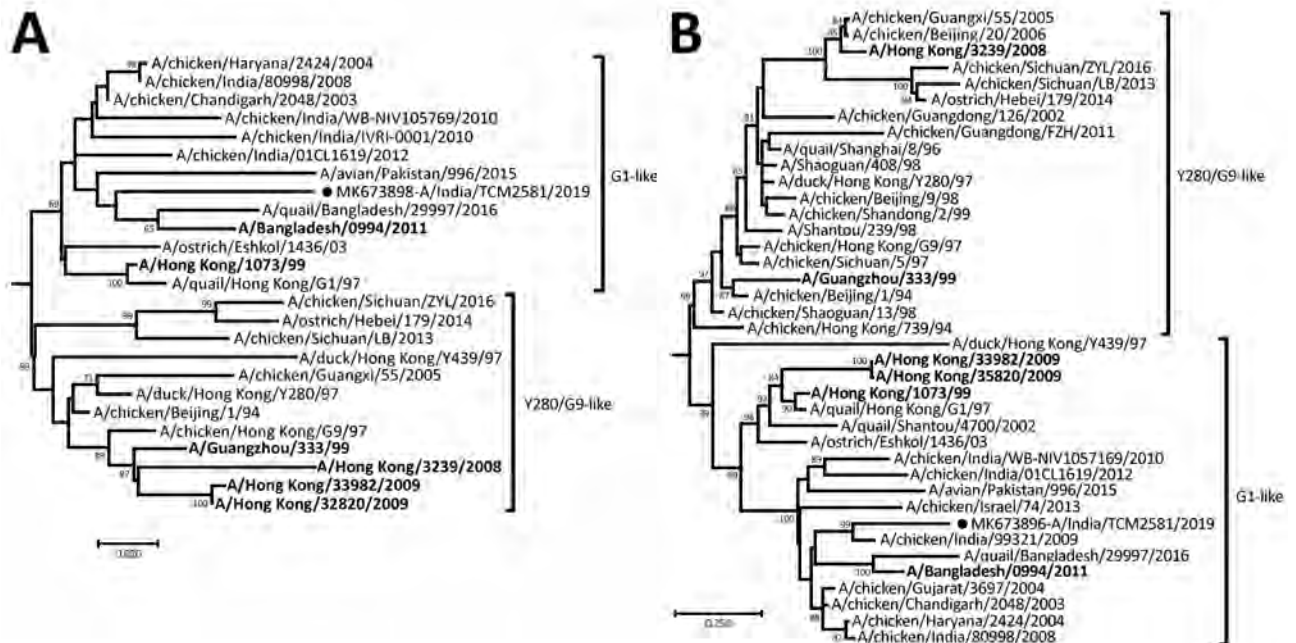
Figure. Phylogenetic tree of hemagglutinin gene (A) and neuraminidase gene (B) gene of influenza virus A/India/TCM 2581/2019(H9N2) from India (black circle) and reference strains. The numbers above the branches are the bootstrap probabilities (%) for each branch, determined by using MEGA 7.0 (https://megasoftware.net). Human cases from other countries are in bold. Scale bars indicate nucleotide substitutions per site.

In conclusion, multiple introductions of H9N2 viruses in poultry have been observed in India. The identification of a human case of H9N2 virus infection highlights the importance of systemic surveillance in humans and animals to monitor this threat to human health.

Acknowledgments

About the Author

Dr. Potdar is senior scientist heading the Influenza Group at the National Institute of Virology, Pune, India. Her primary research interest is molecular characterization and antiviral susceptibility of influenza viruses.

References

1. Malik Peiris JS. Avian influenza viruses in humans. Rev Sci Tech. 2009;28:161–73. https://doi.org/10.20506/rst.28.1.1871
2. Pawar SD, Jamgaonkar AV, Umarani UB, Kode SS. Seroepidemiology of avian influenza H5N1, H9N2 and Newcastle disease viruses during 1954 to 1981 in India. Indian J Med Res. 2016;144:472–6. https://doi.org/ 10.4103/0971-5916.198666
3. Pawar SD, Tandale BV, Raut CG, Parkhi SS, Barde TD, Gurav YK, et al. Avian influenza H9N2 seroprevalence among poultry workers in Pune, India, 2010. PLoS One. 2012;7:e36374. https://doi.org/10.1371/journal.pone.0036374
4. Pan Y, Cui S, Sun Y, Zhang X, Ma C, Shi W, et al. Human infection with H9N2 avian influenza in northern China. Clin Microbiol Infect. 2018;24:321–3. https://doi.org/10.1016/j.cmi.2017.10.026
5. Butt KM, Smith GJ, Chen H, Zhang LJ, Leung YH, Xu KM, et al. Human infection with an avian H9N2 influenza A virus in Hong Kong in 2003. J Clin Microbiol. 2005;43:5760–7. https://doi.org/10.1128/JCM.43.11.5760-5767.2005
6. Shanmuganatham K, Feeroz MM, Jones-Engel L, Smith GJ, Fourment M, Walker D, et al. Antigenic and molecular characterization of avian influenza A(H9N2) viruses, Bangladesh. Emerg Infect Dis. 2013;19. https://doi.org/10.3201/eid1909.130336
7. Ali M, Yaqub T, Mukhtar N, Imran M, Ghafoor A, Shahid MF, et al. Avian influenza A(H9N2) virus in poultry worker, Pakistan, 2015. Emerg Infect Dis. 2019;25:136–9. https://doi.org/10.3201/eid2501.180618
8. Mourya DT, Yadav PD, Nyayanit DA, Majumdar TD, Jain S, Sarkale P, et al. Characterization of a strain of quaranfil virus isolated from soft ticks in India. Is quaranfil virus an unrecognized cause of disease in human and animals? Heliyon. 2019;5:e01368. https://doi.org/10.1016/j.heliyon.2019.e01368
9. Iqbal M, Yaqub T, Reddy K, McCauley JW. Novel genotypes of H9N2 influenza A viruses isolated from poultry in Pakistan containing NS genes similar to highly pathogenic H7N3 and H5N1 viruses. PLoS One. 2009;4:e5788. https://doi.org/10.1371/journal.pone.0005788
10. Kumar S, Stecher G, Tamura K. MEGA7: Molecular Evolutionary Genetics Analysis Version 7.0 for bigger datasets. Mol Biol Evol. 2016;33:1870–4. https://doi.org/ 10.1093/molbev/msw054
11. Govorkova EA, Baranovich T, Seiler P, Armstrong J, Burnham A, Guan Y, et al. Antiviral resistance among highly pathogenic influenza A (H5N1) viruses isolated worldwide in 2002–2012 shows need for continued monitoring. Antiviral Res. 2013;98:297–304. https://doi.org/10.1016/j.antiviral.2013.02.013
12. Li X, Shi J, Guo J, Deng G, Zhang Q, Wang J, et al. Genetics, receptor binding property, and transmissibility in mammals of naturally isolated H9N2 avian influenza viruses. PLoS Pathog. 2014;10:e1004508. https://doi.org/ 10.1371/journal.ppat.1004508
13. Potdar VA, Hinge DD, Dakhave MR, Manchanda A, Jadhav N, Kulkarni PB, et al. Molecular detection and characterization of influenza 'C' viruses from western India. Infect Genet Evol. 2017;54:466–77. https://doi.org/ 10.1016/j.meegid.2017.08.005

Address for correspondence: Varsha Potdar, National Institute of Virology, Ministry of Health and Family Welfare, 20-A Dr. Ambedkar Rd, Post Box 11, Pune, Maharashtra 411001, India; email: potdarvarsha9@gmail.com

Nodular Human Lagochilascariasis Lesion in Hunter, Brazil

Flavio Queiroz-Telles,[1] Gabriel L.O. Salvador[1]

Author affiliation: Federal University of Paraná, Curitiba, Brazil

Lagochilascariasis is a rare helminthic infection caused by *Lagochilascaris minor* nematodes and found in Latin America; most cases are reported in the Amazon region. We report on a case observed in a hunter in southern Brazil and describe scanning electron microscopy results for *L. minor* adult forms.

Lagochilascariasis is a rare tropical helminthic anthropozoonotic disease caused by the nematode *Lagochilascaris minor* (*1,2*). Cases were described by Leiper on the island of Trinidad in 1909; since that report, several cases have been reported in tropical and subtropical zones of a few countries in Latin America, affecting mostly rural inhabitants from Mexico to Argentina, in both genders. Patients range from 2 to 67 years of age but are predominantly children and teenagers (*2*). Although the genus *Lagochilascaris* covers 6 species, *L. major*, *L. buckleyi*, *L. turgida*, *L. sprenti*, *L. multipapillatum*, and *L. minor*, only *L. minor* is related to human disease (*3–5*). Wild felines (*Felis onca, F. nebulosi*, and *F. pardalis*) are suspected to be the parasite's natural reservoirs (*4*).

A 54-year-old male rural worker from the state of Mato Grosso, Brazil, on the border of the Amazon forest, sought medical attention for a 6-month history of a nodular lesion on the right side of the neck. He was a hunter and reported sporadic ingestion of domestic and wild feline raw meat, including meat from jaguars (*Panthera onca*). He was in good general health, except for a tumoral lesion measuring 10 cm in diameter surrounded by an irregular and erythematous skin surface in the left submandibular region, with fistulous tracts expelling 5–15-mm worms (Figure, panel A). We performed a skin biopsy for histopathologic studies and scanning electron microscopy (SEM) of the worms collected.

We tentatively identified the worms as *L. minor* nematodes on the basis of the following features. The skin biopsy showed multiple sinus tracts containing eggs measuring 50–90 μm and having thick shells with coarse, pitted surfaces. Larval fragments were also observed in a granulomatous reaction (Figure, panel B). Optic microscopy of 1 adult worm showed the ejaculatory duct in the posterior surrounded by spicules; the ratio of the ejaculatory duct length to the spicule length was ≈2, strongly suggestive of *L. minor* (Figure, panel C).

SEM of the anterior end of the worms showed 2 subventral lips, 1 subdorsal lip, 2 interlabia, 1 postlabial groove, papillae, and 1 amphidial pore (Figure, panel D), compatible with previous reports of *L. minor* nematodes (*1–5*). The 3 lips were concentrically located around the oral opening.

Eosinophil count in the peripheral blood, together with biochemical and hematologic laboratory examinations, showed no abnormalities. Results of imaging evaluation of the patient's chest and skull were also normal. We treated the patient with levamizole (300 mg/d); after 1 week, improvement in the inflammatory signs and a reduction of the purulent discharge were seen. We performed surgical resection of the lesion and continued administering levamizole at the same dosage for 2 more weeks. We then decreased the dosage by half for another 2 weeks. Follow-up biopsies showed improvement of the inflammation and absence of worms and eggs.

More than 100 human cases of lagochilascariasis have been reported (*5*). Most cases were characterized by cervical, mastoid, middle ear, pharynx, and brain nodules (*5–7*).

Recently, several studies have proposed that when wild cats (definitive hosts) ingest infecting eggs orally, the parasites do not reach sexual maturity (*7*). Other studies have proposed that when felines ingest rodent carcasses infected with third-stage (L3) larvae, larval hatching from cysts occurs in the stomach (*5*). After hatching, larvae migrate to upper regions of the digestive tract, reaching the adult stage in tissues of the nose and oropharynx. Some studies also suggested the idea of autoinfection, as many biopsy studies found larvae in several stages of development and eggs (*8,9*). The uncommon eating habits of this patient corroborate the theory of infection resulting from ingestion of raw feline meat with L3 larvae together with an autoinfection process.

SEM of *L. minor* nematode, as described in a study by Lanfredi et al. (*10*), shows the anterior end with 2 subventral papillae and lips with 1 dorsal papilla, 1 amphidial pore, and triangular interlabial prolongations (*10*). The longitudinal ventral view of the anterior region shows an excretory pore and a lateral line. The lateral view of the lips shows a deep groove around the lips forming the interlabial projection, 1 subventral lip with 1 papilla, and 1 amphidial pore (*10,11*). Morphologic features suggestive of *L. minor* are provided (Appendix Table, https://wwwnc.cdc.gov/EID/article/25/12/19-0737-App1.pdf).

Treatment for lagochilascariasis involves thiabendazole, cambendazole, mebendazole, albendazole, praziquantel, and invermectine (*8,9*). Most series report initial treatment with thiabendazole, followed by diethylcarbamazine or mebendazole and, finally, levamisole (*9*). Most reports

---

[1]Both authors contributed equally to this article.
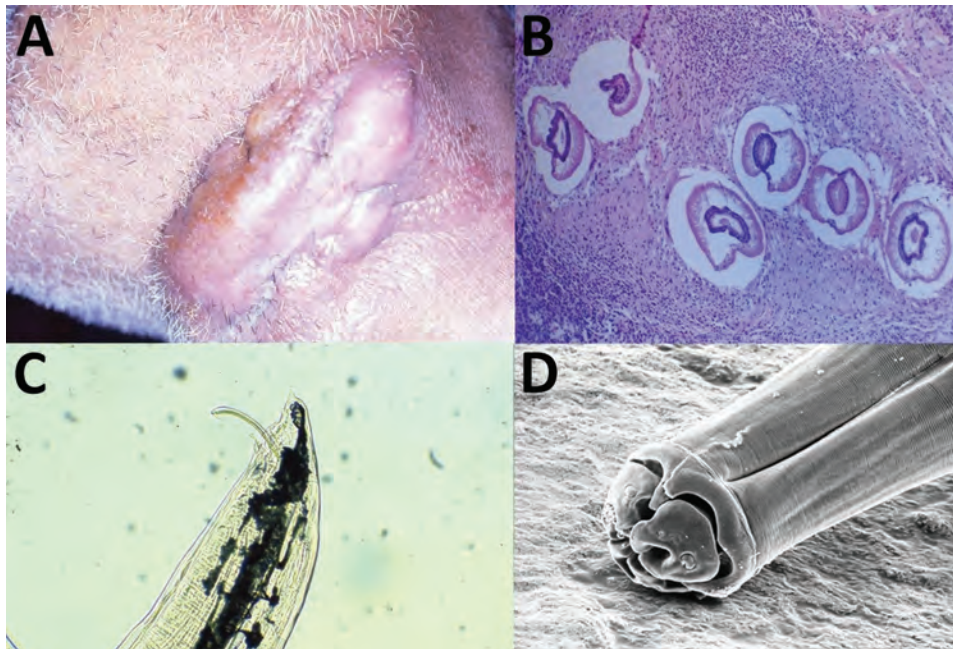
Figure. Lagochilascariasis in a 54-year-old male hunter in Brazil. A) Nodular tumorous lesion on cervical region caused by *L. minor* infection. B) Biopsy specimen of nodular lesion showing granuloma and larvae of *L. minor* nematode. Hematoxylin and eosin staining. Original magnification ×50. C) Optic microscopy shows the ejaculatory duct with spicule and lateral alae of *L. minor*. The ratio of ejaculatory duct length to spicule length of the worms is ≈2. Original magnification ×50. D) Scanning electron microscopy of the anterior end of *L. minor* nematode showing 2 subventral lips, 1 subdorsal lip, 2 interlabia, postlabial groove, papillae, and 1 amphidial pore. Original magnification ×800.

describe recurrent and refractory infections, often because when the presence of *L. minor* nematodes is reduced and the lesion heals, physicians consider the infection resolved (*8*). However, relapses occur when inadequate treatment is given, because of the autoinfective life cycle. Although the life cycle of *L. minor* nematodes is still unknown, patients should be treated for ≥1 month after the clinical cure to avoid relapses.

About the Authors

Dr. Queiroz-Telles is an associate professor of infectious diseases at the Federal University of Parana in Brazil, with lines of research in the areas of neglected diseases and medical mycology. Dr. Salvador is a physician at the Federal University of Parana, with a concentration in head and neck and central nervous system infections.

References

1. Barrera-Pérez M, Manrique-Saide P, Reyes-Novelo E, Escobedo-Ortegón J, Sánchez-Moreno M, Sánchez C. *Lagochilascaris minor* Leiper, 1909 (Nematoda: Ascarididae) in Mexico: three clinical cases from the peninsula of Yucatan. Rev Inst Med Trop São Paulo. 2012;54:315–7. https://doi.org/10.1590/S0036-46652012000600005
2. Sprent JFA. Speciation and development in the genus *Lagochilascaris*. Parasitology. 1971;62:71–112. https://doi.org/10.1017/S0031182000071316
3. Roig JL, Roig-Ocampos Forteza JL, Granato L, Poletti Serafini D. Otomastoidititis with right retroauricular fistula by *Lagochilascaris minor*. Rev Bras Otorrinolaringol (Engl Ed). 2010;76:407. https://doi.org/10.1590/S1808-86942010000300025
4. Vieira MA, de Oliveira JA, Ferreira LS, de Oliveira V, Barbosa CA. A case report of human lagochilascariasis coming from Pará State, Brazil [in Portuguese]. Rev Soc Bras Med Trop. 2000;33:87–90. https://doi.org/10.1590/S0037-86822000000100014
5. Campos DM, Freire Filha LG, Vieira MA, Paçô JM, Maia MA. Experimental life cycle of *Lagochilascaris minor* Leiper, 1909. Rev Inst Med Trop São Paulo. 1992;34:277–87. https://doi.org/10.1590/S0036-46651992000400003
6. Aguilar-Nascimento JE, Silva GM, Tadano T, Valadares Filho M, Akiyama AM, Castelo A. Infection of the soft tissue of the neck due to *Lagochilascaris minor*. Trans R Soc Trop Med Hyg. 1993;87:198. https://doi.org/10.1016/0035-9203(93)90491-8
7. Bento RF, Mazza CC, Motti EF, Chan YT, Guimarães JR, Miniti A. Human lagochilascariasis treated successfully with ivermectin: a case report. Rev Inst Med Trop São Paulo. 1993;35:373–5. https://doi.org/10.1590/S0036-46651993000400012
8. Vargas-Ocampo F, Alvarado-Aleman FJ. Infestation from *Lagochilascaris minor* in Mexico. Int J Dermatol. 1997;36:56–8. https://doi.org/10.1111/j.1365-4362.1997.tb03307.x
9. Falcón-Ordaz J, Iturbe-Morgado JC, Rojas-Martínez AE, García-Prieto L. *Lagochilascaris minor* (Nematoda: Ascarididae) from a wild cougar (*Puma concolor*) in Mexico. J Wildlife Dis. 2016;52:746–8. http://doi.org/10.7589/2015-09-232
10. Lanfredi RM, Fraiha Neto H, Gomes DC. Scanning electron microscopy of *Lagochilascaris minor* Leiper, 1909 (Nematoda: Ascarididae). Mem Inst Oswaldo Cruz. 1998;93:327–30. https://doi.org/10.1590/S0074-02761998000300009
11. Campos DMB, Barbosa AP, Oliveira JA, Tavares GG, Cravo PVL, Ostermayer AL. Human lagochilascariasis—a rare helminthic disease. PLoS Negl Trop Dis. 2017;11:e0005510. https://doi.org/10.1371/journal.pntd.0005510

Address for correspondence: Flavio Queiroz-Telles, Federal University of Paraná, General Carneiro 181, Alto da Glória, Curitiba, Paraná, 80060-900, Brazil; email: queiroz.telles@uol.com.br

MERS-CoV in Camels but Not Camel Handlers, Sudan, 2015 and 2017

Elmoubasher Farag,[1] Reina S. Sikkema,[1]
Ahmed A. Mohamedani, Erwin de Bruin,
Bas B. Oude Munnink, Felicity Chandler,
Robert Kohl, Anne van der Linden,
Nisreen M.A. Okba, Bart L. Haagmans,
Judith M.A. van den Brand, Asia Mohamed Elhaj,
Adam D. Abakar, Bakri Y.M. Nour,
Ahmed M. Mohamed, Bader Eldeen Alwaseela,
Husna Ahmed, Mohd Mohd Alhajri,
Marion Koopmans, Chantal Reusken,[2]
Samira Hamid Abd Elrahman[2]

Author affiliations: Ministry of Public Health, Doha, Qatar
(E. Farag, M.M. Alhajri); Erasmus Medical Centre, Rotterdam,
the Netherlands (R.S. Sikkema, E. de Bruin, B.B.O. Munnink,
F. Chandler, R. Kohl, A. van der Linden, N.M.A. Okba,
B.L. Haagmans, M. Koopmans, C. Reusken); University of
Gezira, Wad Medani, Sudan (A.A. Mohamedani,
S.H. Abd Elrahman); Utrecht University, Utrecht, the Netherlands
(J.M.A. van den Brand); Blue Nile National Institute for
Communicable Diseases, Wad Medani (A.M. Elhaj,
A.D. Abakar, B.Y.M. Nour, A.M. Mohamed, S.H. Abd Elrahman);
Tamboul Camel Research Centre, Tamboul, Sudan
(B.E. Alwaseela, H. Ahmed); National Institute |for Public Health
and the Environment, Bilthoven, the Netherlands (C. Reusken)

We tested samples collected from camels, camel workers, and other animals in Sudan and Qatar in 2015 and 2017 for evidence of Middle East respiratory syndrome coronavirus (MERS-CoV) infection. MERS-CoV antibodies were abundant in Sudan camels, but we found no evidence of MERS-CoV infection in camel workers, other livestock, or bats.

Middle East respiratory syndrome coronavirus (MERS-CoV) is a zoonotic virus from camels that can cause serious respiratory disease and death in humans (1). Camel populations across the Middle East and Africa are highly seropositive. However, the only known human cases of clinical MERS-CoV infection in Africa were related to travel from Qatar and Saudi Arabia (https://ecdc.europa.eu/sites/portal/files/media/en/publications/Publications/RRA_MERS-CoV_7th_update.pdf), and serologic evidence for infections in humans resulting from camel exposure in Africa is limited (2).

[1]These first authors contributed equally to this article.

[2]These authors were co–principal investigators.

The only published report of MERS-CoV circulation in camels in Sudan involved the testing of camel samples from 1983; that study found a seroprevalence of 82% (49/60) (3). Two publications from Egypt describe evidence of possible MERS-CoV circulation in Sudan, reporting a seroprevalence of 91% (543/594) in camels originating from Sudan and a seroprevalence of 92% (48/52), combined with a reverse transcription PCR positivity rate of 5.6%, in camels originating from Ethiopia and Sudan (3). Neither study presented conclusive evidence for MERS-CoV circulation in Sudan. Here, we provide the results of a study conducted in the Butana region of Al Gezira, Sudan, to investigate the local point prevalence of MERS-CoV and MERS-CoV antibodies among camel handlers, camels, and other animals in 2015 and 2017. We also report the results of a MERS-CoV screening in camels from Sudan sampled in Qatar directly upon importation.

We collected samples from humans and animals at a live animal market, an outdoor slaughter area adjacent to that market, and the Tamboul Camel Research Centre (TCRC), all located in Tamboul, Sudan. Overall, ≈1,660 camels and additional other livestock are usually present at the animal market; these camels come from individual small farms, where they are largely kept under free-roaming conditions. At the TCRC, ≈100 camels are generally present and kept out of contact with other camels. Before their arrival at the TCRC, they were herded on the Butana Plain. We also collected samples from 90 Sudan camels that were imported into Qatar in 2015. After arriving at the Hamad International Airport in Doha, Qatar, these camels were directly transported to the Al Shahaniya animal market in Doha. We sampled them immediately after their arrival. We stored all samples locally (1–1.5 years in Sudan, 1 month in Qatar) and tested them after shipment to the Netherlands.

We tested 56 human, 190 camel, 3 bat, 14 donkey, 15 cow, 15 sheep, and 15 goat serum samples for antibodies against MERS-CoV spike S1 using the protein microarray technique (4). We performed a virus neutralization test and a spike S1 protein–based ELISA (human serum samples only) to confirm the detection of MERS-CoV antibodies by protein microarray (5). In confirmatory tests, we included equal numbers of negative serum samples of the same species, when available. We considered samples positive if results of all tests were positive (protein microarray cutoff 1:20, 50% plaque-reduction neutralization titer cutoff 1:20, ELISA cutoff optical density 0.5). To resolve problems with possible mislabeling, we tested all animal serum samples collected in 2017 with a cytochrome B gene PCR to confirm species origins (6). We tested camel nasal (n = 168), nasopharyngeal (n = 24), and rectal (n = 61) swab specimens and milk (n = 33), urine (n = 30), and fecal (n = 42) samples for MERS-CoV RNA using a reverse

Table. MERS-CoV RNA and antibody positivity among humans, bats, camels, and other livestock, Sudan, 2015 and 2017*

Sample type	Location of sample collection	2015			2017		
		No. samples	MERS-CoV RNA, no. positive/total no. (%)	MERS-CoV antibody, no. positive/total no. (%)	No. samples	MERS-CoV RNA, no. positive/total no. (%)	MERS-CoV antibody, no. positive/total no. (%)
Camel worker serum	Tamboul slaughter area	3	NT	ND	35	NT	ND
	Tamboul market	8	NT	ND	NA		
	TCRC	7	NT	ND	3	NT	ND
Camel serum†	Tamboul slaughter area‡§	4	ND	4/4 (100)	13	ND	13/13 (100)
	Tamboul market‡§¶	27	ND	26/27 (96)	NA		
	TCRC¶	31	ND	27/31 (87)	25	ND	25/25 (100)
	Qatar§¶#	90	ND	89/90 (99)	NA		
Camel nasopharyngeal swabs†	TCRC¶	NA			24	ND	NT
Camel nasal swabs†	Tamboul slaughter area‡§	11	ND	NT	NA		
	Tamboul market‡§¶	11	ND	NT	NA		
	TCRC¶	31	ND	NT	25	ND	NT
	Qatar§¶#**	90	3/90 (3)	NT	NA		
Camel ticks (*Hyalomma dromedarii*) from 25 camels	TCRC	155	ND	NT	NA		
Other animal serum							
Cattle	Tamboul slaughter area	6	ND	ND	9	NT	ND
Goat	Tamboul slaughter area	5	ND	ND	10	NT	ND
Sheep	Tamboul slaughter area	5	ND	ND	10	NT	ND
Donkey	Tamboul slaughter area	5	ND	ND	9	NT	ND
Bat††	TCRC	3	ND	NT	NA		
Bat tissue‡‡	TCRC	13	ND	NT	NA		

*MERS-CoV, Middle East respiratory syndrome coronavirus; NA, not available; ND, not detected; NT, not tested; TCRC, Tamboul Camel Research Centre.
†From camels >2 years of age.
‡Serum and swab samples received from the slaughter field and live animal market were not matched.
§Sample set included meat camels.
¶Sample set included milk camels.
#Sample set included race camels.
**Just imported into Qatar from Sudan.
††Genus unknown.
‡‡*Tadarida* spp.; lung, intestine, and brain tissues stored in formalin.

transcription PCR targeting the upstream of envelope and nucleocapsid genes, as described previously (*7,8*). In addition, we tested legs of camel ticks (*Hyalomma dromedarii*) and bat (*Tadarida* spp.) tissues collected at the TCRC in 2015 for MERS-CoV RNA.

In 2015, a total of 92% of camels in Sudan and 99% of camels exported to Qatar from Sudan were MERS-CoV seropositive (Table). In 2017, all camels tested in Sudan were seropositive. No MERS-CoV antibodies were found in human or bat serum samples or serum samples from livestock other than camels. MERS-CoV RNA was detected in the nasal swabs from 3 camels imported into Qatar in 2015 but in no other samples.

The results of this study are in agreement with other seroepidemiologic studies performed in Africa. The camel population was highly seropositive for MERS-CoV, and none or a low percentage of nasal or nasopharyngeal swabs from camels were positive for MERS-CoV RNA. As shown before in other countries in Africa, human serum samples did not show neutralizing activity against MERS-CoV (*2*). In 1 study in Kenya, 2 of 1,122 livestock handlers were found positive for MERS-CoV neutralizing antibodies (*9*).

Other livestock were also seronegative for MERS-CoV in our study, a finding in agreement with most serosurveys, although some sheep, goats, and donkeys and 1 cow have been reported to have MERS-CoV antibodies (*3,10*).

The number of human and livestock samples tested was low in this investigation. Therefore, the results of this study are not conclusive. However, this study provides preliminary insight into MERS-CoV circulation in Sudan, the country with the third largest dromedary camel population in the world (http://www.fao.org/faostat/en/#data/QA). We show evidence of extensive MERS-CoV circulation in camels but no evidence of circulation in other livestock, bats, and humans.

About the Author

Mr. Farag is acting head of the Communicable Diseases Control Programs, Ministry of Public Health, Doha, Qatar, and a doctoral

candidate at the Erasmus Medical Centre. His research interests are mainly the epidemiology of MERS-CoV and spread of MERS-CoV at the human–animal interface. Ms. Sikkema is a doctoral candidate at the Erasmus Medical Centre, Rotterdam, the Netherlands. Her research interests are mainly focused on the risk-based surveillance of MERS-CoVs in animals and humans.

References

1. Reusken CB, Raj VS, Koopmans MP, Haagmans BL. Cross host transmission in the emergence of MERS coronavirus. Curr Opin Virol. 2016;16:55–62. https://doi.org/10.1016/j.coviro.2016.01.004
2. So RT, Perera RA, Oladipo JO, Chu DK, Kuranga SA, Chan KH, et al. Lack of serological evidence of Middle East respiratory syndrome coronavirus infection in virus exposed camel abattoir workers in Nigeria, 2016. Euro Surveill. 2018;23. https://doi.org/10.2807/1560-7917.ES.2018.23.32.1800175
3. Sikkema RS, Farag EABA, Islam M, Atta M, Reusken CBEM, Al-Hajri MM, et al. Global status of Middle East respiratory syndrome coronavirus in dromedary camels: a systematic review. Epidemiol Infect. 2019;147:e84. http://dx.doi.org/10.1017/S095026881800345X
4. Reusken CBEM, Haagmans BL, Müller MA, Gutierrez C, Godeke G-J, Meyer B, et al. Middle East respiratory syndrome coronavirus neutralising serum antibodies in dromedary camels: a comparative serological study. Lancet Infect Dis. 2013;13:859–66. https://doi.org/10.1016/S1473-3099(13)70164-6
5. Okba NMA, Raj VS, Widjaja I, Geurts van Kessel CH, de Bruin E, Chandler FD, et al. Sensitive and specific detection of low-level antibody responses in mild Middle East respiratory. Emerg Infect Dis. 2019;25:1868–77. http://dx.doi.org/10.3201/eid2510.190051
6. Kocher TD, Thomas WK, Meyer A, Edwards SV, Pääbo S, Villablanca FX, et al. Dynamics of mitochondrial DNA evolution in animals: amplification and sequencing with conserved primers. Proc Natl Acad Sci U S A. 1989;86:6196–200. https://doi.org/10.1073/pnas.86.16.6196
7. Corman VM, Eckerle I, Bleicker T, Zaki A, Landt O, Eschbach-Bludau M, et al. Detection of a novel human coronavirus by real-time reverse-transcription polymerase chain reaction. Euro Surveill. 2012;17:20285. https://doi.org/10.2807/ese.17.39.20285-en
8. Corman VM, Müller MA, Costabel U, Timm J, Binger T, Meyer B, et al. Assays for laboratory confirmation of novel human coronavirus (hCoV-EMC) infections. Euro Surveill. 2012;17:20334. https://doi.org/10.2807/ese.17.49.20334-en
9. Liljander A, Meyer B, Jores J, Müller MA, Lattwein E, Njeru I, et al. MERS-CoV antibodies in humans, Africa, 2013–2014. Emerg Infect Dis. 2016;22:1086–9. https://doi.org/10.3201/eid2206.160064
10. Kandeil A, Gomaa M, Shehata M, El-Taweel A, Kayed AE, Abiadh A, et al. Middle East respiratory syndrome coronavirus infection in non-camelid domestic mammals. Emerg Microbes Infect. 2019;8:103–8. https://doi.org/10.1080/22221751.2018.1560235

Recombination between Vaccine and Field Strains of Porcine Reproductive and Respiratory Syndrome Virus

Anping Wang, Qi Chen, Leyi Wang, Darin Madson, Karen Harmon, Phillip Gauger, Jianqiang Zhang, Ganwu Li

Author affiliations: Jiangsu Agri-animal Husbandry Vocational College, Taizhou, China (A. Wang); Iowa State University, Ames, Iowa, USA (A. Wang, Q. Chen, D. Madson, K. Harmon, P. Gauger, J. Zhang, G. Li); University of Illinois, Urbana, Illinois, USA (L. Wang); Chinese Academy of Agricultural Sciences, Harbin, China (G. Li)

DOI: https://doi.org/10.3201/eid2512.191111

We isolated and plaque-purified IA76950-WT and IA70388-R, 2 porcine reproductive and respiratory syndrome viruses from pigs in the same herd in Iowa, USA, that exhibited coughing and had interstitial pneumonia. Phylogenetic and molecular evolutionary analysis indicated that IA70388-R is a natural recombinant from Fostera PRRSV vaccine and field strain IA76950-WT.
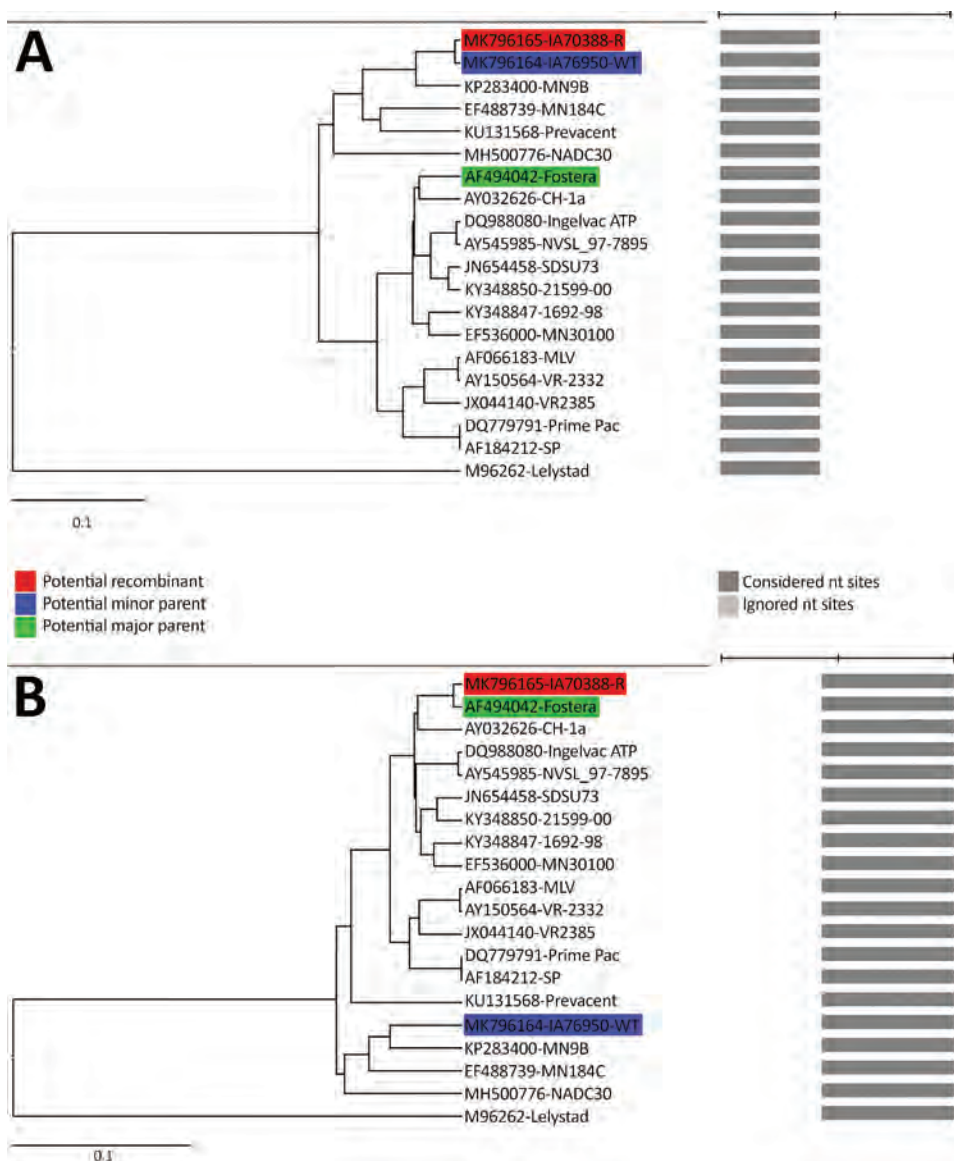
Porcine reproductive and respiratory syndrome (PRRS), characterized by reproductive failure in sows and respiratory distress in pigs of all ages, causes substantial economic loss to the worldwide swine industry. PRRS virus (PRRSV) is an enveloped, single-stranded, and positive-sense RNA virus belonging to the family *Arteriviridae* (*1*). Historically, PRRSV comprises type 1 (PRRSV-1) and type 2 (PRRSV-2); recently, PRRSV-1 was taxonomically classified into the species *Betaarterivirus suid 1* and PRRSV-2 into the species *Betaarterivirus suid 2*. PRRS has remained the most important disease of swine throughout the world, and live attenuated vaccines are used to reduce the clinical impact of PRRSV infection. Several studies have reported that recombinant PRRSV strains emerged in China, Korea, and France because of recombination between wild-type and vaccine strains (*2–6*). Nevertheless, recombination between a live attenuated vaccine strain and a circulating strain has not been reported in the United States.

In October 2018, a farm with a history of using Fostera PRRSV vaccine had been experiencing an ongoing problem with porcine respiratory disease. Histopathologic examination of 2 samples (lungs A and B) revealed the lungs of both pigs demonstrated significant interstitial pneumonia. Open reading frame (ORF) 5 Sanger sequencing identified a wild-type PRRSV from sample A

and a vaccine Fostera-like PRRSV from sample B. However, the Fostera-specific real-time PCR, which targets the nonstructural protein (NSP) 2 region in the virus, was consistently negative for both samples. The viruses were isolated, plaque-purified, and sequenced on the Illumina MiSeq platform (Illumina, https://www.illumina.com) (Appendix, https://wwwnc.cdc.gov/EID/article/25/12/19-1111-App1.pdf). The 2 plaque-purified PRRSV isolates, IA76950-WT from pig A and IA70388-R from pig B, had 100% nt identities to those directly sequenced from the lung tissues.

We determined 14,980 and 14,987 nt of the full-length genomes of IA76950-WT (GenBank accession no. MK796164) and IA70388-R (GenBank accession no. MK796165). The whole genomes of IA76950-WT and IA70388-R shared 81.5% and 85.4% nt identity with the PRRSV-2 prototype strain VR-2332 but only 60.7% and 60.8% with the PRRSV-1 representative Lelystad strain, indicating that both isolates belonged to PRRSV-2. To evaluate the genomic characteristics of IA76950-WT and IA70388-R, we compared their genomes with all PRRSV-2 strains in GenBank and 12 representative strains, including NADC30, CH-1a, SDSU73, VR-2332, and selected 5 US vaccine strains for further analysis in detail (Appendix Table). IA70388-R had >99% nt identity to IA76950-WT in Nsp1α, Nsp1β, and Nsp2~5 and demonstrated much lower nucleotide identities (74.8%–89.8%) in the 3′ region encoding from Nsp6 to ORF7. In contrast, IA70388-R showed high nucleotide identities (99.3%–100%) to the Fostera PRRSV vaccine strain in Nsp6 to ORF7 and lower nucleotide identities in Nsp1α, Nsp1β, and Nsp2~5. These results suggested that

Figure. Genome recombination analysis of the IA70388-R strain of porcine reproductive and respiratory syndrome virus, United States, 2018. A) UPGMA of region derived from major parent (1–6742). B) UPGMA of region derived from major parent (6743–15642 nt). Phylogenies of the parent strains were identified using RDP version 4.24 software (http://web.cbio.uct.ac.za/~darren/rdp.html). Red indicates the recombinant (IA70388-R); green indicates the major parent strain (the Fostera vaccine strain); blue indicates the minor parent strain (IA76950-WT). Scale bars indicate nucleotide substitutions per site.

IA70388-R might be a recombinant that evolved from IA76950-WT and the Fostera vaccine virus.

We further constructed a phylogenetic tree of the NSP2 gene, ORF5 gene, and whole-genome sequences using 12 representative field strains and 5 vaccine strains (Appendix Figure 1). IA76950-WT, IA70388-R, and Fostera vaccine strains were located in 3 different lineages based on the whole-genome sequences. For analysis of NSP2 sequence, IA76950-WT and IA70388-R formed a minor branch and clustered close to the MN184A and NADC30 but remotely from the lineages formed by Fostera, SDSU73, VR2332, and Ingelvac MLV. In contrast, the ORF5 sequence-based phylogenetic tree showed that IA70388-R clustered with Fostera vaccine strain in lineage L8, and the IA76950-WT clustered with NADC30, MN184, and Prevacent vaccine strains in lineage L1 (Appendix Figure 1). These results also suggested that IA70388-R might be a mosaic.

Finally, we aligned the complete genomes of IA76950-WT, IA70388-R, and the Fostera strains using ClustalX (http://www.clustal.org) and conducted a similarity plot analysis using SimPlot software (7). One recombination breakpoint was identified in the Nsp5 (nucleotide position 6742) separating the genome into 2 regions (Appendix Figure 2). IA70388-R was highly similar to that of IA76950-WT in the 5′ region with 99%–99.8% nt identities; however, IA70388-R had high similarity with the Fostera vaccine strain in the 3′ region with 99.3%–100% nt identities (Appendix Figure 2). In addition, we used RDP version 4.24 (http://web.cbio.uct.ac.za/~darren/rdp.html) to evaluate potential recombinants, and it completely confirmed the results of SimPlot analysis (Figure).

All thus far reported recombinant strains from vaccine and field strains in Europe and Asia were based solely on the bioinformatics prediction, and their wild-type parent strains were only theoretically deduced but not actually identified (8–10). In this study, we provide solid evidence that a natural recombinant virus evolved from a vaccine strain and a field strain in the United States. The virulence of the recombinant appeared to be reversed, although a pathogenicity study is still needed to confirm. Our study emphasizes the importance of monitoring recombination between vaccine and field strains in swine herds and reiterates the limitations of ORF5-based sequencing for PRRSV characterization, highlighting that full-length genome sequencing is more reliable.

About the Author

Dr. Wang is a professor in the Jiangsu Agri-animal Husbandry Vocational College and a visiting scholar in the College of Veterinary Medicine, Iowa State University. Her research interests focus on diagnosis of viral infectious diseases and new pathogen discovery.

References

1. Cavanagh D. Nidovirales: a new order comprising Coronaviridae and Arteriviridae. Arch Virol. 1997;142:629–33.
2. Bian T, Sun Y, Hao M, Zhou L, Ge X, Guo X, et al. A recombinant type 2 porcine reproductive and respiratory syndrome virus between NADC30-like and a MLV-like: genetic characterization and pathogenicity for piglets. Infect Genet Evol. 2017;54:279–86. https://doi.org/10.1016/j.meegid.2017.07.016
3. Li B, Fang L, Xu Z, Liu S, Gao J, Jiang Y, et al. Recombination in vaccine and circulating strains of porcine reproductive and respiratory syndrome viruses. Emerg Infect Dis. 2009;15:2032–5. https://doi.org/10.3201/eid1512.090390
4. Zhou L, Kang R, Yu J, Xie B, Chen C, Li X, et al. Genetic characterization and pathogenicity of a novel recombined porcine reproductive and respiratory syndrome virus 2 among Nadc30-like, Jxa1-like, and Mlv-like strains. Viruses. 2018;10:10. https://doi.org/10.3390/v10100551
5. Eclercy J, Renson P, Lebret A, Hirchaud E, Normand V, Andraud M, et al. A field recombinant strain derived from two type 1 porcine reproductive and respiratory syndrome virus (PRRSV-1) modified live vaccines shows increased viremia and transmission in SPF pigs. Viruses. 2019;11:11. https://doi.org/10.3390/v11030296
6. Liu J, Zhou X, Zhai J, Wei C, Dai A, Yang X, et al. Recombination in JXA1-R vaccine and NADC30-like strain of porcine reproductive and respiratory syndrome viruses. Vet Microbiol. 2017;204:110–20. https://doi.org/10.1016/j.vetmic.2017.04.017
7. Lole KS, Bollinger RC, Paranjape RS, Gadkari D, Kulkarni SS, Novak NG, et al. Full-length human immunodeficiency virus type 1 genomes from subtype C-infected seroconverters in India, with evidence of intersubtype recombination. J Virol. 1999;73:152–60.
8. Franzo G, Cecchinato M, Martini M, Ceglie L, Gigli A, Drigo M. Observation of high recombination occurrence of porcine reproductive and respiratory syndrome virus in field condition. Virus Res. 2014;194:159–66. https://doi.org/10.1016/j.virusres.2014.08.005
9. Martín-Valls GE, Kvisgaard LK, Tello M, Darwich L, Cortey M, Burgara-Estrella AJ, et al. Analysis of ORF5 and full-length genome sequences of porcine reproductive and respiratory syndrome virus isolates of genotypes 1 and 2 retrieved worldwide provides evidence that recombination is a common phenomenon and may produce mosaic isolates. J Virol. 2014;88:3170–81. https://doi.org/10.1128/JVI.02858-13
10. van Geelen AGM, Anderson TK, Lager KM, Das PB, Otis NJ, Montiel NA, et al. Porcine reproductive and respiratory disease virus: evolution and recombination yields distinct ORF5 RFLP 1-7-4 viruses with individual pathogenicity. Virology. 2018;513:168–79. https://doi.org/10.1016/j.virol.2017.10.002

Address for correspondence: Ganwu Li, Iowa State University, Department of Veterinary Diagnostic and Production Animal Medicine, College of Veterinary Medicine, 1907 ISU C-Dr, VMRI #1, Ames, IA 50011, USA; email: liganwu@iastate.edu

Genetic Characterization of Avian Influenza A(H5N6) Virus Clade 2.3.4.4, Russia, 2018

Ivan M. Susloparov, Natalia Goncharova, Natalia Kolosova, Alexey Danilenko, Vasiliy Marchenko, Galina Onkhonova, Vasiliy Evseenko, Elena Gavrilova, Rinat A. Maksutov, Alexander Ryzhikov

Author affiliation: State Research Center of Virology and Biotechnology Vector, Koltsovo, Russia

Timely identification of pandemic influenza threats depends on monitoring for highly pathogenic avian influenza viruses. We isolated highly pathogenic avian influenza A(H5N6) virus clade 2.3.4.4, genotype G1.1, in samples from a bird in southwest Russia. The virus has high homology to human H5N6 influenza strains isolated from southeast China.

Highly pathogenic avian influenza (HPAI) H5 virus continues to evolve and pose a threat to animals and humans. Since 2008, HPAI H5 viruses of clade 2.3.4.4 with various neuraminidase (NA) subtypes have become widespread throughout the world and have caused mass epizootics, including in Russia, where these viruses have been reported since 2014 (*1*). In 2013, H5N6 virus began circulating in China (*2*), and a case of human disease was recorded there in 2014. Since then, 23 cases of H5N6 infection in humans, including 7 fatalities, have been confirmed in China (*3*).

In October 2018, we collected cloacal swab samples from aquatic birds around the Volga River Basin in the Saratov region of Russia (51°26′11.7″N, 46°06′49.9″E). We isolated avian H5 influenza virus from 1 sample from a common gull (*Larus canus*) by using embryonic chicken eggs. We used whole-genome sequencing to extract the virus DNA and conducted a phylogenetic analysis against strains available in the GISAID EpiFlu database (http://www.gisaid.org). We submitted genetic data on the virus, A/common gull/Saratov/1676/2018, to the GISAID EpiFlu database (identification no. EPIISL336925).

Using H5 clade nomenclature designated by the World Health Organization/World Organisation for Animal Health/Food and Agriculture Organization H5 Evolution Working Group (*4*), our phylogenetic analysis showed that hemagglutinin (HA) gene of A/common gull/Saratov/1676/2018 clusters with HPAI viruses in clade 2.3.4.4 H5N6-H5/Major lineage. Our analyses also show this strain belongs to a new HA subgroup that includes human H5N6 viruses isolated in Guangxi and Guangdong Provinces, China, in 2018 (Appendix Figure 1, Table 1, https://wwwnc.cdc.gov/EID/article/25/12/19-0504-App1.pdf). This subgroup is not represented by existing candidate vaccine viruses (CVVs) (*5,6*).

The NA gene of A/common gull/Saratov/1676/2018 appears to originate from H6N6 viruses circulating in Asia during 2010–2011 (Appendix Figure 2) and contains the deletion from positions 59–69 in the stalk region. The polymerase basic (PB) 2 gene segment also appears to have originated from an H6 subtype (Appendix Figure 3). The internal gene segments PB1, polymerase (PA), nucleoprotein (NP), matrix (M), and nonstructural protein (NSP) appear to have evolved from HPAI H5 virus clade 2.3.2.1 (Appendix Figures 4–8). The 8-segment constellation leads us to classify this strain into a G1.1 genotype, as described by Bi et al. (*6*).

We conducted a comparative genomic analysis of A/common gull/Saratov/1676/2018 against H5N6 CVVs; the most pronounced differences were several amino acid substitutions associated with potential changes in antigenic properties. We also detected unique mutations in HA D54N, L115Q, L/Q138T, P141A, N183S, and N189D, including a combination of S121Y and I151T. We noted other mutations, including HA L129S, K/M/T140V (H5 numbering), and NA N86K (N6 numbering), which could be associated with antigenic drift.

A/common gull/Saratov/1676/2018 had an HA polybasic proteolytic cleavage site, PLRERRRKR/G, and showed highly pathogenic properties by killing chicken embryos within 48 hours. We also identified amino acid changes associated with increased virulence to mammals (*7,8*), including 9 mutations in the PB2 gene, 8 in the PB1 gene, 7 in the NSP gene, 3 in the M gene, 2 in the PA gene, 1 in the HA gene, and 1 in the NA gene, along with the 59–69 deletion, an 80–84 deletion in NS1, and an NS1 ESEV terminal motif. These changes also appear in most H5N6 CVVs (Appendix Table 2).

Comparative analysis of A/common gull/Saratov/1676/2018 against H5N6 CVVs revealed similarity in the presence of genetic elements associated with receptor binding properties. A/common gull/Saratov/1676/2018 and most CVVs had the motif QS(R)G at the receptor-binding site (nt 222–224), which is associated with an avian-like α2,3-SA receptor-binding preference (*6*). The amino acid changes in D94N, S133A, and T156A in the HA of A/common gull/Saratov/1676/2018 and most H5N6 CVVs are associated with increased binding of the virus to human-like α2,6-SA receptors (*7*). Our analysis suggests that A/common gull/Saratov/1676/2018 retains its avian status but has several mutations that potentially increase its affinity for α2,6-SA, which could indicate an affinity for both avian- and human-type receptors.

We evaluated the phenotypic properties of the virions by kinetics measurement with surface plasmon resonance to assess their ability to bind to receptor analogs α2,3-SA

and α2,6-SA (*9*). The equilibrium dissociation constant for 3′-Sialyl-N-acetyllactosamine is 12.2 (SD ± 0.7 nmol/L) and for 6′-Sialyl-N-acetyllactosamine is 43.3 (SD ± 2.8 nmol/L) (Appendix). These values show that A/common gull/Saratov/1676/2018 has prevalent affinity for the avian-like receptor with lower, but increased, affinity for the human-like receptor, compared with H5N1 strain A/rook/Chany/32/2015 clade 2.3.2.1.C.

Analysis of homology of A/common gull/Saratov/1676/2018 with H5N6 strains available from GISAID showed that all 8 gene segments clustered with human H5N6 strains isolated in southeast China in 2018. We noted 99% homology with human strain A/Guangxi/32797/2018 for all genes, a genetic similarity that raises the question of which pathway led to the spread of the virus. We believe A/common gull/Saratov/1676/2018 was transferred to eastern Russia through northeast Siberia, where HPAI H5N8 clade 2.3.4.4.A was detected in 2018 (*10*), the same pathway through which H5N8 virus was transferred from Southeast Asia to Europe. These viral pathogens could be spread by migratory birds over long distances along flyways from southern China to southwestern Russia during a migration season. Our study indicates that emerging H5N6 viruses are a potential threat to public health.

About the Author

Dr. Susloparov is a senior researcher at the Zoonosis Infections and Influenza Department, State Research Center of Virology and Biotechnology Vector, Koltsovo, Russia. His research interests include the molecular genetics, epidemiology, and host–pathogen interaction of avian influenza viruses.

References

1. Marchenko V, Goncharova N, Susloparov I, Kolosova N, Gudymo A, Svyatchenko S, et al. Isolation and characterization of H5Nx highly pathogenic avian influenza viruses of clade 2.3.4.4 in Russia. Virology. 2018;525:216–23. https://doi.org/10.1016/j.virol.2018.09.024
2. Bi Y, Liu H, Xiong C, Di Liu, Shi W, Li M, et al. Novel avian influenza A (H5N6) viruses isolated in migratory waterfowl before the first human case reported in China, 2014. Sci Rep. 2016;6:29888. https://doi.org/10.1038/srep29888
3. World Health Organization. Regional Office for the Western Pacific. Avian Influenza Weekly Update Number 671. Geneva: the Organization; 2019 Jan 11 [cited 2019 Jan 11]. https://apps.who.int/iris/bitstream/handle/10665/279855/AI-20190111.pdf
4. Smith GJ, Donis RO; World Health Organization/World Organisation for Animal Health/Food and Agriculture Organization (WHO/OIE/FAO) H5 Evolution Working Group. Nomenclature updates resulting from the evolution of avian influenza A(H5) virus clades 2.1.3.2a, 2.2.1, and 2.3.4 during 2013–2014. Influenza Other Respir Viruses. 2015;9:271–6. https://doi.org/10.1111/irv.12324
5. World Health Organization. Antigenic and genetic characteristics of zoonotic influenza viruses and development of candidate vaccine viruses for pandemic preparedness. Geneva: the Organization; February 2019 [cited 2019 Feb 21]. https://www.who.int/influenza/vaccines/virus/201902_zoonotic_vaccinevirusupdate.pdf
6. Bi Y, Chen Q, Wang Q, Chen J, Jin T, Wong G, et al. Genesis, evolution, and prevalence of H5N6 avian influenza viruses in China. Cell Host Microbe. 2016;20:810–21. https://doi.org/10.1016/j.chom.2016.10.022
7. Guo F, Luo T, Pu Z, Xiang D, Shen X, Irwin DM, et al. Increasing the potential ability of human infections in H5N6 avian influenza A viruses. J Infect. 2018;77:349–56. https://doi.org/10.1016/j.jinf.2018.07.015
8. Yang L, Zhu W, Li X, Bo H, Zhang Y, Zou S, et al. Genesis and dissemination of highly pathogenic H5N6 avian influenza viruses. J Virol. 2017;91:e02199–16. https://doi.org/10.1128/JVI.02199-16
9. Meng B, Marriott AC, Dimmock NJ. The receptor preference of influenza viruses. Influenza Other Respir Viruses. 2010;4:147–53. https://doi.org/10.1111/j.1750-2659.2010.00130.x
10. Verhagen JH, Herfst S, Fouchier RA. Infectious disease. How a virus travels the world. Science. 2015;347:616–7. https://doi.org/10.1126/science.aaa6724

Address for correspondence: Ivan M. Susloparov, State Research Center of Virology and Biotechnology Vector, 630559, Koltsovo, Novosibirsk Region, Russia; email: imsous@vector.nsc.ru

Human Parasitism by *Amblyomma parkeri* Ticks Infected with *Candidatus* Rickettsia paranaensis, Brazil

Ana Beatriz P. Borsoi, Karla Bitencourth, Stefan V. de Oliveira, Marinete Amorim, Gilberto S. Gazêta

Author affiliations: Instituto Oswaldo Cruz, Rio de Janeiro, Brazil (A.B.P. Borsoi, K. Bitencourth, M. Amorim, G.S. Gazêta); Universidade Federal de Uberlândia, Uberlândia, Brazil (S.V. de Oliveira); Ministério da Saúde do Brasil, Brasília, Brazil (S.V. de Oliveira)

Spotted fever is the main rickettsial disease in Brazil. We report 12 cases of human parasitism by *Amblyomma parkeri* in the Atlantic rainforest, an area of Brazil to which spotted fever is endemic. Nine of the ticks were infected with *Candidatus* Rickettsia paranaensis.

Spotted fever is considered the main tickborne disease in South America (*1*). In Brazil, spotted fever has been reported since the 1920s and is known to show great clinical diversity and ecoepidemiologic scenario complexity, involving *Rickettsia rickettsii* transmitted by *Amblyomma sculptum* and *A. aureolatum* ticks and *Rickettsia parkeri* strain Atlantic rainforest vectored by *A. ovale* ticks (*2*). However, several studies have identified different *Rickettsia* species infecting a variety of tick species in Brazil, indicating the possibility of newly emerging spotted fever scenarios in Brazil (*1–3*).

In southern Brazil, in addition to the scenario already established for the Atlantic forest region, studies indicate the possibility of a unique cycle developing in the Pampa biome, in which *R. parkeri* sensu stricto might be associated with spotted fever cases involving an *A. tigrinum* tick vector (*3*). Accordingly, to expand the understanding of the spotted fever scenario in Brazil, we conducted a molecular study of *Rickettsia* in *A. parkeri* ticks as parasites of humans in an area of Brazil to which spotted fever is endemic.

During 2013–2018, in an investigation and surveillance of spotted fever cases in urban areas near Atlantic rainforest fragments in the Parana, Santa Catarina, and Rio Grande do Sul states in southern Brazil, we collected 12 tick nymphs parasitizing humans and morphologically identified these ticks as *A. parkeri* (*4*). We individually processed 11 specimens for DNA extraction (*5*), subjected this DNA to PCR for molecular confirmation of tick species (*6*), and isolated *glt*A, *htr*A, *omp*A, and *omp*B gene fragments (Appendix Table, https://wwwnc.cdc.gov/EID/article/25/12/19-0988-App1.pdf). We purified PCR products, sequenced them, and compared them with rickettsial sequences available in GenBank. We subjected concatenated aligned rickettsial sequences to maximum-likelihood analysis.

We identified *A. parkeri* ticks with containing rickettsia in all 3 states studied. Nine samples amplified fragments from ≥1 of the 4 rickettsia gene markers studied. All sequences for *omp*B and *omp*A gene fragments showed 100% similarity with *Candidatus* Rickettsia paranaensis (GenBank accession nos. KX018050, JN126322, and
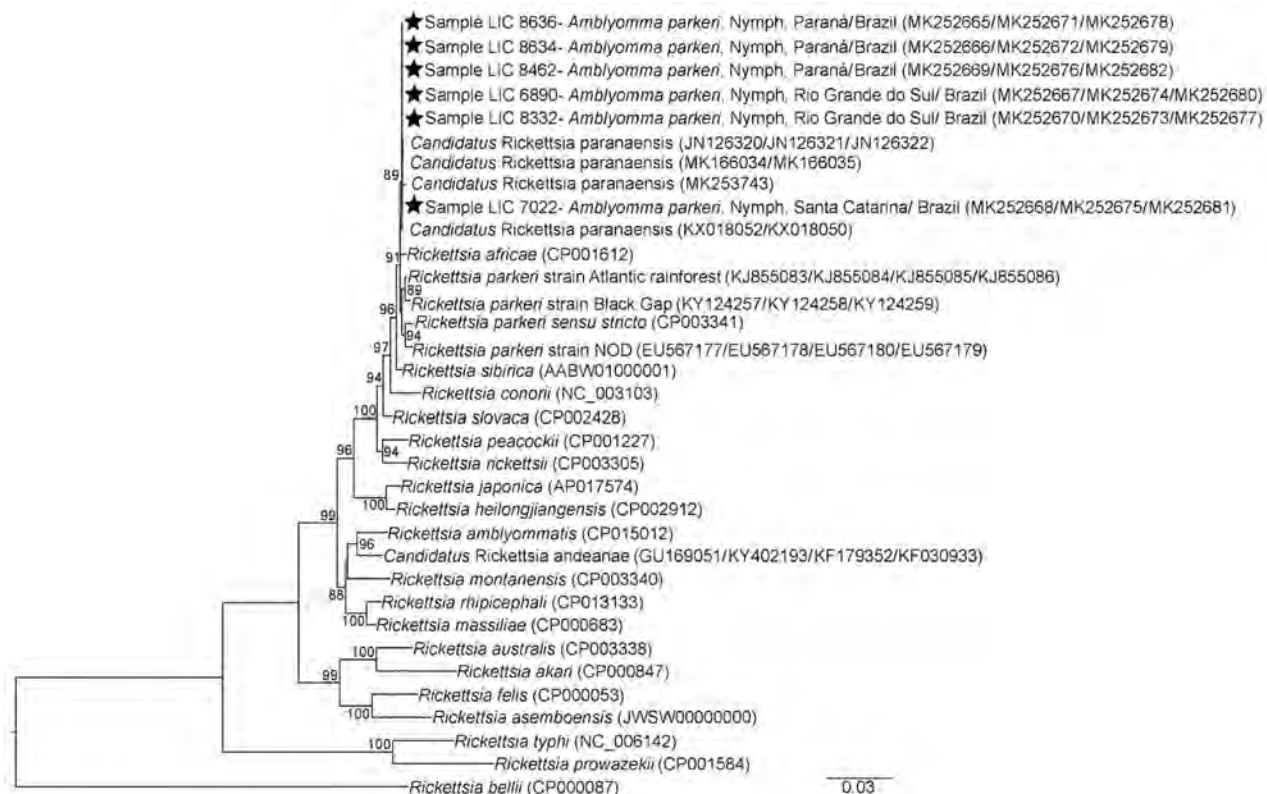
Figure. Concatenated phylogenetic analysis of rickettsia gene fragments detected in *Amblyomma parkeri* ticks in Brazil. Gene fragments *glt*A (1,013 bp), *htr*A (370 bp), *omp*A (494 bp), and *omp*B (822 bp) were inferred by maximum-likelihood analysis with the evolution model T92 + G (Tamura model). Values on the branches indicate bootstrap values (cutoff value 70%). Stars indicate sequences obtained in this study. GenBank accession numbers are given in parentheses. Scale bar indicates nucleotide substitutions per site.

JN126321). The *htr*A and *glt*A sequences had 100% similarity to many of the spotted fever group rickettsia, including *Candidatus* R. paranaensis (GenBank accession nos. KX018052 and JN126320). Phylogenetic analysis showed that bacteria detected in *A. parkeri* ticks from southern Brazil were in the same clade as *Candidatus* R. paranaensis (Figure).

The pathogenicity of *Candidatus* R. paranaensis is unknown. However, Peckle et al. (*7*) placed it close to the Old World species *R. africae* and *R. sibirica*, both of which are proven pathogenic species (*1*). *A. parkeri* nymphs infected by *Candidatus* R. paranaensis are not uncommon (*7*) and might have high frequencies of infection. Luz et al. (*8*) reported that 75% of passariform birds in southeastern Brazil were infected with ticks, a value similar to that obtained in this study (81.81%) for humans in the southern region. Thus, circulation of *Candidatus* R. paranaensis in the Atlantic Forest biome might be closely associated with the presence of *A. parkeri* immature tick stages and passeriform birds.

Although reports of human parasitism by tick species of the genus *Amblyomma* are increasing, *A. parkeri* ticks have been rarely reported from humans, although there are reports of parasitism in the Atlantic rainforest area of southeastern Brazil, including a high prevalence of this ixodid (nymphs) on humans in Rio Grande do Sul State (*9,10*). Although these reports were for a region to which spotted fever is endemic, there was no study of the associated rickettsia. However, our results show 12 humans parasitized by *A. parkeri* nymphs in the 3 states that comprise the southern region of Brazil, indicating that the parasitism of humans by such ticks is more common than that reported. Examples of *Candidatus* R. paranaensis in *A. parkeri* parasitizing humans in an area to which spotted fever is endemic, with milder clinical characteristics (*2*), highlight the need to investigate the role of vector and rickettsia in spotted fever in southern Brazil. This investigation should help in formulating appropriate public health responses by existing surveillance programs.

About the Author

Ms. Borsoi is a PhD student at the Oswaldo Cruz Institute, Rio de Janeiro, Brazil. Her primary research interests are tick taxonomy and rickettsia, with an emphasis on tick–human interactions.

References

1. Parola P, Paddock CD, Socolovschi C, Labruna MB, Mediannikov O, Kernif T, et al. Update on tick-borne rickettsioses around the world: a geographic approach. Clin Microbiol Rev. 2013;26:657–702. https://doi.org/10.1128/CMR.00032-13
2. de Oliveira SV, Guimarães JN, Reckziegel GC, Neves BM, Araújo-Vilges KM, Fonseca LX, et al. An update on the epidemiological situation of spotted fever in Brazil. J Venom Anim Toxins Incl Trop Dis. 2016;22:22. https://doi.org/10.1186/s40409-016-0077-4
3. Weck B, Dall'Agnol B, Souza U, Webster A, Stenzel B, Klafke G, et al. Spotted fever group *Rickettsia* in the pampa biome, Brazil, 2015–2016. Emerg Infect Dis. 2016;22:2014–6. https://doi.org/10.3201/eid2211.160859
4. Martins TF, Onofrio VC, Barros-Battesti DM, Labruna MB. Nymphs of the genus *Amblyomma* (Acari: Ixodidae) of Brazil: descriptions, redescriptions, and identification key. Ticks Tick Borne Dis. 2010;1:75–99. https://doi.org/10.1016/j.ttbdis.2010.03.002
5. Aljanabi SM, Martinez I. Universal and rapid salt-extraction of high quality genomic DNA for PCR-based techniques. Nucleic Acids Res. 1997;25:4692–3. https://doi.org/10.1093/nar/25.22.4692
6. Mangold AJ, Bargues MD, Mas-Coma S. Mitochondrial 16S rDNA sequences and phylogenetic relationships of species of *Rhipicephalus* and other tick genera among Metastriata (Acari: Ixodidae). Parasitol Res. 1998;84:478–84. https://doi.org/10.1007/s004360050433
7. Peckle M, Luz HR, Labruna MB, Serpa MCA, Lima S, Maturano R, et al. Multi-locus phylogenetic analysis groups the New World bacterium *Rickettsia* sp. strain ApPR with the Old World species *R. africae*; proposal of "*Candidatus* Rickettsia paranaensis". Ticks Tick Borne Dis. 2019;10:101261. https://doi.org/10.1016/j.ttbdis.2019.07.005
8. Luz HR, Faccini JLH, McIntosh D. Molecular analyses reveal an abundant diversity of ticks and rickettsial agents associated with wild birds in two regions of primary Brazilian Atlantic Rainforest. Ticks Tick Borne Dis. 2017;8:657–65. https://doi.org/10.1016/j.ttbdis.2017.04.012
9. Martins TF, Scofield A, Oliveira WBL, Nunes PH, Ramirez DG, Barros-Battesti DM, et al. Morphological description of the nymphal stage of *Amblyomma geayi* and new nymphal records of *Amblyomma parkeri*. Ticks Tick Borne Dis. 2013;4:181–4. https://doi.org/10.1016/j.ttbdis.2012.11.015
10. Reck J, Souza U, Souza G, Kieling E, Dall'Agnol B, Webster A, et al. Records of ticks on humans in Rio Grande do Sul state, Brazil. Ticks Tick Borne Dis. 2018;9:1296–301. https://doi.org/10.1016/j.ttbdis.2018.05.010

Address for correspondence: Karla Bitencourth, Laboratório de Referência Nacional em Vetores das Riquetsioses, Anexo Posterior ao Pavilhão Lauro Travassos, Sala 8, Instituto Oswaldo Cruz, Fundação Oswaldo Cruz, Av. Brasil, 4.365, Manguinhos, Rio de Janeiro RJ 21040-900, Brazil; email: karlabitencourth@gmail.com

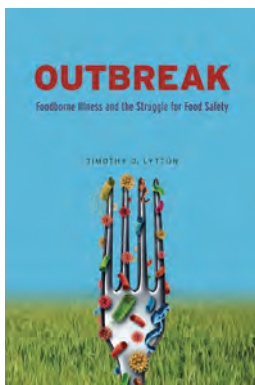# Outbreak: Foodborne Illness and the Struggle for Food Safety

Public health advances step by step, as hazards are recognized and better control and prevention strategies are developed. How this happens, how new safety measures come into being, and how they are improved and become part of the way we live are the focus of this new book, Outbreak: Foodborne Illness and the Struggle for Food Safety.

Professor Timothy D. Lytton, a keen scholar of regulatory evolution, provides a lively and well-documented guide to 150 years of major advances in food safety regulation and prevention in the United States. He starts with the early efforts to cleanse and regulate the milk supply in the 19th century that ultimately led to near-universal pasteurization. Efforts to make canned food free of botulism in the 1920s led to a new focus on critical control steps in processing, using sufficient time and heat to eliminate the risk, and thus to a new general approach based on process control. Modernizing meat inspection with process control logic in the 1990s and the recent efforts to make fresh produce safer in the 2000s take the reader to the controversies of the present day.

This book fills a critical gap, weaving the history of public health, regulatory agencies, and the food industry together with issues of immediate concern today. It is an innovative perspective that captures the complexity of the system beyond the scientific report or published regulation. The book should be of interest to students and practitioners of public health and food science and anyone interested in making food reliably safe.

With fresh examples and detailed interviews, Lytton illustrates the dynamic interplay of outbreak investigations, better prevention strategies developed by industry, consumer advocacy, and regulations. He explains why the resulting balance is a punctuated equilibrium, with longer steady states ending in momentous rapid change. Large and catastrophic outbreaks come as the final trigger, as "focusing events" that, with media coverage, increase public attention and create pressure for change. Lytton tells the striking and less well-known story of what happens behind the scenes as food safety champions within the industry push new solutions and voluntary standards forward, show how they could reduce contamination, and gain adherents up and down the food supply chain, thus leading the way for others in industry and regulators to follow. He also deftly outlines the complex roles of third-party auditors, who provide information to one company about the safety practices of its suppliers, and provides a fresh perspective on the growing role that liability insurers may play in the future.

This is history that uplifts, showing how we honor those who suffered from and died of a foodborne disease that is now preventable in the form of better practices and safer food today. In the crucible of public action, it reminds us all how these advances begin and, with feedback and learning, how they can succeed.

Robert Tauxe

Author affiliation: Centers for Disease Control and Prevention, Atlanta, Georgia, USA

Address for correspondence: Robert Tauxe, Centers for Diseases Control and Prevention, 1600 Clifton Rd NE, Mailstop C-09, Atlanta, GA 30329-4027, USA; email: rvt1@cdc.gov

Antimicrobial Resistance in Bacteria from Livestock and Companion Animals

In this era of "superbugs" and rising antimicrobial resistance, *Antimicrobial Resistance in Bacteria from Livestock and Companion Animals* is a valuable resource to better understand the contribution of animal-derived pathogens to this growing public health crisis. The use of antimicrobial drugs in animal populations is not without controversy; the underlying concern, of course, is that antimicrobial use in animals results in illness and death in humans. This text does not seek to specifically condemn or exonerate. Instead,
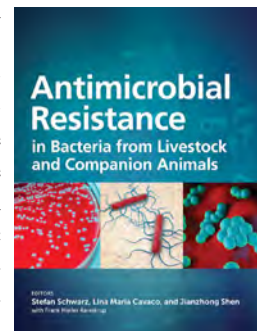
it provides a comprehensive account of a very complicated topic, delving into the nuances needed to understand the what, where, when, and why of antimicrobial resistance in companion animals and livestock.

The text begins with a historical overview of the discovery of antimicrobial drugs and a detailed characterization of the indications for and regulation of their use in veterinary medicine. Salient technical issues are discussed, including antimicrobial susceptibility testing in veterinary pathogens, diagnostic methods for detecting antimicrobial resistance, and licensing of antimicrobial drugs. Overviews of the mechanisms of resistance to antimicrobial agents, including antibiotics, metals, and biocides, provide context to the main substance of the text: an exhaustive report of current antimicrobial resistance in a wide range of pathogens of veterinary and medical importance. The text closes with a look into the future of mitigating antimicrobial resistance in veterinary and production settings through monitoring, surveillance, and antimicrobial stewardship.

Antimicrobial Resistance in Bacteria from Livestock and Companion Animals presents a wealth of information and is a critical resource for anyone who studies, treats, or is affected by antimicrobial resistance in domesticated animals or the food products that come from them. Contributing authors are globally renowned experts in the field who have composed thoughtful and insightful accounts that generally walk the line between technically thorough and accessible to a broad audience. Whether one is interested in a specific pathogen or in policy to mitigate antimicrobial resistance, this text offers a comprehensive review of the increasingly urgent topic that is antimicrobial resistance in animal-derived pathogens.

Laurel Redding

Author affiliation: University of Pennsylvania, Kennett Square, Pennsylvania, USA

Address for correspondence: Laurel Redding, University of Pennsylvania New Bolton Center Hospital for Large Animals, 382 W Street Rd, Kennett Square, PA 19348-1691, USA; email: lredding@vet.upenn.edu

NEWS AND NOTES

Emerging Infectious Diseases Is Moving to Online Only

Starting with the January 2020 issue, *Emerging Infectious Diseases* (EID) will join the growing ranks of journals published online only. We made the decision to stop publishing on paper with the recognition that our readers increasingly access the journal only online, and not through paper copies. In addition, we think the move offers at least three advantages to the journal and its readers. First, we can use budget dollars saved for other important journal functions, such as editing and production. EID is now recruiting a new assistant editor, who will help speed up the review of submitted manuscripts.

Second, we can "go green." Printing and mailing paper issues of the journal carry environmental costs. In recent years, we have come to believe that these costs are not outweighed by whatever advantages remain to printed pages.

Third, we can place even more emphasis on online-only materials included as supplements or appendices to articles published in the journal. These materials now represent a substantial portion of all the pages that we publish. We think that, in the future, they will become an even more important part of the journal.

Readers should rest assured that EID articles will continue to be available online as they have before, along with supplemental materials and appendices. Entire issues of the journal will continue to be available in the PDF format. Readers who have enjoyed browsing a full printed issue of EID can continue to so by using any Web-connected desktop or laptop computer, tablet, or smartphone.

We invite all readers to subscribe to our monthly table of contents alerts on the journal's Web site at https://wwwnc.cdc.gov/eid/subscriptions and to follow us on Twitter at https://twitter.com/CDC_EIDjournal.

D. Peter Drotman
Editor-in-Chief

# A Fanciful Juxtaposition, a Reimagined Farm

Byron Breedlove

Detecting the emergence of novel pathogens before they spread from local sites, where they first appear in animals or humans, is crucial for responding effectively to zoonotic health threats. In *The Tilled Field*, which appears as this month's cover art, internationally acclaimed artist Joan Miró Ferra was not, of course, offering a lesson in how zoonoses such as anthrax, brucellosis, cryptosporidiosis, hantavirus pulmonary syndrome, leptospirosis, orfs, rabies, or salmonellosis may be spread. Nonetheless, his painting reminds viewers of the interdependent relationship among people, animals, plants, and their shared environment.

The Fundació Joan Miró notes that Miró "avoided academicism in his constant quest for a pure, global art that could not be classified under any specific movement." Throughout his long career, Miró's deliberate approach to, and tenacious experimentation with forms of expression enabled him to complete a vast, diverse collection of works, estimated to include some 2,000 oil paintings, 500 sculptures, 400 ceramic objects, 5,000 drawings and collages, and 250 illustrated books. Miró said, "I work like a labourer on a farm or in a vineyard. Things come to me slowly. My vocabulary of forms, for instance, has not been the discovery of a day. It took shape in spite of myself.... That is why I am always working on a hundred different things at the same time."

During the summer of 1923, Miró started painting *The Tilled Field*, an homage to his family's farm in Montroig del Camp, Catalonia, Spain. Miró had previously approached the same subject in an earlier painting called *The Farm* (1921–1922). (Writer Ernest Hemingway, who purchased *The Farm*, wrote that "After Miró had painted *The Farm* and after James Joyce had written *Ulysses*, they had a right to expect people to trust the further things they did even when the people did not understand them.")

The Tilled Field is noteworthy both for being among Miró's earliest surrealistic works and for marking his
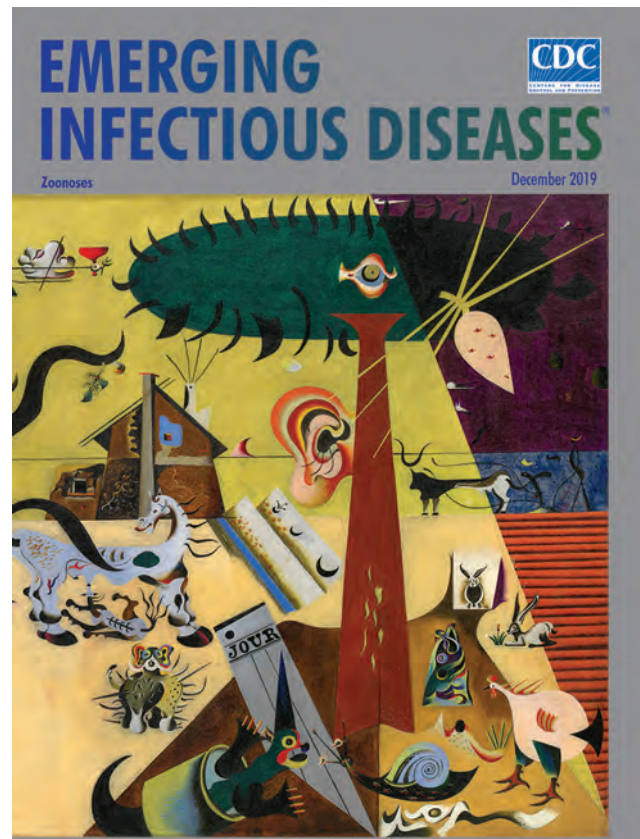
Joan Miró (1893–1983), *The Tilled Field* (*La Terre Labourée*), **1923–1924.** Oil on canvas; 26 in × 36.5 in/66 cm × 92.7 cm. © 2018 Successió Miró / Artists Rights Society (ARS), New York / ADAGP, Paris 2019. Photo Credit: The Solomon R. Guggenheim Museum/Art Resource, New York, New York, USA.

nascent use of an evolving pictorial language of symbols and creatures he employed throughout the rest of his career. Nancy Spector, chief curator and art director at the Guggenheim Museum, notes that the "fanciful juxtaposition of human, animal, and vegetal forms and its array of schematized creatures constitute a realm visible only to the mind's eye and reveal the great range of Miró's imagination."

Miró organized the painting into distinct areas defined by geometric shapes. Subdued, smooth trapezoid panels of

Author affiliation: Centers for Disease Control and Prevention, Atlanta, Georgia, USA

dark and pale yellow converge at the center and fill most of the canvas, functioning as sky and earth, respectively. Six rippled furrows in the bottom left represent one tilled field. The crisp diagonal line that slices down the right side creates a triangle, subdivided into three distinct sections: another tilled field in the bottom right, a small blue trapezoid of blue sky (daylight) in the center, and a larger purple trapezoid (night) situated in the top right.

The large tree dominating the right side of the painting features an all-seeing eye centered in its biomorphic crown and a human ear attached to its trunk. The French word *jour* (day) appears on folded sheet of newsprint at the base of the tree; a farmhouse with cracked walls and a straight chimney—perhaps Miro's family home—occupies the center of the canvas. To the left, a stylized tree cradles a flagpole with the flags of France, Spain, and Catalonia emerging from its crook. Another flag hangs between the tree limb that juts to the upper left of the canvas and the stalk thrusting up from the sawtooth aloe plant.

A menagerie of multicolored creatures, including a dog, snail, horse and foal, chicken, rabbits, birds, a fish half out of the water, and a lizard, are scattered across the painting. Many were inspired by various Catalan ceramics that Miró collected. Historical and cultural sources were also important to the artist, and the farmer following a cattle-drawn plough is styled on the Altamira cave paintings. Though Miró employs a surrealistic perspective, the overall impression is that his painting still evokes normal life on a family farm before the Spanish Civil War. Art historian Janis Mink notes that "the animals, house, fields, and plants have become disquieting presences, stretched, swollen, and barbed sometimes even into ugliness. At the same time, they insist on their identities."

Miró's reimagined, surreal farm depicts a setting in which humans and animals would be in close proximity.

It is the type of environment where emerging and reemerging zoonotic infections could be spread from between animals and humans via viruses, bacteria, parasites, or fungi. Zoonotic diseases are spread in myriad ways, from direct contact with animals or their blood, birth products, urine, or feces; being bitten or scratched by animals; encountering water or soil contaminated with pathogens spread by animals; or consuming unsafe or contaminated foods. All are possibilities on a small family farm or scaled-up modern agricultural enterprises.

Bibliography

1. Bird BH, Mazet JA. Detection of emerging zoonotic pathogens: an integrated One Health approach. Annu Rev Anim Biosci. 2018;6:121–39. https://doi.org/10.1146/annurev-animal-030117-014628
2. Centers for Disease Control and Prevention. Zoonotic diseases [cited 2019 Oct 22]. https://www.cdc.gov/onehealth/basics/zoonotic-diseases.html
3. Centers for Disease Control and Prevention. One Health [cited 2019 Oct 26]. https://www.cdc.gov/onehealth/index.html
4. Fundació Joan Miró. Biography [cited 2019 Oct 23]. https://www.fmirobcn.org/en/joan-miro/
5. Guggenheim Museum. Joan Miró. The tilled field (*La terre labourée*) [cited 2019 Aug 23]. https://www.guggenheim.org/artwork/2934
6. Hemingway E. The Farm. Paris: Cahiers d'Art, IX, No. 1-4; 1934. p. 28–9.
7. Mink J. Joan Miró: 1893–1983. Cologne (Germany): Taschen; 2000. p. 37–9.
8. Rattray J. A delicious imaginary journal with Joan Miró and Jose Maria Hinjosa. In: Havard R, editor. Companion to Spanish surrealism. Rochester (NY): Tamesis Books; 2004. p. 33–4.
9. World Health Organization. Managing public health risks at the human-animal-environment interface [cited 2019 Oct 27]. https://www.who.int/zoonoses

Address for correspondence: Byron Breedlove, EID Journal, Centers for Disease Control and Prevention, 1600 Clifton Rd NE, Mailstop H16-2, Atlanta, GA 30329-4027, USA; email: wbb1@cdc.gov

EMERGING INFECTIOUS DISEASES®

Emerging Infectious Diseases thanks the following reviewers for their support through thoughtful, thorough, and timely reviews in 2019. Please contact us if your name is missing from this list.

Tande Aaron
John Aaskov
Preben Aavitsland
Abu Abdul-Quader
Sam Abraham
Joseph Abrams
Anna Acosta
Goutam Adak
Lisa Adams
Oyelola Adegboye
Bishwa Adhikari
Jennifer Adjemian
Cornelia Adlhoch
Charlene Africa
Rakesh Aggarwal
Patricia Aguilar
Ayman Ahmed
Faruque Ahmed
Cesar Albariño
Randy Albrecht
Kathleen Alexander
Afsar Ali
Ibne Ali
Sheikh Ali
Michael Alifrangis
Marc Allard
Samantha Allen
Franz Allerberger
Sonia Almería
Sandy Althomsons
Benjamin Althouse
Barry Alto
Gerardo Alvarez
Venancio Alves
Brian Amman
Neil Ampel
Cheryl Andam
Albert Anderson
Benjamin Anderson
Kathryn Anderson
Larry Anderson
Maureen Anderson
Voahangy Andrianaranjaka
Emmanouil Angelakis
Kristina Angelo
Andrea Angheben

Spinello Antinori
Daniela Antolová
Denise Antona
Charles Apperson
Brian Appleby
Yoshichika Arakawa
Wildo Araujo
Bob Arbeit
Matthew Arduino
Kevin Ariën
Yuzo Arima
Lisa Armitige
Benjamin Arnold
Garret Asay
Stephanie Ascough
Katie Atkins
Barry Atkinson
Robert Atmar
Houssam Attoui
Christian Auer
Jonathan Auguste
Francisco Javier
    Adroher Auroux
Paul Auwaerter
Andrew Azman
Hilary Babcock
Laura Bachmann
P. Byron Backenson
John Baddley
Edgar Badell
Sékéné Badiaga
Lilian Bahia-Oliveira
Justin Bahl
Tamás Bakonyi
Mark Ballard
Sapna Bamrah
Bettina Bankamp
Keith Baptiste
Gio Baracco
Lindley Barbee
Dulcinea Maria
    Barbosa Campos
Galileu Barbosa Costa
Alan Barbour
Sophie Baron
Thierry Baron
Ian Barr

Joel Barratt
Roberto Barrera
Alan Barrett
Drue Barrett
Albert Barskey
Luisa Barzon
Sridhar Basavaraju
Nicole Basta
Daniel Bausch
Iacopo Baussano
Lauren Bayliss
Magdalena Baymakova
Marlon Bayot
Jose Bazan
Bernard Beall
David Beasley
Scott Beatson
Paul Becher
Alyssa Beck
Emilie Bédard
Emily Beeler
Karlyn Beer
Martin Beer
Nancy Beerens
Jelena Bekvalac
Melissa Bell
Jessica Belser
Jeff Bender
Kaitlin Benedict
John Bennett
Sarah Bennett
Kimberley Benschop
John Berezowski
Elizabeth Berkow
Kyle Bernstein
Robert Bernstein
Eric Bertherat
Kateri Bertran
Julu Bhatnagar
Brad Biggerstaff
Gabriel Birgand
Zeno Bisoffi
Paritosh Biswas
Jason Blackburn
Stuart Blacksell
Carol Blair

David Blair
Lucas Blanton
William Bleser
Bradley Blitvich
Sandra Blome
Patrick Boerlin
Andrea Boggild
Jérôme Boissier
Guy Boivin
Sameh Boktor
Alexandro Bonifaz
Manuel Borca
Andrew Borman
Benny Borremans
Arnold Bosman
Katharine Bossart
Amar Bouam
Daisy Bougard
Herve Bourhy
Michel Boussinesq
Anna Bowen
Asha Bowen
Richard Bowen
Andrew Bowman
Dwight Bowman
David Boyd
Catherine Bozio
Doug Brackney
Richard Bradbury
Catriona Bradshaw
Oliver Brady
Marieta Braks
Mary Brandt
Aaron Brault
Mike Bray
Byron Breedlove
Edward B. Breitschwerdt
Ben Brennan
Maximo Brito
Stefan Brockmann
Els Broens
Sharon M. Brookes
James Brooks
Tim Brooks
Roland Brosch
Clive Brown

Julia Brotherton
Colin Brown
Corrie Brown
Ian Brown
Justin Brown
Kevin Brown
Roberta Bruhn
Vincent Bruno
Peter Burbelo
Brandy Burgess
Jason Burnham
Felicity Burt
Carlos Buscaglia
Anne Buschmann
Aleksandr Butenko
Thomas Butler
Viktoria Cabanova
Daniel Cadar
Fabio Cafini
Olga Calatayud Martínez
Rafael Calero-Bernal
Charles Calisher
Guilherme Calvet
Sébastien Calvignac-Spencer
José Cano
Wuchun Cao
Van-Mai Cao-Lormeau
Julien Cappelle
Jonathan Carapetis
Carolina Carballo
Cristina Cardemil
Philip Carling
Scott Carver
Kelsie Cassell
Pamela Cassiday
Jesús Castilla
Kenneth Castro
Marcio Castro
Adriano Casulli
Joseph Cavanaugh
Maria Carolina Ceriani
Martin Cetron
Allison Chamberlain
Ben Chan
Martin C.W. Chan
Jagdish Chander
Rémi Charrel
Vishnu Chaturvedi
Kalyan Chavda
Liang Chen
Lin Chen
Szu-Chieh Chen
Zhiming Chen

Zhongdan Chen
Zhuo Chen
Erika Chenais
Tom Chiller
Sadegh Chinikar
Chien-Shun Chiou
Eun Hwa Choi
Min Hyuk Choi
B.B. Chomel
Terence Chorba
Olivier Chosidow
Nancy Chow
Anuradha Chowdhary
Gerardo Chowell
Bryan Christensen
Rebecca Christofferson
Daniel Chu
Kaw Bing Chua
Hee Kyoung Chun
Holly Ciesielczuk
Hannah Clapham
C. Graham Clark
Kristie Clarke
Oliver Clay
Jan Clement
Murray Cohen
Charsey Cole Porse
Robert Colebunders
Dan Colley
Peter Collignon
Simon Collin
Mathew Collins
Iñaki Comas
Emilyn Conceicao
Bruce Conn
Neeta Connally
Andrea Conroy
Laura Cooley
Jennifer Cope
Victor Corman
Vincent Cornelisse
Sofia Cortes
Valerie Cortez
Caitlin Cossaboom
Carlos Costa
Solenne Costard
Matthew Cotten
Paul Coussens
Logan Cowan
Benjamin Cowling
James Crainey
John Croese
Zulma Cucunuba Perez

Manuel Cuenca-Estrella
Jie Cui
Matthew Cummings
Nigel Cunliff
Bart Currie
Daniel Curtis
Juliana Da Silva
Cristina Da Silva Carias
Andrei Dadu
Charles Daley
Clarissa Damaso
Delesa Damena
Alexandra Dangel
Eric Dannaoui
M. Carolina
    Danovaro-Holliday
Céline Dard
Marie Laure Dardé
Akbar Dastjerdi
Victoria Davey
Charles Davis
Richard Dawood
Miranda de Graaf
Jesus de Pedro Cuesta
Nick De Regge
Daniela de Souza Rajao
Annabelle de St. Maurice
Henriette de Valk
Alex de Voux
Henry de Vries
Rory de Vries
Kevin DeCock
Alexis Delabouglise
Pascal Delaunay
Mark Delorey
Eric Delwart
Zygmunt Dembek
Walter Demczuk
Xiangyu Deng
David Denning
Gordana Derado
Christina Deschermeier
Abhishek Deshpande
Ulrich Desselberger
Divya Dhasmana
Elisabetta Di Giannatale
Georges Diatta
Francisco Diaz
James Diaz
Sabine Diedrich
Binh Diep
Elizabeth Dietrich
Marta Diez-Valcarce

Sabine Dittrich
Armel Djenontin
Gaston Djomand
Gerhard Dobler
Ulrich Dobrindt
Pete Dodd
Yohei Doi
Rodney Donlan
Paul Douglas
Walter Dowdle
Scott Dowell
Christine Doyle
Michel Drancourt
Michael Drebot
Jan Drexler
Robert Drillien
Francis Drobniewski
Casey Droscha
Christian Drosten
Mignon du Plessis
Grégory Dubourg
Edward Dubovi
Mariette Ducatez
Oana Dumitrescu
John Stephen Dumler
Ghinwa Dumyati
Clare Dykewicz
Gregory Ebel
Hideki Ebihara
Chris Edens
Kathryn Edwards
Morven Edwards
Androulla Efstratiou
Lars Eisen
Karen Elkins
Sascha Ellington
Alex Elliot
Sean Elliott
Joanna Empel
David Engelthaler
J.A. Englund
Francis Ennis
Jonathan Epstein
Lauren Epstein
Guliz Erdem
Dean Erdman
Marina Eremeeva
Bobbie Erickson
Jim Evermann
Anna Fagre
Jessica Fairley
Joseph Falkinham
Ann Falsey

Dennis Falzon
Hongxin Fan
Seamus Fanning
Noha Farag
Nuno Faria
Rhys Farrer
Herman Favoreel
Martin Faye
Beth Feingold
Katherine Feldman
Heinz Feldmann
Leora Feldstein
Ingrid Felger
Yaoyu Feng
Florence Fenollar
Cynthia Ferre
Màrius Fuentes Ferrer
Ezio Ferroglio
Amy Parker Fiebelkorn
Vanessa Field
William Fischer II
Marc Fischer
Thea Fischer
Emily Flies
Anthony Flores
Jason Folster
Anthony Fooks
Stephen Forsythe
Jeffrey Foster
Monique Foster
Guillaume Fournié
Pierre-Edouard Fournier
Brian Foy
Bart Fraaije
Rafael Franca
Neil Franklin
Giovanni Franzo
John Frean
David Freedman
Adelino Freire
Nigel French
Conrad Freuling
Scott Fridkin
King-Wa Fu
Irene Fuertes de Vega
Jennifer Furin
Luis Furuya-Kanamori
Tetsuya Furuya
Alice Fusaro
Ana Gales
Jason Gallagher
Renee Galloway
Shantini Gamage

Pierluigi Gambetti
Manoj Gambhir
Adolfo García-Sastre
Shikha Garg
Giuliano Garofolo
Joy Gary
Robert Gaynes
Thomas Geisbert
Kathleen Gensheimer
Sue Gerber
Antoine Gessain
Giovanni Gherardi
Katherine Gibney
Martin Gilbert
James Gilkerson
Peter Gilligan
Brent Gilpin
John Glasser
Judith Glynn
Gauri Godbole
Jerome Goddard
Jacques Godfroid
Jeremy Gold
Mindy Goldman
Natalia Golender
Diego Gomez
Aubree Gordon
Catherine Gordon
Neela Goswami
Michihiko Goto
Eduardo Gotuzzo
Carolyn Gould
Ernest Gould
Jane Gould
Nelesh Govender
Yonatan Grad
Luigi Gradoni
Christine Graham
Simon Grandjean Lapierre
Gregor Grass
Nicholas Grassly
Stephen Graves
Gregory Gray
Kim Green
David Greenberg
William Greendyke
Luisa Gregori
David Griffith
Kevin Griffith
Ardath Grills
Martin Grobusch
Jacques Grosset
Paolo Grossi

Roland Grunow
Jeannette Guarner
Ania Gubala
Larisa Gubareva
Johnathon Gubbay
Duane Gubler
Vanina Guernier
Claire Guinat
Nicole Guiso
Danielle Gunn-Moore
Stephan Günther
Fangjian Guo
Neil Gupta
Emily Gurley
Bart Haagmans
Andrew Haddow
Stephen Hadler
Ferry Hagen
Deanna Hagge
Stephen Hajduk
Aron Hall
Ian Hall
Roy Hall
Scott Halstead
Davidson Hamer
Christopher Hamilton-West
Timm Harder
Dag Harmsen
Aaron Harris
Emma Harris
John Harris
Reid Harris
Heli Harvala
Latiffah Hassan
Jan Hattendorf
Ben Hause
Karyn Havas
Michael Hawkes
William Hawley
Amber Haynes
Qiushui He
Craig Hedberg
Maged Hemida
Petr Heneberg
Emily Henkle
Ian Hennessee
Monica Henry
Ronnie Henry
Vanessa Herder
Jesús Hernández-Orts
Roger Hewson
David Heymann
Graham Hickling

Lauri Hicks
Sarah Hill
Vincent Hill
Susan Hills
Alison Hinckley
Takahiro Hiono
Yingfen Hisa
Michele Hlavsa
Charlotte Hobbs
Thomas Hoenen
Nicole Hoff
Mike Holbrook
David Holland
Steven Holland
Edward Holmes
Margaret Honein
Jaeyong Hong
Edward Hook
Taisuke Horimoto
Daniel Horton
Jennifer House
Li-Ting Huang
Gwenda Hughes
Holly Hughes
Ralph Huits
John Humphrey
Chien-Ching Hung
Yuen Wai Hung
Elizabeth Hunsperger
Dan Hurnik
A.C. Hurt
Yvan Hutin
Jimee Hwang
Kashef Ijaz
Alexandros Ikonomidis
Allison Imrie
Tim Inglis
Catherine Inizan
Seth Inzaule
Jonathan Iredell
Seth Irish
Badrul Islam
Michael Ison
Danielle Iuliano
Jacques Izopet
Brendan Jackson
Mark Jackwood
Jesse Jacob
Yunho Jang
Lauren Jatt
Emily Jenkins
Amy Jennison
Jørgen Skov Jensen

Khuzwayo Jere
Cecilia Jernberg
Wei Jia
Miguel Jimenez-Clavero
Michael Johansson
Nur Alia Johari
Alan Johnson
Barbara Johnson
James Johnson
Nick Johnson
Paul Johnson
Lisa Jones-Engel
Somchai Jongwutiwes
Kieran Jordan
Tomy Joseph
M. Patricia Joyce
Rebekah Kading
Ayesha Kadir
Laura Kahn
Adriana Kajon
Alexander Kallen
Nassim Kamar
Mary Kamb
Biao Kan
Ed Kaplan
Shahid Karim
Erik Karlsson
Haru Kato
Midori Kato-Maeda
Alan Katz
Louis Katz
Mark Katz
Alexa Kaufer
Ghazi Kayali
Paul Keim
Dervla Kenna
Joan Kenney
Anusak Kerdsin
Ali Khan
Salah Khan
Christine Khosropour
Yury Khudyakov
Mariana Kikuti
James Kile
Marie Killerby
Kenneth Kim
Linda Kimsey
Donald King
Luke Kingry
Martyn Kirk
Robert Kirkcaldy
Hannah Kirking
Peter Kirkland

Laura Kirkman
Carl Kirkwood
Uriel Kitron
Jeffrey Klausner
Steven Kleinman
John Klena
Jonas Klingstrom
Amy Klion
Keith Klugman
Barbara Knust
Albert Ko
Guus Koch
Paula Kocher
Marleen Kock
Anson Koehler
Aaron Kofman
Nicholas Komar
Igor Koralnik
Gulay Korukluoglu
Jasna Kovac
Barbara Kowalcyk
Phyllis Kozarsky
Vicki Kramer
Kristen Kreisel
Erna Kroon
Andi Krumbholz
Steven Kubiski
Adam Kucharski
Roman Kuchta
Amy Kuenzi
Kiersten Kugeler
Thijs Kuiken
Sanjai Kumar
Satu Kurkela
Julianne Kus
Preeta Kutty
Ivan Kuzmin
Bernard La Scola
Marcelo Labruna
Sarah Labuda
Philippe Lagacé-Wiens
Jean-Christophe Lagier
Yingqi Lai
Theresa Lamagni
Amy Lambert
Ben Lambert
Laura Lamberti
Ruiting Lan
J. Michael Lane
Adam Langer
Alfred Lardizabal
Maureen Laroche
Karine Laroucau

Cornelia Lass-Floerl
Colleen Lau
Eric Lau
Rachel Lau
Susanna K.P. Lau
Ana Lauer
Kevin Lawrence
Franziska Layer
Kirsty Le Doare
Soizick Le Guyader
Tan Le Van
Tuan Le Van
Rodolfo Leal
Camille Lebarbenchon
Hakan Leblebicioglu
Karin Leder
James LeDuc
Deog-Yong Lee
Dong-Hun Lee
Keun Hwa Lee
Fabian Leendertz
Pedro Legua
Andrew Leidner
M.J. Leitão
Laetitia Lempereur
Justin Lessler
Anthony Levasseur
Michael Levin
Min Levine
Rosamund Lewis
Joseph Lewnard
Feng Li
Sheng Li
Shu-Ying Li
Yu Li
Zejun Li
Guodong Liang
Mauricio Lima
Jiun-Nong Lin
Michael Lindsay
Robbin Lindsay
Anastasia Litvintseva
Shelan Liu
Manuel Lluberas
Laura Lochlainn
Shawn Lockhart
Latania Logan
Eric Loker
Andrés Londoño
Kanya Long
S. Wesley Long
L. López-Cerero
Ahide Lopez-Merino

Job Lopez
Benjamin Lopman
Olivier Lortholary
Patricia Lozano-Zarain
Stephen Luby
Naomi Lucchi
Yaniv Lustig
Laurence Luu
Marshall Lyon
Neil Mabbott
Kevin Macaluso
C. Raina MacIntyre
John Mackenzie
Douglas MacPherson
Hugo Madrid
Lola Madrid
Anna-Pelagia Magiorakos
Ayesha Mahmud
Saajida Mahomed
Taronna Maines
Donna Mak
Richard Malik
Alexander Malogolovkin
Burkhard Malorny
Anna Mandra
Ghislain Manet
Sylvie Manguin
Lisa Manhart
Barbara Mann
Gabriele Margos
Kevin Markey
Michael Marks
Ernesto Marques
Theodore Marras
Tom Marrie
Laurent Marsollier
Douglas Marthaler
Irene Martin
Javier Martin
Roosecelis Martines
Sandra Regina Maruyama
Grace Marx
Santiago Mas-Coma
Amy Mathers
Blaine Mathison
Yasufumi Matsumura
Max Maurin
Alison Mawle
Sarah A. Mbaeyi
Placide Mbala-Kingebeni
Andrea McCollum
Orion McCotter
Michael McCracken

L. Clifford McDonald
Juan Mcewen
Peter McIntyre
James McKenna
James McKinnell
Donald McLean
Alan McNally
Lucy McNamara
Jonathon McNeil
Jennifer McQuiston
Paul Mead
Samir Mechai
Oleg Mediannikov
Freddy Medina
Jennifer Meece
Adam Meijer
Jacques Meis
Roberto Melano
Martin Meltzer
Ziad Memish
Leonel Mendoza
Stefano Merler
Becky Merrill
Kevin Messacar
Wieland Meyer
Georgies Mgode
Claire Midgley
Amy Mikhail
Susan Mikota
Jackie Miller
Michele Miller
William Miller
James Mills
Jesus Mingorance
Oriol Mitja
John Modlin
Fawzi Mohamed
Igor Mokrousov
Noelle-Angelique Molinari
Phillip Molloy
Abelardo Moncayo
Isabella Monne
Steve Monroe
Ana Margarita Montalvo
Martha Montgomery
Amanda Moodie
Andrew Moon
Patrick Moonan
Patrick Moore
Susan Moore
Hector Mora-Montes
Aurelie Morand
David Morens

Maria Moretti
Oliver Morgan
Kozo Morimoto
Kouichi Morita
Diane Morof
Lillian Morris-Manahan
Joan Morris
Amy Morrison
Kathleen Moser
Eric Mossel
Rafal Mostowy
Damien Mouly
Yi Mu
Marcel Mueller
Barbara Mühlemann
U.G. Munderloh
Muhammad Munir
Kamalich Muniz-Rodriguez
Vincent Munster
David Murdoch
Frederick Murphy
Kristy Murray
David Muscatello
Jukka Mustonen
Khin Myint
Nilson N. Mendes Neto
Pierre Nabeth
Irving Nachamkin
Sharon Nachman
Robyn Nadolny
Prenilla Naidu
Rajeshwari Nair
Satoshi Nakano
Ho Namkoong
Srinivas Nanduri
Sebastian Napp
Avindra Nath
Ruvandhi Nathavitharana
Yuki Nawa
Mark Nelder
Christina Nelson
Martha Nelson
Christopher Netherton
Andreas Neumayr
Catherine Neuwirth
Paul Newton
Sophia Ng
Terry Fei Fan Ng
Michele Nguyen
Mya Ngwe-Tun
Kristen Nichols Heitman
Megin Nichols
Ainsley Nicholson

Loredana Nicoletti
Matthias Niedrig
Eva Møller Nielsen
Stine Nielsen
Sandra Niendorf
Andreas Nitsche
Allan Nix
Susan Noh
Melissa Nolan
Dawn Nolt
Romolo Nonno
Norbert Nowotny
Andrew Noymer
Corrie Ntiforo
Thomas Nutman
Ikwo Oboho
Sophie Octavia
Myoung-don Oh
Makoto Ohnishi
Thelma Okay
Kevin Olival
John Elmerdal Olsen
Rikke Olsen
Sonja Olsen
Donald Olson
Victoria Olson
Oddvar Oppegaard
Walter Orenstein
Anthony Orvedahl
Hitoshi Oshitani
Richard Ostfeld
Stephen Ostroff
Domenico Otranto
Nao Otsuka
Margaret Oxtoby
Egon Ozer
Christopher Paddock
Wendy Page
John Paget
Gustavo Palacios
Peter Palese
Mark Pallansch
Alberto Paniz Mondolfi
Anna Papa
Costas Papagiannitsis
Igor Paploski
John Papp
Sydel Parikh
Benjamin Park
Jane Parmley
Philippe Parola
Gabriel Parra
Colin Parrish

Ben Pascoe
Jotam Pasipanodya
Frank Pasmans
Daniel Pastula
Priti Patel
Samir Patel
Sarad Paudel
Richard Paul
Nicole Pavio
Janusz Paweska
Daniel Payne
Gabriela Paz-Bailey
Carl Pearson
Malik Peiris
Steve Pelton
Pasi Penttinen
Rapm Perera
José-Antonio Pérez-Molina
Janice Perez-Padilla
Steven Pergam
Alex Perkins
Kiran Perkins
David Perlin
Stanley Perlman
Stephanie Perniciaro
Brett Petersen
Christine Petersen
Emily Petersen
Helen Petousis-Harris
Michael Pfaller
Christopher Pfeiffer
Anastasia Pharris
Michael Phelippeau
Mathieu Picardeau
Jamison Pike
Tamara Pilishvili
Allan Pillay
Rachael Piltch-Loeb
Sébastien Pion
Sara Pires
Johann Pitout
Ludovic Plee
Katherine Plewes
Mateusz Plucinski
Maurizio Pocchiari
Laura Podewils
Stefan Pöhlmann
Laurent Poirel
Philippe Poirier
Maria Politis
Marjorie Pollack
Leo Poon
Yong Poovorawan

Sam Posner
Rebecca Poulson
Ann Powers
John Prescott
Rebecca Prevots
Bobbi Pritt
Carolina Probst
Mattia Prosperi
Lisa Prosser
Amy Pruden
Catharine Prussing
Michael Purdy
Pilaipan Puthavathana
Hua-Ji Qiu
Flávio Queiroz-Telles
Yvonne Qvarnstrom
Lewis Radonovich
Gabriel Rainisch
Jayant Rajan
Andrew Ramey
David Ramilo
Mario Ramirez
Adrienne Randolph
Stéphane Ranque
Brian Raphael
Giammarco Raponi
Sonja Rasmussen
Giovanni Ravasi
Mario Raviglione
Simon Rayner
Adam Readhead
Sujan Reddy
Rachel Reeves
Joanna Regan
Gili Regev-Yochay
Arthur Reingold
Paul Reiter
Chantel Reusken
Kelly Reveles
Randall Reves
Katherine C. Reyes
Allen Richards
Jan Hendrik Richardus
Joachim Richter
Hans Rieder
Emmanuel Robesyn
Jennifer Robson
Ignasi Roca
Joacim Rocklöv
Guenael Rodier
Jesús Rodríguez-Baño
Pierre Rollin
Sara Romano-Bertrand

Daniel Romero-Álvarez
Thomas Romig
Hannah Romo
Shannon Ronca
Kimberlyn Roosa
Dale Rose
Gary Roselle
Kyle Rosenke
John Ross
Shannan Rossi
Janell Routh
Sharon Roy
Jose Rubio
Horacio Ruiseñor-Escudero
Charles Rupprecht
Brandy Russell
Thomas Russo
Daniel Ruzek
Laura Ryan
Sukhyun Ryu
Jamal Saad
Fabian Saenz
Yoshihiro Sakoda
Max Salfinger
Joshua Salomon
Vartul Sangal
Nuno Santos
Sarah Sapp
George Sarosi
R. Tedjo Sasmono
Maria Scaturro
Charles Schable
Gereon Schares
Silke Schelenz
Susanne Schjørring
Robert Schlaberg
Patricia Schlagenhauf
William Schluter
Axel Schmidt
Jonas Schmidt-Chanasit
Dennis Schmitt
Eileen Schneider
Monica Schoch-Spana
Betsy Schroeder
Amy Schuh
Constance Schultsz
Tom Schwan
Ilan Schwartz
Jessica Schwind
Doug Scott
Isaac See
Harald Seifert
James Sejvar

Rangaraj Selvarangan
Parham Sendi
Sang Heui Seo
Varadan Sevilimedu
Jessica Sexton
Shokoofeh Shamsi
Manjunath Shankar
Eugene Shapiro
Karen Shapiro
Tyler Sharp
Frederic Shaw
Zizhang Sheng
Samuel Shepard
Zhengli Shi
Jennifer Shield
Tom Shimabukuro
Nahoko Shindo
Hirito Shinomiya
Hiroaki Shirafuji
Marta Shocket
Trevor Shoemaker
Affan Shoukat
Susan Shriner
Massinissa Si Mehand
Carol Sibley
Catarina Silva-Costa
Rodrigo Silva
Simone Silveira
Peter Simmonds
Gustave Simo
Gunnar Simonsen
Amy Sims
Les Sims
Andreas Sing
Balbir Singh
Ria Sinha
Theresa Sipe
Tarja Sironen
Shawn Skerrett
Robert Skov
Kim Skrobarcek
Monica Slavin
Rachel Slayton
Robert Smith
Tara Smith
James Snyder
Heidi Soeters
Olusegun Soge
Cheikh Sokhna
Rami Sommerstein
Jin-Won Song
Lynn Soong
Frank Sorvillo

Giovanni Sotgiu
Erica Spackman
Jessica Spengler
Adel Spotin
Philip Spradling
Armand Sprecher
Shiranee Sriskandan
Siddhartha Srivastava
Kirby Stafford
David Stallknecht
J. Erin Staples
Lindsay Starkey
Anneke Steens
Laura Steinhardt
Amir Steinman
Ivo Steinmetz
Werner Stenzel
Dennis Stevens
O. Colin Stine
Shannon Stokley
Gregory Storch
Susan Stramer
Marc Strassburg
Franc Strle
Jonathan Strysko
Bertrand Sudre
A. Suffredini
Giorgia Sulis
Patrick Sullivan
Xiang-Jie Sun
Rebecca Sunenshine
Temmy Sunyoto
Amitabh Suthar
Tohru Suzuki
Robert Swanepoel
David Swayne
M. Szabo
Shigeru Tajima
Sarah Talarico
G.S. Tan
Kennard Tan
Kenneth Tan
Julian Tang
Robert Tanz
Dennis Tappe
Arnaud Tarantola
Cheryl Tarr
Robert Tauxe
Steve M. Taylor
Andrew Taylor-Robinson
Sarah Teatero
Anders Tegnell
Maria Gloria Teixeira

Rosane Teles
Sam Telford
Kiran Thakur
Elitza Theel
Stephen Thomas
George Thompson
Sharmi Thor
Natalie Thornburg
Guy Thwaites
Peter Timoney
Tejpratap Tiwari
Eugenia Tognotti
Kentaro Tohma
Rafael Toledo
Steven Tong
Suxiang Tong
Mia Torchetti
Paul Torgerson
Montserrat Torremorell
Fernando Torres
Elizabeth Torrone
Anna Maria Tortorano
Mathieu Tourdjman
Jonathan Towner
Antoni Trilla
Sharon Tsay
Sarah Tschudin-Sutter
Ye Tun
Mike Turell
Filippo Turrini
Kenneth Tyler
Rainer Ulrich
Julio Urbina
Timothy Uyeki
Ronald Valdiserri
Braulio Valencia
Marta Valenciano
Snigdha Vallabhaneni
Chris Van Beneden
Wendy van de Sande
Annemiek van der Eijk

Wim van der Hoek
Mark van der Linden
Stijn van der Veen
H. Rogier van Doorn
Monique van Hoek
Jakko van Ingen
Maria Van Kerkhove
Kristien Van Reeth
Debby van Riel
Arnoud van Vliet
Kavin Vanikieti
Daisy Vanrompay
Olli Vapalahti
Andrea Varela-Stokes
George Varghese
Pedro Vasconcelos
Shawn Vasoo
Alexander Vaux
Marietjie Venter
Jose Venzal
Sten Vermund
Andrew Vernon
Pauline Vetter
Luigi Vezzulli
Antonio Vieira
Nadja Alexandra Vielot
Nele Villabruna
Jan Vinjé
Leo Visser
Charles Vitek
Erika Vlieghe
Sophie Von Dobschuetz
Duc Vugia
Supaporn Wacharapluesadee
Timothy Wade
Jesse Waggoner
Sherrilyn Wainwright
Heather Walden
David Walker
Larry Walker
Julia Walochnik

Henry Wan
Dayan Wang
Jianwei Wang
Lin-Fa Wang
Tina Wang
Xin Wang
Marine Wasniewski
Tokiko Watanabe
John Watson
Matthew Watts
Scott Weaver
Cameron Webb
Mark Webber
Richard Webby
J. Todd Weber
Michael Weigand
Daniel Weinberger
Hana Weingartl
Don Weiss
Louis Weiss
Will Weldon
Nancy Wengenack
Mike Whelan
David Whiley
Jennifer White
Lewis White
Gudrun Wibbelt
Andreas Widmer
Joost Wiersinga
Rebecca Wilkes
Diana Williams
Mary Wilson
Jonas Winchell
Kevin Winker
Thomas E. Wittum
David Wohl
Mahlet Woldetsadik
Cameron Wolfe
Nicole Wolter
Darren Wong
Frank Wong

Sunny Wong
Erica Wood
Douglas Woodhams
Gary Wormser
Jonathan Wortham
William Wright
Xianfu Wu
Zhixun Xie
Guang Xu
Zhi-Hong Xu
Zhiwei Xu
Hayley Yaglom
Dafna Yahav
Reina Yamaji
Dan Yamin
Cedric Yansouni
Jiro Yasuda
Hui-Ling Yen
Jingjing Yin
Benediktus Yohan
Hongjie Yu
Victor Yu
Xuejie Yu
Yun-song Yu
Lijuan Yuan
Hans Zaaijer
Mark Zabel
Ruth Zadoks
Fabio Zampieri
Gianluigi Zanusso
Hervé Zeller
Danielle Zerr
Xinyan Zhang
Duping Zheng
Zhiyong Zhou
Bingqing Zhu
Rosalie Zimmermann
Kate Zinszer
Armineh Zohrabian
Alimuddin Zumla

EMERGING INFECTIOUS DISEASES®

Upcoming Issue

- *Candidatus* Mycoplasma haemohominis in Human, Japan
- Spatial Epidemiologic Trends and Hotspots of Leishmaniasis, Sri Lanka, 2001–2018
- Nutritional Care for Patients with Ebola Virus Disease
- Paid Leave and Access to Telework as Work Attendance Determinants during Acute Respiratory Illness, United States, 2017–2018
- Elephant Endotheliotropic Herpesvirus Hemorrhagic Disease in Asian Elephant Calves in Logging Camps, Myanmar
- High Azole Resistance in *Aspergillus fumigatus* Fungal Isolates from Strawberry Field, China, 2018
- High Pathogenicity Nipah Virus in *Pteropus lylei* Fruit Bats, Cambodia
- Effect of Pediatric Influenza Vaccination on Antibiotic Resistance, England and Wales
- Varicella in Adult Foreigners at a Referral Hospital, Central Tokyo, Japan, 2012–2016
- Distribution of Japanese Encephalitis Virus, Thailand and Southeast Asia Islands, 2016–2018
- Geographic Distribution and Incidence of Melioidosis, Panama
- Novel Reassortant Highly Pathogenic Avian Influenza Virus A(H5N2) in Broiler Chickens, Egypt
- Syphilitic Bilateral Papillitis Mimicking Papilloedema
- Emergence of *Vibrio cholerae* O1 Sequence Type 75 in Taiwan
- Influenza A Virus Infections among Dromedary Camels, Nigeria and Ethiopia, 2015–2016
- Autochthonous Human Fascioliasis, Belgium
- Risk Factors and Seroprevalence of Tickborne Zoonoses among Livestock Owners, Kazakhstan
- Training Foodborne Outbreak Investigations by Using the Structured Learning Experience
- Hantavirus Pulmonary Syndrome in a Returning Traveler, Spain
- *Legionella pneumophila* as a Cause of Severe Community-Acquired Pneumonia

Complete list of articles in the January issue at
http://www.cdc.gov/eid/upcoming.htm

Upcoming Infectious Disease Activities

January 28–30, 2020
American Society for Microbiology
2020 ASM Biothreats
Arlington, VA, USA
https://www.asm.org/Events/ASM-Biothreats/Home

February 20–23, 2020
International Society for Infectious Diseases
Kuala Lumpur, Malaysia
https://www.isid.org/

March 8–11, 2020
Conference on Retroviruses and Opportunistic Infections
Boston, MA, USA
https://www.croiconference.org/

March 9–13, 2020
African Society for Laboratory Medicine
7th African Network for Influenza Surveillance Epidemiology
Livingstone, Zambia
http://www.anise2020.org

March 26–30, 2020
Society for Healthcare Epidemiology of America
Decennial 2020
6th International Conference on Healthcare Associated Infections
Atlanta, GA, USA
https://decennial2020.org

April 18–21, 2020
The European Congress of Clinical Microbiology and Infectious Diseases
Paris, France
https://www.eccmid.org/eccmid_2020/

Announcements
Email announcements to EID Editor (eideditor@cdc.gov). Include the event's date, location, sponsoring organization, and a website.

Earning CME Credit

To obtain credit, you should first read the journal article. After reading the article, you should be able to answer the following, related, multiple-choice questions. To complete the questions (with a minimum 75% passing score) and earn continuing medical education (CME) credit, please go to http://www.medscape.org/journal/eid. Credit cannot be obtained for tests completed on paper, although you may use the worksheet below to keep a record of your answers.

You must be a registered user on http://www.medscape.org. If you are not registered on http://www.medscape.org, please click on the "Register" link on the right hand side of the website.

Only one answer is correct for each question. Once you successfully answer all post-test questions, you will be able to view and/or print your certificate. For questions regarding this activity, contact the accredited provider, CME@medscape.net. For technical assistance, contact CME@medscape.net. American Medical Association's Physician's Recognition Award (AMA PRA) credits are accepted in the US as evidence of participation in CME activities. For further information on this award, please go to https://www.ama-assn.org. The AMA has determined that physicians not licensed in the US who participate in this CME activity are eligible for AMA PRA Category 1 Credits™. Through agreements that the AMA has made with agencies in some countries, AMA PRA credit may be acceptable as evidence of participation in CME activities. If you are not licensed in the US, please complete the questions online, print the AMA PRA CME credit certificate, and present it to your national medical association for review.

Article Title

Seroprevalence and Risk Factors Possibly Associated with Emerging Zoonotic Vaccinia Virus in a Farming Community, Colombia

CME Questions

1. You are advising a local public health department in Colombia about emerging cases of vaccinia virus (VACV). According to the serosurvey and risk factor assessment by Styczynski and colleagues, which of the following statements about demographics and descriptive characteristics of persons with VACV in the municipality of Medina in Cundinamarca Department, Colombia, is correct?

A. Nearly one-quarter of 134 farmworkers tested had anti-orthopoxvirus (OPXV) antibodies
B. 34% had a history of smallpox vaccination; 96% reported contact with cows; and 86% participated in the milking process
C. More than half of seropositive individuals reported a history of a vaccinia-like lesion
D. Among the 56 farms studied, less than one-quarter reported animals with vaccinia-like lesions

2. According to the serosurvey and risk factor assessment by Styczynski and colleagues, which of the following statements about risk factors associated with VACV disease exposure in the municipality of Medina in Cundinamarca Department, Colombia, is correct?

A. Age <44 years was predictive of anti-OPXV seropositivity
B. In-country travel was predictive of anti-OPXV seropositivity
C. Use of commercial feed and feeding cattle after milking were protective against anti-OPXV seropositivity
D. Duration of time working on the current farm was not associated with anti-OPXV seropositivity

3. According to the serosurvey and risk factor assessment by Styczynski and colleagues, which of the following statements about clinical and public health implications of demographics and descriptive characteristics of the burden of VACV and risk factors associated with disease exposure in the municipality of Medina in Cundinamarca Department, Colombia, is correct?

A. This study supports possible emergence of VACV as a zoonosis in South America through independent emergence events or expanding reservoir habitats in the setting of waning immunity
B. VACV-like infections had no economic consequences
C. Smallpox vaccination status was not related to risk for symptomatic disease
D. The study proves that infected cows transmitted VACV to farm workers

Earning CME Credit

To obtain credit, you should first read the journal article. After reading the article, you should be able to answer the following, related, multiple-choice questions. To complete the questions (with a minimum 75% passing score) and earn continuing medical education (CME) credit, please go to http://www.medscape.org/journal/eid. Credit cannot be obtained for tests completed on paper, although you may use the worksheet below to keep a record of your answers.

You must be a registered user on http://www.medscape.org. If you are not registered on http://www.medscape.org, please click on the "Register" link on the right hand side of the website.

Only one answer is correct for each question. Once you successfully answer all post-test questions, you will be able to view and/or print your certificate. For questions regarding this activity, contact the accredited provider, CME@medscape.net. For technical assistance, contact CME@medscape.net. American Medical Association's Physician's Recognition Award (AMA PRA) credits are accepted in the US as evidence of participation in CME activities. For further information on this award, please go to https://www.ama-assn.org. The AMA has determined that physicians not licensed in the US who participate in this CME activity are eligible for AMA PRA Category 1 Credits™. Through agreements that the AMA has made with agencies in some countries, AMA PRA credit may be acceptable as evidence of participation in CME activities. If you are not licensed in the US, please complete the questions online, print the AMA PRA CME credit certificate, and present it to your national medical association for review.

Article Title
Streptococcus suis–Associated Meningitis, Bali, Indonesia, 2014–2017

CME Questions

1. Your patient is a 50-year-old male pig farmer in Indonesia admitted for suspected bacterial meningitis. According to the case series in Bali, Indonesia, by Susilawathi and colleagues, which of the following statements about the epidemiology and clinical signs of *Streptococcus suis* meningitis is correct?
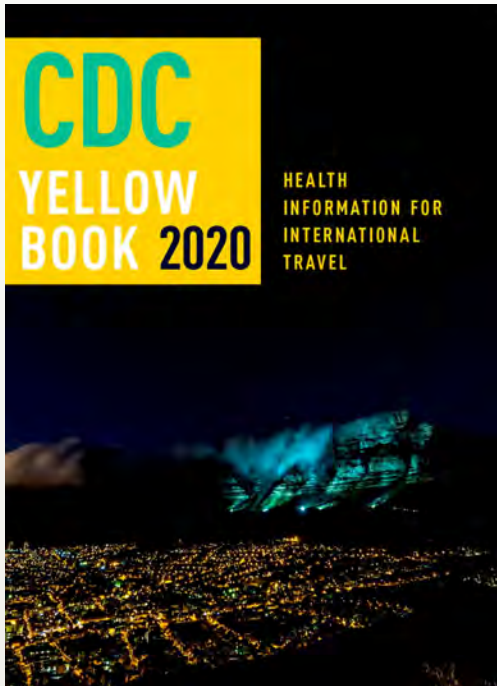
A. Of a total of 71 acute bacterial meningitis cases, *S. suis* was confirmed in cerebrospinal fluid (CSF) culture of 14 patients.
B. Case-fatality rate in confirmed cases was 5%
C. All patients received 2 g intravenous (IV) ceftriaxone every 12 hours for 14 days and 10 mg IV dexamethasone every 6 hours for 4 days
D. Sensorineural hearing loss was the most common presenting sign

2. According to the case series in Bali, Indonesia, by Susilawathi and colleagues, which of the following statements about laboratory findings and microbiology of *S. suis* meningitis is correct?

A. CSF cultures were positive for S. suis, sensitive to ceftriaxone, and resistant to all other drugs tested
B. PCR serotyping showed that most cases were *S. suis*, serotype 1
C. CSF analysis showed pleocytosis with normal glucose levels
D. All glutamate dehydrogenase and recombination/repair protein sequences of *S. suis* generated in this study were identical

3. According to the case series of *S. suis* meningitis in Bali, Indonesia, by Susilawathi and colleagues, which of the following statements about clinical and public health implications of the findings would be correct?

A. Human *S. suis* infections are mostly linked to contact with goats and eating goat's milk or meat
B. The study was likely to overestimate the percentage of bacterial meningitis cases caused by *S. suis*
C. The presence of *S. suis* in Indonesia was first confirmed in 2014, but suspected bacterial meningitis was reported earlier and diagnosed as viridans streptococci
D. The specific signs and symptoms of *S. suis* infection facilitate diagnosis of this type of bacterial meningitis

Summary of Authors' Instructions

Authors' Instructions. For a complete list of EID's manuscript guidelines, see the author resource page: http://wwwnc.cdc.gov/eid/page/author-resource-center.

Manuscript Submission. To submit a manuscript, access Manuscript Central from the Emerging Infectious Diseases web page (www.cdc.gov/eid). Include a cover letter indicating the proposed category of the article (e.g., Research, Dispatch), verifying the word and reference counts, and confirming that the final manuscript has been seen and approved by all authors. Complete provided Authors Checklist.

Manuscript Preparation. For word processing, use MS Word. Set the document to show continuous line numbers. List the following information in this order: title page, article summary line, keywords, abstract, text, acknowledgments, biographical sketch, references, tables, and figure legends. Appendix materials and figures should be in separate files.

Title Page. Give complete information about each author (i.e., full name, graduate degree(s), affiliation, and the name of the institution in which the work was done). Clearly identify the corresponding author and provide that author's mailing address (include phone number, fax number, and email address). Include separate word counts for abstract and text.

Keywords. Use terms as listed in the National Library of Medicine Medical Subject Headings index (www.ncbi.nlm.nih.gov/mesh).

Text. Double-space everything, including the title page, abstract, references, tables, and figure legends. Indent paragraphs; leave no extra space between paragraphs. After a period, leave only one space before beginning the next sentence. Use 12-point Times New Roman font and format with ragged right margins (left align). Italicize (rather than underline) scientific names when needed.

Biographical Sketch. Include a short biographical sketch of the first author—both authors if only two. Include affiliations and the author's primary research interests.

References. Follow Uniform Requirements (www.icmje.org/index.html). Do not use endnotes for references. Place reference numbers in parentheses, not superscripts. Number citations in order of appearance (including in text, figures, and tables). Cite personal communications, unpublished data, and manuscripts in preparation or submitted for publication in parentheses in text. Consult List of Journals Indexed in Index Medicus for accepted journal abbreviations; if a journal is not listed, spell out the journal title. List the first six authors followed by "et al." Do not cite references in the abstract.

Tables. Provide tables within the manuscript file, not as separate files. Use the MS Word table tool, no columns, tabs, spaces, or other programs. Footnote any use of boldface. Tables should be no wider than 17 cm. Condense or divide larger tables.

Figures. Submit editable figures as separate files (e.g., Microsoft Excel, PowerPoint). Photographs should be submitted as high-resolution (600 dpi) .tif or .jpg files. Do not embed figures in the manuscript file. Use Arial 10 pt. or 12 pt. font for lettering so that figures, symbols, lettering, and numbering can remain legible when reduced to print size. Place figure keys within the figure. Figure legends should be placed at the end of the manuscript file.

Videos. Submit as AVI, MOV, MPG, MPEG, or WMV. Videos should not exceed 5 minutes and should include an audio description and complete captioning. If audio is not available, provide a description of the action in the video as a separate Word file. Published or copyrighted material (e.g., music) is discouraged and must be accompanied by written release. If video is part of a manuscript, files must be uploaded with manuscript submission. When uploading, choose "Video" file. Include a brief video legend in the manuscript file.

Types of Articles

Perspectives. Articles should not exceed 3,500 words and 50 references. Use of subheadings in the main body of the text is recommended. Photographs and illustrations are encouraged. Provide a short abstract (150 words), 1-sentence summary, and biographical sketch. Articles should provide insightful analysis and commentary about new and reemerging infectious diseases and related issues. Perspectives may address factors known to influence the emergence of diseases, including microbial adaptation and change, human demographics and behavior, technology and industry, economic development and land use, international travel and commerce, and the breakdown of public health measures.

Synopses. Articles should not exceed 3,500 words in the main body of the text or include more than 50 references. Use of subheadings in the main body of the text is recommended. Photographs and illustrations are encouraged. Provide a short abstract (not to exceed 150 words), a 1-line summary of the conclusions, and a brief biographical sketch of first author or of both authors if only 2 authors. This section comprises case series papers and concise reviews of infectious diseases or closely related topics. Preference is given to reviews of new and emerging diseases; however, timely updates of other diseases or topics are also welcome. If detailed methods are included, a separate section on experimental procedures should immediately follow the body of the text.

Research. Articles should not exceed 3,500 words and 50 references. Use of subheadings in the main body of the text is recommended. Photographs and illustrations are encouraged. Provide a short abstract (150 words), 1-sentence summary, and biographical sketch. Report laboratory and epidemiologic results within a public health perspective. Explain the value of the research in public health terms and place the findings in a larger perspective (i.e., "Here is what we found, and here is what the findings mean").

Policy and Historical Reviews. Articles should not exceed 3,500 words and 50 references. Use of subheadings in the main body of the text is recommended. Photographs and illustrations are encouraged. Provide a short abstract (150 words), 1-sentence summary, and biographical sketch. Articles in this section include public health policy or historical reports that are based on research and analysis of emerging disease issues.

Dispatches. Articles should be no more than 1,200 words and need not be divided into sections. If subheadings are used, they should be general, e.g., "The Study" and "Conclusions." Provide a brief abstract (50 words); references (not to exceed 15); figures or illustrations (not to exceed 2); tables (not to exceed 2); and biographical sketch. Dispatches are updates on infectious disease trends and research that include descriptions of new methods for detecting, characterizing, or subtyping new or reemerging pathogens. Developments in antimicrobial drugs, vaccines, or infectious disease prevention or elimination programs are appropriate. Case reports are also welcome.

Research Letters Reporting Cases, Outbreaks, or Original Research. EID publishes letters that report cases, outbreaks, or original research as Research Letters. Authors should provide a short abstract (50-word maximum), references (not to exceed 10), and a short biographical sketch. These letters should not exceed 800 words in the main body of the text and may include either 1 figure or 1 table. Do not divide Research Letters into sections.

Letters Commenting on Articles. Letters commenting on articles should contain a maximum of 300 words and 5 references; they are more likely to be published if submitted within 4 weeks of the original article's publication.

Commentaries. Thoughtful discussions (500–1,000 words) of current topics. Commentaries may contain references (not to exceed 15) but no abstract, figures, or tables. Include biographical sketch.

Another Dimension. Thoughtful essays, short stories, or poems on philosophical issues related to science, medical practice, and human health. Topics may include science and the human condition, the unanticipated side of epidemic investigations, or how people perceive and cope with infection and illness. This section is intended to evoke compassion for human suffering and to expand the science reader's literary scope. Manuscripts are selected for publication as much for their content (the experiences they describe) as for their literary merit. Include biographical sketch.

Books, Other Media. Reviews (250–500 words) of new books or other media on emerging disease issues are welcome. Title, author(s), publisher, number of pages, and other pertinent details should be included.

Conference Summaries. Summaries of emerging infectious disease conference activities (500–1,000 words). They should be submitted no later than 6 months after the conference and focus on content rather than process. Provide illustrations, references, and links to full reports of conference activities.

Online Reports. Reports on consensus group meetings, workshops, and other activities in which suggestions for diagnostic, treatment, or reporting methods related to infectious disease topics are formulated. These should not exceed 3,500 words and should be authored by the group. We do not publish official guidelines or policy recommendations.

Photo Quiz. The photo quiz (1,200 words) highlights a person who made notable contributions to public health and medicine. Provide a photo of the subject, a brief clue to the person's identity, and five possible answers, followed by an essay describing the person's life and his or her significance to public health, science, and infectious disease.

Etymologia. Etymologia (100 words, 5 references). We welcome thoroughly researched derivations of emerging disease terms. Historical and other context could be included.

Announcements. We welcome brief announcements of timely events of interest to our readers. Email to eideditor@cdc.gov.

Joan Miró (1893–1983), *The Tilled Field (La Terre Labourée)*, **1923–1924.** Oil on canvas; 26 in × 36.5 in/66 cm × 92.7 cm. © 2018 Successió Miró/ Artists Rights Society (ARS), New York/ADAGP Paris 2019. Photo Credit: The Solomon R. Guggenheim Museum/Art Resource, New York, New York, USA